SC-CAMLR-SSP/5

SCIENTIFIC COMMITTEE FOR THE CONSERVATION OF ANTARCTIC MARINE LIVING RESOURCES

SELECTED SCIENTIFIC PAPERS
PART I

COMMUNICATIONS SCIENTIFIQUES SELECTIONNEES
PARTIE I

ИЗБРАННЫЕ НАУЧНЫЕ РАБОТЫ
ЧАСТЬ I

DOCUMENTOS CIENTIFICOS SELECCIONADOS
PARTE I

CCAMLR
25 Old Wharf
Hobart
Tasmania 7000
AUSTRALIA

Telephone : 61 (02) 31 0366
Facsimile : 61 (02) 23 2714
Telex : AA 57236

August 1989

Copies of this document are available on request to the CCAMLR Secretariat at the above address.

Abstract

This volume contains a selection of the scientific papers presented at meetings of the Scientific Committee and Working Groups of the Scientific Committee in 1988. The volume is published in two parts. Part I contains papers related to Antarctic krill. Part II contains papers on other Antarctic Marine Living Resources. The text of the papers is reproduced in the original language of submission; abstracts of the papers and captions of tables and figures are translated into the official languages of the Commission (English, French, Russian and Spanish).

Résumé

Le présent tome contient une sélection de communications scientifiques présentées aux réunions du Comité Scientifique et aux Groupes de travail du Comité Scientifique en 1988. Ce tome est publié en deux parties. La première partie contient les communications qui se rapportent au krill antarctique. La deuxième partie contient les communications sur les autres ressources marines de l'Antarctique. Le texte de ces communications est reproduit dans la langue originale dans laquelle celles-ci ont été présentées; les résumés des communications ainsi que les titres des tableaux et des figures ont été traduits dans les langues officielles de la Commission (anglais, français, russe et espagnol).

Резюме

Настоящий том содержит подборку научных работ, представленных на совещаниях Научного комитета и Рабочих групп Научного комитета в 1988 г., и состоит из двух частей. Первая часть содержит документы, имеющиеся отношение к антарктическому крилю. Вторая часть содержит документы касающиеся других морских живых ресурсов Антарктики. Они представляются на языке оригинала; резюме докладов, название таблиц и подписи к рисункам переведены на официальные языки Комиссии (английский, французский, русский и испанский).

Resumen

Este volumen contiene una selección de los documentos científicos presentados en las reuniones del Comité Científico y de los Grupos de Trabajo del Comité Científico en 1988. Se publica en dos partes. La Parte I comprende los trabajos relacionados con el krill. La Parte II comprende los trabajos sobre los otros recursos vivos marinos antárticos. El texto de estos documentos está reproducido en el idioma original; los resúmenes de éstos y los títulos de los cuadros y figuras están traducidos a los idiomas oficiales de la Comisión (inglés, francés, ruso y español).

TABLE OF CONTENTS

TABLE DES MATIERES

СОДЕРЖАНИЕ

INDICE

LIST OF AUTHORS
LISTE DES AUTEURS
СПИСОК АВТОРОВ
LISTA DE AUTRES

D.G. Bone	British Antarctic Survey High Cross Madingley Road Cambridge CB3 0ET UNITED KINGDOM
D.S. Butterworth	Department of Applied Mathematics University of Cape Town Rondebosch 7700 South Africa
V.N. Dolzhenkov	Laboratory of Antarctic Resources VNIRO Research Institute 17a, V. Krasnoselskaya MOSCOW 107140 USSR
I. Everson	British Antarctic Survey High Cross Madingley Road Cambridge CB3 0ET UNITED KINGDOM
K.G. Foote	Institute of Marine Research PO Box 1870 - NORDNES 5024 Bergen NORWAY
I. Hampton	Department of Environment Affairs Chief Directorate: Marine Development Private Bag X2 Roggebaai, 8012 South Africa
G.M. Jolly	38 Silverknowes Terrace Edinburgh EH4 5HJ UNITED KINGDOM
K. Kawasaki	Science and Engineering Research Institute Doshisha University Kyoto 606 JAPAN
S.A. Levin	Center for Environmental Research, and Section of Ecology and Systematics Cornell University Ithaca, New York, 14853 USA

T.G. Lubimova
Laboratory of Antarctic Resources
VNIRO Research Institute
17a, V. Krasnoselskaya
MOSCOW 107140
USSR

M.C. Macaulay
Northwest and Alaska Fisheries Center
Resource Assessment and Conservation Engineering Division
7600 Sand Point Way Northeast
BIN C15700, Bldg 4
Seatlle, Washington 98115-0070
USA

R.R. Makarov
Laboratory of Antarctic Resources
VNIRO Research Institute
17a, V. Krasnoselskaya
MOSCOW 107140
USSR

M. Mangel
Zoology Department and Center for Population Biology
University of California
Davis
California, 95616
USA

A. Morin
Department of Biology
University of Ottawa
Ottawa, Ontario KIN 6N5
CANADA

A. Okubo
Marine Sciences Research Center
State University of New York
Stony Brook, NY 11794-5000
USA

T.R. Osborn
Chesapeake Bay Institute
The Johns Hopkins University
The Rotunda, Suite 340
711 W40th Street
Baltimore, MD 21211
USA

S.S. Parfenovich
Laboratory of Antarctic Resources
VNIRO Research Institute
17a, V. Krasnoselskaya
MOSCOW 107140
USSR

T.M. Powell
Division of Environmental Studies
University of California, Davis
Davis, California, 95616
USA

V.A. Spiridonov
Laboratory of Antarctic Resources
VNIRO Research Institute
17a, V. Krasnoselskaya
MOSCOW 107140
USSR

J.L. Watkins
British Antarctic Survey
High Cross
Madingley Road
Cambridge CB3 0ET
UNITED KINGDOM

H. Yamazaki
Chesapeake Bay Institute
The Johns Hopkins University
The Rotunda, Suite 340
711 W40th Street
Baltimore, MD 21211
USA

SC-CAMLR-VII/BG/37

A SIMULATION STUDY OF KRILL FISHING BY AN INDIVIDUAL JAPANESE TRAWLER[*]

D.S. Butterworth

Abstract

A model is set up for the operation (which includes both searching and fishing) of a Japanese krill trawler over a half-month period. It is based on an underlying krill distribution model whose parameters are determined primarily from the scientific FIBEX surveys. Output from the model of the operation is compared with (and partially tuned to) statistics for a sample of data from the commercial fishery. A major inconsistency is found: haul times are a factor of 4-5 times greater in reality than in the model. Two *ad hoc* model modifications are introduced to eliminate this inconsistency: artificially elongating krill swarms, and allowing hauls to continue through more than one swarm. Twenty four candidate abundance indices (generally of a CPUE form) for krill biomass in the 600 n mile square oceanic sector modelled are considered, and their performance in response to a variety of ways in which the overall krill biomass might decline is investigated. Generally the indices respond by dropping relatively less than the proportional biomass decrease. Catch statistics collected at present (centred primarily on catch per fishing time) are of low utility in detecting biomass decline. Combination catch rate indices incorporating within-concentration search time give improved performances, but are able to monitor changes in within-concentration krill distribution parameters only. Indices that distinguish primary searching time from secondary searching time (searching while waiting to finish processing) within concentrations perform better, but collection of the requisite data may not be practical. Other approaches (e.g. research vessel surveys) need to be considered to monitor changes in the number, distribution and size of krill concentrations, both because there are doubts about the reliability of indices based on concentration searching time (which do respond to such changes), and because such indices are relatively imprecise. Priority needs to be given to improving the krill distribution model underlying the analysis; this probably requires that scientific surveys be planned to operate in small areas concurrently with fishing vessels.

---

[*] Revised and extended.

Résumé

Un modèle est établi pour l'opération (qui inclut la recherche ainsi que la pêche) d'un chalutier de krill japonais sur une période d'un demi-mois. Il est basé sur un modèle fondamental de répartition du krill, dont les paramètres sont déterminés essentiellement d'après les études scientifiques FIBEX. Les résultats du modèle de l'opération sont comparés aux (et en partie ajusté selon les) statistiques d'un échantillon de données de la pêcherie commerciale. L'on remarque une inconsistance majeure: les heures de trait sont un facteur 4 à 5 fois plus grand en réalité que dans le modèle. Deux modifications du modèle *ad hoc* sont introduites pour éliminer cette inconsistance: allonger artificiellement les bancs de krill et permettre aux traits de se poursuivre sur plus d'un essaim. Vingt-quatre indices d'abondance proposés (généralement sous forme de CPUE) sont considérés pour la biomasse de krill dans le secteur océanique de 600 milles carrés du modèle, et leur performance en réponse à une variété de manières dont la biomasse totale de krill peut baisser est l'objet de recherches. En général les indices répondent en baissant relativement moins que la baisse proportionelle de la biomasse. Les statistiques de capture recueillies à ce jour (concentrées principalement sur la capture par heure de pêche) sont de peu d'utilité pour détecter la baisse de la biomasse. Les indices de taux de pêche combinée, comprenant le temps de pêche dans la concentration, donnent de meilleurs performances mais peuvent uniquement contrôler les paramètres de répartition du krill dans la concentration. Les indices qui distinguent le temps de recherche primaire du temps de recherche secondaire (recherche dans l'attente de la fin du traitement) dans les concentrations donnent de meilleurs résultats mais il se peut que la collecte des données requises présente des difficultés. D'autres méthodes (par ex. des études des navires de recherche) doivent être considérées pour surveiller les changements dans le nombre, la répartition et la taille des concentrations de krill, en raison, d'une part, des doutes sur la fiabilité des indices basés sur le temps de recherche d'une concentration (qui répondent à de tels changements), et d'autre part, parce que d'autres indices sont relativement imprécis. Il faut accorder la priorité à l'amélioration du modèle de base de répartition du krill de l'analyse; ceci nécessite probablement de prévoir que les recherches scientifiques opèrent dans de petites zones concurrement avec les navies de pêche.

Резюме

Модель разработана для операции японского крилевого траулера, которая расчитана на полумесячный срок и влючает как поисковые, так и рыболовные действия. Эта модель базируется на модели распределения основного криля, параметры которой определены в основном из съемок по программе "FIBEX" Выходные данные модели операции сравнимы (и частично приведены в соответствие) со статистическим набором данных промышленного рыболовства. Главное несоответствие найдено: время траления - фактор в 4-5 раз больший в реальности, чем в модели. Для того, чтобы устранить это несоответствие, созданы две специальные модификации модели, которые удлинняют скопления криля и позволяют продолжать траления через более чем одно скопление криля. Учитываются двадцать четыре индекса вероятной численности (обычно формы CPUE) биомассы криля, смоделированной в квадратном секторе океана площадью в 600 морских мили., и изучается изменение этих индексов, в зависимости от разнообразных путей, по которым общая биомасса криля может уменьшаться. Как правило, индексы отвечают относительно меньшим понижением на соответствующие уменьшения биомассы криля. Статистические данные по динамике уловов, собранные в настоящее время (касающиеся главным образом улова на единицу промыслового усилия) мало используются в выявлении уменьшения биомассы. Обобщенные индексы интенсивности вылова, объединяющие время поиска в пределах концентрации, дают более совершенные результаты, однако, они дают возможность контролировать изменения параметров только в пределах границ концентрации. Индексы, различающие первичное время поиска от вторичного (поиска в течение ожидания окончания обработки собранных данных), в пределах концентраций работают лучше, но сбор необходимых данных может быть практически невозможным. Другие методы (например, съемки с Научно-исследовательского судна) должны учитываться для мониторинга изменений в числе, распределении и размерах криля, так как имеются сомнения по поводу надежности индексов, основанных на времени поиска концентрации (которые в действительности реагируют на такие изменения), и в связи с тем также, что эти индексы относительно неточны. В первую очередь необходимо усовершенствовать модель распределения криля, которая лежит в основе исследования; это, возможно, потребует, чтобы научные съемки проводились в небольших районах одновременно со съемками с промысловых судов.

Resumen

Se establece un modelo para la operación (que incluye tanto la búsqueda como la pesquería) de un arrastrero de krill japonés durante una quincena. Se basa en un modelo subyacente de distribución del krill cuyos parámetros están determinados principalmente por las prospecciones científicas FIBEX. El resultado de este modelo de operación se compara con (y parcialmente se ajusta a las estadísticas de una muestra de datos de la pesquería comercial. Se encuentra una anomalía mayor: la duración del arrastre es 4-5 veces mayor en realidad que en el modelo. Se introducen dos modificaciones al modelo ad hoc para eliminar esta anomalía: alargar los cárdumenes de krill artificialmente, y permitir que los lances se realicen en más de un cardumen. Se consideran veinticuatro índices posibles de abundancia (generalmente en forma de CPUE) para la biomasa de krill en el sector oceánico modelado de 600 millas náuticas cuadradas, se investigan sus funcionamientos en respuesta a las diferentes maneras en que la biomasa total del krill podría

declinar. Generalmente los índices reaccionan bajando relativamente menos que la disminución proporcional de la biomasa. Las estadísticas de captura recopiladas actualmente (centradas principalmente sobre captura por tiempo de pesca) son de poca utilidad para detectar la disminución de la biomasa. Los índices de la tasa de captura de combinación que incorporan tiempo de búsqueda dentro de la concentración dan resultados mejores, pero solamente pueden controlar cambios en los parámetros de la distribución del krill dentro de una concentración. Los índices que distinguen entre el tiempo de búsqueda primario y el tiempo de búsqueda secundario (explorando mientras se está terminando la elaboración) dentro de una concentración funcionan mejor, pero la recopilación de datos precisos puede que no sea práctica. Otros enfoques (por ej. prospecciones de buques de investigación) tienen que ser considerados para controlar cambios en el número, distribución y tamaño de las concentraciones del krill, tanto porque hay dudas sobre la exactitud de los índices basados en el tiempo de búsqueda de una concentración (los cuales responden a tales cambios), como porque tales índices son relativamente imprecisos. Se debe dar prioridad a mejorar el modelo de distribución del krill siendo la base del análisis; esto probablemente requiere que las prospecciones científicas sean planeadas para operar en zonas pequeñas al mismo tiempo que los buques de pesca.

1. INTRODUCTION

This document reports the results of a simulation study of krill distribution and the krill fishery in the Antarctic. The exercise is being undertaken on a contractual basis for CCAMLR to determine the (possible) utility of CPUE (catch-per-unit-effort) as an index of changes in krill biomass. A major objective is to provide insight regarding which particular catch statistics might most appropriately be collected to construct (CPUE-like) abundance indices with the greatest potential to reflect such changes.

This paper details an attempt to model the Japanese Antarctic krill fishing operation. This operation is strategically very different from the Soviet fishery, models of which have been presented in Mangel (1987, 1988). In the Soviet fishery, the activities of locating and of fishing krill concentrations are largely the separate responsibilities of different vessels, and a large number of vessels works in close collaboration. In contrast, in the current Japanese fishery (at least as a first approximation), the trawlers operate singly and independently of each other [see Butterworth (1988)], and have each to find the krill concentrations as well as to fish them.

The model developed has attempted to mimic the Japanese fishery in the "high season" (January-February). The reasons for this choice are discussed in Butterworth (1988); essentially, since catch rates are best in this period, it seems likely that future krill fishing will be concentrated in these months (as is already the case). A particular characteristic of the fishery over these months is that most hauls are reported to fish upon a single swarm of krill only.

The model is intended to reflect the operation of a single trawler off Wilkes Land. Butterworth (1988) sets out in some detail the reasons for choosing this area in preference to the Scotia Sea (where most Japanese krill fishing now takes place). The overriding concern was that initial modelling attempts should be aimed at an operation and area with as few complicating factors as possible.

The paper first describes the setting up of the underlying krill distribution model (section 2.1) for a 600 n mile square sector of the Southern Ocean and the basis for the choice of the distribution parameter values (section 2.2). The distribution model with these particular parameter values is designated the "base case". Chapter 2 then goes on to give a detailed description of the models used for the searching (both for concentrations, and for swarms within concentrations) and fishing operations.

A sample of the standard data collected in the commercial fishery was provided for the 1980/81 and 1981/82 seasons for a Japanese trawler that operated off Wilkes Land. Summary statistics are extracted from these data (section 3.1), and then compared to the "base case" simulation model output to check the realism of the model. This realism is improved by "tuning" some of the fishing operation model parameters to obtain better agreement between the data and the model output (section 3.2).

This exercise highlights a fundamental inconsistency between the model and the data: typical swarm sizes and densities, together with mean catches per haul, cannot be reconciled with average haul times and towing only a single swarm per haul. Compatibility is restored by modifying the model in two different ways (section 3.3):

(i) Artificially elongating swarms in the direction in which they are towed.

(ii) Allowing hauls to tow through more than one swarm.

For each of these approaches, the base case model krill distribution parameters are then adjusted in a variety of ways, each of which corresponds to reducing the overall krill biomass in the 600 n mile square sector under consideration by 50%. The change in the average value (over 100 simulations) of a number of potential abundance indices (developed in section 3.4) is determined for each of these adjustments, to examine the abilities of these indices to detect a biomass decline. Further, the behaviour of each of these indices is examined over a range of krill biomass values, where the change in the krill biomass from its original level is effected by a randomly chosen combination of changes in distribution parameters (sections 3.5 and 3.6).

Finally, shortcomings of the model are discussed (section 3.7), and conclusions are summarised and recommendations made in Chapter 4.

2. THE SIMULATION MODEL

The basic structure of the simulation model is set out in flow-diagram form in Figure 1. A trawler steams from its offloading point towards the southernmost limit ("ice-edge") of the 600 n mile square oceanic sector under consideration. Once a concentration of swarms is found, either *en route* to the ice-edge or following searching once the edge has been reached, the trawler will seek suitable swarms to fish in that concentration, and continue fishing in this way until either the catch-rate becomes too low, bad weather intervenes, or the time has come to return to offload (15 days after commencement). In the case of either of the first two of these reasons, searching will continue (after a period has elapsed in the event of bad weather) until another concentration is found, and the process above is then continued.

The sections of this Chapter that follow set out the details of each major element of the model as characterised in Figure 1, together with the rationale underlying that particular specification.

2.1 The Krill Distribution Model

In the first instance, it must be emphasised that the model developed here is a simplification of the real situation; it attempts to capture the main qualitative features of typical krill distribution patterns which would be relevant to the utility of catch statistics based indices as measures of biomass, but does not try to incorporate all the detailed knowledge about krill aggregation behaviour that is available. If certain abundances indices are indeed found not to have utility in this simplified situation, it is highly unlikely that the introduction of more detail into the distribution model would change this conclusion. On the other hand, if some promising candidate indices are revealed by this analysis, then the suitability of those indices should also be checked by simulation for more detailed krill distribution models; however, such an exercise is outside the scope of this initial investigation.

The largest scale considered in the model is a "sector" of the Southern Ocean. This sector is a square with sides of 600 n miles and approximates an area between, say, latitudes 60°S and 70°S spanning 20° of longitude. Clearly the simplest assumption to make would be that there is a uniform average density of krill in the area. However, a stratified habitat distribution as shown in Figure 2 has been used.

One of the reasons for deciding to use a stratified habitat is that scientific sighting surveys of minke whales (a major krill predator) carried out by the International Whaling Commission have shown that this species preferentially congregates close to the Antarctic ice-edge during the summer months [Butterworth *et al* (1987)]. It has therefore been presumed that the southernmost subsector S_1 (see Figure 2) is the most preferred habitat, and that preference for habitats decreases with movement northward.

This description is more representative of the south Indian and southwest Pacific Oceans (e.g. off Enderby Land and off Wilkes Land). For an initial modelling study, it is more convenient and appropriate to deal with such regions of simpler geography rather than, say, the complexities of the Scotia Sea with its island related krill distributional patterns [see Butterworth (1988)].

The South African FIBEX survey, which covered latitudes 60°S to 69°S in the Indian Ocean sector off Antarctica, did not show a correlation of krill abundance with latitude [Hampton (1985)], which argues against the habitat structure adopted for this krill distribution model. However, Hampton (pers. commn) suggests that it would be inadvisable to attach too much importance to this result. Although the survey in question commenced with its southernmost transect very close to the ice-edge, a major storm occurred within hours, changing conditions and rendering it impossible for the survey vessel to resume its original east-west trackline, so that it is questionable whether it really managed representative coverage of the near-ice-edge area. Further, discussions with the Captain of a Japanese krill trawler (Captain Fukui, pers. commn, September 1987) confirmed that his operations off Wilkes Land are generally within 100 n miles of the ice-edge, and often much closer (f 10 n miles) than that, which provides support for the form of habitat structure adopted.

The basic model for the krill within this sector is one of "patches within patches": the sector contains a number of *concentrations* of krill, and these concentrations consist in turn of collections of *swarms*, whose size is smaller than that of a typical concentration. The justification for a distributional model of this type is based on the more detailed hierarchical classification proposed by Kalinowski and Witek (1982, 1985) [see Butterworth and Miller (1987), Appendix I]. Attention has been restricted to swarms, as layers have too low a density for fishing them to be economic, and fishing on superswarms seems to be a relatively infrequent phenomenon [Butterworth (1988)].

The sector is taken to contain N_c concentrations of krill (see Figure 3). These concentrations are assumed to be circular with radius L_c, where L_c varies from one concentration to the next. Each concentration contains some number of swarms of krill. It is assumed that the number of swarms in a concentration (given a fixed total biomass in the sector) is proportional to its area. Thus, if L_c denotes the radius of the i^{th} concentration, the number of swarms in that concentration is given by:

$$N_{si} = D_{ci} \cdot \pi(L_{ci})^2 \qquad (1)$$

where D_{ci} is the density of that concentration in swarms per unit area. Although D_c may vary between concentrations, it is not (in terms of the assumption above) correlated with concentration size.

Individual swarms in the concentrations are characterised by physical location, length scale, density, and the nature ("quality") of the krill in the swarm. The centre of each swarm is assumed to be located uniformly and randomly within its concentration, i.e. any possible spatial correlation in the distribution of swarms within a concentration has been ignored. Each swarm is assumed to be circular in the horizontal plane with a radius r, and to contain krill of density δ measured as a biomass per unit area; both r and δ vary from swarm to swarm within a concentration.

Krill quality is a major concern for the Japanese fishery. Generally the larger sized krill are preferred, and "green" krill are avoided [see Butterworth (1988)]. It is not clear whether size and greenness are swarm or concentration properties, [although comments by Captain Fukui (pers. commn) suggest that they tend to be the latter] and the time scale over which greenness persists is unknown [Captain Fukui commented that this is definitely at least a few days, and that he suspects it is a few weeks]. For simplicity here, these quality factors will be ignored, though they should be an aspect for attention in subsequent studies. There is some further justification for ignoring greenness in this particular case, as the commercial data sample to which the simulation model output is to be compared was deliberately selected for a period where greenness was not a concern for the parent company of the vessel concerned [see Butterworth (1988)].

Although concentrations and swarms within concentrations undoubtedly do move, the model used for this study is quasi-static. For computational simplicity, general movement of the krill concentration field will be mimicked by keeping the position of the concentrations fixed and moving the fishing vessel (for example, during periods of bad weather - see section 2.4). Very large scale movements cannot be taken into account at this stage, because the simulation is restricted to a "sector" within which the krill biomass remains fixed (apart from the effects of fishing). Again, if a candidate abundance index proves to have no utility for monitoring biomass for this simple model, it is most unlikely that it would perform any better for a more complex model of krill movement.

However, in order to capture some effects of motion, a random search formula, rather than exhaustive search, will be used to characterise search both for concentrations, and for swarms within concentrations. This is discussed in more detail in section 2.6.

2.2 Setting the Krill Distribution Parameter Values

The following notation is used in this and following sections:

U[A,B]	indicates a uniform distribution over the range [A,B] (from which a random number is drawn)
$N[0,\sigma^2]$	indicates a normal distribution of mean zero with a standard deviation σ.

2.2.1 Habitat Stratification

It is assumed that the ratio of the densities of krill in subsectors S_1: S_2: S_3: S_4: S_5 is 12:6:4:3:2. Note that the two southernmost subsectors have narrower widths than the others, so that the corresponding abundance ratios are 6:3:4:3:2. There is little specific justification for the numerical choices made here (which could of course be varied), though the International Whaling Commission Antarctic minke whale surveys do indicate minke whale densities within ~ 1° of latitude of the ice-edge (cf: stratum S_1) are typically 2-4 times the densities further north [Butterworth *et al* (1987)].

2.2.2 Number of Concentrations

The estimate of the number of concentrations in the 600 n mile square sector that has been used in this study is:

$$N_c = 36 \qquad (2)$$

This estimate is based in the first instance on diagrams in Ichii (1987) of the operations of a Japanese trawler off Wilkes Land, which suggests a typical inter-concentration distance of about 100 n miles. It was then (partially) tuned so that the simulation model output produced values for total concentration searching time (TCST) roughly equivalent to those evident from the sample of commercial fishing data available.

2.2.3 Radius of (Circular) Concentrations of Swarms

The radii of concentrations are drawn at random from the following distribution:

$L_c = U[10/\sqrt{\pi},\ 20/\sqrt{\pi}]$ n miles

The basis for this choice is to be found in Butterworth and Miller (1987), Appendix I [which is essentially extracted from information in Kalinowski and Witek (1982, 1985)], which describes concentrations as extending over distances of 1 to 100 km. The $\sqrt{\pi}$ factor is an historical anomaly; it originated from maintaining equal concentration areas in two earlier analyses, one of which had modelled concentrations as square in shape. It has been maintained here to preserve some consistency with earlier work.

2.2.4 Surface (Areal) Density of Krill Within a Swarm

The surface densities (i.e. integrated over the vertical dimension) of krill swarms within concentrations are drawn at random as follows:

$$\delta = 150e^{\varepsilon}\ \text{g/m}^2 \qquad \varepsilon \text{ from } N[0,(1.4)^2] \tag{4}$$

Butterworth and Miller (1987) quote a range of 10 to several hundred g/m^3 for the volume density of krill in a swarm. The combined results from FIBEX [BIOMASS (1986), Table XI] give a mean krill volume density $\rho = 59$ g/m^3 and a mean swarm thickness of 5 m; this corresponds to a mean surface density $\delta \cong 300$ g/m^2. Kalinowski and Witek (1983) fit the ρ distribution with a log-normal distribution corresponding to $N[4.28,(1.40)^2]$, for which the median ρ is 72 g/m^3.

BIOMASS (1986), Table XI also indicates that:

c.v.(swarm thickness) ~ 0.25 c.v.(horizontal dimension)

so that the variability of swarm thickness is relatively negligible for the purposes of these calculations.

Accordingly, this suggests:

$$\delta = 300e^{\varepsilon}\ \text{g/m}^2 \qquad \text{where } \varepsilon \text{ from } N[0,(1.4)^2]$$

However, it should be noted that most of the data that contributed to the estimates above were collected in the Antarctic Peninsula area. Butterworth (1988) quotes Japanese Captains' statements that krill catch rates (which seem to relate primarily to within-swarm density) are higher in the Scotia Sea compared to the area off Wilkes Land. Further, Shimadzu (pers. commn) advises that swept-area experiments off Wilkes Land yielded density estimates of 5-10 g/m^3 over a 20 m deep net mouth, which correspond to surface densities $\delta = 100\text{-}200$ g/m^2.

Since the sample of commercial data with which the results of this simulation are to be compared was taken from an operation off Wilkes Land, the median density value suggested above was halved to the 150 g/m^2 used.

2.2.5 Radius of (Circular) Swarms Within a Concentration

The radii of swarms within concentrations are drawn at random from the distribution:

$$r = 50\, e^{\varepsilon} \qquad \varepsilon \text{ from } N[0,(1.1)^2] \tag{5}$$

Butterworth and Miller (1987) [extracted from Kalinowski and Witek (1982, 1985)] state "swarms are several tens of metres long". The FIBEX data [BIOMASS (1986), Table XI] give the mean intersected swarm length $\lambda = 73$ m. Kalinowski and Witek (1983) fit intersected swarm length by a log-normal distribution corresponding to $N[3.69,(1.09)^2]$, for which the median $\lambda \sim 40$ m.

If swarms are assumed to be circular, the radius r is related to λ by:

$$r = (2/\pi)\lambda \tag{6}$$

so that the FIBEX data correspond to a mean $r \sim 47$ m, and Kalinowski and Witek's (1983) results to a mean $r \sim 25$ m.

This would seem to suggest that the median value for r of 50 m adopted for this analysis may be rather too high, particularly as the estimates extracted from the data should be modified further by the $e^{-\sigma^2/2}$ factor for mean-to-median conversion for a log-normal distribution. Further, intercept survey [on which the BIOMASS (1986) results were based] is size biased, and will give a positively biassed estimate of the average radius of circular swarms. On the other hand, the non-circularity of swarms that occurs in practice will introduce a bias in the other direction [Hampton (1985)]. A further fact which suggests this median value choice may be too large is that Kalinowski and Witek (1983) fit the distribution of swarm biomasses by a log-normal corresponding to $N[6.03,(2.54)^2]$, for which the median swarm biomass $B_s = 0.42$ tonnes. This corresponds to a mean $\bar{B}_s = 10.5$ tonnes, which is somewhat less than the $\bar{B}_s = 35$ tonnes to which the chosen distribution model parameters correspond (see summary subsection following). These aspects have not been pursued further at this stage, but merit more investigation in due course.

2.2.6 Density of Swarms Per Unit Area in a Concentration

Swarm densities within concentrations have been generated from:

$$D_c = 20e^{\varepsilon} \text{ (n miles)}^{-2} \qquad \varepsilon \text{ from } N[0,(0.1)^2] \tag{7}$$

The rationale which follows for estimating the median value, was drawn to the author's attention by I. Hampton.

Consider an area A containing N_s circular swarms each of radius r. If F is the fraction of the area A that is covered by the swarms, then:

$$F = N_s \cdot \pi\, r^2/A \tag{8}$$

For an echosounder based line intercept survey of krill swarms, the echosounder beam width is much less than the typical swarm diameter (~100 metres), so that if s is the average distance between swarms detected on the echosounder, and given that these swarms have been assumed to be circular, an estimate of fractional cover F is provided by:

$$F = [2r \cdot \pi/4]/s \qquad \text{(for } s >> r\text{)} \qquad (9)$$

so that:

$$D_c = N_s/A = 1/(2rs) \qquad (10)$$

Inspection of the sample of data provided from the Japanese krill fishery suggests that $s \sim 3$ n miles [see distance between successive hauls (DBH) in Table 1)]. However, application of equation (10) is inappropriate in this case, as it seems from comments made to the author by Mr Ichii and Captain Fukui that sonars (of much wider effective search width than echosounders) do play a major role in swarm detection by the fishing vessels [in contrast to the impression given in Butterworth (1988)], and also because it seems that there is considerable selection taking place in the choice of swarms for fishing (see section 2.7). Nevertheless, equation (10) can be applied to the FIBEX results which report an average inter-swarm spacing of 2.2 km [BIOMASS (1986)]. Taking $r = 50$ m then, gives $D_c = 15.6$ swarms per (n mile)^2.

The $s = 2.2$ km FIBEX figure includes some effective between-concentration as well as the within-concentration spacings, and hence is positively biased for the purpose used here. Accordingly, the median value in (7) was rounded upwards from the estimate obtained using equation (10). The choice of a value for the variance is semi-arbitrary; some variation seems appropriate to allow for differences in D_c from concentration to concentration, which must exist in practice.

2.2.7 Summary and Relation to Circumpolar Krill Biomass

The krill distribution model parameters chosen (for what will subsequently be referred to as the "base case") are therefore:

Relative densities of strata: $S_1{:}S_2{:}S_3{:}S_4{:}S_5 = 12{:}6{:}4{:}3{:}2$
Number of concentrations: $N_c = 36$ (11)
Concentration radius: $L_c = U[10/\sqrt{\pi},\ 20/\sqrt{\pi}]$ n miles
Swarm density: $D_c = 20e^{\varepsilon}\ (s)^{-2}$ ε from $N[0,(0.1)^2]$
Swarm radius: $r = 50e^{\varepsilon}$ metres ε from $N[0,(1.1)^2]$
Swarm (areal) density: $\sigma = 150e^{\varepsilon}$ g/m^2 ε from $N[0,(1.4)^2]$

These parameter values can be used to compute the overall abundance of krill to which the distribution model then corresponds. Using the median values for the parameter distributions yields:

Swarm biomass: $B_s = \sigma \pi r^2 = 1.18$ tonnes
Number swarms in concentration: $N_s = D_c \pi L_c^2 = 4\ 500$
Concentration biomass: $B_c = N_s B_s = 5\ 300$ tonnes
Sector biomass: $B_{sec} = N_c B_c = 0.19$ million tonnes
Biomass around Antarctica: $B_{Ant} = 18\ B_{sec} = 3.4$ million tonnes.

This last figure seems at least an order of magnitude too small. Estimates of (historic) krill consumption by predators have been in the 100-200 million tonne range. Growth rate and longevity estimates for krill [see Rosenberg *et al* (1986)] suggest a production:biomass ratio for krill certainly rather less than unity, so that 500 million tonnes might be an appropriate order of magnitude estimate for the circumpolar krill biomass.

However, the calculations above need to be amended to take into account the bias factors that arise when distributions rather than single values are used for the parameters. For example, the mean of a log-normal distribution (used above for D_c, r and δ) is not equal to its median as utilised in the preceding calculation, but is a factor $e^{\sigma^2/2}$ larger. Revised multiplications along these lines yield mean values:

$\bar{B}_s$ = 35.3 tonnes

$\bar{N}_s$ = 4 690

$\bar{B}_c$ = 166 000 tonnes
B_{sec} = 6 million tonnes
B_{Ant} = 108 million tonnes

which appear to be far more realistic figures.

The basic distribution model, and the rationale for the choice of parameter sp16 values, were presented to participants at a BIOMASS SIBEX Workshop in Cambridge in July 1988. While the obvious shortcomings of the model were recognised, it was generally agreed that existing data were neither adequate to allow substantial improvements to the model at this time, nor radically in conflict with any aspect of the model.

2.3 Generation of the Krill Concentration Field

The total of N_c = 36 concentrations is located in the basic 600 n mile square sector with its stratified habitat, where the southernmost strata are the more preferred regions for krill concentrations. The east-west coordinate of each concentration centre is selected on a uniform random basis from [0,600] n miles; the north-south coordinate is also selected at random from [0,600] n miles, but from a step-wise uniform distribution corresponding to the relative densities chosen for the stratified habitats. A particular realisation of the procedure is shown in Figure 3.

For computational convenience in simulating the fishing operation, two constraints are applied in generating this distribution: potential concentrations whose position and radius (selected from $L_c = U[10/\sqrt{\pi}, 20/\sqrt{\pi}]$ n miles) are such that they overlap the sector boundaries are disallowed, and potential concentrations which overlap those already placed in the sector are similarly excluded.

The chosen parameters are such that a considerable fraction of the potential concentrations (typically some 15% of the desired total number) can be excluded by these constraints. Accordingly, in scenarios (see section 3.5) where the L_c range is reduced for comparative abundance index studies, the original $[10/\sqrt{\pi}, 20/\sqrt{\pi}]$ n miles range is used in applying the constraints when setting up the concentration field, and only then are the concentration radii all diminished by the desired fraction.

2.4 Bad Weather Periods

Ichii (*in litt.*, 30 May 1988) has provided information on the frequency with which bad weather led to suspension of Japanese krill fishing operations. In his compilation, drawn from the 1973/74 to 1985/86 seasons, a total of 37 out of 1472 days, or 2.5%, were affected. The frequencies of the durations of these bad weather periods were:

one day : 68%
two days : 28%
three days : 4%

In the simulation, the probability that bad weather commences (as distinct from occurs) on a particular day within the 15 day (half-month) period under consideration is accordingly taken to be 0.02. The duration of that period is chosen at random to be 24, 48, or 72 hours according to probabilities of 0.68, 0.28 and 0.04 respectively. The time of onset of a particular period of bad weather during the day concerned is selected at random. Bad weather will not, however, recommence on the same day that a previous period of bad weather abated. [Note that this is a slightly more complex prescription than in the study by Mangel (1987), where the bad weather periods all commence and end at midnight.]

Once bad weather commences, the vessel can neither search for concentrations nor seek and fish swarms within a concentration (though a trawl in progress at the time of commencement will be completed); however, transit both to and from offloading remains possible. One minor exception to this (for computational convenience) is that if bad weather occurs while the vessel is *en route* to its chosen spot on the ice-edge, and its track intersects a concentration during that bad weather period, it waits at that position and commences fishing once good weather returns. If bad weather occurs on the way back to the offloading point, this is counted as transit time rather than loss to bad weather; this is because the vessel continues searching/fishing until the last possible moment that will allow it to get back (travelling at 10 knots) to the offloading point within the 15-day deadline, and so would be unable to fish on any concentrations that might be detected on the return trip - hence bad weather at such a time does not result in the loss of any opportunity to fish.

A vessel affected by a 24/48/72 hour period of bad weather is moved 50 n miles in a random direction (reselected if it would move the vessel outside the sector boundaries), and has to recommence searching for a concentration at the end of that period. To a limited extent, this mimics movement of the krill concentration field. (This movement does not occur in the case of the minor exception discussed in the preceeding paragraph.)

The model feature of "losing" concentrations during bad weather is not entirely realistic, as echo sounders do enable vessels to search and keep track of swarms during such periods. However, no allowance has been made in the model for temporal variability in the parameters describing a concentration and the distribution of krill within it, because of the absence of pertinent data to parameterise such effects. Dispersion of a concentration would lead to a vessel leaving to search for another concentration because of a drop in catch rate, so that the manner in which bad weather consequences are modelled can be considered in part as a surrogate for the effect of such temporal variability.

2.5 Initial Searching Strategy for Concentrations

Ichii (pers. commn) advises that a Japanese krill trawler needs to offload at a cargo vessel typically twice a month; accordingly, a 15 day period (a "half-month") was chosen for this simulation study. The trawler commences operations for the half-month from the offloading position, which is assumed to be on the western boundary of the sector at a distance 100 miles from the ice-edge [i.e. the point (0,100)]. This choice may be rather larger than is realistic, as Ichii (*in litt.*, 30 May 1988) advises that his experience is that the cargo transfer is carried out close to the ice-edge to take advantage of the calmer conditions there.

Butterworth (1988) reports that "the opening strategy is often to move to an area where good catches were made the previous season". This "area" is assumed in the simulation model to be close to the ice-edge and near the east-west midpoint of the sector, so that the vessel sets an initial course for the point (300,0), steaming at the searching speed of 10 knots.

If no krill concentration is encountered, the vessel commences its general search strategy once the ice-edge is reached. However, if an encounter takes place - determined in the simulation model by checking whether the transit line intersects the circular boundary of any of the concentrations placed in the sector - fishing commences on the first concentration found in this manner. Once fishing on this concentration has concluded, the vessel commences its general search strategy from the position of that concentration, i.e. the original strategy of heading for the ice-edge is "forgotten"; having found krill in that vicinity, the vessel would regard it as a "good area" and so consider it worthwhile to seek further concentrations in that region.

The period steaming to the ice-edge (except insofar as bad weather intervenes) is regarded as "concentration searching time" (CST) commensurate with that incurred during the exercise of the general search strategy described in the next section.

2.6 General Search Strategy for Concentrations

In order to capture some of the effects of concentration movement, a random search formula rather than an exhaustive search process is used to characterise the search for concentrations. Suppose that an area A contains a krill concentration and that this area is searched at rate W_s units of area per unit time, so that after t units of time the area searched is W_st. In exhaustive search, if W_st is greater than A, the concentration is detected with probability 1. In circumstances where the concentration moves relative to the searcher, it could move back into a region which has already been searched. Such a situation can be regarded as a random search, and under very general conditions random search is characterised by the formula (see Figure 4):

$$\text{Prob \{detecting the object after t time units\}} = 1 - \exp(-W_st/A) \tag{12}$$

For this analysis, this formula becomes:

$$\text{Prob \{detecting a concentration after t hours\}} = p(t) = 1 - e^{-wdvt} \tag{13}$$

where:
w is the effective search width (n miles)
d is the density of concentrations (per n mile^2)
v is the searching speed (knots).

Since echosounder and sonar beam widths are much less than the modal concentration radius used ($15/\sqrt{\pi} \cong 8.5$ n miles), the effective search width is taken to be the modal concentration diameter:

$w = 17$ n miles

(i.e. a concentration is detected if the vessel crosses its boundary).

For the searching speed:

$v = 10$ knots

and for the southernmost stratum in the base case:

$$d = 12/(75 \times 600) = 1/3750 \text{ (n miles)}^{-2}$$

so that the random search formula becomes:

$$p(t) = 1 - e^{-0.045t} \qquad (14)$$

which corresponds to a mean search time to find a new concentration of 22 hours.

This formula must be adjusted for strata with different concentration densities, or simulations where the modal L_c value is changed; in general, it becomes:

$$p(t) = 1 - \exp\{-0.045\ (3750d)\ (L_c/8.5)\ t\} \qquad (15)$$

The search for concentrations is considered in blocks of time which are each of 8 hours duration. The reason for this limitation is to allow the value of d in equation (15) to be changed if the vessel's search moves it into a stratum with a different concentration density. Thus, a random number u from U[0,1], coupled with a value for d corresponding to the vessel's position at the start of that search time block, is used together with equation (15) to determine the time t until a concentration was found as follows:

$$t = -\ [ln(1 - u)]/[0.045(3750d)(L_c/8.5)] \qquad (16)$$

If equation (16) provides a value $t > 8$ hours, the vessel is moved to a new position, and the process repeated until a value of $t < 8$ hours is obtained.

As the vessel would not necessarily steam along a single straight line over such an 8 hour period, 80 n miles is the maximum distance the vessel could have moved from its position at the start of the search time block. For simplicity, it is assumed that the actual distances in n miles moved by the vessel from its various starting points are drawn at random from the uniform distribution U[0,80]. The vessel is then moved the selected distance in a randomly chosen direction, and the calculations are repeated for the next search time block. (The direction is reselected if it is such as would move the vessel outside the sector boundaries.)

Once equation (16) yields a value of $t < 8$ hours, the simulation model program determines which concentrations (i) have their centres a distance s_i from the vessel's starting point for that search time block, where $s_i < 10t$. Note that 10t n miles is the maximum radial distance that the vessel could have steamed from the starting point in t hours. If there are no such concentrations, the vessel is moved some distance within a circle of radius 10t n miles. This distance is calculated on the same basis as described in the preceding paragraph, and another 8 hour search time block then commences at a time t hours later.

Alternatively, one or more concentrations are found within this 10t n mile radius. If only one is found, this is the concentration taken to be discovered. If more than one possibility exists, a choice (using random number generation) is made between those concentrations based on the relative weightings:

$$w_i = L_{ci}/(s_i + 10) \qquad (17)$$

The rationale for the L_{ci} term is that larger concentrations are more likely to be discovered, as the effective search width is proportional to concentration radius. In the absence of any concentration within a 10t n mile radius, the vessel would move a distance drawn from U[0,10t], so that the distribution of distances to concentrations actually found should have a similar form. However, because of the expanding area effect, the number of concentrations possibly discovered will increase linearly with s (on average), so that larger values of s from the [0,10t] range would be favoured. The denominator term involving s in equation (17) was introduced to compensate for this effect; the added 10 n miles is an *ad hoc* adjustment to deaccentuate what would otherwise be very high weights accorded to concentrations very close by.

In cases where the previous concentration has been left because of a poor catch rate, the simulation model program precludes the vessel from rediscovering this same concentration during this search process (though it could be rediscovered later after another concentration has been fished). This restriction does not apply to cases where bad weather has interrupted the fishing, however.

Throughout these calculations, checks are made regarding the onset of bad weather and the need to return to the offloading point [identical to the (0,100) commencement point] before the end of the 15 day period. In circumstances where either of these deadlines occur at a time t^* after commencement of a search time block, and $t^* \leq \min[t,8]$ where t is determined from equation (16), only t^* hours is added to the "concentration searching time" (CST) and this period of search is regarded as unsuccessful.

2.7 Generation of the Krill Swarm Field Within a Concentration - Fishing Selectivity

To save on computer time requirements, the swarm field within a concentration is only set up if that particular concentration is discovered in the searching activities during a specific simulation run. Values of the parameters of the distributions of δ , r and D_c are needed for this process and are generated using equations (11).

The question arises of whether swarm radius and density are correlated, i.e. do larger swarms tend to be more (or less) dense than average? From the Kalinowski and Witek (1983) log-normal fits to ρ and λ, it follows that:

$$\sigma_\rho^2 + (2\sigma_\lambda)^2 = (2.59)^2 \qquad (18)$$

This is very close to the variance of their log normal fit to swarm biomass $[(2.54)^2]$, suggesting little covariance between swarm size and density. This provides some justification for the simulation model procedure of generating the r and δ parameters for a particular swarm from independent distributions.

What would be the average catch per swarm taken from a swarm distribution with the parameter values of equation (11), by a typical fishing net of size 20 m by 20 m? The vertical range of most swarms would be completely encompassed by such a net, so that a well directed tow on a circular swarm would yield on average:

$$\begin{aligned} C &= 20 \cdot 2\,\bar{r} \cdot \bar{\delta} \\ &= 20 \cdot 2 \cdot 50 \exp\{(1.1)^2/2\} \cdot 150 \exp\{(1.4)^2/2\} \text{ g} \qquad (19) \\ &= 1.46 \text{ tonnes} \end{aligned}$$

This cannot be reconciled with data in Shimadzu (1984) that the average number of swarms trawled per haul is 1.5, and in Shimadzu (1985) that the average catch per haul of the Japanese independent trawlers is about 6 tonnes (8 tonnes for the specific commercial data set examined in this study - see Table 1), unless (as indeed might be expected) considerable selection is taking place.

The simulation model program assumes that only those swarms whose biomass exceeded a certain limit (B_{min}) are selected by the fishery. In reality, the Captain does not, of course, make a quantitative estimate of the actual swarm biomass, but rather exercises his judgement based on the indications of swarm size and density evident from his echosounder and sonar. Swarm biomass is a simple and convenient way of combining the measures that will contribute to the Captain's decision into a single quantity. The limit is chosen to provide an average catch per swarm in the vicinity of 8 tonnes (as in Table 1 - see section 3.2), and further incorporates a stochastic component to allow for the fact that there will be imprecision involved in a Captain's estimate of whether a swarm is sufficiently large to warrant its being fished. Thus, the biomass of each swarm generated in the swarm field creation procedure is compared with:

$$B_{min}\, e^{\varepsilon} \text{ tonnes} \qquad \varepsilon \text{ from } N[0,(0.2)^2] \qquad (20)$$

and only those swarms of greater biomass are regarded as "fishable".

The value chosen for the variance in equation (20) is the same as used in modelling the precision with which the Captain estimates the amount of krill caught while the haul is taking place, the basis for which is discussed in section 2.8 [immediately preceding equation (22)].

The limitation of equation (20) means that only a smallish proportion of the total number of krill swarms are fishable (about 7% and about 30% for two modified models eventually considered - see sections 3.2 and 3.3). The simulation model program only needs to retain the parameter values of this subset of all the swarms in the concentration, which saves considerably on storage needs and calculation time.

The positions of the centres of each fishable swarm within the concentration are selected at random (i.e. possible spatial correlation is ignored). This is the only constraint applied; the swarms are not precluded from overlapping each other or the perimeter of the concentration. A particular realisation of this process is shown in Figure 5.

For reasons discussed earlier, the simulation model does not take into account any krill quality aspects - neither "greenness" nor size.

2.8 Searching and Fishing for Swarms Within a Concentration

The initial swarm fished in the concentration discovered is selected at random from all the swarms, irrespective of its position in the concentration. [Note: for terminological convenience, "swarm" is used in this section in the sense of a "fishable swarm", as defined in section 2.7, unless specifically indicated otherwise]. Fishing on this swarm is assumed to commence immediately upon discovery of the concentration, without expenditure of any further search time.

The catch made during a tow is given by:

$$C = \min[40r\delta,\ B_s] \qquad (21)$$

This assumes that swarms are towed along their diameter using a net with 20m x 20m mouth opening, that this net encompasses the complete vertical range of the swarm, and that there is no substantial net avoidance behaviour by the krill. In earlier work the inclusion of an adjustment factor to allow for larger swarms being more easily towed close to their diameter was considered. However, the typical size of those swarms which are ultimately selected as fishable swarms is >> 20m, so that this aspect (whose quantitative parametrisation is problematic anyway) has been disregarded because such large swarms are probably easily targeted. Note that as swarms are assumed to be circular, no allowance "needs" to be made for the Japanese trawlers having to carry out their tows with the wind behind them [Butterworth (1988)].

The simulation model program does also allow for tows being curtailed before the net has passed through the whole swarm. This occurs on occasions because the vessels have limited processing capacity, and the complete catch from a haul has to be processed within a certain period before the krill deteriorates. Because the turnaround time from one haul to the next is roughly two hours, the Captain will aim to make a catch that is about twice the vessel's hourly processing capability. Data on vessels' exact processing capabilities are not available (the information is classified for commercial reasons), but Ichii (pers. commn) advises that for the vessel for which the data sample was provided, the processing capability was in the vicinity of 5 tonnes/hour.

It is therefore assumed in the simulation model that the Captain aims for a catch of a maximum of 10 tonnes, and curtails his fishing time accordingly. The Captain's estimate of the curtailment time will, however, be subject to error, and Captain Fukui (pers. commn) suggested that the catch made could typically differ from that intended by some 20%. Thus, the maximum catch permitted in a haul by the model is:

$$C_{max} = 10\, e^{\varepsilon} \text{ tonnes} \qquad \varepsilon \text{ from } N\,[0,(0.2)^2] \tag{22}$$

The hauling time that is recorded in the standard data reported for the krill fishery corresponds to the period from the net reaching the desired towing depth to the moment when the net starts to be raised; this will be referred to as the "fishing time" (FISHT). Captain Fukui (pers. commn) advised that the net generally reaches the intended depth about 300 m before entering the krill swarm itself. If b metres is the length of the swarm towed through [calculated from equations (21) and (22)], then as the trawlers tow at 2 knots, the fishing time is calculated as:

$$\text{FISHT} = b/(2 \times 1852) + 0.08 \text{ hours} \tag{23}$$

Allowance must also be made for the time required to lower the net to the desired depth, and later to recover it back on deck with the catch. Rough estimation using a small sample of some very detailed data collected by one particular Japanese trawler during the 1986/87 season (and kindly provided by Dr Shimadzu) suggested:

$$\begin{aligned} t_{lower} &= 0.33\, e^{\varepsilon_1} \text{ hours} \qquad \varepsilon_1 \text{ from } N[0,(0.35)^2] \\ t_{raise} &= 0.33\, e^{\varepsilon_2} \text{ hours} \qquad \varepsilon_2 \text{ from } N[0,(0.12)^2] \end{aligned} \tag{24}$$

where the lowering time is measured from the moment the swarm is first detected to the instant the net reaches the desired depth (and FISHT begins). Ichii (*in litt.*, 30 May 1988) advises that both these times are correlated with the depth of the haul. The model has therefore, pending further analysis of available data, assumed the extreme of exact correlation [i.e. generate ε_1, then $\varepsilon_2 = 0.12\, \varepsilon_1/0.35$].

The effect of fishing on a swarm is assumed to be only a reduction in that swarm's radius. The position and surface density δ are taken to be unchanged, and the revised radius is calculated to correspond to the original biomass of the swarm less the catch made.

The initial version of the simulation model restricts hauls to towing through a single swarm. For reasons discussed in section 3.2, this restriction has been relaxed in a subsequent modification. In this modification, once a concentration is found, the parameters of the fishable swarms only are stored as before, but if after towing through one of these fishable swarms, the "Captain" estimates that he has yet to obtain the desired total catch of 10 tonnes, he continues the haul. He then fishes on further swarms which he finds in his path until either a maximum towing distance TOW_{max} (taken here to be 4 n miles) is reached, or he estimates that the additional krill taken from these further swarms has resulted in his catch now having reached 10 tonnes.

To effect this in the modified simulation model for cases where towing continues beyond the initial swarm, further swarms (of any size, not only fishable swarms) are generated in the manner described in section 2.7 in a rectangular area. This area is of length TOW_{max} less the distance already towed at the point of exiting the initial swarm, and width 0.5 n miles either side of the vessel's trackline. Only the parameters of those swarms which intersect the trackline, or whose perimeters come to within 17.5 metres of the trackline (corresponding to an assumed sonar detection width), are stored. For the computational convenience of avoiding having to deal with overlapping swarms, the distances between swarms intersecting this "sonar band" around the trackline are increased so that swarms which did intersect in this band consequently only touch at their boundaries; any swarms overlapping the TOW_{max} distance as a result are excluded. The vessel then fishes each swarm in turn along its longest chord within the sonar band (i.e. deviation by the vessel up to 17.5 metres either side of the trackline to effect this is allowed), until TOW_{max} is reached or the estimated catch exceeds 10 tonnes (this may involve ending the haul midway through one of the subsequent swarms). A particular realisation of this process is shown in Figure 6.

Once the net has been raised, searching commences for another swarm on which to tow. [Strictly, this searching starts at some stage during the raising of the net (Ichii, pers. commn), but this factor is ignored in the model for simplicity.] If a good catch rate has been obtained from the swarm just fished, attempts will be made to relocate and refish that swarm. [A further criterion in practice is whether the catch contained the larger sizes of krill, though this is beyond the scope of this model which ignores krill quality aspects.] Ichii (pers. commn), in the light of observations made on a Japanese krill trawler, estimates that such attempts are made after some 40% of the hauls, but that only about half of these are successful in relocating the swarm just fished. In the program, therefore, whenever:

$$C/FISHT > (C/FISHT)_{rpt} \qquad (25)$$

the swarm just fished is refished with a probability of 0.5. When refishing occurs, a fixed period of 0.2 hours was added to the "total primary searching time" for swarms (TPST).

The value of $(C/FISHT)_{rpt}$ in constraint (25) is chosen to have the program produce a refishing attempt probability in the vicinity of Ichii's 40% estimate (see section 3.2). The 0.2 hours is slightly less than the average interswarm searching time recorded for a Japanese trawler in the 1986/87 season [see discussion following equation (27)]. More than one sequential retowing of a swarm is possible; the model program repeats the above procedure until constraint (25) is not satisfied, or the swarm is not relocated (as determined by random number generation and the 0.5 relocation probability).

If refishing of a swarm does not occur, search has to be conducted for a new swarm to fish. The computational procedure used is basically identical to that described for concentrations in section 2.6. The random search formula used [analogous to equation (15), with t again in hours] is:

$$p(t) = 1 - \exp\{-4\ (D_c/20)\ \ (S/S_b)\ t\} \qquad (26)$$

where: D_c is the density of swarms per (n mile)^2

S is the selectivity, which is the ratio of the number of fishable swarms [from equation (20)] to the total number of swarms in the concentration

S_b is the selectivity for the base case krill distribution parameters.

Mangel (1988) considers a more detailed model for searching for swarms within a concentration, and reports that it results in distributions of search times that are well fitted by exponential distributions of the form of equation (26).

For the base case, $D_c = 20$ and $S = S_b$ so that:

$$p(t) = 1 - e^{-4t} \tag{27}$$

which corresponds to an average search time of 0.25 hours. The value of 4 was in fact chosen on the basis that a sample from the time-budget data collected on a Japanese trawler during the 1986/87 season, and provided to the author by Dr Shimadzu, indicated a mean interswarm searching time of about 15 minutes. Ichii (*in litt.*, 30 May 1988) advises that he observed interswarm searching times of about 10-15 minutes off Wilkes Land in the 1985/86 season, and that the time to rediscover the same swarm was comparable. Note that this implies less efficiency than the random search formula [equation (13)] indicates, the equivalent parameter values for model modifications to be considered (see sections 3.2 and 3.3) being:

$$\left.\begin{array}{l} w = \text{1 n mile (see following paragraph)} \\ v = \text{10 knots} \\ d = D_cS = 20 \times (0.07 - 0.30)\ (\text{n. mile})^{-2} \end{array}\right\} wdv = 14 - 60 \text{ hrs}^{-1} \tag{28}$$

However, the value of an appropriate estimate for w is uncertain, and use of the empirical data seems a more secure approach.

The exponent in equation (26) is taken to be proportional to the density of fishable swarms in the concentration (D_cS); note that S will change in those of the scenarios to be considered (section 3.5) where the parameters of the r or δ distributions are altered. An argument could be made that the exponent should also contain a term proportional to the median of the swarm radius (r) distribution. However, comments to the author by Ichii and Captain Fukui (pers. commn, Sept. 1987) indicate that sonar is quite important in finding swarms. Sonar can have an effective search width of up to 2 n miles, which is rather larger than typical swarm radii (even for the fishable swarms only). It is therefore assumed that the effective search width for swarms is invariant, and the effects of changes in r on search times are manifest only through the selectivity term S.

The "primary search time" (PST, measured in hours) to the next swarm is thus determined by use of a random number u from U[0,1] and equation (20):

$$PST = -[ln(1-u)]/[4(D_c/20)(S/S_b)] + 0.01 \tag{29}$$

The additional 0.01 hours is added to avoid unrealistically small divisions occurring for certain CPUE indices. Unlike the situation with concentrations, no search time block approach needs to be applied, because there is no swarm density gradient within any of the simulated concentrations.

A search is then made by the program for all swarms whose centres are within a distance of 10*PST n miles of the swarm previously fished (excluding that last swarm).

[Strictly the centre point of the swarm previously fished is not always used; this occurs particularly in the model modification which allows for a tow through more than one swarm. Provided the tow proceeds further than half way through the initial swarm, the point from which searching commences for a new swarm upon which to set the net allows for the distance moved by the vessel beyond the centre of the initial swarm, including the time needed to raise the net. The tow direction is taken to be random, but the movement is precluded from taking the vessel beyond the concentration boundary.] If there are no swarms within this distance, fishing is assumed to take place on the nearest swarm in the concentration (for simplicity of programming; this happens only very rarely, and is not unfeasible because of the possibility of swarm movement). If one or more swarms are present, the selection procedure to determine which swarm is actually discovered is as for concentrations (see section 2.6); the relative weighting factors for each swarm (j) [analogous to equation (17)] are:

$$w_j = r_j/(s_j + 0.1) \qquad (30)$$

where s_j is the distance in n miles to the j^{th} swarm, 0.1 is an *ad hoc* adjustment to deaccentuate weights accorded to swarms very close by.

However, a further complication can arise with the discovery of this next swarm, as fishing may need to be delayed to allow processing of the previous catch to progress sufficiently. Processing can continue while a new haul is in progress, but to avoid problems with deterioration of the new catch, processing of the previous catch should be complete by the time the new catch arrives on deck.

This creates a non-trivial problem, as it is not clear beforehand how long the next haul will take, though there is the option of leaving the net in the water longer to slow deterioration of the krill while processing of the catch from the previous haul is completed. However, to simplify matters in constructing the simulation, it is assumed that, given the typical interhaul turnaround time of about 2 hours, the Captain allows for a fixed maximum 1.5 hours of processing during the forthcoming tow.

Even so, by the time the next swarm is discovered, the amount of the previous catch left to process may still exceed 7.5 tonnes (corresponding to 1.5 hours processing at 5 tonnes/hour), so that commencement of the next haul has to be delayed. [The processing rate depends on the particular krill product being produced, but this complication is ignored here for simplicity.] The period from discovery of the swarm until the haul can commence is termed "secondary searching time" (SST). In practice, it is spent keeping track of the swarm found, deciding the best strategy for fishing it, and possibly also examining other swarms seen nearby which may be chosen for towing instead. For simplicity, however, the simulation model assumes that the haul is always carried out on the swarm first found.

The initial version of the simulation model assumes that all hauls are made on a single swarm only. Data (see section 3.1 and Table 1) and comments received from vessel Captains [Butterworth (1988)] indicate that this is the predominant pattern in the Japanese krill fishery during the "high season" (January-February). While the placement of the swarms in the concentration does not preclude overlapping, the simulated tows in the initial implementation ignore this possibility, taking krill from only the single swarm "discovered".

Figure 5 shows a particular realisation of a vessel moving within a concentration while both towing and searching (note that the tow lengths shown correspond to the model modification with f = 8 - see section 3.3).

Fishing on a concentration may end for one of three possible reasons in the simulation model: the need to return to offload, the onset of bad weather, or a poor catch rate. A check on elapsed time is maintained throughout the model program, so that the vessel breaks off fishing with enough time remaining to return to the offloading point (steaming in transit at 10 knots) before the end of the 15 day period. If bad weather occurs, the vessel is moved 50 n miles in a random direction, and has to start searching again for a concentration when the bad weather ends.

Ichii (pers. commn) advises that the catch rate (per overall time) is regarded as too poor if it falls below about half the vessel's processing rate capability. This is usually assessed on a daily basis, as not all fishing occurs at times and places where there is 24 hour daylight (as assumed in the simulation model), and there is a diurnal pattern in krill availability. In the simulation, a continuous check is kept of the ratio of total catch per time elapsed for the previous 10 hauls (close to a 24 hour period for normal operations); fishing on the concentration is ended if this ratio falls below CR_{min}. The value of CR_{min} has been tuned to obtain improved agreement between the simulation model output and the commercial vessel data sample provided (see section 3.2), with this exercise commencing with CR_{min} = 2.5 tonnes/hour (i.e. half the 5 tonnes/hour processing rate assumed).

It is possible that future searching (for concentrations) may return the vessel to a concentration that has been fished earlier during that same half-month (the only exclusion by the simulation model is immediate return to a concentration just left because of poor catch rate). In such a case, that concentration's biomass has been reduced by the previous fishing activity. The swarm distribution within that concentration is then set up anew, as swarms would have intermingled during the intervening period, by repeating the process described in section 2.7. However, to adjust for the catch already taken, all swarm radii are reduced by the square root of the proportion of the original biomass of the concentration still remaining. In practice though, for the chosen parameter values, this adjustment is negligible.

2.9 Moving the Vessel

At certain times during the simulation, it is necessary to adjust the vessel's position in a random direction - this arises either because of a bad weather period, or during the general search for concentrations.

In these cases, the distance to be moved is specified as described in sections 2.4 and 2.6. The compass direction of the movement is chosen using a random number generator. Only one constraint is imposed: the movement may not take the vessel outside the 600 n mile square sector. If a compass direction is selected which has this result, it is disregarded and a further selection is made until the direction obtained will keep the vessel within the sector.

3. RESULTS AND DISCUSSION

3.1 Fishing Operation Statistics Extracted from the Commercial Data Sample

A sample of the data collected routinely during the Japanese krill fishing operations was kindly supplied to the author by Dr Shimadzu. The basis for the vessel and the period chosen is described in detail in Butterworth (1988). Briefly, the vessel is a fairly typical independent trawler, and the data pertains to operations off Wilkes Land in the 1980/81 and 1981/82 seasons.

Summary parameters of these fishing operations extracted from the data are shown in Table 1. The object of the extraction is to provide values to compare with the simulation model output, as a test of the realism of the model developed. As the intention has been to model a "high season" operation, the Table shows data extracts for the months of January and February only.

An explanation for the basis of the entries in Table 1 is necessary. Some of the statistics constitute a single value: thus, the ratio of the total catch during the month (TC) divided by the total time spent "fishing" (note the definition in section 2.8) (T/FISHT), provides one number for each month. However, the ratio catch-per-fishing-time (C/FISHT) can also be evaluated for each haul, and provides a large set of numbers for a particular month; in such cases, Table 1 shows the mean and standard deviation for this set.

An average column has been presented for ease of comparison of these statistics to the simulation model output, and gives the mean of the four monthly values shown. Where only a single statistic was provided each month, the standard deviation shown is that of the four values concerned. However, in cases where a mean and standard deviation are given for each month, the "standard deviation" figure shown with the average was calculated by taking the average of the four monthly coefficient of variation values, and then multiplying this by the average of the four monthly means. (This procedure may give a better impression of the degree of variation than some other averaging methods which are more influenced by mean-variance correlations.)

The distances between successive hauls (DBH) were calculated from the latitude and longitude given for the position of each haul. The shorter of such estimated distances may be rather imprecise, as position is only recorded to the nearest minute of latitude and longitude. The values may also be inflated compared to the actual situation in the concentration, as no allowance can be made for both the swarm and the fishing vessel moving with the current (insofar as the two may be similarly influenced thereby).

A movement from one concentration to another was inferred when both the time between successive hauls (TBH) and DBH showed much larger values than normal. "Bad weather" was assumed when only the TBH (and not the DBH) value was much greater than usual (this could, of course, reflect other aspects such as repairs to machinery). It is difficult to distinguish transiting to offload from inter-concentration movement by inspection of the data; only one clear case of transiting was evident, and added to the bad weather time.

Overall, this exercise involved some guesswork and the results from it should be regarded with caution, particularly in relation to the "independent searching for concentrations" process assumed in the simulation model (section 2.6). There were 7 instances during the 4 months examined of movement (generally in an east-west direction) of over 200 n miles; these hardly seem likely to reflect true searching, but rather probably correspond to movement on the basis of external information received of good fishing in another area. Sometimes a few (typically < 5) hauls were made at an intermediate position between two areas which were both intensively fished. Presumably these constitute some trial tows made in transit, where the locality was left almost immediately because of poor krill quality or catch rate. Also, there were occasions where the vessel clearly moved to another concentration nearby, but returned to the concentration previously fished after only a few tows. In Table 1, the figure shown for number of concentrations fished reflects inclusion of the former but not the latter of these last two instances in the total count; the minimum excludes, while the maximum includes both.

The overall average of 8 concentrations fished per month seems high when compared to a statement by Ichii to the author that typically only 2-3 concentrations would be fished during such a period. Ichii (*in litt.,* 30 May 1988) has also investigated five Japanese mothership type operations over the high season, and found that typically 1-3 concentrations were fished per month on these occasions. It is also clear from the data that, if "bad weather" periods have been correctly interpreted, they do not necessarily result in the vessel losing contact with the concentration as is assumed in the simulation model structure (though note also the comments made in section 2.4 about this feature of the simulation model mimicking the effect of temporal changes in krill distribution parameters).

The position of the ice-edge during these operations was not known, so that distances therefrom could not be calculated. The values shown for the north-south fishing extent are probably a positively biased measure of the range of vessel distance from the ice, as the latitude values from which they were deduced showed a southerly trend with time, presumably related to the ice-edge's summer retreat.

The overall time budget deduced from these data is:

TCST : 23%
TFISHT : 32%
BW + TRANS : 13%
TPST + TSST + (TTOWT - TFISHT) : 32% (by subtraction)

where

CST	is the time searching for a concentration (the prefix "T" indicates total, i.e. summation over the period of interest)
FISHT	is fishing time (with the net at the desired depth)
BW	is time lost to bad weather
TRANS	is transit time
PST	is primary search time for a swarm within a concentration
SST	is secondary search time (time needed to complete processing). [Note that (TPST + TSST) measures total search time within concentrations; the two constituents cannot be distinguished from the data available.]
TOWT	is the total period the net is in the water (including FISHT) during a haul
(TOWT-FISHT)	is thus the net lowering and raising time.

The above may be compared to the detailed records kept by another Captain and listed in Butterworth (1988), which in this terminology correspond to:

TCST + TPST + TSST = TAST : 45%
TFISHT : 18%
TTOWT - TFISHT : 24%
BW + TRANS : 13%

where TAST is the total of all searching time, both for concentrations and for primary and secondary searching for swarms within concentrations.

A further comparison may be made to the time budget data collected during the 1986/87 season throughout the Japanese fleet. Dr Shimadzu has advised the author that this corresponds approximately to:

TCST + TPST + TSST = TAST : 25%
TTOWT : 50%
BW + TRANS : 25%

Certainly these schedules indicate considerable variation, though in a very general sense it is probably true to say that the fractions of time devoted to searching (TCST + TPST + TSST= TAST) and to fishing plus net handling (TTOWT) are roughly the same.

3.2 Tuning the Model Parameters Using the Commercial Data Statistics - the FISHT Problem

Table 2 lists the parameters of the fishing operation model. A number of these have already been fixed, as discussed in Chapter 2. A few remain for adjustment (or "tuning") to have the simulation model output show better agreement with the commercial data sample (Table 1) and other information available on the Japanese krill fishery, as set out in the first column of Table 3 (though now amended where relevant to reflect the half-month period pertinent to the simulation model). These few, which include one (N_c) which is strictly a distribution model rather than a fishing operation model parameter, are:

$(C/FISHT)_{rpt}$	:	the minimum catch rate to attempt to refish a swarm
B_{min}	:	the minimum estimated biomass for a swarm to be selected for fishing
CR_{min}	:	the minimum catch rate per total elapsed time for the vessel not to stop fishing and search for another concentration
N_c	:	the number of concentrations in the sector.

The statistics in the first column of Table 3 are not all independent; for example, parameter values that give a reasonable fit to the figures for mean catch per haul ($\overline{C/H}$) and mean fishing time per haul ($\overline{FISHT}$) are also going to fit the catch rate expressed as TC/TFISHT. While the effects of changing the values of the parameters available for tuning are not totally independent, for practical purposes the tuning amounts to adjusting:

$(C/FISHT)_{rpt}$	to fit the fraction of attempted repeated hauls
B_{min}	to fit mean catch per haul (C/H)
N_c and CR_{min}	to fit total concentration searching time (TCST) and the number of concentrations fished (TNC).

The first column under the heading "Simulation Model Output" in Table 3 corresponds to a fit of the fishing/distribution model as presented in Chapter 2. As pointed out in section 2.6, a non-zero value of B_{min} (i.e. some selectivity) is essential to raise the $\overline{C/H}$ value to the 6-10 tonnes range compatible with the data sample used here and statistics quoted in Shimadzu (1985).

Immediately, one major discrepancy between the simulation model output and the actual data stands out. This is the five-fold difference between the average fishing time per haul ($\overline{\text{FISHT}}$) for the data sample of 1.23 hours, compared to 0.23 hours in the simulation output. [Note also from equation (23) that 0.08 of those 0.23 hours is made up by a fixed contribution comprising the time between the net reaching the desired depth and its entering the swarm.]

This reflects the problem of reconciling the typical length of Japanese trawlers' tows (~ 2 n miles at 2 knots) with typical dimensions of krill swarms reported from scientific surveys (~ 100 metres), together with the fact that the Japanese report most of their tows to be through a single swarm. Introducing the selectivity criterion of equation (20) does reduce this discrepancy to a limited extent by extending the average length of swarm towed per haul to some 550 metres, but by no means removes it. Increasing B_{min} would not solve this problem because even though a smaller fraction still of the swarms with a yet larger average radius would then be selected, the desired catch limit of 10 tonnes per haul would mean suspension of tows before the complete extent of the larger swarms had been traversed, so that FISHT would not increase markedly.

Obviously a fundamental inconsistency exists somewhere in the distribution-operation model which was developed in Chapter 2 with the intention of its being representative of the krill fishery, and this casts some doubt on using any results emanating from that model as a basis to judge the potential utility of alternative abundance indices as measures of krill biomass. In the following section, some possible resolutions of the inconsistency are discussed, and two different model modifications are introduced to achieve reasonable agreement between the simulation model output and the commercial data.

[Strictly, it is not entirely correct to describe the first column under simulation model output in Table 3 as corresponding to a fit of the model precisely as it has been presented in Chapter 2. First, because the mean tow time ($\overline{\text{TOWT}}$ - which includes time for lowering and raising the net) is 0.91 hours, it would be unrealistic for the model to have the "Captain" allow for 1.5 hours of processing during the forthcoming tow (see section 2.8). Thus this period was shortened to 0.75 hours. Secondly, because it is the model modifications developed in the next section that are ultimately used for investigating the response of abundance indices to krill biomass decline, it is actually these modified versions which were tuned. For ease of comparison purposes, the B_{min} and N_c values adopted above for the original (Chapter 2) model are as for the elongated ($f = 8$ - see next section) modification; only $(\text{C/FISHT})_{rpt}$ and CR_{min} were further adjusted.]

3.3 Two Model Modifications

There are a number of possible explanations for the inconsistency revealed in the previous section:

(i) The commercial data (see Table 1) do not reflect a single swarm only towed for every haul. It could be, therefore, that tows in the fishery through more than one swarm are much longer than those through a single swarm. Further inspection of the data, however, does not support this hypothesis. Table 1 shows that the differences in such average FISHT values are small and of variable sign; none of the four cases examined corresponds to a difference that is statistically significant at the 5% level.

(ii) The swarms observed during FIBEX (the results from which contributed substantially to the distribution parameter values chosen for the model developed here) are not typical of those upon which the fishery operates. Ichii (*in litt.*, 30 May 1980) comments that the latter "are much bigger", and are also presumably less dense. It should be borne in mind as well that quoting single summary statistics for the FIBEX data can be misleading. For example, Table XI of BIOMASS (1986) shows that different vessels in the FIBEX exercise recorded very different values for mean intersected swarm length λ . The smallish mean $\lambda = 73$ m quoted in section 2.2 is a reflection of the total FIBEX sample being dominated in number terms by the typically small swarms recorded in the surveys by the *S.A. Agulhas*, *Professor Siedlecki* and *Walther Herwig*. In contrast, the surveys by the *Dr Eduardo L. Holmberg* and *Itzumi* reported mean λ values ~ 500 m, which correspond to much larger swarms [though I Hampton (pers. commn) considers that this might rather reflect differing criteria used to distinguish swarms from layers].

(iii) The definition of a "swarm" used by the fishermen in recording commercial data differs substantially from that used in scientific publications [such as BIOMASS (1986)], and typically rather more than one "scientific" swarm is towed in a haul. Ichii (*in litt.*, 30 May 1988) comments that he often observed fishermen record a haul as fishing a single swarm only even though several swarms were towed, and suggests that their data are less reliable in this respect because their interest centres on the catch-per-haul rather than the number of swarms towed. Ichii has also shown the author an echo chart of a krill aggregation fished by a commercial vessel and recorded thereby as a single swarm, which could readily be interpreted as up to six separate swarms. Failure to discriminate "scientific" swarms may also reflect spatial correlation effects (absent from the model of Chapter 2), with individual swarms clustered together being regarded as one swarm only.

(iv) Non-circularity of swarms. Although an exercise in section 2.2 showed that the krill distribution parameters used were consistent with a circumpolar krill biomass of about one hundred million tonnes, the results from FIBEX [BIOMASS (1986)] give a much lower value. This is "surprising", since those same FIBEX results were used to choose a number of the krill distribution parameter values used for this model. A possible reason for this discrepancy is that swarms are distinctly non-circular, contrary to the assumptions of the model in Chapter 2.

(v) Net avoidance. If the effective net width is less than the 20 m assumed, hauls would need to be longer to achieve the same catch. However, this effect would need to be very large to rectify the inconsistency found in the previous section.

Unfortunately little information is available, or has yet been analysed, that would allow either a choice between the hypotheses above, or their independent quantification to allow, say, fixed revised krill distribution parameter values to be set. Instead two somewhat *ad hoc* model modifications have been introduced drawing on the suggested explanations in (ii) - (iv) above.

(a) Elongated swarms

This modification combines the ideas of (ii) and (iv). The restriction to one swarm per haul is maintained. However, the (fishable) swarms are artificially elongated in the direction in which they are towed by a "fudge factor", f:

$$\begin{array}{lll} r \text{ (perpendicular to tow direction)} & \rightarrow & r \\ r \text{ (along tow direction)} & \rightarrow & r\,f \\ \delta & \rightarrow & \delta / f \end{array} \qquad (31)$$

This form of transformation means that B_{min} can be kept fixed in a tuning exercise [having being used be fix a realistic average catch per haul ($\overline{C/H}$) simulation model output figure], while f provides the extra degree of freedom needed to increase the average time required to make such a catch ($\overline{FISHT}$) in the simulation model. In practice a value of $f = 8$ was found to be appropriate (see Table 3). It could be argued that introduction of this factor necessitates adaptions to other elements of the model; for example, the derivation of equation (26) for the swarm search operation might be modified, but since the factor of 4 in that equation was empirically motivated, the net result might not reflect any eventual change to equation (26).

(b) More than one swarm towed per haul

The rationale for this modification is provided by (iii) above. As described in section 2.8, tows do not necessarily end after traversing the swarm (here assumed again to be circular) initially selected for fishing; instead they continue up to a maximum total distance (TOW_{max}) chosen here to be 4 n miles. Other swarms (any swarms, not only "fishable" ones) intersecting a 17.5 m "sonar band" either side of the trackline are also then fished in that haul. A feature of note in tuning the fishing operation parameters for this modification is that it proves necessary to reduce B_{min} to 5 tonnes [one tenth of its value for (a)] to secure a realistic simulation model output value for the catch rate TC/TFISHT, which is otherwise much too large. Given more than one swarm per haul, an average catch per haul ($\overline{C/H}$) of 6-10 tonnes is much less difficult to achieve, and swarm selectivity increases from 8% in (a) to 29% here. It seems unrealistic to assume that the simulated vessels would "forego" a potentially much higher catch rate by being prepared to start towing on smaller swarms, but in terms of the simulation model this may be a means of compensating for the limitations of the model's two-dimensional nature - not all swarms intersecting the "sonar band" around the trackline may be fished readily because of depth variation. The modified simulation model suggests an average of about 5 swarms fished per haul (see Table 3).

The fishing operation parameter values eventually chosen and listed in the second and third columns of Table 2 reflect only a partial tuning of the model output to the commercial statistics available. Tuning is carried out using the average of the output for a number of simulation runs; as many as 100 runs have been used in this analysis, but this nevertheless gives rise to not insubstantial standard errors for the estimated means, which range up to 7%. This precision could be improved by using a larger number of runs, but this would be unrealistic in computer time terms. Typically 100 half-month runs of the one-swarm-per-haul model require 20 minutes on a mainframe computer (a Sperry UNIVAC 1108 was used), or some 20 times that period on a microcomputer. The more-than-one-swarm-per-haul modification requires about 40 minutes on the mainframe for 100 runs. The aspect of the simulation model that consumes most of the computer time is the generation of the swarm field within a concentration; when tows are continued beyond the initial swarm, the additional swarm field generation procedure then needed adds further to the computer time requirements. Because of this, the computer time requirements for a set of runs depend critically on the average number of concentrations fished per half-month. Thus, although still better agreement could be achieved between model output and commercial statistics than is reflected in Table 3 by further tuning of parameters, this was not considered warranted because of the additional computer time requirements and because, given the simplified model being used (ignoring krill quality considerations, for example), the levels of differences reflected in the comparisons in Table 3 were not considered a serious impediment to use of the model to draw conclusions about the potential utility of alternative abundance indices as measures of krill biomass.

The more-than-one-swarm-per-haul model modification developed in section 2.8 restricts vessel deviation to the "sonar band" 17.5 m either side of its trackline when towing swarms encountered after the initial swarm, so that these swarms are towed offcentre. The results of a complete relaxation of this condition, whereby deviation is unrestricted so that all such subsequent swarms are also towed along their diameters, are shown in the final column of Table 3. The principal features of these results are increases in the total catch (TC) and catch rate (TC/TFISHT) to values yet further above the commercial data statistics. While better agreement could be restored by reducing B_{min} and increasing CR_{min}, it was considered more realistic to retain the feature of offcentre towing of the subsequent swarms for further analysis.

The major remaining discrepancy between the commercial data sample and the output from the two modifications of the simulation model is the average number of concentrations fished per half-month (TNC): 4 and about 2 respectively (see Table 3). Higher TNC values could be achieved in the simulation model outputs by increasing the number of concentrations in the sector (N_c), or improving the concentration searching efficiency of the vessels. The latter could be rationalised as a reflection of "external" information received from other vessels or based on experience of persistent concentrations in certain areas in previous seasons. [This may be the reason for the longer inter-concentration distances indicated by the commercial statistics compared to the model outputs (see Table 3).] However, the identification of the number of concentrations fished from the commercial data sample was problematic (see section 3.1). Further, the values provided by Ichii (section 3.1) of TNC ~ 1-2 compare well with the simulation model outputs. Accordingly, possible further adjustments to the models in this respect were not pursued.

Some other aspects of the comparisons of Table 3 merit mention. The simulation model outputs show greater variability in the total catch (TC) and number of hauls (TH) than do the commercial data statistics. This is a reflection of the greater variability of the number of concentrations fished (TNC) for the former. On the other hand the catch rate TC/TFISHT is more variable in reality than for the model - perhaps a reflection of temporal variability in the krill distribution parameters in the real world. The total times spent searching (TAST) and fishing plus net handling (TTOWT) are very similar as seems appropriate for a fit to commercial data (see final paragraph of section 3.1). The mean of the simulated distances between successive hauls of about 2.6 n miles is slightly less than the 3 n miles indicated by the commercial data, but this may reflect the effect of currents as alluded to in section 3.1.

3.4 Potential Indices of Abundance

The simulation model output provides values for a number of indices (mainly of the CPUE type) which may reflect a change in the sector biomass. These fall under a number of headings, and are listed below together with the direction of response to decreases in the values of some (or all) of the krill distribution parameters which might be expected *a priori*. (Recall that the prefix "T" used in the following implies summation over the half-month period under consideration.)

(A) Total measures related to catching:

(1) TC^{+++}: Total catch: decrease for N_c, L_c, D_c, r or δ decrease.

(2) TH^{+++}: Total number of hauls: decrease in response either to more time being required for searching, or to longer FISHT being needed on a haul to obtain the desired catch, i.e. for N_c, L_c, D_c, r or δ decrease.

(B) Total time related measures:

(Here only the anticipated direction of primary response is indicated; since the total time in the half-month is fixed, the resultant negative correlations will cause secondary responses to other measures in the reverse direction.)

(1) TFISHT^{+++}: Total time spent fishing swarms: increase for δ decrease.

(2) TPST: Total primary searching time for swarms within concentrations: increase for D_c decrease [note: not for r in a primary sense, insofar as the motivation for equation (26) is justified, though there would be secondary effects through the selectivity S of an increase for an r or δ decrease].

(3) $\text{TPST} + \text{TSST}^{+}$: Total primary and secondary searching time (the latter for processing needs, in terms of the model) within concentrations: increase for D_c decrease.

(4) TCST^{+}: Total searching time for concentrations: increase for N_c or L_c decrease.

(5) TAST^{++}: Total of all searching time (= TPST + TSST + TCST): increase for N_c, D_c, and L_c decrease: unclear for r as FISHT would also be affected.

(C) Catch per time CPUE measures:

(1) TC/TFISHT^{+++}: Total catch for all hauls divided by total fishing time for all hauls: decrease for δ decrease.

(2) $\overline{\text{C/FISHT}}^{+++}$: Catch per fishing time for each haul, averaged over the half-month: decrease for δ decrease.

(3) TC/TPST: Total catch for all hauls divided by total primary searching time for all hauls: decrease for D_c decrease.

(4) $\overline{\text{C/PST}}$: Catch per primary searching time for each haul, averaged over the half-month: decrease for D_c decrease.

(5) $\text{TC/(TPST+TSST)}^{+}$: Total catch divided by sum of total primary and secondary searching time within concentrations: decrease for D_c decrease.

(6) $TC/TCST^{+}$: Total catch divided by total searching time for concentrations: decrease for N_c or L_c decrease.

(D) Combination catch-time indices:

Note that each index in (C) is anticipated to respond to changes in only one or two of the five krill distribution parameters, a decrease in any one of which could reflect a biomass decline. The motivation for combination indices is to have a measure that will respond to changes in a greater number of these parameters.

(1) $TC/TFISHT/\overline{PST}$: Catch per fishing time, divided by the average primary searching time for each swarm fished: decrease for D_c, r or δ decrease.

(2) $TC/TFISHT/(\overline{PST+SST})^{+}$: Catch per fishing time, divided by average primary plus secondary searching time for each swarm fished: decrease for D_c, r or δ decrease.

(3) $TC/TFISHT/\overline{PST}/\overline{CST}$: D.1 divided by the mean concentration searching time (i.e. total concentration searching time TCST divided by number of concentrations found and fished TNC): decrease for N_c, L_c, D_c, r or δ decrease.

(4) $TC/TFISHT/(\overline{PST+SST})/(\overline{CST})^{+}$: D.2 divided by the mean concentration searching time: decrease for N_c, L_c, D_c, r or δ decrease.

(5) $TC/TFISHT/TAST^{++}$: Catch per fishing time, divided by the total of search times of all types (TAST = total of all search time = TPST + TSST + TCST): decrease for N_c, L_c, D_c, r or δ decrease.

(E) Indices related to the number of concentrations fished:

(1) TNC^{+}: Total number of concentrations fished: increase for D_c, r or δ decrease, but decrease for N_c or L_c decrease.

(2) TH/TNC^{+}: Number of hauls per concentration: decrease for D_c, r or δ decrease.

(F) Per haul measures:

(1) $\overline{C/H}^{+++}$: Average catch per haul: decrease for r or δ decrease, but this could be offset by saturation effects arising from curtailment of hauls due to processing rate limitations.

(2) $\overline{FISHT}^{+++}$: Average fishing time per haul: increase for r or δ decrease.

(3) $\overline{\text{TOWT}}^{++}$: Average fishing plus net raising and lowering time per haul: increase for r or δ decrease.

(4) $\overline{\text{TBH}}^{++}$: Average inter-haul time: increase for D_c, r or δ decrease.

For each index above, an indication has been made regarding the possibility of collecting such data in practice as follows:

+ + + : Data are already collected.

+ + : Data could be collected (and have been for some experimental periods), but such collection is onerous.

+ : Data could be collected, but there would be difficulties of definition, and considerable difficulties with collection.

Blank : Extreme difficulties of definition and collection.

These indications are based on impressions gathered by the author during discussions in Japan with krill fishery scientists and vessel Captains and Commanders [see Butterworth (1988)]. Generally the problems centre on the practicalities of collecting searching time information. Total searching time (TAST) can be obtained essentially by subtraction of the total time spent on other activities, which is more readily recorded. Separating out concentration searching from swarm searching time would run into a field definition problem. Distinguishing primary and secondary searching time while operating within a concentration would be almost impossible in practice. This is the reason why a number of indices listed above combine primary and secondary searching time (TPST + TSST); use of primary searching time alone is preferable in principle, but including secondary searching time may be a practical necessity. In general, there is a trade-off between collection practicality, and the anticipated magnitude of the reaction of the index to overall biomass changes, which one would expect to be damped by the inclusion of extraneous contributions (such as secondary searching time). (Note: TBH data are already collected, but would need censoring for bad weather, inter-concentration movement, and so forth - hence the ++ designation.)

3.5 Biomass Reduction Scenarios Examined

In the first instance, six variations of the base case distribution model parameter values, and the resultant influence on various potential abundance indices, have been considered. Each of these scenarios corresponds to a reduction of 50% in the total biomass of krill in the 600 n mile square sector. The variations are:

(i) Number of concentrations drops by 50% (by the same proportion in each stratum):

$$N_c = 36 \rightarrow 18$$

(ii) Number of concentrations drops by 50% with a "Pelagic Shift" (P.S.) (number of concentrations in the southernmost two strata unaltered; no concentrations in three northernmost strata:

$$N_c = 36 \rightarrow 18$$

(iii) Concentration radius drops by 30% (i.e. to $1/\sqrt{2}$ of original value):

$$L_c = U[5.6,11.3] \rightarrow U[4.0,8.0] \text{ n miles}$$

(iv) Density of swarms per unit area in a concentration drops by 50%:

$$D_c = 20e^{\varepsilon} \rightarrow 10e^{\varepsilon} \qquad \varepsilon \text{ still from } N[0,(0.1)^2]$$

(v) Swarm radius drops by 30% (i.e. to $1/\sqrt{2}$ of original value):

$$r = 50e^{\varepsilon} \rightarrow 35.4e^{\varepsilon} \qquad \varepsilon \text{ still from } N[0,(1.1)^2]$$

(vi) Surface density of krill within a swarm drops by 50%:

$$\delta = 150e^{\varepsilon} \rightarrow 75e^{\varepsilon} \qquad \varepsilon \text{ still from } N[0,(1.4)^2].$$

The "Pelagic Shift" change envisaged in scenario (ii) is by analogy with pelagic fish populations, whose response to biomass reduction is to decrease their geographical extent while local density in the most favoured habitat (where catch rates would be best) may scarcely be affected [e.g. the northern anchovy off California, MacCall (1983)].

In each of the scenarios, all parameters except the one indicated are unchanged from their base case values. The selection criterion for a fishable swarm [B_{min}: equation (20)], the condition for attempting to refish a swarm [$(C/FISHT)_{rpt}$: constraint (25)], the criterion for leaving a concentration because of poor catch rate (per total time elapsed) [$< CR_{min}$ tonnes per hour averaged over the last ten hauls], and (where appropriate) the swarm elongation "fudge factor" [f: equation (31)] remain unchanged from the pertinent values listed in Table 2.

Comparisons of the output from the base case model and these six alternative scenarios corresponding to different ways in which the overall krill biomass could fall by 50%, are given for the two model modifications under consideration in Tables 4, 6, and 7. Table 5 is a rerepresentation of the information in Table 4.

Table 4 compares the performance of the 24 candidate abundance indices suggested in section 3.4. It is important to be clear as to the meaning of the standard errors given in this Table. For each scenario, the simulation model was run 100 times. Thus, in the base case instance for example, 100 values of half-month catch (TC) were generated. These 100 values have a mean and a standard deviation. This mean will, however, differ from the expected value [i.e. the average which would be obtained if model runs were repeated a very large (infinite) number of times], because the mean of the 100 values will be subject to sampling variation. The size of this variation must be known so that true differences from scenario to scenario are not confused with sampling variability. A measure of this variation is the standard error of the mean (1/10 of the standard deviation of the 100 values that contribute to the mean TC in this case). It is this standard error of the mean which is shown with the mean values of the base case indices.

Such standard errors of the mean can be used to estimate the precision of the estimated change in mean value of an index from one scenario to another. This precision has been expressed as the standard error of the percentage change in an index from the base case to an alternative scenario, which is calculated by:

$$\text{s.e.} = 100\ a/b\sqrt{[\text{s.e.m.}(a)/a]^2 + [\text{s.e.m.}(b)/b]^2}\ \% \qquad (32)$$

where b is the mean value of the index for the base case over 100 simulation runs, and s.e.m.(b) is the associated standard error of the mean

a is similarly the mean, and s.e.m. (a) the standard error of the mean, for the same index for the alternative scenario.

[Note: Strictly, equation (32) is an approximation which could be corrected for bias, but this adjustment is likely to be small for most of the indices considered. Later, the assumption of normality is made in relating ± 1.96 of these standard errors to a 95% confidence interval. Again, this is approximate because the distributions of the indices (and also their ratios) are skew. However, making detailed corrections for these effects does not seem critical for what is only an initial investigation of this problem at this stage.]

These precision levels could be improved by increasing the number of simulation runs from 100 used, though that would be expensive in terms of computer time as discussed in section 3.3. Table 4 shows that for most indices, value changes between scenarios have been determined up to a standard error of 10% or better, which seems adequate for this analysis for which interest centres on biomass changes as large as 50%. All the exceptions involve concentration searching time (CST), with associated standard errors up to 28%. The reason is that far fewer concentrations (~ 200) are fished than hauls (~ 10 000) are made over 100 simulations, so that the precision with which concentration-linked indices can be assessed is necessarily relatively poorer.

Some runs of the simulation model result in no concentrations at all being discovered in the half-month period, and so no catch being made. This is a very infrequent occurrence for the base case, but can occur up to 20% of the time for scenario I) above where the number of concentrations (N_c) is decreased by 50%. Such instances remain included in the statistics quoted in Table 4 for summation-type indices A.1-2, B.1-5 and E.1, and also for the ratio index TC/TCST (C.6); however, since they provide no pertinent data, they are excluded from other ratio indices such as C.1-5 and D.1-5.

Table 5 summarises the information in Table 4 in a less quantitative manner (which is described in detail in the Table caption) to provide a clearer overall comparative perspective. Note that "significant" is used in Table 5 in its statistical sense, and does not necessarily imply "substantial", In fact some differences, although detected to be statistically significant at the 5% level, are no more than 2% in magnitude.

If krill biomass was to drop, it is more likely that this would be manifest by some combination of changes in the various krill distribution parameters, rather than a change in one only as examined thus far. However, there is no basis at present to determine whether some parameters would be more likely to change than others. Thus a further scenario is examined where a random combination of changes in N_c, L_c, D_c, r and δ is chosen to effect a fixed net reduction in the overall krill biomass in the sector [a possible change in the relative distribution of concentrations with habitat - such as the Pelagic Shift of (ii) above - is ignored here for simplicity]. Accordingly, a reduction factor α (the krill sector biomass as a fraction of the base case level) is chosen, and simulations are run for 100 different combinations of changes in N_c, L_c, D_c, r and δ that effect this same reduction. The proportion of change attributed to each parameter is specified by choosing four numbers from U[0,1] and then ordering them, with the resultant five intervals on [0,1] providing the proportions (except that these proportions are adjusted to allow for rounding the changed value of N_c to the nearest integer).

Table 8 shows the results of simulation model outputs for such scenarios. The values of potential abundance indices are expressed as fractions of their estimated base case levels. (The inverse of such fractions has been taken wherever this was necessary to have the statistics listed show a generally increasing trend with α). The results are given for $\alpha = 0.1(0.1)0.9$, i.e. for biomass reductions down to 10% of the base case level. The standard errors shown for the estimated relative levels of the abundance indices reflect both the sampling error pertinent to 100 runs of the simulation model for fixed parameters, and also the variation associated with the random allocation of the biomass reduction amongst the five krill distribution parameters.

Figure 7 plots the results of Table 8 for a selected subset of the potential abundance indices examined. In these plots, mean abundance index estimates have been normalised to the estimates of their respective mean base case levels. The error bars shown are estimates of the central 68% interval of the index distributions (i.e. distributions of the indices for vessel-half-months); the ranges of ± one standard error of the mean will be about one-tenth of the sizes of these intervals. Note that while the error bars for the base case ($\alpha = 1$) estimate reflect sampling error only, the error bars for other values of *a* also incorporate variation arising from the differing contributions of changes in the various krill distribution model parameters to the overall krill biomass reduction, and so are typically larger.

Curves of the form:

$$\text{index} = a + (1-a)\alpha^b \qquad (33)$$

have been fitted to the normalised mean abundance index estimates. Such curves are constrained to pass through the point (1,1), so that only the estimates for $\alpha = 0.1$ to $\alpha = 0.9$ were used in the fitting process. The curve parameters a and b were estimated using weighted least squares and a non-linear optimisation program, where the weights were chosen to be the squared inverses of the standard errors of the mean of the mean abundance index estimates.

Note that equation (33) provides a convex or concave curve depending on whether the parameter b is less than or greater than 1 respectively. As $\alpha \to 0$, all the indices must also $\to 0$. However, fits of equation (33) were not constrained in this way (i.e. the fits did not force $a = 0$) so as to achieve a better representation of the relationship over the α range of [0.1, 1.0]. The equations shown on Figure 7 cannot be extrapolated reliably beyond this range, particularly for $\alpha < 0.1$.

Figure 9 shows similar plots to Figure 7, but for the case where α (the relative level to which the biomass is reduced) is occasioned by a decrease in within-swarm krill surface density δ only. The index vs α equations shown for those fits have been determined in exactly the same manner as described above.

3.6 The Performance of Alternative Abundance Indices in Detecting Biomass Decline

In view of the somewhat *ad hoc* nature of the model modifications introduced in section 3.3 to reconcile the simulation model outputs with the commercial data, the question must immediately arise: how much reliance can be placed on conclusions that are drawn from the outputs of these modified models, particularly as regards the utility of alternative abundance indices as measures of krill biomass? Even given reservations about these modifications, the model nonetheless still hopefully incorporates the major factors that need to be taken into account in a Japanese krill fishing vessel's strategy. Thus, the effects of changing the krill distribution parameters on various candidate abundance indices, together with these indices' likely variability, may still be reasonably reflected in a qualitative and relative sense, although quantitative results such as the assessed magnitudes of non-linearities in index-biomass relationships should be regarded as much less reliable.

Tables 4 and 5 show essentially only two counter-intuitive sets of results in relation to the directions of change of indices under various biomass reduction scenarios, which were hypothesised *a priori* in section 3.4. The first set all relate to FISHT when the swarm radius r is reduced; contrary to expectation TC/TFISHT, $\overline{\text{C/FISHT}}$ and $\overline{\text{C/H}}$ increase, while FISHT and $\overline{\text{TOWT}}$ decrease. The reason, presumably, is the inter-relation with the selectivity criterion of equation (20), which means that fishing remains restricted to the larger swarms. This anomaly occurs only for the one swarm-per-haul situation; the direction of change is as expected when more than one swarm can be towed.

The second set of counter-intuitive results relate to situations where a decrease in the number of concentrations (N_C) is accompanied by a "Pelagic Shift". It might have been anticipated that the increase in TCST, and decreases in TC, TH, TC/TCST and indices involving $\overline{(\text{CST})^{-1}}$, would be less marked than when all strata are similarly affected by the N_c decrease, as is evident for the one swarm-per-haul case. However, when more than one swarm may be towed, the directions of change are the reverse of those expected, with catch rates per concentration searching time (CST) increasing despite the N_c decrease. This is presumably an artefact of the concentration searching procedure (section 2.6) implemented in the simulation model. Once equation (16) has provided the time until the next concentration is found, movement may occur to any concentration within a 10 knot steaming range for that period. In the absence of a "Pelagic Shift", such movement may be selected to be to a concentration north of the highest density strata S_1 and S_2 (see Figure 2); once the vessel has moved to a more northern stratum where the concentration density (d) is lower, more time becomes required for possible further concentration searching in terms of equation (16).

However, for the "Pelagic Shift" example considered, there are no concentrations north of strata S_1 and S_2, so that the simulated vessel remains in the high densities of the southernmost strata and needs, on average, to expend less of the available time on searching for concentrations, thus enhancing many catch-rate indices. Why the quantitative effect of this should be larger for the case of towing more than one swarm-per-haul is not immediately clear. Future model modifications might perhaps build a positive bias towards southward movement into the concentration selection weighting factors of equation (17) to compensate for this effect. This would produce a more realistic representation of the actual fishing strategy, which would be to move preferentially towards areas known from previous seasons to provide higher densities of concentrations (i.e. to move southward in the context of the krill distribution pattern assumed for the model).

There are what might seem to be some other counter-intuitive results if the point estimates only of Table 4 are considered, but such apparent anomalies are attributable either to sampling variation (note the high standard errors associated with such estimates) or, where total-time-related measures are concerned, to secondary responses as described in section 3.4, part B].

The primary concern of this study is the ability of candidate abundance indices to detect biomass declines. A number of important features that emerge from Tables 4, 5 and 8 are discussed under the seven subheadings that follow.

3.6.1 Non-Proportional Response

It is immediately clear from Tables 4 and 5 that the number of instances where an index responds to a 50% biomass drop by a change approaching that same magnitude is relatively rare. For certain indices, the response never reaches 20% for any of the biomass reduction scenarios examined. Thus, from a resource monitoring perspective, there is the undesirable situation that the indices generally respond to biomass drops by proportionately smaller changes. The effects of saturation and compensation on the indices, which arise from the complexity of the overall operation, are evidently of more than a little importance.

It does seem, however, from these Tables that most indices do detect significant and substantial change when the krill surface density δ drops by 50% for either model modification considered. Further, when more than one swarm-per-haul may be towed, changes in swarm radius (r) and areal density (D_c) are similarly well detected. The last result is not surprising, as the rate of finding subsequent swarms in the "sonar band" in such extended tows will be proportional to both r and D_c.

The positive impression given by such results may, however, be misleading. The essential reason for the changes in many of these indices is that the vessel finds considerably greater difficulty in meeting the catch rate per overall elapsed time criterion (CR_{min} - see section 2.8) in these situations, and consequently leaves concentrations much more frequently to search for others. (Table 7 shows that approaching 90% of concentration departures are because of poor catch rate in these instances, compared to the values of typically 60-70% otherwise. Note also the associated large changes in TNC and TH/TNC in Table 4.) However, it may well be that by lowering CR_{min}, the vessel could achieve a larger total catch over the half-month than by spending more time steaming between concentrations in search of better catch rates (see Figure 8 and discussion in section 3.7). This would have the effect of reducing the magnitude of the differences indicated in Table 4 for these scenarios.

3.6.2 Indices Based on Data Currently Being Collected

The indices available from data currently being collected are TC, TH, TFISHT, TC/TFISHT, $\overline{C/FISHT}$, $\overline{C/H}$ and $\overline{FISHT}$. Of these, the crudest indices TC and TH give generally the best responses over the range of biomass reduction scenarios considered (see Tables 4 and 5, and Figure 7 (i). Their responses are nearly identical, which is essentially a reflection of the very poor performance of $\overline{C/H}$ as an index of biomass; $\overline{C/H}$ reacts only to a few of the reduction scenarios (and then weakly), because it is determined primarily by processing rate limitations (see section 2.8). A disadvantage of TC and TH is that they show typically 2-3 times the variability of some other indices [the (C) and (D) catch rate indices that do not involve $\overline{CST}$], so that they would not be able to determine biomass declines as precisely. Much of this additional variability, and the apparent good performance of these indices in detecting changes in the number of concentrations (N_c), is related to concentration searching time (CST), and so they need to be considered in the context of the reservations in this regard expressed under the next subheading. Similarly the performance of TFISHT, changes in which are essentially reflections of an inevitable negative correlation with TCST, must be considered reservedly.

The performances of ratio indices related to FISHT are very poor. Only a decrease in δ is detected consistently, and even then there is some doubt about the realism of those particular results for the reasons discussed under the previous subheading. This is a matter for some concern, as these particular ratio indices are the primary CPUE-type measures presently collected for the Japanese krill fishery.

3.6.3 Detecting Changes in the Number of Concentrations N_c

Tables 4 and 5 show that effective detection is achieved only by indices incorporating concentration searching time (CST). (This incorporation may be indirect in the sense of TC, TH, TNC and total-time-related indices.)

However, there are two problems in regard to such indices. First, their variance is relatively larger (particularly for indices using CST directly), because of the small number of concentrations (compared to swarms) fished per half-month. Secondly, as discussed in section 3.1, the author suspects that, in reality, a substantial fraction of inter-concentration movements of a vessel reflect receipt of external information, rather than the vessel's own searching activities.

To obtain some idea of how serious this second source of concern might be, calculations were repeated for the "One elongated ($f = 8$) swarm per haul" case with concentration searching efficiency increased 7.5 times [by appropriate multiplication of the exponent in equation (15)], to mimic availability of external information on concentration positions. The results are shown in Table 9, which is to be compared to Table 5a. Such a comparison shows that abundance indices change by much lesser amounts in response to a reduction in N_c given greater efficiency in searching for concentrations.

The TC/TCST index appears to have the potential to detect changes in N_c as well as many of the other distribution parameters, even it if is relatively imprecise. There is though a further problem with this index, at least in the context of the model developed. Cases do arise of a concentration being found almost immediately after the vessel leaves its starting point, and fishing continuing for the rest of the half-month in this same concentration (until the time comes to return to offload) because the catch rate never drops below CR_{min}. Such instances provide very high TC/TCST values, so that this statistic has a very long tailed distribution. "Outlier" values from this tail have considerable influence on mean and variance estimates, and it may be necessary to consider trimmed means or harmonic means to obtain estimates with greater precision, if an index of this type is to be considered further.

Detection of changes in N_c by various indices may be confounded by simultaneous changes in the relative density of concentrations between strata, such as the "Pelagic Shift" examined here. However, for reasons discussed at the beginning of this section, the quantitative results for the "Pelagic Shift" shown in Tables 4 and 5 are probably an artefact of an over-simplistic concentration search model, and so should not be considered as reliable.

3.6.4 Detecting Changes in the Concentration Radius L_c

Again it is only indices involving CST which change by non-minimal amounts in response to changes in L_c, but the magnitudes of the changes in such indices are considerably less than for changes in N_c (see Tables 4 and 5).

This confirms the concern expressed in Butterworth (1988) about the likely inability of catch-statistics-based indices to monitor average concentration size. (Note that the typical catch by a vessel from a concentration over the half-month period considered makes no substantial impact on the concentration's total biomass.)

3.6.5 Precision of Indices of Krill Biomass in Practice

Even given estimates of the proportional change in various abundance indices under certain biomass depletion scenarios, a pertinent question is: what is the ability of the "Japanese krill fleet" to detect such changes from one year to the next, given the sampling variability associated with any single abundance measure? The standard errors of the differences shown in Table 4 would also apply to the case of detecting differences between two successive years in each of which 100 vessel-half-months of krill fishing effort was expended. This would correspond to, say, 20 vessels working 2.5 months each year and catching an annual total approaching 100 000 tonnes of krill. This is perhaps twice the size of the current Japanese krill fishery, so that estimates of inter-annual sampling variability would be about $\sqrt{2}$, or approximately 1.5 times as large as the figures in parenthesis in Table 4.

These, however, would be minimum estimates. In practice greater variability would arise because of inter-month and inter-vessel cooperation correlations, catchability fluctuations and so forth. This means that detection of any significant change in an index, and hence in the krill biomass, would be more difficult.

In practice, therefore, the inter-annual variance of abundance indices will not be negligible for the present level of catching. This means that it is important to compare alternative abundance indices in the context of the precision with which they can estimate biomass decline, as well as considering the extent of non-proportionality in the index-biomass relationship.

3.6.6 Choice of the "Best" Index

To simplify the comparison of the large number (24) of potential abundance indices listed in section 3.4, these have been reduced to six for further consideration:

(i) A.1: TC
(ii) C.1: TC/TFISHT
(iii) C.3: TC/TPST

(iv) D.1: TC/TFISHT/$\overline{\text{PST}}$

(v) D.2: TC/TFISHT/($\overline{\text{PST+SST}}$)

(vi) D.3: TC/TFISHT/$\overline{\text{PST/CST}}$

"Per haul" measures (F.1-4) have been rejected because they detect very few distribution parameter changes, and even for those they change by only small amounts. The direction of change for total time measures (B.1-5) is not always clear, and these indices are also influenced by the uncertainty surrounding CST, so that they have not been included. Most indices involving CST directly (e.g. TC/TCST) or indirectly (e.g. TNC) have been omitted because of their imprecision, while "total/total" ratio indices are preferred because they are more precise than the corresponding "average individual ratios" indices (e.g. TC/TFISHT is preferred to $\overline{\text{C/FISHT}}$). The performances of TC and TH are very similar, but where they differ the magnitude of the TC change is greater, so that TC has been chosen.

Comparisons between these six choices enable most of the pertinent considerations to be addressed as adequately as might be possible using alternative or additional choices. Important considerations amongst these are:

(a) Do combination catch-time indices detect biomass decline more effectively by being sensitive to more possible sources of such falls?

(b) How seriously does failure to differentiate PST and SST compromise indices using within-concentration search time?

(c) What is the bias-variance trade-off in incorporating CST into an abundance index?

For ease of comparison of these indices, the corresponding point estimates of proportional changes from Tables 4a and 4b have been set out in a consolidated form in Table 10. Further, Figure 7 provides graphical representations of the results in Table 8 (which presents results for random combinations of changes in the krill distribution parameters) for both model modifications considered.

Consideration (a) is addressed by comparing D.1 with C.1 and C.3 in Table 10, and also Figure 7 (iv) with Figures. 7 (ii) and (iii). The combination index TC/TFISHT/$\overline{\text{PST}}$ performs better than either TC/TFISHT or TC/TPST separately in terms of general magnitude of response, though at the expense of a slight variance increase. TC/TPST performs better than TC/TFISHT, which does not reflect changes in D_c and r as effectively. This result is, however, certainly in part a consequence of the (invariant) criterion used for fishable swarm selectivity [equation (20)] TC/TPST responds to a δ decrease because this reduces the proportion of fishable swarms), and consequently is subject to the reservations discussed in section 3.7. All these indices, however, respond only to changes in within-concentration krill distribution parameters, and are insensitive to N_c and L_c.

Regarding consideration (b), the results for D.1 and D.2 in both Table 10 and in Figures 7 (iv) and (v) suggest that failure to distinguish primary and secondary searching time degrades the effectiveness of the combination index by about one third, where "effectiveness" is measured by the slope of the curve of index against biomass. [Compare also Figs 9 (iii) and (iv) in this regard.] One compensating advantage, however, is that the variance of TC/TFISHT/($\overline{\text{PST+SST}}$) is slightly less than that of TC/TFISHT/$\overline{\text{PST}}$.

Finally, regarding consideration (c), the TC index has a large variance, and fails to reflect D_c or r changes for the one elongated swarm-per-haul model modification. Incorporation of $\overline{\text{CST}}$ into the combination catch-time index D.3 does provide a measure which responds to changes in N_c and L_c, but at the expense of a 3-5 fold standard deviation increase. While D.3 could, of course, be used in conjunction with, say, D.1 in assessing trends in krill biomass, this high variance together with uncertainties in the reliability of $\overline{\text{CST}}$ statistics as representative of a truly random search strategy suggest that indices incorporating CST would have limited utility.

Thus, the analysis suggests that the choice of a "best" index lies between TC/TFISHT/$\overline{\text{PST}}$ and TC/TFISHT/($\overline{\text{PST+SST}}$). Data other than those likely to arise from the Japanese krill fishery as it operates at present would be needed to detect changes in extra-concentration krill distribution parameters such as N_c and L_c.

3.6.7 The Trade-Off Between Effectiveness and Practicality of Collection

Tables 4 and 5 in general, as well as the specific indices extracted for Table 10, reflect the supposition in section 3.4 that there is a trade-off between the effectiveness of an index in detecting biomass decline and the practicality of collection of the requisite data. In particular, indices based on primary searching time (PST) alone reflect the magnitude of biomass changes better than when they are combined (as may be practically necessary) with secondary searching time (SST).

Care must be taken not to over-interpret this result, as the model simplifies what is a very complex searching process within a concentration; PST and SST are idealisations, and given field definition problems, statistics collected during commercial operations might not perform nearly as effectively as the model indicates.

As an initial test of the effect of difficulties of definition, the model runs were repeated allowing for a random error chosen with uniform probability over the range (-30%, +30%) in the allocation of time to PST from the total (PST+SST) period between each successive pair of hauls in a concentration. The results are shown in Table 10, and suggest that introduction of this misallocation effect has virtually no influence on the extent of the greater effectiveness of indices using PST compared to those not needing to differentiate between the two types of within-concentration searching. (The variance increase in the PST indices arising from the misallocation effect is marginal only.)

While the result of this initial test is promising, it is certainly not conclusive. It does, nevertheless, suggest that it may be premature to consider abandoning the use of PST based indices at this stage because of potential data collection problems.

3.7 Reservations About the Model

Obviously, numerous parameter value variations and further model modifications are possible and may merit investigation. However four particularly important problem areas stand out.

3.7.1 Krill Distribution Model

The model modifications adopted in section 3.3 to solve the "FISHT problem" were of an *ad hoc* nature, and so are not particularly satisfactory. If one is to be confident about the magnitudes predicted for the extent of the non-proportionality between abundance indices and overall krill biomass, rather than have to be satisfied with qualitative predictions only, equal confidence is needed in the krill distribution model adopted. Such confidence is impossible given comments (see section 3.3) to the effect that the distribution statistics from FIBEX (upon the results of which many of the choices for distribution parameter values for this exercise were based) are atypical of the swarms on which the Japanese krill fishery operates. While there is scope for further analysis of krill distribution data from previous scientific surveys, the greatest need would seem to be for additional intensive hydroacoustic surveys by research vessels over small areas in which fishing vessels are operating concurrently. Such surveys should be planned and the results analysed with a view to developing more realistic "within-concentration" krill distribution models. In particular they might provide information on the important aspect of temporal variability of the distribution parameters, which is pertinent to more realistic modelling of the process of diminishing catch rates which causes a vessel to leave a concentration, as discussed further below.

The concentration-swarm distinction is also a simplification of a more complex spatially aggregated distribution pattern. Here further analysis of existing data may provide the basis for a more realistic distribution model (on a larger length scale than was the concern of the previous paragraph), and an investigation of whether this would affect the conclusions on the performance of various potential abundance indices should then be carried out.

3.7.2 Swarm Selectivity

The considerable difference between the tuned values of B_{min} for the two model modifications (see Table 2) suggests that at least one of these modifications is not a realistic representation of the actual situation. Empirical data from actual fishing operations on the proportion of swarms considered fishable would provide a valuable constraint for further model development.

Of more concern is whether the swarm selectivity criterion (the B_{min} value) would change if krill biomass declined, rather than remain invariant as assumed in the calculations reported. The sensitivity of the TC/TPST index to a decline in δ for the one swarm-per-haul model, for example, is essentially just a reflection of this assumption. It is arguably logically more consistent (internal to the model) to choose B_{min} and other selectivity related parameters [$(C/FISHT)_{rpt}$ and CR_{min}] for each scenario that maximise the total catch per half-month under those distributional conditions. This would, however, be a very lengthy exercise in computer time terms.

If the selectivity arguments in this paper are reasonably close to reality, the fishery operates on only the upper 7% (or 30%, if more than one swarm may be towed in a haul) of the swarm biomass distribution, which is very long-tailed. How will the shape of this distribution change in response to biomass depletion? One would be rather more confident about model robustness to the assumption in this analysis of relative shape invariance and a change only in the modal value of a distribution, if the fishery covered the centre rather than only the tail of the krill swarm biomass distribution.

3.7.3 The Criterion to Leave a Concentration

Figure 8 shows how sensitive the base case model output is to the choice of a value for the parameter CR_{min}. Over a narrow range of about [1.5, 2.5] for CR_{min}, the behaviour of the simulated vessel changes from the one extreme of remaining in the concentration first found for the balance of the half-month period, to fishing as many concentrations as possible and waiting only long enough in each to conduct sufficient hauls to establish that the CR_{min} criterion has not been met. Though Figure 8 is for the "One elongated ($f = 8$) swarm per haul" model modification, similar results follow if more than one swarm may be towed in a haul.

Figure 8 also points to a weakness of the model, viz. TC is maximal for the extreme of remaining in the concentration first found, rather than for moving between concentrations as does occur in the real world. This points to the need to take one or both of temporal variability of distribution parameters and krill quality considerations into account. (In the latter respect, "greenness" also would vary with time.) The argument in section 2.4 that the manner in which the model deals with the occurrence of bad weather mimics temporal variation of within-concentration distribution parameter values is neither strong nor satisfactory.

The ogive-like nature of the plot shown in Figure 8 (ii) has an important bearing on the shapes of the relationships between abundance indices and biomass, because the effect of changing within-concentration distribution parameter values is similar to changing CR_{min}, and so has a large influence on the proportion of total available time spent in searching for concentrations (CST). Figure 9 shows similar plots of abundance index vs biomass to

Figure 7, but for the case where only the swarm density parameter δ changes. Note that these relationships, although generally closer to proportionality than in Figure 7 because most indices are able to reflect changes in δ well, range from convex to near-linear to concave, rather than showing only the convexity expected from saturation effects. These complicated shapes are a reflection of the manner in which swarm-selectivity and concentration-leaving have been modelled, and may well prove not to be robust to variations in the models of such processes.

3.7.4 Concentration Searching

There is considerable doubt that searching for concentrations resembles random search in reality; rather, some information is passed (directly or indirectly) between vessels, and some concentrations are associated with oceanographic features whose positions have become known as vessel Captains have gained experience. Model modifications to reflect such features might be considered to examine their effect on CST-related abundance indices.

4. CONCLUSIONS AND RECOMMENDATIONS

(a) The simulation indicates that the catch statistics data routinely collected at present would be of low utility in detecting biomass decline. Catch per vessel-day (cf: TC) responds to the widest variety of biomass reduction scenarios, but is an imprecise index. Catch per fishing time indices (e.g. TC/TFISHT) perform very poorly.

(b) This utility might be improved by the collection of search time data to allow calculation of the index TC/TFISHT/($\overline{\text{PST+SST}}$), for example. This could be achieved by keeping records of the times spent on various other vessel activities, so that searching time could be deduced by subtraction. It would be desirable also to have an indication of the periods spent steaming between or searching for concentrations, so that within-concentration search time could be distinguished.

(c) Indices distinguishing primary searching time (PST) for swarms within concentrations, such as TC/TFISHT/$\overline{\text{PST}}$, perform better than those which do not. However, collection of such data would be much more onerous than would be the case for what is proposed in (b) above, and practical field definitions to distinguish PST and SST (secondary searching time) may not be achievable. Before considering routine implementation of such data collection:

   (i) small scale experiments to test collection viability should be performed, and

   (ii) further model tests of the robustness of PST based indices to errors in recording should be carried out.

(d) The priority for further research is improving the krill distribution model underlying the calculations presented here, as there are sound reasons for considerable misgivings about this model. Existing scientific data bases may not be adequate for this purpose, and intensive hydroacoustic surveys by research vessels in areas in which fishing vessels are operating concurrently merit consideration.

(e) Only indices including concentration searching time (CST) seem capable of responding to changes in the number of krill concentrations, and even these remain rather insensitive to concentration size. There are, however, important reservations about the utility of any CST data that might be extracted from the Japanese krill fishing operations. Thus, while these operations may be able to provide information on changes in krill abundance per unit area within concentrations, monitoring of changes in the number, distribution and size of the krill concentrations themselves will probably need to be effected by other means, such as research vessel surveys.

(f) While the model developed has ignored considerations of krill quality and product targeting thus far, nevertheless immediate consideration should be given to possibly requiring the routine recording of a vessel's product targeting and sensitivity to "greenness". Discussion in Butterworth (1988) indicates that is it quite likely that these factors may influence the values of CPUE-like abundance indices, and data should be collected to allow for empirical analysis of this possibility.

ACKNOWLEDGEMENTS

This work was supported principally by contracts from CCAMLR, and also by funding for periods of leave at Imperial College, London during which much of the work was carried out. This latter funding was provided by the Foundation for Research Development of the CSIR, South Africa and the University of Cape Town which generously granted the leave periods. Further to those with whom discussions were held in Japan in 1986 regarding the krill fishery, and who are acknowledged in Butterworth (1988), the author is appreciative of discussions in September 1987 with Captain Fukui, Commander Furukawa, Mr T. Ichii, Commander Kanoh and Dr Y. Shimadzu in Tokyo. Further valuable discussions with Messrs I. Hampton and D. Miller in South Africa, and Drs J. Beddington, I. Everson, J. Gulland, G. Kirkwood, M. Mangel, A. Rosenberg and J. Watkins in the UK are acknowledged, together with correspondence received from Mr T. Ichii and Dr J. Kalinowski. Mrs J. De Decker and Mr A. Punt assisted with preparation of the Figures and Tables, and Ms A. Goddard typed the document in record time.

REFERENCES

BIOMASS. 1986. Report on the post-FIBEX acoustic workshop, Frankfurt, Federal Republic of Germany, 3-14 September 1984. BIOMASS Report Series No. 40: 106 pp.

D.S. BUTTERWORTH. 1988. Some aspects of the relation between Antarctic krill abundance and CPUE measures in the Japanese krill fishery (Report of discussions with Japanese industry and fishing agency members and scientists: 11-16 October, 1986). This volume.

BUTTERWORTH, D.S.,S.T. BUCKLAND, H. KISHINO, and M.J. SILBERBAUER. 1987. Revised sighting estimates of Antarctic minke whale abundance from the 1978/79 to 1984/85 IWC/IDCR assessment cruises. IWC Document SC/39/Mi18: 37 pp.

BUTTERWORTH, D.S. and D.G.M. MILLER 1987. A note on relating Antarctic krill catch-per-unit-effort measures to abundance trends. S. Afr. J. Antarct. Res. 17(2): 112-116. (Earlier version circulated as CCAMLR Document KRILL WG/1985/Doc.3, 15 pp.)

HAMPTON, I. 1985. Abundance, distribution and behaviour of *Euphausia superba* in the Southern Ocean between 15° and 30°E during FIBEX. Antarctic Nutrient Cycles and

Food Webs (ed. by W. R. Siegfried, P. R. Condy, and R. M. Laws), Springer-Verlag, Berlin Heidelberg: 294-303.

ICHII, T. 1987. Observations of fishing operations on a krill trawler and distributional behaviour of krill off Wilkes Land during the 1985/86 season. Selected papers presented to the Scientific Committee of CCAMLR 1987: 337-368.

KALINOWSKI, J. and Z. WITEK. 1982. Forms of Antarctic krill aggregations. ICES Biological Oceanography Committee C.M. 1982/L: 60 (mimeo), 8 pp.

KALINOWSKI, J. and Z. WITEK. 1983. Elementy biologii, formy grupowego wystepowania i zasoby antarktycznego kryla *Euphausia superba* /Dana/Crustacea/. Sea Fisheries Institute, Gdynia, 207 pp.

KALINOWSKI, J. and Z. WITEK. 1985. Scheme for classifying aggregations of Antarctic krill. BIOMASS Handbook No 27: 9 pp.

MANGEL, M. 1987. Simulation of Southern Ocean krill fisheries. CCAMLR Document SC-CAMLR/VI/BG/22, 86 pp.

MANGEL, M. 1988. Analysis and modelling of the Soviet Southern Ocean krill fleet. This volume.

MACCALL, A.D. 1983. Population models of habitat selection, with application to the northern anchovy. Ph.D. Dissertation, University of California at San Diego, 170 pp.

ROSENBERG A.A., J.R. BEDDINGTON and M. BASSON. 1986. Growth and longevity of krill during the first decade of pelagic whaling. Nature 324 (6093): 152-154.

SHIMADZU, Y. 1984. A brief summary of Japanese fishing activity relating to Antarctic krill, 1972/73-1982/83. Selected papers presented to the Scientific Committee of CCAMLR 1982-1984 Part 1: 439-452.

SHIMADZU, Y. 1985. An updated information of the Japanese krill fishery in the Antarctic. CCAMLR Document KRILL WG/1985/Doc.5: 7 pp.

GLOSSARY OF ACRONYMS AND SYMBOLS

Note: (i) A prefix "T" indicates summation over the period considered (a half-month in the simulation).

(ii) A bar (—) over a symbol indicates an average.

(I) Krill distribution related

N_c : Number of concentrations in 600 n mile square sector

L_c : Radius of (circular) concentration

D_c : Density of swarms within a concentration (number per unit area)

r : Radius of (circular) swarm

δ : Surface (areal) density of krill within a swarm (biomass per unit area)

ρ : Volume density of krill within a swarm (biomass per unit volume)

B_s : Biomass of krill in a swarm

λ : Intersected swarm length in a survey

s : Distance to a swarm (or concentration)

f : Swarm elongation factor in modified model - see equations (31)

α : Fraction of base case level to which sector biomass is reduced

P.S. : Pelagic Shift in krill concentration distribution - see section 3.5

$U[A,B]$: Uniform distribution between A and B

$N[0,\sigma^2]$: Normal distribution with mean zero and standard deviation σ.

(II) Fishing operation related

S : Selectivity - fraction of swarms in a concentration considered to be fishable

B_{min} : Minimum biomass for swarm to be considered fishable

$(C/FISHT)_{rpt}$: Minimum catch rate per fishing time for repeat tow on a swarm to be attempted

CR_{min} : Minimum catch rate per total elapsed time (average over last 10 hauls) to continue fishing in a concentration

v : Vessel speed (10 knots searching: 2 knots towing)

w : Effective search width (also used to indicate relative weight)

(III) Fishery statistics

C : Catch (by mass)

H : Haul

DBH : Distance between successive hauls (within the same concentration)

TBH : Time between successive hauls (within the same concentration)

TNC : Total number of concentrations fished in period under consideration

PST : Primary search time for a swarm in a concentration

SST : Secondary search time for a swarm (while waiting to complete processing)

CST : Search time for a concentration

TAST : Total of all search time (TPST + TSST + TCST)

FISHT : Fishing time with net at desired depth (as recorded routinely at present)

TOWT : Total period net is in the water during a haul

TOWT-FISHT : Sum of net lowering and raising times

BW : Time lost to bad weather

TRANS : Time in transit to offload.

Table 1: Summary statistics from a sample of data from a Japanese commercial krill trawler. A number followed by another in parenthesis corresponds to mean (standard deviation), except where indicated otherwise or where only a single statistic is involved.

	JAN 1981	FEB 1981	JAN 1982	FEB 1982	AVERAGE
Number of hauls (TH)	227	163	185	174	187 (28)
Swarms fished per haul	1.34 (0.67)	1.36 (0.69)	1.05 (0.23)	1.09 (0.34)	1.21 (0.46)
Total catch (TC) (tons)	1502	1085	1485	1935	1502 (347)
Catch per haul (C/H) (t)	6.62 (4.70)	6.66 (5.14)	8.03 (4.76)	11.12 (5.43)	8.11 (5.20)
Total fishing time (TFISHT) (hours)	236.5	226.2	162.1	278.5	225.8 (48.1)
TC/TFISHT (t/h)	6.35	4.80	9.16	6.95	6.82 (1.81)
C/FISHT (t/h)	9.08 (10.71)	5.88 (5.29)	15.06 (17.48)	9.01 (9.48)	9.76 (10.46)
FISHT per haul (h)	1.042 (.578)	1.388 (.672)	0.876 (.573)	1.601 (.742)	1.227 (.661)
FISHT per haul (Swarms = 1) (h)	1.034 (.591)	1.416 (.695)	0.874 (.583)	1.604 (.754)	1.232 (.678)
FISHT per haul (Swarms > 1) (h)	1.066 (.543)	1.317 (.593)	0.908 (.372)	1.556 (.566)	1.212 (.526)
Time between hauls (TBH) (h)	2.14 (0.95)	2.68 (1.02)	2.39 (1.13)	2.95 (1.40)	2.54 (1.13)
C/TBH (t/h)	3.66 (2.81)	3.00 (2.50)	4.51 (3.66)	4.30 (2.30)	3.87 (2.85)
Average C/TBH (over 10 successive hauls) (t/h)	3.61 (1.38)	2.84 (0.92)	3.82 (1.00)	3.77 (0.81)	3.51 (1.04)
Distance between hauls (DBH) (n.m.)	2.35 (2.37)	3.39 (3.51)	2.51 (2.08)	3.62 (2.76)	2.97 (2.70)
Speed of haul (knots)	2.01 (0.03)	2.00 (0.02)	2.01 (0.03)	2.00 (0.02)	2.01 (0.02)
No. concentrations fished (TNC) [min, max]	7 [7,10]	7 [4, 8]	11 [10,11]	7 [5, 7]	8 [6.5, 9]
Total concn search time (TCST) (h)	195.7	117.5	276.1	75.3	166.2 (88.7)
Search time per concn (CST) (h)	21.7 (13.1)	16.8 (15.2)	25.1 (37.8)	12.6 (8.1)	19.1 (17.5)
Inter-concentration distance (n.m.)	115 (106)	138 (122)	100 (87)	70 (68)	106 (96)
North-South fishing extent (n.m.)	100	71	108	119	100 (21)
Bad weather and transit time (h)	57.2	113.2	91.0	107.8	92.3 (25.2)
Balance time (net raising, lowering; searching for swarms; processing) (h)	254.6	215.1	214.8	210.4	223.7 (20.7)

Table 2: Values of fishing operation parameters for various modifications. Where a value of a "partially tuned" parameter is shown in square brackets, the value was not tuned for that modification, but set equal to the tuned value for a related modification.

PARAMETER	MODEL			
	One Swarm per Haul		More than One Swarm per Haul	
	No elongation**	Elongation++	Off-Centre++	Through Centre
Fixed				
Start search position (n.m.)	(0,100)	(0,100)	(0,100)	(0,100)
Initial search aim point (n.m.)	(300,0)	(300,0)	(300,0)	(300,0)
Dist moved bad weather (n.m.)	50	50	50	50
Process rate (t/h)	2.5	2.5	2.5	2.5
Process time estimated available during next haul (h)	0.75	1.5	1.5	1.5
Target catch per haul (t)	10	10	10	10
No swarms per haul	1	1	(free)	(free)
Max length haul TOW_{max} (n.m.)	(free)	(free)	4	4
Sonar detection width (m)	N.A.	N.A.	35	35
Partially Tuned				
Swarm elongation factor, f	(1)	8^1	(1)	(1)
Swarm Selectivity, B_{min} (t)	[50]	50^2	5^3	[5]
Repeat haul criterion $(C/FISHT)_{rpt}$ (t/h)	50^4	10^4	10	[10]
Leave concentration criterion CR_{min} (t/h)	3.2^5	2.0^5	3.2^5	[3.2]
(No concentrations N_c)	[36]	36^5	[36]	[36]

Principal fishing operation statistic to which tuned:

1) Mean fish time per haul ($\overline{FISHT}$)
2) Mean catch per haul ($\overline{C/H}$)
3) Catch per fishing time (TC/TFISHT)
4) Fraction attempted repeated hauls
5) Concentration searching time (TCST) and number of concentrations fished (TNC)

++ Modifications used for further analysis

** Corresponds to original model developed in Chapter 2.

Table 3: Comparison of statistics for the Japanese commercial krill fishery from the data sample provided and other sources with the simulation model outputs for the base case. The simulation model results reflect the mean over 100 runs. (NB: All statistics apply to a half-month period.) The numbers in parenthesis are c.v.'s, except for time budget percentages where they are standard deviations.

CATCH STATISTICS	COMMERCIAL DATA				SIMULATION MODEL OUTPUT							
	80/81 + 81/82 Data Sample (Table 1)		Other Sources		One Swarm per Haul				More than One Swarm per Haul			
					No elongation** (f=1)		Elongated swarms++ (f=8)		Non-Initial Off-Centre++		Swarms towed Through Centre	
Number of hauls (TH)	94	(0.15)			121	(0.42)	93	(0.38)	86	(0.40)	100	(0.39)
Swarms fished per haul	1.21	(0.38)			1^*		1^*		4.97	(0.55)	4.63	(0.55)
Total catch (TC) (t)	751	(0.23)			856	(0.43)	666	(0.40)	784	(0.41)	944	(0.40)
Catch per haul (C/H) (t/h)	8.11	(0.64)			$7.08^{(+)}$	(0.46)	7.17^+	(0.45)	9.14	(0.28)	9.43	(0.27)
Total fishing time (TFISHT) (h)	113	(0.21)			27	(0.41)	112	(0.35)	98	(0.38)	107	(0.36)
TC/TFISHT (t/h)	6.82	(0.27)			31.54	(0.14)	5.87	(0.17)	7.92^+	(0.10)	8.66	(0.11)
C/FISHT (t/h)	9.76	(1.07)			43.75	(0.12)	11.85	(0.21)	17.82	(0.22)	18.31	(0.21)
FISHT per haul (h)	1.23	(0.54)			0.22	(0.65)	1.20^+	(0.90)	1.14	(0.60)	1.07	(0.61)
Fraction attempted repeated hauls			0.4^1		0.40^+	(0.20)	0.44^+	(0.21)	0.44^+	(0.16)	0.48	(0.16)
Time between hauls (TBH) (h)	2.54	(0.44)			1.70	(0.32)	2.28	(0.49)	2.34	(0.34)	2.29	(0.34)
Distance between hauls (DBH) (n.m.)	2.97	(0.91)			1.27	(1.09)	2.61	(0.89)	2.57	(0.79)	2.40	(0.82)
Number concentrations fished (TNC)	4	(0.25)	$1-2^1$		2.09^+	(0.45)	2.13^+	(0.36)	2.37^+	(0.41)	1.83	(0.44)
Total concn search time (TCST) (h)	83	(0.53)			$125^{(+)}$	(0.63)	116^+	(0.57)	$132^{(+)}$	(0.54)	102	(0.77)
Search time per concn (CST) (h)	19.1	(0.92)			73.4	(0.94)	64.0	(0.83)	62.0	(0.91)	58.7	(1.01)
Inter-concentration distance (n.m.)	106	(0.91)			85	(0.74)	75	(0.62)	76	(0.72)	78	(0.62)
North-south fishing extent (n.m.)	100	(0.21)	$< 100^2$		52	(1.01)	40	(0.93)	57	(0.85)	55	(0.96)
Distance from ice-edge (n.m.)					66	(0.72)	67	(0.65)	64	(0.67)	65	(0.74)
<u>TIME BUDGET (%)</u>												
TPST+TSST+(TTOWT-TFISHT)	32	(3)			49	(21)	28	(15)	28	(11)	34	(13)
TCST	23	(12)			35	(22)	32	(18)	37	(20)	28	(22)
TAST=TPST+TSST+TCST			45^3	25^4	61	(11)	42	(15)	48	(15)	43	(16)
TFISHT	32	(7)	18		8	(3)	31	(11)	27	(10)	30	(11)
TTOWT (includes TFISHT)			42	50	30	(13)	49	(17)	44	(17)	49	(18)
BW+TRANS	13	(4)	13	25	9	(5)	9	(6)	8	(6)	8	(6)

* Fixed by design
\+ Partially tuned
(+) Partially tuned for related modification

1) T Ichii (pers. commn, Sept 1987)
2) Captain Fukui (pers. commn, Sept 1987)
3) Butterworth (1987)
4) Y Shimadzu (pers. commn, Sept. 1987)

** Corresponds to original model developed in Chapter 2

++ Modifications used for further analysis

Table 4: Comparison of abundance indices for the base case simulation model run with those from six alternative krill distribution scenarios, each corresponding to a 50% overall biomass drop. For the base case, the mean over the 100 simulations is shown, together with the standard error of this mean in parenthesis. For the alternative scenarios, the percentage difference from the base case mean is given, together with the standard of error that difference in parenthesis. (Units, where appropriate, are tonne-hour combinations.)

(a) One elongated (f=8) swarm per haul

INDEX	Base case	$N_c \times 0.5$	$N_c \times 0.5$ + P.S.	$L_c \times 1/\sqrt{2}$	$D_c \times 0.5$	$r \times 1/\sqrt{2}$	$\delta \times 0.5$
A.1: TC^{+++}	666 (27)	−40 (9)	+1 (6)	−16 (7)	−17 (6)	+9 (6)	−60 (7)
2: TH^{+++}	93 (4)	−39 (9)	+2 (6)	−16 (7)	−17 (6)	+8 (5)	−52 (6)
B.1: TFISHT^{+++}	111.8 (3.9)	−38 (8)	+3 (5)	−15 (6)	−17 (5)	−4 (5)	−32 (5)
2: TPST	22.8 (0.9)	−39 (8)	−1 (6)	−17 (7)	+44 (6)	+63 (5)	−27 (6)
3: TPST + TSST^{+}	36.0 (1.4)	−40 (9)	+1 (6)	−17 (7)	+18 (6)	+39 (6)	−44 (6)
4: TCST^{+}	116.2 (6.6)	+68 (7)	−2 (9)	+29 (8)	+20 (8)	−8 (9)	+73 (6)
5: TAST^{++}	152.2 (5.3)	+42 (5)	−1 (5)	+18 (5)	+19 (5)	+3 (5)	+45 (4)
C.1: TC/TFISHT^{+++}	5.87 (0.10)	−8 (3)	−2 (3)	−4 (3)	−0 (3)	+15 (2)	−42 (3)
2: $\overline{\text{C/FISHT}}^{+++}$	11.85 (0.24)	−6 (4)	+1 (3)	−1 (3)	+5 (3)	+13 (3)	−39 (4)
3: $\overline{\text{TC/TPST}}$	28.99 (0.39)	−1 (3)	+5 (2)	+1 (2)	−43 (2)	−33 (2)	−45 (3)
4: $\overline{\text{C/PST}}$	64.59 (1.02)	−2 (3)	+2 (2)	+2 (3)	−31 (3)	−25 (3)	−34 (3)
5: TC/(TPST+TSST)$^{+}$	18.56 (0.18)	+3 (3)	+1 (1)	+0 (1)	−31 (2)	−22 (2)	−29 (2)
6: TC/TCST^{+}	13.07 (2.15)	−64 (23)	+12 (23)	−22 (24)	−37 (22)	+57 (24)	−87 (19)
D.1: TC/TFISHT/$\overline{\text{PST}}$	23.31 (0.52)	−6 (4)	+4 (4)	−1 (4)	−42 (4)	−24 (3)	−62 (4)
2: TC/TFISHT/($\overline{\text{PST+SST}}$)$^{+}$	14.84 (0.25)	−3 (3)	+1 (3)	−2 (3)	−30 (3)	−11 (3)	−52 (3)
3: TC/TFISHT/$\overline{\text{PST}}$/$\overline{\text{CST}}$	0.724 (0.085)	−57 (16)	+3 (15)	−17 (16)	−49 (15)	−8 (16)	−77 (14)
4: TC/TFISHT/($\overline{\text{PST+SST}}$)/$\overline{\text{CST}}^{+}$	0.459 (0.056)	−57 (16)	+1 (15)	−20 (16)	−39 (15)	+5 (16)	−71 (14)
5: TC/TFISHT/TAST^{++}	0.045 (0.002)	−27 (7)	+4 (6)	−11 (7)	−18 (6)	+9 (6)	−62 (6)
E.1: TNC^{+}	2.13 (0.07)	−38 (8)	−7 (6)	−9 (6)	+7 (5)	0 (6)	+41 (5)
2: TH/TNC^{+}	43.6 (2.4)	−1 (9)	+9 (8)	−7 (8)	−22 (8)	+8 (8)	−66 (6)
F.1: $\overline{\text{C/H}}^{+++}$	7.17 (0.03)	−2 (1)	−1 (1)	−1 (1)	+0 (1)	+2 (1)	−17 (1)
2: $\overline{\text{FISHT}}^{+++}$	1.20 (0.01)	+2 (1)	+1 (1)	+1 (1)	−0 (1)	−11 (1)	+41 (2)
3: $\overline{\text{TOWT}}^{++}$	1.89 (0.01)	+1 (1)	+1 (1)	+1 (1)	−0 (1)	−7 (1)	+26 (1)
4: $\overline{\text{TBH}}^{++}$	2.28 (0.01)	+0 (1)	+0 (1)	+0 (1)	+7 (1)	−1 (1)	+25 (1)

+++	Data currently collected
++	Data collectable, but onerous
+	Data collectable with difficulty
blank	Extreme difficulties data collection

Table 4: Comparison of abundance indices for the base case simulation model run with those from six alternative krill distribution scenarios, each corresponding to a 50% overall biomass drop. For the base case, the mean over the 100 simulations is shown, together with the standard error of this mean in parenthesis. For the alternative scenarios, the percentage difference from the base case mean is given, together with the standard of error that difference in parenthesis. (Units, where appropriate, are tonne-hour combinations.)

(b) More than one swarm per haul

INDEX	Base case		$N_c \times 0.5$		$N_c \times 0.5$ + P.S.		$L_c \times 1/\sqrt{2}$		$D_c \times 0.5$		$r \times 1/\sqrt{2}$		$\delta \times 0.5$	
A.1: TC^{+++}	784	(32)	-41	(9)	+25	(5)	-10	(6)	-62	(6)	-51	(6)	-64	(6)
2: TH^{+++}	86	(3)	-42	(4)	+24	(5)	-11	(6)	-53	(6)	-46	(6)	-57	(6)
B.1: TFISHT^{+++}	98.0	(3.8)	-42	(8)	+26	(4)	-10	(6)	-41	(6)	-34	(6)	-42	(6)
2: TPST	20.7	(0.8)	-42	(9)	+22	(5)	-14	(6)	-18	(6)	-30	(6)	-43	(6)
3: TPST + TSST^{+}	42.9	(1.8)	-40	(9)	+26	(5)	-10	(6)	-49	(6)	-48	(6)	-61	(6)
4: TCST^{+}	131.5	(7.1)	+55	(7)	-36	(8)	+12	(7)	+64	(6)	+59	(6)	+70	(6)
5: TAST^{++}	174.4	(5.5)	+32	(4)	-21	(4)	+ 6	(4)	+37	(4)	+33	(4)	+38	(4)
C.1: TC/TFISHT^{+++}	7.92	(0.08)	+ 0	(2)	- 0	(1)	+ 0	(2)	-35	(2)	-26	(2)	-38	(2)
2: $\overline{C/FISHT}^{+++}$	17.82	(0.40)	- 4	(4)	- 5	(3)	- 2	(3)	-26	(4)	-19	(4)	-46	(5)
3: TC/TPST	37.96	(0.51)	+ 3	(2)	+ 3	(2)	+ 5	(2)	-51	(3)	-30	(2)	-36	(3)
4: $\overline{C/PST}$	86.52	(1.67)	- 1	(4)	+ 7	(2)	+ 4	(3)	-43	(4)	-22	(3)	-29	(4)
5: TC/(TPST+TSST)$^{+}$	18.39	(0.14)	+ 0	(1)	- 1	(1)	- 1	(1)	-23	(2)	- 7	(1)	- 7	(2)
6: TC/TCST^{+}	10.18	(1.04)	-37	(27)	+98	(16)	+17	(28)	-84	(13)	-79	(13)	-86	(12)
D.1: TC/TFISHT/$\overline{PST}$	32.08	(0.57)	+ 3	(3)	+ 2	(2)	+ 4	(3)	-63	(4)	-44	(3)	-55	(3)
2: TC/TFISHT/$(\overline{PST+SST})^{+}$	15.50	(0.18)	- 0	(2)	- 2	(1)	- 2	(2)	-42	(3)	-26	(2)	-34	(2)
3: TC/TFISHT/$\overline{PST}/\overline{CST}$	0.883	(.071)	-45	(17)	+85	(11)	-11	(16)	-76	(11)	-62	(10)	-72	(11)
4: TC/TFISHT/$(\overline{PST+SST})/\overline{CST}^{+}$	0.421	(.032)	-48	(15)	+79	(10)	-18	(14)	-62	(11)	-49	(10)	-59	(11)
5: TC/TFISHT/TAST^{++}	0.051	(.002)	-18	(6)	+20	(4)	- 6	(5)	-55	(4)	-49	(4)	-59	(4)
E.1: TNC^{+}	2.37	(0.10)	-43	(8)	+27	(5)	-15	(6)	+42	(6)	+45	(6)	+38	(6)
2: TH/TNC^{+}	36.2	(1.8)	+ 3	(9)	- 2	(7)	+ 5	(7)	-67	(5)	-62	(6)	-69	(5)
F.1: $\overline{C/H}^{+++}$	9.14	(0.03)	+ 1	(1)	+ 1	(0)	+ 1	(0)	-17	(1)	-11	(1)	-17	(1)
2: $\overline{FISHT}^{+++}$	1.14	(0.01)	- 1	(1)	+ 2	(1)	+ 2	(1)	+27	(1)	+21	(1)	+35	(1)
3: $\overline{TOWT}^{++}$	1.83	(0.01)	- 0	(1)	+ 1	(1)	+ 1	(1)	+17	(1)	+13	(1)	+22	(1)
4: $\overline{TBH}^{++}$	2.34	(0.01)	+ 0	(1)	+ 1	(1)	+ 1	(1)	+17	(1)	+11	(1)	+16	(1)

+++	Data currently collected
++	Data collectable, but onerous
+	Data collectable with difficulty
blank	Extreme difficulties data collection

Table 5: Efficiency of abundance indices in detecting changes in krill biomass :

blank : 100 simulations detect no change significant at 5%
+ / - : direction of change if difference significant at 5% level detected
* : Index (or its inverse) drops by > 20%
* * : index (or its inverse) drops by > 45% (within 95% limits)

(a) One elongated (f=8) swarm per haul

INDEX	$N_c \times 0.5$	$N_c \times 0.5$ + P.S.	$L_c \times 1/\sqrt{2}$	$D_c \times 0.5$	$r \times 1/\sqrt{2}$	$\delta \times 0.5$
A.1: TC^{+++}	-**		-	-		-**
2: TH^{+++}	-**		-	-		-**
B.1: TFISHT^{+++}	-**		-	-		-*
2: TPST	-**		-	+*	+**	-*
3: TPST + TSST^{+}	-**		-	+	+*	-*
4: TCST^{+}	+**		+*	+		+**
5: TAST^{++}	+*		+	+		+*
C.1: TC/TFISHT^{+++}	-				+	-**
2: $\overline{C/FISHT}^{+++}$					+	-**
3: TC/TPST		+		-**	-*	-**
4: $\overline{C/PST}$				-*	-*	-*
5: TC/(TPST+TSST)$^{+}$				-*	-*	-*
6: TC/TCST^{+}	**	**	**	**	+**	-**
D.1: TC/TFISHT/$\overline{PST}$				-**	-*	-**
2: TC/TFISHT/($\overline{PST+SST}$)$^{+}$				-*	-	-**
3: TC/TFISHT/$\overline{PST}$/$\overline{CST}$	-**		**	-**		-**
4: TC/TFISHT/($\overline{PST+SST}$)/$\overline{CST}^{+}$	-**		**	-**		-**
5: TC/TFISHT/TAST^{++}	-*			-		-**
E.1: TNC^{+}	-**					+*
2: TH/TNC^{+}				-*		-**
F.1: $\overline{C/H}^{+++}$	-				+	-
2: $\overline{FISHT}^{+++}$			+		-	+*
3: $\overline{TOWT}^{++}$			+		-	+*
4: $\overline{TBH}^{++}$			+	+		+

Table 5: Efficiency of abundance indices in detecting changes in krill biomass :

blank : 100 simulations detect no change significant at 5%
+ / - : direction of change if difference significant at 5% level detected
* : Index (or its inverse) drops by > 20%
* * : index (or its inverse) drops by > 45% (within 95% limits)

(b) More than one swarm per haul

INDEX	$N_c \times 0.5$	$N_c \times 0.5$ + P.S.	$L_c \times 1/\sqrt{2}$	$D_c \times 0.5$	$r \times 1/\sqrt{2}$	$\delta \times 0.5$
A.1: TC^{+++}	-**	+*		-**	-**	-**
2: TH^{+++}	-**	+		-**	-**	-**
B.1: TFISHT^{+++}	-**	+*		-**	-**	-**
2: TPST	-**	+	-	-	-*	-**
3: TPST + TSST^{+}	-**	+*		-**	-**	-**
4: TCST^{+}	+**	-**		+**	+**	+**
5: TAST^{++}	+*	-*		+*	+*	+*
C.1: TC/TFISHT^{+++}				-*	-*	-*
2: $\overline{C/FISHT}^{+++}$				-*	-	-**
3: TC/TPST			+	-**	-*	-*
4: $\overline{C/PST}$		+		-**	-*	-*
5: TC/(TPST+TSST)$^{+}$				-*	-	-
6: TC/TCST^{+}	**	+**	**	-**	-**	-**
D.1: TC/TFISHT/$\overline{PST}$				-**	-**	-**
2: TC/TFISHT/($\overline{PST+SST}$)$^{+}$				-**	-*	-*
3: TC/TFISHT/$\overline{PST}$/$\overline{CST}$	-**	+**		-**	-**	-**
4: TC/TFISHT/($\overline{PST+SST}$)/$\overline{CST}^{+}$	-**	+**	**	-**	-**	-**
5: TC/TFISHT/TAST^{++}	-	+		-**	-**	-**
E.1: TNC^{+}	-**	+*		+*	+*	+*
2: TH/TNC^{+}				-**	-**	-**
F.1: $\overline{C/H}^{+++}$	+	+	+	-	-	-
2: $\overline{FISHT}^{+++}$		+		+*	+	+*
3: $\overline{TOWT}^{++}$		+		+	+	+
4: $\overline{TBH}^{++}$		+	+	+	+	+

Table 6: Further comparative statistics from 100 model runs for the base case and for six alternative scenarios each corresponding to a 50% overall biomass drop. The format is as for Table 4 except that values in parenthesis for the base case are standard deviations (<u>not</u> standard errors of the mean).

(a) One elongated (f-=8) swarm per haul

	Base case		N_c × 0.5		N_c × 0.5 + P.S.		L_c × $1/\sqrt{2}$		D_c × 0.5		r × $1/\sqrt{2}$		δ × 0.5	
Proportion of fishable swarms per concentration	0.075	(0.004)	+ 1	(0.6)	+ 1	(0.5)	0	(0.7)	+ 1	(0.6)	-40	(0.6)	-41	(0.5)
Mean biomass of fishable swarms (t)	439	(4920)	- 1	(5)	+ 1	(5)	+ 1	(6)	+ 1	(6)	-19	(5)	-21	(5)
Mean radius of fishable swarms (m) (before elongation)	370	(331)	- 0	(0.5)	- 0	(0.4)	- 0	(0.6)	+ 0	(0.5)	-14	(0.5)	+21	(0.4)
Mean length of swarm towed through (m)	4160	(4003)	+ 2	(2)	+ 1	(1)	+ 1	(1)	- 0	(1)	-12	(1)	+44	(2)
Proportion of attempted refishing of swarm*	0.44	(0.09)	-10	(4)	- 2	(3)	- 4	(4)	+ 0	(3)	+11	(3)	-43	(5)
Mean distance between swarms fished (n.m.) ($\overline{DBH}$)	2.61	(2.34)	+ 2	(2)	+ 1	(1)	- 5	(1)	+13	(1)	+ 1	(1)	+41	(2)
Mean distance between concentrations fished (n.m.)	75	(47)	+20	(11)	-18	(9)	- 3	(10)	- 4	(10)	- 4	(10)	- 4	(9)
Proportion of concentrations found that had previously been fished that half-month	0.09	(0.29)	-65	(54)	-49	(39)	-47	(39)	-31	(34)	-31	(35)	+30	(27)
Mean distance to ice-edge of concentrations fished (n.m.)	67	(44)	+ 1	(7)	-13	(6)	- 8	(6)	+ 0	(7)	- 4	(7)	+ 8	(6)
Mean distance excluding case where no concentration was found during initial transit to ice	85	(56)	-14	(14)	-41	(13)	-22	(12)	-17	(13)	-33	(13)	-10	(13)

*Standard deviation is of set of 100 estimated proportions.

Table 6: Further comparative statistics from 100 model runs for the base case and for six alternative scenarios each corresponding to a 50% overall biomass drop. The format is as for Table 4 except that values in parenthesis for the base case are standard deviations (<u>not</u> standard errors of the mean).

(b) More than one swarm per haul

	Base case	$N_c \times 0.5$	$N_c \times 0.5$ + P.S.	$L_c \times 1/\sqrt{2}$	$D_c \times 0.5$	$r \times 1/\sqrt{2}$	$\delta \times 0.5$
Proportion of fishable swarms per concentration	0.290 (0.007)	+ 0 (0.3)	0 (0.3)	- 0 (0.3)	+ 0 (0.3)	-29 (0.3)	-29 (0.3)
Mean biomass of fishable swarms (t)	127 (1972)	+ 2 (5)	+ 2 (5)	- 7 (4)	+ 8 (8)	-29 (5)	-28 (4)
Mean radius of fishable swarms (m)	204 (213)	- 0 (0.4)	- 0 (0.3)	- 0 (0.4)	+ 0 (0.3)	-16 (0.3)	+18 (0.3)
Mean length of tow from entering first swarm (m)	3935 (2531)	- 1 (1)	+ 2 (1)	+ 2 (1)	+29 (1)	+23 (1)	+38 (1)
Number of swarms fished per haul	4.97 (2.76)	+ 0 (1)	+ 4 (1)	+ 3 (1)	-24 (1)	+ 3 (1)	+27 (1)
Proportion of attempted refishing of swarm*	0.44 (0.07)	- 3 (3)	- 3 (2)	- 2 (2)	-41 (4)	-33 (3)	-55 (5)
Mean distance between swarms fished (n.m.) (DBH)	2.57 (2.03)	- 2 (1)	+ 2 (1)	- 2 (1)	+40 (1)	+26 (1)	+41 (1)
Mean distance between concentrations fished (n.m.)	76 (55)	+14 (12)	-32 (8)	+13 (10)	-4 (8)	+ 7 (8)	+ 8 (8)
Proportion of concentrations found that had previously been fished that half-month	0.06 (0.23)	-33 (52)	+95 (32)	- 0 (40)	+196 (30)	+160 (30)	+156 (30)
Mean distance to ice-edge of concentrations fished (n.m.)	64 (43)	+ 1 (8)	- 1 (5)	+ 9 (7)	+13 (6)	+20 (6)	+20 (6)
Mean distance excluding case where no concentration was found during initial transit to ice	50 (29)	+48 (12)	+28 (16)	+52 (10)	+53 (11)	+67 (13)	+57 (12)

*Standard deviation is of set of 100 estimated proportions.

Table 7: Additional comparative statistics from simulation model runs for the base case and six alternative scenarios each corresponding to a 50% overall biomass drop. The values given are means over 100 runs, with the standard errors of those means given in parenthesis.

(a) One elongated (f=8) swarm per haul

	Base case		$N_c \times 0.5$		$N_c \times 0.5$ & P.S.		$L_c \times 1/\sqrt{2}$		$D_c \times 0.5$		$r \times 1/\sqrt{2}$		$\delta \times 0.5$	
Proportion occasions fishing concentration terminated due to: bad weather	0.10	(.02)	0.07	(.02)	0.07	(.02)	0.05	(.02)	0.08	(.02)	0.07	(.02)	0.03	(.01)
poor catch rate	0.55	(.03)	0.68	(.04)	0.62	(.04)	0.60	(.03)	0.73	(.03)	0.53	(.04)	0.86	(.02)
Proportion of runs where concentration found prior to initial transit reaching ice-edge	0.74	(.04)	0.47	(.05)	0.72	(.05)	0.54	(.05)	0.66	(.05)	0.73	(.05)	0.67	(.05)
TIME BUDGET (%)														
BW + TRANS	9	(1)	10	(1)	8	(1)	9	(1)	9	(1)	8	(1)	9	(1)
TAST	42	(1)	60	(2)	42	(2)	50	(2)	50	(2)	43	(1)	61	(1)
TTOWT	49	(2)	30	(2)	50	(2)	41	(2)	40	(2)	48	(2)	30	(1)

(b) More than one swarm per haul

	Base case		$N_c \times 0.5$		$N_c \times 0.5$ & P.S.		$L_c \times 1/\sqrt{2}$		$D_c \times 0.5$		$r \times 1/\sqrt{2}$		$\delta \times 0.5$	
Proportion occasions fishing concentration terminated due to: bad weather	0.06	(.02)	0.09	(.03)	0.09	(.02)	0.06	(.02)	0.03	(.01)	0.03	(.01)	0.01	(.01)
poor catch rate	0.70	(.03)	0.66	(.04)	0.64	(.02)	0.69	(.03)	0.91	(.01)	0.86	(.02)	0.89	(.02)
Proportion of runs where concentration found prior to initial transit reaching ice-edge	0.66	(.05)	0.40	(.05)	0.93	(.03)	0.58	(.05)	0.70	(.05)	0.79	(.04)	0.63	(.05)
TIME BUDGET (%)														
BW + TRANS	8	(1)	11	(1)	7	(1)	9	(1)	10	(1)	9	(1)	10	(1)
TAST	48	(2)	64	(2)	38	(1)	52	(2)	66	(1)	64	(1)	67	(1)
TTOWT	44	(2)	25	(2)	55	(1)	39	(2)	24	(1)	27	(1)	23	(1)

Table 8: Abundance indices as a proportion of their values for the base case simulation model run. When the overall krill biomass is decreased to a fraction α of its base case level through a random combination of changes in N_c, L_c, D_c , r and δ. Results relate to the means over 100 simulations in every case. The figures in parenthesis are standard errors of the proportions estimated. Note that some of the indices listed are the inverses of those shown in Tables 4 and 5; the inverse has been taken whenever necessary to make the index an increasing function of α - such cases are indicated by *.

(a) One elongated (f=8) swarm per haul

INDEX \ α		0.1	0.2	0.3	0.4	0.5	0.6	0.7	0.8	0.9
A.1: TC^{+++}		0.55 (.08)	0.63 (.07)	0.70 (.07)	0.70 (.07)	0.79 (.07)	0.83 (.06)	0.86 (.06)	1.00 (.05)	0.95 (.06)
2: TH^{+++}		0.59 (.07)	0.67 (.07)	0.73 (.06)	0.72 (.07)	0.81 (.07)	0.84 (.06)	0.88 (.06)	1.00 (.05)	0.95 (.06)
B.1: TFISHT^{+++}		0.63 (.06)	0.71 (.06)	0.76 (.06)	0.76 (.06)	0.82 (.06)	0.86 (.06)	0.89 (.06)	1.03 (.05)	0.97 (.05)
2: TPST		0.94 (.07)	1.01 (.07)	1.02 (.06)	0.92 (.07)	0.98 (.07)	0.96 (.06)	0.97 (.06)	1.09 (.05)	0.96 (.06)
3: TPST + TSST^{+}		0.77 (.07)	0.83 (.07)	0.87 (.06)	0.82 (.07)	0.90 (.07)	0.91 (.06)	0.92 (.06)	1.04 (.05)	0.96 (.06)
4: [TCST^{+}]$^{-1}$	*	0.62 (.07)	0.66 (.07)	0.71 (.07)	0.70 (.08)	0.77 (.08)	0.79 (.08)	0.85 (.08)	1.01 (.08)	0.92 (.09)
5: [TAST^{++}]$^{-1}$	*	0.71 (.04)	0.74 (.05)	0.78 (.04)	0.78 (.05)	0.83 (.05)	0.85 (.05)	0.90 (.05)	1.00 (.05)	0.94 (.05)
C.1: TC/TFISHT^{+++}		0.85 (.03)	0.88 (.03)	0.92 (.03)	0.92 (.04)	0.95 (.03)	0.96 (.03)	0.96 (.03)	0.97 (.02)	0.96 (.02)
2: $\overline{C/FISHT}^{+++}$		0.90 (.04)	0.90 (.04)	0.90 (.03)	0.92 (.04)	0.97 (.03)	0.99 (.03)	0.99 (.03)	1.00 (.03)	0.97 (.03)
3: TC/TPST		0.62 (.03)	0.65 (.03)	0.71 (.03)	0.76 (.03)	0.82 (.03)	0.86 (.02)	0.89 (.02)	0.94 (.02)	0.99 (.02)
4: $\overline{C}/\overline{PST}$		0.74 (.04)	0.73 (.03)	0.78 (.03)	0.80 (.03)	0.87 (.03)	0.90 (.03)	0.93 (.03)	0.97 (.02)	1.01 (.03)
5: TC/(TPST+TSST)$^{+}$		0.73 (.02)	0.77 (.03)	0.81 (.02)	0.85 (.02)	0.89 (.02)	0.91 (.01)	0.93 (.02)	0.97 (.01)	0.99 (.02)
6: TC/TCST^{+}		0.24 (.20)	0.43 (.28)	0.34 (.20)	0.46 (.22)	0.78 (.28)	0.55 (.20)	0.72 (.22)	1.06 (.23)	1.11 (.28)
D.1: TC/TFISHT/$\overline{PST}$		0.56 (.05)	0.61 (.05)	0.68 (.04)	0.72 (.05)	0.80 (.04)	0.84 (.04)	0.88 (.03)	0.92 (.03)	0.96 (.03)
2: TC/TFISHT/($\overline{PST+SST}$)$^{+}$		0.66 (.04)	0.72 (.04)	0.77 (.03)	0.80 (.03)	0.87 (.03)	0.89 (.03)	0.92 (.03)	0.95 (.02)	0.96 (.02)
3: TC/TFISHT/$\overline{PST}$/$\overline{CST}$		0.29 (.16)	0.41 (.18)	0.39 (.15)	0.49 (.16)	0.67 (.17)	0.63 (.15)	0.82 (.16)	0.96 (.15)	0.96 (.17)
4: TC/TFISHT/($\overline{PST+SST}$)/$\overline{CST}^{+}$		0.34 (.16)	0.49 (.18)	0.46 (.15)	0.54 (.16)	0.73 (.18)	0.66 (.15)	0.86 (.16)	1.01 (.15)	0.94 (.17)
5: TC/TFISHT/TAST^{++}		0.58 (.07)	0.67 (.07)	0.69 (.06)	0.73 (.07)	0.82 (.07)	0.82 (.06)	0.89 (.06)	0.96 (.06)	0.96 (.07)
E.1: [TNC^{+}]$^{-1}$	*	1.00 (.06)	1.00 (.06)	0.96 (.06)	1.02 (.06)	1.04 (.06)	1.02 (.05)	0.96 (.06)	0.96 (.05)	1.06 (.06)
2: TH/TNC^{+}		0.59 (.08)	0.67 (.08)	0.70 (.08)	0.74 (.08)	0.84 (.08)	0.86 (.08)	0.84 (.08)	0.97 (.08)	1.01 (.08)
F.1: $\overline{C/H}^{+++}$		0.94 (.01)	0.95 (.01)	0.96 (.01)	0.97 (.01)	0.98 (.01)	0.99 (.01)	0.98 (.01)	0.99 (.01)	1.00 (.01)
2: [$\overline{FISHT}^{+++}$]$^{-1}$	*	0.93 (.01)	0.94 (.01)	0.96 (.01)	0.95 (.01)	0.99 (.01)	0.98 (.01)	0.99 (.01)	0.98 (.01)	0.98 (.01)
3: [$\overline{TOWT}^{++}$]$^{-1}$	*	0.95 (.01)	0.96 (.01)	0.97 (.01)	0.97 (.01)	0.99 (.01)	0.99 (.01)	0.99 (.01)	0.99 (.01)	0.99 (.01)
4: [$\overline{TBH}^{++}$]$^{-1}$	*	0.91 (.01)	0.93 (.01)	0.94 (.01)	0.95 (.01)	0.98 (.01)	0.98 (.01)	0.99 (.01)	0.99 (.01)	0.99 (.01)

Table 8: Abundance indices as a proportion of their values for the base case simulation model run. When the overall krill biomass is decreased to a fraction α of its base case level through a random combination of changes in N_c, L_c, D_c, r and δ. Results relate to the means over 100 simulations in every case. The figures in parenthesis are standard errors of the proportions estimated. Note that some of the indices listed are the inverses of those shown in Tables 4 and 5; the inverse has been taken whenever necessary to make the index an increasing function of α - such cases are indicated by *.

(b) More than one swarm per haul

INDEX	α	0.1	0.2	0.3	0.4	0.5	0.6	0.7	0.8	0.9
A.1: TC^{+++}		0.36 (.07)	0.35 (.07)	0.43 (.08)	0.48 (.07)	0.57 (.07)	0.59 (.06)	0.77 (.06)	0.76 (.07)	0.93 (.06)
2: TH^{+++}		0.42 (.07)	0.40 (.07)	0.47 (.07)	0.52 (.07)	0.60 (.07)	0.62 (.06)	0.62 (.06)	0.78 (.07)	0.93 (.06)
B.1: $TFISHT^{+++}$		0.52 (.07)	0.49 (.06)	0.56 (.07)	0.61 (.06)	0.68 (.06)	0.69 (.06)	0.83 (.06)	0.81 (.06)	0.96 (.06)
2: TPST		0.60 (.08)	0.55 (.07)	0.59 (.07)	0.62 (.07)	0.67 (.06)	0.69 (.06)	0.81 (.06)	0.78 (.07)	0.92 (.06)
3: $TPST + TSST^{+}$		0.42 (.07)	0.40 (.07)	0.46 (.07)	0.50 (.07)	0.59 (.07)	0.61 (.07)	0.78 (.06)	0.76 (.07)	0.93 (.06)
4: $[TCST^{+}]^{-1}$	*	0.57 (.06)	0.56 (.06)	0.59 (.06)	0.60 (.06)	0.65 (.06)	0.66 (.06)	0.77 (.07)	0.78 (.07)	0.92 (.08)
5: $[TAST^{++}]^{-1}$	*	0.70 (.03)	0.69 (.03)	0.72 (.04)	0.73 (.04)	0.77 (.04)	0.77 (.04)	0.86 (.04)	0.87 (.04)	0.96 (.05)
C.1: $TC/TFISHT^{+++}$		0.71 (.03)	0.71 (.03)	0.79 (.03)	0.78 (.02)	0.83 (.02)	0.88 (.04)	0.91 (.02)	0.93 (.02)	0.94 (.02)
2: $\overline{C/FISHT}^{+++}$		0.72 (.06)	0.72 (.06)	0.81 (.06)	0.75 (.05)	0.79 (.04)	0.87 (.05)	0.89 (.04)	0.90 (.04)	0.87 (.04)
3: TC/TPST		0.66 (.04)	0.67 (.03)	0.74 (.03)	0.79 (.03)	0.86 (.02)	0.88 (.02)	0.97 (.02)	0.99 (.02)	1.01 (.02)
4: $\overline{C/PST}$		0.74 (.05)	0.73 (.05)	0.80 (.04)	0.83 (.04)	0.87 (.03)	0.88 (.03)	0.99 (.03)	0.99 (.03)	1.03 (.03)
5: $TC/(TPST+TSST)^{+}$		0.88 (.02)	0.90 (.02)	0.92 (.01)	0.96 (.01)	0.98 (.02)	0.98 (.01)	1.00 (.01)	1.01 (.01)	1.01 (.01)
6: $TC/TCST^{+}$		0.14 (.13)	0.14 (.14)	0.20 (.16)	0.26 (.23)	0.31 (.19)	0.29 (.14)	0.61 (.19)	0.64 (.19)	1.10 (.17)
D.1: $TC/TFISHT/\overline{PST}$		0.53 (.05)	0.54 (.05)	0.62 (.05)	0.66 (.04)	0.74 (.03)	0.79 (.04)	0.89 (.03)	0.93 (.03)	0.96 (.03)
2: $TC/TFISHT/(\overline{PST+SST})^{+}$		0.69 (.03)	0.72 (.04)	0.77 (.03)	0.79 (.02)	0.84 (.02)	0.88 (.03)	0.92 (.02)	0.94 (.02)	0.95 (.02)
3: $TC/TFISHT/\overline{PST}/\overline{CST}$		0.24 (.11)	0.24 (.12)	0.34 (.12)	0.38 (.12)	0.45 (.14)	0.44 (.10)	0.70 (.12)	0.74 (.12)	0.87 (.12)
4: $TC/TFISHT/(\overline{PST+SST})/\overline{CST}^{+}$		0.33 (.10)	0.32 (.11)	0.43 (.12)	0.47 (.11)	0.51 (.12)	0.50 (.10)	0.73 (.12)	0.76 (.11)	0.86 (.12)
5: $TC/TFISHT/TAST^{++}$		0.45 (.04)	0.45 (.05)	0.53 (.05)	0.55 (.05)	0.61 (.05)	0.65 (.05)	0.76 (.05)	0.80 (.05)	0.94 (.05)
E.1: $[TNC^{+}]^{-1}$	*	0.90 (.07)	0.96 (.07)	0.91 (.07)	0.84 (.06)	0.90 (.06)	0.96 (.06)	0.88 (.06)	0.94 (.06)	1.05 (.06)
2: TH/TNC^{+}		0.38 (.06)	0.38 (.06)	0.43 (.06)	0.44 (.07)	0.54 (.07)	0.56 (.07)	0.69 (.07)	0.73 (.07)	0.98 (.08)
F.1: $\overline{C/H}^{+++}$		0.86 (.01)	0.87 (.01)	0.91 (.01)	0.91 (.01)	0.95 (.01)	0.96 (.01)	0.98 (.01)	0.98 (.01)	1.00 (.01)
2: $[\overline{FISHT}^{+++}]^{-1}$	*	0.80 (.01)	0.81 (.01)	0.85 (.01)	0.85 (.01)	0.89 (.01)	0.90 (.01)	0.94 (.01)	0.95 (.01)	0.97 (.01)
3: $[\overline{TOWT}^{++}]^{-1}$	*	0.87 (.01)	0.87 (.01)	0.90 (.01)	0.90 (.01)	0.93 (.01)	0.94 (.01)	0.96 (.01)	0.97 (.01)	0.98 (.01)
4: $[\overline{TBH}^{++}]^{-1}$	*	0.88 (.01)	0.89 (.01)	0.92 (.01)	0.92 (.01)	0.94 (.01)	0.95 (.01)	0.97 (.01)	0.98 (.01)	0.98 (.01)

Table 9: Efficiency of abundance indices in detecting changes in krill biomass:

blank : 100 simulations detect no change significant at 5% level
+ / _ : direction of change if difference significant at 5% level detected
* : index (or its inverse) drops by > 20%
* * : index (or its inverse) drops by > 45% (within 95% limits)

This table corresponds to Table 5a for the "One elongated (f=8) swarm per haul" case, except that concentration searching efficiency has been increased 7.5 times.

INDEX	$N_c \times 0.5$	$N_c \times 0.5$ + P.S.	$L_c \times 1/\sqrt{2}$	$D_c \times 0.5$	$r \times 1/\sqrt{2}$	$\delta \times 0.5$
A.1: TC^{+++}	-*			-	+	-**
2: TH^{+++}	-*			-	+	-*
B.1: TFISHT^{+++}	-*			-	-	
2: TPST	-*			+*	+*	+
3: $\mathrm{TPST} + \mathrm{TSST}^{+}$	-*			+*	+*	-
4: TCST^{+}	+**					+*
5: TAST^{++}	+*			+		+
C.1: $\mathrm{TC/TFISHT}^{+++}$					+	-**
2: $\overline{\mathrm{C/FISHT}}^{+++}$					+	-*
3: TC/TPST				-**	-*	-**
4: $\overline{\mathrm{C/PST}}$				-*	-*	-*
5: $\mathrm{TC/(TPST+TSST)}^{+}$				-*	-*	-*
6: $\mathrm{TC/TCST}^{+}$	-**			*	*	-**
D.1: $\mathrm{TC/TFISHT/}\overline{\mathrm{PST}}$				-**	-*	-**
2: $\mathrm{TC/TFISHT/(}\overline{\mathrm{PST+SST}}\mathrm{)}^{+}$				-*	-	-**
3: $\mathrm{TC/TFISHT/}\overline{\mathrm{PST}}\mathrm{/}\overline{\mathrm{CST}}$	-**			-**	-	-**
4: $\mathrm{TC/TFISHT/(}\overline{\mathrm{PST+SST}}\mathrm{)/}\overline{\mathrm{CST}}^{+}$	-**			-*		-**
5: $\mathrm{TC/TFISHT/TAST}^{++}$	-*			-	+	-**
E.1: TNC^{+}	-*			+	-	+*
2: $\mathrm{TH/TNC}^{+}$				-*	+	-**
F.1: $\overline{\mathrm{C/H}}^{+++}$					+	-
2: $\overline{\mathrm{FISHT}}^{+++}$	-			+	-	+*
3: $\overline{\mathrm{TOWT}}^{++}$		-		+	-	+*
4: $\overline{\mathrm{TBH}}^{++}$		-		+		+*

Table 10: A consolidated version of Table 4 for the six abundance indices selected for detailed comparison in section 3.6. Only the point estimates of the percentage difference from the estimated base case mean are given for the six alternative krill distribution scenarios (each corresponding to a 50% overall biomass drop). The first figure shown corresponds to the "One elongated (f=8) swarm per haul" and the second figure to the "More than one swarm per haul" model modification.

INDEX	$N_c \times 0.5$	$N_c \times 0.5$ + P.S.	$L_c \times 1/\sqrt{2}$	$D_c \times 0.5$	$r \times 1/\sqrt{2}$	$\delta \times 0.5$
A.1: TC^{+++}	-40; -41	+ 1; +25	-16; -10	-17; -62	+ 9; -51	-60; -64
C.1: $TC/TFISHT^{+++}$	- 8; + 0	- 2; - 0	- 4; + 0	- 0; -35	+15; -26	-42; -38
3: TC/TPST	- 1; + 3	+ 5; + 3	+ 1; + 5	-43; -51	-33; -30	-45; -36
D.1: TC/TFISHT/PST	- 6; + 3	+ 4; + 2	- 1; + 4	-42; -63	-24; -44	-62; -55
2: $TC/TFISHT/(PST+SST)^{+}$	- 3; - 0	+ 1; - 2	- 2; - 2	-30; -42	-11; -26	-52; -34
3: TC/TFISHT/PST/CST	-57; -45	+ 3; +85	-17; -11	-49; -76	- 8; -62	-77; -72

Table 11: Estimates of the percentage decrease in abundance indices incorporation PST for a 50% overall krill biomass drop are compared with and without random error (see text - section 3.6) in the allocation of within concentration search time between PST and SST. The comparisons are shown for the biomass drop due to falls in each of D_c, r and δ, and are for the "One elongated (f=8) swarm per haul" case.

	$D_c \times 0.5$		$r \times 1/\sqrt{2}$		$\delta \times 0.5$	
INDEX	No error	Error	No error	Error	No error	Error
B.2: TPST	+44	+32	+63	+55	-27	-27
3: TPST+TSST$^+$	+18	+ 5	+39	+32	-44	-43
|Difference|	26	27	24	23	17	16
C.3: TC/TPST	-43	-44	-33	-32	-45	-44
5: TC/(TPST+TSST)$^+$	-31	-31	-22	-21	-29	-29
|Difference|	12	13	11	11	16	15
D.1: TC/TFISHT/$\overline{\text{PST}}$	-42	-47	-24	-23	-62	-61
2: C/TFISHT/($\overline{\text{PST+SST}}$)$^+$	-30	-34	-11	-11	-52	-51
|Difference|	12	13	13	12	10	10
D.3: TC/TFISHT/$\overline{\text{PST}}$/$\overline{\text{CST}}$	-49	-61	- 8	-10	-77	-76
4: TC/TFISHT/($\overline{\text{PST+SST}}$)/$\overline{\text{CST}}^+$	-39	-51	+ 5	+ 4	-71	-69
|Difference|	10	10	13	14	6	7

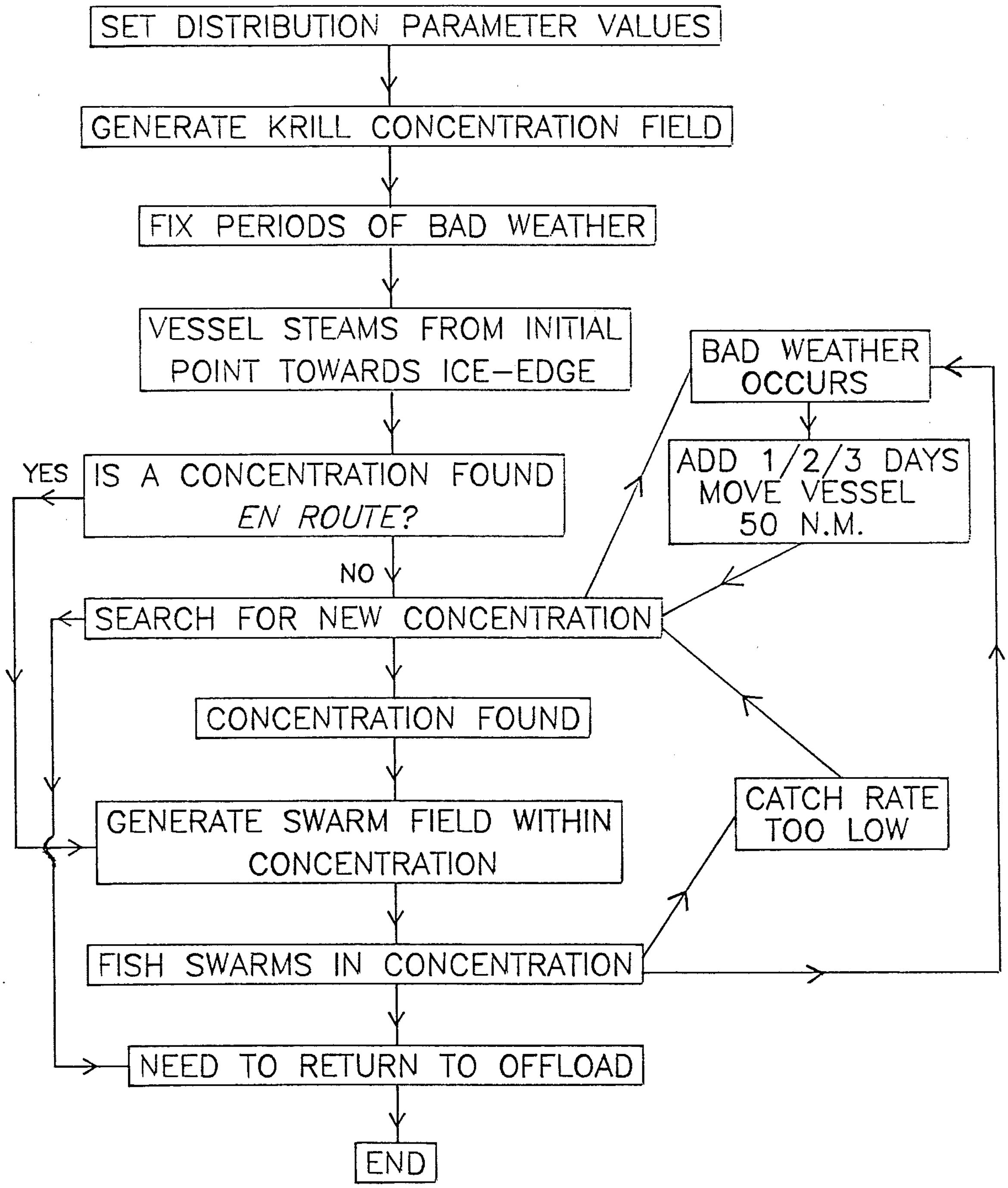

Figure 1: A flow diagram of the basic structure of the simulation model.

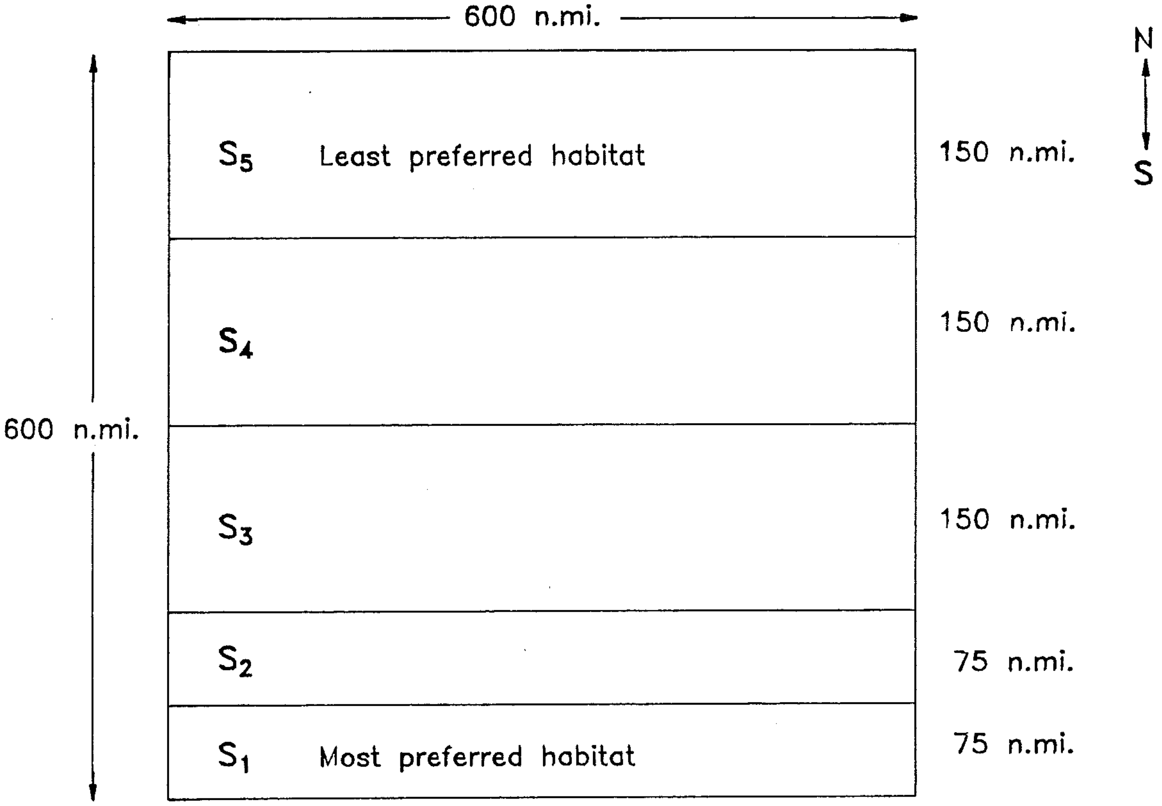

Figure 2: The stratified habitat chosen for the krill distribution model in a 600 n mile square sector of the Southern Ocean.

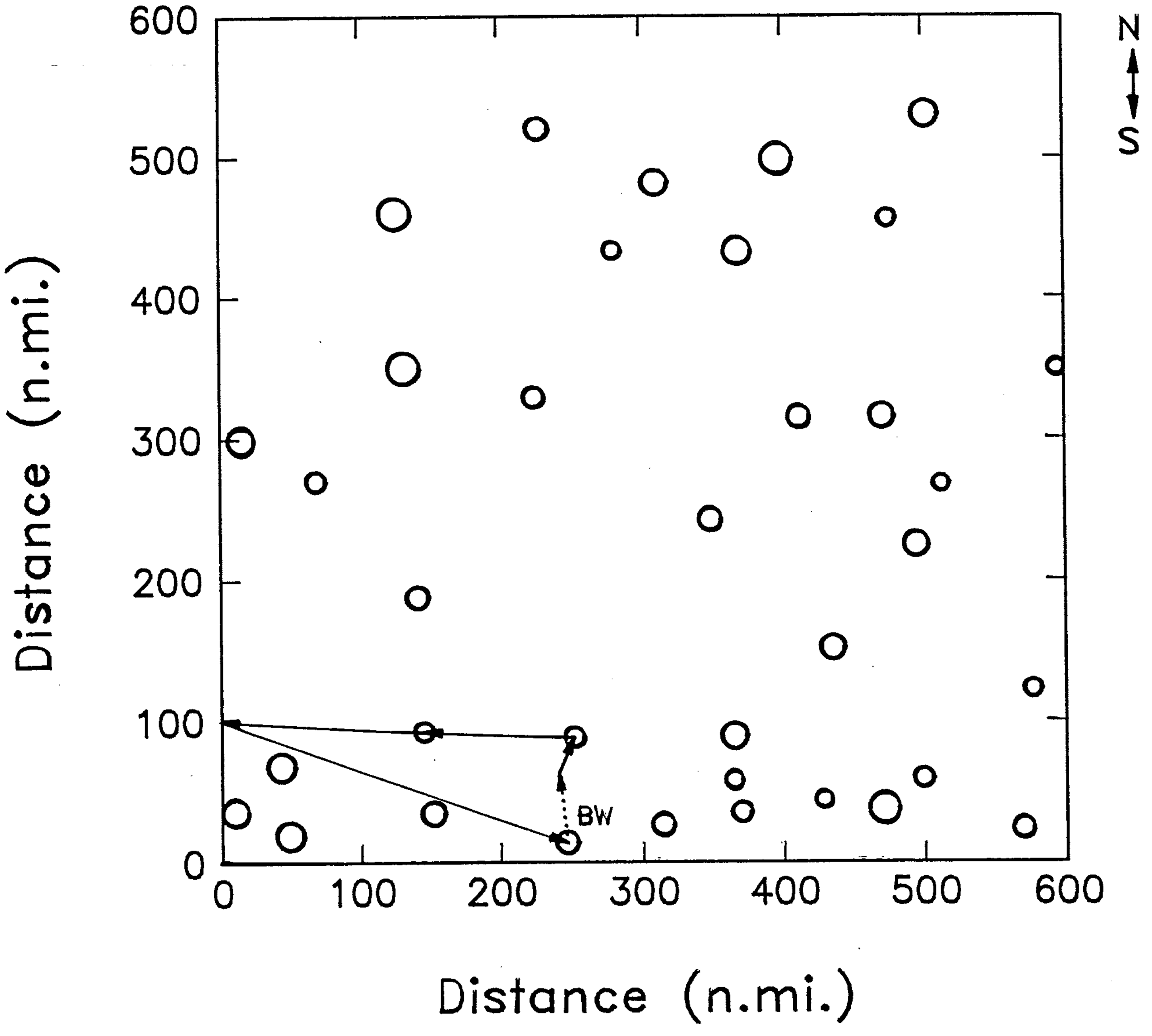

Figure 3: An example of the distribution of krill concentrations in the 600 n mile square Southern Ocean sector chosen, which has been generated as described in section 2.3. The radii of the concentrations are to scale. The arrowed lines indicate the concentrations fished sequentially during a half-month period. The dotted line represents movement during a period of bad weather (see section 2.4).

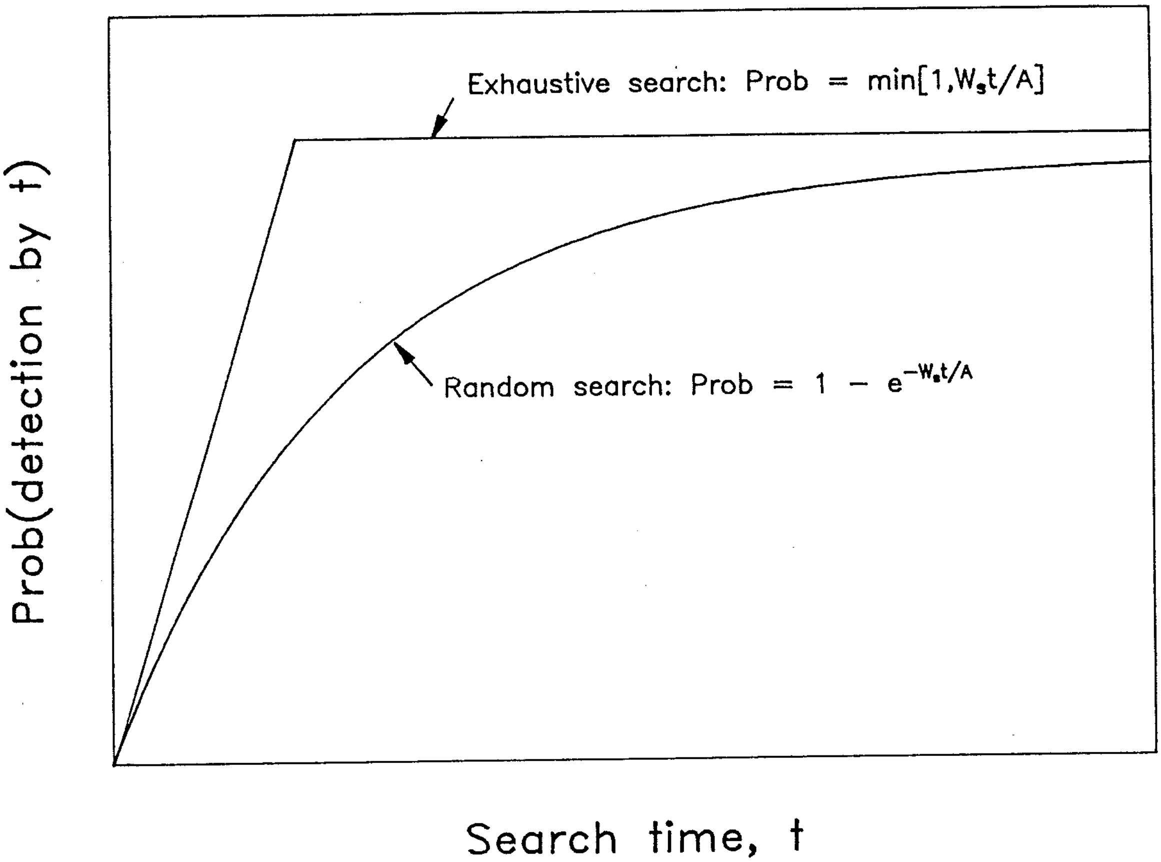

Figure 4: Detection probability as a function of time for the exhaustive search and random search models.

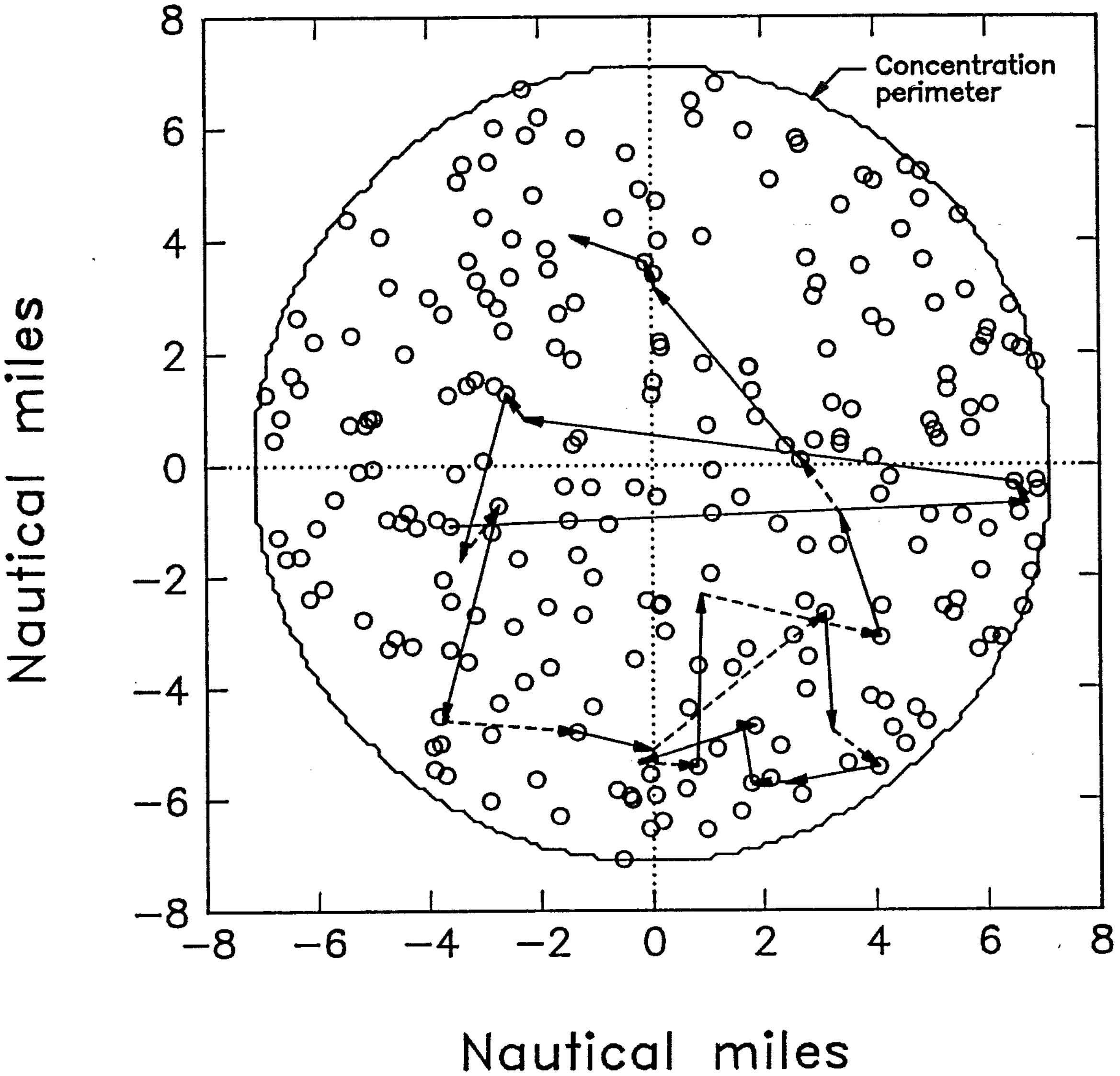

Figure 5: An example of the distribution of fishable swarms in a concentration, generated as described in section 2.7. The radii of the swarms are NOT to scale. This example corresponds to the "One elongated (f=8) swarm per haul" model modification, with the symbol for each fishable swarm placed at the centre point chosen for that swarm prior to elongation. The arrowed lines reflect the sequential towing of swarms in the concentration by a fishing vessel. Note that only the initial swarms are towed, even though these lines may intersect the symbols for other swarms. The full lines represent the length and direction of each haul (to scale), while the dashed lines indicate net movement in searching for the following swarm to tow.

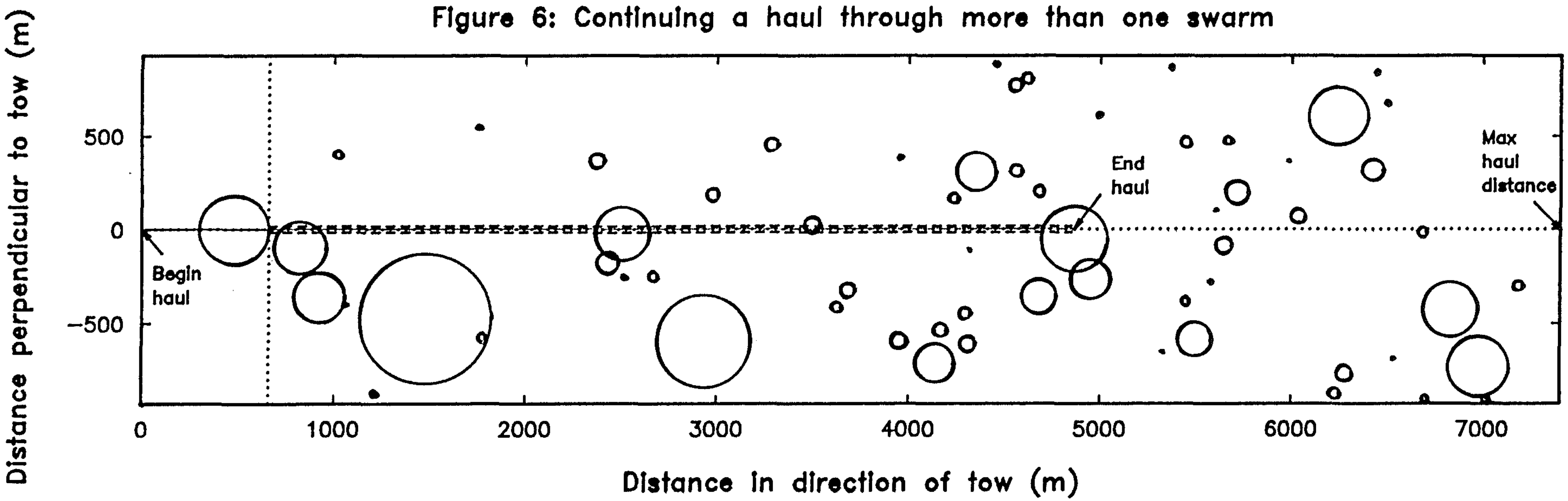

Figure 6: An example of a single haul for the model modification where more than one swarm may be towed per haul (see sections 2.8 and 3.3). The swarms shown are to scale. While the initial swarm towed is a "fishable" swarm in terms of criterion (20), all swarms in the area to the right of this original swarm are shown. The dashed lines to the right of the initial swarm define the "sonar band"; swarms intersecting this band are also fished until the haul is ended because (in this example) the Captain estimates the catch has reached 10 tonnes.

Figure 7: Plots of abundance indices as a function of α (the proportion of the base case level to which the krill biomass has been reduced), where biomass reduction occurs as a result of a random combination of decreases in the distribution parameters N_C, L_C, D_C, r and δ. The abundance indices have been normalised to their estimated base case mean levels. The error bars shown represent estimates of the central 68% of the distribution of the index in question for a vessel-half-month, while the symbol is the estimate of the distribution mean, for each particular value of α. A formula is shown for the curve fitted to the relationship between the index and *a* by the method described in section 3.5. Plots a) and b) are for the "One elongated (f=8) swarm per haul" and "More than one swarm per haul" model modifications respectively, and correspond to the indices :

(i) TC
(ii) TC/TFISHT
(iii) TC/TPST
(iv) TC/TFISHT/$\overline{\text{PST+SST}}$
(v) TC/TFISHT/($\overline{\text{PST+SST}}$)
(vi) TC/TFISHT/$\overline{\text{PST/CST}}$

Figure 7 i) a)

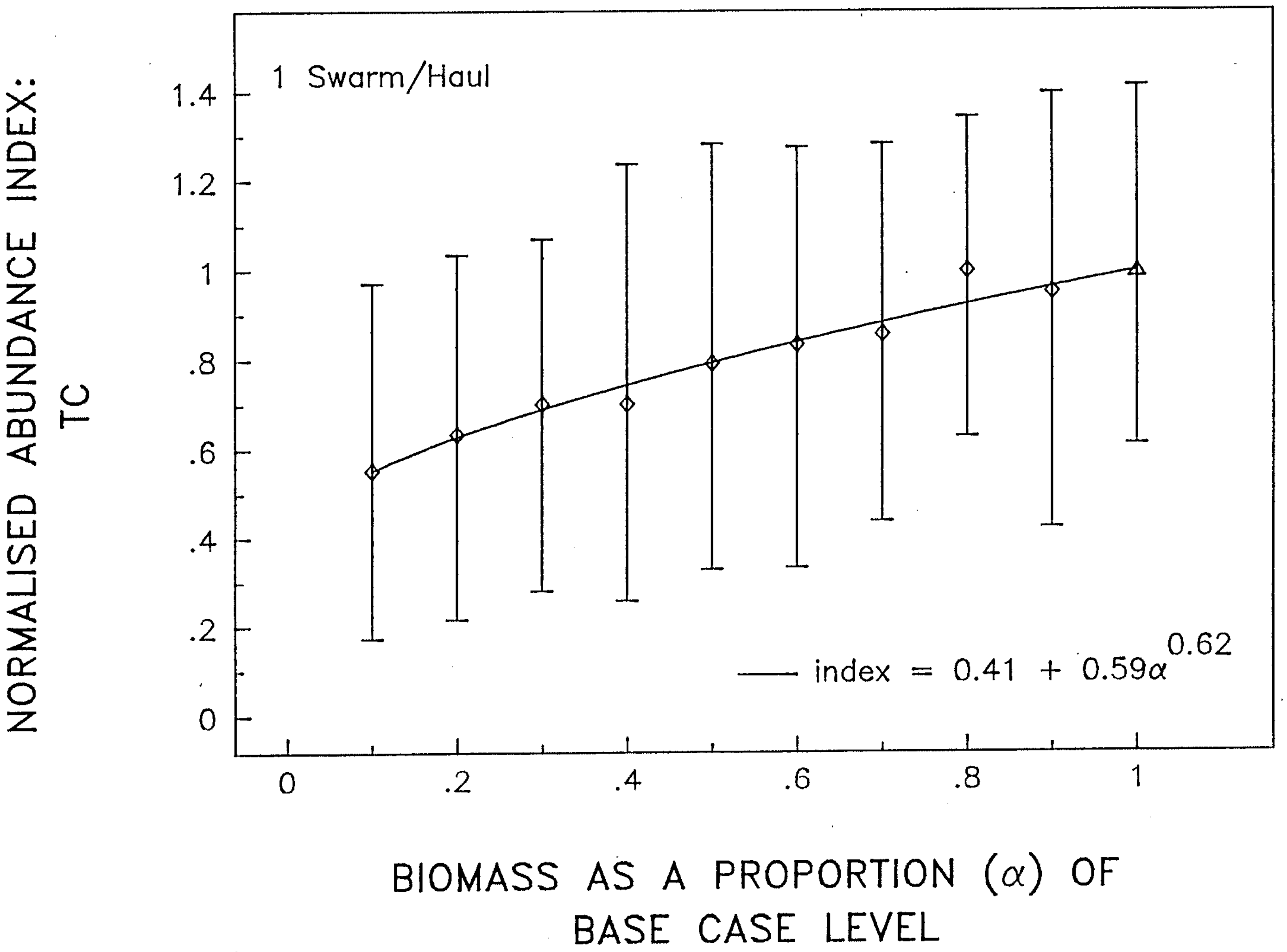
1 Swarm/Haul
NORMALISED ABUNDANCE INDEX: TC
1.4
1.2
1
.8
.6
.4
.2
0
0
.2
.4
.6
.8
1
— index = 0.41 + 0.59α^0.62
BIOMASS AS A PROPORTION (α) OF BASE CASE LEVEL

Figure 7 i) b)

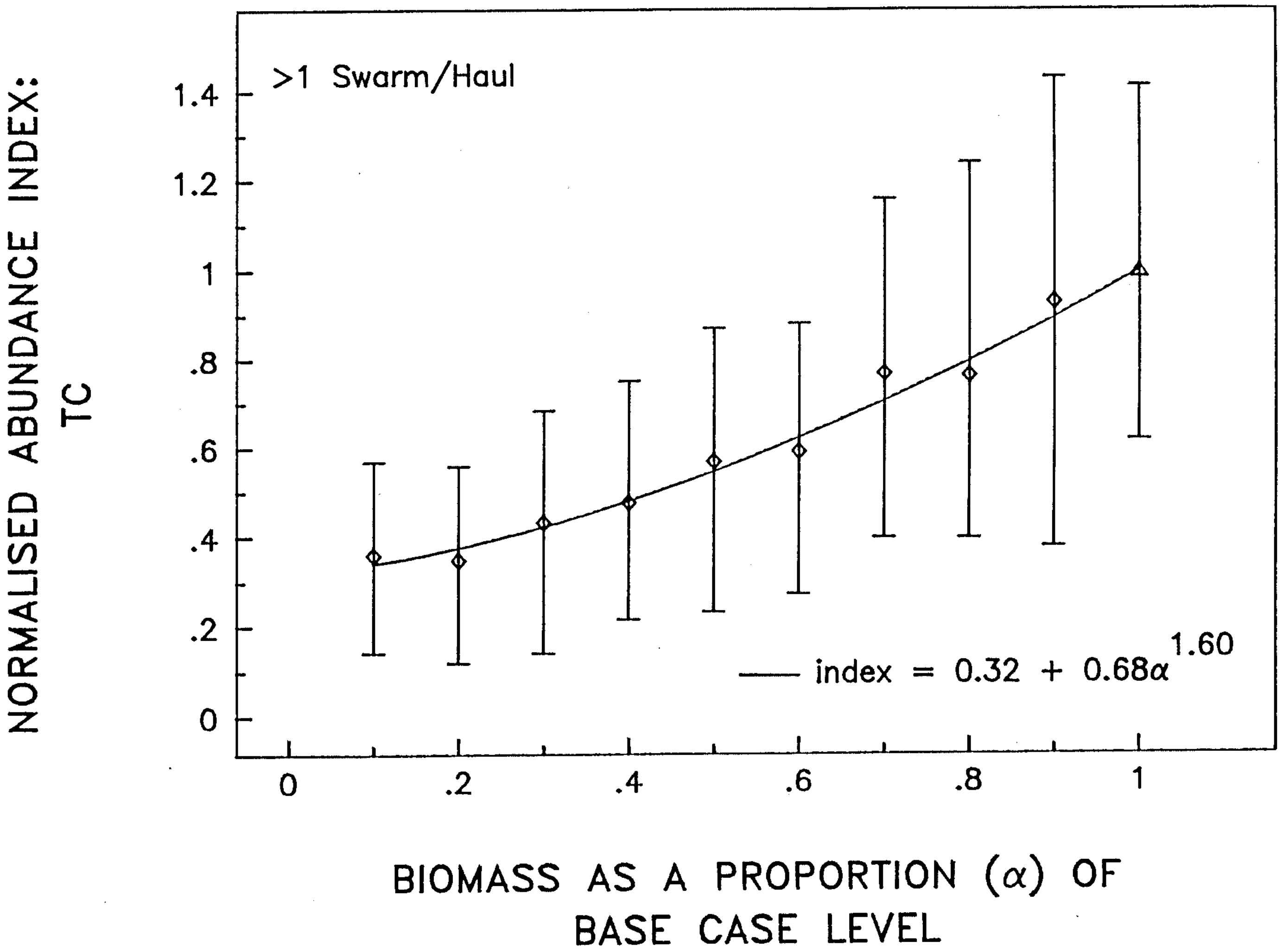
>1 Swarm/Haul
NORMALISED ABUNDANCE INDEX: TC
1.4
1.2
1
.8
.6
.4
.2
0
0
.2
.4
.6
.8
1
index = 0.32 + 0.68α^1.60
BIOMASS AS A PROPORTION (α) OF BASE CASE LEVEL

Figure 7 ii) a)

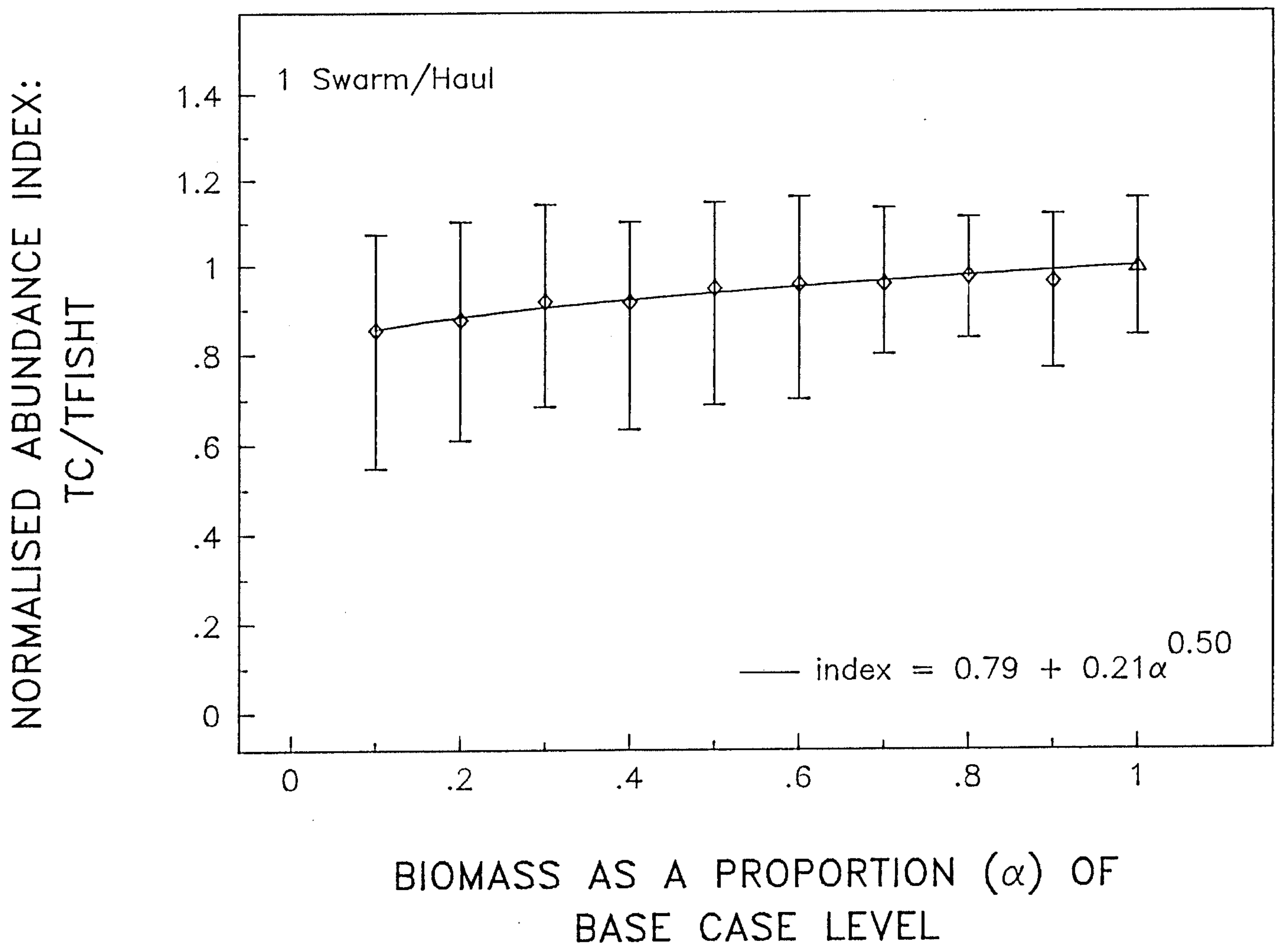
1 Swarm/Haul
1.4
1.2
1
.8
.6
.4
.2
0
0
.2
.4
.6
.8
1
index = 0.79 + 0.21α^0.50
NORMALISED ABUNDANCE INDEX:
TC/TFISHT
BIOMASS AS A PROPORTION (α) OF
BASE CASE LEVEL

Figure 7 ii) b)

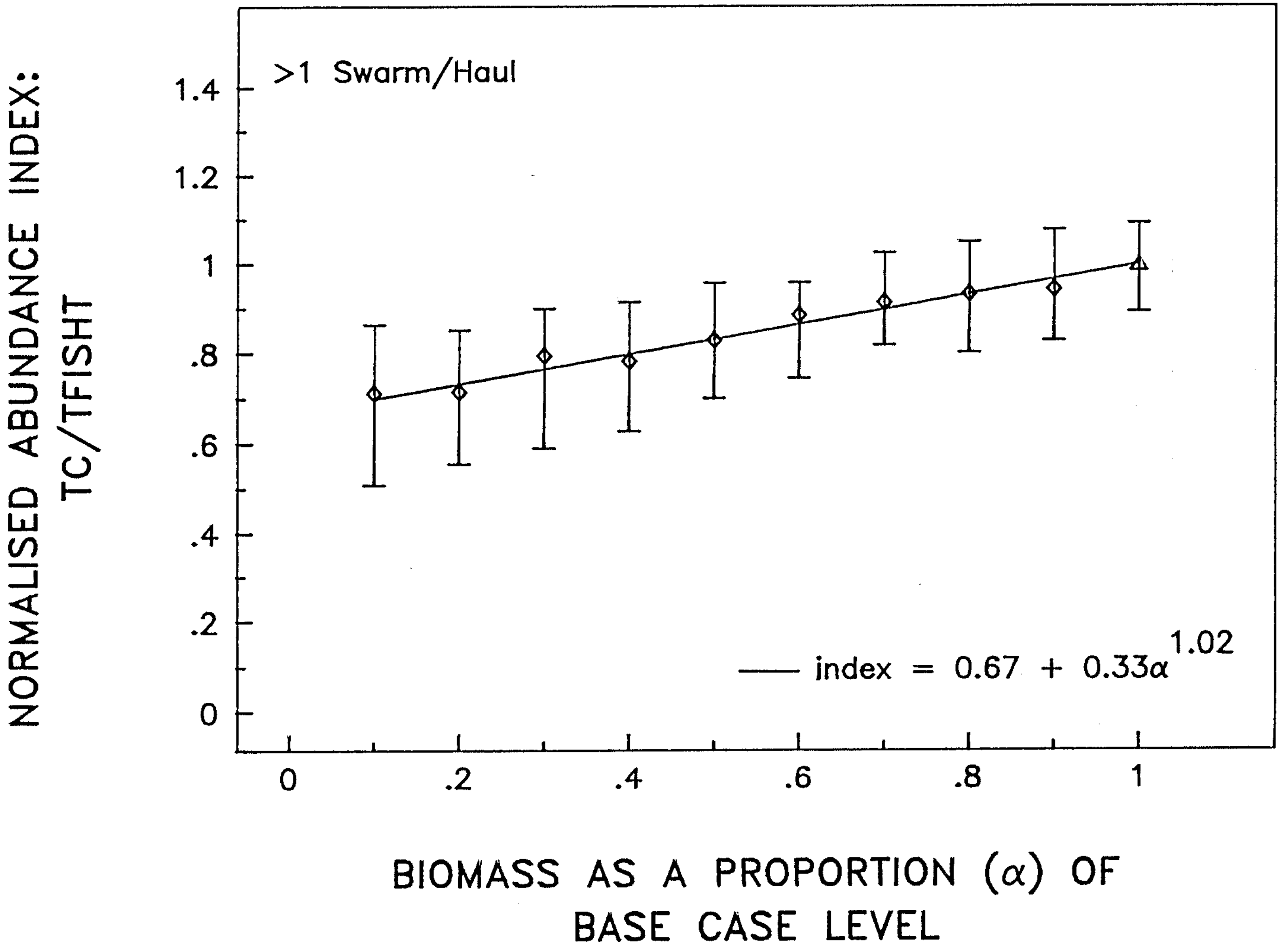
NORMALISED ABUNDANCE INDEX:
TC/TFISHT
>1 Swarm/Haul
1.4
1.2
1
.8
.6
.4
.2
0
0
.2
.4
.6
.8
1
index = 0.67 + 0.33α^1.02
BIOMASS AS A PROPORTION (α) OF
BASE CASE LEVEL

Figure 7 iii) a)

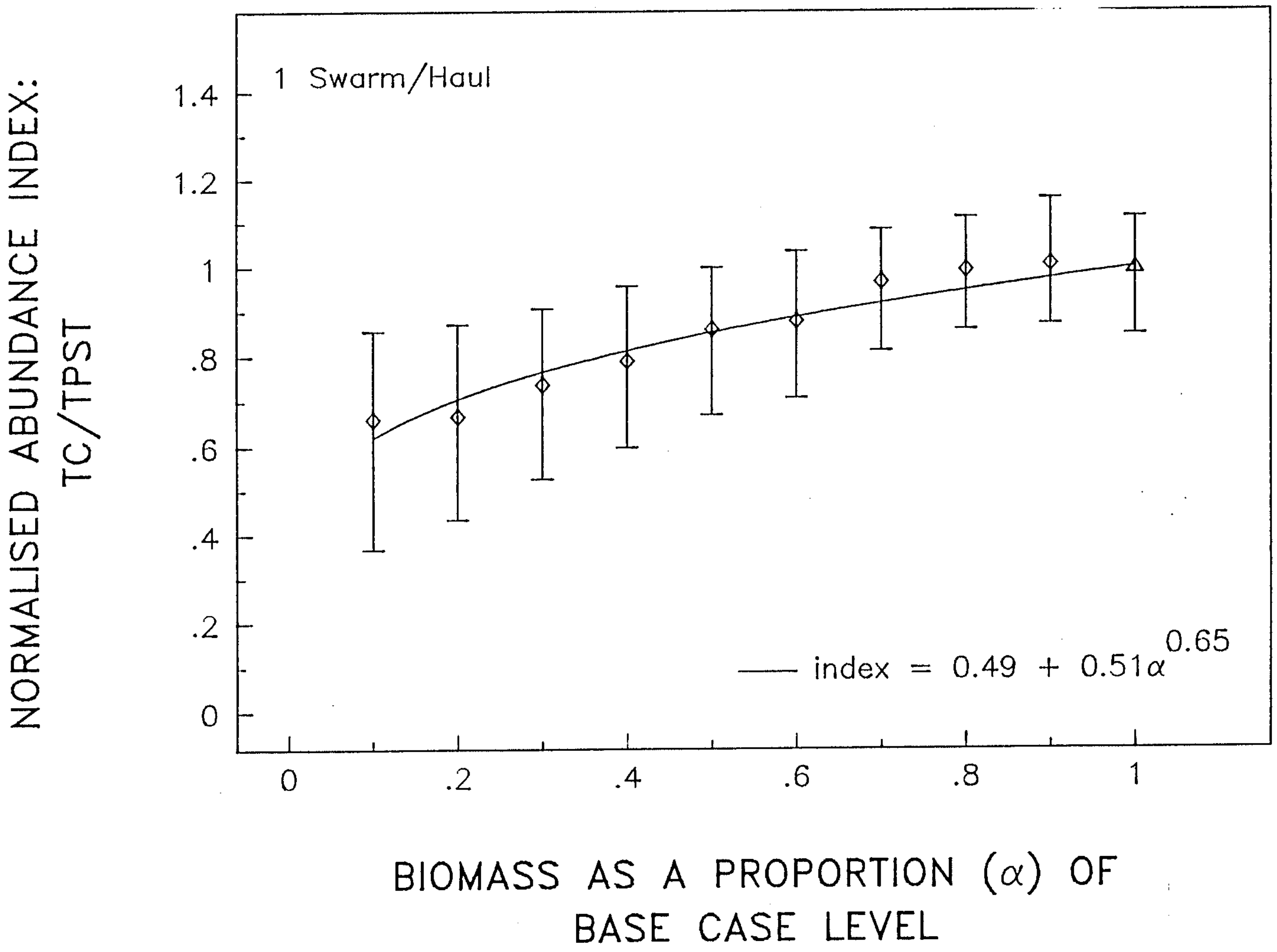

Figure 7 iii) b)

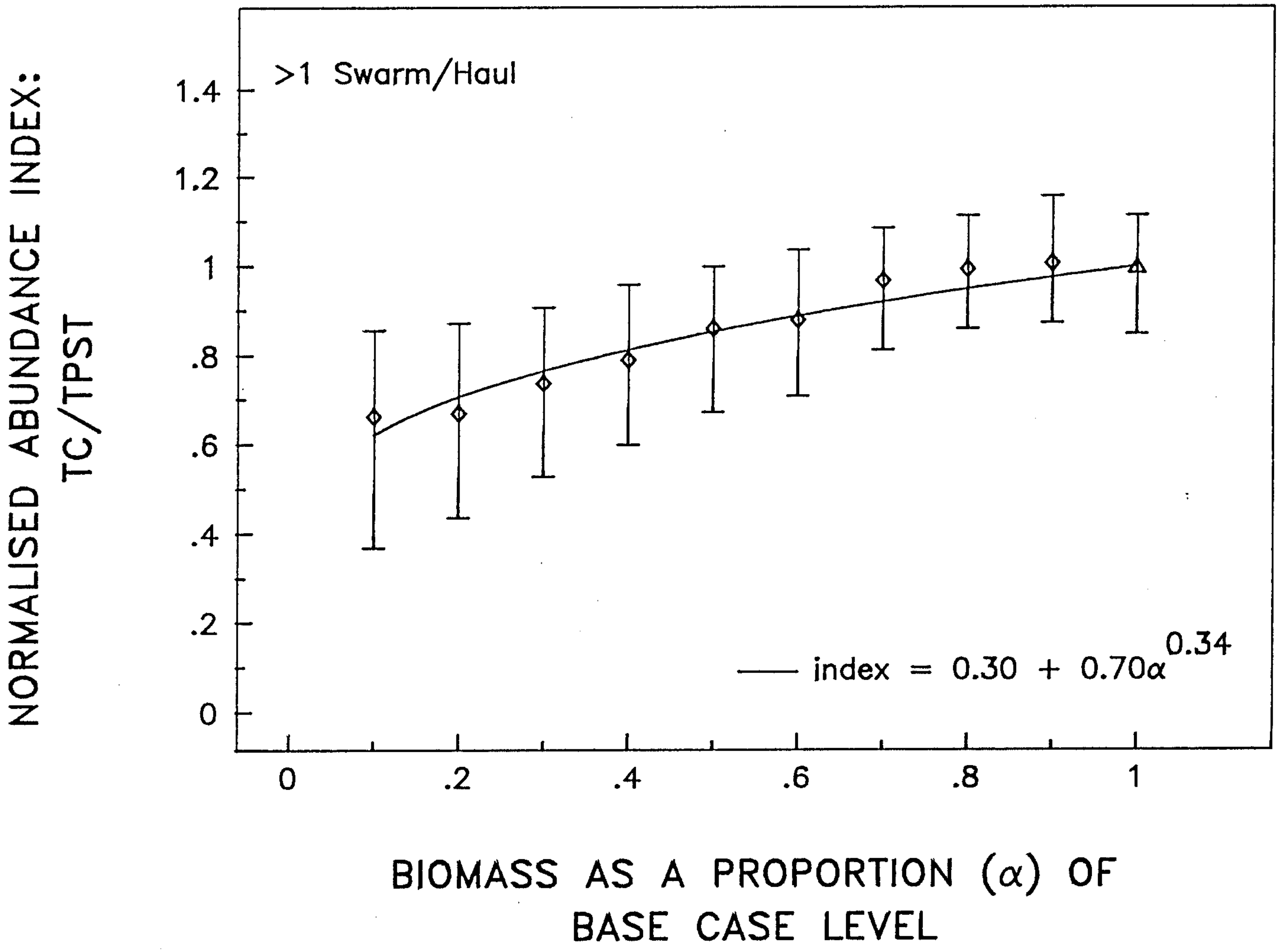

Figure 7 iv) a)

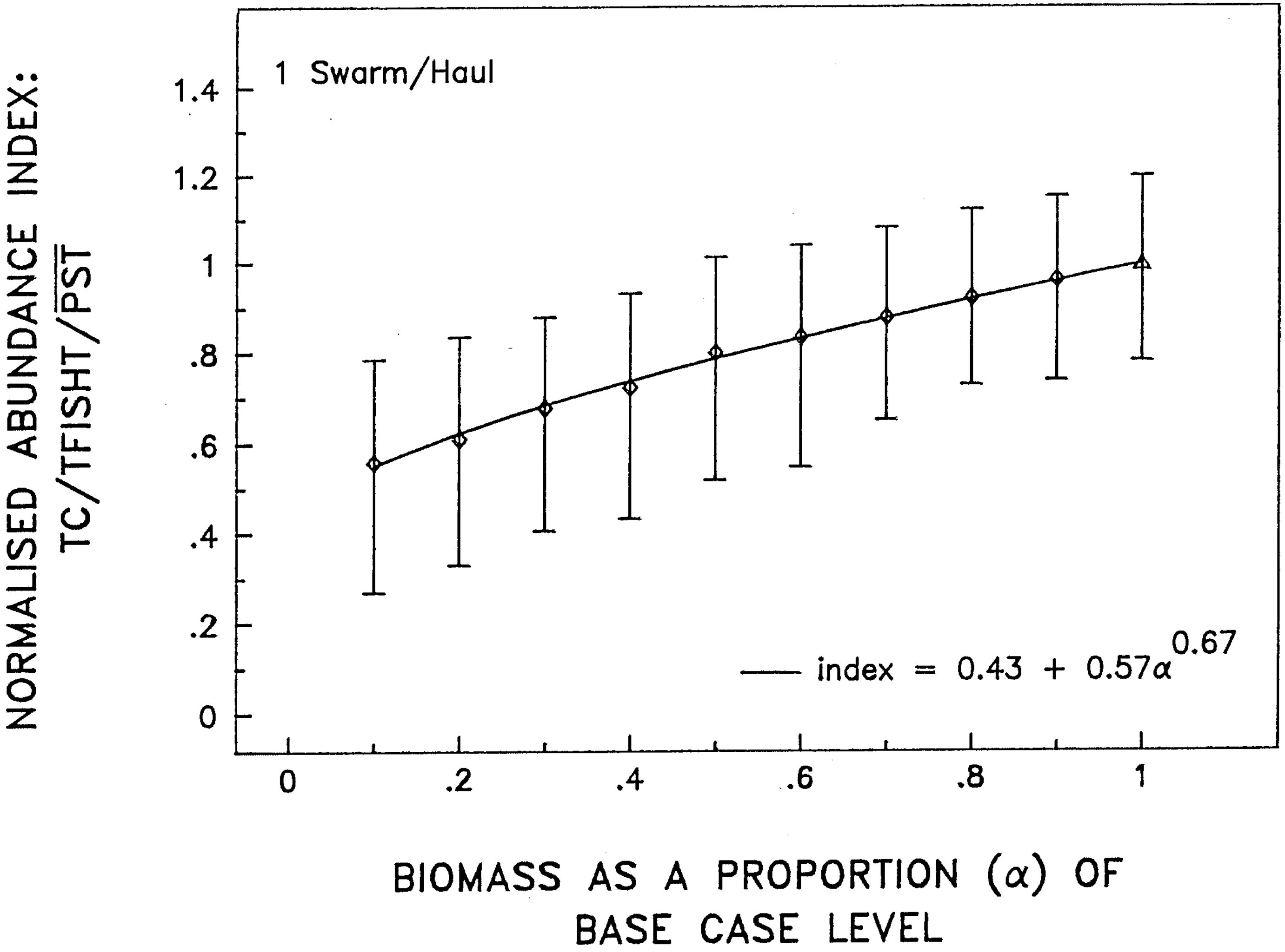
1 Swarm/Haul
NORMALISED ABUNDANCE INDEX:
TC/TFISHT/$\overline{PST}$
1.4
1.2
1
.8
.6
.4
.2
0
index = 0.43 + 0.57$\alpha^{0.67}$
0
.2
.4
.6
.8
1
BIOMASS AS A PROPORTION (α) OF
BASE CASE LEVEL

Figure 7 iv) b)

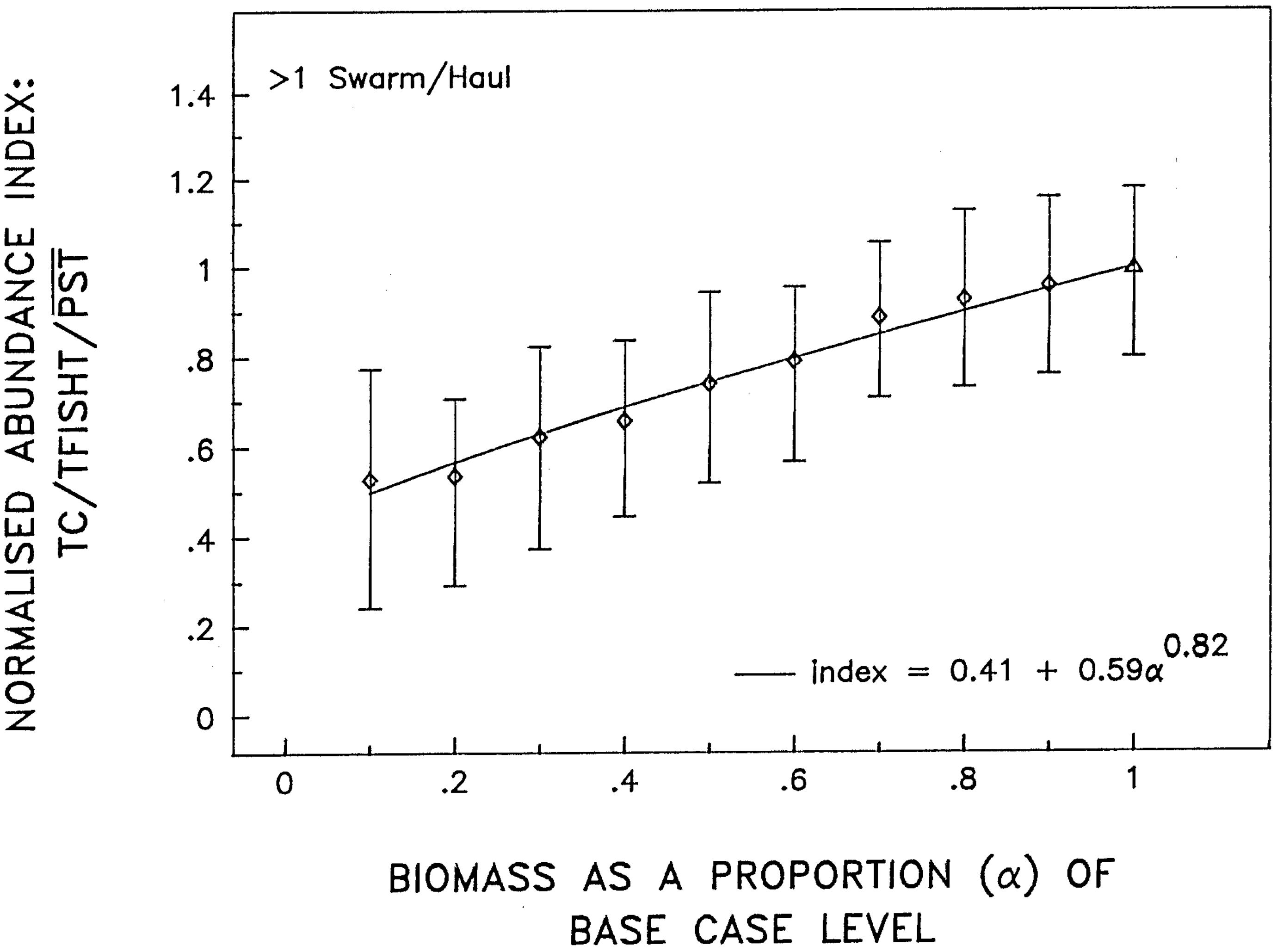
>1 Swarm/Haul
NORMALISED ABUNDANCE INDEX: TC/TFISHT/$\overline{PST}$
1.4
1.2
1
.8
.6
.4
.2
0
index = 0.41 + 0.59α^0.82
0
.2
.4
.6
.8
1
BIOMASS AS A PROPORTION (α) OF BASE CASE LEVEL

Figure 7 v) a)

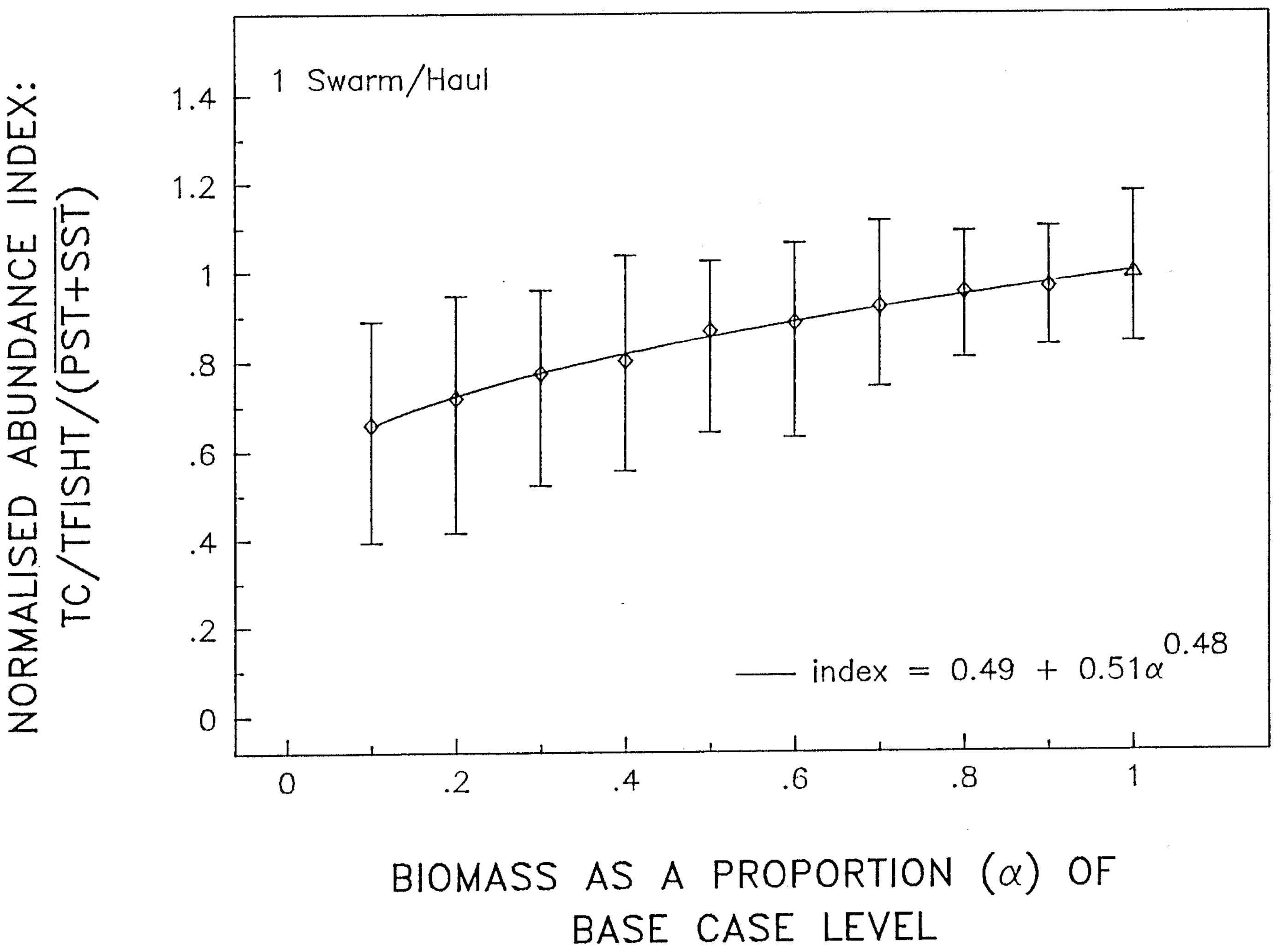
1 Swarm/Haul
NORMALISED ABUNDANCE INDEX:
TC/TFISHT/$\overline{(PST+SST)}$
1.4
1.2
1
.8
.6
.4
.2
0
0
.2
.4
.6
.8
1
index = 0.49 + 0.51α^0.48
BIOMASS AS A PROPORTION (α) OF
BASE CASE LEVEL

Figure 7 v) b)

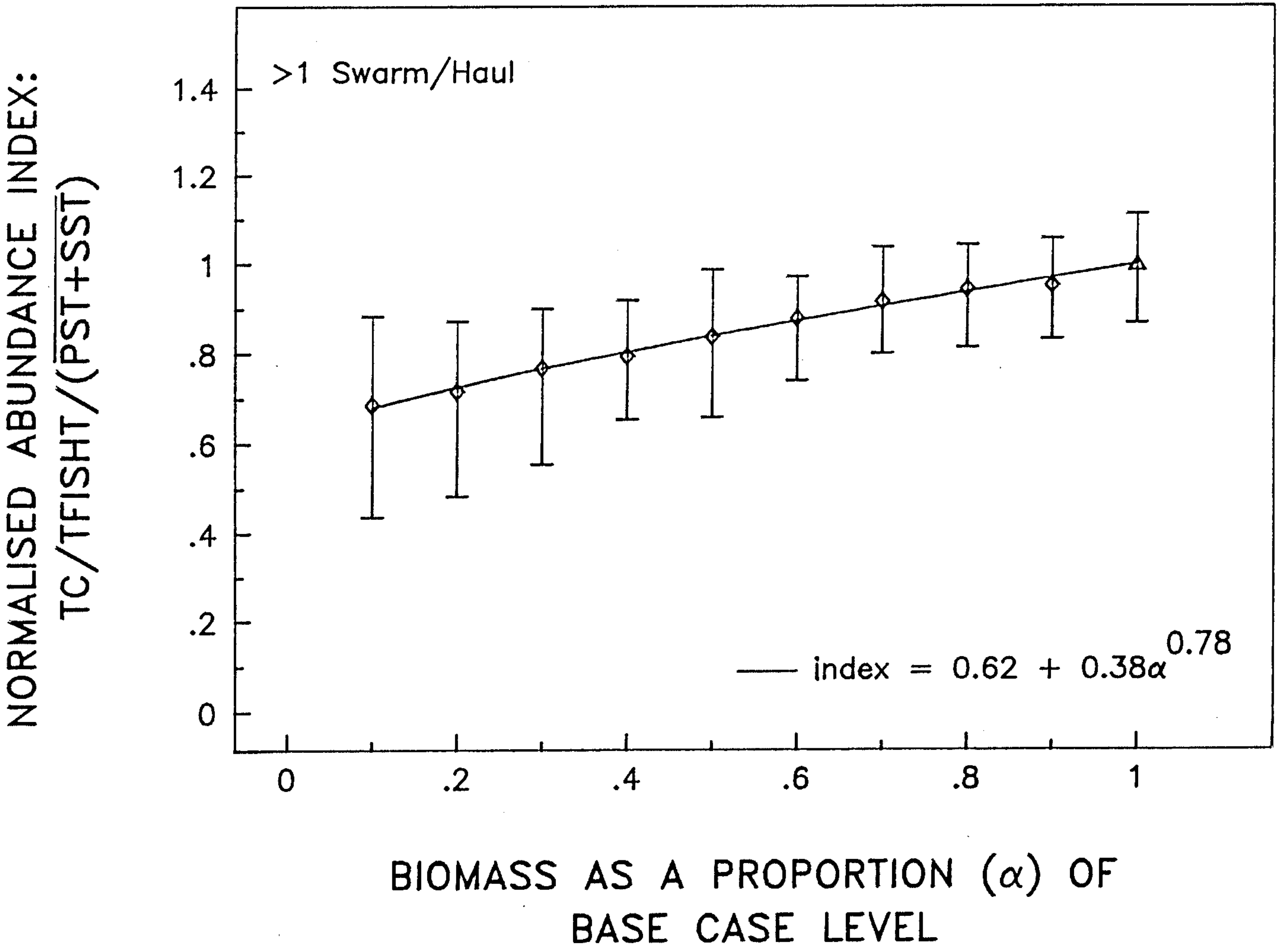
>1 Swarm/Haul
NORMALISED ABUNDANCE INDEX:
TC/TFISHT/(PST+SST)
1.4
1.2
1
.8
.6
.4
.2
0
0
.2
.4
.6
.8
1
index = 0.62 + 0.38α^0.78
BIOMASS AS A PROPORTION (α) OF
BASE CASE LEVEL

Figure 7 vi) a)

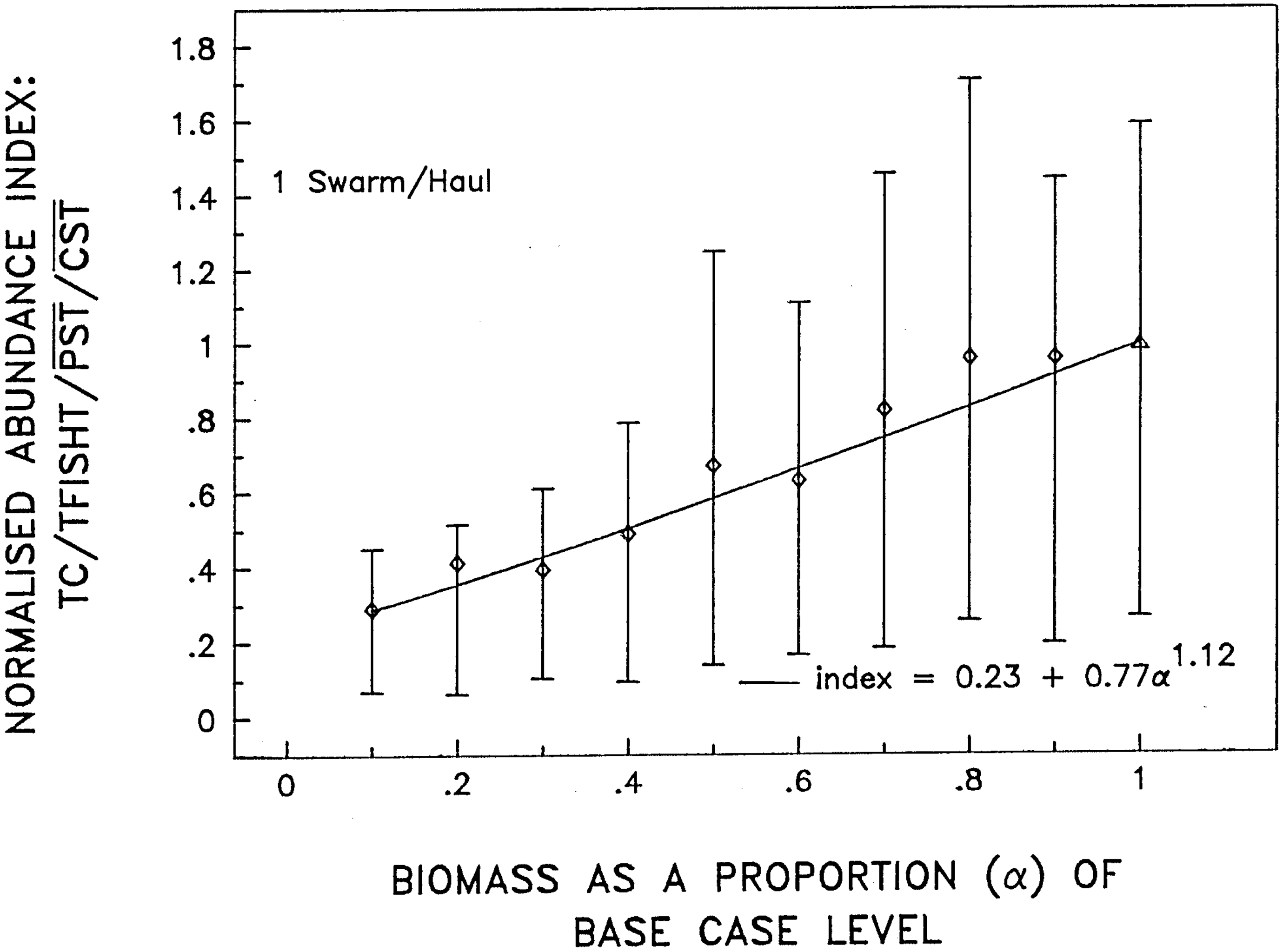
1 Swarm/Haul
index = 0.23 + 0.77α^1.12
NORMALISED ABUNDANCE INDEX:
TC/TFISHT/PST/CST
1.8
1.6
1.4
1.2
1
.8
.6
.4
.2
0
0
.2
.4
.6
.8
1
BIOMASS AS A PROPORTION (α) OF
BASE CASE LEVEL

Figure 7 vi) b)

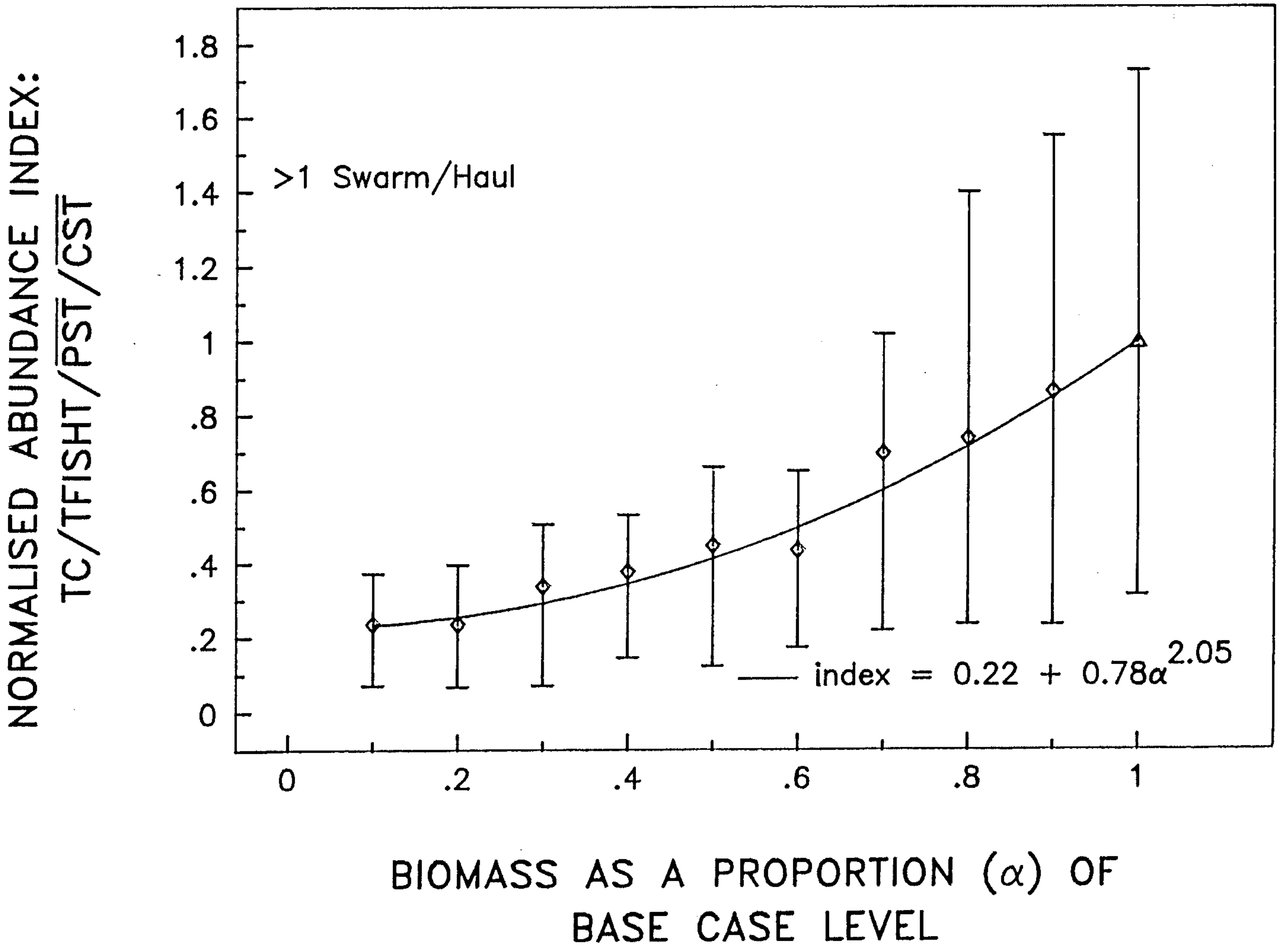
NORMALISED ABUNDANCE INDEX:
TC/TFISHT/$\overline{PST}$/$\overline{CST}$
1.8
1.6
1.4
1.2
1
.8
.6
.4
.2
0
>1 Swarm/Haul
index = 0.22 + 0.78α^2.05
0
.2
.4
.6
.8
1
BIOMASS AS A PROPORTION (α) OF
BASE CASE LEVEL

Figure 8: Plots of (i) total half-monthly catch (TC) and (ii) number of concentrations fished (TNC) against the minimum catch rate per overall elapsed time (CR_{min}) required to be achieved for a vessel not to leave a concentration. The plots are for the base case krill distribution and the "One elongated (f=8) swarm per haul model modification. The error bars indicate one standard deviation.

Figure 8 i) TC *vs* CR$_{min}$

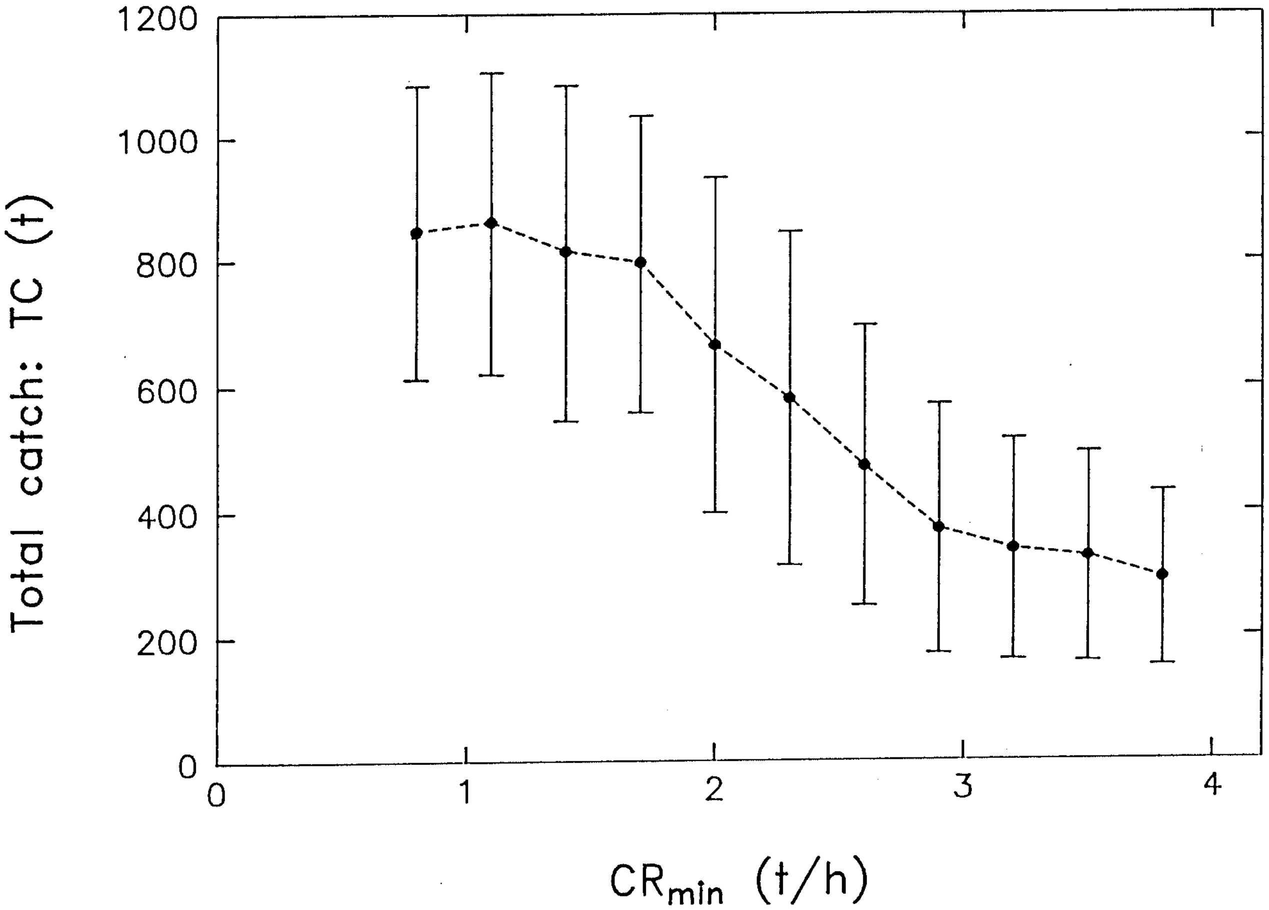

Figure 8 ii) TNC *vs* CR_{min}

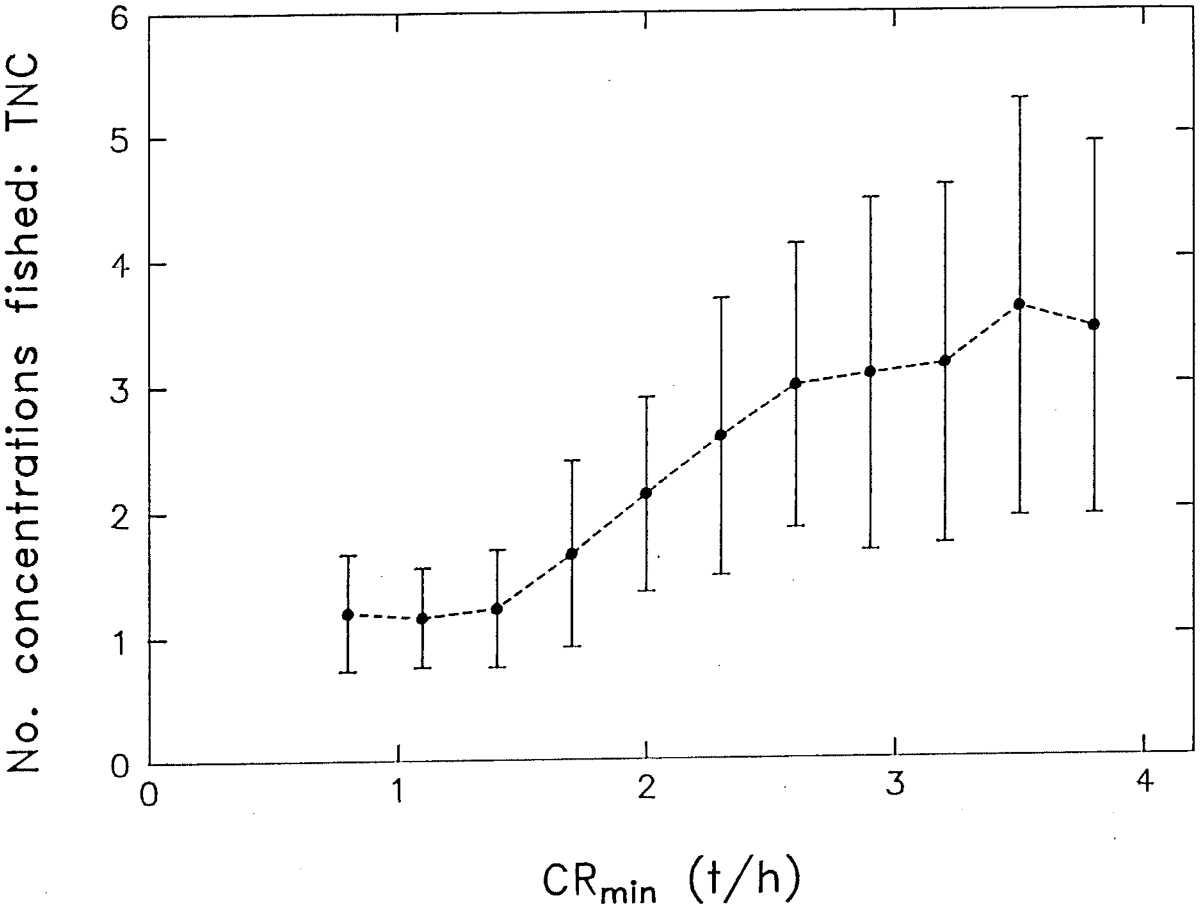

Figure 9: Plots of abundance indices against α as in Figure 7, except that the overall biomass decline is the result of a change in krill swarm surface density δ only. The plots are for the "One elongated (f=8) swarm per haul" model modification, and correspond to the indices :

(i) TC
(ii) TC/TFISHT
(iii) TC/TPST
(iv) TC/(TPST+TSST)
(v) TC/TFISHT/$\overline{\text{PST+SST}}$
(vi) TC/TFISHT/$\overline{\text{PST/CST}}$

Figure 9 i)

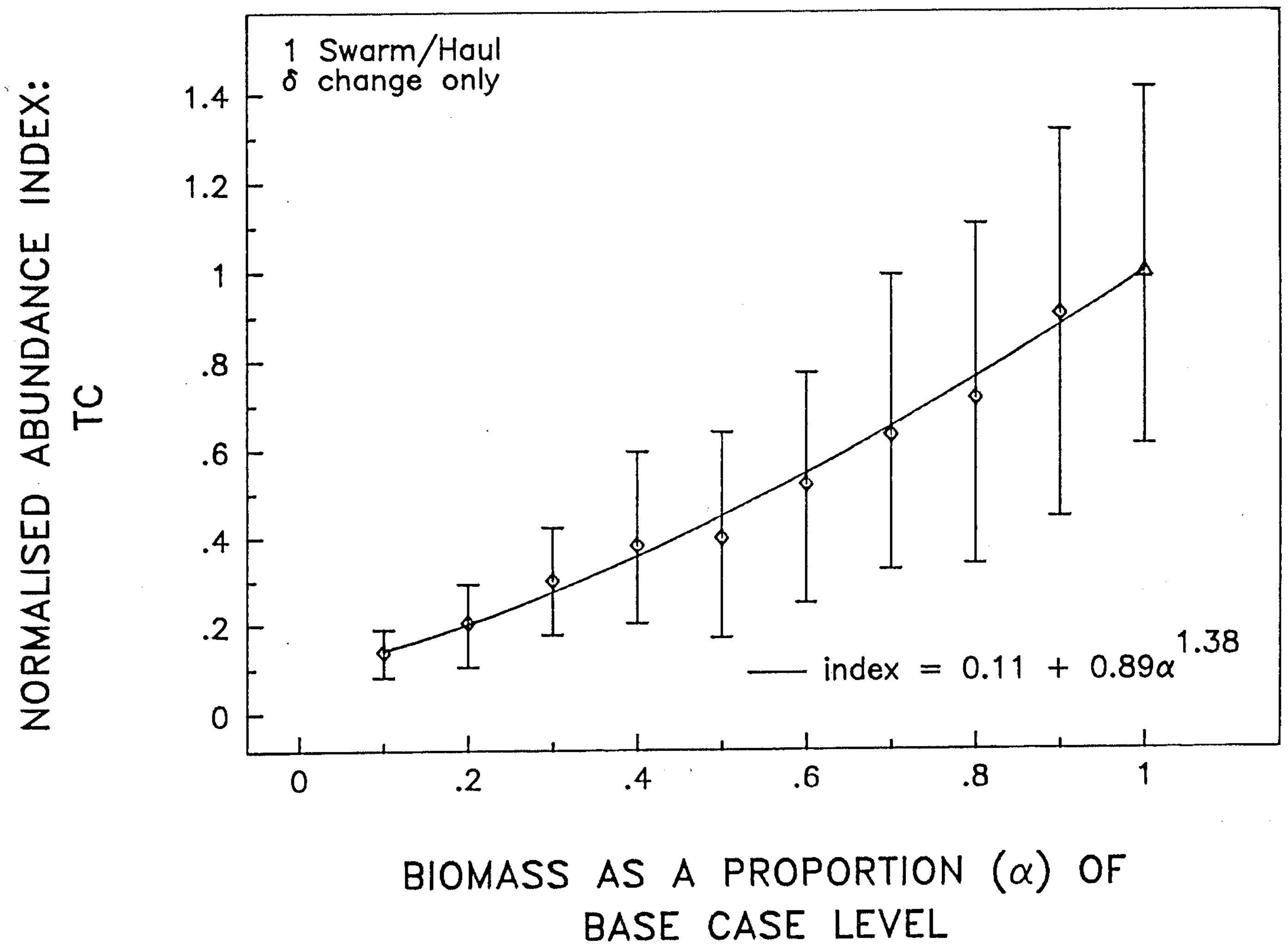
1 Swarm/Haul
δ change only
NORMALISED ABUNDANCE INDEX:
TC
1.4
1.2
1
.8
.6
.4
.2
0
0
.2
.4
.6
.8
1
— index = 0.11 + 0.89α^1.38
BIOMASS AS A PROPORTION (α) OF
BASE CASE LEVEL

Figure 9 ii)

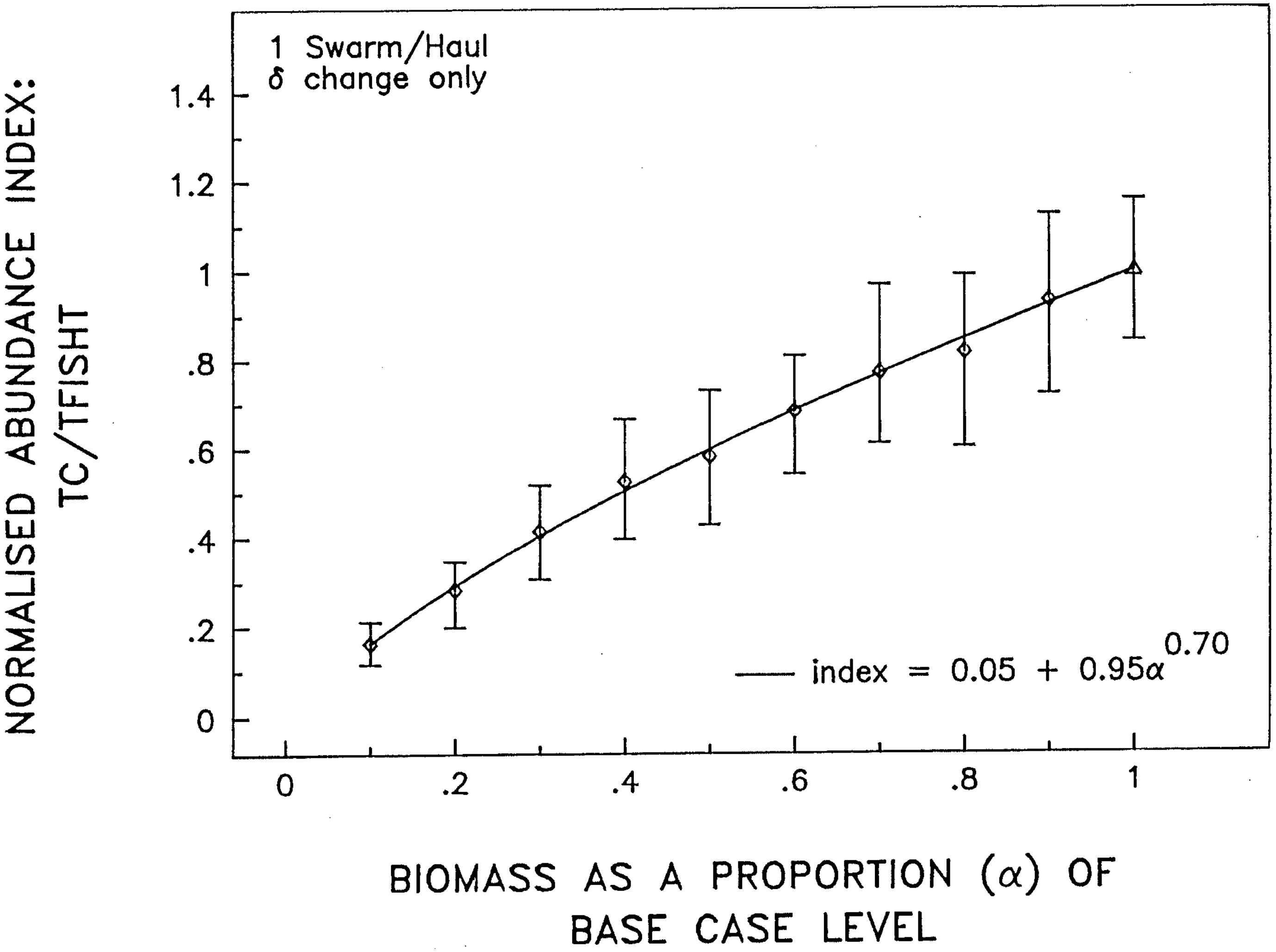
1 Swarm/Haul
δ change only
NORMALISED ABUNDANCE INDEX:
TC/TFISHT
1.4
1.2
1
.8
.6
.4
.2
0
0
.2
.4
.6
.8
1
index = 0.05 + 0.95α^0.70
BIOMASS AS A PROPORTION (α) OF
BASE CASE LEVEL

Figure 9 iii)

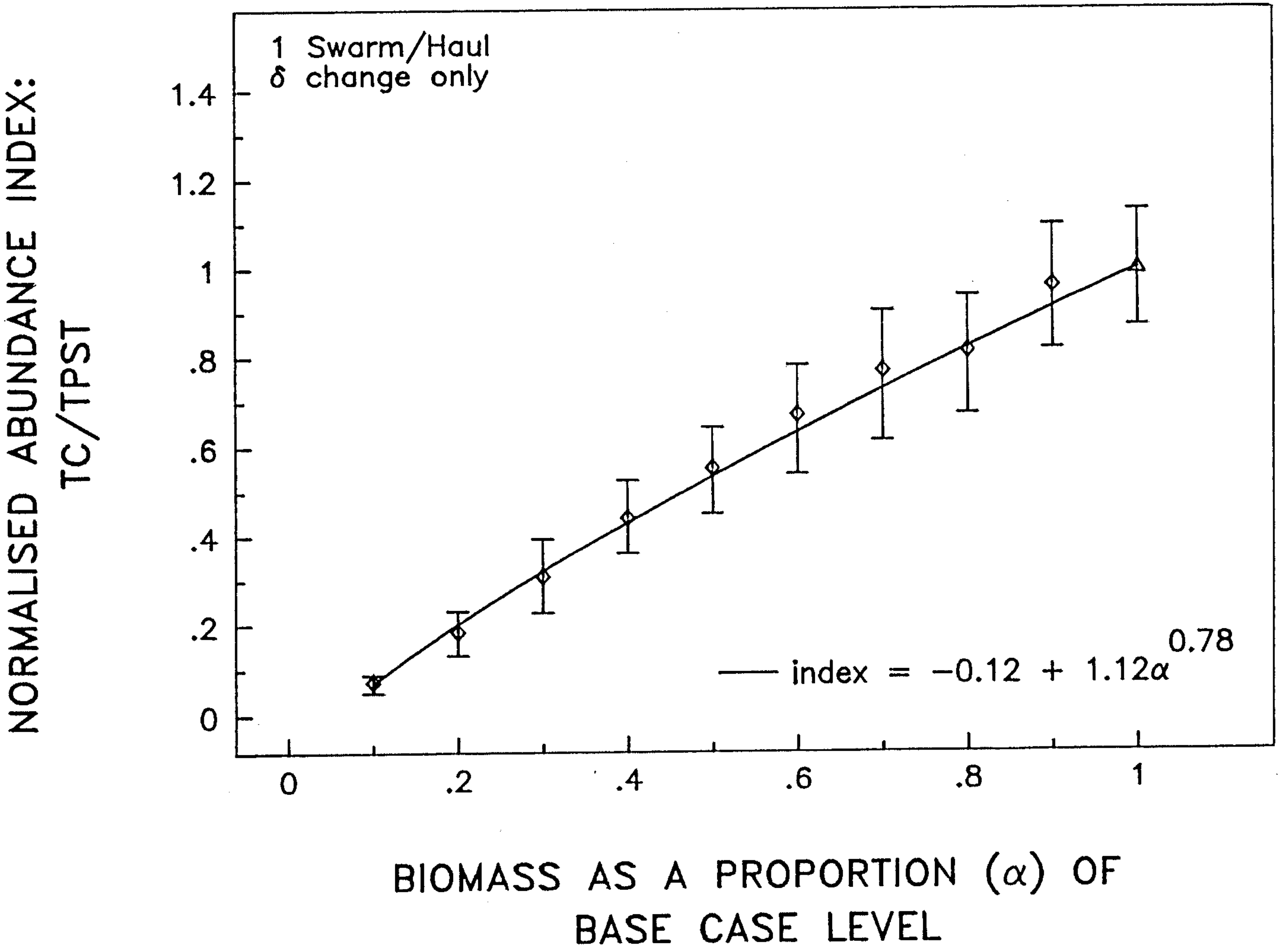
1 Swarm/Haul
δ change only
NORMALISED ABUNDANCE INDEX:
TC/TPST
1.4
1.2
1
.8
.6
.4
.2
0
0
.2
.4
.6
.8
1
index = −0.12 + 1.12α^0.78
BIOMASS AS A PROPORTION (α) OF
BASE CASE LEVEL

Figure 9 iv)

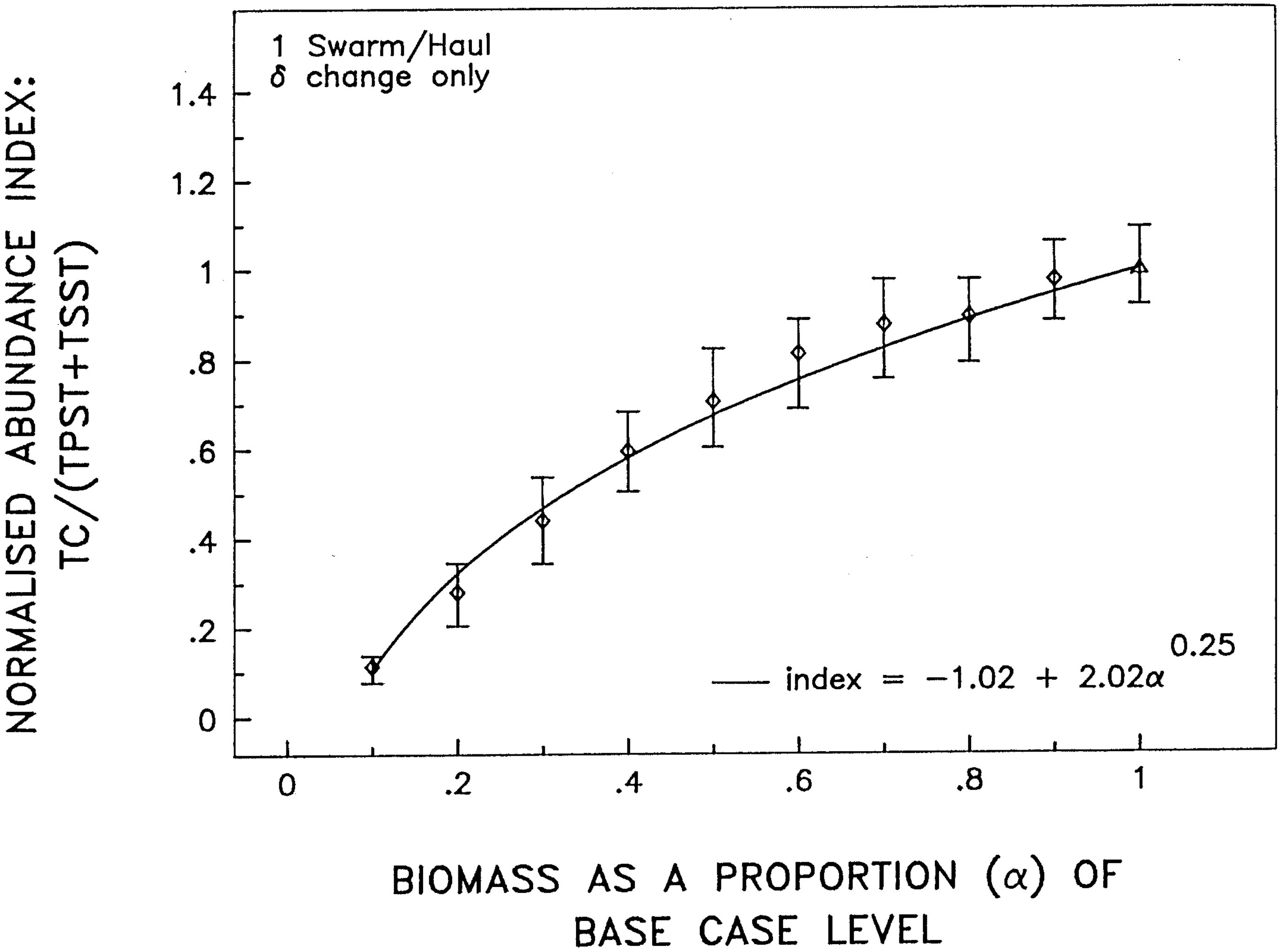
1 Swarm/Haul
δ change only
NORMALISED ABUNDANCE INDEX:
TC/(TPST+TSST)
1.4
1.2
1
.8
.6
.4
.2
0
index = −1.02 + 2.02α 0.25
0
.2
.4
.6
.8
1
BIOMASS AS A PROPORTION (α) OF
BASE CASE LEVEL

Figure 9 v)

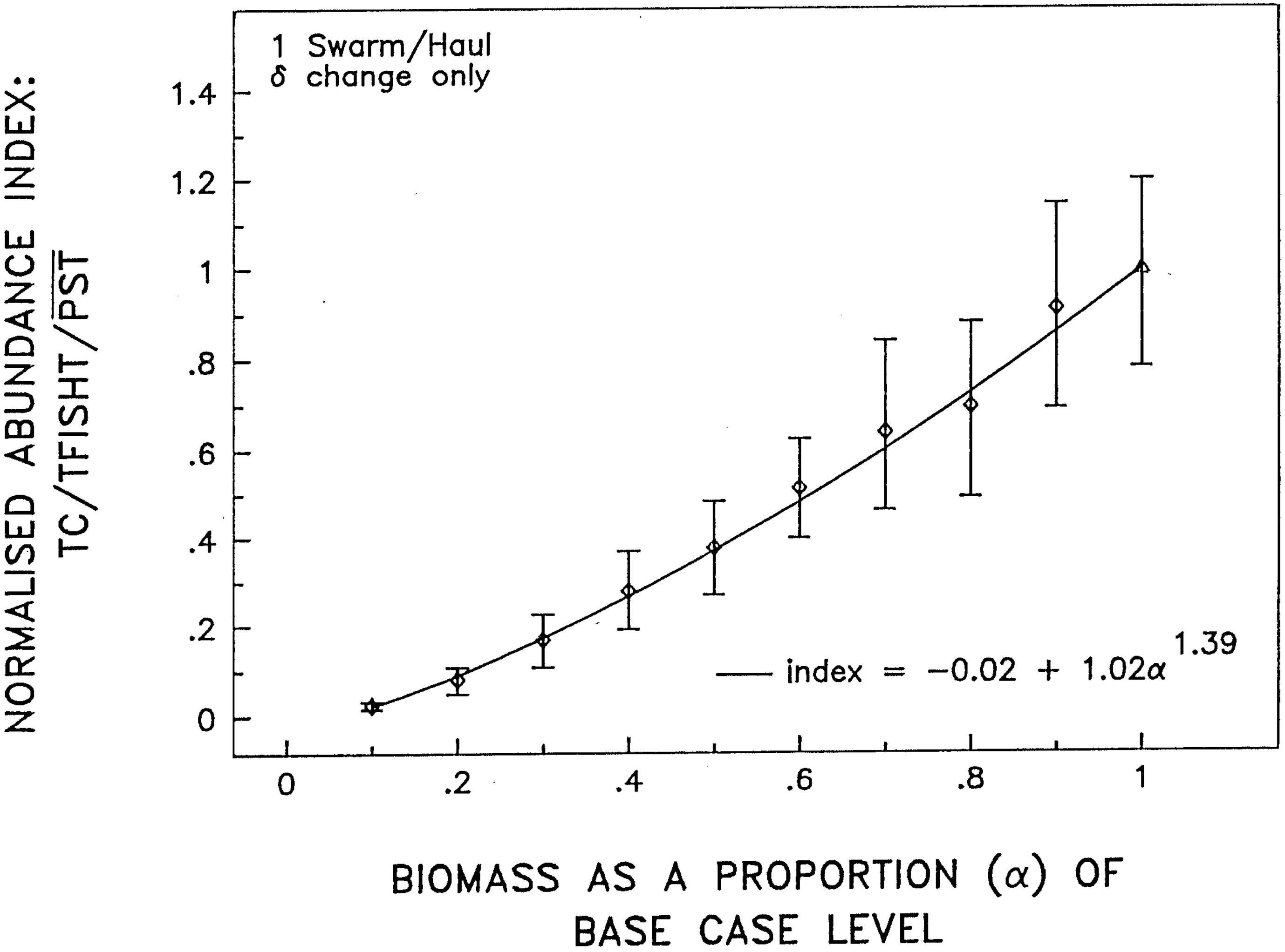
1 Swarm/Haul
δ change only
NORMALISED ABUNDANCE INDEX:
TC/TFISHT/$\overline{PST}$
1.4
1.2
1
.8
.6
.4
.2
0
0
.2
.4
.6
.8
1
— index = $-0.02 + 1.02\alpha^{1.39}$
BIOMASS AS A PROPORTION (α) OF
BASE CASE LEVEL

Figure 9 vi)

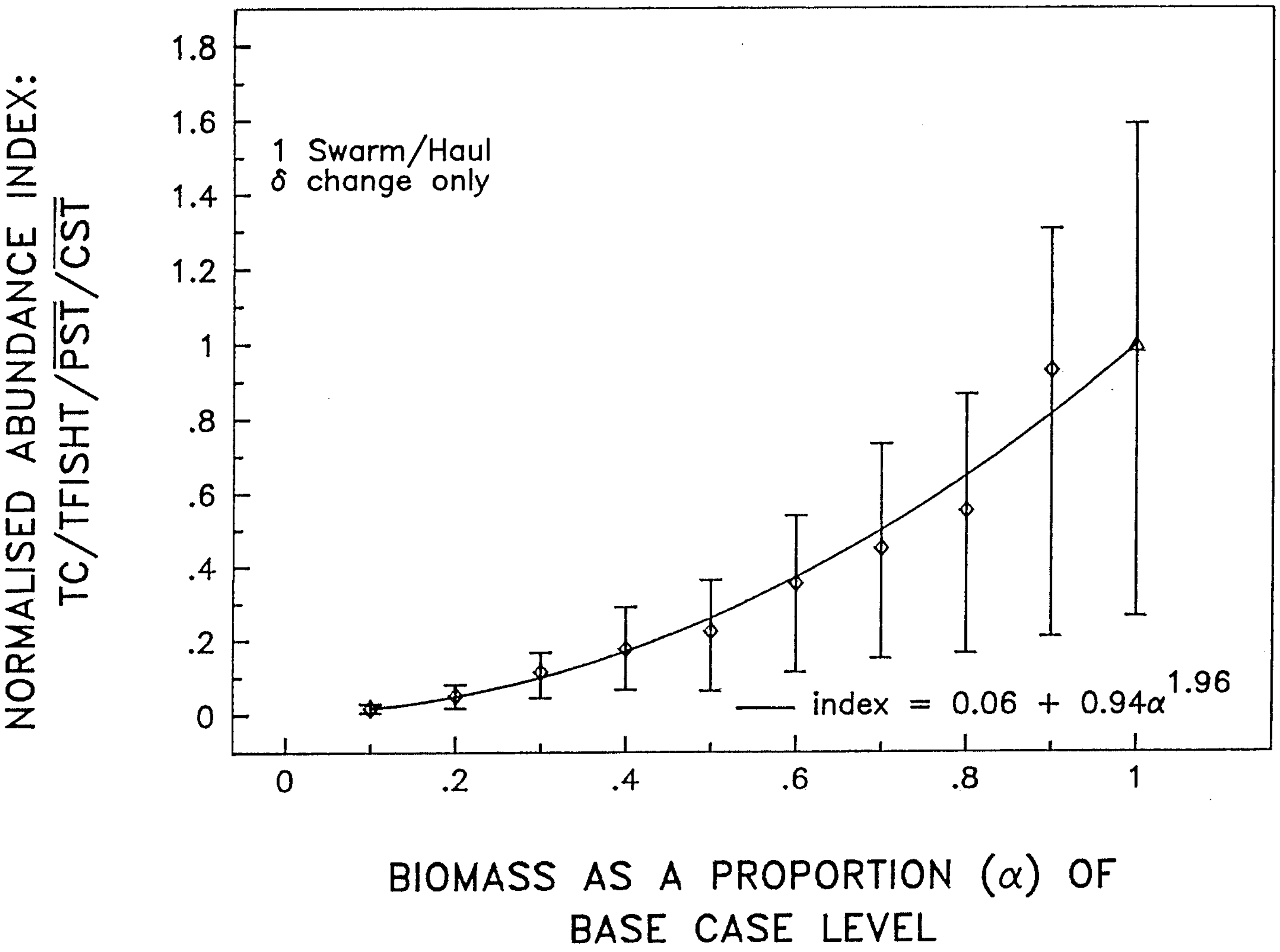
1.8
1.6
1.4
1.2
1
.8
.6
.4
.2
0
NORMALISED ABUNDANCE INDEX:
TC/TFISHT/$\overline{\text{PST}}$/$\overline{\text{CST}}$
1 Swarm/Haul
δ change only
— index = 0.06 + 0.94$\alpha^{1.96}$
0
.2
.4
.6
.8
1
BIOMASS AS A PROPORTION (α) OF
BASE CASE LEVEL

Légendes des tableaux

Tableau 1	Statistiques de synthèse d'un échantillon de données recueillies par un chalutier industriel de krill japonais. Un nombre suivi par un autre entre parenthèses correspond à une moyenne (écart-type), sauf indication contraire ou lorsqu'une seule statistique est en jeu.
Tableau 2	Valeurs des paramètres d'opérations de pêche pour différentes modifications de modèle. Lorsqu'une valeur d'un paramètre "partiellement affiné" est mise entre parenthèses carrées, la valeur n'a pas été ajustée pour cette modification, mais égalisée à la valeur ajustée pour une modification connexe.
Tableau 3	Comparaison de statistiques pour la pêcherie commerciale japonaise de krill établies à partir de l'échantillon de données reçues et d'autres sources, avec les résultats du modèle de simulation du cas de base. Les résultats du modèle de simulation reflètent la moyenne sur 100 cas. (NB: Toutes les statistiques ont trait à une période d'un demi-mois.) Les chiffres entre parenthèses sont les coefficients de variation sauf les pourcentages de bilan temporel qui sont les écarts-types.
Tableau 4	Comparaison des indices d'abondance pour l'expérience du modèle de simulation du cas de base avec ceux de six autres scenarios de répartition du krill, correspondant chacun à une baisse totale de 50% de la biomasse. Pour le cas de base, la moyenne sur les 100 simulations est représentée avec l'erreur standard de cette moyenne entre parenthèses. Pour les autres scenarios, la différence de pourcentage du cas de base moyen est donnée entre parenthèses, avec l'erreur standard. (Les unités, le cas échéant, sont en combinaisons tonne-heure.) (a) Un Essaim Allongé (f=8) Par Trait (b) Plus d'Un Essaim Par Trait
Tableau 5	Efficacité des indices d'abondance à détecter les changements de la biomasse de krill: blanc : 100 simulations ne détectent pas de changement significatif à un intervalle de confiance de 5% + / - : significative à un intervalle de confiance de 5% * : indice (ou son inverse) baisse de > 20% * * : indice (ou son inverse) baisse de > 45% (dans des limites de 95%) (a) Un Essaim Allongé (f=8) Par Trait (b) Plus d'Un Essaim Par Trait
Tableau 6	Statistiques comparatives complémentaires de 100 expériences de modèles de simulation pour le cas de base et pour six autres scenarios correspondant chacun à une baisse totale de 50% de la biomasse. Le format est le même que celui du tableau 4 mais les valeurs entre parenthèses pour le cas de base sont les écarts-types (et non pas les erreurs standard de la moyenne.)

(a) Un Essaim Allongé (f=8) Par Trait

(b) Plus d'Un Essaim Par Trait

Tableau 7 Statistiques comparatives supplémentaires des expériences de modèles de simulation pour le cas de base et six autres scenarios correspondant chacun à une baisse totale de 50% de la biomasse. Les valeurs données sont des moyennes sur 100 expériences, avec les erreurs standard de ces moyennes données entre parenthèses.

(a) Un essaimallongé (f=8) par trait

(b) Plus d'un essaim par trait

Tableau 8 Indices d'abondance comme proportion de leurs valeurs pour l'expérience de modèle de simulation du cas de base quand la biomasse totale de krill est réduite à une fraction a de son niveau du cas de base par une combinaison au hasard de changements en N_c, L_c, Dc,r et δ. Les résultats se rapportent aux moyennes sur 100 simulations dans chaque cas. Il faut noter que quelques uns des indices mentionnés sont les inverses de ceux indiqués sur les tableaux 4 et 5; l'inverse a été utilisé si nécessaire, pour faire de l'indice une fonction croissante de α - ces cas sont indiqués par un *.

(a) Un Essaim Allongé (f=8) Par Trait

(b) Plus d'Un Essaim Par Trait

Tableau 9 Efficacité des indices d'abondance à détecter les changements de la biomasse de krill:

blanc : 100 simulations ne détectent pas de changement significatif à un intervalle de confiance de 5%
+/- : direction de changement en cas de détection d'une différence significative à un intervalle de confiance de 5%
* : indice (ou son inverse) baisse de > 20%
* * : indice (ou son inverse) baisse de > 45% (dans des limites de 95%)

Tableau 10 Une version consolidée du Tableau 4 pour les six indices d'abondance selectionnés pour une comparaison détaillée dans la section 3.6. Seules les estimations ponctuelles de différence de pourcentage par rapport à la moyenne estimée du cas de base sont données pour les six autres scenarios de répartition du krill (correspondant chacun à une baisse totale de 50% de labiomasse). Le premier chiffre indiqué correspond à "Un essaim allongé(f=8)-par-trait" et le second chiffre à la modification du modèle "Plus d'un essaim-par-trait".

Tableau 11 Des estimations de la baisse du pourcentage des indicesd'abondance incorporant le temps de recherche primaire(PST)pour une baisse totale de 50% de la biomasse de krill sont comparées avec et sans erreur aléatoire (voir texte - section 3.6) dans l'allocation du temps de recherche de concentrations entre temps de recherche primaire et secondaire (PST et SST). Les comparaisons sont indiquées pour la baisse de la biomasse dûe à des baisses en D_c, r et δ respectivement, et sont pour le cas d'"Un essaim (f=8)allongé-par-trait".

Légendes des figures

Figure 1	Organigramme de la structure de base du modèle de simulation.
Figure 2	L'habitat stratifié choisi pour le modèle de répartition du krill dans un secteur de 600 milles nautiques carrés de l'océan Austral.
Figure 3	Un exemple de la répartition des concentrations de krill dans le secteur choisi de l'océan Austral de 600 milles nautiques carrés qui a été engendré selon la description de la section 2.3. Les rayons de concentrations sont représentés à l'échelle. Les lignes fléchées indiquent les concentrations pêchées séquentiellement pendant une période d'un demi-mois. La ligne pointillée représente le mouvement pendant une période de mauvais temps (voir sectionè.4).
Figure 4	Probabilité de détection comme fonction de temps pour la recherche approfondie et les modèles de recherche au hasard.
Figure 5	Un exemple de la répartition d'essaims pêchables dans une concentration engendrée selon la description de la section 2.7. Les rayons d'essaims ne sont PAS représentés à l'échelle. Cet exemple correspond à la modification du modèle "Un essaim allongé (f=8) par trait", avec le symbole, pour chaque essaim pêchable, placé au point central choisi pour cet essaim avant l'élongation. Les lignes fléchées reflètent le chalutage séquentiel de bancs dans la concentration par un navire de pêche. Il faut noter que seuls les bancs initiaux sont chalutés, bien que ces lignes puissent entrecouper les symboles d'autres bancs. Les lignes continues représentent la longueur et la direction de chaque trait (à l'échelle), tandis que les lignes en tirets indiquent le mouvement net de recherche du prochain essaim à chaluter.
Figure 6	Un exemple d'un seul trait pour la modification du modèle lorsque plus d'un essaim peut être chaluté par trait (voir sections 2.8 et 3.3). Les bancs représentés sont à l'échelle. Tandis que le premier banc chaluté est un banc "pêchable" en termes de critère (20), tous les bancs dans la zone à la droite de ce banc d'origine sont représentés. Les lignes en tirets à la droite de l'essaim initial délimitent la "bande de sonar"; les essaims intersectant cette bande sont aussi pêchés jusqu'à ce que le trait soit terminé parce que (dans cet exemple) le Capitaine estime que la capture a atteint 10 tonnes.
Figure 7	Courbes des indices d'abondance comme fonction d' a (la proportion du niveau du cas de base auquel la biomasse de krill a été réduite), où la réduction de la biomasse se produit par suite d'une combinaison au hasard de baisse dans les paramètres de distribution N_c, Lc, Dc, r et δ. Les indices d'abondance ont été normalisés à leurs niveaux moyens estimés pour le cas de base. Les barres d'erreur représentent les estimations des 68% centraux de la distribution de l'indice en question pour un navire par demi-mois, tandis que le symbole est l'estimation de la moyenne de distribution pour chaque valeur particulière de α. Une formule est présentée pour la courbe ayant trait à la relation entre l'indice et a par la méthode décrite dans la section 3.5. Les courbes a) et b) se rapportent respectivement aux modifications du modèle "Un essaim allongé (f=8) par trait" et "Plus d'un essaim par trait" et correspondent aux indices:

(i) TC
(ii) TC/FISHT
(iii) TC/TPST
(iv) $\mathrm{TC/TFISHT}/\overline{\mathrm{PST+SST}}$
(v) $\mathrm{TC/TFISHT}/(\overline{\mathrm{PST+SST}})$
(vi) $\mathrm{TC/TFISHT}/\overline{\mathrm{PST/CST}}$

Figure 8 Courbes de (i) capture totale par demi-mois (TC) et (ii) nombre de concentrations pêchées (TNC) par le taux de capture minimum par temps total écoulé (CR_{min}) requis pour qu'un navire n'abandonne pas une concentration. Les courbes ont trait à la répartition du krill du cas de base et à la modification du modèle "Un essaim allongé (f=8) par trait". Les barres d'erreur indiquent un écart-type.

Figure 9 Courbes des indices d'abondance par α sur la figure 7, sauf que le déclin de la biomasse totale provient uniquement d'un changement de la densité δ de surface d'un banc de krill. Les courbes sont celles de la modification du modèle "Un essaim allongé (f=8) par trait", et correspondent aux indices:

(i) TC
(ii) TC/FISHT
(iii) TC/TPST
(iv) TC/(TPST+TSST)
(v) $\mathrm{TC/TFISHT}/\overline{\mathrm{PST+SST}}$
(vi) $\mathrm{TC/TFISHT}/\overline{\mathrm{PST/CST}}$

Заголовки к таблицам

Таблица 1 Сводка избранных статистических данных, полученных с японского коммерческого крилевого траулера. Цифра с последующей в скобках другой цифрой соответствует среднему числу (среднему квадратическому отклонению), за исключением тех примеров, где цифры стоят в другом порядке, или где приведен только один показатель.

Таблица 2 Значения параметров промысловой операции для различных модификаций модели. Там, где значение частично "приведенного в соответствие" параметра показано в квадратных скобках, означает, что значение не было приведено в соответствие для данной модификации, а было оставлено равным приведенной в соответствие величине для соседней модификации.

Таблица 3 Сравнение статистических результатов, касающихся японского коммерческого промысла криля, полученных из выборки данных и других источников, с выходными данными имитационной модели для базисного варианта. Результаты имитационной модели отражают среднюю величину, полученную за 100 прогонов модели. (Примечание: Вся статистика относится к периоду полумесяца.) Цифры в скобках являются коэффициентами вариации, за исключением процентных величин затраченного времени, где они соответствуют среднему квадратическому отклонению.

Таблица 4 Сравнение индексов численности для имитационной модели базисного варианта с индексами численности, полученными из шести различных комбинаций параметров распределения криля, каждая из которых соответствует общему уменьшению биомассы на 50%. Для базисного варианта дается средняя величина, полученная в результате 100 прогонов модели, в скобках указана средняя квадратическая ошибка этой средней величины. Для различных комбинаций параметров распределения криля дается процентная разница по отношению к средней величине базисного варианта, в скобках указана средняя квадратическая ошибка этой процентной разницы. (Единицы в сотвествующих местах выражены в тоннах/час.).

(a) одно удлиненное (f=8) скопление за одно траление.

(b) больше одного скопления за одно траление.

Таблица 5 Показатель эффективности индексов численности при обнаружении изменений в биомассе криля:

пустое место : за 100 прогонов модели никаких статистически значимых изменений не обнаружено при 5% уровне
+/- : направление изменений, когда статистически значимое различие обнаружено при 5% уровне
* : индекс (или обратная величина индекса) снижается на > 20%
** : индекс (или обратная величина индекса) снижается на > 45% (в пределах 95%)

(a) одно удлиненное (f=8) скопление за одно траление.

(b) больше одного скопления за одно траление.

Таблица 6 Дополнительная сравнительная статистика по 100 прогонам имитационной модели для базисного варианта и для шести различных комбинаций параметров, соответстующих общему уменьшению биомассы на 50%. Обозначения те же, что и в таблице 4 кроме того, что цифры в скобках для базисного варианта являются средними квадратическими отклонениями (а не средними квадратическими ошибками средней величины).

(a) одно удлиненное (f=8) скопление за одно траление.

(b) больше одного скопления за одно траление.

Таблица 7 Дополнительная сравнительная статистика по прогонам имитационной модели для базисного варианта и для шести различных комбинаций параметров, соответствующих общему уменьшению биомассы на 50%. Данные значения являются средними числами, полученными за 100 прогонов модели, в скобках указаны средние квадратические ошибки этих значений.

(a) Одно удлиненное (f=8) скопление за одно траление.

(b) Больше одного скопления за одно траление.

Таблица 8

Индексы численности, выраженные в процентном отношении к их величинам, для прогона имитационной модели базисного варианта, когда общая биомасса криля уменьшается до доли α от ее базисного уровня вследствие случайного сочетания изменений в N_c, L_c, D_c, r и δ. В каждом случае результаты относятся к средним числам, полученным за 100 прогонов имитационной модели. Цифры в скобках являются средними квадратическими ошибками подсчитанных средних величин. Обратите внимание, что некоторые из нижеследующих индексов являются обратными величинами индексов, указанных в таблицах 4 и 5; когда необходимо превращать индекс в возрастающую функцию α дается его обратная величина, такие примеры отмечены значком *.

(a) одно удлиненное (f=8) скопление за одно траление.

(b) больше одного скопления за одно траление.

Таблица 9

Показатель эффективности индексов численности в обнаружении изменения биомассы криля:

пустое место : за 100 прогонов модели никаких статистически значимых изменений не обнаружено при 5% уровне
+/- : направлениеизменений, когда статистически значимое различие обнаружено при 5% уровне
* : индекс (или обратная величина индекса) снижается на > 20%
** : индекс (или обратная величина индекса) снижается на > 45% (в пределах 95%)

Эта таблица соответствует таблице 5a ("одно удлиненное (f=8) скопление за одно траление"), за исключением того, что эффективность концентрированного поиска увеличена в 7.5 раз.

Таблица 10

Обобщенный вариант таблицы 4 для шести индексов численности, выбранных для подробного сравнения в разделе 3.6. Для шести различных комбинаций параметров распределения криля (каждая такая комбинация соответствует общему уменьшению биомассы на 50%) дается только оценка процентного различия отдельных результатов базисного варианта Первая цифра соответствует модификации модели "одно удлиненное (f=8) скопление за одно траление", вторая цифра - "больше одного скопления за одно траление".

Таблица 11

Сравнение оценок процентного снижения индексов численности (с ошибкой случайного выбора и без нее), включающих первичное время поиска (PST), соответствующее 50% снижению биомассы криля при распределении в пределах времени поиска концентрации от первичного времени поиска (PST) до вторичного времени поиска (SST). Сравнения касаются уменьшения биомассы вследствие понижения в каждом из D_c, r и δ и относятся к случаю "одно удлиненное (f=8) скопление за одно траление".

Подписи к рисункам

Рисунок 1	Схема основной структкры имитационной модели.
Рисунок 2	Стратифицированный ареал обитания криля, использованный для модели его распределения в участке Южного океана площадью 600 квадратных морских миль.
Рисунок 3	Пример распределения концентраций криля в выбранном квадратном участке Южного океана площадью 600 квадратных морских миль, рассчитанный как показано в разделе 2.3. Радиусы концентраций пропорциональны. Линии со стрелками показывают концентрации, последовательно облавливаемые в течение полутора месяцев.Точечная линия изображает передвижение в период плохой погоды (см. раздел 2.4).
Риунок 4	Вероятность обнаружения как функция времени для моделей всеобъемлющего и случайного поиска.
Рисунок 5	Пример распределения скоплений промыслового размера в пределах концентрации рассчитан как описано в разделе 2.7. Радиусы скоплений НЕ пропорциональны. Этот пример соответствует модификации модели "одно удлиненное (f=8) скопление за одно траление", где обозначение для каждого пригодного для промысла скопления находится в центральной точке, выбранной для этого скопления до его удлинения. Линиями со стрелками.показано последовательное траление промысловым судном скоплений в пределах этой концентрации. Обратите внимание на то, что, хотя эти линии могут пересекать обозначения для других скопленйй, облавливаются только исходные скопления. Непрерывные линии обозначают длину и направление каждого траления (пропорциально), а пунктирные линии изображают движение сети в ходе поиска следующего скопления для лова.
Риунок 6	Пример отдельного траления для модификации модели, где улов может составить больше одного скопления за одно траление (см. раздел 2.8 и 3.3). Данные скопления пропорциальны. Хотя, в соответствии с критерием 20, только исходное скопление является "пригодным для промысла", показаны все скопления, находящиеся в районе направо от этого исходного скопления. Пунктирные линии направо от исходного скопления определяют "звуковую полосу"; скопления, пересекающие эту полосу также облавливаются, так как (в этом случае) капитан оценивает улов в 10 тонн.
Рисунок 7	Графики индексов численности как функция α (процентная величина базового уровня, к которому сведена биомасса криля), где уменьшение биомассы является результатом случайного

сочетания снижений параметров распределения N_C, L_C, D_C, r и δ. Индексы численности были приведены к вычисленным средним уровням базисного варианта. Размер указанных на графике статистических ошибок представляет собой оценки центральной части распределения 68% данного индекса для судна в течение полумесяца, а обозначение является оценкой средней величины распределения для каждого отдельного значения α. Дается формула для кривой, скорректированной в отношение связи между индексом и α по методу, описанному в разделе 3.5. Графики (a) и (b) соответственно относятся к модификациям модели "одно удлиненное (f=8) скопление за одно траление" и "больше одного скопления за одно траление", и соответствуют нижеследующим индексам:

(i) TC
(ii) TC/TFISHT
(iii) TC/TPST

(iv) TC/TFISHT/$\overline{\text{PST+SST}}$

(v) TC/TFISHT/($\overline{\text{PST+SST}}$)

(vi) TC/TFISHT/$\overline{\text{PST/CST}}$

Рисунок 8 Графики (i) общего улова в течение полумесяца (TC) и (ii) количества облавливаемых концентраций (TNC) по отношению к минимальному коэффициенту уловистости на единицу общего протекшего времени ($КУ_{мин}$), который необходимо достичь для того, чтобы судно не отплыло от концентрации. Графики касаются распределения криля базисного варианта и модификации модели "одно удлиненное (f=8) скопление за одно траление". Размер указанных на графике статистических ошибок свидетельствует об одном среднем квадратическом отклонении.

Рисунок 9 Графики индексов численности по отношению к α такие же, как на рисунке 7, за исключением того, что общее уменьшение биомассы является результатом изменения только в плотности поверхностного слоя скопления криля δ. Графики касаются модификации модели "одно удлиненное (f=8) скопление за одно траление", и соответствуют нижеследующим индексам:

(i) TC
(ii) TC/TFISHT
(iii) TC/TPST

(iv) TC/TFISHT/$\overline{\text{PST+SST}}$

(v) TC/TFISHT/($\overline{\text{PST+SST}}$)

(vi) TC/TFISHT/$\overline{\text{PST/CST}}$

Encabezamientos de las Tablas

Tabla 1 Resumen de las estadísticas de una muestra de datos de un arrastrero comercial de krill japonés. Un número seguido de otro, entre paréntesis, corresponde a un promedio (desviación estándar), salvo indicación contraria o donde una sola estadística está implicada.

Tabla 2 Valores de los parámetros de operaciones de pesca para diferentes modificaciones del modelo. Donde el valor de un parámetro "parcialmente ajustado" se indica en corchetes, el valor no fue ajustado para esta modificación, pero igualado al valor ajustado para una modificación relacionada.

Tabla 3 Comparación de las estadísticas para la pesquería comercial japonesa del krill a partir de una muestra de datos suministrada y de otras fuentes con los resultados del modelo de simulación para el caso de base. Los resultados del modelo de simulación reflejan el promedio sobre 100 ejecuciones. (NB: Todas las estadísticas se aplican a un período de 15 días). Los números entre parémtesis con coeficientes de variaciones, excepto los porcentajes del presupuesto temportal que son desviaciones estándar.

Tabla 4 Comparación de los índices de abundancia para la ejecución del modelo de simulación del caso de base con aquellos de los seis escenarios alternativos de la distribución del krill, correspondiendo cada uno a un descenso del 50% del total de la biomasa. Para el caso de base, se indica el promedio sobre las 100 simulaciones, junto con el error estándar de este promedio entre paréntesis. Para los escenarios alternativos, se da la diferencia del porcentaje del caso de base promedio, junto con el estándar de error de esta diferencia entre paréntesis. (Las unidades, cuando corresponda, son combinaciones de toneladas-hora).

(a) Un cardumen por lance alargado (f=8)

(b) Más de un cardumen por lance

Tabla 5 Eficiencia de los índices de abundancia para detectar cambios en la biomasa del krill:

blanco : 100 simulaciones no detectan un cambio importante al nivel del 5%
+ / - : dirección de cambio si se detecta una diferencia importante al nivel del 5%
* : índice (o su inverso) baja un > 20%
* * : índice (o su inverso) baja un > 45% (dentro de los límites del 95%)

(a) Un cardumen por lance (f=8)

(b) Más de un cardumen por lance

Tabla 6 Estadísticas comparativas adicionales de 100 ejecuciones del modelo de simulación para el caso de base y para seis escenarios alternativos, cada uno correspondiendo a un descenso del 50% del total de la biomasa. El formate es el mismo que el de la tabla 4 excepto que los valores entre paréntesis para el caso de base son desviaciones estándar (no errores estándar del promedio).

(a) Un cardumen por lance alargado (f=8)

(b) Más de un cardumen por lance

Tabla 7

Estadísticas comparativas adicionales de las ejecuciones del modelo de simulación para el caso de base y seis escenarios alternativos cada uno correspondiendo a un descenso del 50% de la biomasa total. Los valores dados son promedios sobre 100 ejecuciones, con los errores estándar de estos promedios dados entre paréntesis.

(a) Un cardumen por lance alargado (f=8)

(b) Más de un cardumen por lance

Tabla 8

Indices de abundancia como una proporción de sus valores para la ejecución del caso de base del modelo de simulación, cuando la biomasa total del krill disminuye a una fracción α del nivel del caso de base a través de una combinación aleatoria de cambios en N_c, L_c, D_c r y δ. Los resultados se relacionan a los promedios sobre 100 simulaciones en cada caso. Las cifras entre paréntesis son errores estándar de las proporciones estimadas. Observese que algunos de los índices en la lista son los inversos de los indicados en las Tablas 4 y 5; el inverso se ha tomado siempre que ha sido necesario para hacer del índice una función creciente de α - tales casos están indicados con un *.

(a) Un cardumen por lance alargado (f=8)

(b) Más de un cardumen por lance.

Tabla 9

Eficiencia de los índices de abundancia para detectar cambios en la biomasa del krill:

blanco : 100 simulaciones no detectan un cambio importante al nivel del 5%
+ / - : dirección de cambio si se detecta una diferencia importante al nivel del 5%
* : el índice (o su inverso) desciende un > 20%
* * : el índice (o su inverso) desciende un > 45% (dentro de los límites del 95%)

Esta Tabla corresponde a la Tabla 5a del caso "Un cardumen alargado (f=8) por lance" excepto que la eficiencia de búsqueda de la concentración ha sido aumentada 7.5 veces.

Tabla 10

Una versión consolidada de la Tabla 4 para los seis índices de abundancia seleccionados para una comparación detallada en la sección 3.6. Sólo se dan las estimaciones de la diferencia del porcentaje del promedio del caso de base estimado para los seis escenarios alternativos de distribución del krill (correspondiendo cada uno a un descenso del 50% del total de la biomasa). La primera cifra indicada corresponde a "Un cardumen-por-lance" alargado (f=8) y la segunda cifra a la modificación del modelo "Más de un cardumen-por-lance".

Tabla 11

Se comparan estimaciones de la disminución del porcentaje en los índices de abundancia que incorporan PST para un descenso del 50% del total de la biomasa del krill con y sin error aleatorio (ver texto -sección 3.6) en la adjudicación de tiempo de búsqueda entre PST y SST dentro de una concentración. Las comparaciones se indican para el descenso de la biomasa debido a disminuciones en cada uno de D_c , r y δ, y son para el caso de "Un cardumen por lance" alargado (f=8).

Leyendas de las Figuras

Figura 1	Un diagrama de flujo de la estructura básica del modelo de simulación.
Figura 2	Habitat estratificado seleccionado para el modelo de distribución del krill en un sector de 600 millas náuticas cuadradas del Océano Austral.
Figura 3	Un ejemplo de la distribución de las concentraciones de krill en el sector seleccionado del Océano Austral de 600 millas náuticas cuadradas, el cual ha sido producido tal como se describe en la sección 2.3. Los radios de las concentraciones están a escala. Las flechas indican las concentraciones pescadas secuencialmente durante un período de 15 días. La línea de puntos representa movimiento durante un período de mal tiempo (ver sección 2.4).
Figura 4	Probabilidad de detección como una función de tiempo para los modelos de búsqueda exhaustiva y búsqueda aleatoria.
Figura 5	Un ejemplo de la distribución de los carúmenes explotables en una concentración, producidos tal como se describe en la sección 2.7. Los radios de los cardúmenes NO están a escala. Este ejemplo corresponde a la modificación del modelo "Un cardumen por lance" alargado (f=8), con el símbolo para cada cardumen explotable situado en el punto central escogido para este cardumen antes del alargamiento. Las flechas reflejan el arrastre secuencial de los cardúmenes en la concentración por un buque de pesca. Observese que sólo los cardúmenes iniciales son arrastrados, aunque las líneas pueden cruzar los símbolos para otros cardúmenes. Las líneas sólidas representan la longitud y dirección de cada lance (a escala), mientras las líneas quebradas indican movimiento de las redes en la búsqueda del cardumen que se arrastrará a continuación.
Figura 6	Un ejemplo de un solo lance para la modificación del modelo donde más de un cardumen puede ser arrastrado por lance (ver las secciones 2.8 y 3.3). Los cardúmenes representados están a escala. Aunque el cardumen inicial arrastrado es un cardumen "explotable" en términos de criterio (20), todos los cardúmenes situados a la derecha de este cardumen original están representados. Las Líneas quebradas a la derecha del cardumen inicial determinan la "banda sonar"; los cardúmenes que cruzan esta banda también se pescan hasta que el lance termina porque (en este ejemplo) el Capitán estima que la captura ha alcanzado las 10 toneladas.
Figura 7	Curvas de los índices de abundancia como una función de α (la proporción del nivel del caso de base para el cual la biomasa del krill ha sido reducida), donde la reducción de la biomasa ocurre como un resultado de una combinación aleatoria de disminuciones en los parámetros de distribución N_c , L_c , D_c r y δ. Los índices de abundancia han sido normalizados a sus niveles promedios estimados para el caso de base. Las barras de error representadas indican estimaciones del 68% central de la distribución del índice en cuestión para un buque durante una quincena, mientras el símbolo es la estimación del promedio de la distribución, para cado valor particular de α. Se presenta una fórma para la curva ajustada a la relación entre el índice y α por el método descrito en la sección 3.5. Las curvas (a) y (b) corresponden a las modificaciones del modelo "Un cardumen por lance" alargado (f=8) y "Más de un cardumen por lance" respectivamente, y corresponden a los índices:

(i) TC
(ii) TC/TFISHT
(iii) TC/TPST
(iv) TC/TFISHT/$\overline{\mathrm{PST+SST}}$
(v) TC/TFISHT/($\overline{\mathrm{PST+SST}}$)
(vi) TC/TFISHT/($\overline{\mathrm{PST/CST}}$)

Figura 8 Curvas de (i) captura total en una quincena (TC) y (ii) número de concentraciones pescadas (TNC) como función de la tasa de captura mínima por el tiempo total transcurrido (CR_{min}) requerido para que un buque no abandone una concentración. Las curvas corresponden a la distribución del krill del case de base y al modelo de modificación "Un cardumen por lance (f=8) alargado". Las barras de error indican una desviación estándar.

Figura 9 Curvas de los índices de abundancia como una función de α como en la Figura 7, excepto que la disminución total de la biomasa es solamente el resultado de un cambio en la densidad de superficie del cardumen de krill. Las curvas corresponden a la modificación del modelo "Un cardumen por lance" alargado (f=8), y corresponde a los índices:

(i) TC
(ii) TC/TFISHT
(iii) TC/TPST
(iv) TC/(TPST+TSST)
(v) TC/TFISHT/$\overline{\mathrm{PST+SST}}$
(vi) TC/TFISHT/$\overline{\mathrm{PST/CST}}$

SC-CAMLR-VI/BG/4

SOME ASPECTS OF THE RELATION BETWEEN ANTARCTIC KRILL ABUNDANCE AND CPUE MEASURES IN THE JAPANESE KRILL FISHERY

D.S. Butterworth

Abstract

The history of the Japanese krill fishery is reviewed briefly. Important aspects of the fishing operation are the constraints imposed by processing rate limitations on the vessels, and product quality considerations - in particular the increasing tendency to avoid catching "green" krill. These factors result in Catch-per-Day and Catch-per-Haul measures being unlikely to index krill abundance. During the high season, Catch-per-Towing-Time seems likely to index only within-swarm density. Search time data may be needed to assess the density of swarms in a concentration, but may be difficult to record in practice, and a number of other factors may complicate any analysis. The possibility of indexing the extent of the krill distribution through routine oceanographic monitoring merits attention. A data sample from the Japanese krill fishery statistics data-base has been selected for further studies.

Résumé

L'historique de la pêcherie de krill japonaise est résumée brièvement. Les aspects importants de l'opération de pêche sont les contraintes imposées par les limites du taux de traitement sur les navires et les considérations de qualité du produit - en particulier la tendance croissante à éviter le krill de "teinte verte". En raison de ces facteurs, les mesures de Prise-par-jour et de Prise-par-trait risquent d'être impropres à indiquer l'abondance du krill. Pendant la haute saison, la Prise-par-durée-de-trait n'indique vraisemblablement que la densité à l'intérieur des essaims. L'on pourrait avoir besoin de données sur le temps de recherche pour évaluer la densité d'essaims dans une concentration, mais, sur le plan pratique, il pourrait être difficile de les enregistrer, et un certain nombre d'autres facteurs pourraient compliquer l'analyse. La possibilité d'indiquer l'étendue de la distribution du krill par un contrôle océanographique régulier mérite d'être étudiée. Un échantillon de données provenant de bases de données statistiques de la pêcherie de krill japonaise a été sélectionné pour une étude ultérieure.

Резюме

Дается краткий обзор истории японского промысла криля. Наиболее важными аспектами промысла являются требования, вызванные ограничениями мощности судна по обработке криля и вопросами качества продукта - в частности увеличивающаяся тенденция избегать промысел "зеленого" криля. Результатом этих факторов является малая вероятность использования параметров "Улов за день" и "Улов за траление" в качестве показателей численности криля. В течение сезона, когда промысел достигает наивысшего размера, параметр "Улов за время траления", вероятно, служит показателем плотности криля только внутри скопления. Данные по времени поиска могут быть необходимы для оценки плотности скопления внутри концентрации, но, возможно, что их сбор будет на практике затруднен, а также ряд других факторов может осложнить анализ. Заслуживает внимания возможность получения индекса распределения криля на основе данных стандартных океанографических съемок. Для будущих исследований была сделана выборка данных из статистического банка данных по японскому промыслу криля.

Resumen

Se analiza brevemente la historia de la pesquería japonesa del krill. Los aspectos importantes de la operación pesquera son las restricciones impuestas por los límites de las tasas de procesamiento en los buques, y las consideraciones de calidad del producto - particularmente la tendencia creciente de evitar la captura del krill “verde”. A razón de estos factores, las medidas Captura-por-día y Captura-por-lance pueden ser inadecuadas para indicar la abundancia del krill. Durante la temporada alta, parece que la Captura-por-tiempo-de-arrastre sólo indica la densidad en el interior de cardúmenes. Los datos del tiempo de búsqueda pueden ser necesarios para evaluar la densidad de cardúmenes en una concentración, pero en la práctica, pueden ser difíciles de registrar, además, otros factores pueden complicar cualquier análisis. La posibilidad de indicar la extensión de la distribución del krill por medio del control oceanográfico regular merece ser estudiada. Se ha seleccionado una muestra de datos de la base de datos de las estadísticas de la pesquería de krill japonesa para estudios ulteriores.

1. INTRODUCTION

This document summarises information provided in discussions held with Captains and other executives of Japanese krill fishing companies, and also Japan Fishing Agency officials and scientists involved in research on krill and the krill fishery, during October 1986. These discussions constituted the initial phase of a simulation study of krill distribution and the krill fishery to determine the utility of CPUE as an index of changes in krill abundance, which is being undertaken on a contractual basis for CCAMLR.

Details of the persons with whom discussions were held are listed in the Appendix. The material presented is drawn from those discussions and written information provided by Japanese scientists - in particular various documents authored by Dr Y. Shimadzu and Mr T Ichii. A number of the comments made during the discussions are anecdotal in nature, and should not be regarded as the conclusions of a detailed scientific analysis. Nevertheless they provide extremely useful background for developing an understanding of the way the fishery operates, and hence a basis to formulate hypotheses to test, and to choose the most appropriate approach for modelling purposes - such comments have been recorded and should be viewed in that context.

Nomenclature in general use for the different types of krill aggregations is somewhat varied. The terminology in this document will be kept consistent with that of Butterworth and Miller (1987): krill aggregate into "concentrations"; different modes of concentration are a "number of swarms", a "layer", and a "super-patch". Swarms are typically several tens of metres long with densities between 10 and several hundred g/m^3; layers may exceed 1 000 m in length with densities of several tens of g/m^3; super-patches may extend over several km with densities of several hundred g/m^3. Conventional translations of certain of the standard Japanese terms differ somewhat from the above: they use the terms "patch" and "layer" for alternative manifestations of what is indicated above (and in what follows) as a "swarm" (see also Section 3.2).

Throughout this document attempts are made to relate the information presented to the question of obtaining a measure (or set of measures) from data collected (or potentially collected) in the fishery, which would provide an annual index of krill abundance. As discussed subsequently, the fishery provides no information on layers because their densities are too low for fishing on them to be economic, while fishing on super-patches seems a relatively rare phenomenon. Comments will accordingly be directed towards monitoring the abundance of krill aggregating in the "swarm" mode (K_s). Butterworth and Miller (1987) express this as:

$$K_s = A_t D_c A_{cs} d_s A_s \delta_{ks} \qquad (1)$$

where A_t = total management area

A_{cs} = average area of a concentration of swarms

A_s = average swarm area for swarms comprising a concentration of swarms

D_c = density of concentrations of swarms (no. concentrations per unit area)

d_s = average density of swarms within a concentration (no. swarms per total area of concentration)

δ_{ks} = average density of krill in a swarm (mass krill per surface area of swarm)

[Note: While these Butterworth and Miller (1987) symbols are used in this paper, a slightly different set are used in Butterworth (1988). Essentially the equivalences are, with the Butterworth (1988) symbols on the right hand sides:

$A_{cs} = \pi L_c^2$
$A_s = \pi r^2$
$D_c A_t = N_c$
$d_s = D_c$
$\delta_{ks} = \delta]$

Since changes in krill abundance could be reflected by changes in any one of the factors in equation (1) (see Section 4.5 for the sense in which a "change" in A_t is implied), it is important to attempt to relate data collected in the fishery to each of these factors. [Note that although δ_{ks} is defined as an areal density, subsequent discussions will for simplicity tacitly treat it as a volume density. Average swarm thickness is a further factor which should perhaps also be included in equation (1).]

This document first gives a brief overview of the history of the Japanese krill fishery, and then discusses details of the nature of the fishing operation. This is followed by a section on possible specific relations between data which are (or might be) routinely collected in the fishery and the factors in equation (1). A final section summarises the more important impressions, conclusions and recommendations.

2. AN OVERVIEW

2.1 A Brief Historical Perspective

The history of the Japanese fishery for Antarctic krill has been detailed by Shimadzu (1984) from 1972/73 to 1982/83. That document has been updated to cover the following two seasons by Shimadzu (1985).

In brief, some experimental fishing first took place in the 1972/73 season by a single vessel using side-towing nets designed for near-surface fishing, a method found to be inefficient. Commercial operations started in 1973/74 with stern trawlers using surface-midwater trawl nets. Unlike the USSR fishery, where catchers are guided by research vessels, the Japanese fishery has essentially been an individual ship operation (except for a five year period where a "mothership" also operated, as described in the next section). Between 1 and 10 vessels have operated on this individual basis from 1973/74 to 1984/85, and nearly all of these (90% of the vessel-years) have been 2 000-3 000 tonne class trawlers.

For the first three seasons, catches totalled only a few thousand tonnes, but rose rapidly over the next three years as effort expanded, including the introduction of the mothership operation in 1977/78. Since that time, seasonal catch totals have averaged 37 thousand tonnes, with a maximum of 50 thousand tonnes in 1983/84.

The fishery has been conducted in three areas, which are generally referred to as "off Enderby Land", "off Wilkes Land", and "the Scotia Sea". The greatest catches in these areas (Shimadzu 1985, Figure 4) have been taken between longitudes 50°E-70°E, 110°E-150°E, and 65°W-40°W (from the South Shetland to South Orkney islands) respectively, although effort has extended over wider ranges than these limits indicate. For the first three seasons the fishing took place off Enderby Land, but in 1976/77 started moving further east to the area off Wilkes Land. In 1979/80 further movement into the western hemisphere occurred, and since 1980/81 there has been an increasing transfer of fishing effort into the Scotia Sea area, which now contributes almost all the Japanese krill harvest. (The reasons for this are discussed in Section 3.5).

Although fishing has taken place from early November to the start of April, most activities have been concentrated in the mid-December to end-February period (i.e. an effective season of 70-80 days), for reasons primarily related to krill's swarming behaviour.

Further details of the history of the fishery are given in Shimadzu (1984), Shimadzu (1985), and Shimadzu and Ichii (1985).

2.2 The Mothership Operation

This operation took place during the five seasons from 1977/78 to 1981/82, fishing off Wilkes Land throughout this period. The venture was partly subsidised, and consisted of an 8 000 tonne class trawler with freezing and processing capabilities as the mothership, together with from 7-10 catchers (349 tonne class) each with limited freezing capacity.

Two detailed examples of this operation are provided in Shimadzu and Ichii (1985). Typically the catchers did not move more than 30 n.miles from the mothership (except for one vessel used for searching); this small radius was because processed product quality requirements necessitated their harvests to be transferred to the mothership within 2-3 hours of capture. Economically the operation did not compare favourably with the individual trawler performances - the fleet caught typically 200-300 tonnes per day compared to the 50-70 tonne average for a 3 000 tonne class vessel (Shimadzu, 1984) - and accordingly was discontinued.

Although this activity accounted for some 50% of the total Japanese catch while it operated, it is not felt appropriate to attempt a detailed model of the exercise. This is because the constraints of processing limitations would likely render interpretation of the data more difficult and the modelling quite complicated; further it seems unlikely that this operational mode would be recommenced by the Japanese in the future. This viewpoint might merit reconsideration if a detailed study would aid in analysing the USSR operation (which may have more similarities with this fleet-mode procedure), or if felt necessary to provide more information on areal swarm distribution than is available from individual fishing vessel records and research surveys.

3. THE FISHING OPERATION

3.1 Comparison with Other Trawling Operations

Gulland (1985) suggested that from a CPUE analysis perspective, the individual Japanese krill fishing vessels operate very much like a demersal trawler. Both the vessels used in the krill fishery and their Captains participate in mid-water or demersal trawling for other species over the remainder of the year, so the Captains present at the discussions were asked to comment on the differences in strategy between krill and other trawling operations.

The difference most strongly stressed was the limitations imposed by processing and quality considerations for krill. In other fisheries, maximising catch rate (in terms of total time) is the primary consideration. With krill, catches per haul are limited to prevent the product being crushed, and to allow time for processing while the krill remains fresh - generally only 2-3 hours for the fresh-frozen product. Towing times can therefore be quite short. This "quality" aspect and its implications for analysis are discussed further in Sections 3.3 and 4.1.

Another difference emphasised was that krill fishing involves much more searching (predominantly using an echo sounder). This contrasts with demersal operations where bottom features are considered of more importance in locating promising areas, and where there is in any case more accumulated experience on the location of preferential areas.

Comments were also made that krill trawling is sometimes very close to the surface, particularly with swarms so positioned in poor light conditions, and sonar is important in establishing the appropriate angle to tow through a swarm.

3.2 Fishing Strategies

The importance of the echosounder in locating swarms upon which to fish was stressed repeatedly. Ichii (1987) records this as the most frequent means of krill detection, both for surface and underwater swarms, and whether the area is of low or high abundance. Predator cues and direct sighting of swarms near the surface are location methods that appear not to be used very frequently.

The main role of sonar appears to be to determine the shapes and orientations of swarms and hence the appropriate towing direction. This also applies when swarms are small (generally earlier in the season), and tows are continued through a number of swarms. Sonar is also used for initial detection of underwater swarms, but is apparently limited in this role as it can be set to cover only a small depth range. Nevertheless one Captain ascribed the lack of success of the mothership operation as due in part to only one of the vessels having being equipped with sonar - echosounders having a much narrower horizontal effective search width. Another Captain commented that swarming behaviour was quite different in the Scotia sea (deep and dense swarms) compared to the near continuous echos off Wilkes Land; thus sonar was used far more in the Scotia Sea.

There are also favoured areas to find krill concentrations (the distribution is not random), and some relations between oceanographic features and the likelihood of finding krill swarms were suggested. Catch rates suffered in the earliest years until experience in these respects was developed.

Ichii (pers. commn) advises that such areas tend to be to the west of islands or glaciers (the downstream side in the East Wind Drift). Fronts and areas of water convergence (detected by observing movements of icebergs) were suggested as good signs, and water colour as a useful cue (clear water generally bad, green water generally good). Varying rather than flat bottom depth is another positive index, possibly because of associated upwelling currents carrying nutrients.

The vessels search at 10 knots, but the towing speed is only about 2 knots. Wind is an important aspect, and trawling requires a wind speed of less than 20 metres/sec (about 10 knots) for an average sized vessel. Ichii's (1985) report on repeated tows on the same swarm shows that such tows are nearly parallel to each other. The primary reason for this is that unless wind speeds are less than about 2-3 on the Beaufort scale (about 5-10 knots), the vessel must steam with the wind from behind when trawling. Accordingly the reverse traverse of the swarm is used to recheck the position of the swarm (which may be moving) and the optimum direction for towing; attempts are made to avoid the previous trackline when re-towing, as passage of the vessel tends to disperse the krill, although this can be difficult if the swarm has moved, and demarcation of the line may be problematic as air bubbles from the original tow vanish within 15 minutes. [The Soviet operations differ in this respect; their net design allows for faster towing at 4-5 knots, and they are less influenced by wind factors.]

In the initial part of the fishing season - until late December - krill swarms tend to be small and catch rates low. In the high season from late December to the end of February, the number of swarms and their sizes increase, and catch rates are high. In March icing starts, and after sunset the krill swarms rise to the surface and disperse with a consequent large drop in catch rates. The fishing takes place 24 hours a day, until later in the season when there is a period of darkness.

The records kept of the fishing operation distinguish between "patches" and "layers" (Japanese terminology); the separation is based on the ratio of vertical to horizontal dimensions of the aggregation - greater than 0.2 for a "patch", and less for a "layer". However either of these categorisations would seem to be "swarms" in the sense of Butterworth and Miller (1987). The larger dispersed "layers" [as defined by Butterworth and Miller (1987)] were indicated to be very common (though less so in the Scotia Sea), but their densities are too low to render fishing on them an economic proposition. Nevertheless, it is believed that these layers comprise a considerable fraction of the total krill biomass; since it seems that this component will not be sampled by the fishing vessels, some attention should perhaps be given to the possibilities of monitoring it during research activities.

Only one of the Captains with whom discussions were held, had experience of fishing on a super-patch (off the South Orkney islands during the 1985/86 season). Another stated that most super-patches were reported in the area off Enderby Land. From comments in Ichii (1985), it seems that the main difference in operational procedures when fishing on a super-patch, is the major reduction of the proportion of time spent actively searching.

3.3 Quality Aspects and "Green" Krill

Six types of products are prepared on the krill trawlers. Dried krill and boiled-and-peeled krill are very rare - the latter was only produced on an exploratory basis. Meal production is now increasing. The three major products are boiled-and-frozen krill (for human consumption), fresh-frozen krill (used as fishing bait and for food in rearing fish, though a part is used to produce a seasoning liquid for human consumption), and fresh-peeled krill consisting of the tail portion only (for human consumption). Processing constraints differ for the various products: fresh-frozen krill must be processed within 2-3 hours of capture, whereas peeled or boiled-and-frozen krill can wait for 3-4 hours.

The size of the krill is categorised by length class: LL (larger than 45 mm), L (between 35 and 45 mm), and M (below 35 mm in length). The largest size class has been targeted throughout the history of the fishery. This is because it is easier to peel, and the larger sizes are preferred both for human consumption and for use as bait.

However, in the course of time certain other important consumer preferences have developed. Over the past two years there has been a Government campaign to promote human consumption of krill, and the market has developed a clear preference for firm rather than soft krill.

The most important quality consideration though is (avoidance of) "green" krill. "Green" krill have been feeding intensively on phytoplankton, which accumulates in the head section (specifically in the hepatopancreas inside the carapace). This is of no relevance if fresh-peeled krill (or meal) is being produced, but "green" krill are actively avoided if the other two major products are required because they are dirty in appearance, smell bad on cooking, and are inferior in taste. The smaller sized krill tend to be less "green", so that L and M size classes may be fished preferentially if "green" krill are abundant. Egg-carrying females may also be sought in such circumstances, as this diminishes the greenish appearance.

Avoiding "green" krill was not always a feature of the fishery. The first season it became a factor was 1978/79. However, not all companies involved became concerned about this aspect simultaneously. A survey of the companies (Shimadzu, pers. commn) has indicated a steady progression with time in the number of companies taking "greenness" into account, with the final company joining this list as recently as the 1985/86 season; the market preference for "white" krill is now very strong. The first haul made by a vessel on moving to a new area is often small to provide a sample test for quality (both size and colour).

"Green" krill is more prevalent in the Scotia Sea than off Wilkes Land. It is more likely to be found early in the season, and closer inshore in relation to the Scotia Sea islands (possibly a consequence of upwelling). Swarms of krill in the Scotia Sea were reported usually to be close inshore and "green".

It seems very likely that any model of an individual trawler's operation would have to allow for change with time as krill "greenness" has become more relevant. Catch-length based analyses may also be affected, with age-specific-selectivity patterns influenced by this factor. Even though all the companies participating in the fishery are now "green" - sensitive however, this is not a constraint for all vessels at all times - it depends on the product(s) required on a particular day. For example, one multi-vessel company had one of its vessels dedicated to fresh-peeled krill production throughout the 1985/86 season, for which "greenness" would have been of no concern.

The data-base contains records of daily krill production by size category and product-type, though no details of "greenness". There seems to be a need to examine whether CPUE measures are substantially affected by desired-product-related targeting, and whether the existing data is adequate to allow targeting to be inferred - if not, a request might need to be made to consider possible routine recording of product-related targeting and "greenness" in future.

3.4 Cooperation with Other Vessels

The role of cooperative inter-vessel communication in determining fishing patterns is important to establish. The average time it takes to find a new swarm or new concentration upon which to trawl, may be an important contributing index in monitoring krill abundance trends (see Section 4.3); but this only applies to independent searching, which is quite different from moving directly to a high density region under the specific direction of another vessel already fishing there. Models of the fishing operation may yield very different results depending on the extent of such cooperation.

The Captains advised that during the first four seasons of the commercial fishery (essentially the operations off Enderby Land), there had been very frequent communication between the vessels, essentially to speed the development of expertise as all were then "new boys".

However the situation has since changed, and because of competition between the fishing companies, it seems that as a general rule there is no active communication between vessels from different companies. In contrast, vessels from the same company communicate and cooperate very closely - one company advised their vessels usually operate within sight of each other. The vessels from the company that also conducts whaling operations maintain close contact with the whaling fleet, which provides information on oceanographic conditions which may favour krill fishing as well as data on krill quality (size class) from minke whale stomach content inspection.

While the distinctions just indicated seem to be the case on a "microscale", and probably provide an appropriate basis for the stratification of data from various vessels in initial modelling exercises, they should not be understood to imply that vessels from different companies are kept completely ignorant of the activities of each other. The Captains advised that they are eager to collect information from other companies on catch rates and catch compositions (size and quality) in previous seasons. While fishing is in progress, general information about whether an area is good or bad for catching may be passed on if vessels accidentally approach each other, or hints of appropriate areas to which to move may be relayed to vessels following communication between company offices in Japan. The vessels are aware of each other's approximate positions, and may consult with others before deciding whether to move east or west in searching for a new fishing area. "Areas" in this sense may be typically of the order of 100 n.miles apart, i.e. reflecting different "concentrations" as the term is used in this document.

Ichii (1987), following observations on a krill trawler off Wilkes Land, reports that communication with another vessel (from a different company in this instance) was the primary determinant of fishing area location in about 20% of cases - a not insubstantial proportion.

3.5 Macroscale Ground Selection

Ichii (1987) contrasts the features of the fishing grounds in the Scotia Sea and off Wilkes Land. In broad terms, the quality of krill off Wilkes Land is better: there is less "green" krill, and the krill tend to be transparent and firm rather than of red-pink colour and soft, so that processing of the fresh-frozen product need only be completed in 3 hours, compared to 2 hours in the Scotia Sea. By-catches of salps and of fish larvae are also problems in the Scotia Sea.

In this context, the almost complete transfer of effort from off Wilkes Land to the Scotia Sea over the past few years may seem surprising, but has been brought about for more important logistic/economic reasons. Recent increased product demand has been primarily for peeled krill, for which "greenness" is not relevant; and the better catch rates (and also larger sized krill) in the Scotia Sea compared to those off Wilkes Land are important favourable factors.

The profit levels in the krill fishery are not high, so that cost-reducing strategies are adopted. The various companies' vessels operating in the Scotia Sea generally share the same freezer-cargo ship, reducing the options for more widespread operation. (The whaling factory ship is used in this capacity off Wilkes Land). In earlier years many of the trawlers were based in Japan, so that the grounds off Enderby and Wilkes Lands involved the least transit times. Now most of the vessels involved are engaged in other fishing activities off New Zealand, Africa and South America over the remainder of the year (for example, squid fishing off the Falklands/Malvinas); the vessels are based in foreign ports (in Chile, for example) so that fishing in the Scotia Sea for krill becomes a much more practical proposition.

4. THE RELATION BETWEEN CATCH RATES AND ABUNDANCE

4.1 The Utility of Catch-per-Haul and Catch-per-Towing-Time Indices

Catch-per-day holds little promise as a krill abundance indicator, because of limitations imposed by vessels' processing capabilities. Also it seems very clear that Catch-per-Haul will not constitute a usable index in monitoring abundance trends. When vessels move to a new area, the first haul is usually deliberately small, as the immediate concern is to determine the quality of the krill at that location. But more importantly, hauls are generally kept to a maximum of 5-10 tonnes (assessed while towing by use of net sounders). This is for two reasons: product quality suffers in larger hauls because the krill is crushed, and operations need to be linked to the vessel's processing rate capabilities. Thus Catch-per-Haul exhibits a form of gear saturation.

Gulland's (1985) initial impression of the Japanese krill fishery was that it was rather similar to demersal trawlers operating on dispersed fish, and that fishing on a single swarm was far from being the standard practice. Accordingly he concluded that Catch-per-Towing-Time might give a fair index of krill density over a wide area. In consequence Butterworth and Miller (1987) suggested that Catch-per-Towing-Time would index within-concentration krill density ($d_sA_s\delta_{ks}$) rather than within swarm density (δ_{ks}) alone.

However, following discussions, the author suspects that this conclusion may be incorrect. Shimadzu (1984) reports the average number of swarms trawled per haul as 1.5. One company advised that a single swarm was generally adequate to obtain the maximum catch required in a single haul (though also quoted the South Shetland Islands area in 1985/86 as an exception); another advised that about 80% of hauls in the high season were made on a single swarm alone. Clearly this needs to be investigated in detail by analysis of the Japanese krill data base, but the immediate implication seems to be that Catch-per-Towing-Time will provide only an index of within swarm density (δ_{ks}) - the data base contains records of the number of swarms trawled each haul, so that multi-swarm tows could be excluded when making such a calculation.

The situation may be different in the earlier part of the season when swarms are smaller, and hauls tend rather to traverse a number of swarms. Sonar (forward range 1/2-1 km) is used to detect swarms ahead of the vessel. Responses differed as to the strategy adopted if no further swarms were immediately visible on the sonar once towing through a particular swarm was complete: some advised it was more efficient to keep towing the net in such circumstances; others stated that in areas with a small number of swarms, it was preferable to increase the number of hauls rather than keep the net in the water. The latter instance would complicate interpretation of Catch-per-Towing-Time as an index of within-concentration krill density ($d_s A_s \delta_{ks}$).

Even if this measure could be used to index $d_s A_s \delta_{ks}$ in the earlier part of the season, this may nevertheless prove to be of limited utility. One company advised that operations are now being concentrated in the high-season (January-February), primarily to maximise efficiency by taking advantage of higher catch rates at that time. Thus in future years, data pertinent to the early part of the season may well be very sparse.

Accordingly the existing data collection procedures seem likely only to provide an index of within-swarm krill density (δ_{ks}), through Catch-per-Towing-Time. While searching time measures may allow monitoring of average swarm density within a concentration (d_s) (see Section 4.3), a concern is that this would nevertheless leave average swarm area (A_s) unmeasured (in the high season maximum haul sizes apparently usually being obtained, and nets being raised, before the whole swarm has been traversed).

4.2 Reasons for Vessel Movement

If the density of swarms within a concentration (d_s), or the density of concentrations (D_c), are to be indexed by operational data other than Catch-per-Towing-Time, it is important that the various reasons that may lead to movement of a vessel be appreciated. Accordingly one question asked of the Captains was what were the main determinants of a decision to move to another "area" to fish. Although the question was intended to apply both to within-concentration and between-concentrations scales, the author suspects that most of the comments made were more applicable to the latter.

The principal consideration appears to be an economic one. However, comments differed as to whether catch rate or krill quality (white rather than green, large size class, and avoidance of by-catch of salps and/or fish larvae) was the dominant factor in the economic equation. This must depend on the final product required, which may differ from vessel to vessel, and even for the same vessel at different times of the season. If catch rate or quality (whichever is relevant at the time) is satisfactory, a vessel will attempt to keep track of the swarm while completing processing to allow for subsequent re-towing, but will otherwise undertake searching for new swarms.

Bad weather also plays a role; the low power of vessels restricts their ability to catch in adverse conditions (see Section 3.2), so they will move to avoid these unless the area being fished is particularly good. Further, poor weather is often accompanied by a change in the distribution of the krill swarms, so that searching may have to be started anew once such periods are over, although the echosounder is monitored continually through these periods despite towing being impossible.

Communication with other vessels (see Section 3.4) can lead to a decision to move to another area. Also movements must take into account the need to transfer catch and take on fuel and water from a freezer-cargo vessel (or whaling factory ship for some vessels) - this occurs typically 5 times for a vessel during one krill fishing season. The opening strategy is often to move to an area where good catches were made the previous season, although locations favoured by krill can change from year to year.

From observations made aboard one particular vessel, Ichii (1987) lists the following relative frequencies of reasons to move to new fishing areas:

Areas that provided good yields the previous season:	34%
Communication with other vessels:	22%
Return to areas previously located that season (in the hope, perhaps, of quality improvement):	22%
Cues to krill concentrations (e.g. ice conditions, predators)	22%

The reason for leaving an area during the period of these observations was usually poor catch rates.

Ichii (1985) provides an example of fishing on a super-patch. Vessel movement on that occasion appears essentially to have involved no more than maintaining contact with the super-patch in its counter-migration against the current.

4.3 Time Budgeting and Search Time

As discussed in Section 4.1, it appears that in the high season for krill fishing, Catch-per-Towing-Time is likely to relate only to the average density of krill within a swarm (δ_{ks}), rather than the product $d_s A_s \delta_{ks}$ representing the density of krill within a concentration of swarms. Some index is needed of the density of swarms within a concentration (d_s) (as well as, if possible, the density of concentrations, D_c). For example, one company stated that in the vicinity of the South Orkney islands in the 1985/86 season, although the within swarm density was very high, the number of swarms per unit area had been rather low; thus Catch-per-Towing-Time alone might give an over-optimistic impression of the krill abundance in that area on that occasion.

Measuring the search time to find swarms could provide an index of d_s (and also possibly D_c). Certainly a large fraction of operational time is spent searching, and the Captains emphasised that the echosounder is watched all the time (even when transferring cargo). One Captain (who had previous experience of the time budget data recorded in whaling operations) had had his quartermaster keep records in a notebook on a similar basis over the krill fishing season. His vessel's time had been divided as follows:

Searching:	45%
Net handling (entry to and withdrawal from water):	24%
Towing:	18%
Idling (due to bad weather, engine kept going):	6%
Transferring cargo:	4%
Drifting (engine stopped):	3%

Note: (a) The searching time above was not measured directly, but was obtained by subtracting the time spent on other activities from the total operation time. It includes both "primary" and "secondary" searching (as defined subsequently in this section).

(b) The towing time refers only to when catching is taking place, as indicated by the net recorder; about 1.5% of the total time was spent adjusting the net to the desired water depth, and this is included in the searching time above. Drifting occurs for several reasons, for example engine repair; only a small proportion of this time corresponds to waiting to end processing (without searching) because swarms are known to be in the area.

This indicates that the great majority of the time is spent in searching and net handling. A Captain from a different company independently offered this comment, although not possessing as detailed quantitative data.

However, the definition of searching is not as straightforward as the tabulation above suggests, in particular since it is only the “primary searching” component of this time relating to finding a new swarm (or new concentration) that is relevant as an index of d_s (or D_c). Ichii (1987) comments that while searching time is almost equivalent to the time between finishing one haul and starting the next in low density areas, definition becomes very difficult in higher densities when the constraint imposed by processing time requirements delays the onset of further trawling. Sometimes the trawl net may be deliberately kept under water until processing of the catch from the previous tow has been completed. Also Ichii (1985) suggests that judgements that repeated towing on a patch is taking place (such data has been recorded since 1984/85) may not be entirely reliable.

The Captains, while appreciating the relevance of a measure of primary searching effort, were doubtful how practical it would be to record this. One problem (unlike in the case of whaling) is that it would not always be possible to decide easily and unequivocally what a vessel's primary activity was at a particular time. Further, it was stressed that the quartermaster already has considerable data recording duties to which to attend, and would not welcome further work; this aspect has to be kept in mind, as unrealistic further requests of the crews may lead only to a decline in data quality.

Nevertheless because of the importance of this issue, two experimental recording procedures were discussed with Dr Shimadzu and his colleagues, and Dr Shimadzu was to investigate further whether it might be possible to implement them during the 1986/87 season. (Shimadzu, pers. commn, advises that some trial recordings similar to those discussed below were duly made.)

The first was to request all vessels to keep a record of the start and end times of periods of "primary searching effort" during a limited period of the fishing season (mid-January to mid-February during the high season was suggested). "Primary searching" was defined as the time spent looking for a new swarm on which to trawl, and excluding time spent preparing to tow again on the same swarm or to complete processing after a new swarm had been found. It would be requested that if there were periods when the crew was too busy to record this information, they note such times on the forms to be provided. The objective of this exercise was to serve as a feasibility study of whether primary searching information could be collected in practice and would prove suitable for use in calculations.

The second experiment would involve a request to the company whose vessel had collected time budget data previously (as summarised above) to continue this exercise using a form that would facilitate subsequent encoding and analysis of the data. This would constitute continuous recording of the vessel's operational activity. In discussion with Dr Shimadzu and colleagues after the meetings with company personnel, the following provisional list of activities was constructed:

(I) Searching:

  (a) Primary searching:

    (i) Searching for new swarm within concentration
    (ii) Searching for new concentration (undirected)
    (iii) Searching following external communication
    (iv) Searching in transit to/from cargo transfer

  (b) Secondary searching:

    (i) Confirming swarm dimensions after finding it
    (ii) Searching for swarm just trawled to trawl again
    (iii) Maintaining contact with swarm until processing ends

(II) Net Handling:

  (a) Net entering water
  (b) Aiming net to correct depth
  (c) Withdrawing net from water onto deck

(III) Towing (actively fishing)

(IV) Idling (due to bad weather)

(V) Transferring cargo

(VI) Drifting (engine off):

  (a) Drifting while finishing processing, with swarms in the area
  (b) Drifting because of bad weather
  (c) Drifting for other reasons (e.g. engine repair).

The objective of this was again a feasibility study of the practicality of collecting such information. The resultant data could be used, for example, to develop a model such as that of Cooke and Christensen (1983) to assess the magnitude of possible non-linearities in the CPUE-abundance relation arising from catchability fluctuations.

4.4 Large-scale Density Trends

Another component in the expression to calculate total krill abundance is the total management area (A_t). A concern is that changes in total abundance could be reflected mainly by expansions or contractions of the overall extent of the krill concentrations, rather than in the smaller scale features [such as within-swarm density (δ_{ks})] to which indices discussed earlier would relate (Butterworth and Miller, 1987). Information on larger-scale trends in krill density is therefore of interest.

The close vicinity of the continental ice-edge was not regarded by the Captains as necessarily a preferred area to catch krill, but this must be considered in the context that drifting ice is avoided because of the danger of damage to the fishing gear. One strategy when new concentrations are sought, is to move to the ice-edge and then search northwards, which is suggestive of a large-scale general fall-off in density moving away from the ice.

A feature mentioned more than once is that krill remains within the cold water masses as the ice retreats in the early stages of the season, so that fishing tends to move closer to the continent with time. The prospects that a routine monitoring of oceanographic features might provide an annual index of the overall krill distributional area perhaps merit attention.

In the Scotia Sea, most fishing is carried out within sight of an island. Islands can be approached to within 1/2 n.mile for fishing, but the nearer regions tend to be avoided because of the greater likelihood of encountering "green" krill. Fishing extends to about 30 n.miles from shore in the South Orkneys, and as far as 80 n.miles in the South Shetlands. The Captains could not suggest any general trend in density within these areas, though a belief was expressed that krill were rather far from the islands at the start of January, and tended to move closer as the season progressed. However, the distribution in the zone between the South Shetlands and South Orkneys was described as very sparse, suggesting that there must be a fall off in density once a certain distance from the islands is exceeded.

4.5 The Choice of a Data Sample for Further Studies

The CCAMLR Scientific Committee has requested that Japan make available a sample of the detailed data that has been collected on their krill fishing operations, to facilitate further investigations in this study. In choosing such an initial sample, the primary consideration was to search for a vessel whose operation was categorised by as few complicating factors as possible. Any initial model of the fishing operation needs to be kept simple; the data choice strategy was intended in that sense, to enhance the possibility of identifying the basic features of the operation - attempts to take account of complicating factors can be made later.

The sample chosen comprised the operation of a particular vessel off Wilkes Land in the 1980/81 and 1981/82 seasons. The vessel is only slightly larger than the average, both in terms of size and its harvest in each of the two seasons. Also the nets used by the vessel were virtually identical over the two seasons. The vessel's parent company had previous Antarctic krill fishing experience prior to the 1980/81 season.

There are several advantages to this particular choice:

(i) This was the only vessel operated by its parent company over those two seasons, so that searching behaviour was probably influenced relatively little by inter-vessel communication.

(ii) The parent company indicates the "green" krill catch quality aspect was not a factor it took into consideration until some years after these two seasons.

(iii) The vessel fished for a lengthy period in both seasons (about 3.5 months - late November to mid-March - in each case), which allows scope for inter-month comparisons.

(iv) Another vessel from the same company fished in the same area in 1982/83 - this allows for further comparisons in future work.

(v) The area off Wilkes Land does not have the complications of the numerous islands of the Scotia Sea; krill distribution and fishing patterns in the Scotia Sea seem to be closely linked to these islands, which would complicate modelling.

(vi) There is a longer history of Japanese operations off Wilkes Land compared to the Scotia Sea.

However the choice also has some disadvantages:

(i) The great majority of current Japanese krill fishing takes place in the Scotia Sea, rather than off Wilkes Land as previously.

(ii) Little of the fishing area off Wilkes Land was surveyed by research vessels in the FIBEX and SIBEX programmes.

(iii) Records have been kept of whether a tow was on a new swarm or repeated on the same swarm - but only from the 1984/85 season. Such data would be useful for modelling.

Consideration was given to choosing the vessel for which certain time-budget data had been collected (see Section 4.3). However it was felt that this was offset by the complications of that vessel's searching behaviour being influenced by communication with the whaling fleet, and being sensitive to a certain extent to "green" krill quality considerations.

5. SUMMARY OF CONCLUSIONS

(a) Investigations of the Japanese krill fishery should concentrate on the analysis of individual vessel activities. The mothership-type operation was complicated by processing constraints, would be difficult to model, and seems unlikely to be repeated in the immediate future.

(b) Catch-statistics analysis will be concerned with fishing on concentrations of swarms. Super-patches seem to be relatively rare. Layers of krill are of densities that are too low for fishing to be economic; consideration should be given to the possibilities of monitoring these layers during research activities.

(c) It seems likely that future krill fishing will be concentrated in the January-February "high-season" period, which yields the best catch-rates. Modelling should therefore concentrate on the circumstances typical of this period.

(d) Processing rate limitations are a major feature of the krill fishery, so that Catch-per-Day indices are unlikely to relate to abundance.

(e) Product quality considerations lead to haul sizes being restricted, so that Catch-per-Haul is not a reliable index of abundance.

(f) Advice was that most tows in the high-season are completed before the first swarm fished has been traversed completely. This merits checking against available data, and would imply that Catch-per-Towing-Time is likely to index only within-swarm density (δ_{ks}).

(g) Primary search time information (pertaining to finding a new swarm) would be desirable to obtain to attempt to index within concentration swarm densities (d_s), and perhaps also the density of concentrations (D_c). However, there are practical and definition difficulties in recording such data. Some feasibility experiments in this regard may be attempted (and were indeed subsequently instituted, Shimadzu, pers. commn). Other important difficulties for analysis of this aspect are:

   (i) The overall krill distribution is non-random; there are favoured areas, possibly linked to oceanographic features.

   (ii) There is communication between vessels. Vessels from the same company cooperate very closely, but on the other hand communication between vessels from different companies is very limited.

   (iii) Searching often has to start "*ab initio*" after bad weather.

   (iv) Over the years, market preference development has led to an increasing tendency to avoid catching "green" krill, unless the fresh-peeled product is required. Analysis should attempt to determine the extent to which this influences various CPUE measures, and whether routine recording of "greenness" and product-targeting is needed. This aspect of the fishing strategy may also have implications for catch-length-frequency-based assessment methods such as Virtual Population Analysis.

(h) A concern is that high-season catch rates and associated data seem unlikely to index average swarm area (A_s) (see 6. above), or the average area of a concentration of swarms (A_{cs}).

(i) There are indications that (in a very broad sense) krill density falls-off moving north from the continental ice-edge, and away from island coastlines in the Scotia Sea. The possibility of routine oceanographic monitoring being used to demarcate and so index the extent of the krill distribution (reported to remain within the cold water masses as they retreat during the fishing season) should be investigated.

(j) Data from an individual vessel which operated off Wilkes Land in the 1980/81 and 1981/82 seasons have been selected for initial study; the choice was aimed at an operation affected by as few complicating factors as possible, to simplify initial modelling attempts.

ACKNOWLEDGEMENTS

The willing cooperation I received from all parties, and the hospitality extended to me during the period of the discussions reported above, can only be described as outstanding. My thanks are extended to all who participated in the discussions - their names are listed in the Appendix detailing my schedule. In particular I must thank Mr Kumatani and Dr Shimadzu who made the arrangements for the various meetings, and Dr Shimadzu for his sterling efforts as a translator throughout long periods of discussions with the representatives of the various fishing companies. Documents and written information prepared by Mr Ichii and Dr Shimadzu proved extremely helpful in compiling this report. Dr Shimadzu also kindly checked an earlier version of the text, and a number of his comments have been incorporated. Financial support during the period of these discussions was provided by CCAMLR; my travel costs to Japan had been covered by the International Whaling Commission to attend an IWC Meeting immediately preceding this period.

REFERENCES

BUTTERWORTH, D.S. 1988. A simulation study of krill fishing by an individual Japanese trawler. This volume.

BUTTERWORTH, D.S. and D.G.M. MILLER. 1985. A note on relating Antarctic krill catch-per-unit-effort measures to abundance trends. S. Afr. J. Antarct. Res. 17(2): 112-116. (Earlier version circulated as CCAMLR Document KRILL WG/1985/DOC.3, 15 pp.)

COOKE, J.G. and I. CHRISTENSEN. 1983. A model of the operation of the Norwegian whale fishery in the Barents Sea. IWC Document SC/35/Mi3, 7 pp.

GULLAND, J.A. 1985. Krill - Catch per unit effort. CCAMLR Document KRILL WG/1985/DOC.2, 4 pp.

ICHII, T. 1985. Some aspects of repeated operation on the same patch in Japanese krill fishery. CCAMLR Document KRILL WG/1985/DOC.6, 6 pp.

ICHII, T. 1987. Observations of fishing operations on a krill trawler and distributional behaviour of krill off Wilkes Land during the 1985/86 season. Selected papers presented to the Scientific Committee of CCAMLR 1987: 337-368.

SHIMADZU, Y. 1984. A brief summary of Japanese fishing activity relating to Antarctic krill, 1972/73 - 1982/83. Selected papers presented to the Scientific Committee of CCAMLR 1982-1984 Part I: 439-452.

SHIMADZU, Y. 1985. An updated information of the Japanese krill fishery in the Antarctic. CCAMLR Document KRILL WG/1985/DOC.5, 7 pp.

SHIMADZU, Y. and T. ICHII. (1985). Some considerations on the usefulness of CPUE data from Japanese krill fishery in the Antarctic. CCAMLR Document KRILL WG/1985/DOC.4, subsidised.

SC-CAMLR-VII/BG/12

ANALYSIS AND MODELLING OF THE SOVIET SOUTHERN OCEAN KRILL FLEET

M. Mangel

Abstract

The first part of this document contains an analysis of data pertaining to the Soviet krill fleet. The data base consists of the records of 12 different cruises by 8 different research vessels between 1981 and 1984. The data are analyzed according to operational characteristics of the fishing process such as trawl duration, krill catch, or between trawl movement. Correlation analyses are presented as a means of understanding the within trawl and between trawl features of the operation. The data support the notion of a "patches within patches" model for the distribution of krill in the southern oceans.

The second part of this document contains the development and use of a simulation model of a Southern Ocean krill fleet. The objective of the work is to answer questions such as: what information do catch and effort data provide about krill abundance or how easily can significant changes in krill biomass be detected? The krill distributional model begins with individual krill which are assumed to aggregate into swarms of krill. The swarms then aggregate into concentrations, which are the foci for the fishing operation. Parameters of the model are motivated by study of the literature and FIBEX results. A model is developed for a survey vessel that does no fishing, but simply locates concentrations of krill for the fishing fleet. The fishery model involves finding concentrations, finding swarms within concentrations and fishing individual swarms. Wherever possible, operational data from Part I are used to provide distributions in Part II. General considerations about the theory of abundance indices for pelagic, schooling species are discussed. In particular, the importance of the time spent searching for swarms is highlighted. A theory for detecting changes in krill biomass is developed. Forty-four different abundance indices are considered and their effectiveness in detecting changes in krill biomass is studied. The best indices involve two separate measures: one in which survey vessel discoveries are used to track the number of concentrations and a measure of the form catch/swarm/search-time to track swarm density within concentrations and krill density within swarms. Operational recommendations are given: (i) I propose an experiment in which survey and fishing vessels operate simultaneously but independently in the same region, (ii) I recommend that fishing vessels begin to indicate in their log books the amount of between trawl time spent searching, (iii) I propose that CCAMLR consider sending a Ph.D. level modeller to sea in order to develop a truly operational model of the fishing process, and (iv) I propose abundance indices that could be used to track krill biomass.

Résumé

La première partie de ce document contient une analyse des données concernant la flottille de pêche au krill soviétique. La base de données

consiste de registres de 12 campagnes d'étude différentes menées par 8 navires de recherche différents entre 1981 et 1984. Les données ont été analysées selon les caractéristiques d'opération du processus de pêche, tels que la durée du chalutage, la prise du krill, ou les déplacements entre chalutages. Des analyses de corrélation sont présentées comme moyen de compréhension des caractéristiques de l'opération pendant les chalutages et entre les chalutages. Les données corroborent la notion d'un modèle de "regroupements à l'intérieur de regroupements" pour la distribution du krill dans les océans australs.

La seconde partie de ce document contient le développement et l'utilisation d'un modèle de simulation d'une flotille de pêche au krill dans l'océan austral. L'objectif de ce travail est de répondre aux questions telles que: quelles informations sont fournies par les données de capture et d'effort sur l'abondance du krill, ou avec quelle facilité peut-on détecter des changements importants dans la biomasse du krill? Le modèle de distribution du krill commence avec le krill individuel, que l'on présume se concentrer dans des essaims de krill. Les essaims se regroupent alors en concentrations qui sont les objets de l'opération de pêche. Les paramètres du modèle sont motivés par une étude de la littérature et des résultats de la FIBEX. Un modèle est développé pour un navire de recherche qui ne pêche pas, mais détermine simplement la position des concentrations de krill pour la flotille de pêche. Le modèle de la pêcherie implique la localisation des concentrations et des essaims à l'intérieur des concentrations, et la pêche des essaims individuels. Partout où cela est possible, des données sur les opérations de la première partie sont utilisées pour fournir les distributions dans la partie II. Des considérations générales en ce qui concerne la théorie des indices d'abondance pour les espèces pélagiques grégaires sont discutées. En particulier, l'importance du temps passé à la recherche des essaims est soulignée. Une théorie sur la détection des changements de la biomasse du krill est développée. Quarante-quatre indices d'abondance différents sont considérés et leur efficacité dans la détection des changements dans la biomasse du krill est étudiée. Les meilleurs indices entraînent deux mesurages séparés: l'un où les découvertes faites par le navire de recherche sont utilisées pour contrôler, de façon continue, le nombre de concentrations, et un mesurage de capture/essaim/temps de recherche pour un contrôle suivi de la densité des essaims à l'intérieur des concentrations et la densité du krill au sein des bancs. Les recommandations opérationnelles données sont les suivantes: (i) je propose une expérience où les navires de recherche et de pêche opèrent simultanément mais indépendamment dans la même zone, (ii) je recommande que les navires de pêche commencent à indiquer dans leurs journaux de bord le temps entre chalutages passé à la recherche, (iii) je propose que la CCAMLR envoie en mer un modeleur d'un niveau de doctorat afin de développer un modèle vraiment opérationnel du processus de pêche, et (iv) je propose des indices d'abondance qui pourraient être utilisés pour déterminer, d'une manière continue, la biomasse du krill.

Резюме

Первая часть данного документа содержит анализ данных, относящихся к советской промысловой крилевой флотилии. Данные основаны на результатах 12 различных рейсов 8 разных научно-исследовательских судов в период между 1981 и 1984 г. Данные проанализированы в соответствии с фактическими характеристиками, такими, как длительность траления, улов криля, или время между тралениями. Корреляционный анализ представлен как ключ к пониманию характеристик операции во время траления и между тралениями. Данные подтверждают идею модели "пятно в пятне" распределения криля в Южном океане.

Вторая часть этого документа включает развитие и использование моделирования южноокеанской промысловой крилевой флотилии. Цель работы заключается в ответе на следующие вопросы: какие выводы можно сделать на основании данных по улову и промысловому усилию о численности криля и о том, насколько легко можно обнаружить значительные изменения в биомассе криля. Первичным звеном в модели распределения криля являются отдельные экземпляры криля, которые образуют скопления. Скопления образуют концентрации, которые являются центром промысловой операции. Параметры модели зависят от изучения опубликованных результатов и результатов программы "FIBEX". Модель разработана для поискового судна, не занимающегося промыслом, но ведущего поиск концентраций криля для рыболовных судов. Модель промысла включает нахождение концентраций, нахождение скоплений внутри концентраций и промысел отдельных скоплений. Где возможно, фактические данные из Части 1 использованы в Части 2. Обсуждены основные аспекты теории индексов численности пелагических стайных видов. В частности придается большое значение времени, потраченому на поиск скоплений.Разработана теория выявления изменений в биомассе криля. Рассмотрены сорок два различных индекса численности и изучена их эффективность в выявлении изменений в биомассе криля. Наилучшие индексы состоят из двух отдельных частей: первая - когда результаты работы поискового судна используются для выявления количества концентраций и вторая часть по форме улов/скопление/время поиска заключается в выявлении плотности скоплений внутри концентраций и плотности криля внутри скоплений. Даны следующие оперативные рекомендации: (i) я предлагаю эксперимент, в котором поисковые и рыболовные суда работали бы одновременно, но независимо друг от друга в одном и том же районе, (ii) я рекомендую, чтобы рыболовные суда начали отмечать в судовом журнале количество времени поиска между тралениями, (iii) я предлагаю, чтобы CCAMLR рассмотрел возможность направления специалиста по моделированию на уровне доктора наук в морскую экспедицию для того, чтобы разработать полностью действующую модель процесса промысла, и (iv) я предлагаю, чтобы индексы численности использовались для выслеживания биомассы криля.

Resumen

La primera parte de este trabajo contiene un análisis de los datos relacionados con la flota de krill de la Unión Soviética. La base de datos se compone del registro de 12 cruceros diferentes realizados por 8 buques de investigación entre 1981 y 1984. Se analizan los datos según las características operativas de proceso de pesca, tales como duración del arrastre, captura de krill o movimientos entre arrastre.

Los análisis de correlación se presentan como un medio para entender las características de la operación durante el arrastre, y entre un arrastre y otro. Los datos corroboran la noción de un modelo de "manchas dentro de manchas" en la distribución del krill en el Océano Austral.

La segunda parte de este trabajo contiene el desarrollo y utilización de un modelo de simulación para una flota de krill en el Océano Austral. El objetivo del mismo es responder a cuestiones tales como: ¿Qué información proporcionan los datos de captura y esfuerzo sobre la abundancia del krill? o ¿Con qué facilidad pueden detectarse cambios significativos en la biomasa del krill? El modelo de distribución del krill se inicia con krill individual que se supone se concentra en cardúmenes. Los cardúmenes forman a continuación concentraciones, las cuales son el objetivo de la operación de pesca. Los parámetros del modelo se fundamentan en el estudio de la documentación existente y en los resultados de FIBEX. Se desarrolla un modelo para un buque de investigación que no faena, sino que solamente localiza concentraciones de krill para la flota pesquera. El modelo de pesca implica la búsqueda de concentraciones, de cardúmenes dentro de concentraciones y la pesca de cardúmenes individuales. Siempre que es posible, los datos oeprativos de la Parte I se emplean para proporcionar distribuciones en la Parte II. Se discuten las consideraciones generales sobre la teoría de los indices de abundancia para especies pelágicas que se agrupan en bancos. Se destaca, en particular, la importancia del tiempo empleado en la búsqueda de cardúmenes. Se desarrolla una teoría para detectar cambios en la biomasa del krill. Se consideran cuarenta y cuatro índices de abundancia, y se estudia su efectividad a la hora de detectar cambios en la biomasa del krill. Los mejores índices requieren dos medidas distintas: una en la que se utilizan los descubrimientos del buque de investigación para rastrear el número de concentraciones, y otra sobre la forma de la captura/cardumen/tiemp de búsqueda, para rastrear la densidad de un cardumen en las concentraciones y la densidad del krill en los cardúmenes. Se ofrecen recomendaciones operativas: (i) propongo un experimento en el cual buques de investigación y de pesca operen simultánea pero independientemente en la misma zone, (ii) recomiendo que los buques de pesca empiecen a indicar en sus cuadernos de pesca el tiempo, entre un arrastre y otro, empleado en la búsqueda, (iii) propongo que la CCRVMA considere

enviar a un modelador cualificado para que desarrolle un modelo realmente operativo para el proceso pesquero, y (iv) propongo índices de abundancia que podrían ser empleados en el rastreo de la biomasa del krill.

1. INTRODUCTION AND RECOMMENDATIONS

This document contains two distinct parts. In the first part, I present an analysis of data provided by Professor Lubimova (VNIRO Rresearch Institute, Moscow) on the Soviet krill (*Euphausia superba*) fleet. The analysis presented is based on data collected over a number of different seasons by about 10 different vessels. The second part contains a description of the krill simulation model developed in conjunction with Professor Butterworth and Dr Beddington's group in London. This document supercedes and modifies the model and results in Mangel (1987) and Mangel and Butterworth (1987).

The overall objective of this work is to provide an answer to the question: Can fishery generated data be used to monitor krill abundance? If so, what kinds of data need to be collected. Any such procedure, which is based on derived data (versus direct surveys), must also be based on the assumption that changes in abundance occur relatively quickly after periods of relative constancy. If changes occur slowly over many years or biomass fluctuates wildly from year to year, then it is unlikely, if not impossible, to detect such changes with fishery derived data.

1.1 Recommendations

Based on the statistical analysis and modelling described in the body of the report, the following three recommendations are presented:

1. Fishing and survey vessels should indicate in their log books approximately how much of the between trawl times are spent in search for swarms of krill. If possible, vessels should indicate the number of swarms fished in a haul. This would require a consistent definition of swarm (in terms of sonar ping threshold, for example).

2. CCAMLR should consider an "experiment" in which a research vessel and a fishing fleet travel together, but work independently. In particular, the fishing fleet should operate as if the survey vessel were not present, and the survey vessel should conduct krill surveys in the vicinity of regions in which the fleet fishes. By doing this, one can obtain a distributional model for krill that are considered fishable by the fleet.

3. If a detailed operational model of krill fisheries is desired, CCAMLR should consider sending a Ph.D. level modeller to sea with the fleets. This is in the best traditions of operational analysis (see, e.g. Tidman 1984) and will most likely be the only way that accurate operational models can be developed. In particular, such a field assignment will lead to accurate understanding of search operations while fishing and while not fishing and to an accurate understanding of operational fishing decisions.

4. The following indices can be used, at least temporarily, to track krill abundance:

    (a) Use the number of discoveries of fishing foci or large scale concentrations of krill by the survey vessel to track changes in the number of concentrations and the characteristic radii of concentrations.

    (b) Use one of the following indices to track within concentration changes in swarm density and krill abundance within swarms:

(Total Catch/Total Hauls) / Average {Searchtime}
(Total Catch/Swarms Fished) / Average {Searchtime}
(Total Catch/Swarms Encountered) / Average {Searchtime}.

PART I : ANALYSIS OF SOVIET DATA

2. SOVIET DATA SOURCES AND DEFINITION OF TERMS

Professor Lubimova provided a number of different sets of data obtained from research/survey vessel cruises. Table 2.1 contains a summary of the sources.

The vessels listed in Table 2.1 have similar characteristics. All except *Globus* are freezer-trawlers; the *Globus* is listed as PTMC but I could not interpret that code. The displacement of all vessels except *Globus* is about 3 800 tonnes; the displacement of the *Globus* is about 5 400 tonnes. The propulsion of all vessels except *Globus* is 2 000 horsepower; the propulsion of *Globus* is 3 880 tonnes. Table 2.2 shows net characteristics of the different vessels.

Some explanations about Table 2.1 and the associated computations are needed: (1) In the analyses described below, one degree of latitude is assumed to equal 60 n miles. and one degree of longitude is assumed to equal 30 n miles. (2) A "record" is, essentially, a trawl and concomittant information. Four different reporting methods were used, but the following information was contained in all records:

- Date
- Starting point (S,W)
- Trawling duration (starting time and ending time)
- Trawling depth
- Trawling tack
- Trawling speed (kts)
- Catch (kg) and krill catch (i.e., catch composition)

In addition, some of the data sheets contained the following information:

- Krill length (mm)
- Cloudiness (presumed to be measured in oktas)
- Wind direction and strength
- Air and water temperatures.

(3) In a few instances, multiple tacks were recorded. In such cases, the final direction was used in analysis. In a few instances multiple depths were recorded. In such cases, the largest depth was used in the analysis. Whenever a range of krill size was reported, the average was used in the analysis.

From the information contained in the data, the following quantities were constructed for each data set:

- The number of trawls per day
- Trawltime
- Trawling length
- Krill catch per trawl
- Distance moved between trawls
- Time elapsed between trawls

- Average speed of vessel between trawls (distance between trawls divided by time between trawls)
- Trawling depth
- Trawling speed
- Mean length of krill

(Some of these, obviously, need no "construction" and are simply the data entries themselves.)

For the statistical analysis reported in this part of the document, the following were computed for each of the quantities listed above:

- The mean of the quantity, over trawls within the same data set
- The standard deviation of the quantity, over trawls within the same data set
- Qualitative properties of the distribution of the quantity, particularly whether the distribution is unimodal or bimodal.

In addition, correlations between different quantities were computed. The correlation between quantity x and quantity y, denoted by r_{xy}, is defined by

$$r_{xy} = \Sigma\ (x_i - \langle x \rangle)(y_i - \langle y \rangle) \ /\ [\ \Sigma\ (x_i - \langle x \rangle)^2\ \Sigma\ (y_i - \langle y \rangle)^2\ ]^{1/2} \tag{2.1}$$

In this equation, x_i and y_i denote the values of the quantities x and y on the i^{th} trawl, <x> and <y> are the averages of the quantities x and y and the summation is taken over the trawls in the data set. The quantity r_{xy} can be considered a "same point" correlation, since both quantities are evaluated on the i^{th} trawl. A lagged correlation can be computed in a similar fashion by evaluating the quantities on different trawls. In the analysis reported here, only single lags for the correlations were considered. The lagged correlation coefficient denoted by $r_{xy}{}^{lag}$ is defined by

$$r_{xy}{}^{lag} = \Sigma\ (x_i - \langle x \rangle)(y_{i-1} - \langle y \rangle) \ /\ [\ \Sigma\ (x_i - \langle x \rangle)^2\ \Sigma\ (y_i - \langle y \rangle)^2\ ]^{1/2} \tag{2.2}$$

Although it is a mistake to interpret correlation as causation, the use of correlation coefficients allows one to make inferences about the operations of the vessel. For example, one could assume as a null hypothesis that all of the quantities listed above are independent. Suppose then that a value of the correlation coefficient r_{ob} is observed. The probability of obtaining a value of the correlation coefficient greater than or equal to r_{ob} if the null hypothesis were true is given by (Press et. al. 1985)

$$\text{Prob}\ \{\ |\ r\ | > r_{ob}\ ,\ \text{given that the null hypothesis is true}\ \} = \text{Erfc}\ (r_{ob}(N/2)^{1/2}) \tag{2.3}$$

In this equation, N is the number of trawls in the data set and Erfc(z) is the complementary error function. It is related to the cumulate normal distribution by $\text{Erfc}(z) = 2(1\Phi(z/\sqrt{2}))$, where $\Phi(z)$ is the probability that a normally distributed random variable with mean 0 and variance 1 is less than z.

3. RESULTS OF ANALYSIS OF THE SOVIET DATA

Preliminary analysis of the data showed that 11 of the 12 data sets were bimodal. For this reason, cutoff values for quantities were introduced in the course of statistical analysis.

The following cutoff values were chosen for the quantities that required them:

- Trawling depth: 250 m
- Trawling time: 4 hours
- Trawling length: 8 n miles
- Time elapsed between trawls: 40 hours
- Distance moved between trawls: 100 n miles.

Table 3.1 contains a summary of the means and standard deviations of the particular quantities. In this table, the first entry in a column is the mean and the second entry is the variance. Thus, for example, for data set 1, the mean number of trawls per day is 1.78 and the standard deviation is 0.91. If two sets of numbers are given, then the first set are the mean and standard deviation when the cutoff values were used in the computations and the second set is the mean when no cutoff was used and the number of data points greater than the cutoff. The second set of numbers is included only if there is a significant difference (at least 20%) between the mean when the cutoff value is applied and when it is not applied. Thus, for example, for data set 1 when the cutoff values are used, the mean value of trawl depth is 44.9 m and the standard deviation is 22.2; there are 4 data points greater than the cutoff value of 250 m and the mean value of trawl depth using all data points is 58 m.

In rest of this chapter, the statistical analysis of the Soviet data will be reported. Implications for modelling are described in the next chapter. The results presented in Table show that all but Data Set 6 exhibit some form of bimodality of the data. Figure 3.1 shows an example of the bimodal distribution of between trawl movement for data set 10 (which has the largest differential between mean movement when the cutoff is applied and when it is not applied). There are very many small movements - less than 10 n miles, fewer moderate movements and again many large movements between trawls.

Correlations were computed as described in the previous chapter. The correlations are presented in Tables 3.2 - 3.25. In these tables, the following notation is used:

- TT = trawling time
- TL = trawling length
- KC = krill catch
- BTM = distance moved between trawls
- BTT = time elapsed between trawls
- D = trawling depth
- L = krill length (not always available in the data).

The correlations will be presented in matrix form. Each data set has two tables associated with it: the first table contains correlation information when no cutoff values were applied in the computation of statistics and the second table contains correlation information when cutoff values were applied in the computation of statistics. Each pair of quantities in the correlation table has two entries associated with it. The upper entry is the unlagged correlation. The lower entry is the lagged correlation, with the column quantity corresponding to the i+1st trawl and the row quantity corresponding to the ith trawl. Correlations are reported according to the supposition of the null hypothesis described in the previous chapter. That is, if the value of the correlation is such that the probability of observing it when the null hypothesis is true is greater than .05, then a 0 is reported. If the probability is less than .05, then the sign of the correlation is reported. For example, for data set 1 when all data are used (Table 3.2) the unlagged correlation between trawl time and krill catch has a value such that the probability of observing it if the null hypothesis is true is greater than .05. On the other hand, the lagged correlation between trawl time on trawl i-1 and krill catch on trawl i has a value such that the probability of observing it if the null hypothesis is true is less than .05 and the correlation is positive.

When reading these tables, a number of issues should be kept in mind. First, there are obvious positive correlations. The non-lagged correlation of a quantity with itself is always 1. Second, as the number of data points increases (so that the value of N increases in Eqn 2.3) the probability that the correlation will be judged significant at the .05 level increases. Thus, data sets with many records may, in fact, have spurious correlations. Third, the presence of zeroes in the correlation matrix suggests that the trawls are independent, or at least that the quantities derived from the trawls are independent.

4. IMPLICATIONS FOR MODELLING

The results presented in the previous chapter have a number of implications for the modelling of Southern Ocean krill fisheries described in the second part of this document. Perhaps most important is the bimodal nature of the data. This bimodality, especially for between trawl times and movement, suggests that the fundamental distributional model developed in the following chapters is feasible.

It is not clear from the data analyzed thus far if the vessels used vertical echo sounders or directional sonars. Since the latter have much larger detection widths, this would impact the search process.

It is also not clear from the data how one can estimate the time in active search between trawls. One of the recommendations is that vessels record search times or estimates of search times between trawls.

It must also be kept in mind that the data analyzed here were provided by research, and not commercial fishing, vessels. Thus processing time and considerations are minimal. This may account for some of the exceptionally large trawl times and distances as well as krill catches far in excess of 10 tonnes, the limit used by Mangel (1987) and Butterworth (1987).

In some cases, the net was trawled at two, three or four depths. In the model described in the next sections, veering and hauling times are assumed to be drawn from a probability distribution characterizing depths.

PART II : SIMULATION MODEL OF A SOUTHERN OCEAN KRILL FLEET

5. OBJECTIVES AND GUIDING PRINCIPLES

The overall objective of this work is to develop a framework in which one can ask questions such as:

- What information do catch and effort data provide about abundance levels of krill. In particular, what kinds of abundance indices can be developed from data that would be generated by a fishery?
- How easily can significant changes in krill biomass be detected? In particular, what are the properties of the abundance indices? The most important properties are linearity (so that changes in abundance indices accurate reflect changes in krill biomass) and variability (so that mean changes are not swamped by variance, i.e. "noise").

The krill are fished when they are in dense aggregations, which will be called swarms in this document. The swarms are scattered over the ocean in a non-uniform manner and thus the fishing process involves search for concentrations of aggregations (fishing foci) and fishing aggregations once concentrations and aggregations within the concentrations are found. The simplest biomass estimates for krill population in swarms is:

$$\text{Total Biomass} = (\text{Number of Swarms}) \times (\text{Biomass per swarm}) \qquad (5.1)$$

and the question then becomes how one estimates both the number of swarms and the biomass per swarm.

A model of any natural system must, be necessity, be less complicated than the true system. We should strive to build sufficient realism into the model so that it captures the main features of the system of interest, but is still as parsimonious as possible. Thus, for example, the model described in this document does not attempt to simulate the entire Southern Ocean, or even a large portion of it, in the computer nor does the model simulate the decisions of skippers on a very short time scale (say 5 minutes). Instead, a relatively featureless section of ocean is considered and larger time scales for vessel motion and decisions are used. In a study such as this one, it is large qualitative changes in abundance indices that are most important for operational recommendations.

6. BASIC DEFINITIONS AND SCALES

The Southern Ocean fishery for krill is a pelagic fishery operating on dense aggregations of krill. There are many different temporal and spatial scales associated with the fishery. It is this wide variety of scales, in fact, that makes analysis of the problem as difficult as it is. Thus, it is important to consider and identify all of the the scales of interest from the outset.

To begin, there are individual krill. These organisms have a length of the order of 40-70 mm and are assumed to move at about 15 cm/sec ≈ 500 m/hr. The lifetime of a krill may be many years (Rosenberg et. al. 1986).

Individual krill aggregates into swarms of krill. In this document, a swarm is assumed to consist of krill in surface densities in excess of about 100 g/m^2, over a surface spatial extent on the order of 50 m. The swarms can be envisioned in the following way: Krill are actually distributed in an aggregation at a certain volume density (e.g. 5 g/m^3) and we "integrate" over that volume to concentrate the entire volume in a surface layer (e.g. if the volume is 20 m deep, this gives a surface density of 20 m x 5 g/m^3 = 100 g/m^2). Swarms persist on a temporal scale of at least a few days. (For the model here, swarms are presumed to persist for over the course of 14 days.) The actual operational definition of a swarm is determined by the interaction of the krill, the echosounder or sonar used to detect them, and the operator. For example, Everson (1982, Figure 1) gives excellent examples of the difference between swarms of krill at night and during the daytime. During the daytime, krill are typically "compact, discrete swarms" (Watkins 1986). In addition, Watkins et. al. (1986) report that "variability between swarms in close temporal or spatial proximity suggests that the swarm is the basic unit of organization of the krill population" .

Swarms of krill are further aggregated into concentrations or fishing foci. Concentrations are thus collections of swarms of krill over a large spatial extent, of the order of 10 nautical miles = 20 000 m (here and in the rest of this document, the conversion of 1 n miles = 2 000 m is adopted). A concentration with a length scale of 15 n miles is presumed to contain of the order of 5 000-10 000 individual swarms of krill, randomly placed within the concentration. The temporal scale of the concentration is assumed to be constant for the entire 14 day period considered in this report, although concentrations are allowed to move. The basic model thus consists of "patches within patches".

For the model developed in this document, a sector of the Southern Ocean consists of a "featureless" area of ocean 600 n miles on a side. The sector is treated as a square, so that its area, denoted by A_s , is 1.44×10^{12} m^2. In this context, featureless means that there are no large land masses in the sector and that there are no large scale oceanic currents that would move either concentrations or individual krill across the sector. Including large scale oceanic currents is a natural extension of the model and easily done. The motivation for adopting a featureless sector of ocean is the following: If catch and effort indices are not effective in detecting changes in krill biomass in a featureless ocean, they most likely will not be effective in detecting changes in krill biomass in an ocean with large land masses and currents. If the indices do appear to be effective in detecting changes, then a further modelling effort could couple many sectors by linking them with currents and adding land masses to the sectors.

Fishing for krill is done by a fleet of 5 fishing vessels, a research/survey vessel and sufficient processing vessels that backlogs do not occur. In this document, a fishing period of 14 days is considered. The fishing process consists of two main activities: search for concentrations and swarms of krill and fishing individual swarms. The fishing vessels and survey vessel each have temporal and spatial scales. The survey vessel is assumed to move constantly at 10 n miles/hour for the entire 14 day period in which the fishing fleet is operating. The survey vessel is assumed to use a forward looking sonar with a detection width of about 500 m (further details are given in the next chapter).

The fleet of 5 commercial vessels are assumed to operate in perfect cooperation, so that they search for concentrations of krill together and share information about discovered concentrations. All vessels are assumed to fish in the same concentration. When searching for concentrations, the commercial vessels are assumed to have the same equipment as the survey vessel. Once within a concentration, and thus searching for individual swarms of krill, the survey vessels are assumed to use a vertical echosounder with a detection width of 35 m. The width of the net used by the fishing vessels is assumed to be 20 m.

7. KRILL DISTRIBUTIONAL MODEL

This chapter contains a description of the model for the spatial and temporal distribution of krill in the sector of ocean of interest. As mentioned above, the basic model is a "patches within patches" model: the large sector of ocean contains concentrations (fishing foci) of swarms of krill. Parameters described in this chapter correspond to the "base case" scenario; in succeeding chapters ways that the biomass of krill in the sector could change are documented.

The number of concentrations in the sector is denoted by N_c and in the base case

- $N_c = 36$.

Throughout this document, concentrations are indexed by the letter i, thus i runs from 1 to 36 in the base case. The location of concentrations within the sector is specified by the location of the center of the concentration. I assume that there is a "habitat structure" to the sector, defined in the following way. The sector is divided into 5 different habitats, stratified in the North-South direction, but not the East-West direction. If the southern-most edge of the sector is taken to be 0, the boundaries for the habitats are 75 n miles, 150 n miles, 300 n miles , 450 n miles and 600 n miles. Thus, for example, habitat H_1 consists of the "rectangle" 600 n miles in the EW direction and the southern most 75 n miles in the NS direction and habitat H_2 consists of the "rectangle" 600 n miles in the EW direction and contains the region from 76 n miles to 150 n miles in the NS direction.

Centers of concentrations are randomly placed in the sector, using habitat structure to determine the probability that a concentration is placed in a particular sector. The following probability distribution for habitat structure is adopted, motivated by distributions of krill predators (cetaceans and birds) and fishing boats in the Southern Ocean. Define the probability p_k by

$$p_k = \text{Probability that a concentration is placed in habitat } k \tag{7.1}$$

The following values are assumed:

Habitat	Value of p_k
1	1 / 3
2	1 / 6
3	2 / 9
4	1 / 6
5	1 / 9

Thus, when N_c= 36, there are on average 12 concentrations in habitat 1, 6 concentrations in habitat 2, 8 concentrations in habitat 3, 6 concentrations in habitat 4 and 4 concentrations in habitat 5. Note that the NS extent of the first two habitats is half of the NS extent of the other three habitats. The per unit area krill density in habitat H_2 is thus twice as great as the krill density in habitat H_4, although the two habitats contain the same number of concentrations. The center of the i^{th} concentration is denoted by (x_i,y^i). The value of x_i is chosen randomly from a uniform distribution on [0,600 nmi] and the value of y_i is chosen according to the probability distribution given above.

Each concentration has a radius that determines the number of swarms in the concentration. The radius of the i^{th} concentration is denoted by L_i. The radius is given by

$$L_i = L_c(1 + \mathbf{U}) \tag{7.2}$$

In this equation **U** denotes a randomly variable uniformly distributed on [0,1] and L_c denotes the <u>concentration characteristic radius</u>. For the base case, it is

- $L_c = 10/(\pi)^{.5}$ n miles = 5.64 n miles.

Thus, on average the radius of a concentration is about 8.5 n miles.

The number of swarms in the i^{th} concentration is denoted by N_i and is assumed to be given by

$$N_i = D_i \pi \ (L_i)^2 \tag{7.3}$$

In this equation, D_i is the per unit area density of swarms in the i^{th} concentration. It is given by

$$D_i = D_c \exp(\mathbf{X}_{.1}) \tag{7.4}$$

In this equation D_c is the <u>concentration characteristic density</u>. For the base case, it is

- $D_c = 20 \quad (\text{n miles})^{-2}$.

Also in Eqn (7.4), $\mathbf{X}_\sigma$ denotes a normally distributed random variable with mean 0 and standard deviation σ. In the sequel, it is useful to know that the expected value of $\exp(k\,\mathbf{X}_\sigma)$ is given by $E\{\exp(k\,\mathbf{X}_\sigma)\} = \exp(.5\,k^2\,\sigma^2)$. Thus, using Eqn (7.3) on average a concentration will contain $(20)(\exp(.5(.01)))\,\pi\,(8.46)^2$ swarms or about 4 500 swarms.

Swarms within concentrations are indexed by j, so that the subscript ij denotes the j^{th} swarm within the i^{th} concentration. Swarms are characterized by their radii and the density of krill within them. The radius of the j^{th} swarm within the i^{th} concentration is denoted by r_{ij} and is given by

$$r_{ij} = r_c \exp(\mathbf{X}_{1.1}) \tag{7.5}$$

In this equation, r_c denotes the swarm characteristic radius. It is

- $r_c = 50$ meters.

The density of krill within the j^{th} swarm in the i^{th} concentration is denoted by δ_{ij} and is given by

$$\delta_{ij} = \delta_c \exp(\mathbf{X}_{1.4}) \tag{7.6}$$

In this equation, δ_c denotes the swarm characteristic density of krill. It is

- $\delta_c = 150$ g/m^2

The model described above shows that the density of swarms, the radii of swarms and the density of krill within swarms all follow a log-normal distribution. This distributional model is based on extensive study of the literature, use of FIBEX data and conversations with numerous scientists involved in both FIBEX and SIBEX. In particular, Professor Butterworth and I spent a morning with SIBEX participants discussing this distributional model. The following issues were raised:

- FIBEX, taken around Elephant Island, may not be representative of the entire Antarctic area. In particular, the density of krill may be higher than on average. On the other hand, commercial fishing was occurring independently of but concommitant with the FIBEX data collection. This supports the use of the distributional model.

- Swarms may aggregate in concentrations, so that swarms are not randomly distributed within the concentration. This would affect the number of swarms that a vessel tows through.

- The actual definition of a swarm is not clear, since it depends on the threshold used with the sonar. Thus what appears to be one large swarm at a given ping threshold may be separated into a number of smaller swarms at a different threshold.

- The radii of concentrations and the density of swarms within concentrations may depend upon the location of the concentration within the habitat structure. In particular, concentrations may be more densely aggregated near the ice edge.

- One can't guarantee that the fishing vessels actually fish the swarm that they target on.

Even with these caveats, the general feeling of SIBEX participants was that the distributional model described above, while undoubtedly flawed, cannot be significantly improved upon at this time. (Naturally changes in the model could be implemented, but it is not clear that the resulting model would be superior.)

The FIBEX study estimated that the standing biomass of krill in the Southern Ocean is 90 million tonnes. How does that compare with the krill distributional model just described? There are 36 swarms, each with about 4 500 concentrations. The average area of a swarm is $\pi \, E \{ (50 \exp(\mathbf{X}_{1.1})^2) \} = \pi \, (50)^2 \exp(2.42) = 8.64 \times 10^4 \, m^2$. The average density of krill in a swarm is $150 \exp(.98) = 4 \times 10^2 \, g/m^2$. Thus, the average biomass of krill in the swarm is 34.6×10^6 g. Using the conversion of 1 tonne = 1 000 kg, the average swarm contains about 35 tonnes of krill. This value is low when compared to other reported values (e.g. Witek et. al. 1987) but may be due to a selection process in which only the larger swarms are targeted. A selection mechanism is described in the fishing submodel. A concentration then contains $35 \times 4\,500 = 15.8 \times 10^4$ tonnes of krill and the sector considered in this document thus contains $36 \times 15.8 \times 10^4 = 5.7 \times 10^6$ tonnes of krill. Since the Southern Ocean would contain 18 sectors similar to the one described here, the overall estimate for krill biomass in the Southern Ocean is about 100 million tonnes. This is consistent with the FIBEX results.

8. SURVEY VESSEL MODEL

This chapter contains a description of the operational model for the research survey vessel. At the extreme interpretation,which is adopted here, a research vessel does no fishing. Instead, the operation of the research vessel consists entirely of large scale surveying of the oceanic sector and detecting concentrations of krill.

The path of the research vessel is modelled on a daily basis, assuming that the vessel executes an "exhaustive search" (Koopman 1980) of the region. That is, the vessel starts at the southwest corner or the sector and traverses the sector in an easterly direction. When the eastern boundary of the sector is reached, the vessel moves north and traverses the sector in a westerly direction. The speed of the vessel is assumed to be 10 kts, so that in 24 hours the vessel's track length is 240 n miles. As a lower bound for search effectiveness, the assumption used in the model is that the vessel covers a block of 200 n miles in each day. The remaining track length is assumed to be used for investigation of discoveries of possible concentrations; although the discovery process is not explicitly modelled here. Since the length of the sector is 600 n miles, it takes three days for the vessel to traverse the sector in the EW direction. After one traverse, assume that the vessel moves 20 n miles north and traverses the sector in the direction opposed to the most recently completed traverse. This survey process is modelled for 14 days, with the vessel starting at the point (0, 15 n miles) on day 1. Other search patterns can easily be incorporated . For example, in the current search pattern Habitats 4 and 5 are not covered at all. This could be changed by modifying northward motion of the vessel at the end of each EW traverse. Detections by the research vessel are monitored on a daily basis. I assume that the vessel uses a forward looking sonar with a detection width 500 m on either side of the search path. Thus, during a single day the vessel sweeps out a rectangular area 200 n miles = 4×10^5 m long and 1 000 m wide. Any concentration that extends into this rectangular area is assumed to be detected by the vessel.

At the end of each survey day, the concentrations are "moved". I assume that the center of each concentration is displaced by a distance corresponding to the krill speed $v_k = 15$ cm/sec in a randomly chosen direction. The daily displacement distance is (15 cm/sec) x (.01 m/cm) x (3 600 sec/hr) x (24 hr/day)∞13 x 10^3 m/day. Thus, if (x_i, y_i) is the location of the center of the concentration on day d, the location of the center of the concentration on day d +1 is (x_i+ 13 x10^3 x cos(ø) , y_i+ 13 x 10^3 x sin(ø)), where ø is a randomly chosen direction. That is, ø is uniformly distributed with range [0, 360°].

The discovery history of the research vessel consists of a daily list of the location of concentrations that it has encountered. The discovery history has two main uses in the model. First, the discovery history is used to place the fishing fleet into a concentration whenever the fleet is not in one (e.g., at the start of the fishing period, if bad weather causes the fleet to lose the concentration, or if the fleet chooses to exit a concentration because catch is low). Second, the discovery history can be used to estimate the number of concentrations present in the oceanic sector. Mangel and Beder (1985) analyzed a problem similar to this one and showed that if a search time t_s lead to n_e encounters with concentrations, then an estimate for the number of concentrations is

$$N = n_e / (\varepsilon_r \; t_s) \qquad (8.1)$$

where ε_r is a search parameter associated with the operation of the research survey vessel. For the model described here, the parameter ε_r is computed according to the rule

$$\begin{aligned} \varepsilon_r &= \text{(Vessel speed) x (Detection Width) / Area of Sector} \\ &= (2 \text{ x}10^4 \text{ m/hr}) \text{ x } (10^3 \text{ m}) / (6 \text{ x}10^2 \text{ x } 2 \text{ x}10^{\,3}\text{m})^2 \\ &= 1.38 \text{ x } 10^{-5} \text{ /hr.} \end{aligned} \qquad (8.2)$$

Note that the search parameter is measured in hours; hence a 14 day search interval corresponds to a search time t_s = 14 days x 24 hrs/day=336 hours. The basis of Eqn (8.2) is the "random search formula" (Koopman 1980, Mangel 1985) and allows for double counting concentrations . is, there is no way to "mark" concentrations after a detection. For example, concentrations may be discovered on day d and on day d+1 in which case it is easily conceivable that the same concentration has been discovered. On the other hand, the same concentration may be discovered on day d and day d+5, due to movement of the vessel and concentration, in which case it is not so obvious that this concentration was discovered once before. The estimate obtained from Eqn (8.2) may thus be larger than the true number of concentrations.

9. FISHERY MODEL

The fishing period considered in this document is 14 days long. Fishing is assumed to occur in mid-summer (e.g. February) and sufficiently far south that daylight is essentially 24 hours. The fishing model consists of the following components:

(i) The cooperative search by the fleet and research vessel for concentrations. This occurs at the start of the fishing period, if the fleet loses the concentration because of bad weather or if the fleet exits a concentration because of low catch rates.

(ii) The search within concentrations by individual vessels for swarms of krill.

(iii) The fishing of swarms of krill.

(iv) The fleet decision process.

Each of these is a submodel of the fishing model.

(i) Finding Concentrations

The model developed in this document treats a "cooperative fishery" consisting of the research survey vessel and 5 identical fishing vessels. The vessels cooperate in that they share search information and all fish in the same concentration when they are fishing.

If the research survey vessel discovers one or more concentrations on the first day of the fishing period, then the fleet simply moves to the first concentration discovered and begins fishing there. Otherwise, the fleet itself begins searching for concentrations. I assume that each vessel in the fleet has both echosounder used for targeting on swarms during the fishing process and a forward looking sonar with a detection width of 500 m on either side of the vessel track used for search for concentrations and that the fishing vessels can also search at 10 n miles/hr. If the fleet must search for a concentration, the following procedure is applied. All concentrations within 24 hours steaming of the current position of the fleet are identified. The five vessels are assumed to search independently for concentrations and the time to detect an individual concentration is assumed to follow an exponential distribution with parameter proportional to the search speed and inversely proportional to the area of the habitat in which the vessel is operating. Thus, more than one concentration may be discovered; I assume that the first one discovered is the one that the fleet moves to. Detection of a concentration is determined by drawing a random number from the appropriate distribution. If at least one concentration is detected, then the concentration selected for fishing is determined by a weighted measure of the distance between the fleet and the different concentrations within 24 hours steaming. If no concentrations are detected, the fleet moves towards the center of habitat H_1.

(ii) Within Concentration Search by Individual Vessels: The Swarm Encounter Model

Once the fleet has encountered a concentration, individual vessels begin searching for swarms within the concentration. This section contains a description for the search by vessels for individual swarms. Since there are 36 concentrations, with about 4 500 swarms in each concentration, there are of the order of 162 000 swarms in the entire sector. Very few of these swarms will be fished, since the fishing period only lasts 14 days and I will assume (in the next section) that each fishing vessel makes no more than 11 hauls per day. Thus, tracking the location of each swarm is unnecessary, and consumes valuable computer time and memory. In order to save memory space in the computer and speed the running of the model, I adopt the following procedure for modelling the within concentration search behavior of individual vessels. First, a detailed model of the within concentration search behavior of the vessels will be described. This search model is called the swarm encounter model and provides parameter estimates that are used in the fishing model of the next section. The model described here actually tracks the detailed motion of a vessel and all 4 500 swarms in a concentration. In the next section, I use the distributions and parameters developed in this section, so that vessel positions and swarm locations do not need to be tracked.

To begin, consider a concentration that has characteristic radius 8.5 n miles and contains about 2 500 swarms. A vessel in this concentration searches at a speed of 2 n miles/hr and uses a sonar with a detection width of 35 m on either side of the vessel. The vessel starts its search at a randomly chosen point in the concentration. The swarms are randomly located within the concentration, swarm radii are log-normally distributed .

Time is explicitly considered in this encounter model, using increments of dt = .01 hours. Both the vessel and swarms of krill are assumed to use "random tour" models (Washburn 1969). Thus, let $(x_v(t), y_v(t))$ and $(x_j(t), y_j(t))$ denote respectively the positions of the vessel and the j^{th} swarm of krill at time t. The dynamics of the motion of the vessel are

$$\begin{aligned} x_v(t+dt) &= x_v(t) + 4000 \cos(\theta)\, dt \\ y_v(t+dt) &= y_v(t) + 4000 \sin(\theta)\, dt \end{aligned} \qquad (9.1)$$

where θ is the direction of search. When t= 0, the value $\theta = 45°$ is chosen. Until a detection occurs, every 10 dt hours the direction of search is changed to a new direction, within 30° of the previous direction. The only constraint on the motion in Eqn (9.1) is that the vessel is not allowed to leave the concentration. The 4 000 in Eqn (9.1) is the vessel speed and dt is the time increment.

Similarly, the dynamics of the center of a swarm are given by

$$\begin{aligned} x_j(t+dt) &= x_j(t) + 540 \cos(\omega)\, dt \\ y_j(t+dt) &= y_j(t) + 540 \sin(\omega)\, dt \end{aligned} \qquad (9.2)$$

where the ω denotes the direction of motion of the swarm of krill. I assume that in each time interval , ω is randomly chosen in the range [0°, 360°].

Detection of a swarm of krill occurs when the distance between the vessel and the center of the swarm is less than the sum of the radius of the swarm and the detection width of the sonar. Since initial location of the swarms and vessel and motion of the swarms and vessel involve random components, the detection times will also be random variables. With the same initial conditions, the encounter model can be iterated many times using Monte Carlo simulation. Hence introduce the detection time distribution function F(t) defined by

$$F(t) = \text{Fraction of iterations in which the detection occurred before time } t \qquad (9.3)$$

The distribution F(t) was determined by simulation, choosing a wide variety of initial conditions on swarm numbers (ranging from 200 to 8 000). In all of the cases studied, the empirical distribution was fit well by an exponential distribution of the form

$$F(t) = 1 - \exp(-\beta t) \qquad (9.4)$$

The mean time to detection for the expotential distribution is $1/\beta$. A "base case" for the swarm encounter model was chosen with the following parameters:

- Number of swarms = N_{base} = 2 500
- Concentration radius = L_{base} = 8.46 n miles
- Characteristic swarm radius = r_{base} = 50 m.

For this case, the mean time to detect a swarm was .0356 hours and the fit between the empirical distribution (based on 110 iterations) and the exponential model is shown below:

Detection interval	Fraction of Detections in the Detection Interval	
	Encounter Simulation	Exponential Model
0 - .05 hours	.70	.75
.06 -.1 hours	.082	.185
.11 - .15 hours	.064	.045
> .16 hours	.154	.02

These results show that the exponential distribution underweights the likelihood of longer detection times.

The exponential distribution arises in the famous random search formula. This formula is based on two assumptions:

1. The time to detection is exponential distributed, so that Prob {detection time < t } = 1 - exp(-βt).
2. The parameter β is given by the formula β = Wv/A, where W is the detection width of the vessel's sonar, v is the speed of the vessel and A is the area in which the vessel is searching.

In this document, the first assumption is retained but the second assumption is dropped and is replaced as follows. Let β_{base} = .05 hours denote the approximate value of the parameter β when the base parameters are used. Consider a concentration of radius L containing N_s swarms in which the characteristic swarm radius is r. The detection parameter for the concentration is assumed to be given by

$$\beta = \beta_{base}\ (N_S/N_{base})(\ L_{base}/\ L)\ ^2(\ [W_{echo} + \ r\exp(.605)]/\ [W_{echo} + r_{base}\exp(.605)]) \tag{9.5}$$

In this equation, W_{echo} is the detection width of the echosounder and the term exp(.605) comes from the expectation of the log-normally distributed swarm radius. The logic behind this equation is the following: the rate of detections should increase as the number of swarms increases or the detection width increases (either from the echo sounder or changes in swarm radius) and should decrease as the area increases.

The actual search time for a swarm will consist of (i) an encounter time t_{enc} following the exponential distribution described above and (ii) an identification time t_{id} in which the signal is determined to be an actual swarm. I assume that identification time consists of a fixed period of 2 minutes and a variable period given by variable $t_{id} = 5(1-\exp(-B_s/10))$ min, where B_s is the biomass of the encountered swarm, measured in tonnes.

Even so, the encounter and total detection time described above appear to be considerably less than what we can infer from logbook data. Consequently, following Butterworth (1987), a selectivity process is introduced. An encountered swarm with biomass B_s is accepted for fishing only if its biomass exceeds a threshold. In particular, the encountered swarm is accepted for fishing only if $B_s > B_{threshold} \exp(\mathbf{X}_{.2})$. Here $B_{threshold}$ is the basic value for the threshold (set to be 50 tonnes in the base case) and $\mathbf{X}_{.2}$ is a normally distributed random variable with mean 0 and variance 0.2.

(iii) Fishing Submodel

It is now possible to describe the fishing submodel. The setup is as follows: The entire fleet is located in a single concentration, ready to begin fishing. Although the vessels are assumed to search cooperatively and pool catches when making decisions about leaving concentrations, the micro-operations of the vessels (i.e. individual trawls) are treated independently. It is thus sufficient to consider a single vessel, with the understanding that the modelling process for the fishing of one vessel is repeated 5 to include all vessels of the fleet. (Naturally, the vessels are treated independently. This means independent draws of random variables during the simulation.)

Fishing is assumed to take place in periods of 24 continuous hours of daylight. Even so, there are limits to the number of hauls and the total catch per vessel. I assume that the vessels make no more than 7 hauls per 24 hours and that because of processing constraints, the vessels draw their nets when the nets contain 20 tonnes of krill. Thus, the maximum catch by a single vessel is 140 tonnes per day, or 700 tonnes for the entire 14 day fishing period. The maximum catch for a fleet of 5 identical vessels is thus 9 800 tonnes for the 14 day period.

I assume that if the fleet is already within a concentration, each fishing day starts with the search for swarms. At the start of the day, the operational time remaining, which is denoted by T_R , is 24 hours. The time until a swarm is detected, which is denoted by T_{search}, is determined as described above. After a swarm is detected and selected for fishing, the vessel lowers its net. In light of the mean surface density (150 g/m^2), it will usually be true that more than one swarm is fished per haul of the net. To take this into account, I use the Poisson approximation to the binomial to determine the number of additional swarms within 35 m of the vessel as it tows for a maximum of 8 n miles. After a swarm is fished, the distance travelled to reach the next swarm is uniformly distributed and is determined by the inter swarm center to center distance (computed from the number of swarms and characteristic radius of the concentration). The haul ends when either (i) more than 4 n miles have been traversed with the net in the water , or (ii) more than 20 tonnes are in the net (presumed to be estimated from the echosounder). The 4 n miles limit is applied with liberty (although it rarely ever is binding).

The actual catch is computed by considering a the tow of a net through a circular swarm. I assume that the towed area can be modelled by a rectangle, that the width of the net is 20 m, so that the maximum area swept is the net width times the diameter of the swarm, i.e. the maximum area swept is 20x 2x r = 40 r m^2. (This assumes that diameter of the swarm exceeds 20 m and must be modified if the diameter of the swarm is less than the width of the net. In general, 40r m^2 is replaced by 2r min(20,2r) m^2.

The time spent towing is determined in the following way. The vessel's speed while towing is assumed to be $v_{tow} = (2.5 + 2\,\mathbf{U})$ m/hour, where **U** is a random variable uniformly distributed on the interval [0,1]. The tow through a swarm with radius r_{ij} takes $(2r_{ij}/v_{tow})$ hr. Let d_{ij} denote the distance between swarm j in concentration i and the next swarm fished. I assume that the tow time is given by

$$T_{tow} = [\Sigma_j \ (2r_{ij}+ d_{ij})/v_{tow}] \qquad (9.6)$$

The summation on the right hand side of Eqn (9.6) is the total time to tow through all of the swarms.

At the end of a tow, the net is hauled. I assume a hauling/veering rate of 150 m/hr and use the empirical distribution of depths from the Soviet data to randomly select an associated veering/hauling time. After the net is brought on board, the vessel has a period of "dead time" in which processing occurs. Dr Ichii (personal communication) provided the following information on processing time:

Catch per haul (tonnes)	Processing time (hours)
0 - 10	1.5
11- 15	2.0
> 15	2.5

The time remaining is then decremented by the total of search time + trawl time + hauling time + processing time. This fishing model is repeated for each vessel each day until either time remaining reaches 0 or the number of hauls exceeds 7. The model is then repeated for the entire fleet for 14 days of fishing. The data generated by this submodel are search times, tow times, and catch times.

(iv) Fleet Decision and Bad Weather Models

Dr Ichii (personal communication) kindly provided information on fleet decisions and on bad weather. Based on this information, I assume that at the end of each day the daily value of catch/haul is computed. If this value exceeds 3 tonnes/haul, then the fleet stays in the current concentration. If the daily value is below 3 tonnes/haul, then the fleet exits the current concentration and begins search for another concentration.

Dr Ichii also provided data on the frequency and duration of bad weather experienced in operations by JAMAC between 1973-74 and 1985-86. Based on these data, the probability of bad weather terminating fishing is assumed to be .02. If bad weather does occur, the duration of the bad weather spell is one day with probability .68., two days with probability .28 and three days with probability .04. I assume that if bad weather occurs, the fleet is displaced 50 n miles from the concentration in which it was fishing and that the fleet must search for a concentration at the end of the bad weather period.

10. GENERAL CONSIDERATIONS ON ABUNDANCE INDICES FOR PELAGIC, SCHOOLED STOCKS

This chapter contains a general discussion of considerations for a theory of abundance indices for pelagic, schooling species. Particular indices will be developed and employed in the next chapter. The objective here is to discuss desirable properties of indices and also to discuss.how indices can be used to detect changes in abundance.

The general question is how one develops a biomass index (or indices) with the following desirable properties:

- Consistency: Changes in actual abundance and changes in the index should always be in the same direction. This is crucial for a system such as the Southern Ocean krill fishery in which many parameters determine ultimate abundance and more than one parameter may change at a time.
- Linearity: Changes in actual abundance should be reflected by proportional changes in the index.
- Small variability: The inherent variability in the index should be small, so that the probability of detecting changes in the index is large.

For the underlying "patches within patches" system as described here, a biomass estimate B_{est} should take the form:

$$B_{est} = \text{(Number of Concentrations) (Swarms Per Concentration) (Biomass Per Swarm)} \quad (10.1)$$

The number of concentrations can clearly be estimated from the data generated by the research/survey vessel, so let us consider estimates of swarms per concentration and biomass per swarm.

10.1 Estimating Swarms per Concentration

The exponential model for detection of swarms is equivalent to the assertion that when N_s swarms are present

$$\text{Prob\{ detect one swarm by time } t \mid N_s \text{ swarms are present \}} = 1 - \exp(\beta t N_s) \quad (10.2)$$

so that the expected value of the search time t_{srch} before a swarm is detected is

$$E\{t_{srch}\} = 1/\beta N_S \qquad (10.3)$$

Eqn (10.3) suggests that the number of swarms present in a concentration could be estimated by

$$N_{s,est} = 1/\beta E\{t_{srch}\} \qquad (10.4)$$

Note that when the exponential distribution is used, the expected value of $1/t_{srch}$ does not exist. That is, $\int_0^\infty (1/t)\beta N_s \exp(-\beta N_s t)\,dt$ is infinite.

The actual search model described above has a fixed identification time, which means that the minimum value of $t_{srch} = t_{id,fixed}$ (which is 2 minutes here). This would lead one to consider changing the exponential distribution in Eqn(10.2) and replacing it by

$$F(t) = \text{Prob}\{\text{ detection in search time} \le t\} = \begin{cases} 0 & \text{if } t \le t_{id} \\ 1 - \exp\{-\beta N_s(t-t_{id})\} & t>t_{id} \end{cases} \qquad (10.5)$$

The search process is now a renewal process and the mean search time (including detection as part of the search process) is

$$E\{t_{srch}\} = (1/\beta N_s) + t_{id} \qquad (10.6)$$

so that the estimate for the number of swarms becomes

$$N_{s,est} = [\, b(E\{t_{srch}\} - t_{id}\,)]^{-1} \qquad (10.7)$$

These considerations show that reciprocal search times may play an important role in estimating the number of swarms per concentration.

10.2 Estimating Biomass/Swarm

"Conventional" wisdom suggests that biomass/swarm can be accurately estimated by some measure of catch rate, e.g. catch per towtime. Such thinking is based on the fundamental premise that the sampled organism is smoothly distributed over the region of interest. For a highly aggregated stock, in which there may be big gaps between swarms, catch per towtime may be a very poor estimator - severely under-diasing estimates of swarm biomass. Alternatives such as catch per selected swarm, catch per fished swarm or catch per encountered swarm may be much better.

10.3 Detecting Changes in Abundance Indices

Suppose now that the same abundance index (e.g. catch/swarm) has been computed in two different situations (e.g. the situation in which all parameters assume their base case values and the situation in which one of the parameters, say characteristic radius, is changed). Let X_b denote the abundance index for the base case parameters and X_c denote the abundance index when the parameters are changed. The simulation model described in the previous section allows one to compute an entire distribution for X_b and X_c. From that distribution, the following information is extracted:

- The mean values of the abundance indices. These are denoted by μ_b and μ_c respectively.
- The standard deviations of the abundance indices. These are denoted by σ_b and σ_c respectively.
- The ranges of the abundance indices observed in the simulation. For the base case, the lowest value of the abundance index will be denoted by $x_{lb,sim}$ and the greatest value by $x_{ub,sim.}$ For the case in which parameters are changed the extremes will be denoted by $x_{lc,sim}$ and $x_{uc,sim}$ respectively.

We are interested in detecting changes in the abundance indices. One natural, and obvious measure is a comparison of the means, so that one would consider the ratio μ_c/μ_b. This was done, for example, by both Butterworth (1987) and Mangel (1987). Various statistical tests can be applied to determine the likelihood that the two means came from the same underlying distribution. There is , however, a fundamental problem with using such a test. In real life, one value of the abundance index will be observed. That is, the Southern Ocean fishery will not be "replicated" fifty times over in a single year. Thus, even if the abundance indices for the base case and changed parameter case do arise from different distributions, a particular value of the index in the changed parameter case may be very close, say, to the mean of the index for the base parameter case. It is here that the observed ranges of the abundance indices become so important.

In general, there will be overlap of the ranges, as shown below:

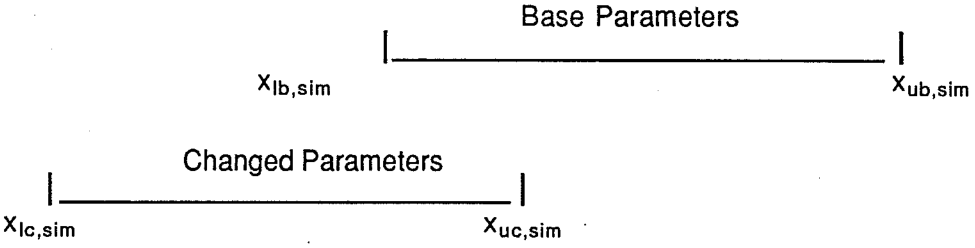

For this situation, the overlap region consists of values of the abundance indices in the range $x_{lb,sim}$ to $x_{uc,sim}$. In addition to comparing the means of the abundance indices, one wants to compute the probability that a shift can be detected. Two methods for computing the probability of detecting a change will now be described.

The first method could be called a "non-parametric" or simulation based computation. In this case,

Prob{detect a change in abundance indices } =
1 - [Number of Data Points in the Overlap Region]/Total Number of Simulations
(10.8)

That is, one simply counts the number of simulation iterations for the case of changed parameters in which the abundance index falls within the range $[x_{lb,sim}, x_{ub,sim}]$ and divides this by the total number of simulation iterations. The resulting value is the fraction of simulation iterations for changed parameters in which the abundance index falls in the range of base case parameters. The probability of detecting a change is defined as 1 minus this fraction.

The second method for computing the probability of detecting a change in abundance indices is based on a normal approximation. That is, one assumes ad hoc that the abundance indices are normally distributed with the mean and standard deviation observed in the simulations. Since a normal distribution with mean μ and variance σ has more than 99% of its probability mass concentrated in the interval $[\mu - 3\,\sigma, \mu + 3\,\sigma]$, the ranges for the base case are redefined as:

$$x_{ub} = \max [\, x_{ub,sim}, \mu_b + \sigma_b] \text{ and } x_{lb} = \max [\, x_{lb,sim}, \mu_b + \sigma_b] \qquad (10.9)$$

Given these new ranges and μ_c and s_c, the probability of detecting a change in this case is defined as

Prob{detect a change in abundance indices}
= 1 - Prob{ a point from the normal distribution with mean and standard deviation μ_c and σ_c falls in the range $[x_{lb}, x_{ub}]$ (10.10)

A small computation shows that

Prob{detect a change in abundance indices}

$$=1- \{\ \Phi([x_{ub} - \mu_c]/\sigma_c) - \Phi([x_{lb} - \mu_c]/\sigma_c)\ \} \qquad (10.11)$$

where $\Phi(z)$ is the cumulative distribution function for a normally distributed random variable with mean 0 and variance 1.

11. ABUNDANCE INDICES FOR THE SOUTHERN OCEAN KRILL FISHERY MODEL AND BASE CASE RESULTS

In this chapter, 44 different abundance indices that could be computed from fishery generated data are described along with the mean, standard deviation and range for the base case parameters. These values are computed from 50 iterations of the simulation model.

Total catch (tonnes). This is the total catch by the 5 vessels over the 14 day fishing period.

Mean	Standard Deviation	Range
4642	428	2585,5270

Total number of hauls. This is also the total number of swarms that were selected for fishing.

Mean	Standard Deviation	Range
394	30.7	230,418

Total number of swarms fished. This index is based on the assumption that the vessels can identify individual swarms during the fishing process.

Mean	Standard Deviation	Range
2088	195	1192,2392

Total number of swarms encountered.

Mean	Standard Deviation	Range
7268	596	4214,7888

Total towtime (hours). This is the total time that the vessels have nets in the water.

Mean	Standard Deviation	Range
415	32.5	252,451

Total searchtime (hours). This is the total time that the vessels are searching for krill.

Mean	Standard Deviation	Range
429	36.7	255,473

Total reciprocal searchtime (1/hours). This is the total of the reciprocal of times spent searching for krill.

Mean	Standard Deviation	Range
813	87.2	425,1002

Total number of discoveries by the research/survey vessel.

Mean	Standard Deviation	Range
11.6	3.5	3,21

Number of different concentrations fished.

Mean	Standard Deviation	Range
1.2	.523	1,4

Total catch per total towtime. (tonnes/hour). This index is computed by dividing the total catch by the total towtime.

Mean	Standard Deviation	Range
11.2	.434	10.1,11.8

Average catch per towtime (tonnes/hour). This index is computed by averaging over individual hauls within a simulation iteration the quantity {catch/towtime}.

Mean	Standard Deviation	Range
13.6	.575	12.3,14.5

Average catch per searchtime (tonnes/hour). This index is computed by averaging over individual hauls within a simulation iteration the quantity {catch/searchtime}.

Mean	Standard Deviation	Range
24.2	1.93	20.2,30.3

Average of catch per towtime per searchtime (tonnes/hour^2). This index is computed by averaging over individual hauls within a simulation iteration the quantity {(catch/towtime)(1/searchtime)}.

Mean	Standard Deviation	Range
27.8	2.52	22.8,35.5

Catch per day (tonnes/day). This index is computed by dividing total catch by the length of the fishing period.

Mean	Standard Deviation	Range
332	30.6	185,376

Catch per haul (tonnes). This index is computed by dividing the total catch in a simulation iteration by the total number of hauls in that simulation iterations.

Mean	Standard Deviation	Range
11.8	.422	10.8,13.0

Hauls per concentration discovered. This index is computed by dividing the total number of hauls in a simulation iteration by the total number of concentrations discovered by the research/survey vessel and fleet.

Mean	Standard Deviation	Range
38.6	18.4	11.5,134

Fraction of swarms selected. This index is computed by dividing the total number of hauls by the total number of swarms encountered.

Mean	Standard Deviation	Range
.054	.0019	.0503,.0595

Average trawl length (n miles).

Mean	Standard Deviation	Range
1.37	.033	1.31,1.44

Discoveries times catch (10^4 tonnes). This index is computed by multiplying the total number of concentrations discovered by the survey vessel and fleet and the total catch.

Mean	Standard Deviation	Range
5.35	1.61	1.44,9.63

Discoveries times hauls times catch (10^7 tonnes). This index is computed by multiplying the total number of concentrations discovered by the total number of hauls and by the total catch.

Mean	Standard Deviation	Range
2.12	.682	.576,3.85

Discoveries times catch per towtime times swarms fished (10^5 tonnes/hour). This index is computed by multiplying the total number of discoveries by the total catch and by the total of swarms fished and dividing by the total towtime.

Mean	Standard Deviation	Range
2.69	8.17	.663,4.88

Discoveries times average catch per towtime times swarms fished (10^5 tonnes/hour). This index is computed by multiplying the total number of discoveries by the average catch per towtime and by the total number of swarms fished.

Mean	Standard Deviation	Range
3.27	.996	.804,6.04

Average catch per towtime divided by average searchtime (tonnes/hr^2).

Mean	Standard Deviation	Range
12.5	.905	10.8,14.7

Average catch per towtime times average reciprocal searchtime (tonnes/hr^2).

Mean	Standard Deviation	Range
28.0	2.06	22.7,34.5

Discoveries times total catch divided by total towtime(tonnes/hour).

Mean	Standard Deviation	Range
129	39.1	32.7,232

Discoveries times average catch per towtime divided by average searchtime (tonnes/$hour^2$).

Mean	Standard Deviation	Range
145	44.8	35.5,255

Discoveries times average catch per towtime times average reciprocal searchtime (tonnes/$hour^2$).

Mean	Standard Deviation	Range
325	103	76.6,605

Discoveries times average {(catch per towtime) (reciprocal searchtime)} (tonnes/$hour^2$).

Mean	Standard Deviation	Range
322	100	74,593

Discoveries times total catch divided by total towtime divided by average searchtime (tonnes/$hour^2$).

Mean	Standard Deviation	Range
119	36.9	29.3,206

Discoveries times total catch times average reciprocal searchtime divided by total towtime (tonnes/hour^2).

Mean	Standard Deviation	Range
267	84.8	63.2,84.9

Discoveries times total catch times number of selected swarms divided by total towtime (10^4 tonnes/hour).

Mean	Standard Deviation	Range
5.07	1.53	1.31,9.23

Discoveries times average catch per towtime times number of selected swarms (10^4 tonnes/hour).

Mean	Standard Deviation	Range
6.17	1.86	1.59,11.1

Discoveries times total catch times number of swarms encountered divided by total towtime (10^5 tonnes/hour).

Mean	Standard Deviation	Range
9.35	2.78	2.78,16.9

Discoveries times average catch per towtime times number of swarms encountered (10^6 tonnes/hour).

Mean	Standard Deviation	Range
1.14	.339	.287,2.09

Discoveries times total catch per total towtime times hauls per concentration fished (10^4.tonnes/hour).

Mean	Standard Deviation	Range
4.75	1.81	1.81,9.23

Discoveries times average catch per towtime times hauls per concentration fished (10^4 tonnes/hour).

Mean	Standard Deviation	Range
5.78	2.2	1.3,11.1

Discoveries times total catch per total towtime times swarms fished per concentration (10^5 tonnes/hour).

Mean	Standard Deviation	Range
2.52	.964	.602,4.88

Discoveries times average catch per towtime times swarms fished per concentration (10^5 tonnes/hour).

Mean	Standard Deviation	Range
3.06	1.17	.724,6.04

Total catch per total hauls divided by average searchtime (tonnes/hour).

Mean	Standard Deviation	Range
10.8	.685	9.24,12.8

Discoveries times total catch per total hauls divided by average searchtime (tonnes/hour).

Mean	Standard Deviation	Range
122	39.1	40.4,207

Total catch per swarms fished per average searchtime (tonnes/hour).

Mean	Standard Deviation	Range
2.03	.088	1.88,2.3

Discoveries times total catch per swarms fished per average searchtime (tonnes/hour).

Mean	Standard Deviation	Range
22.9	7.2	7.92,37.2

Catch per swarms encountered per average searchtime (tonnes/hour).

Mean	Standard Deviation	Range
.581	.0445	.483,.695

Discoveries times catch per swarms encountered per average searchtime (tonnes/hour).

Mean	Standard Deviation	Range
6.56	2.14	2.21,11.3

12. PERFORMANCE OF THE INDICES IN DETECTING CHANGES IN KRILL BIOMASS

This chapter contains results on the efficacy of the different abundance indices in detecting changes in krill abundance. Krill abundance will change if any of the basic parameters change.

Biomass is indexed by the product of characteristic parameters:

- Biomass index = $N_c D_c(L_c)^2 \delta_c(r_c)^2$

Two types of parameter changes were implemented. First, only one parameter was changed at a time, leading to drops in biomass to either 2/3 or 1/3 of the base case level. This was done by changing the parameters as follows:

- L_c multiplied by $\sqrt{2/3}$ or $\sqrt{1/3}$
- r_c multiplied by $\sqrt{2/3}$ or $\sqrt{1/3}$
- δ_c multiplied by 2/3 or 1/3
- N_c multiplied by 2/3 or 1/3
- D_c multiplied by 2/3 or 1/3.

The multiplicative factor is 2/3 (1/3) or $\sqrt{2/3}$ ($\sqrt{1/3}$) depending on the way that the parameter enters into the determination of biomass (linearly or squared).

Second, more than one parameter was changed simultaneously, leading to changed biomass levels that ranged from 0.2 to 1.2 times the biomass in the base case. The parameter values for these cases are shown in Table 12.1 (the base case parameters are also shown, for easy reference).

Finally, the effect of adaptive behavior by the fishing fleet was studied by considering changes in the threshold for accepting a krill swarm for fishing. The other two values of the threshold used were B_{thr} = 40 tonnes and B_{thr} = 0 tonnes. Naturally, changing the threshold for accepting swarms does not change the underlying krill biomass, but it may change the abundance indices and thus lead to a belief that the underlying biomass was indeed changed.

Tables 12.2 to 12.46 show the results. Shown in these tables are the biomasses relative to the base case, the ratio of the mean abundance index for the changed parameters (μ_c) to the mean abundance index for the base case parameters (μ_b) and the probability of detecting the change in biomass based on the simulation (non-parametric) and normal approximation calculations described previously.

13. DISCUSSION OF THE SIMULATION RESULTS

When considering the results presented in the last chapter, it is useful to separate changes in biomass index caused by changes of within concentration parameters (that is D_c, r_c and δ_c) and changes of between concentration parameters (L_c and N_c). No single index is capable of tracking both kinds of changes. Study of the results leads to the following conclusions:

- Many of the indices are ineffective for tracking changes in krill abundance because they have inconsistent changes (both increases and decreases in the abundance index or no change in the abundance index) with the biomass index.

- Even those indices that do exhibit consistent changes also exhibit the problem of "convexity": a change of biomass index to 2/3 or 1/3 of the base case leads to a ratio of μ_c/μ_b that is greater than 2/3 or 1/3. That is, the abundance indices are not linear in the biomass index.

- Even those indices for which μ_c/μ_b is considerably less than 1 and close to 2/3 or 1/3 may have a small probability of detecting the shift. This is caused by the large variability in the abundance indices for fixed krill distributional parameters.

- Simple indices appear to perform better than more complicated indices. This is true at two levels. For example, the index
  (Total Catch / Total Towtime)/ Average {Searchtime}
  performs better than the index

Average { (Catch/Towtime) / {Searchtime }
where the average is taken over individual hauls. Similarly, indices in which the number of discoveries is multiplied by a within-swarm abundance index perform more poorly than indices without that multiplier (compare Tables 12.40, 12.42 and 12.44 with Tables 12.41, 12.43 and 12.45).

- Although a number of abundance indices are effective in tracking changes in biomass caused by single changes in parameters, none is effective when many parameters change at once. This is caused by the confounding effects of multiple changes in parameters. This suggests that determining the most likely sources of biomass change is an important future project. That is, effort should be spent determining the parameters that are most likely to change and the directions in which they will change.

- The most effective tracking of krill abundance could be done with the following abundance indices:

  1. Use the number of discoveries by the survey vessel to track changes in the number of concentrations and the characteristic radii of concentrations.

  2. Use one of the following indices to track within concentration changes of swarm density and krill abundance within swarms:

     (Total Catch / Total Hauls) / Average{Searchtime}
     (Total Catch/Swarms Fished) / Average{Searchtime}
     (Total Catch/Swarms Encountered)/Average{Searchtime}.

  Note that since the total number of hauls equals the number of swarms selected for fishing, all of these indices have the form catch per "swarm" per searchtime. This is consistent with the theoretical concepts presented in Chapter 10.

- The adaptive behavior of fishing vessels may be important for the accurate interpretation of abundance indices. For example, a changing threshold for acceptance of a swarm for fishing or a changing catch continuation parameter might drastically effect abundance indices and lead to inaccurate interpretations of their meaning. Refishing might also affect abundance indices, depending upon the effectiveness of the search procedure during refishing (Butterworth 1987, Mangel 1987)

14. CONCLUSION AND RECOMMENDATIONS

Although the model developed in the body of this report contains many operational uncertainties (e.g. what exactly is search time), it is still possible to make a number of recommendations. In particular the following are suggested :

1. Fishing and survey vessels should indicate in their log books approximately how much of the between trawl times are spent in search for swarms of krill. If possible, vessels should indicate the number of swarms fished in a haul. This would require a consistent definition of swarm (in terms of sonar ping threshold, for example).

2. CCAMLR should consider an "experiment" in which a research vessel and a fishing fleet travel together, but work independently. In particular, the fishing fleet should operate as if the survey vessel were not present, and the survey vessel

should conduct krill surveys in the vicinity of regions in which the fleet fishes. By doing this, one can obtain a distributional model for krill that are considered fishable by the fleet.

3. If a detailed operational model of krill fisheries is desired, CCAMLR should consider sending a Ph.D. level modeller to sea with the fleets. This is in the best traditions of operational analysis (see, e.g. Tidman 1984) and most likely is the only way that accurate operational models can be developed. In particular, such a field assignment will lead to accurate understanding of the role of search in the overall fishing operation and to an accurate understanding of operational fishing decisions.

4. The following indices can be used, at least temporarily, to track krill abundance:

   (a) Use the number of discoveries by the survey vessel to track changes in the number of concentrations and the characteristic radii of concentrations.

   (b) Use one of the following indices to track within concentration changes in swarm density and krill abundance within swarms:

   (Total Catch / Total Hauls) / Average {Searchtime}
   (Total Catch/Swarms Fished) / Average {Searchtime}
   (Total Catch/Swarms Encountered) / Average {Searchtime}.

REFERENCES

BUTTERWORTH, D. 1987. A simulation study of krill fishing by an individual Japanese trawler. This report.

EVERSON, I. 1982. Diurnal variation in mean volume backscattering strength of an Antarctic krill (*Euphausia superba*) patch. Journal of Plankton Research 4: 155-162.

KOOPMAN, B.O. 1980. Search and Screening. Pergamon Press, Oxford, UK.

MANGEL, M. 1985. Search models in fisheries and agriculture. Lecture Notes in Biomathematics 61: 105-138.

MANGEL, M 1987. Simulation of Southern Ocean Krill Fisheries. CCAMLR Document SC-CAMLR-VI/BG/22. 13 October 1987.

MANGEL, M. and D. BUTTERWORTH. 1987. A model of krill distribution and assumptions regarding the effects of fishing. CCAMLR Document.

PRESS, W.H., FLANNERY, B.P., TEUKOLSKY, S.A. and W.T. WETTERING. 1986. Numerical Recipes. Cambridge University Press, New York.

ROSENBERG, A. , J.R. BEDDINGTON and M. BASSON. 1986. Growth and longevity of krill during the first decade of pelagic whaling. Nature 324: 152-154.

TIDMAN, K.R. 1984. The Operations Evaluation Group. Naval Institute Press, Anapolis, Md.

WASHBURN, A. 1969. Probability density of a moving particle. Operations Research 17: 861-871.

WATKINS, J.L., D.J. MORRIS, C. RICKETS and J. PRIDDLE. 1986. Differences between swarms of Antarctic krill and some implications for sampling krill populations. Marine Biology 93: 137-146.

WITEK, J. and A. GRELOWSKI. 1987. Formation of Antarctic krill concentrations in relation to hydrodynamic processes and social behaviour. Preprint obtained from J.L. Watkins, British Antarctic Survey.

Table 2.1: Summary of Soviet Cruise Sources

Data Set	Vessel Name	Region	Period	Number of Records
1	Akademik Knipovich	12.6°E - 56° W 52.1°S -69.8°S	5.3.81- 23.5.81	92
2	Akademik Knipovich	46.1°W-135.7°W 60.3°S - 69.3°S	20.3.82- 7.5.82	39
3	Akademik Knipovich	27.5°E-67.7°E 48.1°S -69°S	12.1.84- 29.3.84	177
4	Odyssey	35.3°W -55.7°W 53.6°S -61.3°S	9.1.81- 19.3.81	39
5	Professor Derugin	59.5°E -94.5°E 61.7°S -69°S	15.1.81- 20.4.81	417
6	Professor Derugin	61.2°E -112.4°E 62.9°S -67.1°S	18.2.82- 5.5.82	188
7	Argus	32.3°W -39°W 51.1°S -54.5°S	23.4.81- 27.6.81	229
8	Argus	44.2°W -55.6°W 59.4°S -61°S	27.1.84- 8.4.84	236
9	Globus	56.9°E - 68.4°E 60.5°S - 67°S	2.2.84- 9.4.84	306
10	Mys Dalniy	105.6°E -163.9°E 64.3° S - 72.1°S	7.2.84- 29.4.83	65
11	Mys Unony	135.5°E - 172.8°E 65.1°S -77.9°S	20.1.82- 9.4.84	47
12	Mys Tihiy	116.7°E -167.6°E 64° S - 68.4°S	2.1.81- 8.4.81	155

Table 2.2: Net Characteristics of the Vessels

	Trawl Mouth Length (m)	Effective Trawl Mouth Section (m^2)	Mesh Size (mm)	Mesh Bar Length (mm)
Akademik Knipovich	87.6	49	40	20
Odysssey	36.6	78	40	20
Argus	66	163	40	20
Professor Derugin	49.5	26	35	12
Globus	110	72	35	12
Mys Dalniy	77.4	50	35	11
Mys Unony	77.4	50	35	11
Mys Tihiy	77.4	50	35	11

Table 3.1: Summary of Means and Variances of Quantities Derived from Soviet Data. (See text for a full discussion of how to read the table.)

Quantity	Data Set					
	1	2	3	4	5	6
Trawls per day	1.78,.91	2,.73	2.8,1.6	1.3,.44	4.6,2.4	4.5,2.4
Trawling depth (meters)	44.9,22.2 (58,4)	64,54	66,47	80,45	20.3,15.3	37,21
Trawling Speed (knots)	4.3,.32	2.8,.26	3.4,.5	2.9,1	2.7,.26	2.9,.22
Trawling time (hours)	1.0,.65	1.1,.52	.89,.53	1.2,.71 (1.8,3)	1.1,.52 (1.3,13)	.72,.52 (.87,1)
Trawling length (n miles)	3.7,1.8 (4.5,24)	3.1,1.4 (3.6,3)	2.9,1.7 (3.1,8)	2.9,2.2 (5.4,10)	3.0,1.5 (3.3,12)	2.1,1.6
Krill Catch (tonnes)	8391, 5822	4053, 3097	2386, 2906	4505, 3778	4008, 8147	5814, 3983
Krill Size (mm)	45,3.5	48,3.6	44,3.7	51,2.9	No data	39,3.6
Between Trawlings Time (hours)	11.4,8.8 (17,8)	9.0,9.0 (24.6,6)	7.2,6.2 (10.8,6)	14,8.2 (36.4,11)	4.6,7.2	4.2,5.2
Between Trawlings Movement (n miles)	18,15.4 (41,13)	6.5,7.6 (58,12)	25.7,17.8 (60,36)	18.5,17.4 (54,5)	13.2,18.5 (20,19)	5.6,9.9

Quantity	Data Set					
	7	8	9	10	11	12
Trawls per day	3.5,1.9	3.4,1.3	5.7,4.9	2.6,1.3	2.7,2.6	3.2,1.9
Trawling depth (meters)	43,36	88.6,27	17,15.7	17.3,16.6	52,45	26,14
Trawling Speed (knots)	3.3,.24	3.5,.14	3.0,.17	2.8,.22	3.6,.28	2.7,.32
Trawling time (hours)	1.41,.86	.77,.66 (.93,2)	.9,.9 (1.1,11)	1.4,.4	2.3,.76 (2.8,5)	1,.6 (1.2,3)
Trawling length (n miles)	3.8,1.9 (4.8,34)	2.2,1.3 (3.0,16)	2.2,2.1 (3.3,8)	4.0,1.4 (4.3,3)	5.7,1.4 (10,30)	2.7,1.7 (3.4,6)
Krill Catch (tonnes)	4133, 4081	2534, 5035	7193, 4876	2192, 2364	10435, 8123	3512, 3205
Krill Size (mm)	39,3.6	48,4.2	No data	No data	No data	No data
Between Trawlings Time (hours)	5.8,7.6 (6.4,1)	5.6,4.6 (5.8,1)	3.0,4.3 (4.6,7)	7.4,10.3 (18,14)	6.2,8.0 (24,6)	6.5,8.9 (13,9)
Between Trawlings Movement (n miles)	9.6,12.8 (11.6,3) (37,15)	21.8,15.6 (25,4)	5.6,9.9 (10.6,5)	15.2,20.5 (83,9)	10,14 (29,3)	12,20

Table 3.2: Correlations for Data Set 1, all Data Used (see text for a discussion of how to read the table)

Quantities	TT	TL	KC	BTM	BTT	D	L
TT	+ +	+ +	0 +	- -	0 0	0 0	0 0
TL	+ +	+ +	0 +	- -	0 0	0 0	0 0
KC	0 +	0 +	+ 0	- -	0 0	0 0	0 0
BTM	- -	- -	- -	+ +	+ 0	0 0	0 0
BTT	0 0	0 0	0 0	+ 0	+ 0	0 0	0 0
D	- 0	0 0	0 0	0 +	0 +	+ 0	0 0
L	0 0	0 0	0 0	0 0	0 0	0 0	+ +

Table 3.3: Correlations for Data Set 1, Cutoff Values applied (see text for a discussion of how to read the table)

Quantities	TT	TL	KC	BTM	BTT	D	L
TT	+ +	+ +	0 +	- -	0 0	- -	0 0
TL	+ +	+ 0	+ 0	- -	0 -	0 0	0 0
KC	0 +	0 0	+ 0	0 -	- 0	- 0	0 0
BTM	- -	- 0	0 0	+ +	+ 0	0 0	0 0
BTT	0 -	0 0	- 0	+ 0	+ 0	0 0	0 0
D	- 0	0 0	0 0	0 +	0 +	+ 0	0 0
L	0 0	0 0	0 0	0 0	0 0	0 0	+ +

Table 3.4: Correlations for Data Set 2, all Data Used (see text for a discussion of how to read the table)

Quantities	TT	TL	KC	BTM	BTT	D	L
TT	+	+	0	0	0	0	0
	+	+	0	0	0	0	0
TL	+	+	0	0	0	0	0
	+	0	0	0	0	0	0
KC	0	0	+	0	0	0	0
	0	0	0	0	0	0	0
BTM	0	0	0	+	+	+	-
	0	0	0	0	0	0	0
BTT	0	0	0	+	+	+	-
	0	0	0	0	0	0	0
D	0	0	0	+	+	+	-
	0	0	0	+	+	0	-
L	0	0	0	-	-	-	+
	0	0	0	-	-	0	+

Table 3.5: Correlations for Data Set 2, Cutoff Values applied (see text for a discussion of how to read the table)

Quantities	TT	TL	KC	BTM	BTT	D	L
TT	+	+	0	0	0	0	0
	0	0	0	0	0	0	0
TL	+	+	0	0	0	0	0
	0	0	0	0	0	0	0
KC	0	0	+	0	0	0	0
	0	0	0	0	0	0	0
BTM	0	0	0	+	+	+	0
	0	0	0	0	0	+	-
BTT	0	0	0	+	+	+	0
	0	0	0	0	0	0	0
D	0	0	0	+	+	+	-
	0	0	0	0	0	0	-
L	0	0	0	0	0	-	+
	0	0	0	0	-	0	+

Table 3.6: Correlations for Data Set 3, all Data Used (see text for a discussion of how to read the table)

Quantities	TT	TL	KC	BTM	BTT	D	L
TT	+	+	+	0	0	0	0
	0	0	0	+	+	0	0
TL	+	+	+	0	0	0	0
	0	0	0	0	+	0	0
KC	+	+	+	-	0	-	0
	0	0	+	0	0	-	0
BTM	0	0	-	+	+	0	0
	0	0	0	+	+	0	0
BTT	0	0	0	+	+	0	0
	+	+	0	0	+	0	0
D	0	0	-	0	0	+	0
	0	0	-	0	0	0	0
L	0	0	0	0	0	0	+
	0	0	0	0	-	0	+

Table 3.7: Correlations for Data Set 3, Cutoff Values applied (see text for a discussion of how to read the table)

Quantities	TT	TL	KC	BTM	BTT	D	L
TT	+	+	+	0	0	0	0
	0	+	0	0	+	0	0
TL	+	+	+	0	0	0	0
	0	0	0	0	+	0	0
KC	+	+	+	-	0	-	0
	0	0	+	-	0	-	0
BTM	-	0	-	+	+	0	0
	0	0	-	+	0	0	0
BTT	0	0	0	+	+	0	0
	0	0	0	+	+	0	0
D	0	0	-	0	0	+	0
	-	-	-	0	0	+	0
L	0	0	0	0	0	0	+
	0	0	0	0	0	0	+

Table 3.8: Correlations for Data Set 4, all Data Used (see text for a discussion of how to read the table)

Quantities	TT	TL	KC	BTM	BTT	D	L
TT	+ 0	+ 0	0 0	0 0	0 0	+ 0	- 0
TL	+ 0	+ 0	0 0	0 0	0 0	+ +	0 0
KC	0 0	0 0	+ 0	0 0	0 0	0 0	0 0
BTM	0 0	0 0	0 0	+ 0	+ 0	0 0	0 0
BTT	0 0	0 0	0 0	+ 0	+ 0	0 0	0 0
D	+ 0	+ 0	0 0	0 0	0 0	+ 0	- 0
L	- -	- -	0 0	0 0	0 0	- -	+ -

Table 3.9: Correlations for Data Set 4, Cutoff Values applied (see text for a discussion of how to read the table)

Quantities	TT	TL	KC	BTM	BTT	D	L
TT	+ 0	+ 0	0 0	0 0	0 0	0 0	0 0
TL	+ 0	+ 0	0 0	0 0	0 0	0 0	0 0
KC	0 0	0 0	+ 0	0 0	0 0	0 +	0 0
BTM	0 0	0 +	0 -	+ +	0 0	- 0	+ +
BTT	0 0	0 0	0 0	+ 0	0 0	0 0	0 0
D	0 0	0 0	0 0	- 0	0 0	+ +	0 -
L	0 0	0 0	0 0	+ +	0 0	0 -	+ +

Table 3.10: Correlations for Data Set 5, all Data Used (see text for a discussion of how to read the table)

Quantities	TT	TL	KC	BTM	BTT	D
TT	+ 0	+ 0	0 0	+ 0	+ +	0 0
TL	+ 0	+ 0	0 0	+ 0	+ +	0 0
KC	0 0	0 0	+ +	0 0	0 0	0 0
BTM	+ 0	+ 0	0 0	+ +	+ 0	+ 0
BTT	+ 0	+ 0	0 0	+ +	+ 0	+ 0
D	0 0	0 0	0 0	+ 0	+ 0	+ +

Table 3.11: Correlations for Data Set 5, Cutoff Values applied (see text for a discussion of how to read the table)

Quantities	TT	TL	KC	BTM	BTT	D
TT	+ +	+ +	0 -	0 0	0 0	0 0
TL	+ +	+ +	0 -	0 0	0 0	0 +
KC	0 0	0 0	+ +	- -	0 0	0 -
BTM	0 0	0 0	- 0	+ +	+ 0	0 0
BTT	0 0	0 0	0 0	+ +	+ 0	+ 0
D	0 0	0 0	0 0	0 0	+ 0	+ +

Table 3.12: Correlations for Data Set 6, all Data Used (see text for a discussion of how to read the table)

Quantities	TT	TL	KC	BTM	BTT	D
TT	+ 0	+ 0	0 0	0 0	0 0	0 0
TL	+ 0	+ 0	0 0	0 0	0 0	0 0
KC	0 0	0 0	+ +	0 0	0 0	0 0
BTM	0 0	0 0	0 +	+ 0	+ 0	0 +
BTT	0 0	0 0	0 0	+ 0	+ 0	+ 0
D	0 +	0 +	0 0	0 0	0 0	+ +

Table 3.13: Correlations for Data Set 6, Cutoff Values applied (see text for a discussion of how to read the table)

Quantities	TT	TL	KC	BTM	BTT	D
TT	+ +	+ +	0 0	0 0	0 +	+ 0
TL	+ +	+ +	+ 0	0 0	0 +	+ 0
KC	0 0	+ 0	+ +	0 -	0 +	0 0
BTM	0 0	0 0	0 0	+ 0	+ 0	0 +
BTT	0 0	0 0	0 0	+ 0	+ 0	0 0
D	+ +	+ +	0 0	0 0	0 0	+ +

Table 3.14: Correlations for Data Set 7, all Data Used (see text for a discussion of how to read the table)

Quantities	TT	TL	KC	BTM	BTT	D	L
TT	+	+	0	0	0	0	0
	+	+	0	0	0	0	0
TL	+	+	0	0	0	0	0
	+	+	0	0	0	0	0
KC	0	0	+	0	0	0	0
	0	0	0	0	0	0	0
BTM	0	0	0	+	+	0	0
	0	0	0	+	0	0	0
BTT	0	0	0	+	+	0	0
	0	0	0	0	0	0	0
D	0	0	0	0	0	+	0
	0	0	0	0	0	+	0
L	0	0	0	0	0	0	+
	0	0	0	0	0	0	0

Table 3.15: Correlations for Data Set 7, Cutoff Values applied (see text for a discussion of how to read the table)

Quantities	TT	TL	KC	BTM	BTT	D	L
TT	+	+	0	0	-	0	0
	+	+	0	0	0	0	0
TL	+	+	+	0	-	0	0
	+	+	0	0	0	0	0
KC	0	+	+	0	0	0	0
	0	0	0	0	+	0	0
BTM	0	0	0	+	+	+	0
	0	0	0	+	0	0	+
BTT	-	-	0	+	+	-	0
	0	0	0	0	0	0	0
D	0	0	0	0	0	+	0
	0	0	0	+	0	+	0
L	0	0	0	0	0	0	+
	0	0	0	0	0	0	0

Table 3.16: Correlations for Data Set 8, all Data Used (see text for a discussion of how to read the table)

Quantities	TT	TL	KC	BTM	BTT	D	L
TT	+ 0	+ 0	0 0	0 0	0 0	- -	0 0
TL	+ 0	+ +	0 +	0 0	0 0	- -	+ 0
KC	0 0	0 0	+ 0	0 0	0 0	- -	0 0
BTM	0 0	0 0	0 0	+ +	+ 0	0 0	0 0
BTT	0 0	0 0	0 0	+ 0	+ 0	0 0	0 0
D	- -	- -	- -	0 0	0 0	+ +	0 -
L	0 0	+ 0	0 0	0 0	0 0	- -	+ +

Table 3.17: Correlations for Data Set 8, Cutoff Values applied (see text for a discussion of how to read the table)

Quantities	TT	TL	KC	BTM	BTT	D	L
TT	+ +	+ +	+ +	- -	0 0	- -	+ +
TL	+ +	+ +	+ +	- -	0 0	- -	0 0
KC	+ +	+ +	+ +	- -	- 0	- -	+ +
BTM	- -	- -	- -	+ +	+ +	+ +	- 0
BTT	0 -	0 0	- 0	+ +	+ 0	+ 0	0 0
D	- -	- -	- -	+ +	+ 0	+ +	- -
L	+ +	0 0	+ +	- -	0 0	- -	+ +

Table 3.18: Correlations for Data Set 9, all Data Used (see text for a discussion of how to read the table)

Quantities	TT	TL	KC	BTM	BTT	D
TT	+ +	+ +	+ +	0 0	+ +	+ +
TL	+ +	+ +	+ +	0 0	+ 0	+ +
KC	+ +	+ +	+ +	0 0	0 0	+ +
BTM	0 0	0 0	0 0	+ +	0 0	0 0
BTT	+ 0	+ 0	0 0	0 0	+ 0	0 0
D	+ +	+ +	+ +	0 0	0 0	+ +

Table 3.19: Correlations for Data Set 9, Cutoff Values applied (see text for a discussion of how to read the table)

Quantities	TT	TL	KC	BTM	BTT	D
TT	+ +	+ +	+ +	+ +	+ +	+ +
TL	+ +	+ +	+ +	+ +	+ +	+ +
KC	+ +	+ +	+ +	0 0	0 0	+ +
BTM	+ +	+ +	0 0	+ +	+ 0	+ 0
BTT	+ 0	+ 0	0 0	+ 0	+ -	0 0
D	+ +	+ +	+ +	+ 0	0 0	+ +

Table 3.20: Correlations for Data Set 10, all Data Used (see text for a discussion of how to read the table)

Quantities	TT	TL	KC	BTM	BTT	D
TT	+ 0	+ 0	+ 0	0 0	0 0	0 0
TL	+ 0	+ 0	+ 0	0 0	0 0	0 0
KC	+ 0	+ 0	+ +	0 -	0 0	0 0
BTM	0 0	0 0	0 0	+ 0	+ 0	0 0
BTT	0 0	0 0	0 0	+ 0	+ 0	0 0
D	0 0	0 0	0 0	0 +	0 0	+ +

Table 3.21: Correlations for Data Set 10, Cutoff Values applied (see text for a discussion of how to read the table)

Quantities	TT	TL	KC	BTM	BTT	D
TT	+ 0	+ 0	0 0	0 0	0 0	0 0
TL	+ 0	+ 0	0 0	0 0	0 0	0 0
KC	0 0	0 0	+ +	0 -	0 0	0 0
BTM	0 0	0 0	0 0	+ 0	+ 0	0 0
BTT	0 0	0 0	0 0	+ 0	+ 0	0 0
D	0 0	0 0	0 0	0 0	0 0	+ +

Table 3.22: Correlations for Data Set 11, all Data Used (see text for a discussion of how to read the table)

Quantities	TT	TL	KC	BTM	BTT	D
TT	+ 0	+ 0	+ +	0 0	0 0	0 0
TL	+ 0	+ 0	+ +	0 0	0 0	0 0
KC	+ +	+ +	+ +	0 -	0 0	0 0
BTM	0 0	0 0	0 0	+ +	+ 0	+ 0
BTT	0 0	0 0	0 0	+ +	+ 0	0 0
D	0 0	0 0	0 0	+ +	0 0	+ 0

Table 3.23: Correlations for Data Set 11, Cutoff Values applied (see text for a discussion of how to read the table)

Quantities	TT	TL	KC	BTM	BTT	D
TT	+ 0	+ 0	0 0	0 0	0 0	0 0
TL	+ 0	+ 0	0 0	0 0	0 0	0 0
KC	0 0	0 0	+ +	0 -	0 0	0 0
BTM	0 0	0 0	0 0	+ 0	+ 0	0 0
BTT	0 0	0 0	0 0	+ 0	+ 0	0 0
D	0 0	0 0	0 0	0 0	0 0	+ 0

Table 3.24: Correlations for Data Set 12, all Data Used (see text for a discussion of how to read the table)

Quantities	TT	TL	KC	BTM	BTT	D
TT	+ +	+ +	+ 0	0 0	0 0	+ +
TL	+ +	+ +	+ 0	0 0	0 0	+ +
KC	+ 0	+ 0	+ 0	0 0	0 0	0 0
BTM	0 0	0 0	0 0	+ +	+ 0	0 0
BTT	0 0	0 0	0 0	+ +	+ 0	0 0
D	+ +	+ +	0 0	0 0	0 0	+ +

Table 3.25: Correlations for Data Set 12, Cutoff Values applied (see text for a discussion of how to read the table)

Quantities	TT	TL	KC	BTM	BTT	D
TT	+ +	+ +	+ 0	0 0	0 0	+ 0
TL	+ +	+ +	+ +	0 0	0 0	+ 0
KC	+ +	+ 0	+ 0	0 0	- 0	0 0
BTM	0 0	0 0	0 0	+ 0	+ 0	0 0
BTT	0 0	0 0	- 0	+ 0	+ 0	0 0
D	+ +	+ +	0 0	0 0	0 0	+ +

Table 12.1: Parameter Values for Multiple Parameter Changes in Biomass

Parameter					Biomass Relative to Base Case
N_c	L_c	δ_c	r_c	D_c	
48	5.11	87.1	44.0	8.09	.20
60	6.60	237.2	16.5	20.4	.40
57	2.66	124.1	77.7	17.2	.61
54	3.84	134.7	84.5	9.05	.81
36	5.60	150	50	20	1.0 (Base Case)
37	6.89	48.9	68.5	25.6	1.2

Table 12.2: Detection Properties of Abundance Index "Total Catch"

Biomass Relative to Base Case	μ_c/μ_b	Probability of Detection	
		Simulation	Normal Approx
Biomass = 2/3 of Base Case			
$L_c \times \sqrt{2/3}$	1.01	0	0
$r_c \times \sqrt{2/3}$	.91	0	0
$\delta_c \times 2/3$	.80	0	0
$D_c \times 2/3$	.91	0	0
$N_c \times 2/3$	1.01	0	0
Biomass = 1/3 of Base Case			
$L_c \times \sqrt{1/3}$	1	0	0
$r_c \times \sqrt{1/3}$	.72	0	0
$\delta_c \times 1/3$	.51	.96	.92
$D_c \times 1/3$	.78	0	0
$N_c \times 1/3$	1	0	0
Multiple Parameter Changes Biomass =			
.2 of Base Case	.53	.62	.68
.4 of Base Case	.63	0	.02
.61 of Base Case	1.05	.08	0
.81 of Base Case	.98	0	0
1.2 of Base Case	.64	0	.01
Adaptive Behavior by Fleet			
B_{thr} = 0 tonnes	.62	.08	.09
B_{thr} = 40 tonnes	.99	0	0

Table 12.3: Detection Properties of Abundance Index "Total Hauls (Total Number of Swarms Selected)"

Biomass Relative to Base Case	μ_c/μ_b	Probability of Detection	
		Simulation	Normal Approx
Biomass = 2/3 of Base Case			
$L_c \times \sqrt{2/3}$	1.01	0	0
$r_c \times \sqrt{2/3}$	.93	0	0
$\delta_c \times 2/3$	.94	0	0
$D_c \times 2/3$	.96	0	0
$N_c \times 2/3$	1.0	0	0
Biomass = 1/3 of Base Case			
$L_c \times \sqrt{1/3}$	.99	0	0
$r_c \times \sqrt{1/3}$	.77	0	0
$\delta_c \times 1/3$	.82	0	0
$D_c \times 1/3$	.88	0	0
$N_c \times 1/3$	.99	0	0
Multiple Parameter Changes Biomass =			
.2 of Base Case	.76	0	0
.4 of Base Case	.59	.22	.30
.61 of Base Case	1.05	.64	0
.81 of Base Case	1.05	.76	0
1.2 of Base Case	.95	0	0
Adaptive Behavior by Fleet			
B_{thr} = 0 tonnes	1.29	.98	.83
B_{thr} = 40 tonnes	1.03	.34	0

Table 12.4: Detection Properties of Abundance Index "Total Number of Swarms Fished"

Biomass Relative to Base Case	μ_c/μ_b	Probability of Detection	
		Simulation	Normal Approx
Biomass = 2/3 of Base Case			
$L_c \times \sqrt{2/3}$	1.02	.02	0
$r_c \times \sqrt{2/3}$	.95	0	0
$\delta_c \times 2/3$	.98	0	0
$D_c \times 2/3$	.84	0	0
$N_c \times 2/3$	1	0	0
Biomass = 1/3 of Base Case			
$L_c \times \sqrt{1/3}$	1	0	0
$r_c \times \sqrt{1/3}$	.79	0	0
$\delta_c \times 1/3$	.88	0	0
$D_c \times 1/3$	.64	.04	.03
$N_c \times 1/3$	1	0	0
Multiple Parameter Changes Biomass =			
.2 of Base Case	.58	.32	.35
.4 of Base Case	.59	.32	.3
.61 of Base Case	1.01	.02	0
.81 of Base Case	.81	0	0
1.2 of Base Case	1.15	.64	.06
Adaptive Behavior by Fleet			
B_{thr} = 0 tonnes	1.4	.98	.91
B_{thr} = 40 tonnes	1.06	.14	0

Table 12.5: Detection Properties of Abundance Index "Total Number of Swarms Encountered"

Biomass Relative to Base Case	μ_c/μ_b	Probability of Detection	
		Simulation	Normal Approx
Biomass = 2/3 of Base Case			
$L_c \times \sqrt{2/3}$	1.01	.04	0
$r_c \times \sqrt{2/3}$	1.17	.9	.14
$\delta_c \times 2/3$	1.19	.98	.24
$D_c \times 2/3$	.93	0	0
$N_c \times 2/3$	1.01	.04	0
Biomass = 1/3 of Base Case			
$L_c \times \sqrt{1/3}$	1	.04	0
$r_c \times \sqrt{1/3}$	1.541	.98	
$\delta_c \times 1/3$	1.67	1	.99
$D_c \times 1/3$	.82	0	0
$N_c \times 1/3$	1	.04	0
Multiple Parameter Changes Biomass =			
.2 of Base Case	1.16	.86	1
.4 of Base Case	1.98	1.99	
.61 of Base Case	.76	0	0
.81 of Base Case	.63	.16	.1
1.2 of Base Case	1.37	1	.95
Adaptive Behavior by Fleet			
B_{thr} = 0 tonnes	.47	1	.99
B_{thr} = 40 tonnes	.93	0	0

Table 12.6: Detection Properties of Abundance Index "Total Trawl Time"

Biomass Relative to Base Case	μ_c/μ_b	Probability of Detection Simulation	Probability of Detection Normal Approx
Biomass = 2/3 of Base Case			
$L_c \times \sqrt{2/3}$	1.01	0	0
$r_c \times \sqrt{2/3}$	.92	0	0
$\delta_c \times 2/3$	.97	0	0
$D_c \times 2/3$	.96	0	0
$N_c \times 2/3$	.99	0	0
Biomass = 1/3 of Base Case			
$L_c \times \sqrt{1/3}$	.99	0	0
$r_c \times \sqrt{1/3}$	.74	0	0
$\delta_c \times 1/3$	.87	0	0
$D_c \times 1/3$	.89	0	0
$N_c \times 1/3$	.99	0	0
Multiple Parameter Changes Biomass =			
.2 of Base Case	.77	0	0
.4 of Base Case	.55	.9	.93
.61 of Base Case	1.11	.7	.02
.81 of Base Case	1.1	.76	.04
1.2 of Base Case	1.06	0	0
Adaptive Behavior by Fleet			
B_{thr} = 0 tonnes	1.23	.94	.48
B_{thr} = 40 tonnes	1.03	.16	0

Table 12.7: Detection Properties of Abundance Index "Total Search Time"

Biomass Relative to Base Case	μ_c/μ_b	Probability of Detection	
		Simulation	Normal Approx
Biomass = 2/3 of Base Case			
$L_c \times \sqrt{2/3}$	1	.02	0
$r_c \times \sqrt{2/3}$	1.24	.92	.42
$\delta_c \times 2/3$	1.19	.86	.21
$D_c \times 2/3$	1.11	.52	.01
$N_c \times 2/3$	.99	0	0
Biomass = 1/3 of Base Case			
$L_c \times \sqrt{1/3}$	.99	.04	0
$r_c \times \sqrt{1/3}$	1.76	1	.99
$\delta_c \times 1/3$	1.66	1	.99
$D_c \times 1/3$	1.41	.98	.95
$N_c \times 1/3$	1	0	0
Multiple Parameter Changes Biomass =			
.2 of Base Case	1.9	1	.99
.4 of Base Case	2.47	1	.99
.61 of Base Case	.69	.06	.01
.81 of Base Case	.71	0	0
1.2 of Base Case	1.12	.72	.01
Adaptive Behavior by Fleet			
B_{thr} = 0 tonnes	.1	1	1
B_{thr} = 40 tonnes	.87	0	0

Table 12.8: Detection Properties of Abundance Index "Total Reciprocal Search Time"

Biomass Relative to Base Case	μ_c/μ_b	Probability of Detection	
		Simulation	Normal Approx
Biomass = 2/3 of Base Case			
$L_c \times \sqrt{2/3}$	1.01	0	0
$r_c \times \sqrt{2/3}$	.76	0	0
$\delta_c \times 2/3$	.81	0	0
$D_c \times 2/3$	.088	0	0
$N_c \times 2/3$	1.01	0	0
Biomass = 1/3 of Base Case			
$L_c \times \sqrt{1/3}$	1	0	0
$r_c \times \sqrt{1/3}$	.44	.96	.95
$\delta_c \times 1/3$	.52	0	.51
$D_c \times 1/3$	.64	.96	.03
$N_c \times 1/3$	.98	0	0
Multiple Parameter Changes Biomass =			
.2 of Base Case	.41	1	.98
.4 of Base Case	.22	1	.99
.61 of Base Case	1.42	.94	.82
.81 of Base Case	1.35	.84	.58
1.2 of Base Case	.86	0	0
Adaptive Behavior by Fleet			
B_{thr} = 0 tonnes	7.91	1	.99
B_{thr} = 40 tonnes	1.15	.12	.03

Table 12.9: Detection Properties of Abundance Index "Number of Discoveries by the Survey Vessel"

Biomass Relative to Base Case	μ_c/μ_b	Probability of Detection	
		Simulation	Normal Approx
Biomass = 2/3 of Base Case			
$L_c \times \sqrt{2/3}$	.76	0	0
$r_c \times \sqrt{2/3}$	.92	0	0
$\delta_c \times 2/3$	.97	0	0
$D_c \times 2/3$	1.01	0	0
$N_c \times 2/3$	.65	0	0
Biomass = 1/3 of Base Case			
$L_c \times \sqrt{1/3}$	.62	.04	0
$r_c \times \sqrt{1/3}$	.96	.02	0
$\delta_c \times 1/3$	1	.97	0
$D_c \times 1/3$	.94	0	0
$N_c \times 1/3$	.35	.18	.05
Multiple Parameter Changes Biomass =			
.2 of Base Case	1.15	0	0
.4 of Base Case	1.95	.62	.54
.61 of Base Case	.77	0	0
.81 of Base Case	.98	0	0
1.2 of Base Case	1.15	.02	0
Adaptive Behavior by Fleet			
B_{thr} = 0 tonnes	1	0	0
B_{thr} = 40 tonnes	.99	0	0

Table 12.10: Detection Properties of Abundance Index "Average {Catch/Towtime}"

Biomass Relative to Base Case	μ_c/μ_b	Probability of Detection	
		Simulation	Normal Approx
Biomass = 2/3 of Base Case			
$L_c \times \sqrt{2/3}$	1	.06	0
$r_c \times \sqrt{2/3}$	1	.04	0
$\delta_c \times 2/3$	.83	.98	.86
$D_c \times 2/3$	.94	.18	.03
$N_c \times 2/3$	1.01	.06	0
Biomass = 1/3 of Base Case			
$L_c \times \sqrt{1/3}$	1	.16	0
$r_c \times \sqrt{1/3}$	.99	.08	0
$\delta_c \times 1/3$	.57	1	.99
$D_c \times 1/3$	.86	.84	.56
$N_c \times 1/3$	1.01	.08	0
Multiple Parameter Changes Biomass =			
.2 of Base Case	.69	1	.99
.4 of Base Case	1.19	.98	.87
.61 of Base Case	.92	.28	.07
.81 of Base Case	.87	.8	.47
1.2 of Base Case	.58	1	.99
Adaptive Behavior by Fleet			
B_{thr} = 0 tonnes	.47	1	.99
B_{thr} = 40 tonnes	.95	.16	.02

Table 12.11: Detection Properties of Abundance Index "Average {Catch/Searchtime}"

Biomass Relative to Base Case	μ_c/μ_b	Probability of Detection	
		Simulation	Normal Approx
Biomass = 2/3 of Base Case			
$L_c \times \sqrt{2/3}$	1	0	0
$r_c \times \sqrt{2/3}$	.8	0	.25
$\delta_c \times 2/3$	.74	.9	.57
$D_c \times 2/3$	.86	.36	.05
$N_c \times 2/3$	1.02	0	0
Biomass = 1/3 of Base Case			
$L_c \times \sqrt{1/3}$	1.01	0 0	
$r_c \times \sqrt{1/3}$	.53	1	.99
$\delta_c \times 1/3$	.39	1	.99
$D_c \times 1/3$	.64	1	.97
$N_c \times 1/3$	1	0	0
Multiple Parameter Changes Biomass =			
.2 of Base Case	.38	1	.99
.4 of Base Case	.39	1	.99
.61 of Base Case	1.33	.86	.87
.81 of Base Case	1.19	.26	.27
1.2 of Base Case	.61	1	.99
Adaptive Behavior by Fleet			
B_{thr} = 0 tonnes	2.77	1	.99
B_{thr} = 40 tonnes	1.08	0	0

Table 12.12: Detection Properties of Abundance Index "Average {(Catch/Towtime)/ Searchtime}"

Biomass Relative to Base Case	μ_c/μ_b	Probability of Detection	
		Simulation	Normal Approx
Biomass = 2/3 of Base Case			
$L_c \times \sqrt{2/3}$	1	0	0
$r_c \times \sqrt{2/3}$	.83	.48	.08
$\delta_c \times 2/3$	.36	1	.99
$D_c \times 2/3$	.87	.2	.01
$N_c \times 2/3$	1.03	0	0
Biomass = 1/3 of Base Case			
$L_c \times \sqrt{1/3}$	1.01	0	0
$r_c \times \sqrt{1/3}$	.56	1	.99
$\delta_c \times 1/3$	.36	1	.99
$D_c \times 1/3$	.63	1	.93
$N_c \times 1/3$	1.01	.02	0
Multiple Parameter Changes Biomass =			
.2 of Base Case	.37	.64	.99
.4 of Base Case	.45	1	.99
.61 of Base Case	1.25	.4	.37
.81 of Base Case	1.11	.04	.04
1.2 of Base Case	.53	1	.99
Adaptive Behavior by Fleet			
B_{thr} = 0 tonnes	2.74	1	.99
B_{thr} = 40 tonnes	1.07	0	0

Table 12.13: Detection Properties of Abundance Index " Catch Per Day"

Biomass Relative to Base Case	μ_c/μ_b	Probability of Detection	
		Simulation	Normal Approx
Biomass = 2/3 of Base Case			
$L_c \times \sqrt{2/3}$	1.01	0	0
$r_c \times \sqrt{2/3}$	.91	0	0
$\delta_c \times 2/3$	.8	0	0
$D_c \times 2/3$	.91	0	0
$N_c \times 2/3$	1.01	0	0
Biomass = 1/3 of Base Case			
$L_c \times \sqrt{1/3}$	1	0	0
$r_c \times \sqrt{1/3}$	.72	0	0
$\delta_c \times 1/3$	.51	.94	.92
$D_c \times 1/3$	.78	0	0
$N_c \times 1/3$	1	0	0
Multiple Parameter Changes Biomass =			
.2 of Base Case	.53	.64	.68
.4 of Base Case	.63	0	.02
.61 of Base Case	1.05	.08	0
.81 of Base Case	.98	0	0
1.2 of Base Case	.64	.96	.01
Adaptive Behavior by Fleet			
B_{thr} = 0 tonnes	.62	.92	.09
B_{thr} = 40 tonnes	.99	0	0

Table 12.14: Detection Properties of Abundance Index "Catch Per Haul"

Biomass Relative to Base Case	μ_c/μ_b	Probability of Detection	
		Simulation	Normal Approx
Biomass = 2/3 of Base Case			
L_c x$\sqrt{2/3}$	.99	0	0
r_c x $\sqrt{2/3}$	.97	0	0
δ_c x 2/3	.85	.98	.87
D_c x 2/3	.94	.18	.05
N_c x 2/3	1	0	0
Biomass = 1/3 of Base Case			
L_c x $\sqrt{1/3}$	1	0	0
r_c x $\sqrt{1/3}$	.94	.26	.03
δ_c x 1/3	.61	1	.99
D_c x 1/3	.87	.98	.81
N_c x 1/3	1	0	0
Multiple Parameter Changes Biomass =			
.2 of Base Case	.7	.1	.99
.4 of Base Case	1.05	.04	.09
.61 of Base Case	.99	0	0
.81 of Base Case	.93	0.	.09
1.2 of Base Case	.67	1	.99
Adaptive Behavior by Fleet			
B_{thr} = 0 tonnes	.48	1	.99
B_{thr} = 40 tonnes	.96	1	.01

Table 12.15: Detection Properties of Abundance Index "Hauls Per Concentration Discovered"

Biomass Relative to Base Case	μ_c/μ_b	Probability of Detection	
		Simulation	Normal Approx
Biomass = 2/3 of Base Case			
$L_c \times \sqrt{2/3}$	1.38	0	0
$r_c \times \sqrt{2/3}$	1.03	0	0
$\delta_c \times 2/3$	.89	0	0
$D_c \times 2/3$	.93	0	0
$N_c \times 2/3$	1.5	.04	0
Biomass = 1/3 of Base Case			
$L_c \times \sqrt{1/3}$	1.66	.04	.03
$r_c \times \sqrt{1/3}$	.77	0	0
$\delta_c \times 1/3$	.80	0	0
$D_c \times 1/3$	.89	0	0
$N_c \times 1/3$	3.1	.28	.45
Multiple Parameter Changes Biomass =			
.2 of Base Case	.63	0	0
.4 of Base Case	.27	.68	0
.61 of Base Case	1.31	0	0
.81 of Base Case	1.02	0	0
1.2 of Base Case	.77	0	0
Adaptive Behavior by Fleet			
B_{thr} = 0 tonnes	1.23	1	0
B_{thr} = 40 tonnes	1	0	0

Table 12.16: Detection Properties of Abundance Index "Fraction of Swarms Selected For Fishing"

Biomass Relative to Base Case	μ_c/μ_b	Probability of Detection	
		Simulation	Normal Approx
Biomass = 2/3 of Base Case			
$L_c \times \sqrt{2/3}$	.99	.02	0
$r_c \times \sqrt{2/3}$	.79	1	.99
$\delta_c \times 2/3$	.79	1	.99
$D_c \times 2/3$	1.04	.12	.05
$N_c \times 2/3$	.99	.04	0
Biomass = 1/3 of Base Case			
$L_c \times \sqrt{1/3}$	.99	.02	0
$r_c \times \sqrt{1/3}$	.5	1	.99
$\delta_c \times 1/3$	.49	1	.99
$D_c \times 1/3$	1.08	.32	.27
$N_c \times 1/3$	.98	.06	0
Multiple Parameter Changes Biomass =			
.2 of Base Case	.65	1	.99
.4 of Base Case	.3	1	1
.61 of Base Case	1.38	1	.99
.81 of Base Case	1.66	1	.99
1.2 of Base Case	.71	1	.99
Adaptive Behavior by Fleet			
B_{thr} = 0 tonnes	2.74	1	.99
B_{thr} = 40 tonnes	1.11	.58	.53

Table 12.17: Detection Properties of Abundance Index "Average Trawl Length"

Biomass Relative to Base Case	μ_c/μ_b	Probability of Detection	
		Simulation	Normal Approx
Biomass = 2/3 of Base Case			
$L_c \times \sqrt{2/3}$	1.01	.04	0
$r_c \times \sqrt{2/3}$	.97	.42	.05
$\delta_c \times 2/3$	1.07	1	.5
$D_c \times 2/3$	.7	.22	0
$N_c \times 2/3$	1	.02	0
Biomass = 1/3 of Base Case			
$L_c \times \sqrt{1/3}$	1.01	.04	.01
$r_c \times \sqrt{1/3}$	.91	1	.78
$\delta_c \times 1/3$	1.16	1	.99
$D_c \times 1/3$	1.01	.12	.02
$N_c \times 1/3$	1	.04	0
Multiple Parameter Changes Biomass =			
.2 of Base Case	1.03	.14	.08
.4 of Base Case	.79	1	.99
.61 of Base Case	1.13	.98	.97
.81 of Base Case	1.11	.98	.94
1.2 of Base Case	1.33	1	.99
Adaptive Behavior by Fleet			
B_{thr} = 0 tonnes	.86	1	.99
B_{thr} = 40 tonnes	1	.02	0

Table 12.18: Detection Properties of Abundance Index "Discoveries x Total Catch"

Biomass Relative to Base Case	μ_c/μ_b	Probability of Detection Simulation	Probability of Detection Normal Approx
Biomass = 2/3 of Base Case			
$L_c \times \sqrt{2/3}$	.77	0	0
$r_c \times \sqrt{2/3}$	.85	.02	0
$\delta_c \times 2/3$	.78	0	0
$D_c \times 2/3$	.93	0	0
$N_c \times 2/3$	.66	.02	0
Biomass = 1/3 of Base Case			
$L_c \times \sqrt{1/3}$	.63	.04	0
$r_c \times \sqrt{1/3}$	.7	0	0
$\delta_c \times 1/3$	.49	.04	0
$D_c \times 1/3$	.74	0	0
$N_c \times 1/3$	.36	.34	.06
Multiple Parameter Changes Biomass =			
.2 of Base Case	.62	0	0
.4 of Base Case	1.24	.04	0
.61 of Base Case	.81	0	0
.81 of Base Case	.97	0	0
1.2 of Base Case	.74	1	0
Adaptive Behavior by Fleet			
B_{thr} = 0 tonnes	.63	0	0
B_{thr} = 40 tonnes	.99	0	0

Table 12.19: Detection Properties of Abundance Index "Discoveries x Total Hauls x Total Catch"

Biomass Relative to Base Case	μ_c/μ_b	Probability of Detection	
		Simulation	Normal Approx
Biomass = 2/3 of Base Case			
$L_c \times \sqrt{2/3}$	.78	0	0
$r_c \times \sqrt{2/3}$	.8	.04	0
$\delta_c \times 2/3$	.74	0	0
$D_c \times 2/3$	.9	0	0
$N_c \times 2/3$	.66	.02	0
Biomass = 1/3 of Base Case			
$L_c \times \sqrt{1/3}$	.63	.06	0
$r_c \times \sqrt{1/3}$	.54	.06	0
$\delta_c \times 1/3$	.41	.04	0
$D_c \times 1/3$	.66	0	0
$N_c \times 1/3$	.36	.36	.03
Multiple Parameter Changes Biomass =			
.2 of Base Case	.47	.12	0
.4 of Base Case	.74	0	0
.61 of Base Case	.86	0	0
.81 of Base Case	1.02	0	0
1.2 of Base Case	.71	0	0
Adaptive Behavior by Fleet			
B_{thr} = 0 tonnes	.82	0	0
B_{thr} = 40 tonnes	1.03	0	0

Table 12.20: Detection Properties of Abundance Index "Discoveries x (Total Catch/Total Towtime) x Swarms Fished "

Biomass Relative to Base Case	μ_c/μ_b	Probability of Detection	
		Simulation	Normal Approx
Biomass = 2/3 of Base Case			
$L_c \times \sqrt{2/3}$	.78	0	0
$r_c \times \sqrt{2/3}$	.88	.02	0
$\delta_c \times 2/3$	.5	.04	0
$D_c \times 2/3$	.81	0	0
$N_c \times 2/3$	.68	.02	0
Biomass = 1/3 of Base Case			
$L_c \times \sqrt{1/3}$	.63	.04	0
$r_c \times \sqrt{1/3}$	.75	0	0
$\delta_c \times 1/3$	.5	.04	0
$D_c \times 1/3$	.53	.02	0
$N_c \times 1/3$	.36	.2	.05
Multiple Parameter Changes Biomass =			
.2 of Base Case	.47	.08	0
.4 of Base Case	1.34	.06	.04
.61 of Base Case	.74	0	0
.81 of Base Case	.71	0	0
1.2 of Base Case	.81	0	0
Adaptive Behavior by Fleet			
B_{thr} = 0 tonnes	.71	0	0
B_{thr} = 40 tonnes	1.02	0	0

Table 12.21: Detection Properties of Abundance Index "Discoveries x Average {Catch/ Towtime} x Swarms Fished "

Biomass Relative to Base Case	μ_c/μ_b	Probability of Detection	
		Simulation	Normal Approx
Biomass = 2/3 of Base Case			
$L_c \times \sqrt{2/3}$	.78	0	0
$r_c \times \sqrt{2/3}$	.89	.02	0
$\delta_c \times 2/3$	.79	0	0
$D_c \times 2/3$	.81	0	0
$N_c \times 2/3$	.68	.02	0
Biomass = 1/3 of Base Case			
$L_c \times \sqrt{1/3}$	.63	.04	0
$r_c \times \sqrt{1/3}$	.77	0	0
$\delta_c \times 1/3$	.49	.04	0
$D_c \times 1/3$	.52	.02	0
$N_c \times 1/3$	.36	.22	.05
Multiple Parameter Changes Biomass =			
.2 of Base Case	.47	.08	0
.4 of Base Case	1.4	.1	.06
.61 of Base Case	.73	0	0
.81 of Base Case	.7	0	0
1.2 of Base Case	.78	0	0
Adaptive Behavior by Fleet			
B_{thr} = 0 tonnes	.67	0	0
B_{thr} = 40 tonnes	1.01	0	0

Table 12.22: Detection Properties of Abundance Index "Total Catch/Total Towtime"

Biomass Relative to Base Case	μ_c/μ_b	Probability of Detection	
		Simulation	Normal Approx
Biomass = 2/3 of Base Case			
$L_c \times \sqrt{2/3}$	1	0	0
$r_c \times \sqrt{2/3}$	.98	.14	0
$\delta_c \times 2/3$	.82	1	.93
$D_c \times 2/3$	.94	.5	.04
$N_c \times 2/3$	1.01	0	0
Biomass = 1/3 of Base Case			
$L_c \times \sqrt{1/3}$	1	0	0
$r_c \times \sqrt{1/3}$	.97	.18	0
$\delta_c \times 1/3$	.58	1	.99
$D_c \times 1/3$	.87	1	.63
$N_c \times 1/3$	1	.04	0
Multiple Parameter Changes Biomass =			
.2 of Base Case	.7	1	.99
.4 of Base Case	1.15	.98	.75
.61 of Base Case	.93	.06	.06
.81 of Base Case	.88	.64	.44
1.2 of Base Case	.6	1	.99
Adaptive Behavior by Fleet			
B_{thr} = 0 tonnes	.5	1	.99
B_{thr} = 40 tonnes	.95	.32	.02

Table 12.23: Detection Properties of Abundance Index "Average {Catch/Towtime} / Average {Searchtime}"

Biomass Relative to Base Case	μ_c/μ_b	Probability of Detection	
		Simulation	Normal Approx
Biomass = 2/3 of Base Case			
$L_c \times \sqrt{2/3}$	1.01	0	0
$r_c \times \sqrt{2/3}$	.75	1	.67
$\delta_c \times 2/3$	.65	1	.99
$D_c \times 2/3$	.82	1	.23
$N_c \times 2/3$	1.02	0	0
Biomass = 1/3 of Base Case			
$L_c \times \sqrt{1/3}$	1	.48	.01
$r_c \times \sqrt{1/3}$	.43	1	.99
$\delta_c \times 1/3$	.28	1	.99
$D_c \times 1/3$	.54	1	.99
$N_c \times 1/3$	1	0	0
Multiple Parameter Changes Biomass =			
.2 of Base Case	.28	1	.99
.4 of Base Case	.29	1	.99
.61 of Base Case	1.43	1	.99
.81 of Base Case	1.28	.86	.73
1.2 of Base Case	.49	1	.99
Adaptive Behavior by Fleet			
B_{thr} = 0 tonnes	5.75	1	.99
B_{thr} = 40 tonnes	1.12	.08	.12

Table 12.24: Detection Properties of Abundance Index "Average {Catch/Towtime} x Average {Reciprocal Searchtime}"

Biomass Relative to Base Case	μ_c/μ_b	Probability of Detection	
		Simulation	Normal Approx
Biomass = 2/3 of Base Case			
$L_c \times \sqrt{2/3}$	1	0	0
$r_c \times \sqrt{2/3}$	.82	.52	.26
$\delta_c \times 2/3$	.71	.9	.82
$D_c \times 2/3$	.83	.16	.19
$N_c \times 2/3$	1.03	0	0
Biomass = 1/3 of Base Case			
$L_c \times \sqrt{1/3}$	1.01	0	0
$r_c \times \sqrt{1/3}$	.56	1	.99
$\delta_c \times 1/3$	.36	1	.99
$D_c \times 1/3$	.63	1	.99
$N_c \times 1/3$	1.01	0	0
Multiple Parameter Changes Biomass =			
.2 of Base Case	.37	1	.99
.4 of Base Case	.44	1	.99
.61 of Base Case	1.25	.54	.59
.81 of Base Case	1.11	0	.08
1.2 of Base Case	.53	1	.99
Adaptive Behavior by Fleet			
B_{thr} = 0 tonnes	2.92	1	.99
B_{thr} = 40 tonnes	1.06	0	0

Table 12.25: Detection Properties of Abundance Index "Discoveries x Total Catch/Total Towtime"

Biomass Relative to Base Case	μ_c/μ_b	Probability of Detection	
		Simulation	Normal Approx
Biomass = 2/3 of Base Case			
$L_c \times \sqrt{2/3}$	.76	0	0
$r_c \times \sqrt{2/3}$	.92	.02	0
δ_c x 2/3	.8	0	0
D_c x 2/3	.97	0	0
N_c x 2/3	.66	.02	0
Biomass = 1/3 of Base Case			
$L_c \times \sqrt{1/3}$	.62	.04	0
$r_c \times \sqrt{1/3}$	.94	0	0
δ_c x 1/3	.56	.02	0
D_c x 1/3	.82	0	0
N_c x 1/3	.36	.22	.05
Multiple Parameter Changes Biomass =			
.2 of Base Case	.3	.4	.59
.4 of Base Case	2.24	.8	.75
.61 of Base Case	.73	0	0
.81 of Base Case	.87	0	0
1.2 of Base Case	.7	0	0
Adaptive Behavior by Fleet			
B_{thr} = 0 tonnes	.5	0	0
B_{thr} = 40 tonnes	.95	0	0

Table 12.26: Detection Properties of Abundance Index "Discoveries x Average {Catch/ Towtime} / Average {Searchtime}"

Biomass Relative to Base Case	μ_c/μ_b	Probability of Detection	
		Simulation	Normal Approx
Biomass = 2/3 of Base Case			
$L_c \times \sqrt{2/3}$	.77	0	0
$r_c \times \sqrt{2/3}$	.69	.04	0
$\delta_c \times 2/3$	.63	0	0
$D_c \times 2/3$	.84	0	0
$N_c \times 2/3$	.67	0	0
Biomass = 1/3 of Base Case			
$L_c \times \sqrt{1/3}$	.62	.04	0
$r_c \times \sqrt{1/3}$	.42	0	0
$\delta_c \times 1/3$	.27	.34	0
$D_c \times 1/3$	.51	.02	0
$N_c \times 1/3$	.35	.22	.03
Multiple Parameter Changes Biomass =			
.2 of Base Case	.32	.12	0
.4 of Base Case	.56	0	0
.61 of Base Case	1.1	.04	0
.81 of Base Case	1.26	.08	.02
1.2 of Base Case	.57	0	0
Adaptive Behavior by Fleet			
B_{thr} = 0 tonnes	5.76	1	.98
B_{thr} = 40 tonnes	1.11	0	0

Table 12.27: Detection Properties of Abundance Index "Discoveries x Average {Catch/ Towtime} x Average {Reciprocal Searchtime}"

Biomass Relative to Base Case	μ_c/μ_b	Probability of Detection	
		Simulation	Normal Approx
Biomass = 2/3 of Base Case			
$L_c \times \sqrt{2/3}$	.76	0	0
$r_c \times \sqrt{2/3}$	.76	.02	0
$\delta_c \times 2/3$	.69	0	0
$D_c \times 2/3$	.88	0	0
$N_c \times 2/3$	.67	.02	0
Biomass = 1/3 of Base Case			
$L_c \times \sqrt{1/3}$	.63	.04	0
$r_c \times \sqrt{1/3}$	.55	.02	0
$\delta_c \times 1/3$	.35	.08	0
$D_c \times 1/3$	.59	0	0
$N_c \times 1/3$	.35	.22	.03
Multiple Parameter Changes Biomass =			
.2 of Base Case	.43	.08	0
.4 of Base Case	.87	0	0
.61 of Base Case	.96	0	0
.81 of Base Case	1.09	0	0
1.2 of Base Case	.61	0	0
Adaptive Behavior by Fleet			
B_{thr} = 0 tonnes	2.91	.86	.86
B_{thr} = 40 tonnes	1.05	0	0

Table 12.28: Detection Properties of Abundance Index "Discoveries x Average {(Catch/Towtime) / Searchtime}"

Biomass Relative to Base Case	μ_c/μ_b	Probability of Detection	
		Simulation	Normal Approx
Biomass = 2/3 of Base Case			
$L_c \times \sqrt{2/3}$	.76	0	0
$r_c \times \sqrt{2/3}$	.76	.02	0
$\delta_c \times 2/3$	.7	0	0
$D_c \times 2/3$	.89	0	0
$N_c \times 2/3$	.68	.02	0
Biomass = 1/3 of Base Case			
$L_c \times \sqrt{1/3}$	.63	.04	0
$r_c \times \sqrt{1/3}$	.54	.02	0
$\delta_c \times 1/3$	.35	.1	0
$D_c \times 1/3$	.6	0	0
$N_c \times 1/3$	.35	.2	.04
Multiple Parameter Changes Biomass =			
.2 of Base Case	.43	.06	0
.4 of Base Case	.88	0	0
.61 of Base Case	.97	0	0
.81 of Base Case	1.09	.02	0
1.2 of Base Case	.61	0	0
Adaptive Behavior by Fleet			
B_{thr} = 0 tonnes	2.74	.82	.83
B_{thr} = 40 tonnes	1.05	0	0

Table 12.29: Detection Properties of Abundance Index "Discoveries x (Total Catch/Total Towtime) / Average {Searchtime} "

Biomass Relative to Base Case	μ_c/μ_b	Probability of Detection	
		Simulation	Normal Approx
Biomass = 2/3 of Base Case			
$L_c \times \sqrt{2/3}$	.77	0	0
$r_c \times \sqrt{2/3}$	.69	.04	0
$\delta_c \times 2/3$	.63	0	0
$D_c \times 2/3$	.83	0	0
$N_c \times 2/3$	.67	0	0
Biomass = 1/3 of Base Case			
$L_c \times \sqrt{1/3}$	.62	.04	0
$r_c \times \sqrt{1/3}$	.41	.06	0
$\delta_c \times 1/3$	.28	.34	0
$D_c \times 1/3$	.51	.02	0
$N_c \times 1/3$	.35	.22	.03
Multiple Parameter Changes Biomass =			
.2 of Base Case	.32	.22	0
.4 of Base Case	.54	0	0
.61 of Base Case	1.11	.04	0
.81 of Base Case	1.28	.08	.03
1.2 of Base Case	.59	0	0
Adaptive Behavior by Fleet			
B_{thr} = 0 tonnes	6.13	1	.98
B_{thr} = 40 tonnes	1.11	0	0

Table 12.30: Detection Properties of Abundance Index "Discoveries x (Total Catch/Total Towtime) x Average {Reciprocal Searchtime}"

Biomass Relative to Base Case	μ_c/μ_b	Probability of Detection	
		Simulation	Normal Approx
Biomass = 2/3 of Base Case			
$L_c \times \sqrt{2/3}$	.76	0	0
$r_c \times \sqrt{2/3}$	.75	.02	0
δ_c x 2/3	.69	0	0
D_c x 2/3	.88	0	0
N_c x 2/3	.67	.02	0
Biomass = 1/3 of Base Case			
$L_c \times \sqrt{1/3}$	.63	.04	0
$r_c \times \sqrt{1/3}$	.53	0	0
δ_c x 1/3	.35	.08	0
D_c x 1/3	.6	0	0
N_c x 1/3	.35	.22	.03
Multiple Parameter Changes Biomass =			
.2 of Base Case	.43	.08	0
.4 of Base Case	.84	0	0
.61 of Base Case	.98	0	0
.81 of Base Case	1.11	0	0
1.2 of Base Case	.63	0	0
Adaptive Behavior by Fleet			
B_{thr} = 0 tonnes	3.1	.9	.89
B_{thr} = 40 tonnes	1.05	0	0

Table 12.31: Detection Properties of Abundance Index "Discoveries x (Total Catch/Total Towtime) x Number of Selected Swarms"

Biomass Relative to Base Case	μ_c/μ_b	Probability of Detection Simulation	Probability of Detection Normal Approx
Biomass = 2/3 of Base Case			
$L_c \times \sqrt{2/3}$	.77	.02	0
$r_c \times \sqrt{2/3}$	.86	.02	0
$\delta_c \times 2/3$	.76	0	0
$D_c \times 2/3$	.94	0	0
$N_c \times 2/3$	.67	.02	0
Biomass = 1/3 of Base Case			
$L_c \times \sqrt{1/3}$	.63	.04	0
$r_c \times \sqrt{1/3}$	.73	0	0
$\delta_c \times 1/3$	.47	.06	0
$D_c \times 1/3$	.73	0	0
$N_c \times 1/3$	.36	.24	.06
Multiple Parameter Changes Biomass =			
.2 of Base Case	.62	.02	0
.4 of Base Case	1.35	.06	.03
.61 of Base Case	.77	0	0
.81 of Base Case	.92	0	0
1.2 of Base Case	.66	0	0
Adaptive Behavior by Fleet			
B_{thr} = 0 tonnes	.66	0	0
B_{thr} = 40 tonnes	.98	0	0

Table 12.32: Detection Properties of Abundance Index "Discoveries x Average {Catch/Towtime} x Number of Selected Swarms"

Biomass Relative to Base Case	μ_c/μ_b	Probability of Detection	
		Simulation	Normal Approx
Biomass = 2/3 of Base Case			
$L_c \times \sqrt{2/3}$	.75	.02	0
$r_c \times \sqrt{2/3}$	.87	.02	0
$\delta_c \times 2/3$	.76	0	0
$D_c \times 2/3$	.94	0	0
$N_c \times 2/3$	.67	.02	0
Biomass = 1/3 of Base Case			
$L_c \times \sqrt{1/3}$	.63	.04	0
$r_c \times \sqrt{1/3}$	.74	0	0
$\delta_c \times 1/3$	.46	.04	0
$D_c \times 1/3$	.73	0	0
$N_c \times 1/3$	.36	.18	.06
Multiple Parameter Changes Biomass =			
.2 of Base Case	.61	0	0
.4 of Base Case	1.4	.1	.05
.61 of Base Case	.76	0	0
.81 of Base Case	.91	0	0
1.2 of Base Case	.65	0	0
Adaptive Behavior by Fleet			
B_{thr} = 0 tonnes	.62	0	0
B_{thr} = 40 tonnes	.98	0	0

Table 12.33: Detection Properties of Abundance Index "Discoveries x (Total Catch/Total Towtime) x Number of Encountered Swarms"

Biomass Relative to Base Case	μ_c/μ_b	Probability of Detection Simulation	Normal Approx
Biomass = 2/3 of Base Case			
$L_c \times \sqrt{2/3}$	.77	.02	0
$r_c \times \sqrt{2/3}$	1.08	.06	.02
$\delta_c \times 2/3$	.97	0	0
$D_c \times 2/3$	.91	0	0
$N_c \times 2/3$	.67	.02	0
Biomass = 1/3 of Base Case			
$L_c \times \sqrt{1/3}$	.63	.04	0
$r_c \times \sqrt{1/3}$	1.45	.16	.18
$\delta_c \times 1/3$	.95	0	0
$D_c \times 1/3$	.68	0	0
$N_c \times 1/3$	.36	.22	.07
Multiple Parameter Changes Biomass =			
.2 of Base Case	.95	0	0
.4 of Base Case	4.48	1	.99
.61 of Base Case	.56	.06	0
.81 of Base Case	.55	0	0
1.2 of Base Case	.93	0	0
Adaptive Behavior by Fleet			
B_{thr} = 0 tonnes	.24	.56	.03
B_{thr} = 40 tonnes	.89	0	0

Table 12.34: Detection Properties of Abundance Index "Discoveries x Average {Catch/ Towtime} x Number of Swarms Encountered"

Biomass Relative to Base Case	μ_c/μ_b	Probability of Detection Simulation	Normal Approx
Biomass = 2/3 of Base Case			
$L_c \times \sqrt{2/3}$	.77	.02	0
$r_c \times \sqrt{2/3}$	1.09	.06	.02
δ_c x 2/3	.96	0	0
D_c x 2/3	.9	0	0
N_c x 2/3	.68	.02	0
Biomass = 1/3 of Base Case			
$L_c \times \sqrt{1/3}$	.63	.04	0
$r_c \times \sqrt{1/3}$	1.49	.16	.21
δ_c x 1/3	.94	0	0
D_c x 1/3	.67	0	0
N_c x 1/3	.36	.24	.07
Multiple Parameter Changes Biomass =			
.2 of Base Case	.94	0	0
.4 of Base Case	4.66	1	.99
.61 of Base Case	.55	.06	0
.81 of Base Case	.54	0	0
1.2 of Base Case	.9	0	0
Adaptive Behavior by Fleet			
B_{thr} = 0 tonnes	.22	.58	.04
B_{thr} = 40 tonnes	.88	0	0

Table 12.35: Detection Properties of Abundance Index "Number of Different Concentrations Fished by the Fleet"

Biomass Relative to Base Case	μ_c/μ_b	Probability of Detection Simulation	 Normal Approx
Biomass = 2/3 of Base Case			
$L_c \times \sqrt{2/3}$	.98	0	0
$r_c \times \sqrt{2/3}$	1.08	0	0
$\delta_c \times 2/3$	1.06	0	0
$D_c \times 2/3$	1.11	0	0
$N_c \times 2/3$	1.13	0	0
Biomass = 1/3 of Base Case			
$L_c \times \sqrt{1/3}$	1.05	0	0
$r_c \times \sqrt{1/3}$	1.10	0	0
$\delta_c \times 1/3$	1	0	0
$D_c \times 1/3$	1.05	0	0
$N_c \times 1/3$	1.08	0	0
Multiple Parameter Changes Biomass =			
.2 of Base Case	.98	0	0
.4 of Base Case	1.03	0	0
.61 of Base Case	1.18	0	0
.81 of Base Case	1.08	0	0
1.2 of Base Case	1.01	0	0
Adaptive Behavior by Fleet			
B_{thr} = 0 tonnes	1	0	0
B_{thr} = 40 tonnes	1.06	0	0

Table 12.36: Detection Properties of Abundance Index "Discoveries x (Total Catch/Total Towtime) x (Hauls/Concentration Fished)"

Biomass Relative to Base Case	μ_c/μ_b	Probability of Detection	
		Simulation	Normal Approx
Biomass = 2/3 of Base Case			
$L_c \times \sqrt{2/3}$	.76	.02	0
$r_c \times \sqrt{2/3}$	.8	.02	0
$\delta_c \times 2/3$	.71	0	0
$D_c \times 2/3$	.83	0	0
$N_c \times 2/3$	.61	.06	0
Biomass = 1/3 of Base Case			
$L_c \times \sqrt{1/3}$	.6	.08	0
$r_c \times \sqrt{1/3}$	.68	.04	0
$\delta_c \times 1/3$	.45	.1	0
$D_c \times 1/3$	.71	.04	0
$N_c \times 1/3$	.34	.36	0
Multiple Parameter Changes Biomass =			
.2 of Base Case	.06	.04	.19
.4 of Base Case	1.29	.06	.02
.61 of Base Case	.67	.04	0
.81 of Base Case	.87	0	0
1.2 of Base Case	.64	.02	0
Adaptive Behavior by Fleet			
B_{thr} = 0 tonnes	.65	.06	0
B_{thr} = 40 tonnes	.95	0	0

Table 12.37: Detection Properties of Abundance Index "Discoveries x Average {Catch/ Towtime} x (Hauls/Concentration Fished)"

Biomass Relative to Base Case	μ_c/μ_b	Probability of Detection Simulation	Probability of Detection Normal Approx
Biomass = 2/3 of Base Case			
$L_c \times \sqrt{2/3}$	.76	.02	0
$r_c \times \sqrt{2/3}$	.81	.02	0
$\delta_c \times 2/3$	.71	0	0
$D_c \times 2/3$	.83	0	0
$N_c \times 2/3$	.61	.16	0
Biomass = 1/3 of Base Case			
$L_c \times \sqrt{1/3}$	.6	.08	0
$r_c \times \sqrt{1/3}$	.70	.02	0
$\delta_c \times 1/3$	.45	.08	0
$D_c \times 1/3$	.70	.04	0
$N_c \times 1/3$	.34	.40	0
Multiple Parameter Changes Biomass =			
.2 of Base Case	.61	.04	0
.4 of Base Case	1.34	.12	.03
.61 of Base Case	.66	.04	0
.81 of Base Case	.86	.02	0
1.2 of Base Case	.62	0	0
Adaptive Behavior by Fleet			
B_{thr} = 0 tonnes	.61	.08	0
B_{thr} = 40 tonnes	.94	0	0

Table 12.38: Detection Properties of Abundance Index "Discoveries x (Total Catch/Total Towtime) x Swarms Fished per Concentration"

Biomass Relative to Base Case	μ_c/μ_b	Probability of Detection	
		Simulation	Normal Approx
Biomass = 2/3 of Base Case			
$L_c \times \sqrt{2/3}$	.77	.02	0
$r_c \times \sqrt{2/3}$	.82	.02	0
δ_c x 2/3	.49	.06	0
D_c x 2/3	.72	0	0
N_c x 2/3	.62	.06	0
Biomass = 1/3 of Base Case			
$L_c \times \sqrt{1/3}$	.61	.08	0
$r_c \times \sqrt{1/3}$	.7	.04	0
δ_c x 1/3	.49	.06	0
D_c x 1/3	.51	.12	0
N_c x 1/3	.34	.36	0
Multiple Parameter Changes Biomass =			
.2 of Base Case	.47	.08	0
.4 of Base Case	1.29	.06	.03
.61 of Base Case	.64	.04	0
.81 of Base Case	.67	0	0
1.2 of Base Case	.77	0	0
Adaptive Behavior by Fleet			
B_{thr} = 0 tonnes	.71	.02	0
B_{thr} = 40 tonnes	.98	0	0

Table 12.39: Detection Properties of Abundance Index "Discoveries x Average {Catch/Towtime} x Swarms Fished per Concentration"

Biomass Relative to Base Case	μ_c/μ_b	Probability of Detection	
		Simulation	Normal Approx
Biomass = 2/3 of Base Case			
$L_c \times \sqrt{2/3}$	.77	.02	0
$r_c \times \sqrt{2/3}$	.83	.02	0
$\delta_c \times 2/3$	.74	0	0
$D_c \times 2/3$	.72	0	0
$N_c \times 2/3$	.62	.06	0
Biomass = 1/3 of Base Case			
$L_c \times \sqrt{1/3}$	.61	.08	0
$r_c \times \sqrt{1/3}$	.72	.04	0
$\delta_c \times 1/3$	.48	.1	0
$D_c \times 1/3$	.5	.12	0
$N_c \times 1/3$	.34	.34	0
Multiple Parameter Changes Biomass =			
.2 of Base Case	.47	.06	0
.4 of Base Case	1.34	.1	.04
.61 of Base Case	.64	.04	0
.81 of Base Case	.66	.06	0
1.2 of Base Case	.69	0	0
Adaptive Behavior by Fleet			
B_{thr} = 0 tonnes	.66	.04	0
B_{thr} = 40 tonnes	.97	0	0

Table 12.40: Detection Properties of Abundance Index "(Total Catch/Total Number of Hauls) / Average {Searchtime}"

Biomass Relative to Base Case	μ_c/μ_b	Probability of Detection	
		Simulation	Normal Approx
Biomass = 2/3 of Base Case			
$L_c \times \sqrt{2/3}$	1.04	.02	.01
$r_c \times \sqrt{2/3}$	.74	.98	.89
$\delta_c \times 2/3$	.66	1	.99
$D_c \times 2/3$	.82	.68	.41
$N_c \times 2/3$	1.01	.02	0
Biomass = 1/3 of Base Case			
$L_c \times \sqrt{1/3}$	1	0	0
$r_c \times \sqrt{1/3}$	.41	1	.99
$\delta_c \times 1/3$	.29	1	.99
$D_c \times 1/3$	.55	1	.99
$N_c \times 1/3$	1.03	0	.01
Multiple Parameter Changes Biomass =			
.2 of Base Case	.28	1	.99
.4 of Base Case	.25	1	1
.61 of Base Case	1.54	1	.99
.81 of Base Case	1.37	.96	.96
1.2 of Base Case	.57	1	.99
Adaptive Behavior by Fleet			
B_{thr} = 0 tonnes	5.88	1	.99
B_{thr} = 40 tonnes	1.12	.18	.21

Table 12.41: Detection Properties of Abundance Index "Discoveries x (Total Catch/Total Number of Hauls) / Average {Searchtime}"

Biomass Relative to Base Case	μ_c/μ_b	Probability of Detection Simulation	Probability of Detection Normal Approx
Biomass = 2/3 of Base Case			
$L_c \times \sqrt{2/3}$	.86	0	0
$r_c \times \sqrt{2/3}$	.77	0	0
$\delta_c \times 2/3$	.66	.04	0
$D_c \times 2/3$	.8	0	0
$N_c \times 2/3$	.7	.06	0
Biomass = 1/3 of Base Case			
$L_c \times \sqrt{1/3}$	.64	.1	0
$r_c \times \sqrt{1/3}$	.38	.3	0
$\delta_c \times 1/3$	.33	.54	0
$D_c \times 1/3$	.56	.04	0
$N_c \times 1/3$	.37	.46	.05
Multiple Parameter Changes Biomass =			
.2 of Base Case	.33	.46	0
.4 of Base Case	.47	.06	0
.61 of Base Case	1.14	.06	.01
.81 of Base Case	1.32	.2	.07
1.2 of Base Case	.8	.02	0
Adaptive Behavior by Fleet			
B_{thr} = 0 tonnes	6.0	1	.98
B_{thr} = 40 tonnes	1.09	.06	0

Table 12.42: Detection Properties of Abundance Index "(Total Catch/Number of Swarms Fished) / Average {Searchtime}"

Biomass Relative to Base Case	μ_c/μ_b	Probability of Detection Simulation	Probability of Detection Normal Approx
Biomass = 2/3 of Base Case			
$L_c \times \sqrt{2/3}$	1.01	.04	0
$r_c \times \sqrt{2/3}$	.72	1	.99
$\delta_c \times 2/3$	.65	1	.99
$D_c \times 2/3$	.93	.32	.11
$N_c \times 2/3$	1	.16	.04
Biomass = 1/3 of Base Case			
$L_c \times \sqrt{1/3}$	1	.12	.02
$r_c \times \sqrt{1/3}$	.39	1	.99
$\delta_c \times 1/3$	.28	1	1
$D_c \times 1/3$	.77	1	.97
$N_c \times 1/3$	1.01	.06	.04
Multiple Parameter Changes Biomass =			
.2 of Base Case	.37	1	.99
.4 of Base Case	.25	1	1
.61 of Base Case	1.62	1	.99
.81 of Base Case	1.76	1	.99
1.2 of Base Case	.48	1	.99
Adaptive Behavior by Fleet			
B_{thr} = 0 tonnes	5.41	1	.99
B_{thr} = 40 tonnes	1.09	.96	.27

Table 12.43: Detection Properties of Abundance Index "Discoveries x (Total Catch/Number of Swarms Fished) / Average {Searchtime}"

Biomass Relative to Base Case	μ_c/μ_b	Probability of Detection Simulation	Probability of Detection Normal Approx
Biomass = 2/3 of Base Case			
$L_c \times \sqrt{2/3}$	.85	0	0
$r_c \times \sqrt{2/3}$	.76	0	0
$\delta_c \times 2/3$	.65	.06	0
$D_c \times 2/3$	.93	0	0
$N_c \times 2/3$	.69	.06	0
Biomass = 1/3 of Base Case			
$L_c \times \sqrt{1/3}$	.63	.1	.01
$r_c \times \sqrt{1/3}$	.37	.42	0
$\delta_c \times 1/3$	.31	.75	0
$D_c \times 1/3$	.78	0	0
$N_c \times 1/3$	.37	.48	.07
Multiple Parameter Changes Biomass =			
.2 of Base Case	.44	.24	0
.4 of Base Case	.48	.1	0
.61 of Base Case	1.2	.82	.02
.81 of Base Case	1.72	.46	.33
1.2 of Base Case	.68	.06	0
Adaptive Behavior by Fleet			
B_{thr} = 0 tonnes	5.5	1	.99
B_{thr} = 40 tonnes	1.06	.04	0

Table 12.44: Detection Properties of Abundance Index "(Total Catch/Swarms Encountered) / Average {Searchtime}"

Biomass Relative to Base Case	μ_c/μ_b	Probability of Detection	
		Simulation	Normal Approx
Biomass = 2/3 of Base Case			
$L_c \times \sqrt{2/3}$	1.04	.06	.01
$r_c \times \sqrt{2/3}$	.59	1	.99
$\delta_c \times 2/3$	.53	1	.99
$D_c \times 2/3$	.86	.32	.12
$N_c \times 2/3$	1.01	0	.01
Biomass = 1/3 of Base Case			
$L_c \times \sqrt{1/3}$	1	.02	.01
$r_c \times \sqrt{1/3}$	.2	1	1
$\delta_c \times 1/3$	.15	1	1
$D_c \times 1/3$	.61	1	.99
$N_c \times 1/3$	1.04	.04	.03
Multiple Parameter Changes Biomass =			
.2 of Base Case	.18	1	1
.4 of Base Case	.07	1	1
.61 of Base Case	2.16	1	.99
.81 of Base Case	2.27	1	.99
1.2 of Base Case	.41	1	.99
Adaptive Behavior by Fleet			
B_{thr} = 0 tonnes	16.11	1	.99
B_{thr} = 40 tonnes	1.24	.76	.55

Table 12.45: Detection Properties of Abundance Index "Discoveries x (Total Catch/Swarms Encountered) / Average {Searchtime}"

Biomass Relative to Base Case	μ_c/μ_b	Probability of Detection	
		Simulation	Normal Approx
Biomass = 2/3 of Base Case			
$L_c \times \sqrt{2/3}$	.87	0	0
$r_c \times \sqrt{2/3}$	.62	0	0
$\delta_c \times 2/3$	.53	.12	0
$D_c \times 2/3$	.85	0	0
$N_c \times 2/3$	.37	.44	.05
Biomass = 1/3 of Base Case			
$L_c \times \sqrt{1/3}$	.64	.02	0
$r_c \times \sqrt{1/3}$	.19	.98	0
$\delta_c \times 1/3$	.16	1	0
$D_c \times 1/3$	.61	.02	0
$N_c \times 1/3$	.37	.44	.05
Multiple Parameter Changes Biomass =			
.2 of Base Case	.21	.96	0
.4 of Base Case	.14	1	0
.61 of Base Case	1.61	.38	.25
.81 of Base Case	2.21	.72	.62
1.2 of Base Case	.58	.12	0
Adaptive Behavior by Fleet			
B_{thr} = 0 tonnes	16.46	1	.99
B_{thr} = 40 tonnes	1.21	.08	.02

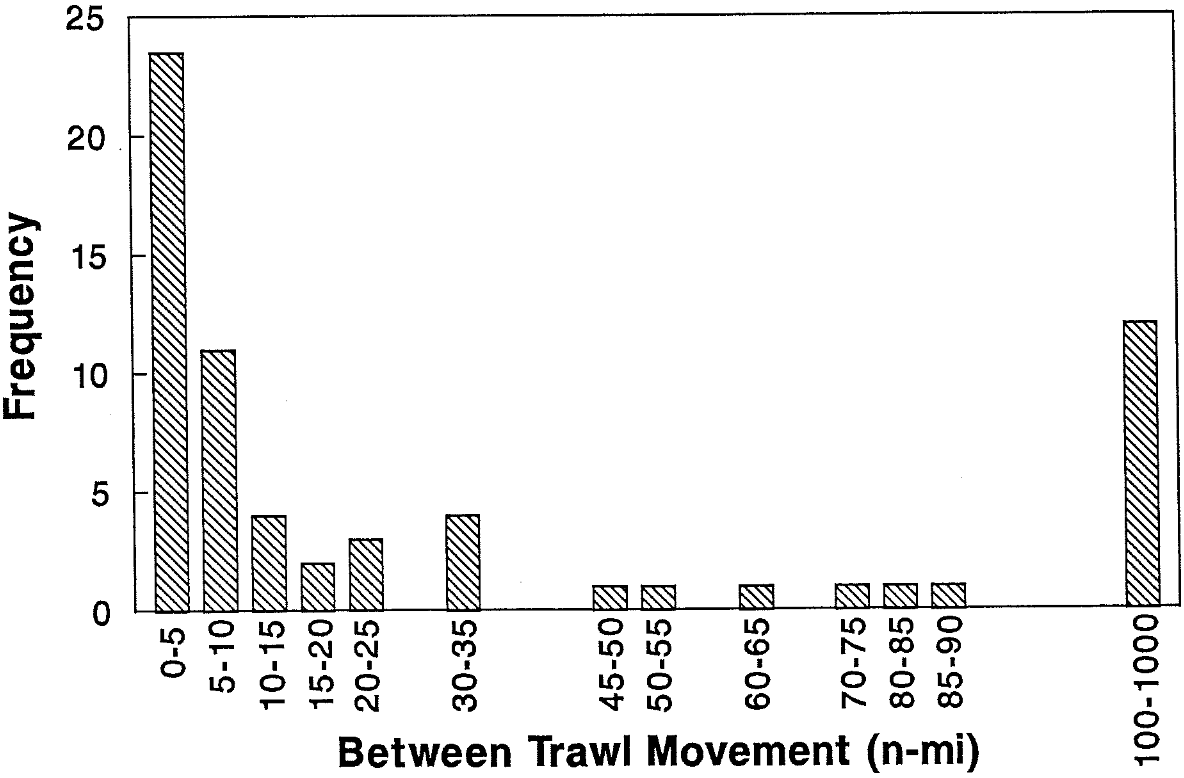

Figure 3.1 Example of the bimodal distributions obtained in the analysis of the between trawl movement data for data set 10

Légendes des tableaux

Tableau 2.1	Résumé des origines des données des campagnes d'étude soviétiques.
Tableau 2.2	Caractéristiques des engins de pêche des navires.
Tableau 3.1	Résumé des moyennes et variances des quantités provenant des données soviétiques. (Voir le texte pour une discussion détaillée sur la manière de lire le tableau).
Tableau 3.2	Corrélations de l'ensemble de données 1, toutes données utilisées (voir le texte pour une discussion détaillée sur la manière de lire le tableau).
Tableau 3.3	Corrélations de l'ensemble de données 1, valeurs limites appliquées (voir le texte pour une discussion détaillée sur la manière de lire le tableau).
Tableau 3.4	Corrélations de l'ensemble de données 2, toutes données utilisées (voir le texte pour une discussion détaillée sur la manière de lire le tableau).
Tableau 3.5	Corrélations de l'ensemble de données 2, valeurs limites appliquéesv(Voir le texte pour une discussion détaillée sur la manière de lire le tableau).
Tableau 3.6	Corrélations de l'ensemble de données 3, toutes données utilisées (voir le texte pour une discussion détaillée sur la manière de lire le tableau).
Tableau 3.7	Corrélations de l'ensemble de données 3, valeurs limites appliquées (voir le texte pour une discussion détaillée sur la manière de lire le tableau).
Tableau 3.8	Corrélations de l'ensemble de données 4, toutes données utilisées (voir le texte pour une discussion détaillée sur la manière de lire le tableau).
Tableau 3.9	Corrélations de l'ensemble de données 4, valeurs limites appliquées (voir le texte pour une discussion détaillée sur la manière de lire le tableau).
Tableau 3.10	Corrélations de l'ensemble de données 5, toutes données utilisées (voir le texte pour une discussion détaillée sur la manière de lire le tableau).
Tableau 3.11	Corrélations de l'ensemble de données 5, valeurs limites appliquées (voir le texte pour une discussion détaillée sur la manière de lire le tableau).
Tableau 3.12	Corrélations de l'ensemble de données 6, toutes données utilisées (voir le texte pour une discussion détaillée sur la manière de lire le tableau).
Tableau 3.13	Corrélations de l'ensemble de données 6, valeurs limites appliquées (voir le texte pour une discussion détaillée sur la manière de lire le tableau).
Tableau 3.14	Corrélations de l'ensemble de données 7, toutes données utilisées (voir le texte pour une discussion détaillée sur la manière de lire le tableau).
Tableau 3.15	Corrélations de l'ensemble de données 7, valeurs limites appliquées (voir le texte pour une discussion détaillée sur la manière de lire le tableau).
Tableau 3.16	Corrélations de l'ensemble de données 8, toutes données utilisées (voir le texte pour une discussion détaillée sur la manière de lire le tableau).

Tableau 12.31	Propriétés de détection de l'indice d'abondance "Découvertes x (prise totale / temps total de chalutage) x nombre d'essaims sélectionnés".
Tableau 12.32	Propriétés de détection de l'indice d'abondance "Découvertes x {prise/temps de recherche} moyen x nombre d'essaims sélectionnés".
Tableau 12.33	Propriétés de détection de l'indice d'abondance "Découvertes x (prise totale/temps total de chalutage) x nombre d'essaims rencontrés".
Tableau 12.34	Propriétés de détection de l'indice d'abondance "Découvertes x moyenne {prise/temps de recherche} x nombre d'essaims rencontrés".
Tableau 12.35	Propriétés de détection de l'indice d'abondance "Nombre de concentrations différentes pêchées par la flotille".
Tableau 12.36	Propriétés de détection de l'indice d'abondance "Découvertes x (prise totale/temps total de chalutage) x (traits/concentrations pêchées)".
Tableau 12.37	Propriétés de détection de l'indice d'abondance "Découvertes x moyenne {prise/temps de chalutage} x (traits/concentrations pêchées)".
Tableau 12.38	Propriétés de détection de l'indice d'abondance "Découvertes x (prise totale/temps total de chalutage) x essaims pêchés par concentration".
Tableau 12.39	Propriétés de détection de l'indice d'abondance "Découvertes x moyenne {prise/temps de chalutage} x essaims pêchés par concentration".
Tableau 12.40	Propriétés de détection de l'indice d'abondance "(Prise totale/nombre total de chalutages) / moyenne {temps de recherche}".
Tableau 12.41	Propriétés de détection de l'indice d'abondance "Découvertes x (prise totale/nombre total de traits) / moyenne {temps de recherche}".
Tableau 12.42	Propriétés de détection de l'indice d'abondance "(Prise totale/nombre d'essaims pêchés) / moyenne {temps de recherche}".
Tableau 12.43	Propriétés de détection de l'indice d'abondance "Découvertes x (prise totale/nombre d'essaims pêchés) / moyenne {temps de recherche}".
Tableau 12.44	Propriétés de détection de l'indice d'abondance "(Prise totale/essaims rencontrés) / moyenne {temps de recherche}".
Tableau 12.45	Propriétés de détection de l'indice d'abondance "Découvertes x (prise totale/essaims rencontrés) / {temps de recherche}".

Légende de la figure

Figure 3.1	Exemple de distributions bimodales obtenues par l'analyse des données sur le déplacement entre chalutages pour l'ensemble de données 10.

Заголовки к таблицам

Таблица 2.1	Сводная таблица исходных данных по рейсам советских судов.

Таблица 2.2	Характеристики орудий лова судов.
Таблица 3.1	Сводная таблица средних величин и средних отклонений показателей, полученных на основе данных, предоставленных СССР. (См. объяснение в тексте как читать таблицу).
Таблица 3.2	Корреляции для серии данных 1; были использованы все данные (см. объяснение в тексте как читать таблицу).
Таблица 3.3	Корреляции для серии данных 1; были использованы предельные величины (см. объяснение в тексте как читать таблицу).
Таблица 3.4	Корреляции для серии данных 2; были использованы все данные (см.объяснение в тексте как читать таблицу).
Таблица 3.5	Корреляции для серии данных 2; были использованы предельные величины (см. объяснение в тексте как читать таблицу).
Таблица 3.6	Корреляции данных подбора 3; были использованы все данные (см. объяснения в тексте как читать таблицу).
Таблица 3.7	Корреляции для серии данных 3; были использованы предельные величины (см. объяснение в тексте как читать таблицу).
Таблица 3.8	Корреляции для серии данных 4; были использованы все данные (см. объяснение в тексте как читать таблицу).
Таблица 3.9	Корреляции для серии данных 4; были использованы предельные величины (см. объяснение в тексте как читать таблицу).
Таблица 3.10	Корреляции для серии данных 5; были использованы все данные (см. объяснение в тексте как читать таблицу).
Таблица 3.11	Корреляции для серии данных 5; были использованы предельные величины (см. объяснение в тексте как читать таблицу).
Таблица 3.12	Корреляции для серии данных 6; были использованы все данные (см. объяснение в тексте как читать таблицу).
Таблица 3.13	Корреляции для серии данных 6; были использованы предельные величины (см. объяснения в тексте как читать таблицу).
Таблица 3.14	Корреляции для серии данных 7; были использованы все данные (см. объяснение в тексте как читать таблицу).
Таблица 3.15	Корреляции для серии данных 7; были использованы предельные величины (см. обЬяснение в тексте как читать таблицу).

Таблица 3.16	Корреляции для серии данных 8; были использованы все данные (см. объяснение в тексте о том как читать таблицу).
Таблица 3.17	Корреляции для серии данных 8; были использованы предельные величины (см. объяснение в тексте как читать таблицу).
Таблица 3.18	Корреляции для серии данных 9; были использованы все данные (см. объяснение в тексте как читать таблицу).
Таблица 3.19	Корреляции для серии данных 9; были использованы предельные величины (см. объяснение в тексте как читать таблицу).
Таблица 3.20	Корреляции для серии данных 10; были использованы все данные (см. объяснение в тексте о том, как читать таблицу).
Таблица 3.21	Корреляции для серии данных 10; были использованы предельные величины (см. объяснение в тексте как читать таблицу).
Таблица 3.22	Корреляции для серии данных 11; были использованы все данные (см. объяснение в тексте как читать таблицу).
Таблица 3.23	Корреляции для серии данных 11; были использованы предельные величины (см. объяснение в тексте как читать таблицу).
Таблица 3.24	Корреляции для серии данных 12; были использованы все данные (см. объяснение в тексте как читать таблицу).
Таблица 3.25	Корреляции для серии данных 12; были использованы все данные (см. объяснение в тексте как читать таблицу).
Таблица 12.1	Величины параметров, используемые в многофакторном анализе изменений биомассы.
Таблица 12.2	Параметры обнаружения (концентраций криля), присущие индексу численности "Общий улов".
Таблица 12.3	Параметры обнаружения (концентраций криля), присущие индексу численности "Все траления (общее число отобранных скоплений".
Таблица 12.4	Параметры обнаружения (концентраций криля), присущие индексу численности "Общее количество облавливаемых скоплений".
Таблица 12.5	Параметры обнаружения (концентраций криля), присущие индексу численности "Общее количество встретившихся скоплений".
Таблица 12.6	Параметры обнаружения (концентраций криля), присущие индексу численности "Общее время траления".

Таблица 12.7	Параметры обнаружения (концентраций криля), присущие индексу численности "Общее время поиска".
Таблица 12.8	Параметры обнаружения (концентраций криля), присущие индексу численности "Общее эквивалентное время поиска".
Таблица 12.9	Параметры обнаружения (концентраций криля), присущие индексу численности "Число обнаружений, сделанных поисковым судном".
Таблица 12.10	Параметры обнаружения (концентраций криля), присущие индексу численности "Средняя величина {улов/время траления}".
Таблица 12.11	Параметры обнаружения (концентраций криля), присущие индексу численности "Средняя величина {улов/время поиска}".
Таблица 12.12	Параметры обнаружения (концентраций криля), присущие индексу численности "Средняя величина {(улов/время траления) / время поиска}".
Таблица 12.13	Параметры обнаружения (концентраций криля), присущие индексу численности "Улов за сутки".
Таблица 12.14	Параметры обнаружения (концентраций криля), присущие индексу численности "Улов за траление".
Таблица 12.15	Параметры обнаружения (концентраций криля), присущие индексу численности "Число тралений на обнаруженную .концентрацию".
Таблица 12.16	Параметры обнаружения (концентраций криля), присущие индексу численности "Доля скоплений, отобранных для промысла".
Таблица 12.17	Параметры обнаружения (концентраций криля), присущие индексу численности "Средняя длина тралений".
Таблица 12.18	Параметры обнаружения (концентраций криля), присущие индексу численности "Обнаружение х общий улов".
Таблица 12.19	Параметры обнаружения (концентраций криля), присущие индексу численности "Обнаружение х все траления њ общий улов".
Таблица 12.20	Параметры обнаружения (концентраций криля), присущие индексу численности "Обнаружение х (общий улов/общее время траления) х облавливаемые скопления".
Таблица 12.21	Параметры обнаружения (концентраций криля), присущие индексу численности "Обнаружение х средняя величина {улов/время траления} х облавливаемые скопления".
Таблица 12.22	Параметры обнаружения (концентраций криля), присущие индексу численности "Общий улов/общее время траления".

Таблица 12.23 Параметры обнаружения (концентраций криля), присущие индексу численности "Средняя величина {улов/время траления}/ средняя величина {время поиска}".

Таблица 12.24 Параметры обнаружения (концентраций криля), присущие индексу численности "Средняя величина {улов/время траления} њ средняя величина {эквивалентное время поиска}".

Таблица 12.25 Параметры обнаружения (концентраций криля), присущие индексу численности "Обнаружение њ общий улов/общее время траления".

Таблица 12.26 Параметры обнаружения (концентраций криля), присущие индексу численности "Обнаружение x средняя величина {улов/время траления} / средняя величина {время поиска}".

Таблица 12.27 Параметры обнаружения (концентраций криля), присущие индексу численности "Обнаружение x средняя величина {улов/время траления} x средняя величина {эквивалентное время поиска}".

Таблица 12.28 Параметры обнаружения (концентраций криля), присущие индексу численности "Обнаружение x средняя величина {(улов/время траления) / время поиска}".

Таблица 12.29 Параметры обнаружения (концентраций криля), присущие индексу численности "Обнаружение x (общий улов/общее время траления) / средняя величина {время поиска}".

Таблица 12.30 Параметры обнаружения (концентраций криля), присущие индексу численности "Обнаружение x (общий улов/общее время траления) x средняя величина {эквивалентное время поиска}".

Таблица 12.31 Параметры обнаружения (концентраций криля), присущие индексу численности "Обнаружение x (общий улов/общее время траления) x количество выбранных скоплений".

Таблица 12.32 Параметры обнаружения (концентраций криля), присущие индексу численности "Обнаружение x средняя величина {улов/время траления} x количество выбранных скоплений".

Таблица 12.33 Параметры обнаружения (концентраций криля), присущие индексу численности "Обнаружение x (общий улов/общее время траления) x количество встретившихся скоплений".

Таблица 12.34 Параметры обнаружения (концентраций криля), присущие индексу численности "Обнаружение x средняя величина {улов/время траления} x количество встретившихся скоплений".

Таблица 12.35 Параметры обнаружения (концентраций криля), присущие индексу численности "Количество различных концентраций, облавливаемых флотилией".

Таблица 12.36	Параметры обнаружения (концентраций криля), присущие индексу численности "Обнаружение х (общий улов/общее время траления) х (количество тралений/облавливаемая концентрация)".
Таблица 12.37	Параметры обнаружения (концентраций криля), присущие индексу численности "Обнаружение х средняя величина {улов/время траления} х (Количество тралений/облавливаемая концентрация)".
Таблица 12.38	Параметры обнаружения (концентраций криля), присущие индексу численности "Обнаружение х (общий улов/общее время траления) х облавливаемые скопления на концентрацию".
Таблица 12.39	Параметры обнаружения (концентраций криля), присущие индексу численности "Обнаружение х средняя величина {улов/время траления} х облавливаемые скопления на концентрацию".
Таблица 12.40	Параметры обнаружения (концентраций криля), присущие индексу численности "(Общий улов/общее количество тралений)/средняя величина { время поиска}.
Таблица 12.41	Параметры обнаружения (концентраций криля), присущие индексу численности "Обнаружение х (общий улов/общее количество тралений)/средняя величина {время поиска}.
Таблица 12.42	Параметры обнаружения (концентраций криля), присущие индексу численности "(Общий улов/количество облавливаемых скоплений)/средняя величина {время поиска}.
Таблица 12.43	Параметры обнаружения (концентраций криля), присущие индексу численности "Обнаружение х (общий улов/количество облавливаемых скоплений) / средняя величина {время поиска}.
Таблица 12.44	Параметры обнаружения (концентраций криля), присущие индексу численности "(Общий улов/встретившиеся скопления)/средняя величина {время поиска}".
Таблица 12.45	Параметры обнаружения (концентраций криля), присущие индексу численности "Обнаружение х (общий улов/встретившиеся скопления)/средняя величина {время поиска}.

Подписи к рисункам

Рисунок 3.1	Пример бимодальных распределений, полученных из анализа данных по движению судна в период между тралениями, для серии данных 10.

Encabezamientos de las Tablas

Tabla 2.1	Resumen de los datos originales del crucero soviético

Tabla 12.32	Propiedades de detección del índice de abundancia "Descubrimientos x promedio {captura/tiempo de arrastre} x número de cardúmenes seleccionados".
Tabla 12.33	Propiedades de detección del índice de abundancia "Descubrimientos x (captura total/tiempo de arrastre total) x número de cardúmenes hallados".
Tabla 12.34	Propiedades de detección del índice de abundancia "Descubrimientos x promedio {captura/tiempo de arrastre} x número de cardúmenes hallados".
Tabla 12.35	Propiedades de detección del índice de abundancia "Número de concentraciones diferentes pescadas por la flota".
Tabla 12.36	Propiedades de detección del índice de abundancia "Descubrimientos x (captura total/tiempo de arrastre total) x (lances/concentraciones pescadas)".
Tabla 12.37	Propiedades de detección del índice de abundancia "Descubrimientos x promedio {captura/tiempo de arrastre} x (lances/concentraciones pescadas)".
Tabla 12.38	Propiedades de detección del índice de abundancia "Descubrimientos x (captura total/tiempo de arrastre total) x cardúmenes pescados por concentración".
Tabla 12.39	Propiedades de detección del índice de abundancia "Descubrimientos x promedio {captura/tiempo de arrastre} x cardúmenes pescados por concentración".
Tabla 12.40	Propiedades de detección del índice de abundancia "(Captura total/número total de lances) / promedio {tiempo de búsqueda}".
Tabla 12.41	Propiedades de detección del índice de abundancia "Descubrimientos x (captura total/número total de lances) / promedio {tiempo de búsqueda}".
Tabla 12.42	Propiedades de detección del índice de abundancia "(Captura total/número de cardúmenes pescados) / promedio {tiempo de búsqueda}".
Tabla 12.43	Propiedades de detección del índice de abundancia "Descubrimientos x (captura total/número de cardúmenes pescados) / promedio {tiempo de búsqueda}".
Tabla 12.44	Propiedades de detección del índice de abundancia "(captura total/cardúmenes hallados) / promedio {tiempo de búsqueda}".
Tabla 12.45	Propiedades de detección del índice de abundancia "Descubrimientos x (captura total/cardúmenes hallados) / promedio {tiempo de búsqueda}".

Leyenda de la Figura

Figura 3.1	Ejemplo de las distribuciones bimodales obtenidas por el análisis de los datos del movimiento entre-arrastres para el conjunto de datos 10.

SC-CAMLR-VII/BG/14

SOME SPECIFIC FEATURES OF THE USSR KRILL FISHERY AND POSSIBILITIES OF APPLYING FISHERY STATISTICS TO STUDIES OF KRILL BIOLOGY AND STOCKS

V.N. Dolzhenkov, T.G. Lubimova, R.R. Makarov, S.S. Parfenovich, V.A. Spiridonov

Abstract

General principles of the USSR krill fishery such as the location of exploited fishing areas and the seasonal regime of their exploitation are considered. Using data obtained by the scouting vessel *Globus* engaged in regular krill fishery, it is shown that the catch-per-haul variables are associated with the fishing regime of the vessel rather than with krill abundance in a certain area. During preparations for regular fishing operations very short hauls (under 15 minutes) are practised. Such fishing practice, together with substantial fluctuations of catches during scouting operations often results in yields which do not correspond to the actual biomass of krill in the place in question. In both cases particular diurnal and long-term behaviour patterns have an impact. All these factors limit the extent to which CPUE can be used in simulation studies of krill distribution and stock assessment. A standard large-scale multi-disciplinary survey, followed by processing of the data obtained using diverse methods may be viewed as a better instrument for studies.

Résumé

Les principes généraux sous-tendant les activités de pêche de krill menées par l'URSS, tels que l'emplacement des zones de pêche et leur régime saisonnier d'exploitation, sont ici considérés. Sur la base de données recueillies par le navire de reconnaissance *Globus*, engagé dans des activités régulières de pêche de krill, l'on remarque que les variables de prise par trait relèvent plutôt du régime des activités de pêche entreprises par le navire que de l'abondance de krill en certains endroits. Lors des préparatifs précédant les opérations de pêche régulières, des traits de courte durée (moins de 15 min.) sont effectués. Cette pratique, ainsi que les fluctuations substantielles des prises pendant les opérations de reconnaissance, a souvent pour résultat l'obtention de rendements ne correspondant pas à la biomasse réelle de krill dans la zone considérée. Dans les deux cas, l'on observe l'incidence de types de comportements particuliers, diurnes et à long terme. Tout ceci limite la possibilité d'utiliser la CPUE dans des études par simulation sur la répartition et l'évaluation des réserves de krill. Une campagne d'étude standard multidisciplinaire à grande échelle, suivie par le traitement des données obtenues à l'aide de méthodes variées, peut être considérée comme un meilleur instrument pour les études entreprises.

Резюме

Обсуждаются общие принципы проводимого СССР промысла криля - такие, как выявление промысловых участков и сезонный режим их эксплуатации. На основании данных, полученных поисковым судном "*Globus*", занятым в регулярном промысле криля, показывается, что значения переменной "улов за траление" связаны скорее с режимом ведения промысла судном, чем с количеством криля в конкретном районе. Во время подготовки к регулярным промысловым операциям проводятся очень короткие (не больше 15 мин) траления. Такая промысловая практика вместе с большими флуктуациями в размерах уловов во время поисковых операций часто дают величины вылова, не соответствующие фактическому объему биомассы криля в данном районе. В обоих случаях наличествует влияние нетипичных закономерностей суточного и долговременного поведения. Все это сужает область применение CPUE при изучении распределения криля методом моделирования и при оценке запасов. Стандартная крупномасштабная многоотраслевая съемка и последующая обработка полученных данных с помощью различных методов могут оказаться лучшим способом проведения таких исследований.

Resumen

Se examinan los prinicipios generales de la pesquería del krill de la URSS, tales como la ubicación de las zonas de pesca explotadas y el régimen de temporadas para su explotación. Basándose en datos obtenidos por el buque de exploración *Globus* que participa en operaciones de pesca regulares, se demuestra que las variables de captura por lance están más bien relacionadas con el régimen de pesca del buque, que con la abundancia del krill en una zona determinada. Durante las preparaciones para las operaciones de pesca regulares se realizan lances de muy corta duración, (menos de 15 minutos). Esta práctica pesquera, junto con las considerables fluctuaciones en las capturas durante las operaciones de exploración, dan a menudo como resultado rendimientos que no corresponden a la biomasa real del krill en el lugar en cuestión. En ambos casos, está presente el efecto de los patrones característicos de comportamiento diurno y de largo plazo. Todo esto limita el grado en que los índices de CPUE pueden ser utilizados en estudios de simulación de distribución del krill y de evaluación de reservas. Se puede considerar una prospección multidisciplinaria estándar a gran escala, seguida por el procesamiento de la información obtenida con la ayuda de diversos métodos, como un instrumento mejor para llevar a cabo estos estudios.

1. INTRODUCTION

The usefulness of statistics on the Antarctic krill (*Euphausia superba*) fishery as a source of information on the distribution and the state of the exploited part of the population is an important item of the present work of the CCAMLR Scientific Committee. In particular, discussions are held of the usefulness of CPUE data for the assessment of krill stocks and the establishment of a future fishery management system. However, it is impracticable to evaluate the extent of possible application of CPUE data for these purposes without knowing specific features of fishing practices of particular countries. In recent years a description of the Japanese krill fishery has been given in several publications (Shimadzu, 1985, 1986; Shimadzu and Ichii, 1985; Ichii, 1987; Butterworth, 1987). A description of the USSR krill fishery was presented at a meeting of a group of experts of the CCAMLR Scientific Committee in Moscow in 1987 and published in this volume (Butterworth, 1989).

Both general and specific features of fishing activities are considered in this paper. The selection of fishing areas, the exploitation of krill concentrations and some important aspects of fisheing operations during the commercial season are included. Information received from fishing vessels is useful in studies of krill distribution patterns and abundance and also in mathematical modelling of the krill fishery.

2. PREPARING AND CONDUCTING KRILL FISHING OPERATIONS

2.1 Distribution of Krill and General Scheme of Krill Fishery

Data obtained from numerous research cruises conducted by the USSR since the 1963, and from commercial krill scouting operations have enabled us to assess patterns of krill distribution over the entire range of its habitat. Data on krill concentrations detected and estimated by hydroacoustics within the range of its distribution are assembled and mapped (see Figure 1). As compared with other maps (Marr, 1962; Mackintosh, 1973; Parfenovich, 1982) this one distinguishes between various Antarctic areas in terms of population density and the probability of occurrence of krill concentrations.

Areas for commercial exploitation are selected in accordance with distribution trends within the range. The areas with more regular occurrences of krill concentrations are chosen, but the choice may also depend on weather and ice conditions, the latter being most favourable in spring and summer.

At present Soviet catches are taken from Statistical Areas 48 and 58, with several subareas being considered as traditional fishing areas. In a number of subareas fishing operations are implemented annually according to a stable balanced schedule incorporating a change of the time and areas of operations during the fishing season.

The master schedule may be modified depending on the situation in the year in question. At least two variables are encountered here. Firstly, in spring, autumn and especially in winter, the fishery may be very limited or closed due to weather and particularly ice conditions, irrespective of the presence of commercial concentrations of krill. Secondly, the density of krill concentrations and the time of the formation of dense concentrations vary to some extent from year to year in the same areas. The biological condition of crustaceans is no less important in determining the quality of the catch. The limitations in processing of so-called feeding "green krill" bring about a decrease in daily catches per day and often cause a delay in the start of the fishery in a particular area.

According to current seasonal fishing strategies, operations in Statistical Area 48 start from Subareas 48.1 and 48.2. At the beginning of the season (November-January), ice conditions of a certain year and plankton bloom, which is responsible for the dominance of "green krill", limit the catches. Experience shows that fishing conditions stabilize at the earliest in Subarea 48.1 (waters off the Antarctic Peninsula in the vicinity of Elephant Island). Although Subarea 48.2 is situated on the same latitude as Subarea 48.1, seasonal plankton succession and the ice cover drift occur there rather late. The situation stabilizes in both areas in January (with some difference in time observed) and continues until April-May and sometimes June. Such time differences are associated with year-to-year fluctuations in the seasonal dynamics of ice cover. In April-May, sometimes earlier, the fishery is moved to the waters off South Georgia (Subarea 48.3). In summer, fishing activities in the subarea are not intensive, but the intensity increases by autumn. This is the only subarea where ice conditions do not interfere with fishing operations. The fishing potential is determined by water dynamics. Under favourable conditions, abundant krill concentrations appear and remain. Favourable conditions may prevail until winter, providing for krill fishery in winter and early spring. In mid-spring the abundance of krill decreases and "green krill" appear due to the increasing spring plankton bloom. Consequently, the krill fishery in Subarea 48.3 is usually closed in spring. On the whole, in spring the fishery in the Antarctic decreases or stops. By late spring, an increase in krill catches occurs at the expense of Subareas 48.1 and 48.2.

Small scale fishing operations are also conducted in other sectors of the Southern Ocean, particularly in the Sodruzhestra Sea (Area 58). Fishing operations are carried out in this area only in summer, due to preclusive ice conditions there throughout the rest of the year.

2.2 Fishing Regime and Its Implementation in a Given Region

To ensure high efficiency and stable catches in the krill fishery, scouting operations are conducted by special vessels in each region at the beginning of the fishing season. These vessels gather data on the size of krill concentrations, their location and probable stability, and inform the fishing fleet. Single concentrations or groups of concentrations are detected, assessed and outlined. Moreover, hydroacoustic and regular control trawling surveys are conducted for scouting purposes. Research vessels can participate in these tasks since the main purpose of research vessels is to carry out multi-disciplinary studies over the vast territory, including fishing grounds.

As a rule, data obtained by research vessels are used by the commercial fleet. Multidisciplinary studies make it possible to meet the current requirements and to consolidate data on yearly and seasonal variations in krill abundance with reference to environmental conditions.

Fishing vessels exchange information to determine precisely fishing conditions and to elaborate tactics for optimum and most stable fishing regime.

Besides data on catches and areas where the catches are taken, fishing vessels should receive information on vertical distribution of crustaceans, dynamics of their diurnal distribution, daily and long-term fluctuations in the density of crustaceans in single concentrations and in the whole area. These parameters, as well as general biological characteristics of krill (size composition, maturity, amount of food in stomachs), are liable to substantial seasonal fluctuations in krill availability which should be taken into account in fishing operations. Substantial fluctuations may be observed during the fishing season.

Scouting vessels, and to some extent research vessels, provide essential information to fishing vessels. Scouting vessels are obliged to explore regions adjacent to fishing areas with a view to future exploitation should fishing conditions deteriorate in areas of current fishing operations. Scouting vessels themselves often work in the fishing regime to find out whether detected concentrations are suitable for commercial exploitation.

2.3 Seasonal Operations of a Krill Trawler

The scouting vessel *Globus*, which took krill in the fishing regime in the Sodruzhestra Sea (Area 58) in February-April 1984, is taken as an example. In the Sodruzhestra Sea, large-scale concentrations usually occur, however, they are very unstable. Fishing operations in this area are always combined with scouting. In accordance with its objective, the vessel combined scouting with fishing for krill. The main working schedule of this vessel is typical enough for fishing operations in high latitudes.

Primary areas in which trawl catches were taken are indicated in Figure 2. Three areas are subdivided into regions (indicated by letters). Thus, there are 11 areas and regions of the operation which are marked in chronological order. Scouting operations were carried out in all areas. Krill was detected by an echosounder and hauls were made if records were reliable. Due to the experience gained, the identification of hydroacoustic records and the assessment of concentration densities were well organized. Catches were not less than one tonne per haul. At the same time, long hauls (over 3 hours) were made when dispersed concentrations were recorded and large catches were also taken. When stable concentrations were detected, hauls became shorter.

Catches taken in each area and region are plotted against the time of day (without calculating CPUE) (Figure 3). The duration of each haul is represented by four grades (see symbols in Figure 3). The fishing regime, in particular the duration of hauls, changed both by regions and seasons because of differences in krill distribution and catch processing objectives.

In the largest Area I (2-29 February) scouting operations predominated. Krill concentrations were dispersed over the vast area. There were no regular hauls: as a rule, hauls at the start were long and consequently large catches were taken. It was characteristic that at night very long hauls had resulted in catches of 7-10 tonnes (e.g. region A1). It should be noted that the tendency continued and night fishing was stopped. Scouting operations accounted for a lot of time in region B1 (12-20 February) and appeared to be more successful with about half the hauls lasting one hour (see Figure 3). The obtained catches (4-8 tonnes) were enough to satisfy the demands of krill processing. It should be emphasized that larger catches were often avoided because of processing limitations. The transition to the stable optimum fishing regime occurred between 20 February and 29 February in region 1C where all but six hauls were carried out in the optimum regime (less than 1 hour, see Figure 3).

When fishing operations were moved to Area II (29 February-8 March) and Area III (8-31 March) the optimum regime was kept, but in regions IIIB and IIIC concentrations lacked stability and high density owing to the earlier onset of the biological autumn and its subsequent effects on krill populations and the whole plankton community. Changes in conditions caused an increase in the duration of some hauls, but the bulk of hauls remained short.

In Area IV and especially in Areas V and VI , krill fishing was relocated northwards at later dates. Therefore, krill catches there were rather small even when long hauls were used. This was most characteristic of Area V where there were no catches exceeding 7 tonnes for hauls over 3 hours. In Areas V and VI, there were no hauls of one hour or less. At that time, the most successful operations were conducted in Area VI where concentrations appeared to be larger than in Area V, but the optimum catch level could not be reached due to unfavourable weather conditions.

We can see that the sequence of changes in the fishing regime undertaken to obtain the optimum level is clearly followed through seasons. This is explained not only by different times spent on scouting operations but also by the stability of concentrations themselves. The transition from Area II to Area III and from Area III to Area IV was associated with a drop in the density of krill concentrations.

Notably, only hauls of one hour were practiced within the optimum fishing regime. Moreover, if differentiated by minutes, the majority of hauls were much shorter. Sometimes, to get the optimum catch of 3-8 tonnes, it was enough to haul for 15 minutes or less (see Table 1).

In conclusion it should be indicated that in other areas of the Scotia Sea fishing operations conducted in the optimum regime similar to that described above, continued for about 2-3 months. This was associated with the fact that these areas were in low latitudes.

3. THE APPLICATION OF FISHERY STATISTICS TO STUDIES OF DISTRIBUTION AND BIOLOGY OF ANTARCTIC KRILL

Data from commercial vessels could be used to some extent in studies of krill distribution and biology. However, difficulties arise when attempts are made to assess quantitatively krill distribution and abundance in areas of different size This primarily concerns catch data which are necessary for simulation studies of krill distribution based on CPUE data from commercial vessels. Catches by the latter, as mentioned above, are not regular and fluctuate for various reasons.

From a seasonal point of view, fishing operations are made difficult or even impossible due to unfavourable weather (and ice) conditions. Even if commercially fishable krill concentrations are found, the unfavourable weather (ice) conditions could prevent vessels from making productive hauls. The appearance of "green krill" in catches brings about a drop in fishing intensity and catches. Catches can vary in the case of temporary dispersion of krill in a particular fishing area associated either with hydrological factors or with natural life patterns of crustaceans. Catches would fluctuate in all these cases but the total biomass of krill in a certain area might remain unchanged.

Catch data from vessels which fish for stable krill concentrations on the contrary could be used in estimates and assessments. However, in this case, each haul is short and catch per haul does not correspond to actual abundance of krill in a certain area. The use of the correction factor for calculating a universal effort unit (e.g. for one hour) might cause the constant over-estimation of totals (over 36-38 tonnes per one hour haul). Sometimes such catches were registered during fishing and particularly during scouting operations. It is doubtful whether regular adjustments to an averaged haul duration should be made under the described conditions. The adjustment to CPUE data taken from areas similar to regions IIA and IIB (see section 2.3) would naturally result in highly inaccurate biomass estimates.

The duration of hauls often depends on echosounder operation. If echosounder recordings are interrupted the trawl is usually lifted. Under these circumstances it is unreasonable to continue trawling. The re-calculation of results of such hauls, which are usually shorter than one hour, would inevitably cause the over-estimation of the catch and consequently the biomass.

Fully comparable are the hauls of the same duration (about half an hour or one hour). Their comparability does not depend on existing limitations because the thickness of the concentration layer is controlled by echosounders.

Thus, it is evident that several independent variables (fishing tactics, fishing regime of a vessel, krill distribution properties, the extent of its dispersion, etc) distort assessments of the density of krill concentrations in a given area. That is why CPUE data reported by fishing vessels, could not be an objective indicator of krill abundance. To discover and to take into account these factors in every case is a problem which sometimes could not be solved. Therefore, simple CPUE statistics taken at any scale would supply deliberately distorted results.

Seasonal catch variables reflecting the extent of stability of krill concentrations are of interest for biological studies, particularly studies of small-scale distribution patterns and distribution dynamics in relation to krill physiological conditions. These data together with data on daily fluctuations of krill distribution in the water column provide substantial information about variations in krill concentrations. Repeated transects of the vessel engaged in fishing through a concentration supply detailed information about its shape and size.

Biological samples obtained from krill catches from a certain group of concentrations supply a valuable information about seasonal fluctuations in physiological conditions of crustaceans.

It should be emphasized that for the majority of biological problems, optimum results could be obtained only by the combination of these data with results of observations of scouting and research vessels which carry out multi-disciplinary surveys of vast areas including fishing grounds.

4. CONCLUSIONS

The presented information on practical work of the USSR commercial fishing vessels appears to be insufficiently detailed when compared with a similar document submitted by Japanese scientists (Ichii, 1987). Routine reporting system of the USSR fishing vessels makes it impossible to compile a document with detailed information on the working regime of a particular commercial vessel for all stages of the cruise. There are no biologists aboard these vessels to collect and properly report comprehensive information.

In the 1987/88 season a biologist joined the crew of one of the Soviet fishing vessels which took and processed krill. He was assigned to collect fishery statistics, the analysis of which would facilitate compilation of a detailed report on all aspects of krill trawler activities.

It should be noted that data reported by fishing vessels could hardly provide a satisfactory as background information for the assessment of krill large-scale distribution and stock status. This information would become, to a certain extent, more valuable if collected systematically by all fishing vessels. Unfortunately this appears to be impossible, partially because of the absence of biologists onboard every fishing vessel. Moreover, Soviet scientists in general, believe that CPUE is neither the sole indicator to be used in simulations, nor the basic means of solving the abovementioned problems.

It would be preferable to collect data simultaneously from scouting and research vessels which carry out specifically designed surveys. In this case, data will be similar to those collected under FIBEX (in case of improved methods) or under the USSR national program in the Sodruzhestva and Kosmonavtov Seas in 1984 (Bibik et al, 1988). Thus, large areas could be covered by several vessels operating in accordance with standard methods and standard parameters. Data exchange, mutual data bank, co-ordinated data analysis at working group meetings etc., should serve as the basic means of solving both the abovementioned and other problems with a view to elaborating conservation measures and principles of rational exploitation of Antarctic krill resources. Consequently, data from the fishery could be used as a supplementary, but not as the decisive element in all simulation models of krill fishery.

REFERENCES

BIBIK, V.A., V.V. MASLENNIKOV, N.G. PETROVA, E.Z. SAMYSHEV, E.V. SOLYANKIN, and V.V. SHEVTSOV. 1988. Distribution of *Euphausia superba Dana* in relation to environmental conditions in the Sodruzhestva and Kosmonavtov Seas. In: Interdisciplinary investigations of pelagic ecosystem in the Sodruzhestva and Kosmonavtov Seas. Collected papers. Moscow: VNIRO. p.109-124 (in Russian).

BUTTERWORTH, D.S. 1989. Some aspects of the relation between Antarctic krill abundance and CPUE measures in the Japanese fishery. Report of discussions with Japanese industry and fishing agency members and scientists. (See this volume).

ICHII, T. Observation of fishing operation and distributional behaviour of krill on a krill trawler off Wilkes Land during the 1985/86 season. SC-CAMLR-VI/BG/35, 25 October 1987: 1-26.

MACINTOSH, N.A. 1973. Distribution of post-larval krill in relation to ice and water conditions. Discover Rep. 36: 95-156.

MARR, J.W.S. 1962. The natural history and geography of the Antarctic krill (*Euphausia superba Dana*). Discover Rep. 32: 33-464.

PARFENOVICH, S.S. 1982. Specific features of spatial distribution of Antarctic krill. Oceanologia 22 (3): 480-485.

SHIMADZU, Y. 1985. A brief summary of Japanese fishing activity relating to Antarctic krill, 1972/73 - 1982/83. Selected papers presented to the Scientific Committee of CCAMLR 1982-1984 Part I: 439-452.

SHIMADZU, Y. 1985. An updated information of the Japanese krill fishery in the Antarctic. CCAMLR. CCAMLR document Krill WG/1985/Doc 5: 7 pp.

SHIMADZU, Y. and T. ICHII. Some considerations on the usefulness of CPUE data from Japanese krill fishery in the Antarctic. CCAMLR Document Krill WG/1985/Doc. 4: 10 pp.

Table 1: Actual duration of hauls under the optimum regime of krill fishery (% from the number of hauls which lasted less than one hour in every area and region), February-April 1984.

Area (region) see Fig. 2	Time	Duration of hauls in minutes				Number of haul total
		below 15	15-30	30-45	45-60	
IB	12-20.2	4.5	36.4	36.4	22.7	22
IC	20-29.2	60.0	27.5	12.5	-	40
IIA	29.2-2.3	86.7	13.3	-	-	15
IIB	2-8.3	75.7	10.8	10.8	2.7	37
IIIA	8-10.3	70.0	10.0	15.0	5.0	20
IIIB	10-23.3	47.1	17.6	25.6	8.8	34
IIIC	23-31.3	-	13.8	41.4	44.8	29
IV	31.3-1.4	-	-	75.0	25.0	4

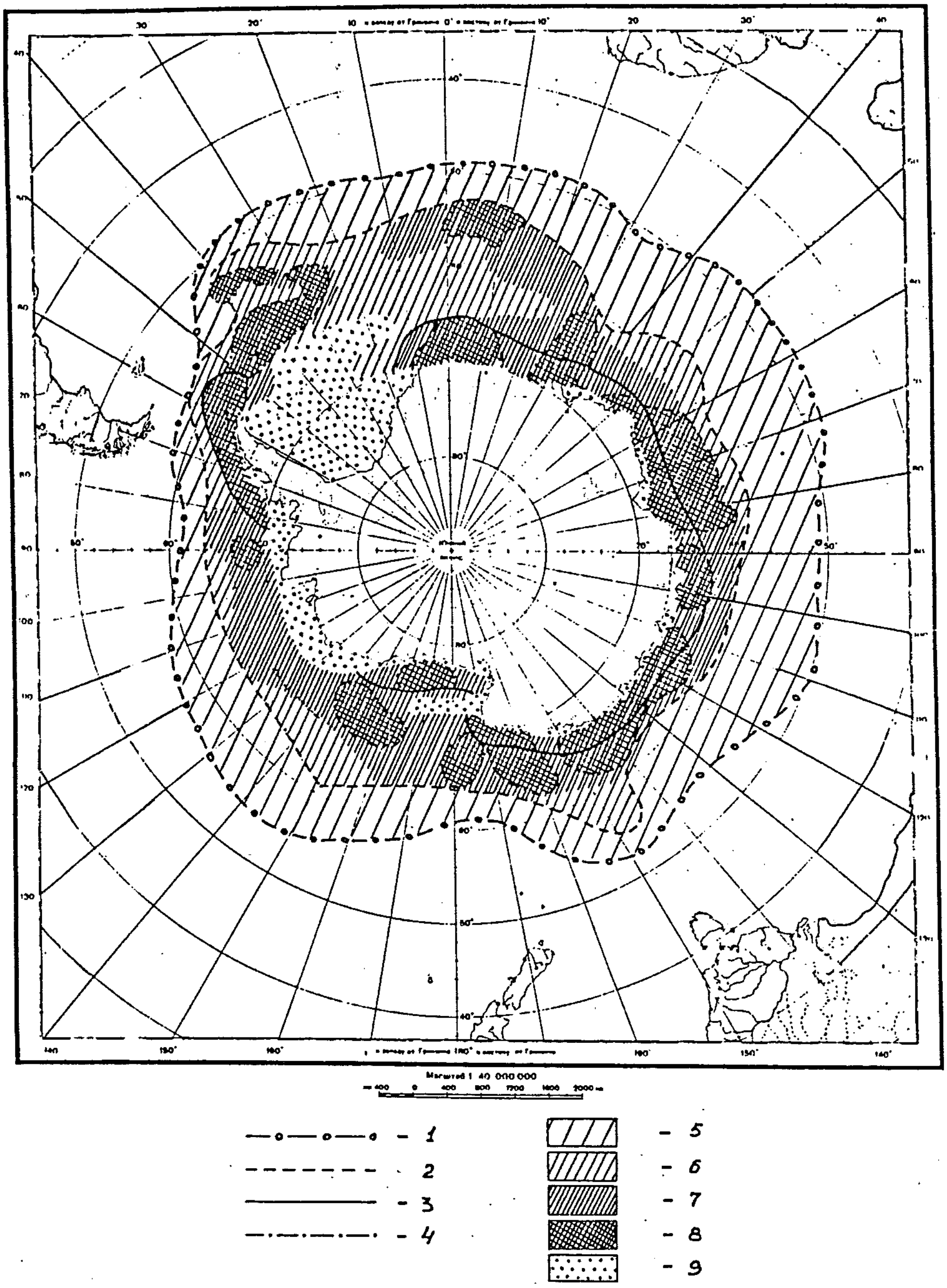

Figure 1: Spatial differentiation of Antarctic krill distribution range mapped by occurrences of concentrations.

1 - northern boundary of the range;
2 - northern boundary of the area of occurrence of krill concentrations;
3 - boundary of subareas
north subarea - the subarea of occurrence of unstable concentrations of the open sea, and south subarea - the subarea of occurrence of stable concentrations in the waters off the continent;
4 - boundaries of areas of most stable and mass concentrations of krill (Parfenovich, 1982 and 1985);
5 - area of distribution of dispersed krill (no catches*);
6 - area of distribution of krill concentrations with low density (catches below 1 t/h*);
7 - area of distribution of krill concentrations with average density (catches 1-5 t/h*);
8 - area of distribution of krill concentrations with high density (catches 5-30 t/h);
9 - area of distribution range inaccessible for observations of concentrations;

---

* Catches taken by midwater trawls of research and scouting vessels.

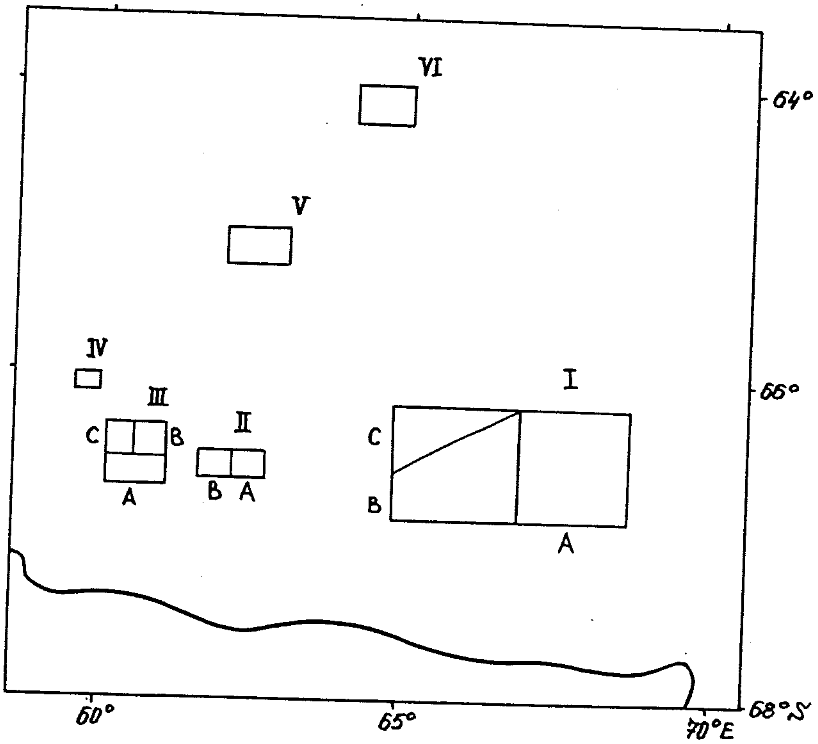

Figure 2: Operation areas of scouting vessel *Globus* in the Sodruzhestva Sea in February-April 1984 (see keys in the text).

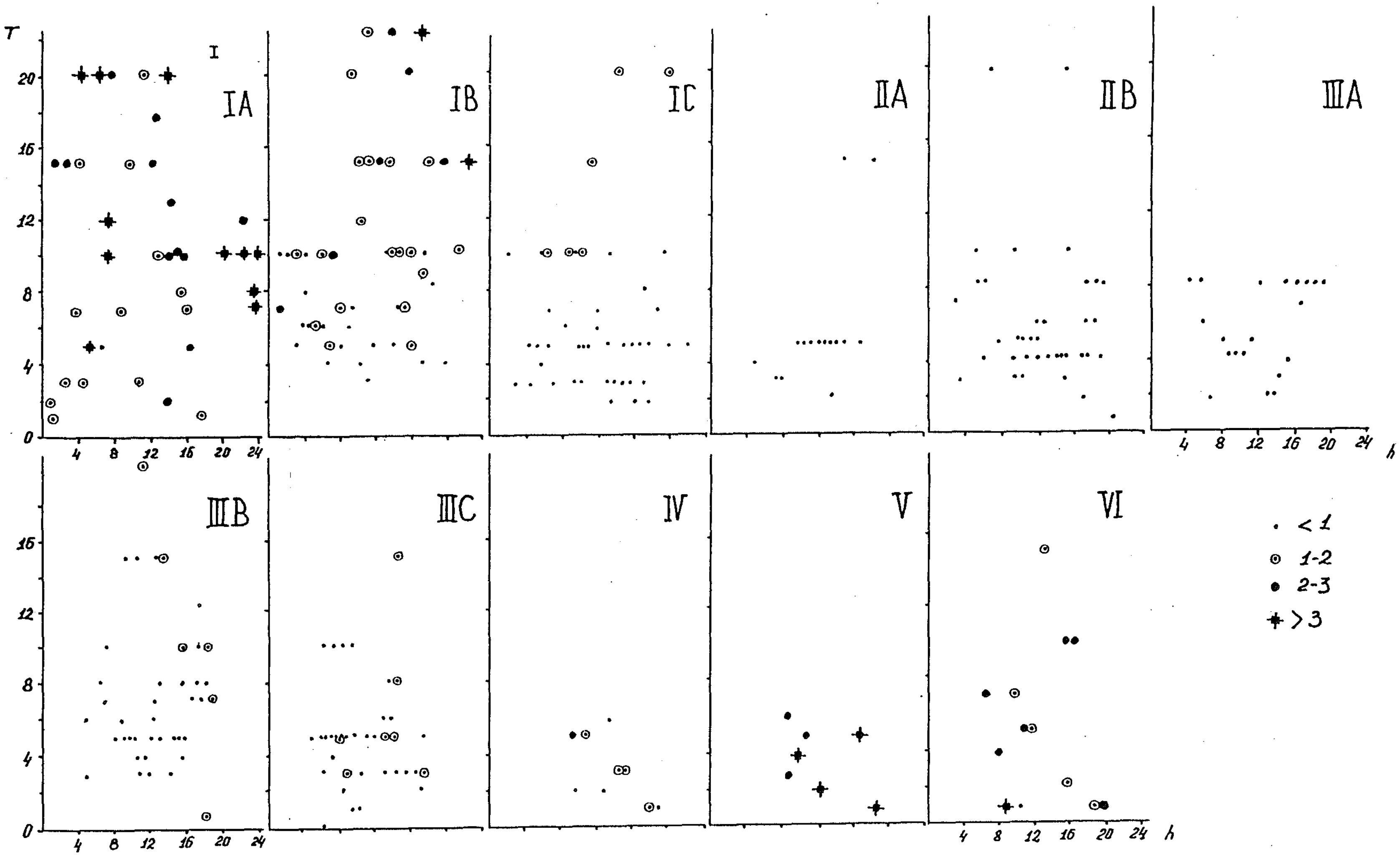

Figure 3: Catching regime of scouting vessel *Globus* which operated in the Sodruzhestva Sea in February-April 1984 by areas and regions (see Figure 2). Dates of operation are indicated in Table 1 or in the text. Key: tonnes per haul.

Légendes des tableaux

Tableau 1	Durée réelle des traits de chalut sous le régime optimal de pêche de krill (% du nombre de traits de moins d'une heure dans chaque zone et région), de février à avril 1984.

Légendes des figures

Figure 1	Différentiation spatiale de l'éventail de distribution du krill antarctique dressée sur une carte des concentrations.
Figure 2	Zones d'opération du navire de reconnaissance *Globus* dans la mer du Sodruzhestva de février à avril 1984 (voir clé dans le texte).
Figure 3	Régime de pêche du navire de reconnaissance *Globus* qui était en activité dans la mer du Sodruzhestva de février à avril 1984, par zones et régions (voir figure 2). Les dates d'opération sont indiquées sur le tableau 1 ou dans le texte. Clé: tonnes par trait.

Заголовки к таблицам

Таблица 1	Действительная продолжительность тралений при оптимальном режиме промысла криля (% от количества тралений, продолжавшихся менее одного часа), с февраля по апрель 1984 г.

Подписи к рисункам

Рисунок 1	Пространственная дифференциация параметров распределения антарктического криля, отмеченная на карте случаями концентраций.
Рисунок 2	Районы работы поискового судна "*Globus*" в море Содружества с февраля по апрель 1984 г. (см. обозначения в тексте).
Рисунок 3	Режим ведения промысла поискового судна "*Globus*", работавшего в определенных районах моря Содружества с февраля по апрель 1984 г. (см. Рисунок 2). Даты операции указаны в Таблице 1 или в тексте. Обозначение: тонны за траление.

Encabezamientos de las Tablas

Tabla 1	Duración real de los lances dentro del régimen óptimo de la pesquería del krill (% del número de lances cuya duración fue menos de una hora en cada área y región), febrero-abril 1984.

Leyenda de la Figura

Figura 1	Diferenciación espacial del rango de distribución del krill antártico representado por la presencia de concentraciones.

Figura 2 Zonas de operación del buque de reconocimiento *Globus* en el mar de la Sodruzhestva , de febrero a abril 1984, (véase clave en el texto).

Figura 3 Régimen de capturas del buque de reconocimiento *Globus* que operó en el mar de la Sodruzhestva de febrero a abril 1984, por áreas y regiones, (véase Figura 2). Las fechas de operación se indican en la Tabla 1 o en el texto. Clave: toneladas por lance.

SURVEY DESIGN TO ESTIMATE KRILL ABUNDANCE DURING FIBEX

I. Everson, I. Hampton, G.M. Jolly

Abstract

One of the primary aims of FIBEX (First International BIOMASS Experiment), 1981 was to study the methodology for assessing the abundance of krill. The survey design used in the southwest Atlantic study area of the FIBEX is described in this papers. Sampling involved the use of echosounders for estimating krill abundance as well as collection of data on the size, density and distribution of krill swarms. In addition, information on surface water temperature, salinity and fluorescence as well as on seabirds was also collected. The study area was subdivided into several geographically distinct subareas in each of which randomly spaced transects were located. Subarea were treated as strata and a stratified random sampling method was used. The survey was done in two phases. In the first phase a fairly evenly dispersed subsample of transects was surveyed and these were also used to fix stratum boundaries. In the second phase the remaining transects were surveyed, using the stratum boundaries defined from the first phase. The design of the survey was directly related to the subsequent method of data analyses, some main aspects of which are discussed. The analytical formulae for the analyses are also presented.

Résumé

L'un des objectifs principaux de la FIBEX (Première expérience internationale BIOMASS), 1981 était d'étudier la méthodologie de l'évaluation de l'abondance du krill. Le modèle de prospection utilisé dans la zone d'étude de l'Atlantique sud-ouest est décrite dans ce document. L'échantillonnage a nécessité l'utilisation d'échosondeurs pour estimer l'abondance du krill ainsi que la collecte des données sur la taille, la densité et la distribution des essaims de krill. En sus, des informations ont été recueillies sur la température de l'eau de surface, la salinité et la fluorescence ainsi que sur les oiseaux de mer. La zone d'étude a été subdivisée en plusieurs sous-zones géographiques distinctes, dans chacune desquelles des transects ont été disposés au hasard. Ces sous-zones ont été considérées comme des strates et une méthode d'échantillonnage au hasard par couche a été utilisée. L'étude a été effectuée en deux phases. Dans la première phase, un sous-échantillon de transects, éparpillés de façon assez uniforme, a été étudié et ceux-ci ont aussi été utilisés pour établir les limites des strates. Dans la deuxième phase, le reste des transects a été étudié en utilisant les limites des strates établies au cours de la première phase. Le modèle de l'étude a un rapport direct avec la méthode subséquente des analyses de données, dont quelques aspects importants sont discutés. Les formules analytiques utilisées dans le traitement des données ont aussi été présentées.

Резюме

Одной из первейших задач программы FIBEX (Первый международный эксперемент BIOMASS), 1981 г., было изучение методологии при оценке численности криля. В этой работе описывается планирование съемки, использованное в юго-восточном атлантическом районе исследования FIBEX. Выборка включала в себя использование гидроакустических приборов для оценки численности криля, а так же для сбора данных о размере, плотности и распространении скоплений криля. Кроме того, была собрана информация о температуре поверхностного слоя воды, солености и флуоресценции, а также о морских птицах. Исследуемый район был разделен на несколько географически обособленных подрайонов, в каждом из которых были произведены гидрологические разрезы на произвольно выбранном расстоянии друг от друга. Подрайоны рассматривались как стратум, и использовался стратифицированный метод произвольной выборки. Съемка производилась по двум этапам. На первом этапе под наблюдением находилась равномерно рассредоточенная часть пробы разрезов, использованных также для определения границ стратума. На втором этапе обследовались оставшиеся разрезы при использовании границ стратума, определенных на первом этапе. Планирование съемки было непосредственно связано с последующим методом анализа данных, некоторые основные аспекты которых здесь обсуждаются. Также представляется аналитическая формула для этого анализа.

Resumen

Uno de los objetivos principales del FIBEX (Primer Experimento Internacional de la BIOMASA), en 1981 fue el estudio de la metodología para evaluar la abundancia del krill. Se describe en este documento el diseño de la prospección utilizado en el área de estudio del FIBEX en el suroeste Atlántico. El muestreo requirió el uso de ecosondas para estimar la abundancia del krill, así como la recopilación de datos sobre la talla, densidad y distribución de los cardúmenes de krill. Asimismo, se recogió información sobre la temperatura, salinidad y fluorescencia de las aguas superficiales así como sobre las aves marinas. El área de estudio fue subdivida en varias subáreas geográficamente distintas, colocándose en cada una de ellas transectos espaciados aleatoriamente. Se trató a las subáreas como estratos y se utilizó un método de muestreo aleatorio estratificado. Se realizó la prospección en dos fases. En la primera fase se prospeccionó una submuestra de transectos dispersados de modo uniforme, los cuales se utilizaron también para determinar los límites del estrato. En la segunda fase se prospeccionaron los transectos restantes, utilizando los límites del estrato definidos en la primera fase. El diseño de la prospección estuvo directamente relacionado con el método subsiguiente de análisis de datos. Se discuten algunos aspectos principales del mismo. Asimismo se plantean las formulas analíticas para el análisis.

1. INTRODUCTION

Increasing interest in the marine living resources of the Southern Ocean has highlighted significant gaps in our knowledge of their basic ecology. This is particularly true of Antarctic krill (*Euphausia superba*). Against this background and in view of the developing fishery for krill it is necessary to provide a sound framework for future research. This has resulted in the formation of BIOMASS (Biological Investigations of Marine Antarctic Systems and Stocks). The principal objective of BIOMASS is to gain a deeper understanding of the structure and dynamic functioning of the Antarctic marine ecosystem as a basis for future management of potential living resources (SCAR 1977).

Estimation of krill abundance was identified as being one of the key topics for study and this became one of the major investigations for FIBEX (First International BIOMASS Experiment). The primary aims of FIBEX (BIOMASS 1980a) were:

1. To study the methodology for assessing the abundance of the total krill population.
2. To map the distribution of krill in parts of the southwest Atlantic, southern Indian and western Pacific sectors of the Southern Ocean and if possible relate the distribution of krill to the distribution of water masses.
3. To obtain a synoptic assessment of the abundance of krill in the south-west Atlantic sector of the Southern Ocean.

It was anticipated that about 12 vessels from 11 nations might participate in the experiment. The coordinated multiship part of the study was scheduled to take 30 days. Two main areas were identified for study, in the southwest Atlantic and the southeast Indian Ocean. A greater level of sampling activity per unit area was expected in the former area and this allowed a more sophisticated survey design, described here, to be used.

2. SAMPLING PROGRAMME

Underway sampling centred on the use of echosounders for estimating krill abundance and also providing information on the size, density and distribution of krill swarms. The requirements in this field were as follows:

1. Data should be integrated along the shortest track interval that practical limitations allow (generally this interval would be one nautical mile).
2. Data should be reported as mean volume back-scattering strength.
3. The depth, size and density of swarms should be estimated either by processing of digitised echosignals or from examination of echocharts with respect to integrator output.
4. The operating frequency of echosounders should be between 50 and 200 kHz. The standard frequency would be 120 kHz.

In addition, underway observations were requested for surface temperature, salinity, fluorescence and observations on seabirds.

3. SURVEY DESIGN

3.1 Anticipated Distribution of Krill

Published information indicated that krill would be distributed northwards from the pack ice zone (Marr 1962; Mackintosh 1973) with the abundance decreasing rapidly some distance from the ice edge.

3.2 Selection of Transects

The design used in the Atlantic Sector of the FIBEX survey was that recommended in BIOMASS (1980b). The Sector was subdivided into several geographically distinct subareas (Figure 1) in each of which parallel, randomly spaced sample transects were located. Subareas were treated as strata, the result being a stratified random sample of transects analysable by standard statistical methods as recommended, for example, by Cochran (1977).

For a given subarea (stratum) the direction of transects was chosen to run across the direction of ocean currents and thus across the probable contour lines of krill abundance. Generally, therefore, transects tended to run north/south, the northern boundary of a stratum being determined by the limit of the krill population. Since this limit had to be defined during the survey, the pre-determined sample of transects was surveyed in two phases.

In the first phase a fairly evenly dispersed subsample of transects was surveyed and these were also used to fix stratum boundaries. The second-phase transects, that is, selected transects not surveyed in the first phase, were surveyed on the return journey to base, using the stratum boundaries defined from the first phase. This meant that second-phase transects tended to be shorter than first-phase transects, which gave strata of the shape seen in Figure 2, the procedure being unbiassed as far as estimation of krill population was concerned and efficient inasmuch as no transect data had to be discarded. In practice, in order to achieve the maximum of survey time in the total available time (about 30 days) each Chief Scientist made calculations throughout the survey as to how many transects could be included in the time remaining, deleting transects as necessary from the list according to pre-assigned random numbers.

A further advantage of the two-phase system was that it allowed a larger number of transects to be sampled in strata of apparently higher density, thus further increasing sampling efficiency (see Cochran 1977).

3.3 Associated Analysis

Since the design of a survey has a direct bearing on the subsequent method of data analyses, some comment on this is desirable here. The main considerations are:

1. Assuming that an unbiassed estimate of mean krill density can be obtained for each sampled transect, the design is capable of providing an unbiassed estimate of density for each stratum.
2. Stratification ensures that major sources of variation are eliminated from the overall estimate of mean density for the region.
3. Randomisation ensures that (a) an unbiassed estimate of the variance of mean density is obtainable, and (b) the possibility of bias, such as might arise if

equally spaced transects were to coincide with a periodicity in the krill distribution, is eliminated.

4. By taking account of the different lengths of the sampled transects, the variance can be further reduced. The appropriate method for the present circumstances is a ratio-to-size estimate in which transect means are weighted by their length in calculating the stratum mean. Although, in general, ratio estimates are subject to small-sample bias, it can be shown that this bias is zero when the ratio of the observed variate (biomass) to the supplementary variate (transect length) for a particular sampling unit (transect) is uncorrelated with the supplementary variate; these conditions can be assumed to apply here as density is unlikely to be related to transect length. This source of bias was considered negligible in the present survey. For a detailed discussion of ratio estimation the reader is referred to Cochran (1977) or other standard texts on sampling methods.

5. Confusion sometimes arises when a variance is estimated from a sum of squares of deviations of transect means from the stratum mean, the procedure is so simple that it is thought not to take account of serial correlations between or within transects or of other features of the distribution pattern (for example, aggregations). Such a belief, of course, is wholly incorrect. These methods make no assumptions whatever as to distribution patterns and are entirely valid for any population, provided of course, that selection of transects is at random within a stratum. A full account of the analytical methods used is given in BIOMASS (1985).

4. ANALYTICAL FORMULAE

The surveyed area contains J strata whose individual areas are denoted by A_j. Each stratum is composed of K transects and each transect contains M distance intervals. The useable length of one of the transects is therefore given by the formula:

$$L_k = \sum_{m=1}^{M_k} (D_k)_m$$

The mean weight density for each transect is given by the formula:

$$\overline{W_k} = \frac{1}{L_k} \sum_{m=1}^{M_k} \overline{(W_k)_m} \cdot (D_k)_m$$

The mean weight density within a stratum is given by the formula:

$$\overline{W_k} = \frac{\sum_{k=1}^{K} \overline{W_k} \cdot L_k}{\sum_{k=1}^{K} L_k}$$

and the mean weight density for J non overlapping strata is given by the formula:

$$\overline{W} = \frac{\sum_{j=1}^{J} (\overline{W_k})_j \, A_j}{\sum_{j=1}^{J} A_j}$$

The variance of the within stratum mean weight density (W_k) is given by the formula:

$$\mathrm{Var}\,(W_k) = \frac{K \bullet \sum_{k=1}^{K} (\overline{W}_k - \overline{W}_K)^2 \; L_k^2}{(K-1) \bullet (\sum_{k=1}^{K} L_k)^2}$$

The deviation of these formulae is given fully in BIOMASS (1986).

5. FIELDWORK

A total of 10 ships from Argentina, Australia, Chile, France, Federal Republic of Germany, Japan, Poland, South Africa, the USA and the USSR participated in the FIBEX acoustic survey. This allowed full coverage of virtually the whole area initially planned with the exception of the South Georgia subarea, allotted to the UK who withdrew due to mechanical breakdown of RRS *John Biscoe.* A part of the South Georgia subarea was covered by scientists from the USSR on the research vessel *Odyssee.*

Inevitably the FIBEX survey generated large datasets which are being analysed by several groups. A resume of the datasets has been published (Hempel 1983) while a detailed analysis on abundance estimation has been prepared (BIOMASS 1986).

REFERENCES

BIOMASS. 1980a. FIBEX Implementation and Coordination Meeting Report, Dammarie-les-Lys, France, 4-6 June 1980. BIOMASS Report Series No. 13: 22 pp, 3 Annex.

BIOMASS. 1980b. FIBEX Acoustic Survey Design Meeting Report, Dammarie-les-Lys, France, June 1980. BIOMASS Report Series No. 14: 11 pp.

BIOMASS. 1986. Report on post-FIBEX Acoustic Workshop, Frankfurt, Federal Republic of Germany, September 1984. BIOMASS Report Series No. 40: 127 pp.

COCHRAN, W.G. 1977. Sampling Techniques. Wiley, New York.438 pp.

HEMPEL, G. 1983. FIBEX - An International survey in the Southern Ocean. Review and Outlook Memoirs of the National Institute of Polar Research No 27: 1-15.

MACKINTOSH, N.A. 1973. Distribution of post larval krill. In: the Antarctic Discovery Reports 36: 96-156.

MARR, J.W.S. 1962. The natural history and geography of the Antarctic Krill (*Euphausia superba*). Discovery Reports 32: 33-464.

NAST. 1982. Krillfrange Wahrend FIBEX 1981. Archiv fur Fischereiwissenschaft 33: 61-84.

SCAR. 1977. Biological investigations of Marine Antarctic Systems and Stocks. Volume 1: Research proposals.

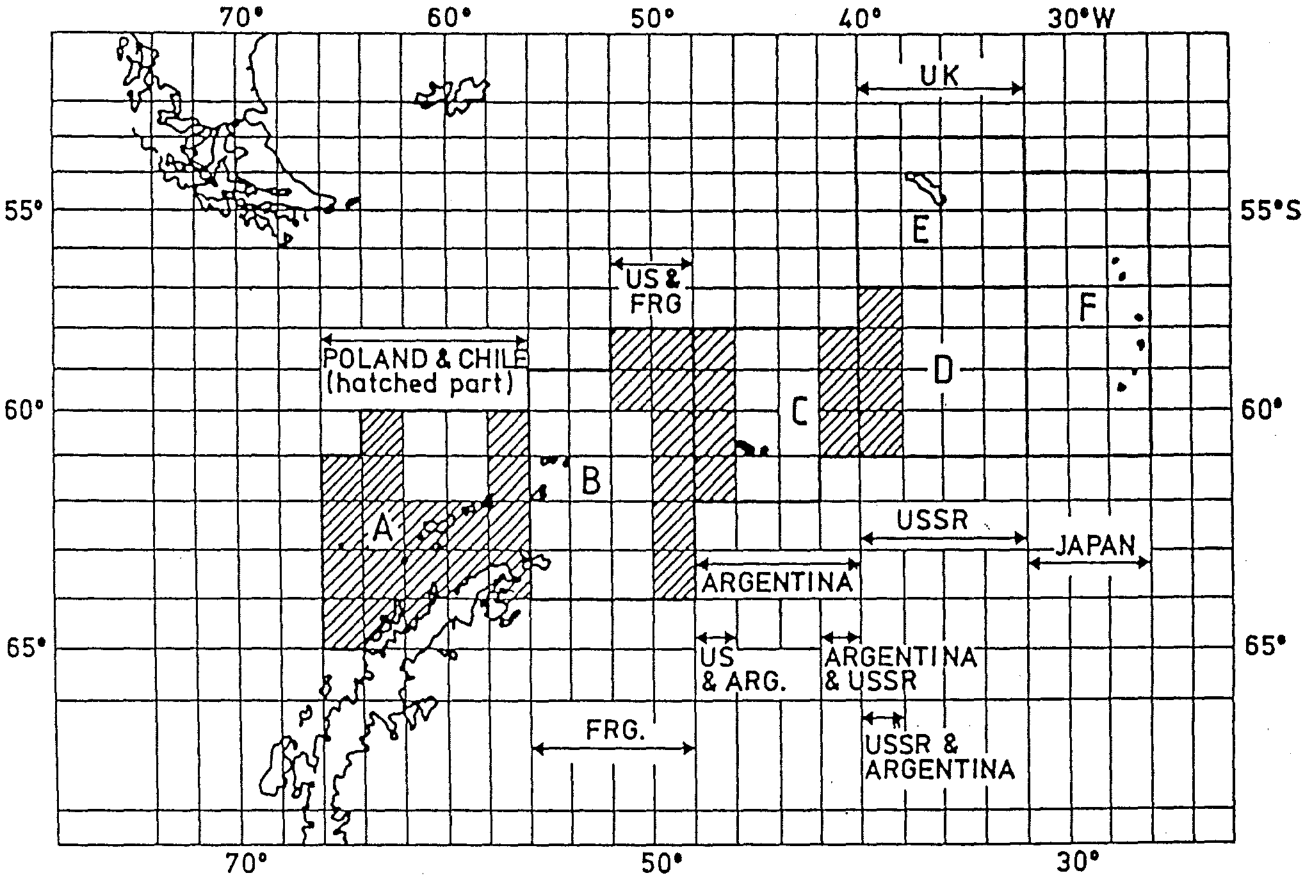

Figure 1: Proposed FIBEX survey areas in the Southwest Atlantic sector of the Southern Ocean (BIOMASS 1980a).

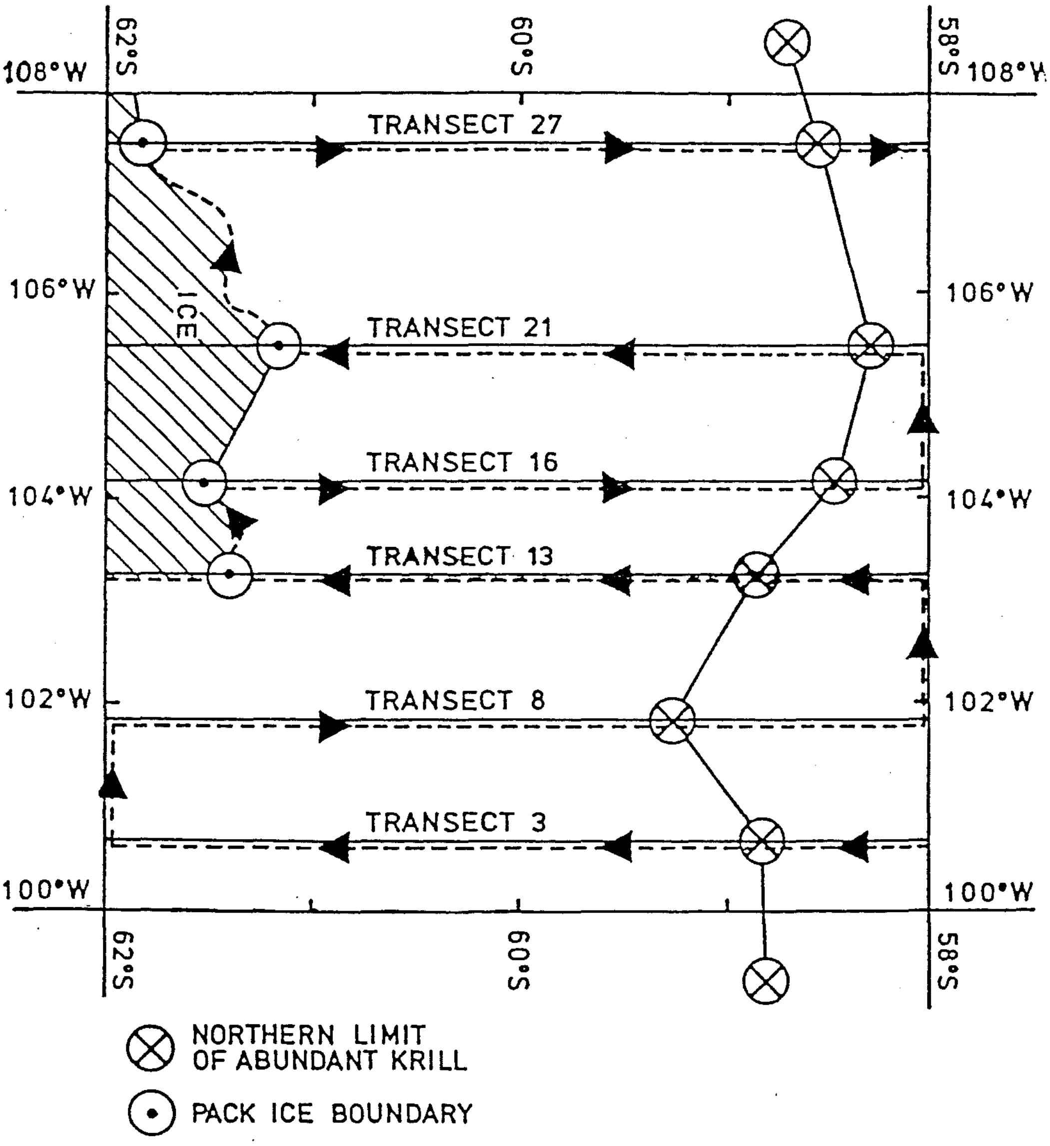

Figure 2: Example of a survey subarea at the end of the primary phase (after BIOMASS 1980b). Phase 2 transects would be run only in the anticipated high density stratum between the pack ice boundary and the northern limit of abundant krill.

Légende de la figure

Figure 1	Zones d'étude proposées de la FIBEX dans le secteur sud-ouest Atlantique de l'océan Austral (BIOMASS 1980a).
Figure 2	Exemple d'une sous-zone d'étude à la fin de la phase primaire (après BIOMASS 1980b). Les transects de la Phase 2 ne seraient effectués que dans la strate de haute densité anticipée entre la limite de la banquise et la limite nord du krill abondant.

Подписи к рисункам

Рисунок 1	Предлагаемые районы съемки (FIBEX) в юго-западном секторе Южного океана (BIOMASS 1980a).
Рисунок 2	Пример съемки подрайона в конце первичной стадии (после BIOMASS 1980b). Поперечные разрезы будут осуществлены только в предполагаемом слое высокой плотности между границей пакового льда и северным лимитом обильного криля.

Leyenda de la Figura

Figura 1	Areas de prospección FIBEX propuestas en el sector del Sudoeste Atlántico del Océano Austral (BIOMASS 1980a).
Figura 2	Ejemplo de una subárea de prospección al final de la primera fase (después de BIOMASS 1980b). Los transectops de la fase 2 se llevarían a cabo únicamente en el estrato de alta densidad anticipado entre el límite del hielo a la deriva y el límite norte de abundancia del krill.

TARGET STRENGTHS OF ANTARCTIC KRILL (*EUPHAUSIA SUPERBA*)

I. Everson, D.G. Bone, J.L. Watkins and K.G. Foote

Abstract

The Mean Volume Backscattering Strength of encaged aggregations of swimming krill have been measured at 38 and 120 kHz in a sheltered bay at South Georgia. The results indicate that the Target Strength values are approximately 10dB lower than previously assumed.

Résumé

Des concentrations encloses de krill mobile ont été mesurées à 38 et 120 kHz. Les résultats indiquent que les valeurs de la réponse acoustique sont nettement moins élevées que l'on supposait jusqu'à présent.

Резюме

Средняя сила обратного рассеивающего объема помещенных в садки агрегаций плавающего криля составляла 38 и 120 кГц в спокойном заливе Южной Георгии. Результаты показывают, что величины силы цели были приблизительно на 10 децибел ниже, чем ранее предполагаемые.

Resumen

Se ha medido la Fuerza de Retrodispersión del Volumen Medio de las agregaciones enjauladas de krill que nada a 38 y 120 kHz en una bahía protegida en Georgia del Sur. Los resultados indican que los valores de la Fuerza de Blanco son aproximadamente 10dB más bajos de lo que previamente se había supuesto.

1. INTRODUCTION

Euphausia superba is recognised to occupy a key position in the Antarctic ecosystem (Everson 1987, Laws 1985). The attempt to quantify its abundance in 1981 over part of its area of occurrence in the Southern Ocean occassioned the "largest acoustic survey of a marine species ever undertaken" (Anon. 1986). Insofar as it was desired to derive absolute measures of stock strength by the traditional echo integration method (Forbes and Nakken 1972, Johannesson and Mitson 1983), knowledge of the target strength is essential.

The problem of the target strength of krill has long been troublesome (Everson 1987). Firstly, only a few measurements on *E. superba* have been reported, and fewer applied, e.g., those by Protaschuk and Lukashova (1982) at 120 kHz and those by Nakayama et al. (1986) at 200 kHz. To supplement such measurements, recourse has been made to measurements on other krill species and fresh water shrimp, on tethered live, defrosted or otherwise preserved specimens, in fresh water as well as sea water. In addition the state of equipment calibration has generally not been reported, notwithstanding use of hydrophones, which method is fraught with errors and whose accuracy "is probably no better than ±1.4 dB" (Blue 1984). This figure is much inferior to that readily obtainable with standard spheres (Foote and MacLennan 1984, Robinson 1984, Foote et al. 1987), which is now the accepted method of calibrating fisheries acoustics instruments.

Recourse has also been made to model calculations, e.g., the scattering model of Greenlaw (1977) or radiation model of Kristensen (1983), to establish the frequency dependence of target strength. The latest calculations (Stanton 1988a, b), however, must cast doubt on the predictability of krill target strength by such models.

It is the aim of this work to describe a new series of measurements of the target strength of *E. superba*, made in January and February 1988. These were performed on encaged, otherwise free-swimming aggregations of krill at 38 and 120 kHz. In anticipation of submitting a detailed account of the experimental method and analysis to a journal, these parts, to the extent that they are complete, are only summarized, the primary objective here being to orient. Likewise, the measurement results are presented without the broader analysis that is evidently required for their explanation.

2. EXPERIMENTAL DESIGN

Earlier studies on the target strength of euphausiids and other small crustaceans convinced the authors of the need to perform all measurements on the animal of interest, *E. superba*. The work of Køgeler et al. (1987) was noted for its finding of systematic variations in density of euphausiids and the copepods *Calanus finmarchicus* and *C. hyperboreus* with size and season. The nominal density of these species, and that of *E. superba* too, is so close to the density of sea water that quite small changes can be very significant in the context of echo formation (Greenlaw et al. 1980). This is why it was necessary to travel south of the Antarctic Convergence, to where *E. superba* is found.

Given the general weakness of acoustic scattering by euphausiids, with physical properties similar to those of sea water, it was widely desired to perform the measurements on known targets. This was the motivation for measuring encaged aggregations of krill.

Several additional wishes contributed to the experimental design. Firstly, the recognised directionality of scattering by euphausiids (Greenlaw 1977) persuaded the authors to attempt concurrent photographic measurements of behaviour during the acoustic observations. Secondly, the desire to characterise the physical properties of the object animal by laboratory measurements of density and longitudinal sound speed, among others, made a shore base highly desirable. Thus it was that the measurement venue became a raft moored in the harbour of the abandoned, and sadly vandalized, whaling station at Stromness on the island of South Georgia.

The decision to measure encaged aggregations of krill allowed a wealth of experience on encaged fish to be tapped, as represented in the bibliography in Foote (1986). In addition, an experiment in fisheries acoustics (Foote 1983) could serve as a model for the present experiment. This was mostly followed, the major exception being acoustic measurements on single animals. Although planned, these were precluded by the lowness of the krill target strengths, which was already obvious from the very first encaged-aggregation measurements.

3. MATERIALS

3.2 Experimental Site

The primary measurements were made from a raft anchored securely 200 m from shore in 50-m-deep water in the harbour at Stromness on South Georgia. The site was protected from the open sea by an island blocking most of the harbour mouth. Swell with amplitude up to 0.5 m did pass through, however. The site was subject to violent catabatic winds rushing down the large and open valley behind Stromness. These reached severe gale force on roughly one out of two days, and hurricane force about once a fortnight. Depending on the wind direction and temperature, the immediate surface layer in the harbour could become quite brackish owing to glacial runoff. However, this light-water layer was seldom thicker than about 1 m, and did not affect the conduct of the measurements, which were performed far below it.

3.3 Krill Supply and Maintenance

Although krill frequently occur around South Georgia, their presence in bays, such as Stromness, is unpredictable. Fresh supplies of good-condition, live krill were obtained by RRS *John Biscoe* at approximately fortnightly intervals throughout the experiment. Krill captured by trawling were immediately put into sea water-filled tanks on the trawling deck. Dead or damaged krill were removed from the tanks while the ship was at sea. Live, good-condition krill were transferred to the holding pens when the ship returned to Stromness.

This supply was augmented by fortuitous swarms of krill in the harbour. On each such occasion it was possible to attract the krill at night by surface lighting to the very edge of the holding pens, where they could be caught and transferred in the freshest condition by dip net. It was estimated that 500 000 krill were secured after about one hour on each occasion.

The krill were kept in a cluster of four holding pens. Each was cylindrical in form, with 2 m diameter and 3 m depth. An air pump, driven by generator ashore, lifted water from 5 m depth to above the surface, where its fall into the pen entrained additional air. The rapid growth of algae on the sidewalls of the pens provided a source of food for the krill, which were frequently observed to be grazing on this.

An enclosure net was hung around the holding pens, this and a fine-mesh covering of the surface openings protected the krill from predators, such as penguins and seals.

3.3 Cage

Useful acoustic measurements were obtained with each of two identical cages. These were right octagonal cylinders of 0.5 m height and 0.5 m diameter measured across the flat sides of the octagon, measured between opposite sides. The volume was thus 0.104 m^3.

The material used in the construction was plastic netting of rectangular grid 3.2 x 3.6 mm. This was procured from Internet Incorporated, Minneapolis, Minnesota, USA. The netting, product number ON-8360, is normally used in reinforcing paper, as for towelling.

The cages were constructed by sewing, with monofilament nylon, pre-cut octagonal end panels of the mesh to the long edges of a pre-cut rectangular panel, which formed the sidewall. The sidewall was closed by sewing with the same monofilament nylon.

3.4 Measurement Configuration

The cage was suspended approximately 6 m below the transducers, which were mounted on a weighty frame from which other gear was suspended. The cage itself was suspended between two lightweight square frames, 3 m on a side. Lines of monofilament nylon were attached to each of sixteen corners. The upper eight were attached to a superior frame, the lower eight to the inferior frame. An underwater television camera was suspended from the inferior frame, pointing upwards towards the cage. The entire rig was suspended by a single rope attached to the transducer frame and allowing raising and lowering by a winch attached to a gantry positioned over one of two identical 4 x 4 m square moon-pools on the raft. The normal operating depth of the transducers was 9 m.

3.5 Acoustic Equipment

It was desired to use the same kind of equipment for the measurements as is typically used during surveys. This was done with the SIMRAD EK-400 echosounder (Brede 1984a) normally used on board RRS *John Biscoe*. The echosounder was used in its dual 38 and 120 kHz modes together with UNIVERSAL SONAR transducers, each with nominal 10 deg beamwidth. Integration of the squared echo signals was performed with the SIMRAD QD digital echo integrator (Brede 1984b). Both echosounder and integrator were housed ashore, in the laboratory, together with other equipment. This included a BAS system for display and logging of data. The cable link was entirely satisfactory. Additional acoustic equipment consisted of three calibration spheres; 60 and 23 mm diameter copper spheres and a 38.1 mm diameter tungsten carbide sphere (Foote and MacLennan 1984).

3.6 Photographic Equipment

The principal photographic equipment that worked consisted of an underwater television camera and programmable videotape units for the display, recording and replay of the television images.

A stereoscopic camera system was also suspended with the television camera. However, for a variety of reasons and in spite of arduous if Sisyphean labours, the system provided few data and none on the particular acoustically measured krill.

3.3 Cage

Useful acoustic measurements were obtained with each of two identical cages. These were right octagonal cylinders of 0.5 m height and 0.5 m diameter measured across the flat sides of the octagon, measured between opposite sides. The volume was thus 0.104 m^3.

The material used in the construction was plastic netting of rectangular grid 3.2 x 3.6 mm. This was procured from Internet Incorporated, Minneapolis, Minnesota, USA. The netting, product number ON-8360, is normally used in reinforcing paper, as for towelling.

The cages were constructed by sewing, with monofilament nylon, pre-cut octagonal end panels of the mesh to the long edges of a pre-cut rectangular panel, which formed the sidewall. The sidewall was closed by sewing with the same monofilament nylon.

3.4 Measurement Configuration

The cage was suspended approximately 6 m below the transducers, which were mounted on a weighty frame from which other gear was suspended. The cage itself was suspended between two lightweight square frames, 3 m on a side. Lines of monofilament nylon were attached to each of sixteen corners. The upper eight were attached to a superior frame, the lower eight to the inferior frame. An underwater television camera was suspended from the inferior frame, pointing upwards towards the cage. The entire rig was suspended by a single rope attached to the transducer frame and allowing raising and lowering by a winch attached to a gantry positioned over one of two identical 4 x 4 m square moon-pools on the raft. The normal operating depth of the transducers was 9 m.

3.5 Acoustic Equipment

It was desired to use the same kind of equipment for the measurements as is typically used during surveys. This was done with the SIMRAD EK-400 echosounder (Brede 1984a) normally used on board RRS *John Biscoe*. The echosounder was used in its dual 38 and 120 kHz modes together with UNIVERSAL SONAR transducers, each with nominal 10 deg beamwidth. Integration of the squared echo signals was performed with the SIMRAD QD digital echo integrator (Brede 1984b). Both echosounder and integrator were housed ashore, in the laboratory, together with other equipment. This included a BAS system for display and logging of data. The cable link was entirely satisfactory. Additional acoustic equipment consisted of three calibration spheres; 60 and 23 mm diameter copper spheres and a 38.1 mm diameter tungsten carbide sphere (Foote and MacLennan 1984).

3.6 Photographic Equipment

The principal photographic equipment that worked consisted of an underwater television camera and programmable videotape units for the display, recording and replay of the television images.

A stereoscopic camera system was also suspended with the television camera. However, for a variety of reasons and in spite of arduous if Sisyphean labours, the system provided few data and none on the particular acoustically measured krill.

4. METHODS

Measurements were made of encaged krill, empty cages, calibration spheres, and volume reverberation. Each series of measurements on a given object is referred to as an event.

4.1 Echosounder Operation

The acoustic measurements were generally made in the same way. Standard settings were used on the EK-400 echosounder. The time-varied-gain (TVG) function was the "20 log r" type. The pulse repetition frequency was a constant 50 pulses/min, with alternating transmissions at 38 and 120 kHz. The nominal pulse duration in the measurements considered here was 1.00 ms. Attenuator and gain settings were adjusted depending on the measurement object.

4.2 Echo Integration

Integration of the squared received voltage was performed over the full range interval corresponding to echoes from the cage. This was [6.0, 8.0] m for nearly all measurements. The exceptional cases with krill involved Event numbers 54 and 55, when the cage was lowered 1 m, for which the integration interval was [7.0, 9.0] m.

Results of echo integration were summed over intervals corresponding to either 0.2 or 1.0 nautical miles at a simulated vessel speed of 10 knots, hence for 1.2 or 6 min, respectively. The cumulative numbers were divided by the interval duration and presented as "mean volume backscattering strength" in decibels (Brede 1984b). These values, together with those from other integration intervals, were displayed on a screen and stored on a BAS data logger at the end of each interval.

4.3 Calibration

On-axis calibration with standard spheres was performed throughout the experiment as often as circumstances permitted. In the absence of the cage, the sphere was lowered to a position intended to be at the centre of the cage. The echosounder and integrator were then operated as during the cage measurement. Adjustments of the attenuator and gain settings during several calibrations established the relative accuracy of these.

To supplement the on-axis calibrations at cage depth, the spare tungsten carbide sphere was suspended at a fixed position below the transducers, but outside of the cage integration interval. This provided a ready means of monitoring the equipment performance.

4.4 Empty Cage and Volume Reverberation Measurements

Empty-cage measurements were also performed as circumstances allowed, but again covering the entire period of the krill measurements. Measurement of the water volume without cage, but with rig in place, established the general lowness of the volume reverberation. Continual monitoring with the underwater television camera confirmed the general absence of visible extraneous scatterers near the cage. The exceptions were provided by several occurrences of krill swarms in Stromness harbour, occasional occurrences of acoustically inevident ctenophores, and rare, brief visits by the odd Gentoo penguin or blue-eyed shag.

4.5 Beam-Pattern Mapping

The tungsten carbide sphere was also used to map the transducer beam patterns. The adopted procedure was that due to Simmonds (1984), although with a deliberately lesser degree of automation.

4.6 Krill Measurement

Measurement of krill began with their capture in a holding pen, by a small dip net, with c. 100 cm^2 opening, and transfer to a 100 litre tub half-filled with surface sea water. After reaching the predetermined number, more or less, the tub was ferried to the measurement raft. Here the krill were introduced into the cage, this having been raised to the surface the krill were syphoned in through a slit in the top panel. Handling of the krill was thus minimal, and their apparently vigorous condition was continually confirmed by television. Emptying of the cage proceeded through a slit in the bottom panel. Both slits were secured by threading monofilament nylon through reinforced meshes on the sides of the opening.

Upon completing an encaged-krill measurement series, the krill were transferred to the laboratory in a tub with sea water. On average, about half of the krill continued swimming vigorously, and nearly all showed signs of life, although the overall condition did vary considerably from event to event. Some of the krill were used in measurements of sound speed, as in Køgeler et al. (1987), but with recognition of the error in their equation, evidently copied from Equation (3.3) in Kristensen (1983). The salinity of the sea water was measured, and the temperature was monitored continually during the sound speed measurements. Measurements of total length of krill and wet weight were performed on the samples used for sound speed measurement and sometimes also on samples taken directly from the tub.

The total number of krill removed from the cage was also determined. This was generally less than the starting number by a few percent, presumably owing to cannibalism. In the worst case, Event number 36, the initial number was reduced by 7%, but over a 42-hour period. In another case, Event number 20, the number increased by two specimens, believed entrapped by the cage during intense swarming observed in the harbour.

A Plessey CTD-sonde was suspended at the nominal 15-m depth of the cage, but from the second moon-pool reserved for such measurements. When working, both salinity and temperature were recorded at 15-second intervals throughout the day. In addition, the light intensity at the same depth was recorded at 2-minute intervals.

5. DATA ANALYSIS

The first step in the analysis was to decide which data were usable. Whole events with encaged krill had to be purged for the following reasons: (1) early use of wrong integration limits, (2) distortion of the cage, with displacement from the usual position in the beam, due to entangling of the cage suspension lines, and (3) damage of the cage, with mass escape of krill, owing to a presumed collision or attack by a seal. Half the data from another event, number 28, had to be purged because of severing of the lifting rope to the underwater rig in heavy-swell conditions.

Data in the remaining events were purged very cautiously owing to these causes: (1) event start-up effects, always of short duration, (2) observed or presumed interference by extraneous scatterers such as fish, penguins, or krill swarms in the harbour attracted deliberately to the measurement raft by using underwater lights at night, (3) radio interference with the receivers during arrival of a yacht under motor power, and (4) trial use of different echosounder settings or transducer beamwidths. For some events no data were purged, and for no event was as much as 15% of the data purged, except for the fourth cause.

In order to extract target strengths or backscattering cross sections from the QD echo integrator data, the "mean volume backscattering strengths" had to be reduced. This entailed a number of analyses.

(1) Conversion factors. To express the echo integrator data as absolute quantities, the calibration data were reduced. Upon combining, the following factors were derived for adding to the logarithmic QD units: - 42.3 and -31.1 dB for the data at 38 and 120 kHz, respectively. The total range of variation of these factors was ±0.4 dB each.

(2) Time-varied-gain (TVG) corrections factors. Several errors were incurred by the use of TVG in the receiver. One is due to the rather short target range, 6-7 m, for which the pulse length, 1.47 m, is not negligibly small. The other error is due to the distributed nature of the cage and krill aggregation, which is to be compared to the compactness of the calibration sphere. The extent of the cage, and krill aggregation too if so dispersed, was 0.5 m vertically and slightly more aslant as viewed from the transducer. For the particular "20 log r" TVG used throughout the measurements, the resulting correction factors are - 0.4 dB for the cage at nominal 6 m range and 1.0 dB for the cage at nominal 7 m range. These figures apply at both frequencies. The estimated uncertainties of the correction factors, due to uncertainty in the precise target ranges, are ±0.2 and ±0.1 dB at the respective 6- and 7-m ranges.

(3) Beam pattern compensation factors. The transducer beams were nonuniform across the cage and unaligned with the cage axis. Each beam center was inferred from the respective beam-pattern-mapping data by a least-squares procedure based on comparison with the theoretical beam patterns. Integration of the squared beam pattern over the cage cross section and normalizing this to the solid angle formed by the cage results in the following compensation factors: 0.9 and 0.7 dB at 38 and 120 kHz, respectively, for the cage at nominal 6-m depth, and 0.7 and 0.6 dB for the cage at nominal 7-m depth. Estimated uncertainties due to uncertainty in both measured and computed beam patterns are ±0.1 dB.

Application of the three factors to the echo integrator data produces a series of numbers for the equivalent target strength of the krill and cage together. This is alternatively expressed through the backscattering cross section σ by the standard relation, $TS=10 \log \sigma/4$ (Urick 1975), but with use of SI units.

The cage contribution can be removed in two different ways. (1) Because of the availability of empty-cage measurements, these can be summarized, and the mean contribution can be subtracted in the appropriate intensity domain (Foote 1983). The effective cage target strengths in uncompensated QD units are -20.3 and -19.3 dB at 38 and 120 kHz, respectively, with respective uncertainties of ±1.2 and ±1.4 dB. Following subtraction, averaging yields the mean backscattering cross section per krill. (2) The effective cage contribution can also be inferred by regressing the equivalent backscattering cross section of cage and krill on the number of encaged krill. The intercept is then the cage contribution, and the slope or regression coefficient is the mean backscattering cross section of a single krill. Both methods of compensating for the cage contribution are used.

6. RESULTS

Some summary results of events with apparently usable krill data are presented in Table 1. The mean target strengths, denoted TS, are determined in the usual fashion. First, the mean backscattering cross section σ is computed; then the mean target strength is derived from the definition TS=10 log $\sigma/4$.

The mean krill target strength, denoted $TS_{1\ \mathrm{krill}}$ in Table 1, is determined by the first method of removing the cage contribution, viz. by subtracting the mean empty-cage contribution in the intensity domain. The missing datum, for Event number 54 at 120 kHz, reveals a flaw in the method if not in the data. Here the actual cage contribution must be less than the number assumed for it. Indeed, the echo strength of cage and krill together is less than the mean cage contribution.

Curiously, or not, the equivalent target strength at 38 kHz of cage and krill together for Event number 54 is greater than that for Event number 55, although the second has twice the number of krill of the first. Given the proximity of the events, their data are not used in the analyses reported in Table 2.

The results of averaging the corresponding single-krill backscattering cross sections in Table 1 is shown in the 'subtraction' row of Table 2. The coefficient of variation of σ is included together with the mean target strength. The additional quantities are defined thus: $TS_{1,2}$=10 log $(\sigma \pm \Delta\sigma)/4$.

The equivalent mean target strength of cage and krill together is denoted $TS_{\mathrm{cage+N\ krill}}$ in Table 1. Regression of the corresponding backscattering cross section on N allows derivation of σ for one krill through the regression coefficient. This is shown in the 'regression' row in Table 2. The coefficient of variation in this case is formed by expressing the standard error of the regression coefficient as a percentage of the regression coefficient, namely σ.

The analyses reported in Table 2 have been repeated for another subset of the data in Table 1. This excludes the data with rms lengths greater than 34.0 mm. The results are not significantly different from their antecedents. Specifically, TS decreases by 0.2 dB at each frequency for the 'subtraction' method, while remaining unchanged for the 'regression' method. The rms length for the two subsets are 33.2 and 31.6 mm, respectively.

7. DISCUSSION

If the reader is looking for a simpler answer to the problem of krill target strength than is contained in Table 2, then so are the authors. The discrepancy between the respective results is uncomfortably, if not discomfitingly, large.

It is to be admitted at once that the present analysis is incomplete for other data from the experiment have not yet been analysed. These include videotape recordings of the krill distribution across the cage, other notes on the behaviour and condition of the encaged krill, data on the light intensity at the cage depth, and measurements of longitudinal sound speed and density of krill removed from the cage.

The importance of behavioural data derives from the recognition of krill as a directional scatterer (Greenlaw 1977). As is the case with another directional scatterer, commercially important fish at ultrasonic frequencies (Nakken and Olsen 1977), systematic changes in tilt angle distribution can have dramatic effect of target strength (Foote 1980, 1987).

At the outset of the experiment it was the authors, firm intention to collect data on the tilt angle distribution of the encaged krill. However, the stereoscopic camera system failed utterly to provide any data bearing on the measured krill.

Clues to possible behavioural effects may be found in the video tape record. A quantitative image analysis by one of the authors (JLW) is underway.

The record of light intensity at cage depth may also elucidate a major determinant of behaviour, if applicable to encaged krill. This is pure speculation at the moment, but correlation with the quantified videotape data or, better, acoustic data themselves, may prove this.

Condition could also be a critical factor affecting or determining target strength. While the quality of encaged krill was often excellent, those krill caught at sea by trawling had a distinctly higher mortality than those caught beside the holding pen by dip net. Only active swimmers were introduced into the cage, but the change in condition over the duration of an event was often considerable.

This change in condition might be expected to affect the measurements in two ways. Firstly, the change in condition may have a behavioural consequence, as in changing the tilt angle distribution. Secondly, a changing condition may affect the physical properties of the animal, as is the case for fish (Gytre 1987). Since these are only slightly different from the respective properties of sea water under any circumstances, a small change in physical properties may have a very big effect of target strength (Greenlaw et al. 1980).

A direct approach to the problem of the influence of krill condition on target strength is to analyse the acoustic record for time variations both within events and from event to event. In the case of intra-event comparisons, this could proceed by averaging the acoustic data over intervals of, say, several hours. The problem would be to distinguish variations due to changing condition from those due to diurnal or other strong effects. This problem might be circumvented through the search for inter-event differences, as, for example, among different events that used krill with the same origin.

Some collateral, still unanalyzed data from the experiment that might shed light on the role of condition are those collected on density and sound speed. These data were planned for use in modelling work, but may serve a more immediate, interpretive function.

The same is true with respect to extinction. A regression analysis of the single-krill target strengths on cage density has been performed. The results are marginally significant at the 0.10-0.05 level, but not at 0.02. Thus the phenomenon of extinction may be noticeable in the data, but determination of the extinction cross section must be rather uncertain. One thing that is certain about extinction is that if it was present to a significant degree, then it will require raising the computed means shown in Table 2.

The mentioned analysis of extinction has been interesting for yielding quite large values for the extinction cross sections, compared to the mean backscattering cross sections, at both frequencies. This is not inconsistent with scattering theory. It may even be as revealing in its way as resonances are in other applications. Again, a fuller analysis should prove the point.

Some other outstanding work of concern to the authors involves describing the various dependences of krill target strength. This is allied with the modelling effort, but also requires more data on acoustic, behavioural, and physical properties. An especially regrettable shortcoming of the experiment is the absence of gravid krill. Controlled acoustic measurement of these in a future experiment is unavoidable for addressing the general survey situation.

8. CONCLUSION

Notwithstanding the noted discrepancies in Table 2 and also the large uncertainties in estimated mean target strengths, the general finding of this study is clear. The target strengths of krill at 38 and 120 kHz are quite low compared to earlier assumed values. Justification for this may be found in basic scattering theory: small euphausiids, even *E. superba*, with physical properties only slightly different from those of sea water, cannot possess target strengths even remotely comparable to those of swimbladder-bearing fish of similar size, which has been the implicit assumption until now.

ACKNOWLEDGEMENTS

Captain John Cole and fellow officers and crew of RRS Bransfield are thanked for logistic support. Captain Malcolm Phelps and fellow officers and crew of RRS John Biscoe are thanked for both logistics support and assistance during the krill-fishing cruises. William Graham is thanked for technical assistance on all electronic matters.

REFERENCES

Anon. 1986. Report on Post-SIBEX acoustic workshop. BIOMASS Rep. Ser., 40: 106 pp.

BLUE, J.E. 1984. Physical calibration. Rapp. P.-v. Reun. Cons. Int. Explor. Mer, 184: 19-24.

BREDE, R. 1984a. SIMRAD EK-400 scientific echosounder. FAO Fish. Circ., 778: 44-56.

BREDE, R. 1984b. SIMRAD QD integrator. FAO Fish. Circ., 778: 100-106.

EVERSON, I. 1977. The living resources of the Southern Ocean. FAO GLO/SO/77/1. 155 pp.

EVERSON, I. 1987. Krill target strength, current status. SC-CAMLR-VI/BG/9. 14 pp.

FOOTE, K.G. 1983. Effect of fish behaviour on echo energy: the need for measurements of orientation distributions. J. Cons. Int. Explor. Mer, 39: 193-201.

FOOTE, K.G. 1983. Linearity of fisheries acoustics, with addition theorems. J. Acoust. Soc. Am., 73: 1932-1940.

FOOTE, K.G. 1986. A critique of Goddard and Welsby's paper "The acoustic target strength of live fish". J. Cons. Int. Explor. Mer, 42: 212-220.

FOOTE, K.G. 1987. Target strength of polarized fish. ICES C.M. 1987/B: 4, 10 pp (mimeo).

FOOTE, K.G. and D.N. MACLENNAN. 1984. Comparison of copper and tungsten carbide calibration spheres. J. Acoust. Soc. Am., 75: 612-616.

FOOTE, K.G., H.P. KNUDSEN, G. VESTNES, D.N. MACLENNAN and E.J. SIMMONDS. 1987. Calibration of acoustic instruments for fish density estimation: a practical guide. ICES Coop. Res. Rep., 144: 69 pp.

FORBES, S.T. and O. NAKKEN. 1972. Manual of methods for fisheries resource survey and appraisal. Part 2. The use of acoustic instruments for fish detection and abundance estimation. FAO Man. Fish. Sci., 5: 1-138.

GREENLAW, C.F. 1977. Backscattering spectra of preserved zooplankton. J. Acoust. Soc. Am., 62: 44-52.

GREENLAW, C.F, R.K. JOHNSON and T. POMMERANZ. 1980. Volume scattering strength predictions for Antarctic krill (*Euphausia superba Dana*). Meeresforsch., 28: 48-55.

GYTRE, T. 1987. Ultrasonic methods for fish tissue characteristics. ICES C.M. 1987/C:14, 6 pp. (mimeo).

JOHANNESSON, K.A. and R.B. MITSON. 1983. Fisheries acoustics. A practical manual for aquatic biomass estimation. FAO Fish. Tech. Pap, 240: 1-249.

KRISTENSEN, A. 1983. Acoustic classification of zooplankton. Thesis. The Norwegian Institute of Technology. 107 pp.

KØEGLER, J.W., S. FALK-PETERSEN, A. KRISTENSEN, F. PATTERSEN and J. DALEN. 1987. Polar Biol., 7: 231-235.

LAWS, R.M. 1985. The ecology of the Southern Ocean. Am. Sci., 73: 26-40.

NAKAYAMA, K., K. SHIRAKIHARA and Y. KOMAKI. 1986. Target strength of krill *in situ* at the frequency of 200 kHz. Mem. Natl. Inst. Polar Res., Spec. Issue 40: 153-161.

NAKKEN, O. and K. OLSEN. 1977. Target strength measurements of fish. Rapp. P.-v. Reun. Cons. int. Explor. Mer, 170: 52-69.

PROTASCHUK, V.A. and T.A. LUKASHOVA. 1982. Determination of Antarctic krill acoustic backscattering cross section. Paper no. 66. Symposium on Fisheries Acoustics, Bergen, Norway.

ROBINSON, B.J. 1984. Calibration of equipment. Subject group C. Rapp. P.-v. Reun. Cons. Int. Explor. Mer, 184: 62-67.

SIMMONDS, E.J. 1984. A comparison between measured and theoretical equivalent beam angles for seven similar transducers. J. Sound Vib., 97: 117-128.

STANTON, T.K. 1988a. Sound scattering by cylinders of finite length. I. Fluid cylinders. J. Acoust. Soc. Am., 83: 55-63.

STANTON, T.K. 1988b. Simple approximate formulas for backscattering of sound by spherical and elongated objects. J. acoust. Soc. Am. (In press).

URICK, R.J. 1975. Principles of underwater sound. Second edition. McGraw-Hill, New York. 384 pp.

Table 1: Summary of krill target strengths by event. The respective sample size is denoted N_s. Each acoustic sample is the result of averaging over a 6-min interval at the effective PRF of 25 pulses/min.

			Krill lengths (mm)				TS (dB) at 38 kHz			TS (dB) at 120 kHz		
Event no.	Duration	Mean no. krill N	$l^{2^{1/2}}$	$\bar{l}$	Δl	n_s	$TS_{1\ krill}$	$TS_{cage+Nkrill}$	n_s	$TS_{1\ krill}$	$TS_{cage+Nkrill}$	n_s
17	16h46m	496	39.2	38.9	4.4	458	-84.1	-55.9	159	-75.9	-46.5	159
19	15h22m	246	31.5	31.3	3.4	100	-82.6	-57.1	132	-74.5	-47.3	132
20	23h16m	351	33.7	33.3	4.8	100	-82.8	-56.1	206	-76.2	-47.4	206
26	23h 1m	752	30.5	30.4	2.4	300	-87.8	-57.3	202	-77.3	-46.2	202
28	38h38m	390	29.7	29.6	2.2	100	-83.6	-56.4	189	-74.6	-46.3	189
30	40h13m	458	34.9	34.8	3.2	200	-85.1	-56.9	376	-74.8	-46.0	376
36	42h31m	1368	31.6	31.5	3.0	500	-85.5	-53.5	424	-75.6	-43.2	424
37	18h13m	787	30.8	30.7	3.2	200	-88.0	-57.3	180	-76.5	-45.7	180
43	37h 3m	398	33.0	32.9	2.8	200	-87.6	-58.8	164	-77.0	-47.5	358
47	64h41m	1593	32.5	32.3	2.9	397	-89.1	-55.9	318	-79.7	-45.7	298
50	42h36m	850	31.1	31.0	2.7	200	-86.6	-56.1	232	-78.0	-46.3	411
52	65h 5m	816	38.1	37.9	3.8	200	-84.2	-54.3	632	-75.4	-44.8	632
54	62h44m	394	31.2	31.0	3.7	200	-86.9	-58.4	619	-	-50.2	619
55	46h 7m	794	31.0	30.8	3.3	200	-88.3	-58.7	459	-80.7	-48.6	461

Table 2: Summary results for each of two methods of removing the empty-cage contribution based on the data in Table 1 exclusive of those for Event numbers 54 and 55.

	38 kHz					120 kHz				
Method	$\bar{\sigma}(mm^2)$	cv(%)	$\overline{TS}$	TS_1	TS^2	$\bar{\sigma}(mm^2)$	cv(%)	$\overline{TS}$	TS_1	TS^2
Subtraction	0.039	47	-85.1	-87.9	-83.4	0.311	31	-76.1	-77.7	-74.9
Regression	0.015	46	-89.4	-92.1	-87.7	0.173	33	-78.6	-80.3	-77.4

Légendes des tableaux

Tableau 1	Résumé des réponses acoustiques du krill par cas. La taille de l'échantillon respectif est dénotée N_s. Chaque échantillon acoustique est le résultat d'une prise de moyenne pour un intervalle de 6 minutes à une fréquence effective de répétition de 25 pulsations/minute.
Tableau 2	Résultats résumés de chacune des deux méthodes pour ôter la contribution de la cage vide, basés sur les données figurant au Tableau 1, à l'exclusion de celles sur les cas numérotés 54 et 55.

Заголовки к таблицам

Таблица 1	Сводка данных отдельных замеров акустической силы цели криля. Соответственный объем пробы отмечен N_s. Каждая акустическая проба является результатом усреднения по 6-минтервалу при действующей частоте повторения импульсов (PRF), которая составляет 25 импульсов/мин.
Таблица 2	Сводка результатов для каждого из двух методов внесения поправки на пустой садок, основанных на данных таблицы 1, за исключением замеров 54 и 55.

Encabezamientos de las Tablas

Tabla 1	Resumen de las fuerzas de blanco del krill en cada caso. El tamaño de la muestra respectiva está indicada N_s. Cada muestra acústica es el resultado de promediar sobre un intervalo de 6 minutos al efectuivo PRF de 25 pulsos/min.
Tabla 2	Resumen de los resultados para cada uno de los dos m´todos de retirar la contribución de la jaula-vacia basada en los datos de la Tabla 1, excepto los datos para el Caso, números 54 y 55.

PATTERNS AND PROCESSES IN THE DISTRIBUTION AND DYNAMICS OF ANTARCTIC KRILL

S.A. Levin, A. Morin and T.M. Powell

Abstract

A general framework is presented to develop, test and integrate component models of the distribution and dynamics of Antarctic krill population at various spatial and temporal scales. We suggest that models of increasing complexity be developed iteratively for variability and patchiness of krill abundance. Incremental models should then be compared to statistical descriptions of the observed distribution patterns at various scales of observation to ascertain the plausibility of the model and identify critical processes to be added. An analysis of spatial distribution of krill in the Bransfield Strait area reveals that purely physical models of turbulent redistribution are not sufficient to explain krill distribution at small scales. We therefore propose to develop a modified diffusion-reaction model incorporating spatially variable growth rates of krill, krill loss rates due to predators, and density-dependent attraction of krill to account for the small-scale aggregations.

Résumé

Une structure générale est présentée afin de développer, de tester et d'intégrer des modèles constitutifs de la répartition et de la dynamique de la population du krill antarctique à différentes échelles spatiales et temporelles. Nous suggérons que soient développés d'une manière itérative des modèles de complexité croissante portant sur la variabilité et la répartition irrégulière de l'abondance du krill. Des modèles incrémentiels devraient ensuite être comparés aux descriptions statistiques des formes de répartition observées à différentes échelles d'observation afin de déterminer la plausibilité du modèle et d'identifier les processus critiques à ajouter. Une analyse de la répartition spatiale du krill dans la région du détroit de Bransfield montre que des modèles purement physiques de redistribution turbulente ne suffisent pas à expliquer la répartition du krill à de petites échelles. Nous proposons donc de développer un modèle modifié de diffusion-réaction incorporant les taux de croissance du krill variables sur le plan spatial, les taux de perte de krill due aux prédateurs, et l'attraction du krill en fonction de la densité pour expliquer les concentrations sur une petite échelle.

Резюме

Представлена общая схема разработки, опробования и интеграции однокомпонентных моделей распределения и динамики популяции антарктического криля по различным пространственным и временным масштабам. Мы предлагаем, чтобы возрастающей сложности модели многообразия и неравномерности распространения криля разрабатывались итеративно, появляющиеся вновь модели должны затем сравниваться со статическим описанием наблюдавшихся картин распределения по различным масштабам, по которым проводились наблюдения, чтобы оценить степень достоверности модели и выявить ключевые процессы, требующие включения в модель. Анализ пространственного распределения криля в районе пролива Брансфилда показал, что чисто физической модели турбулентного перераспределения криля недостаточно для объяснения мелкомасштабного распределения криля. В связи с этим для того,чтобы объяснить существование небольших агрегаций криля, мы предлагаем разработать диффузно-реактивную модель, включающую также и пространственные переменные - такие, как темпы роста криля, смертность криля, зависящая от хищников, и взаимное привлечение криля, обусловленное плотностью скопления.

Resumen

Se presenta una estructura general a fin de desarrollar, analizar e integrar los modelos componentes de la distribución y dinámica de la población de krill antártico a distintas escalas espaciales y temporales. Se sugiere la elaboración de modelos de creciente complejidad en forma iterativa para la variabilidad y discontinuidad de la abundancia de krill. Se deberá comparar luego los modelos de incremento con las descripciones estadísticas de los patrones de distribución obtenidos a distintas escalas de observación para establecer la plausibilidad del modelo e identificar los procesos críticos que deban agregarse. Un ánalisis de la distribución espacial de krill en el área del estrecho de Bransfield revela que los modelos puramente físicos de redistribución turbulenta no son suficientes para explicar la distribución del krill a pequeñas escalas. Por consiguiente se propone desarrollar un modelo modificado de reacción-difusión que incorpore los índices de crecimiento del krill de variación espacial, los índices de pérdidas del krill a causa de predadores, la atracción de krill dependiente de la densidad para explicar el porqué de las concentraciones a pequeña escala.

1. INTRODUCTION

Among the important questions being addressed in scientific studies of living marine resources in the Antarctic are:

1. How important are physical processes, such as the movement of fronts and sea-surface contiguous zones, in determining the distribution and dynamics of krill and fin fish?
2. How important are biological factors such as predation and food availability?
3. What is the interaction between spatial patterns and fishing behavior?
4. How can theoretical approaches to stock assessment and prediction facilitate the estimation of the size of the resource, and aid in the development of optimal harvesting strategies?

In the Antarctic ecosystems, as in other complex ecosystems, physical and biological factors interact to produce patterns of multiple spatial and temporal scales. The initial steps in the development of a quantitative theory of the Antarctic must involve an examination of those scales (Denman and Powell, 1984; Levin, 1988). Spectral analysis and other statistical approaches allow comparison of observed distributions of physical factors, primary producers, and consumers; mechanistic investigations provide complementary information on natural time and space scales for biological and physical processes underlying patterns.

In the equatorial mid-Pacific, over the 2-50 km spatial scales, the range for which the best data are available for comparison with the Antarctic ecosystem, estimation of fractal dimensions of phytoplankton patches suggests that physical factors are the primary determinants of spatial pattern (Slice et al., 1988). Of course, it is quite a leap from the equatorial ocean to the Antarctic, but spectral analyses of data from the Southern Ocean lead to the same conclusion. We turn in the next section to an examination of the evidence. The implications are substantial, since if the proposition is accepted, it means that primary productivity can be modelled as, to a first approximation, a reflection of physical conditions.

2. DISTRIBUTION OF TEMPERATURE AND FLUORESCENCE

In various data sets taken from different regions of the Antarctic, the concordance between physical factors (temperature) and primary productivity (fluorescence) is excellent on intermediate and broader scales. Figure 1, reprinted from Weber et al. (1986), demonstrates the similarity of slopes in the spectral distributions of temperature and fluorescence in the Southern Ocean in austral summer 1981; the middle panels in Figure 2 indicate strong coherence in the distributions. Weber et al. (1986) believe that the slightly steeper slope of the fluorescence spectrum, plus the strong coherence between fluorescence and krill (Figure 2), is evidence that grazing is a factor in the small-scale distribution of phytoplankton. We are not convinced, and in any case, regard physical factors as providing an adequate explanation of the fluorescence spectrum at least on intermediate scales (4-20 km). It is unfortunate that we do not yet have available comparable data for the Elephant Island-Bransfield Strait region. We hope to be able to obtain such data to strengthen our interpretation of krill distributions, reported in the next section.

Our conclusion is that, to a first approximation, it is reasonable to regard phytoplankton abundance as determined by physical processes. Of course, this is based entirely on correlations; nonetheless, it is our null hypothesis. In our modelling approach, this assumption will represent our baseline model. In later versions of the model, grazing will be allowed to modify the basic distribution.

3. PRELIMINARY DATA ANALYSIS OF KRILL SPATIAL DISTRIBUTION

Quantitative descriptions of krill spatial distribution are necessary for two purposes. The first is that the patterns revealed by those descriptions allow the formulation of the simplest models that can reproduce these properties. The second reason is that the descriptions of real spatial distributions will serve as standards to which to compare the output of the candidate models.

The most useful analyses to date are those of Weber et al. (1986) discussed in the previous section and shown in Figures. 1 and 2, for the spatial distributions of temperature, fluorescence, and krill biomass in the Antarctic Ocean south of Africa. The power spectra for temperature and fluorescence, shown in Figure 1 and discussed in the last section, differ markedly from that reported for krill biomass. The variance of fluorescence and temperature declines with increasing wavenumber (decreasing wavelength). The slope of the relationship between the log variance and the log wavenumber approaches previously reported values for these quantities (Powell et al., 1975; Mackas, 1977; Steele and Henderson, 1977; Lekan and Wilson, 1978; Platt and Denman, 1980); these slopes were close to the -5/3 prediction of Kolmogorov (1941) for the inertial subrange of turbulence. In contrast, the krill power spectrum was almost flat, indicating an approximately equal variance at all scales.

The description of Weber et al. (1986) implies that different mechanisms control temperature and fluorescence spatial distributions on the one hand, and krill distribution on the other. As suggested in the previous section, purely physical models may be sufficient to explain fluorescence spatial distribution (at least in the 2-20 km length scales of the Weber et al. study). However, such a model could not reproduce the krill spectral estimates; additional mechanisms must be invoked.

If the description of Weber et al. (1986) were to hold for the Elephant Island-Bransfield Strait region, it could serve as the basis for a preliminary model of that region. The submodel for primary productivity of algal biomass distribution would be primarily physical. The close correspondence of the spectral estimates for temperature and fluorescence suggests that grazing by herbivores has a minimal effect on algal spatial distribution. In contrast, a purely physical model for krill would be inappropriate since it could not produce the relatively high variability at small scales (high wavenumber). Although krill distribution undoubtedly is influenced by physical processes (such as advection and turbulence), other factors (presumably involving krill behavior) must be responsible for the high heterogeneity at small scales. Thus, a krill submodel would have to include additional mechanisms acting predominantly at small scales.

The first step of this analysis was to examine, through spectral analysis, the krill biomass distribution in the vicinity of King George Island and then to compare the resulting power spectrum to the description of Weber et al. (1986) to determine whether the same type of spectrum can describe the krill distribution patterns in different areas.

Acoustic data (provided by M.C. Macaulay), obtained 4-5 January 1987, aboard the RV *Professor Siedlecki*, were analyzed in the following way. The data tapes contained continuous reading of estimated average krill biomass (g m^{-3}; 200 kHz estimates) at each meter of depth (range: 3-185 m) at a horizontal resolution of approximately 200 m for eight transects (Figure 3). Vertical profiles were summed to obtain an areal estimate of krill biomass (g m^{-2}). The resulting traces were then subdivided into 16 series of 64 data points to be analyzed by spectral analysis. The power at each frequency for the 16 transects then was summed, and normalized to the total power of the signal to obtain a normalized power spectrum (Figure 4).

To facilitate comparison with the power spectrum of Weber et al. (1986), we also analyzed the data by first averaging areal biomass into 1 km bins, and subdividing the resulting series into traces of 20 data points. The power estimates then were treated as above to obtain an average power spectrum spanning the same scales as Weber et al. (Figure 5).

The resulting spectra (Figures. 4-5) were closely similar to the published spectra for krill, but much less steep than that which commonly has been observed for fluorescence, salinity and temperature. There is a relatively high variability of krill biomass at small scales that apparently cannot be explained by physical processes alone.

A second descriptor of spatial distribution, the semivariogram (see for example, Mackas, 1984), also was computed from the same data (Figure 6). The results indicate that the variability in krill biomass between pairs of data points is only a weak function of the linear distance between those points. The semivariance of log biomass does not vary significantly over most distances between points except for the smallest distances. This suggests that patch size (swarm size) is smaller than 200 m, the finest resolution of those data.

A third, simple descriptor, the *frequency distribution* of biomass, was computed for the same data set (Figure 7). The resulting frequency distribution is biomodal and appears to be the mixture of two lognormal distributions. About two-thirds of the observations (67%) can be attributed to the first lognormal distribution (mean $\log_{10}$ (biomass) = 0.18, SD = 0.49), and one-third to a second lognormal distribution (mean = 1.76, SD = 0.51). These two distributions may correspond to the between- and within-patch biomass (mean biomass between patches = 2.8 g m^{-2}, apparent mean biomass within patches = 115 g m^{-2}). Note that the biomass within swarms may be substantially higher since it appears that most swarms have a diameter smaller than 200 m, and that the observed biomass is an average for a 200 m trace.

4. COMPARISON OF DATA WITH THE PHENOMENOLOGICAL MODEL PREDICTIONS OF MANGEL

As an example of how we intend to use these descriptions to evaluate the plausibility and adequacy of our models, we have reconstructed the "patch within patch" model of Mangel (1987) with minor modification to account for the low "background" biomass of krill. This model assumes that individual krill aggregate in swarms in surface densities of the order of 300 g/m^2, over a surface spatial extent on the order of 100 m. Swarms of krill are further aggregated into concentrations or patches over a large spatial extent of the order of 10 nautical miles (=20 km). A concentration with a length scale of 15 nautical miles is assumed to have 8000 swarms of krill, randomly placed within the concentration.

Transect data, similar to those analyzed above, were then extracted from the simulated krill spatial distribution, and the three descriptors calculated for 100 sets of 16 transects of 64 points. The results are presented in Figure 8. Not surprisingly, the resulting frequency distribution (Figure 8a) is similar to the one observed for the real data. The semivariogram (Figure 8b) also is both qualitatively and quantitatively similar to the one obtained from real data. The power spectrum of simulated data (Figure 8c) also approximates the one observed for the real data, though it does not mimic the apparent curvature of Figure 4, especially at small scales. Overall, the simple model of Mangel appears to reproduce excellently the patterns observed with real krill biomass data. Of course, this model is phenomenological rather than mechanistic; it is useful as a descriptor of observed patterns, and for evaluating the success of different fishing and sampling strategies. It does not provide a means of relating patterns to underlying processes.

Obviously, a larger set of real data needs to be analyzed not only to produce more precise descriptions, but also to test whether the power spectra, semivariograms, and/or frequency distributions vary in a systematic fashion among the various subareas of the general Bransfield Strait-Elephant Island area. The same descriptors have to be obtained from the other relevant parameters of the integrated model: temperature, salinity, algal biomass, and density of krill predators.

5. DEVELOPMENT OF A PROCESS-BASED MODEL

Statistical analyses, such as those reported in the previous section, are a start, but are limited as devices for prediction. Without some understanding of mechanisms, we have no idea why correlations hold, or when they will fail (e.g., Lehman, 1986). Therefore, we seek to go beyond such statistical analyses, developing mechanistic explanations of observed patterns.

Our basic approach is built upon modification of classical diffusion reaction models. However, that basic approach must be modified in a number of ways to take into account what is known about mechanisms. Thus, we alter the diffusion-reaction model so that:

1. Krill growth rates are spatially variable functions of phytoplankton availability;

2. Krill loss rates are functions of predator abundance;

3. On broad scales, the assumption of diffusion is replaced by the inertial subrange of turbulence;

4. On smaller scales, the assumption of diffusion is replaced for krill by models for aggregation, such as Kawasaki's (1978) model for long-range density-dependent attraction (see Morin et al., 1989).

6. MODEL IMPLEMENTATION

The integrated spatial and temporal model outlined in the previous section relies on a large number of parameters that presently are unknown. The present data base does not suffice to formulate the model in a more quantitative form. Although the final model may require estimates of most of the parameters, we suggest using an iterative approach in the development of working models.

In the first approximation, we still will assume that the physics determines the distribution and abundance of algae, and that krill distribution depends on algal availability. We further assume that krill consume an insignificant fraction of algal biomass, and that predators have a negligible effect on detailed versions of the model. For the first approximation, the driving forces thus will be found in the hydrographic data. The output of such a model will be compared to real data, both by looking at the large-scale distribution of krill obtained by the acoustic surveys and at the three spatial distribution descriptors (power spectra, semivariogram, frequency distribution), for temperature (or salinity), algal biomass, and krill. Discrepancies between the observed and simulated patterns will indicate the major inadequacies of this simplistic model. It already is apparent that such a model will not reproduce krill distribution adequately, although it is less clear whether it will mimic its temporal variability.

The next (and improved) versions of the model will depend on the results of the first iteration. The second iteration will incorporate the krill aggregation model of Kawasaki and Okubo, and more detailed functions for the encounter rates. Subsequent iterations will include the grazing effect of predation by invertebrates, fish, and marine mammals.

REFERENCES

DENMAN, K.L. and T.M. POWELL. 1984. Effects of physical processes on planktonic ecosystems in the coastal ocean. Oceanography and Marine Biology Annual Review 22: 125-168.

KAWASAKI, K. 1978. Diffusion and the formation of spatial distribution. Mathematical Science 183: 47-52.

KOLMOGOROV, A. 1941. The local structure of turbulence in incompressible viscous fluid for very large Reynolds' numbers. Comptes rendus de l'academie des sciences de l'URSS 32: 16-18.

LEHMAN, J.T. 1986. The goal of understanding in limnology. Limnology and Oceanography 31: 1160-1166.

LEKAN, J.F. and R.E. WILSON. 1978. Spatial variability of phytoplankton biomass in the surface water of Long Island. Estuarine and Coastal Marine Science 6: 239-250.

LEVIN, Simon A. 1989. Physical and Biological Scales, and the Modeling of Predator-prey Interactions in Large Marine Ecosystems. In: SHERMAN, Kenneth and L.M. ALEXANDER(Eds.). Patterns, Processes, and Yields of Large Marine Ecosystems. American Association for the Advancement of Science Selected Symposium. (In press). Chapter 17.

MACKAS, D.L. 1977. Horizontal spatial variability and covariability of marine phytoplankton and zooplankton. PhD dissertation. Dalhousie University, 220 pp.

MACKAS, D.L. 1984. Spatial autocorrelation of plankton community composition in a continental shelf ecosystem. Limnology and Oceanography 29: 451-471.

MANGEL, M. 1987. Simulation of southern ocean krill fisheries. SC-CAMLR-VII/BG/22, Report for Commission for the Conservation of Antarctic Marine Living Resources (CCAMLR), 13 October. 86 pp.

MORIN, Antoine, Akira OKUBO and Kohkichi KAWASAKI. 1988. Acoustic data analysis and models of krill spatial distribution. Background paper for Annual Meeting of Commission for the Conservation of Antarctic Marine Living Resources (CCAMLR), October, Hobart, Tasmania, Australia.

PLATT, T. and K.L. DENMAN. 1980. Patchiness in phytoplankton distribution. In: MORRIS, I. (Ed.). The Physiological Ecology of Phytoplankton. Oxford: Blackwell. pp. 413-431.

POWELL, T.M., P.J. RICHERSON, T.M. DILLON, B.A. AGEE, B.J. DOZIER, D.A. GODDEN, and L.O. MYRUP. 1975. Spatial scales of current speed and phytoplankton biomass fluctuations in Lake Tahoe. Science 189: 1088-1090.

SLICE, D., A. OKUBO, and G. FELDMAN. 1988. Scale-dependent structure of open-ocean plankton patch boundaries. Submitted.

STEELE, J.H. and E.W. HENDERSON. 1977. Plankton patches in the northern North Sea. In: STEELE, J.H. (Ed.). Fisheries Mathematics. New York: Academic Press. pp. 1-19.

WEBER, L.H., S.Z. EL-SAYED, and I. HAMPTON. 1986. The variance spectra of phytoplankton, krill and water temperature in the Antarctic Ocean south of Africa. Deep-Sea Research *33* (10): 1327-1343.

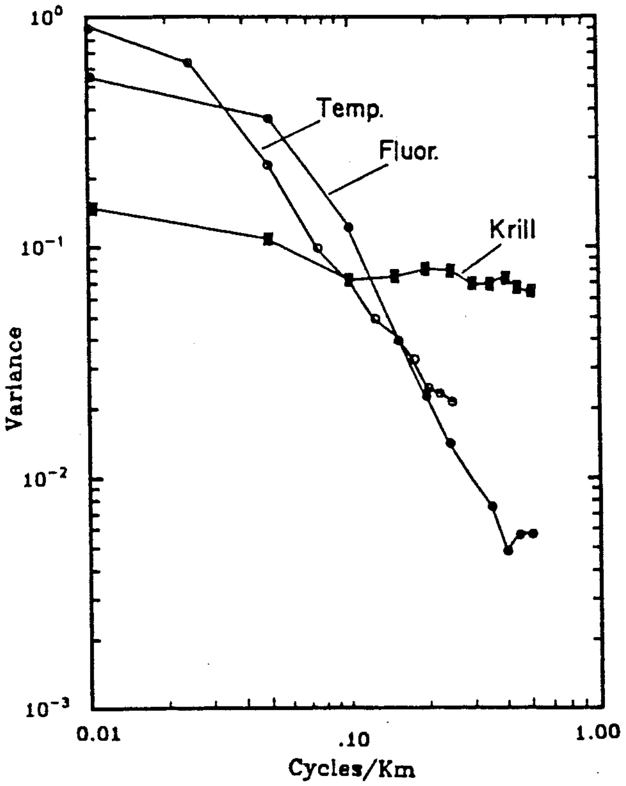

Figure 1: Mean spectral plots for krill, *in vivo* fluorescence, and temperature. (From Weber et al., 1986).

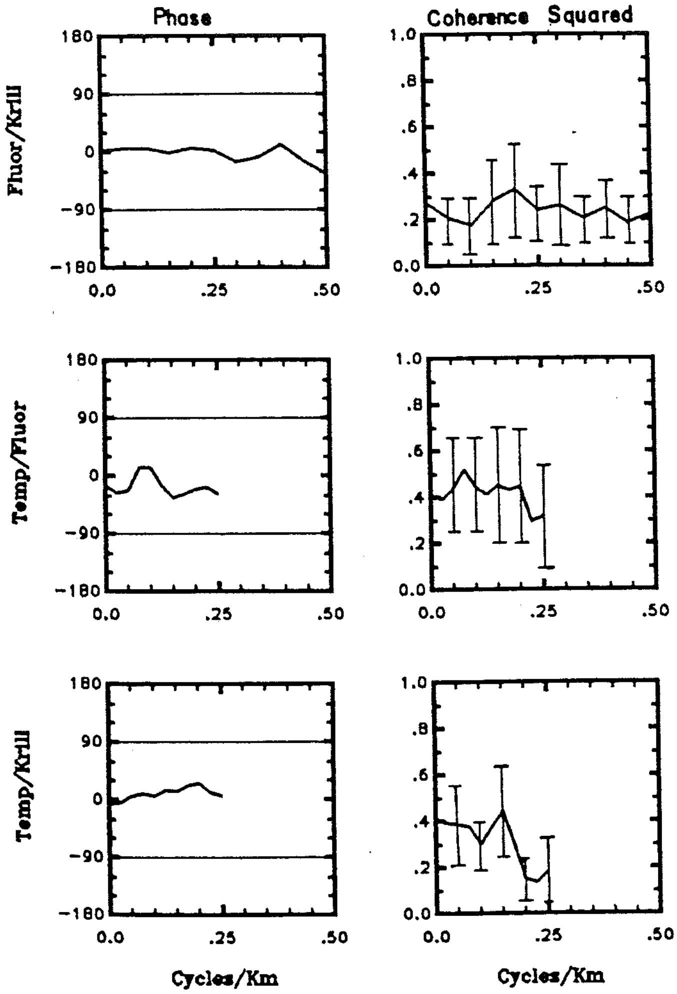

Figure 2: Mean phase and squared coherence spectra for fluorescence-krill, temperature-fluorescence, and temperature-krill. Vertical bars indicate the 95% confidence limits about the mean coherence squared estimates ($\bar{y} \pm (2.2)\ (S.D./\sqrt{12})$). For clarity, confidence limits for temp-fluor and temp-krill are only shown at every other computed frequency. (From Weber et al., 1986).

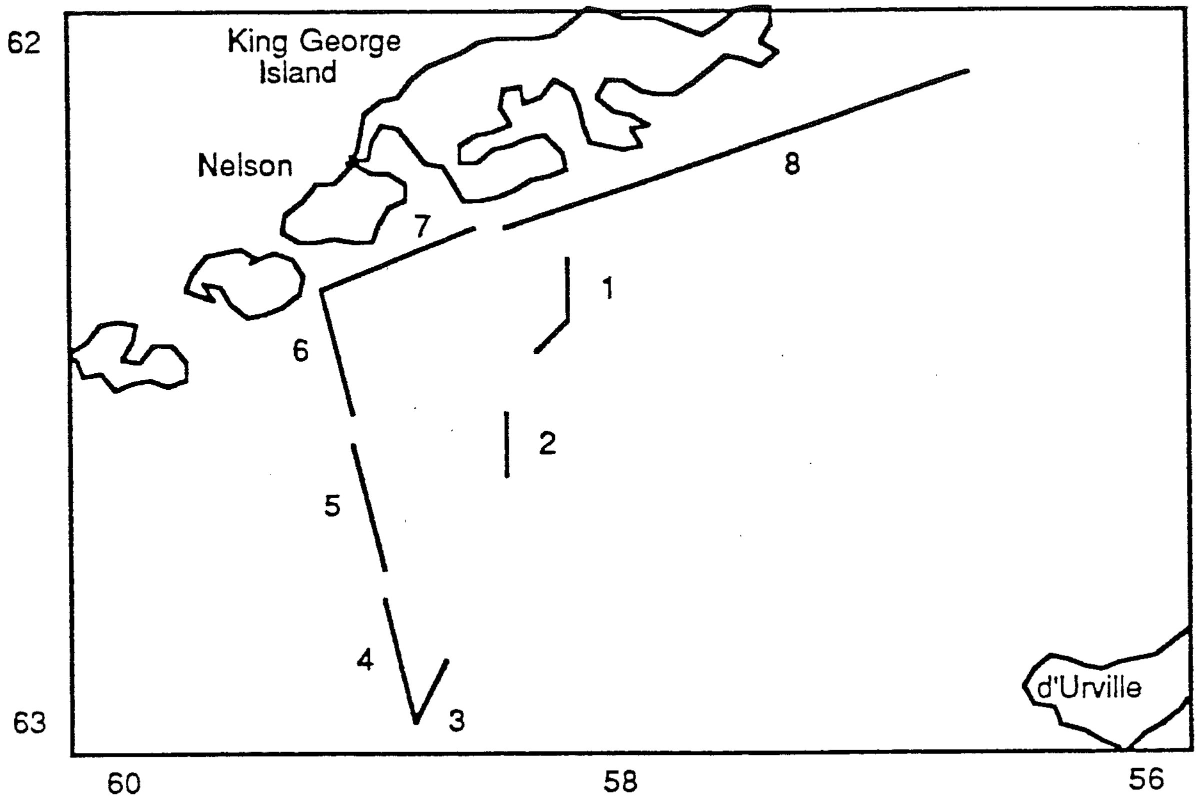

Figure 3: Location of the transects used in the preliminary data analysis. 4-5 January 1987.

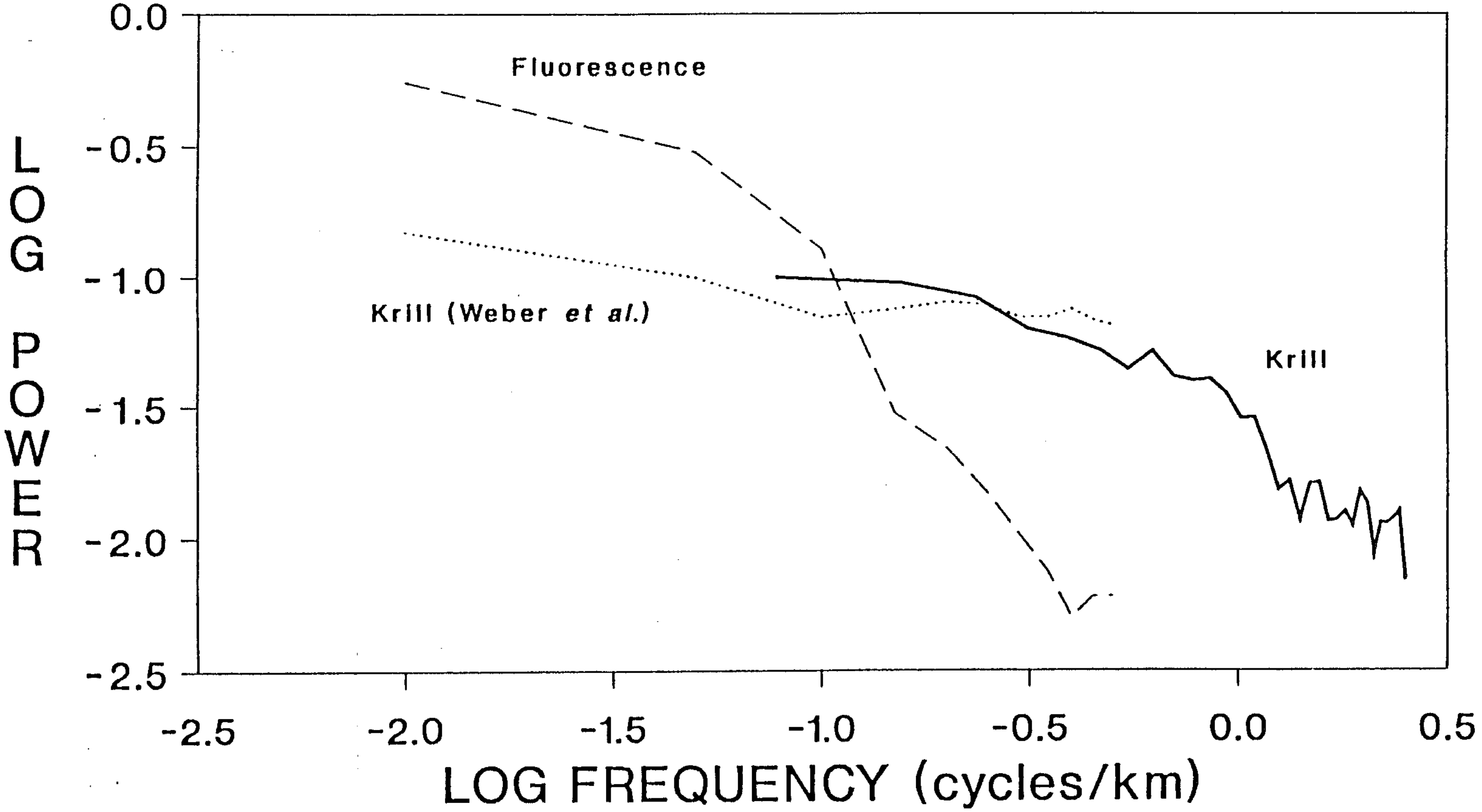

Figure 4: Normalized power spectra of Weber et al. (1986) for fluorescence and krill, compared to the observed spectra for the krill acoustic data.

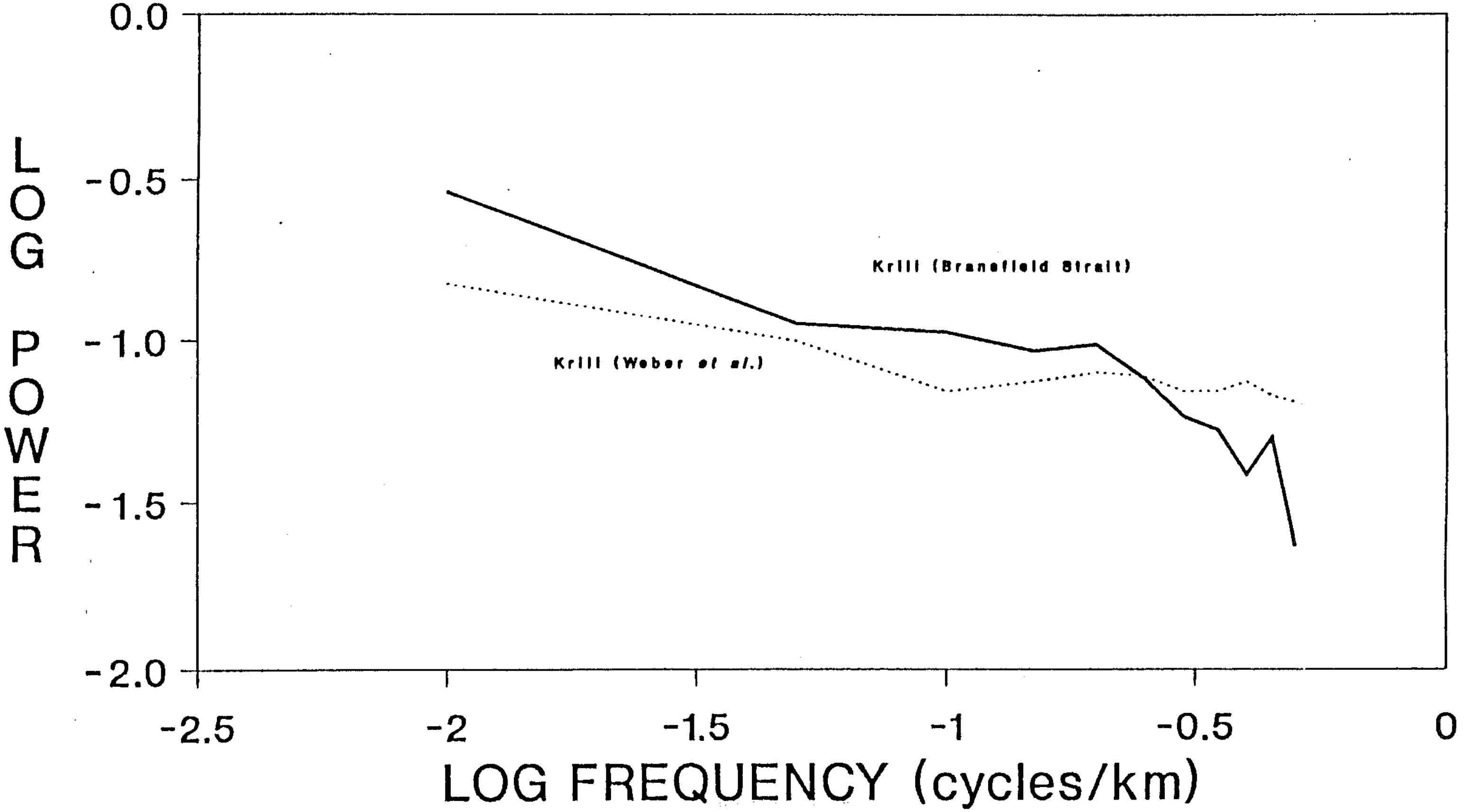

Figure 5: Power spectra for krill at the 2-20 km scale observed in this analysis and by Weber et al. (1986). Krill biomass was averaged over 1 km.

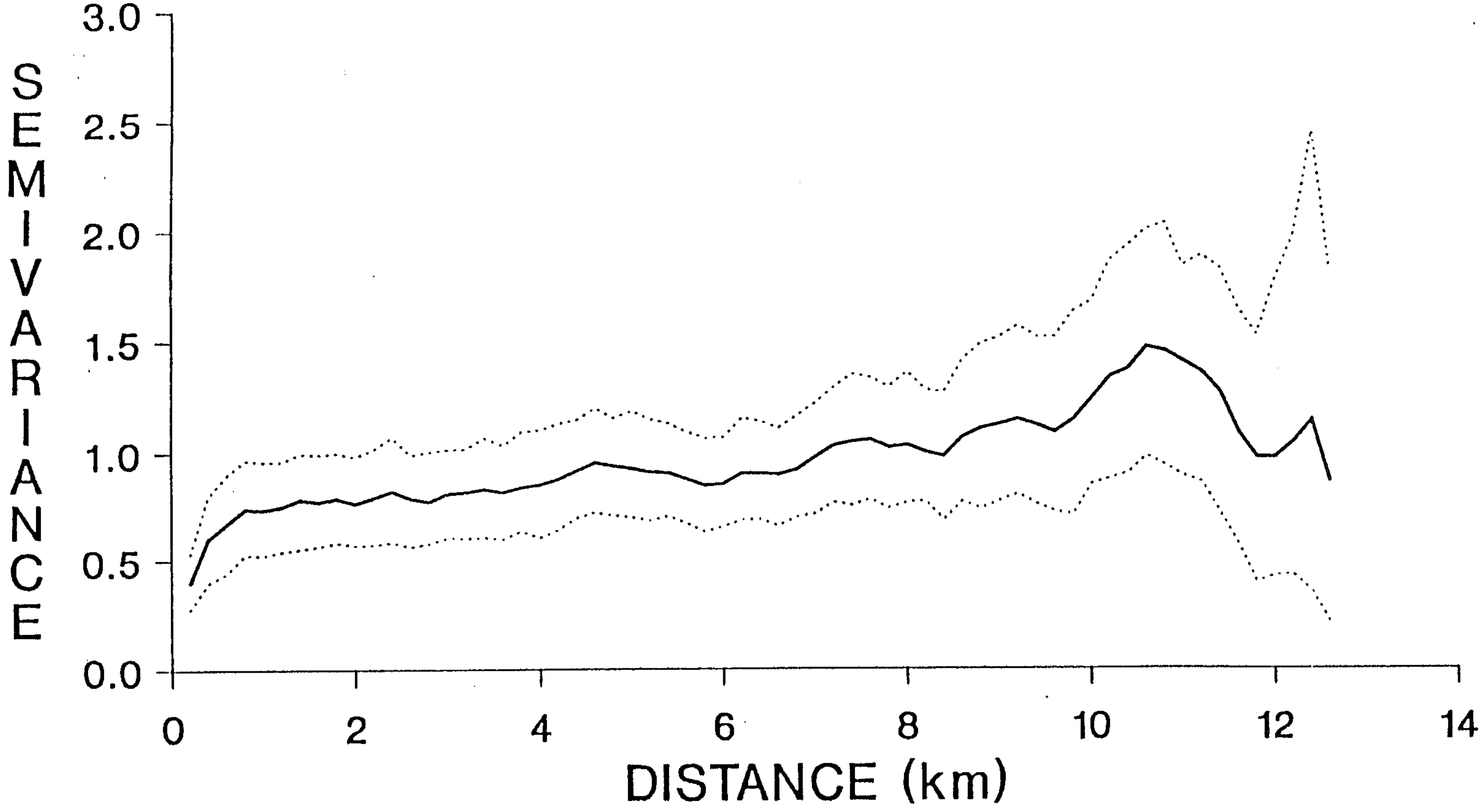

Figure 6: Semivariogram of $\log_{10}$ krill biomass (g/m^{-2}) with bootstrap 95% confidence intervals for the Bransfield Strait data (4-5 January 1987).

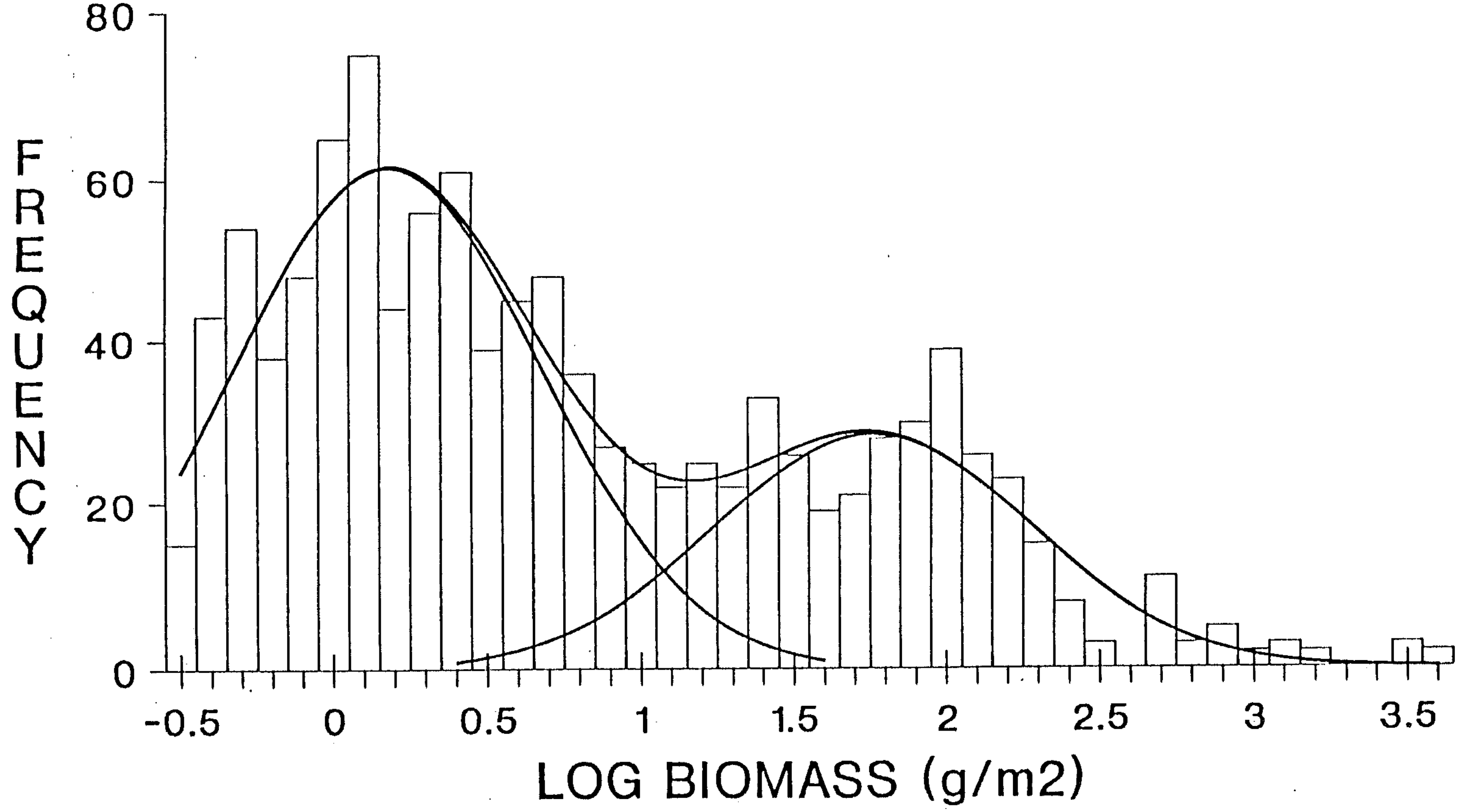

Figure 7: Frequency distribution of $\log_{10}$ biomass estimates (g/m^{-2}) for the Bransfield Strait data (4-5 January 1987).

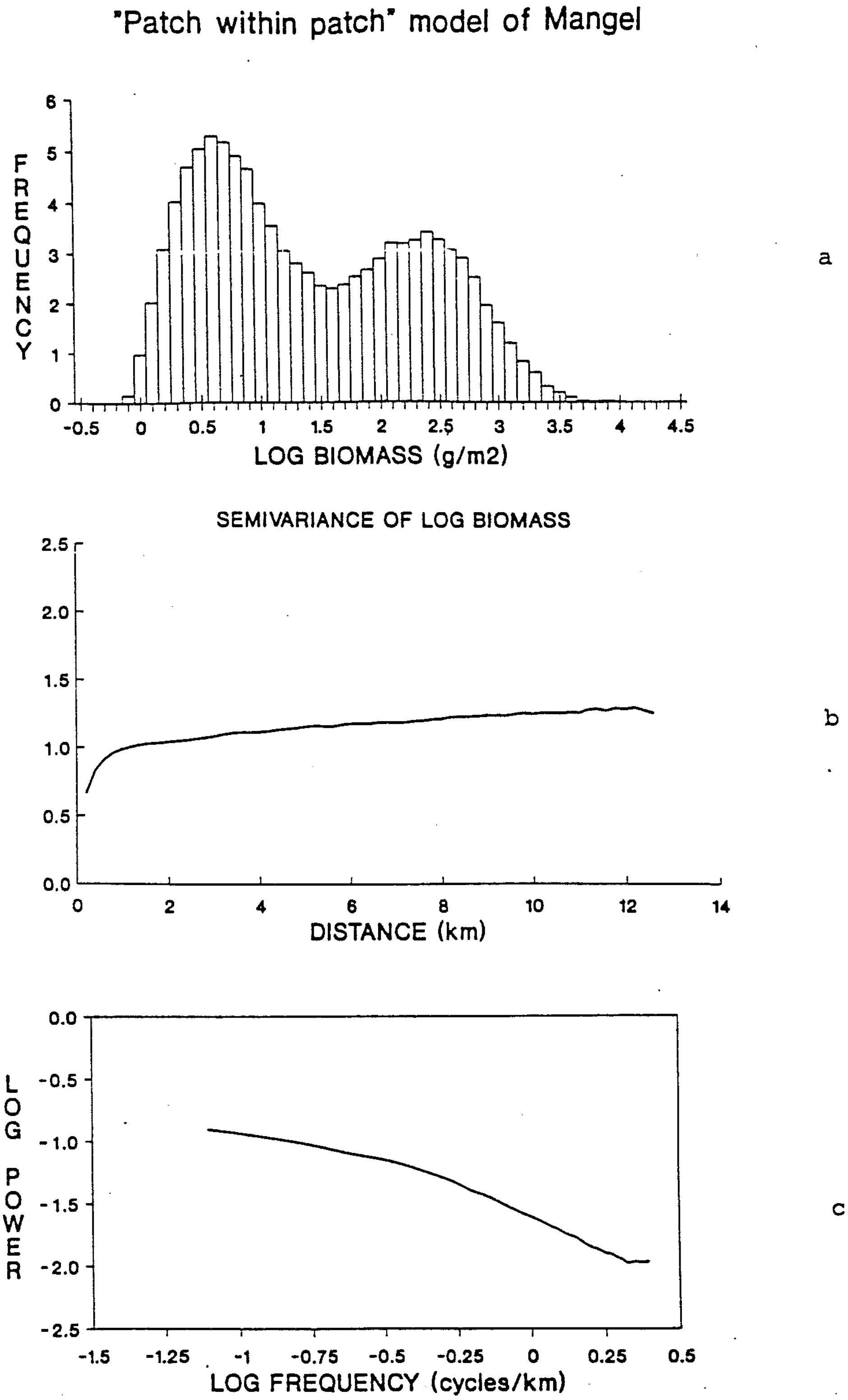

Figure 8: Frequency distribution (a), semivariogram (b), and power spectrum (c) of simulated data using the "patch within patch" model of Mangel (1987).

Légendes des figures

Figure 1	Corrélations spectrales moyennes du krill, de la fluorescence *in vivo*, et de la température. (De Weber et al., 1986).
Figure 2	Spectres de phase transversale moyenne et cohérence carrée de fluorescence-krill, température-fluorescence, et température-krill. Les barres verticales indiquent les limites de fiabilité de 95% en ce qui concerne les calculs carrés de cohérence moyenne $(\bar{y} \pm (2.2)\ (S.D.\sqrt{12}))$. Afin d'être clair, les limites de fiabilité de température-fluor et de température-krill ne sont montrés qu'à une fréquence calculée sur deux. (De Weber et al., 1986).
Figure 3	Emplacement des transects utilisés pour les analyses de données préliminaires. 4-5 janvier 1987.
Figure 4	Spectres normalisés d'intensité de Weber et al. (1986) pour la fluorescence et le krill, et spectres observés des données acoustiques sur le krill analysées.
Figure 5	Spectres d'intensité du krill sur une échelle de 2-20 km observée dans cette analyse et par Weber et al. La moyenne de la biomasse du krill a été prise sur 1 km.
Figure 6	Semivariogramme de la biomasse du krill $\log_{10}$ (g/m^2) avec une zone d'intervalles de confiance de 95% pour les données recueillies dans le détroit de Bransfield (4-5 janvier 1987).
Figure 7	Distribution de fréquences d'estimations $\log_{10}$ de la biomasse (g/m^2) pour les données recueillies dans le détroit de Bransfield (4-5 janvier 1987).
Figure 8	Distribution de fréquences (a), semivariogramme (b), et spectre d'intensité (c) de données simulées utilisant le modèle de "regroupements à l'intérieur de regroupements" de Mangel (1987).

Подписи к рисункам

Рисунок 1	Спектральные графики средних величин для криля, *in vivo* флуоресценции и температуры (по Веберу и др., 1986 г.).
Рисунок 2	Спектры средней кросс-фазовой и квадратичной когерентности для соотношений флуоресценция-криль, температура-флуоресценция, и температура-криль. Вертикальные полосы указывают на доверительные пределы, касающиеся оценок средней квадратичной когерентности $(\bar{y} \pm (2.2)\ (S.D.\sqrt{12}))$. Для ясности, доверительные пределы для соотношений температура-флуоресценция и температура-криль указываются только на каждой второй вычисленной частоте. (по Веберу и др., 1986 г.).
Рисунок 3	Расположение гидрографических разрезов, использованных при анализе предварительных данных. 4-5 января 1987 г.

Рисунок 4 Нормализованная спектральная мощность частотного распределения для флуоресценции и криля, по Веберу и др. (1986 г.), и полученные путем наблюдения спектры для проанализированных акустических данных по крилю.

Рисунок 5 Полученная (Вебером и др.) путем наблюдения в этом анализе спектральная мощность частотного распределения для криля по шкале 2-20 км. Биомасса криля была усреднена по километровому квадрату.

Рисунок 6 Семивариограмма с логарифмической шкалой (log$_{10}$) биомассы криля (г/м^2) с зоной доверительного интервала (95%) для данных по проливу Брансфилда (4-5 января 1987 г.).

Рисунок 7 Распределение частоты с логарифмической шкалой (log$_{10}$) оценок биомассы (г/м^2) для данных по проливу Брансфилда (4-5января 1987 г.).

Рисунок 8 Распределение частоты (a), семивариограмма (b), и спектральная мощность частотного распределения (c) смоделированных данных при использовании модели Мангела "пятна в пределах пятен" (1987 г.).

Leyenda de la Figura

Figura 1 Curvas espectrales promedio para el krill, fluorescencia *in vivo* y temperatura. (Weber et al., 1986).

Figura 2 Frase-cruzada promedio y espectro de coherencia cuadrada para el krill-fluorescencia, fluorescencia-temperatura, y krill-temperatura. Las barras verticales indican los límites de confianza del 95% de las estimaciones promedio de la coherenica cuadrada $(\bar{y} \pm (2.2) \quad (S.D.\sqrt{12}))$. Para mayor claridad, los límites de confianza para el flúor-temperatura y krill-temperatura se indican solamente en las frecuencias computadas alternas. (Weber et el., 1986).

Figura 3 Localización de los transectos utilizados en los análisis de los datos preliminares. 4-5 enero de 1987.

Figura 4 Densidad espectral normalizada de Weber et al. (1986) para fluorescencia y krill, y espectro observado para los datos acústicos analizados del krill.

Figura 5 Densidad espectral para el krill en la escala de 2-20 km observada en este análisis y por Weber et al. La biomasa del krill fue calculada por término medio sobre 1 km.

Figura 6 Semivariograma del log$_{10}$ de la biomasa del krill (g/m^2) con zonas de intervalos de confianza del 95% para los datos del estrecho de Bransfield (4-5 de enero de 1987).

Figura 7 Distribución de la frecuencia del log$_{10}$ de estimaciones de la biomasa (g/m^2) para los datos del estrecho de Bransfield (4-5 de enero de 1987).

Figura 8 Distribución de la frecuencia (a), semivariogram (b), y densidad espectral (c) de los datos simulados usando el modelo de Mangel “mancha dentro de mancha” (1987).

SC-CAMLR-VII/BG/22

STATISTICAL PROBLEMS IN KRILL STOCK HYDROACOUSTIC ASSESSMENTS

M.C. Macaulay

Abstract

Two primary issues are at question for hydroacoustic assessments of krill. The first is the methods applied to establish biomass in a survey area and the second is the improvement in accuracy of target-strength measurements. In the case of statistical methods, there are no clear guidelines for deciding what method is most appropriate, this is made even more difficult by the fact that most survey methods assume the population is fixed in space, relative to the sampling interval. There remain several unsatisfied needs for improvements in sampling design and tests for systematic trends in survey data collected from non-stationary populations, which have not been well addressed by present techniques. However, this does not invalidate the use of available methods to conduct surveys and analyze results. In the case of target-strength accuracy, even if the present values were very accurate, the issue of interest would seem to be not the absolute amount of biomass present in an area, but rather how it is distributed. The issue of patchy years vs more even distribution would seem to have more impact on ecosystem management than absolute accuracy of biomass estimates.

Résumé

Deux questions fondamentales se posent à l'égard des évaluations hydroacoustiques du krill. La première concerne celle des méthodes utilisées pour établir la biomasse d'une zone d'étude et la seconde est celle de l'amélioration de la précision des mesures de la réponse acoustique. Dans le cas des méthodes statistiques, il n'existe aucune directive qui permettrait de choisir sans hésitation le procédé le mieux adapté, et le problème est d'autant plus difficile à résoudre que la plupart des méthodes de recherche présument que la population est fixe sur le plan spatial, en rapport avec l'intervalle d'échantillonnage. Il reste encore beaucoup à faire pour répondre aux besoins d'amélioration des types d'échantillonnage et des tests portant sur les tendances systématiques dans les données d'étude recueillies à partir de populations non-stationnaires, questions auxquelles les techniques actuelles ne sont pas suffisamment intéressées. Cependant, ceci n'exclut pas l'utilisation des méthodes disponibles de recherche et d'analyse des résultats. Pour ce qui est de la précision concernant la réponse acoustique, l'intérêt semble se trouver non pas dans la quantité absolue de biomasse présente dans une région, mais plutôt dans la manière dont elle est répartie, et cela même si les valeurs actuelles étaient très précises. La question des années de répartition irrégulière contre répartition plus régulière semblerait avoir un effet plus important sur la gestion de l'écosystème que la précision absolue des évaluations de la biomasse.

Резюме

Рассматриваются два основных аспекта проведения оценки запасов криля гидроакустическими методами: первый - методы, применяемые для оценки биомассы в районе съемки, и второй - повышение точности при измерении силы цели. В случае статистических методов не имеется четких правил для выбора наиболее подходящего метода, и дело осложняется еще и тем, что при применении большинства методов съемки популяция принимается неподвижной в течение всего времени взятия проб. Все еще требуют усовершенствования некоторые аспекты взятия проб и выявления систематических отклонений от данных, полученных по нестационарным популяциям, чего современными способами на достаточно хорошем уровне сделать нельзя. Но это никак не обесценивает применения имеющихся методов при проведении съемок и анализировании результатов. В вопросе о точности величины силы цели, даже если имеющиеся значения были очень точны, интерес, как кажется, представляла бы не абсолютная величина имеющейся в каком-либо районе биомассы, а скорее то, как она распределена. Представляется, что результаты сравнения данных за годы с очень неравномерным распределением с картиной более равномерного распределения могли бы в вопросе управления экосистемой представить большую ценность, чем абсолютно точные оценки величины биомассы.

Resumen

Se cuestionan dos problemas fundamentales de las evaluaciones hidroacústicas del krill. El primero son los métodos que se aplican para establecer la biomasa de una zona de prospección, y el segundo es el perfeccionamiento de la precisión de medición de la fuerza de blanco. En lo que se refiere a los métodos estadísticos, no existen pautas claras para decidir qué método es el más apropiado, lo cual es otro problema, ya que la mayoría de métodos de prospección suponen que la población se encuentra fija en el espacio con relación al intervalo del muestreo. Quedan todavía varios requisitos no satisfechos en cuanto a mejoras en el diseño de muestreo y en los análisis de tendencias sistemáticas de datos de prospección recolectados sobre poblaciones no estacionarias, todo lo cual no ha sido tratado satisfactoriamente por las técnicas actuales. Sin embargo, esto no invalida el uso de los métodos existentes en la realización de prospecciones y análisis de resultados. En el caso de la precisión de la fuerza de blanco, aún cuando los valores actuales fueran muy precisos, el punto de interés no sería la biomasa absoluta presente en una zona, sino más bien su distribución. El tema de los años de distribución más regular, parece tener más incidencia en la administración del ecosistema que la precisión absoluta de las estimaciones de biomasa.

1. INTRODUCTION

Distribution and abundance estimates for midwater zooplankton and nekton are often obtained using quantitative hydroacoustic methods. The usual method employed is echo integration, producing estimates of abundance by depth and distance along a survey track. These relative estimates of abundance are then converted to absolute estimates of abundance using the target strength of the identified target organisms. Target strength is a measure of how much sound an organism reflects, expressed in terms of the amount of sound reflected per individual or per unit weight of organism. All other electronic and acoustic variables are taken into account in the relative estimate of abundance so that if the target strength employed is later refined or revised, these acoustic estimates may be corrected by adjusting the estimate by the ratio of the old and new target strengths.

Surveys are conducted along pre-determined tracklines of parallel or zigzag pattern which cover the area of interest in a systematic manner. For repeated surveys, the pattern of transects may be refined to better fit the expected distribution of populations, but in all cases, the limiting factor is shiptime to conduct the survey. This constraint usually imposes some compromises on the nature and spacing of the trackline pattern and this may be in conflict with optimum distribution of effort for statistical sampling methods.

Zooplankton and nekton populations are seldom, if ever, random in their distribution with respect to the sampling effort. Thus the use of the random sample mean and random sample variance will often provide a biased estimate of the mean and variance of the population. Because of the high sampling frequency of a hydroacoustic survey (one sample per second), there sometimes is a lack of independence between samples due to overlapping of sampling volume and consequently an expectation of serial correlation or some degree of covariance contributing to the bias. Williamson (1982) addresses the process of accounting for this serial correlation by treating individual clusters of observations (usually an entire transect) as independent and the variance is therefore a function of the number of clusters and the total number of observations. Other authors have used the ratio estimation methods of Cochran (1977) to partition the variance by transect but this method assumes there is no serial correlation or other covariance.

At present, there are no clear guidelines for deciding what method is most appropriate, this is made even more difficult by the fact that most survey methods assume the population is fixed in space, relative to the sampling interval. In fact, this is seldom the case in an aquatic environment. True planktonic organisms may be carried through the sampled area, either in a systematic way due to abiotic factors (e.g. currents and eddies) or biotic ones due to migratory behaviour. Micronekton and nekton (especially large zooplankton and fish) may swim fast enough in a single day to traverse from one transect to another and hence be sampled multiple times. Given the fact that large surveys often take two weeks or more, this migratory behaviour needs to be considered.

In some senses, the collective actions of individuals of a species may produce a combined distribution for a population or subpopulation which makes the aggregation behave as one large patch with variable discontinuities within some definable boundary. These large aggregations may require separate treatment, i.e. separate stratification of sampling, to minimize the variance estimate. Large aggregations of this kind have been observed in the Antarctic (Macaulay, 1984) for krill (*Euphausia superba*) and may be true for segments of fish populations as well. A krill aggregation observed in 1981 covered an area 3 km by 5-6 km and extended from the surface to 250 m (Figure 1a).

2. GENERAL STATUS AND NEEDS

The first issue is that of large statistical variances. Hydroacoustic surveys are often characterized by large to very large confidence intervals. These large variances result from the highly discontinuous distribution of many marine stocks (the patchiness problem) often caused by the contagious distribution of the negative binomial or Poisson type models where mean and variance are proportional or equal. Some degree of post-survey stratification can be used to minimise this effect but more objective methods for such stratification would help to make the confidence in the results of such stratification greater. The tendency to consider many zooplankton as weak swimmers needs to be more carefully analyzed and verified. The problem of a mobile population moving within the survey area still remains and may not be addressable or even known without special surveys designed to examine an area multiple times from different starting points and possibly even different sampling strategies. However, awareness of the problem can at least prompt consideration of prevailing currents (abiotic factors) or known migratory behaviour (biotic factors) in the development of a sampling plan. There remain several unsatisfied needs for improvements in sampling design and tests for systematic trends in survey data collected from non-stationary populations, which have not been well addressed by present techniques. However, this does not invalidate the use of available methods to conduct surveys and analyze results.

The second issue is the improvement of estimates of target-strength for krill. Given that present values are probably within a factor of 2 of being correct, it seems reasonable to consider the following. Even if the present values were very accurate, the issue of interest would seem to be not the absolute amount of biomass present in an area, but rather how it is distributed. Consider as a test case that we have two surveys in two consecutive years giving identical biomass for a surveyed area, in one, the biomass is nearly uniform with only a few small patches and in the other, the biomass is concentrated in some areas and low to absent in others. If a predator (e.g. a penguin) must obtain not only its own daily ration but also sufficient extra to return to feed its offspring, the time spent searching becomes critical. If such an individual encounters a patch (a patch dominated year) it can quickly obtain sufficient food for its needs. If, however, it must spend a great deal of time picking up isolated individuals, it may have to spend too much time just satisfying its own requirements to have sufficient for its offspring too. Figure 1 shows an example of this with abundant patches near Seal Island in 1981 and much lower abundance of patches in 1984. The shaded area is approximately 20 n miles from Seal Island (the estimated foraging range of a penguin, personal communication John Bengtson). The point is that if we can begin to isolate the causes of patchiness and/or areas more typically possessing patches of krill, the implications for ecosystem management of the resource will be more important than just improving our accuracy.

3. CONCLUSIONS

Improvement of the accuracy of target-strength estimates and measurements can and will continue to increase the accuracy of our biomass estimates by the consequences of not surveying and especially not maintaining a temporarily coherent data set will be a longer delay in our understanding of the ecosystem. I would, therefore, recommend that surveys be conducted by those currently involved in such efforts and where possible, other interested parties contribute to this effort. Further delays in obtaining the needed data due to deficiencies in current methods would be counterproductive to the goals of CCAMLR. The time-series information cannot be obtained by any other means and, so long as data are collected and archived in detail, it may be possible to correct for inadequacies in methods at a later date including correcting for errors in target-strength.

EFERENCES CITED

COCHRAN, W.G. 1977. Sampling Techniques, 3rd Ed., John Wiley & Sons, N.Y. 428 p.

MACAULAY, M.C., T.S. ENGLISH and O.A. MATHISEN. 1984. Acoustic characterization of swarms of Antarctic krill (*Euphausia superba*) from Elephant Island and Bransfield Strait. Journ. of Crust. Biology, 4: 16-44.

WILLIAMSON, N.J. 1982. Cluster sampling estimation of the variance of abundance estimates derived from quantitative echosounder surveys. Can Journ. Fish. Aquatic. Sciences, 39(1) 229-231 p.

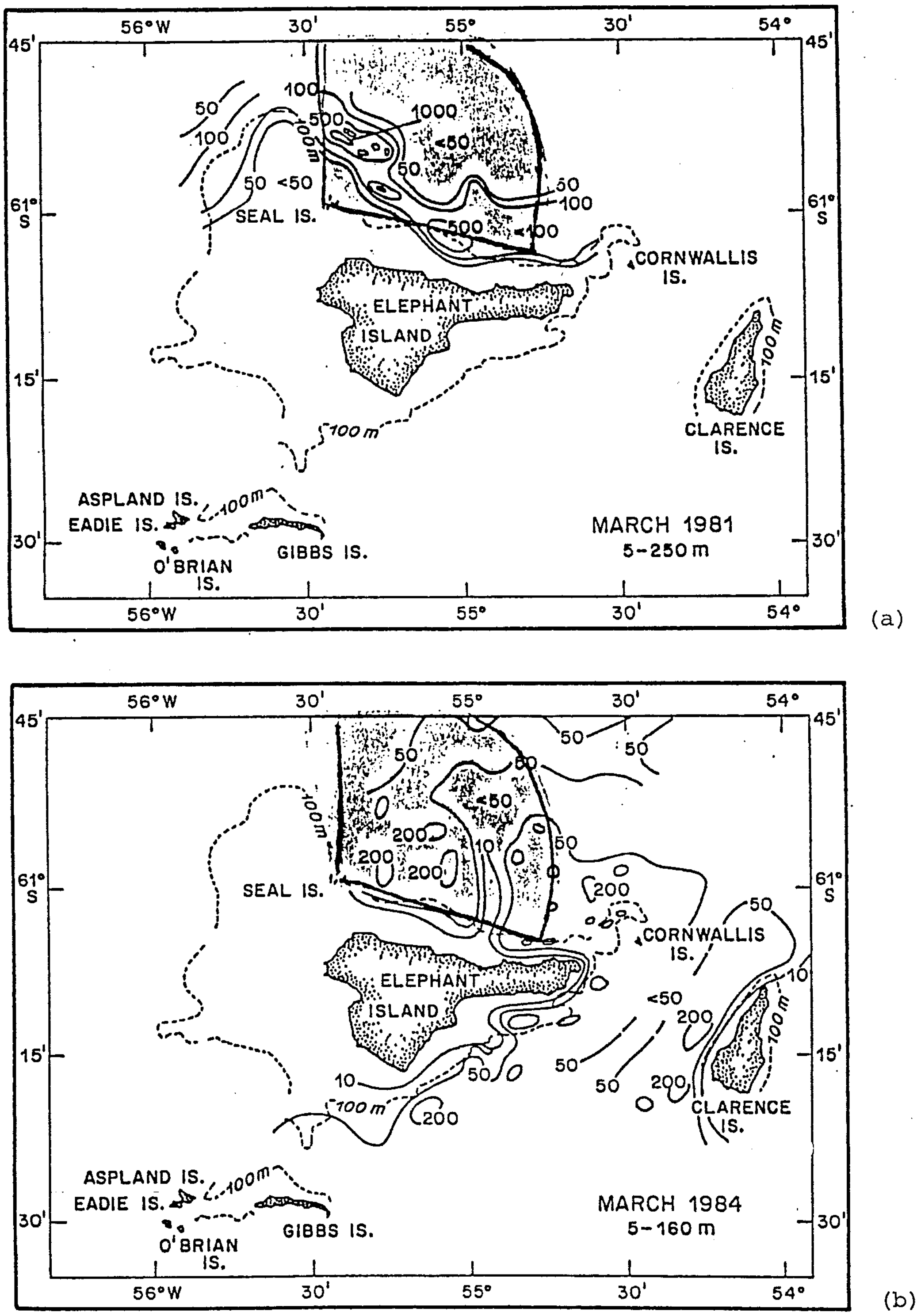

Figure 1: Distribution of krill in the vicinity of Elephant Island in March 1981 (a) and March 1984 (b). The shaded area is approximately 20 n miles from Seal Island, a known penguin rookery. The large swarm observed in 1981 contained over 1 million tonnes of krill. The contour intervals are in kg/m².

Légende de la figure

Figure 1

Distribution du krill aux abords de l'île de l'Eléphant en mars 1981 (a) et mars 1984 (b). La zone hachurée est située à environ 20 milles n de l'île des Phoques, une colonie de manchots reconnue. L'essaim étendu observé en 1981 contenait plus d'un million de tonnes de krill. L'équidistance des courbes est en kg/m^2.

Подписи к рисункам

Рисунок 1

Распределение криля в районе о. Элефант в марте 1981 г. (a) и марте 1984 г. (b). Затушеванный участок на карте находится примерно на растоянии 20 морских миль от о. Сил, известной залежки пингвинов. Большое скопление, наблюдавшееся в 1981 г., насчитывало свыше 1 миллиона тонн криля. Растояние между контурами выражено в кг/м^2.

Leyenda de la Figura

Figura 1

Distribución del krill en los alrededores de la isla Elefante en marzo 1981 (a) y marzo 1984 (b). Las zonas oscuras están aproximadamente a 20 millas náuticas de la isla Seal, una conocida colonia de pingüinos. El extenso cardumen observado en 1981 contenía más de 1 millón de toneladas de krill. Los intervalos contorneados de densidad de krill se expresan en kg/m^2.

SC-CAMLR-VII/BG/25

ACOUSTIC DATA ANALYSIS AND MODELS OF KRILL SPATIAL DISTRIBUTION

A. Morin, A. Okubo and K. Kawasaki

Abstract

Acoustic data obtained on 4-5 January 1987 aboard the R/V *Professor Siedlecki* were used in three descriptors of krill spatial aggregation: power spectra for krill biomass fluctuations in space, semivariogram (spatial autocorrelation of krill biomass) and the frequency distribution of krill biomass estimate. The wavenumber spectrum resembles a white noise at scales of 2-20 km, although at scales smaller than 1 km the spectrum appears to lose its power significantly. The semivariance of biomass does not vary significantly over most distances between points except for the distances smaller than 1 km. The computed frequency distribution of krill biomass is bimodal and appears to be the mixture of two lognormal distributions. These two distributions may correspond to the between and within patch biomass. These results of data analysis suggest that krill patch size or rather a basic swarm size should be smaller than 200 m, finest resolution of our data analyzed, and the real spatial distribution of krill should be the manifestation of the balance between the dispersion of the basic swarm units and long-range density-dependent attraction of the units. Simple dynamical and kinematical models can interpret the observed result.

Résumé

Les données acoustiques recueillies les 4 et 5 janvier 1987 à bord du navire de recherche *Professor Siedlecki* ont été utilisées dans trois descripteurs de répartition spatiale du krill: spectre d'intensité pour les fluctuations de la biomasse du krill dans l'espace, semivariogramme (autocorrélation spatiale de la biomasse du krill) et distribution de fréquences de la biomasse estimée de krill. Le spectre à ondes ressemble à un son blanc aux échelles de 2 à 20 km, mais aux échelles inférieures à 1 km, le spectre semble diminuer considérablement en intensité. La semivariance de la biomasse ne varie pas de manière significative pour la plupart des distances entre les points, sauf pour les distances inférieures à 1 km. La distribution calculée des fréquences de la biomasse du krill est bimodale et semble consister en un mélange de deux distributions logarithmiques normales. Ces deux distributions pourraient correspondre à la biomasse à l'intérieur d'un regroupement, d'une part, et entre les regroupements, d'autre part. Ces résultats de l'analyse des données suggèrent que la taille d'un regroupement de krill, ou plutôt la taille de base d'un banc, devrait être inférieure à 200 m, résolution la plus précise de nos données analysées, et que la répartition spatiale réelle du krill devrait être la manifestation de l'équilibre entre la dispersion des unités de base des bancs et l'attraction des unités à longue portée et dépendant de la densité. Des modèles dynamiques et cinématiques simples peuvent interpréter le résultat observé.

Резюме

Акустические данные, полученные R/V *Professor Siedlecki* 4-5 января 1987 г., использованы в трех типах описания пространственной агрегации криля: спектральной функции пространственных флуктуаций биомассы криля, графике полумногообразия (пространственной автокорреляции биомассы криля) и частотном распределении оценочных величин биомассы криля. В диапазоне 2-20 км спектр волновых чисел напоминает белый шум, хотя в диапазоне меньше 1 км в спектре наблюдается значительная потеря энергии. Полумногообразие массы существенно не меняется при почти любых расстояниях между точками, за исключением расстояний меньше 1 км. Вычисленное частотное распределение биомассы криля оказывается бимодальным и, видимо, является смесью двух типов логнормального распределения. Эти два типа распределения могут соответствовать биомассе между пятнами и биомассе внутри пятна. Полученные результаты анализа данных заставляют предположить, что размер пятна криля, или вернее размер типичного скопления криля должен быть меньше 200 м, - что является пределом разрешающей способности при получении подвергнутых нами анализу данных, и что реальное пространственное распределение криля должно отразить имеющийся баланс между дисперсией типичных скоплений и взаимным привлечением отдельных элементов скопления с большого расстояния, - в зависимости от плотности скопления. Полученные результаты можно интерпретировать с помощью простых динамических и кинематических моделей.

Resumen

Se utilizaron los datos acústicos, obtenidos el 4-5 de enero de 1987 a bordo del B/I *Professor Siedlecki*, en tres descriptores de concentración espacial del krill: densidad espectral de las fluctuaciones espaciales de la biomasa del krill, semivariograma (autocorrelación espacial de la biomasa del krill), y distribución de frecuencias en la estimación de la biomasa del krill. A escalas de 2-20 km, el espectro del número de ondas se parece a un ruido blanco, aunque a escalas menores de 1 km el espectro parece perder su potencia de modo significativo. El semivariograma de la biomasa no parece variar considerablemente en la mayoría de distancias entre puntos, excepto en las distancias menores de 1 km. La distribución de frecuencias calculada de la biomasa del krill es bimodal, y parece ser la combinación de dos distribuciones logarítmicas normales. Estas dos distribuciones pueden corresponder a la biomasa existente dentro de una mancha y entre varias. Estos resultados, obtenidos del análisis de datos, hacen pensar que el tamaño de las manchas de krill, o mejor dicho, el tamaño de un cardumen de krill debería ser menor de 200 m, la resolución más precisa del análisis de nuestros datos, y la distribución espacial real del krill debería ser la manifestación del

equilibrio entre la dispersión de las unidades de cardumen básicas y la atracción a largo alcance dependiente de la densidad de dichas unidades. Modelos dinámicos y kinemáticos sencillos pueden interpretar este resultado observado.

1. INTRODUCTION

The Antarctic krill (*Euphausia superba*) constituting nearly half of the Antarctic zooplankton biomass (Brinton and Antezana 1984), is the dominant herbivores and plays an important role in supporting animal populations such as whales, seals and penguins as well as fish. Krill distribution is highly variable in space and time (Marr 1962), and krill often aggregates into dense swarms, ranging from square meters to vast super swarms, but spherical or laminar swarms of volume 1-10 m^3 may be quite common (Mauchline 1980).

Recently Weber et al. (1986) have used the techniques of spectral analysis to examine the spatial scale dependence of variability in temperature, phytoplankton (chlorophyll-a) and krill biomass in the Antarctic Ocean south of Africa. They found that the power spectra for temperature and chlorophyll fluctuations differed markedly from that of krill biomass. In other words, the spectra of temperature and chlorophyll appeared very similar, and the mean slopes of the temperature and chlorophyll spectra, when plotted on a log-log plot, were -1.66 and -2.04, respectively, whereas the krill spectra were much flatter with near-zero slopes, indicating an approximately equal variance at all scales (white noise).

The result of Weber et al. (1986) implies that mechanisms controlling temperature and chlorophyll spatial distributions are different from those for krill distributions. The spectral slope of -1.66 is quite consistent with the -5/3 power predicted by Kolmogorov (1941) for the inertial subrange of turbulence, and also the slope of -2 for chlorophyll may be interpreted by the turbulence model with a slight modification by biological activities (Fasham, 1978). For krill, a purely physical model would be inappropriate in explaining their high variability at small scales. Although krill distribution is influenced by large scale physical processes, other biological factors, presumably behaviour, must be responsible for the high heterogeneity at small scales. Thus a krill distribution model would have to include additional mechanisms acting predominantly at small scales.

The first step of our approach is to examine the krill biomass distribution in the vicinity of King George Island through spectral analysis, and compare the resulting power spectrum with the description of Weber et al (1986) to see if the same type of spectrum can describe the krill distribution patterns in different areas. Acoustic data provided by M.C. Macaulay were used in our spectral analysis. The same data were also used to compute the semivariogram (Mackas 1984) for further investigation of the spatial variability in krill biomass. The third description is the frequency distribution of biomass estimate, another measure of patchiness in the krill distribution.

2. METHODS

Acoustic data (so-called "Macaulay data") obtained on 4-5 January 1987 aboard the R/V *Professor Siedlecki* were used in the following analysis (Figure 1). The data tapes contained continuous reading of estimated average krill biomass (g/m^3; 200 k kHz estimates) at each meter of depth ranging from 3 to 185 m at a horizontal resolution of approximately 200 m for 8 transects. Vertical profiles were summed to obtain an areal estimate of krill biomass (g/m^2). The resulting traces were then subdivided into 16 series of 64 data points for spectral analysis. The power at each frequency for the 16 transects was then summed and normalized to the total power of the signal to obtain a normalized power spectrum. To facilitate comparison with the power spectrum of Weber et al (1986), the data were also analyzed by first averaging areal biomass into 1 km bins and subdividing the resulting series into traces of 20 data points. The power estimates were then treated in the same way as above to obtain an average power spectra spanning the same scales as Weber et al (Figures 2 and 3).

A second description of spatial distribution, the semivariogram (Mackas 1984) was also computed from the same data (Figure 4). The semivariogram represents the spatial autocorrelation of krill biomass and measures the extent to which the similarity of spatial locations (or samples from those locations) is dependent on their separation.

A third, simpler descriptor, the frequency distribution of biomass estimate was finally computed for the same data set (Figure 5).

3. RESULTS

The resulting spectra shown in Figures 2 and 3 are roughly similar to the spectra of Weber et al. (1986) for krill, but much less steeper than the commonly observed spectra for chlorophyll, temperature or salinity (Steele and Henderson 1977; Lekan and Wilson 1978; Denman 1976). There is a relatively high variability of krill biomass at small scales less than 10 km that cannot be explained by the physical process only. However, the power spectra for krill biomass in the region under study is slightly steeper than that of Weber et al. (1986) in the Weddell Sea. This suggest that either a relatively more important contribution of physical processes or a relatively less important contribution of biological (behavioural) processes to the spatial distribution of krill in the Bransfield Strait-Elephant Island area in the Weddell Sea. Also our data show that at scales smaller than 1 km, the krill spectrum appears to lose its power significantly, indicating the predominance of physical processes or dispersing behaviour of krill.

The spatial autocorrelation of krill biomass (Figure 4) indicates that the variability in krill biomass between pairs of data points is only a weak function of the separation between those points. The semivariance of log biomass does not vary significantly over most distances between points except for the smallest distances. This suggests that patch size or rather a basic swarm size is smaller than 200 m, which is the finest resolution of those data.

The computed frequency of krill biomass estimate (Figure 5) is bimodal and appears to be the mixture of two lognormal distributions. About two thirds of the observations 67%) can be attributed to the first lognormal distribution (mean log (biomass)) = 0.18, SD=0.49) and one third (33%) to a second lognormal distribution (mean=1.76, SD=0.51). These two distributions may correspond to the between and within patch biomass (mean biomass between patches = 2.8 g/m^2, apparent mean biomass within patches = 115 g/m^2). Note that the biomass within swarms may be substantially higher since it appears that most swarms have a diameter smaller than 200 m and that the observed biomass is an average for a 200 m trace.

4. DISCUSSION

According to Mauchline (1980), krill form a patch, i.e. huge aggregation within a defined environmental region, of densities 1 - 10/m^3. Environmental parameters play a more important role than behavioural reactions between individuals in maintaining the aggregation. Within a patch are found shoals, consisting of large groups of individuals. Shoals may be as large as 100 km^2 but are normally much smaller, probably in the range of 0.1-10 km. Average densities of krill in a shoal is 1-100/m^3. The behavioural mechanisms of the animals, rather than the physical environmental parameters, are probably more important in initiating and maintaining shoals. Cohesiveness of individuals is evident in shoals, whereas it is not generally evident in the overall structure of patches. Swarms and schools are often constituent parts of shoals. Cohesiveness reaches its greatest development in swarms and schools. They are small in spatial extent, their area being measured in square meters. Average areal sizes of 10^3-10^4 m^2 can occur, but spherical or laminar sizes of 1-10 m^3 may be quite common. Mean densities of individuals in swarms and schools are 10^3-$10^5/m^3$. Swarms are cohesive groups of individuals without parallel orientation, while schools are cohesive groups of individuals with parallel orientation. In a swarm the centre of mass is more or less stationary relative to the ambient water, while in a school the centre of mass is mobile relative to the water.

Very little has been done on mathematical modelling the dynamics of behaviour of swarms and distribution of krill in space and time. Our data analysis suggests that most swarms (and schools) have a diameter smaller than 200 m, i.e. less than the finest resolution of those data. The result of the semivariogram (Figure 4) supports this concept. We make an attempt to model the krill biomass spectrum on the basis of the dynamical theory of krill aggregation. The basic unit of krill aggregation or shoals is assumed to be a great number of small swarms (or schools) of individual krill. They diffuse as a unit and also attract each other according to Kawasaki's (1978) model for a longrange density-dependent attraction. Krill population dynamics is also incorporated in a simple way. As a result, our basic dynamical equation for the krill concentration fluctuations is given by

$$\frac{\partial s'}{\partial t} = D\frac{\partial^2 S'}{\partial x^2} - \lambda\bar{S}\,\frac{\partial}{\partial x}\,\{\int_{-\infty}^{\infty} \phi\;(x-x')S'(x',t)dx'\}\; -\alpha\; s' \;+\; f' \qquad (1)$$

where s' (x,t): krill biomass fluctuations in space (x) and time (t), D: diffusivity for the swarm unite, $\lambda\bar{S}$: "aggregation speed" for unit swarms, α: intrinsic growth rate at stable equilibrium level $\bar{S}$, or alternatively could be interpreted as a predation rate, f': random local biomass input, and $\phi(x)$ represents a weighting function for a longrange mutual attraction of swarms.

The wavenumber spectrum of krill biomass fluctuations E(k) can be derived from (1) under the assumption that the random input function is white noise of intensity B and the weighting function $\phi(x)$ is exponential with spatial attenuation parameter c. It results

$$E^*(k) \;\equiv\; \frac{E(k)\alpha}{\pi^2 B^2} \;=\; \{Dk^2 \;+\; \alpha \;-\; \lambda\bar{S}\;c\;k^2/(k^2+c^2)\;\}^{-1} \qquad (2)$$

The nondimensionalized spectrum E*(k) is evaluated as a function of wavenumber k, using the following parameter values:

D = 10^3 cm^2/sec (appropriate for the basic swarm unit of the order of 10 m in size after Okubo's (1971) diffusion diagram).

α = 10^{-7}/sec (growth or predation time scale of 100 days)

c = 10^{-3}/cm (mutual attraction distance of the order of the swarm unit)

$\lambda\bar{S}$ = 1cm/sec (aggregation speed = one tenth of krill unit swimming speed).

Figure 6 shows the theoretical spectrum of krill biomass with mutual attraction (solid line), which results in a nearly uniform variance-density in the spatial scale ranging from 1 km to 20 km and relatively sharp decline in the variance below 100 m in scale, approaching the k^{-2} regime at very small scales. In the absence of the mutual attraction of swarms, on the other hand, the spectrum (broken line) decays rapidly in the spatial scale below 10 km and approaches the k^{-2} regime below 1 km. The behaviour of the theoretical spectrum agrees fairly well with that of our observation (Figure 2).

As previously discussed in this section, Mauchline's (1980) "patch within patch", or rather "swarms within schools", concept seems very adequate for interpreting the bimodality of the frequency distribution of biomass (Figure 5) and the behaviour of the semivariograms (Figure 4). To demonstrate this more precisely we have reconstructed the patch within patch model of Mangel (1987) with minor modification to account for the low "background" biomass of krill. Transect data similar to those analyzed previously were then extracted from the simulated krill spatial distribution, and the corresponding descriptors were calculated for 100 sets of 16 transects of 64 points. The results are presented in Figures 7 and 8. Not surprisingly, the resulting frequency distribution of biomass looks similar to the one obtained from the real data. The semivariogram (Figure 8) is also similar to the one from the data. The power spectrum of simulated data (Figure 9) also approximates the one obtained from the real data, although it does not mimic the apparent curvature of Figure 3 as good as the dynamical model of aggregation. Overall the simple kinematic model of Mangel appears to produce the patterns observed with real krill biomass data, and in combination with the dynamical model of krill aggregation we may be able to provide a better understanding of krill spatial distribution.

Obviously a larger set of real data need to be analyzed for testing whether or not power spectra, semivariograms, and biomass frequency distributions vary in a systematic fashion among the various subareas of the general Bransfield Strait-Elephant Island area. At the same time descriptors have to be obtained for the other relevant parameters of the integrated ecosystem model, e.g. temperature, salinity, phytoplankton biomass, and krill predators.

Another important descriptor for determination of krill population dynamics would be the frequency distribution of krill swarm size or aggregation size under given behavioural and environmental constraints. Okubo (1986) introduced the concept of the entropy of swarming, which is a measure of cohesiveness in animal aggregation. The most probably frequency distribution of animal swarm size is the one that maximized the entropy subject to given information or constraints. Thus, if the mean number of individual krill per swarm is specified, the most probably frequency distribution is geometric or exponential. Witek et al (1981) analyzed the data of krill swarms in the Antarctic Peninsula region to show that frequency of swarm size in the range of 10 to 500 m is well represented by an exponential distribution. A similar method should be employed in our data analyses.

REFERENCES

BRINTON, Edward and T. ANTEZANA. 1984. Structures of swarming and dispersed populations of krill (*Euphausia superba*) in Scotia Sea and South Shetland waters during January-March 1981, determined by bongo nets. Journal of Crustacean Biology 4 (Special 1): 45-66.

DENMAN, Kenneth L. 1976. Covariability of chlorophyll and temperature in the sea. Deep-Sea Research 23 (6): 539-550.

FASHAM, M.J.R. 1978. The application of some stochastic processes to the study of plankton patchiness. In: STEELE, J.H. (Ed.). Spatial Pattern in Plankton Communities. New York: Plenum Press. 131-156.

KAWASAKI, Kohkichi. 1978. Diffusion and the formation of spatial distribution. Mathematical Science 183: 47-52.

KOLMOGOROV, A. 1941. The local structure of turbulence in incompressible viscous fluid for very large Reynolds' numbers. Comptes rendus de l'academic des science de l"URSS 32: 16-18.

LEKAN, Jack and R.E. WILSON. 1978. Spatial variability of phytoplankton biomass in the surface water of Long Island. Estuarine and Coastal Marine Science 6: 239-250.

MACKAS, David L. 1984. Spatial autocorrelation of plankton community composition in a continental shelf ecosystem. Limnology and Oceanography 29 (3): 451-471.

MANGEL, Marc. 1987. Simulation of Southern Ocean krill fisheries. SC-CAMLR-VI/BG/22, Report for the Commission for the Conservation of Antarctic Marine Living Resources (CCAMLR), 13 October, 85 pp.

MARR, J.W. 1962. The natural history and geography of Antarctic krill Euphausia superba Dana. Discovery Report 32: 33-464.

MAUCHLINE, J. 1980. Studies on patches of krill, *Euphausia superba* Dana. BIOMASS Handbook 6, 36 pp.

OKUBO, Akira. 1971. Oceanic diffusion diagrams. Deep-Sea Research 18: 789-802.

STEELE, J.H. and E.W. HENDERSON. 1977. Plankton patches in the Northern North Sea. In: STEEL, J.H. (Ed.). Fisheries Mathematics, London-New York: Academic Press, 1-19 p.

WEBER, Larry H., S.Z. EL-SAYED and I. HAMPTON. 1986. The variance spectra of phytoplankton, krill and water temperature in the Antarctic Ocean south of Africa. Deep-Sea Research 33 (10): 1327-1343.

WITEK, Z., J. KALINOWSKI, A. GRELOWSKI nad N. WOLNOMIEJSKI. 1981. Studies of aggregations of krill (*Euphausia superba*). Meeresforsch 28: 228-243.

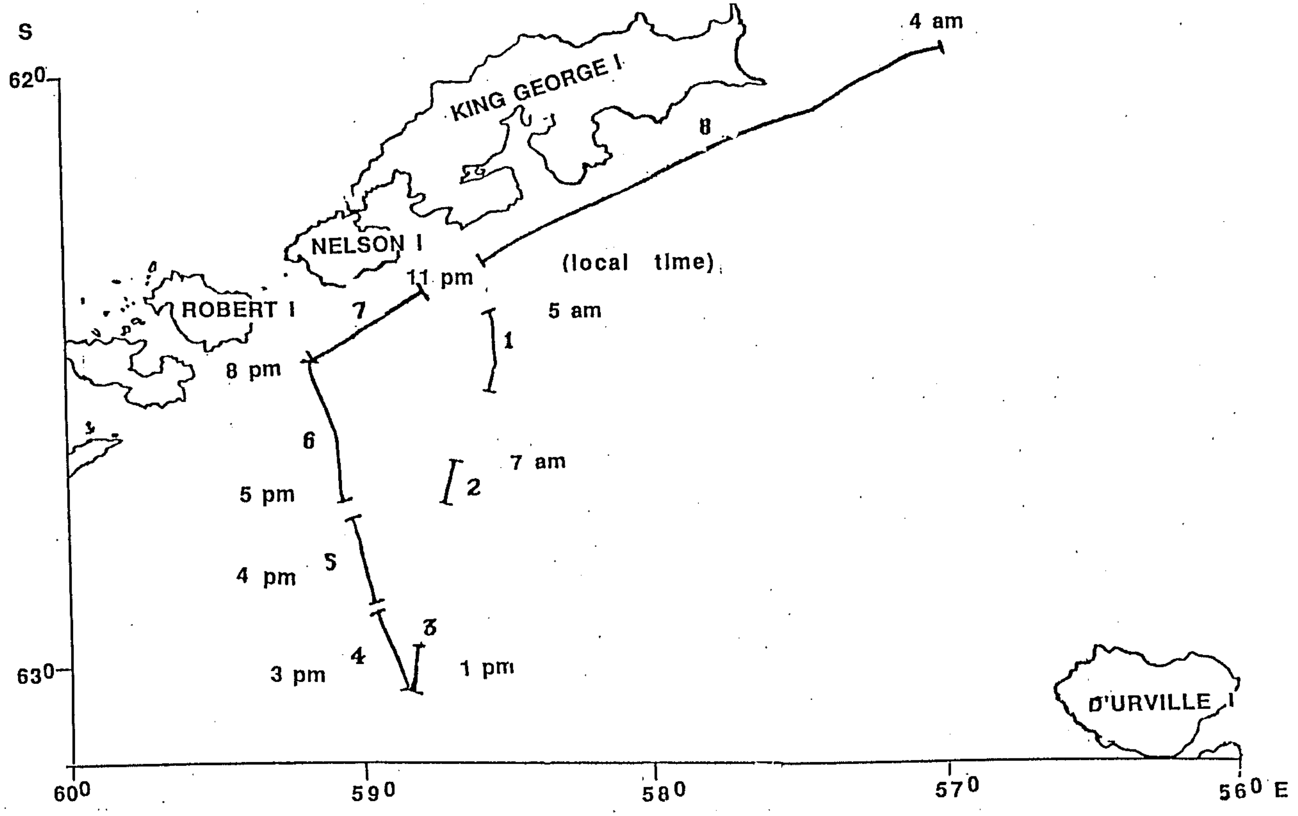

Figure 1: Location of eight transects used in the data analysis 4-5 January 1987.

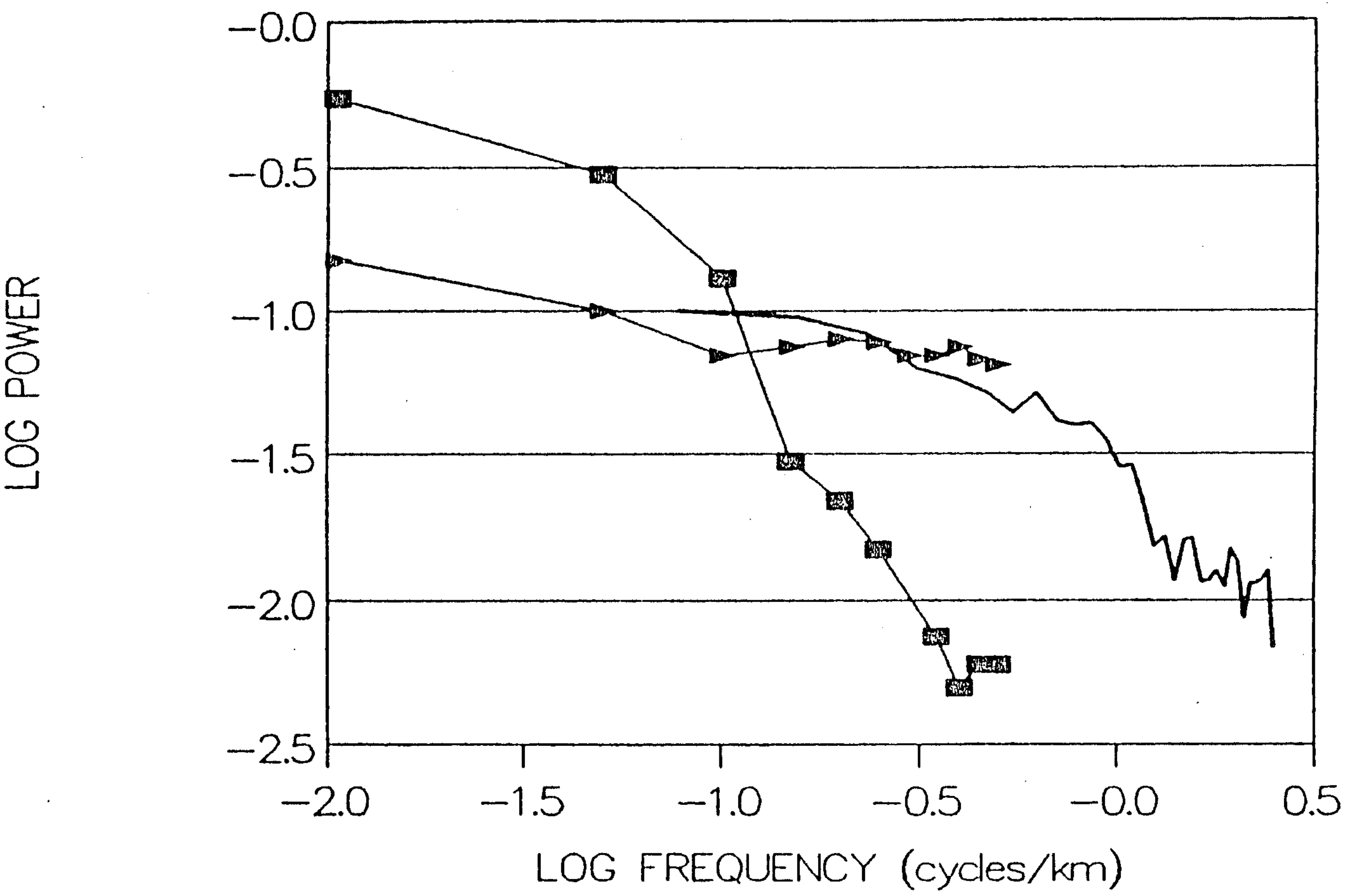

Figure 2: Normalized power spectra for chlorophyll (squares) and krill (triangles) or Weber et al (1986) and for krill acoustic data analyzed in this report (line).

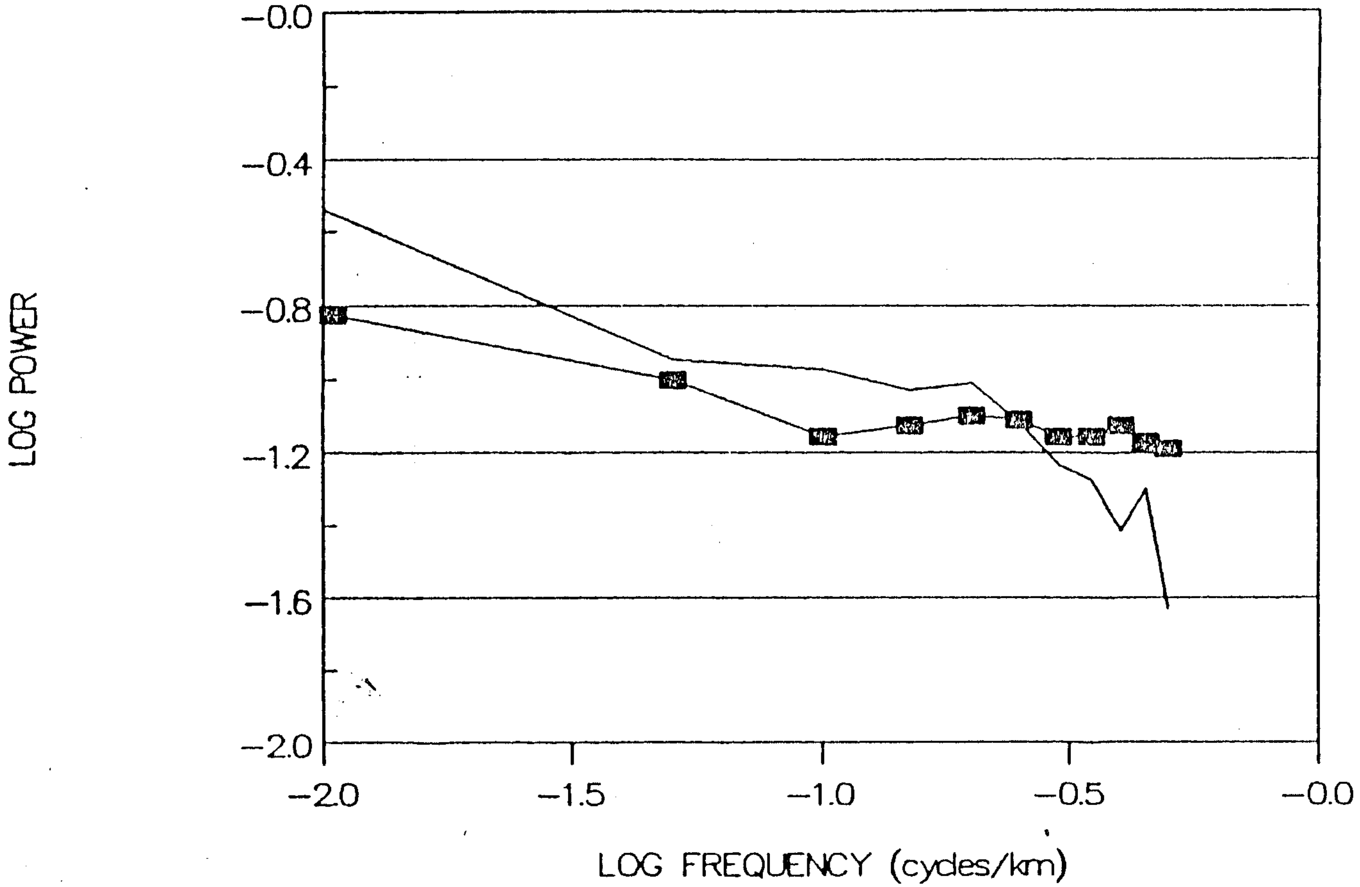

Figure 3: Power spectra for krill at the 2-20 km scale observed in this analysis (line) and by Weber et al (squares). Krill biomass was averaged over 1 km.

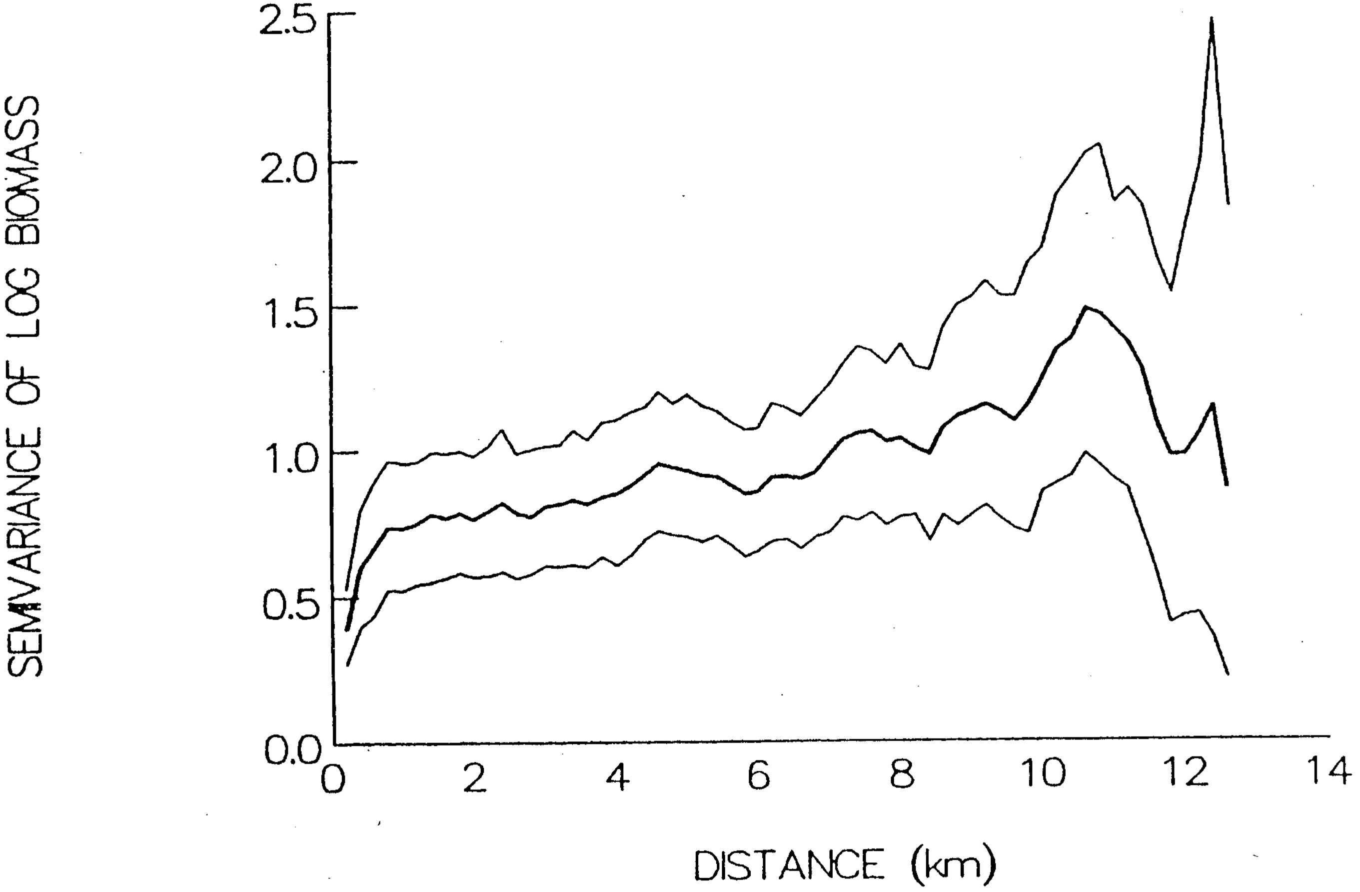

Figure 4: Semivariogram of log (krill biomass) (g/m-2) with bootstrap 95% confidence intervals for the Bransfield Strait data (4-5 January 1987).

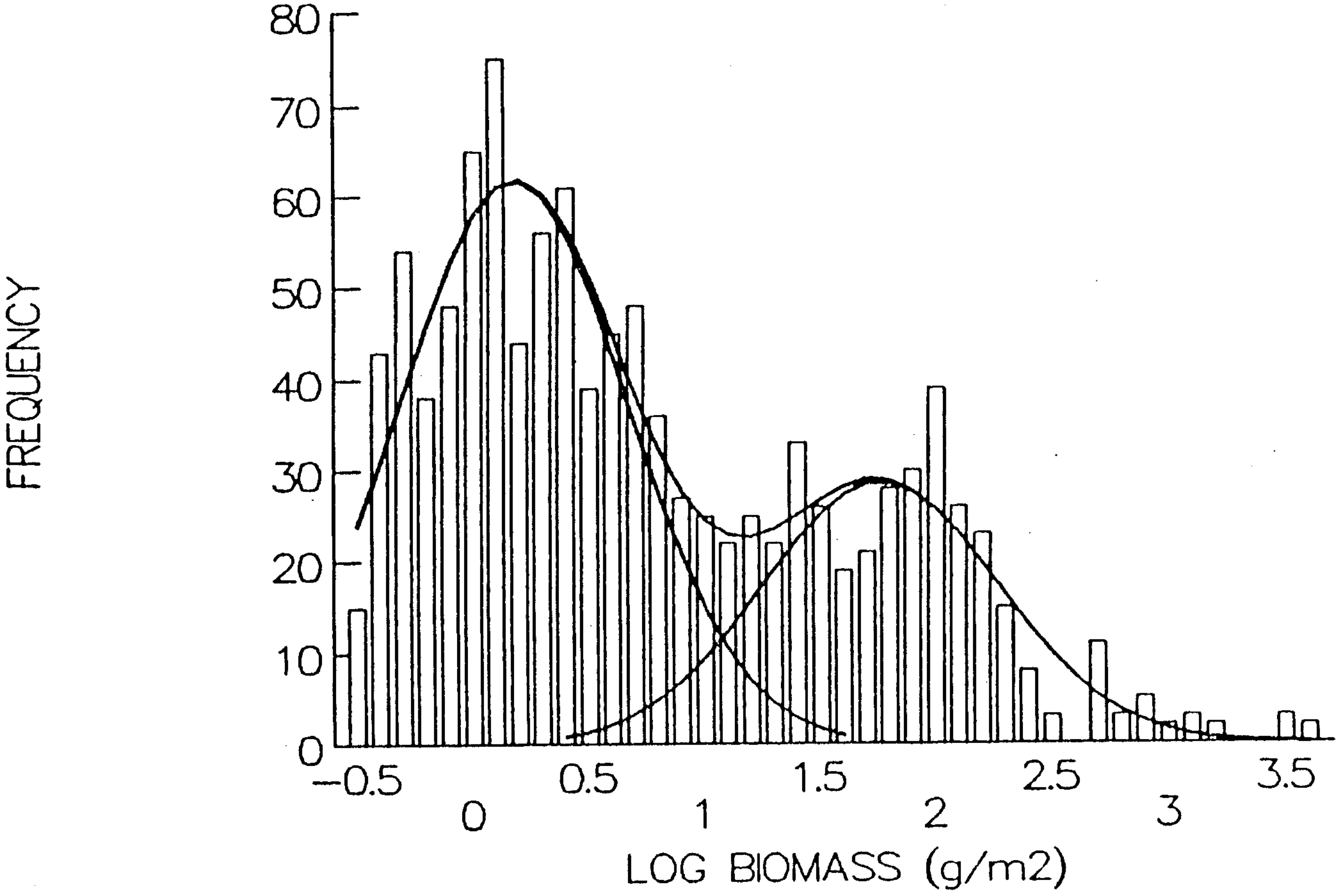

Figure 5: Frequency distribution of log (biomass estimates) (g/m^{-2}) for the Bransfield Strait data. Two lognormal distributions are fitted to the data.

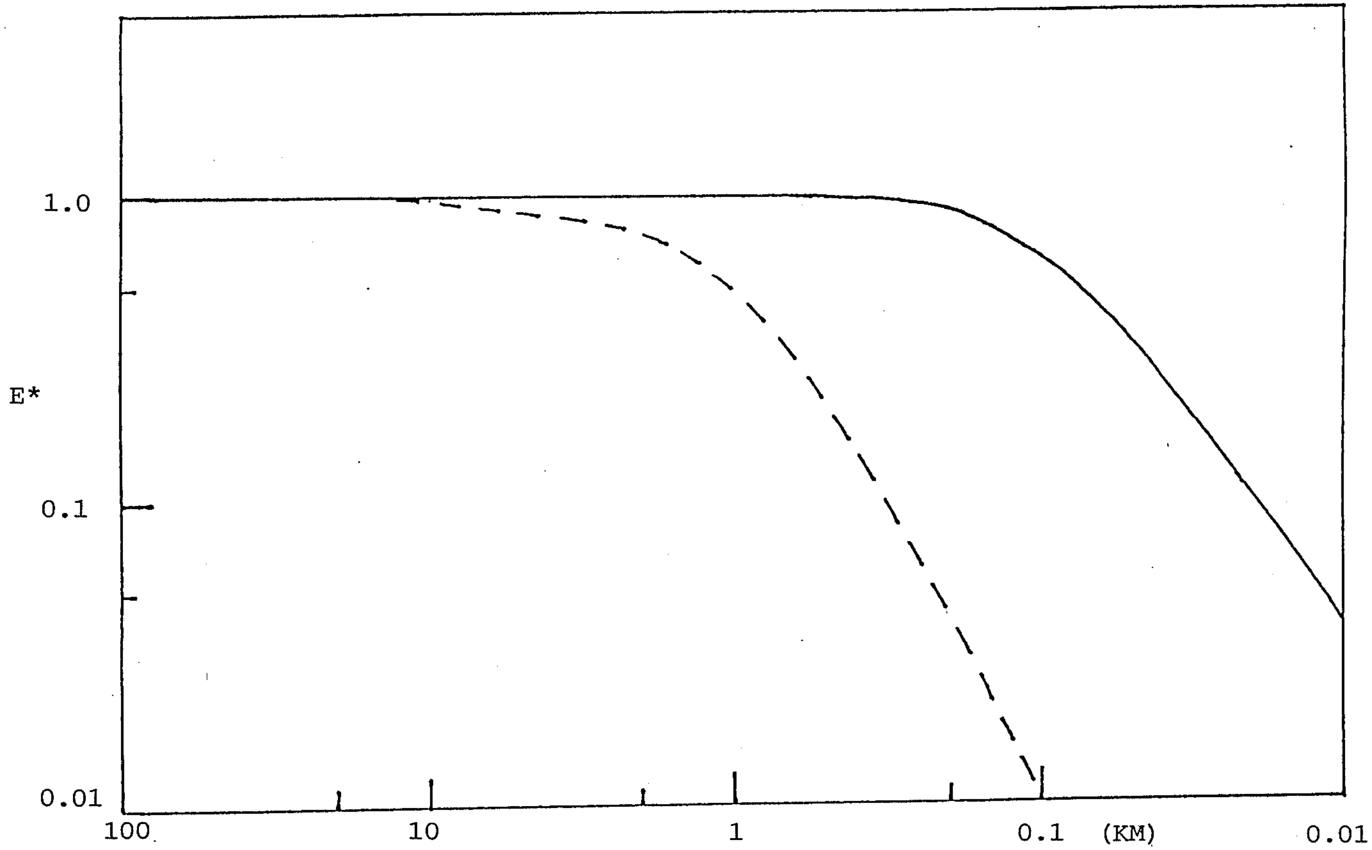

Figure 6: Normalized power spectra for krill biomass based on the dynamical theory of krill aggregation. Solid line: with mutual attraction and dispersion of basic swarm units. Broken line: without mutual attraction.

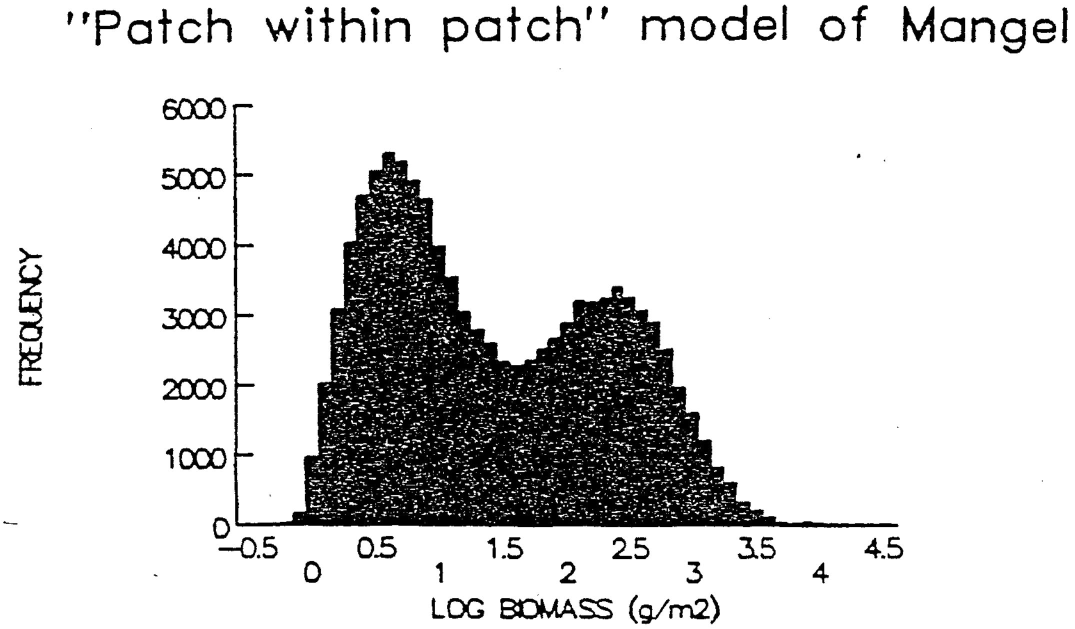

Figure 7: Frequency distribution of krill biomass based on the "patch within patch" model of Mangel (1987).

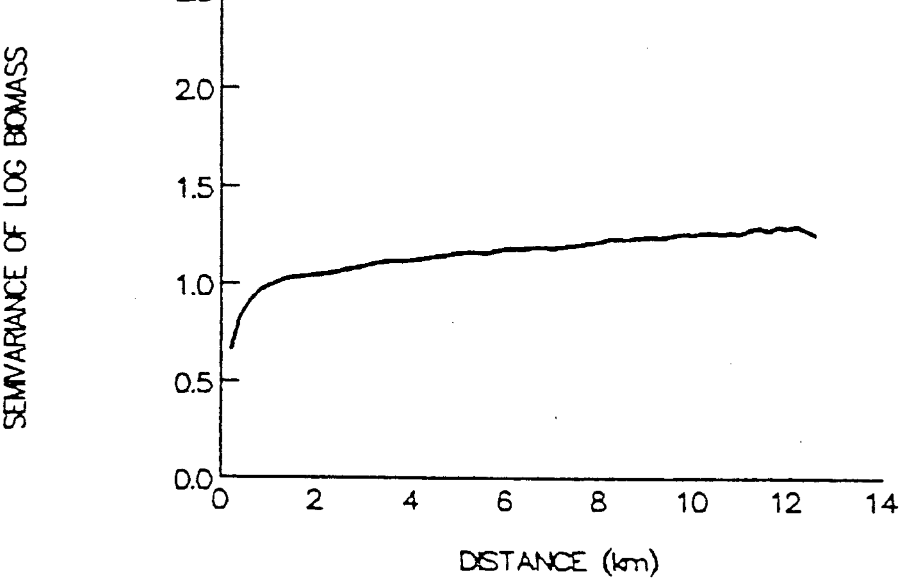

Figure 8: Semivariogram of log (krill biomass) based on the "patch within patch" model of Mangel.

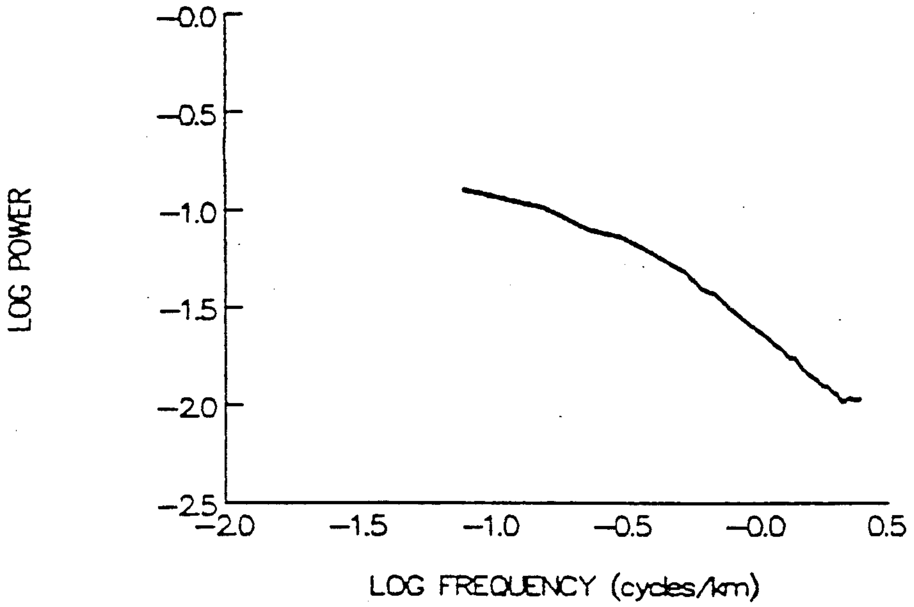

Figure 9: Power spectrum of simulated data using the "patch within patch" model of Mangel.

Légendes des figures

Figure 1	Emplacement de huit transects utilisés dans l'analyse des données les 4 et 5 janvier 1987.
Figure 2	Spectres d'intensité normalisés pour la chlorophylle (carrés) et le krill (triangles) de Weber et al. (1986) et pour les données acoustiques sur le krill analysés dans ce rapport (ligne).
Figure 3	Spectres d'intensité pour le krill sur l'échelle 2-20 km observés dans cette analyse (ligne) et par Weber et al. (carrés). La moyenne de la biomasse du krill a été prise sur 1 km.
Figure 4	Semivariogramme du logarithme (estimations de la biomasse) (g/m^2) avec une zone d'intervalles de confiance de 95% pour les données recueillies dans le détroit de Bransfield (4 au 5 janvier 1987).
Figure 5	Distribution des fréquences du logarithme (estimations de la biomasse) (g/m^2) pour les données recueillies dans le détroit de Bransfield. Deux distributions logarithmiques normales ont été ajustées aux données.
Figure 6	Spectres de puissance normalisés pour la biomasse du krill basés sur la théorie dynamique des mœurs grégaires du krill. Ligne continue: avec attraction mutuelle et dispersion des unités des essaims de base. Tireté: sans attraction mutuelle.
Figure 7	Distribution des fréquences de la biomasse du krill basée sur le modèle "regroupement à l'intérieur d'un regroupement" de Mangel (1987).
Figure 8	Semivariogramme du logarithme (biomasse du krill) basé sur le modèle "regroupement à l'intérieur d'un regroupement" de Mangel.
Figure 9	Spectre d'intensité des données de simulation utilisant le modèle "regroupement à l'intérieur d'un regroupement" de Mangel.

Подписи к рисункам

Рисунок 1	Расположение восьми гидрографических разрезов, использованных при анализе данных 4-5 января, 1987 г.
Рисунок 2	Нормализованная спектральная мощность частотного распределения (по Веберу и др., 1986 г.) для хлорофилла (квадратов) и криля (треугольников) и для проанализированных в этом отчете акустических данных по крилю (линии).
Рисунок 3	Наблюдавшиеся в этом анализе спектральные мощности частотного распределения для криля по шкале 2-20 км.(линия) и спектральные мощности, полученные путем наблюдения Вебером и др.(квадраты). Биомасса криля была усреднена по километровому квадрату.
Рисунок 4	Семивариограмма с логарифмической шкалой (биомассы криля) (г/м^2) с зоной доверительного интервала (95%) для данных по проливу Брансфилда (4-5 января 1987 г.).

Рисунок 5 Частотное распределение логарифма (оценок биомассы) (г/м^2) для данных по проливу Брансфилда. Два логнормальных распределения приложены к данным.

Рисунок 6 Нормализованная спектральная мощность частотного распределения для криля, основанная на динамической теории агрегации криля. Постоянная линия: с взаимным притяжением и рассеянием единиц скопления. Пунктирная линия: без взаимного притяжения.

Рисунок 7 Частотное распределение биомассы криля, основанное на модели Мангела "пятна в пределах пятен" (1987 г.).

Рисунок 8 Семивариограмма логарифма (биомассы криля) основанная на модели Мангела "пятна в пределах пятен".

Рисунок 9 Спектральная мощность частотного распределения смоделированных данных при использовании модели Мангела "пятна в пределах пятен".

Leyendas de las figuras

Figura 1 Ubicación de los ocho transectos utilizados en los análisis de datos, 4-5 de enero de 1987.

Figura 2 Densidad espectral normalizada para la clorofila (cuadrados), para el krill (triángulos) de Weber et al. (1986), y para los datos acústicos del krill que se analizan en este trabajo (línea).

Figura 3 Densidad espectral del krill a la escala 2-20 km observado en este análisis (línea), y por Weber et al. (cuadrados). La biomasa del krill se promedió a lo largo de 1 km.

Figura 4 Semivariograma de log (biomasa del krill) (g/m^2) con una banda de intervalos de confianza del 95% para los datos del estrecho de Bransfield (4-5 de enero de 1987).

Figura 5 Distribución de frecuencias de log (estimaciones de la biomasa) (g/m^2), para los datos del estrecho de Bransfield. Las dos distribuciones logarítmicas normales se adaptan a los datos.

Figura 6 Densidades espectrales normalizadas de la biomasa del krill basados en la teoría dinámica de las concentraciones de krill. Línea solida: con atracción y dispersión mútua de las unidades básicas de cardumen. Línea quebrada: sin atracción mútua.

Figura 7 Distribución de frecuencias de la biomasa del krill basado en el modelo de Mangel (1987) de “manchas dentro de manchas”.

Figura 8 Semivariograma de log (biomasa del krill) basado en el modelo de Mangel de “manchas dentro de manchas”.

Figura 9 Densidad espectral de los datos simulados utilizando el modelo de Mangel de “manchas dentro de manchas”.

SC-CAMLR-VII/BG/26

PHYTOPLANKTON DISTRIBUTION IN THE MIXED LAYER: IMPLICATION TO KRILL ABUNDANCE*

Hidekatsu Yamazaki and Thomas R. Osborn

Abstract

A one dimensional Lagrangian model of random walk is presented to study the distribution of phytoplankton in the Antarctic ocean. Since little is known about mixed layer dynamics in the Antarctic Ocean, we estimate the depth of the mixed layer and its turbulence intensity from an Ekman layer model. Available CTD data suggest that the mixing in the upper layer is less than what we expected. However, the effect on the dynamics is vital, affecting the distribution of particles in the upper ocean.

Résumé

Un modèle uni-dimensionnel de trajet aléatoire de Lagrange est présenté pour permettre l'étude de la distribution du phytoplancton dans l'océan Antarctique. Vu que l'on possède une connaissance réduite de la dynamique des couches mixtes dans l'océan Antarctique, la profondeur de la couche mixte et l'intensité de sa turbulence ont été estimées d'après un modèle de couche d'Ekman. Des données disponibles de conductivité, température, profondeur, suggèrent que le mélange dans la couche supérieure est moindre que l'on ne s'y attendait. Cependant, la répercussion sur la dynamique est vitale, car elle modifie la distribution des particules dans la couche supérieure de l'océan.

Резюме

Для изучения распространения фитопланктона в водах Антарктики представлена одномерная модель Лагренджа (Lagrange) случайного блуждания. Поскольку мало известно о динамике смешанного слоя в водах Антарктики, глубина смешанного слоя и интенсивность турбулентности в нем были оценены с помощью модели слоя Экмана (Ekman layer model). По имеющимся данным по проводимости, температуре и глубине (CTD) можно предположить, что смешение в верхнем слое меньше предполагаемого. Тем не менее, его воздействие на динамику велико, в связи с тем, что оно оказывает влияние на распределение частиц в верхних слоях океана.

Resumen

Se presenta un modelo unidimensional de Lagrange de trayecto aleatorio para estudiar la distribución del fitoplancton en el Océano

---

* (Revised)

Antártico. Ya que se sabe poco sobre la dinámica de las capas mixtas del Océano Antártico, estimamos la profundidad de la capa mixta y su intensidad de turbulencia a partir de un modelo de la capa Ekman. Los datos CTD disponibles, sugieren que la mezcla en la capa superior es menor de lo esperado. Sin embargo, el efecto en la dinámica es vital, afectando a la distribución de partículas en la parte superior del océano.

1. INTRODUCTION

There has been an increasing interest in the variability of biological marine resources, but little progress toward accurate predictions of productivity has been made. The major difficulty arises in variations among the density-dependent populations whose controlling factors are not only the prey-predator interaction and the physiological conditions but also the *in situ* physical environment. The problem, as it now stands, is highly complex with many degrees of freedom.

The basic concept underlying our approach is to use a Lagrangian kinematic model to trace individual organisms in space and time. Historically, Eulerian models have been adapted to study the distribution of plankton. For example, Wroblewski (1982) models copepoda abundance during upwelling off the Oregon coast. The model results agree favorably with observations. Since the Eulerian models inherently deal with averaged spatial distributions, the results may differ considerably from the reality because physical-biological interactions are highly non-linear. Woods and Onken (1982) state that "averaging non-linear equations before integration does not give the same answer as averaging them after integration." An individual life history can only be evaluated by a Lagrangian type model. They also note that "..the power of the Lagrangian ensemble method lies in its potential for testing the consequences of different hypotheses concerning the physiology and behavior of plankton, in a systematic and internally consistent way". They are referring to phytoplankton but the same principal holds for zooplankton. Platt and Gallegos (1980) state that "we need more knowledge about how complex trajectories affect photosynthetic performance by phytoplankton; we need to incorporate these complex trajectories into our experimental designs; and we need to cooperate with physical oceanographer to study how the temporal responses to the phytoplankton are coupled to the temporal scales of mixing found in nature". Lagrangian models require an extensive computational effort compared to Eulerian models, but the models have advantages; namely the coding does not require a sophisticated algorithm; the model can be fairly flexible to variety of environmental conditions; and prey-predator interaction can be "directly" evaluated by the model. Recent advancements of computer technology make the operation time less significant.

Although experiments suggest that krill are omnivorous, the animals extensively feed on phytoplankton. Boyd et al. (1984) estimate that they spend up to 30% of their total respiratory energy collecting food. Morris et al. (1984) suggest that the turnover rate of chlorophyll in a krill's stomach is of the order of minutes. These reports imply that krill are continuously grazing, and that females must continuously consume food to meet the minimum requirement for the production of eggs. To meet the minimum nutrient level they must find high concentrations of food. Another important process is the efficiency of the food capturing and handling. Ross and Quetin (1986) suggest that schooling and swimming behavior of krill may be related to foraging. A strategy to minimize energy requirement for feeding would be expected. A correlation between krill swarms and phytoplankton abundance was discussed by Weber and El-Sayed (1985). Hence, we think that studying the distribution of the food (phytoplankton) is the key to understanding the distribution of krill. The animals are excellent swimmers and velocities of 40 cm s^{-1} are possible. Therefore, small scale turbulence is irrelevant to their swimming ability, but the turbulence can significantly affect the distribution of their food source and their foraging. The goal of our study is to develop a Lagrangian prey-predator model for krill and phytoplankton. Phytoplankton grow in the upper ocean where enhanced mixing due to turbulence can be found. Unfortunately, however, very little is known about mixed layers in the Antarctic ocean.

We deduce the dynamics of the mixed layer in the Antarctic ocean from existing STD data in the next section. Implementation of one-dimensional Lagrangian model is discussed in section 3. The last section summarizes our preliminary results.

2. THE MIXED LAYER IN THE ANTARCTIC

2.1 STD Data

STD data from a hydrographic survey made from R/V *Professor Seidlecki* in January, 1987 near the Antarctic Peninsula were used to investigate the level of turbulence in the mixed layer. A section along 57° W (Figure 1) shows the transition from Pacific water to Bransfield Strait water separated by a frontal zone at near the latitude 61.3 degrees south (Gordon, 1988). In general, the stratification in the Antarctic Ocean, south of the front, is very weak compared to that of the low latitude ocean. The depths of the mixed layer in the Pacific water, north of the front, ranges between 30 and 50 meters. A sharp pycnocline near 40 m in STD237 shows a high buoyancy frequency, N, as is often found at the base of mixed layers at mid-latitude. Stratification in the continental front and Bransfield strait water is weak, and mixed layers are not apparent. Since wind speeds were typically 10 to 15 m s^{-1} (Chapman, personal communication), the buoyancy flux provided by melt water must be suppressing the surface mixing. The Weddell Sea is covered by the sea ice in January.

2.2 Mixed Layer Depth

The depth of mixing is controlled by the surface buoyancy production (cooling promotes convection) and by the surface wind stress, but quantitative relationships between the depth of mixing and surface forcing are still controversial. Since very little is known about surface forcing in the Antarctic ocean, we will use the Ekman depth

$$h_E = \kappa u_{.}/f \qquad (1)$$

as the upper limit to the depth of mixing, where $u_{.} = (t_o/\rho)^{1/2}$, t_o is the surface wind stress, f the Coriolis parameter and ρ the density of water. Turbulence observations at mid-latitudes for wind speeds of 10 m s^{-1} show mixing to approximately 65% of the Ekman depth (Lueck, 1989). Because of the strong surface buoyancy flux provided by melt water, convective mixing is not expected during the southern summer. For current models, the Ekman depth is a sufficient indicator of the depth of mixing.

2.3 Turbulence

Under purely wind-stress forcing, the rate of dissipation of kinetic energy should follow

$$\varepsilon = u_{.}^3/\kappa z \qquad (2)$$

(Gregg, 1987). Figure 2 shows the dissipation profile for U_{10} = 1, 5, 10 and 20 m sec^{-1} at 61°S and the profiles are terminated at the depth of Ekman layer. The dissipation rate decreases inversely from 5×10^{-6} W kg^{-1} at 1 meter to 10^{-7} W kg^{-1} for U_{10}=10 m sec^{-1}. The average dissipation rate $<\varepsilon>$ over the depth range gives 5×10^{-7} W kg^{-1}. In order to exam the scale of turbulent mixing we introduce a universal spectrum for the isotropic turbulence. The energy spectrum $E(k)$ is expressed as follows

$$E(k) = \alpha \varepsilon^{2/3} k^{-5/3} \exp[-1.5\alpha\{\pi\beta\alpha^{-1/2}(kl)^{-4/3} + (k\eta)^{4/3}\}] \qquad (3)$$

where α and β are canonical constants and k is the radian wave number. The spectrum shape has a sharp cut-off at both the energy containing eddy scale l and the Kolmogorov length scale $\eta \equiv (\nu^3/\varepsilon)^{1/4}$. For a scale smaller than $2\pi\eta$ the flow is dominated by the viscosity and is laminar. The integration of $E(k)$ gives the turbulence kinetic energy $q^2 \equiv 3u^2/2$,

$$q^2 = \int_0^\infty E(k)\, dk \qquad (4)$$

where u is the rms turbulent velocity scale.

The dissipation rate spectrum $D(k)$ can be expressed in terms of $E(k)$ as follows

$$D(k) = 2\nu k^2 E(k) \qquad (5)$$

The integration of $D(k)$ gives the kinetic dissipation rate.

$$\varepsilon = \int_0^\infty D(k)\, dk \qquad (6)$$

The dissipation rate can be set from the Ekman layer model. The dissipation rate is also related to the energy containing eddy scale.

$$\varepsilon = A u^3 l^{-1} \qquad (7)$$

where A is a constant of an order one. For the sake of simplicity we have used $A=1$. Therefore by knowing ε, for our case $<\varepsilon>$ from the Ekman layer model, u can be evaluated with l.

The energy containing eddy scale, l, is bounded by the depth of mixed layer and may be proportional the Ozmidov scale $L_o \equiv (\varepsilon N^{-3})^{1/2}$ which is a scale of the largest eddy size in a stratified fluid. Stratification limits the vertical scale of turbulent fluctuations although not necessarily the vertical extent of the patches. Detailed measurements of the three turbulent velocity components (Gargett et al. 1984) from the *Pisces* submersible show the suppression of vertical velocities at scale larger than L_o. The turbulence velocity scale u may be estimated by assuming $l \approx L_o$.

$$u = (<\varepsilon> L_o)^{1/3} = (<\varepsilon> N^{-1})^{1/2}. \qquad (8)$$

where $<\varepsilon>$ is the previously defined average dissipation rate between 1 meter and h_E. Figure 3 shows the shape of turbulent energy spectrum (solid line) and the dissipation spectrum (dotted line) for N=0.001 rad s^{-1} and U_{10}=1, 5, 10 and 20 m sec^{-1} at 61°S. Since N can be an order of magnitude larger than 0.001 Figure 4 is prepared for N=0.01 rad s^{-1} with the same condition. The turbulent eddy sizes vary between the energy containing eddy scale and the Kolmogorov dissipation scale.

Another length scale may be used to describe the turbulence field is the Taylor microscale $l_T \equiv u s^{-1}$, where s^2 is a turbulent strain component $2\varepsilon 15^{-1} \nu^{-1}$. The turbulent field may be considered as an equivalent vortex tube with the size of l_T and the velocity scale u. Although the length scale is not a characteristic length of the strain-rate field and does not represent any group of eddy sizes in which dissipative effects are strong (Tennekes and Lumley, 1972, p 68), the scale has a direct implication to the Lagrangian auto-correlation function and thus makes useful to link the universal spectral theory and the diffusion processes.

It is instructive to show an inter-comparison among four length scales. The Ekman depth h_E is shown in Figure 5 (solid line) with the depth averaged dissipation rate, $<\varepsilon>$. The Ozmidov scale L_o (dotted lines), the Taylor microscale l_T (single- and double-chain-dot lines), and the Kolmogorov scale η (dashed line) are also depicted against $<\varepsilon>$. We used three different buoyancy frequency N=0.001, 0.005, 0.01 rad s^{-1} for L_o.

Since the energy containing eddy size can be set by either h_E or L_o, the Taylor microscales based on both scales are shown in the same figure. For the wind speed higher than 5 m s^{-1} these scales hold the inequality $h_E > L_o > l_\tau > \eta$. The Taylor microscale is insensitive to changes in $<\varepsilon>$, in fact l_T base on L_o is independent from $<\varepsilon>$. The range of l_τ is approximately an order of magnitude around 10^{-1} m. Turbulence eddies within the inertia sub-range are unaffected by the size of the energy containing eddy and the viscous dissipation scale. The Ozmidov scale can be considerably different depending on the stratification but the size of largest eddy is limited by the depth of mixed layer h_E.

2.4 Diffusivity

Particle tracking must be done in a Lagrangian fashion, thus the above discussion is not useful unless we relate the universal spectrum to the Lagrangian statistics. A particle displacement can be investigated with the Lagrangian auto-correlation function $\rho_L(\tau)$. The empirical function is in a simple form,

$$\rho_L(\tau) = \exp(-\tau\lambda^{-1}) \tag{9}$$

where λ is the integral time scale. For this simple form of the auto-correlation function the integral scale is related with the Taylor microscale, namely $\lambda = l_T u^{-1}$ provided the Lagrangian velocity scale is identical to the Eulerian velocity scale. A mean square value of a particle displacement, $<X(t)>^2$, can be expressed in terms of λ.

$$<X(t)>^2 = 2u^2\lambda t. \tag{10}$$

Note that the above expression is valid as an asymptotic result. The diffusion coefficient K_D can be defined as follows (Taylor, 1921),

$$K_D = (1/2)\ \mathrm{d}<X(t)>^2/\mathrm{d}t = u^2\lambda = ul_T. \tag{11}$$

If we employ Eulerian quantities for the above expression we can rewrite K_D as

$$K_D = (15/2)^{1/2}\ (\varepsilon l^4 \nu^3)^{1/6} \tag{12}$$

If we take $l = L_o$,

$$K_D = (15/2)^{1/2}(\varepsilon\nu^{-2})^{1/2} = 7.5\nu s N^{-1}. \tag{13}$$

Since we used the Ozmidov scale for l the formula is only applicable for the vertical diffusion in the stably stratified environment. The equation (13) is considerably different from the empirically suggested form $K_z = \alpha\varepsilon N^{-2}$ where a is an empirical constant. Osborn (1980) suggests the upper bound for a is 0.2, hence

$$K_z = 0.2\varepsilon N^{-2}. \tag{14}$$

Since the diffusion coefficient must have the same dimension with the turbulence velocity scale u times a length scale L, a dimensional argument yields K_z must be a constant times uL. Hence the K_z model can be obtained by setting $L = L_o$. The discrepancy between (13) and (14) is rooted in the original formulation.

Figure 6 shows values of K_D and K_z against ε for three different N (0.001, 0.005 and 0.01 rad s^{-1}). The kinematic viscosity was evaluated at 2°C. The average dissipation rate in the mixed layer is roughly between 10^{-7} and 10^{-6} W Kg^{-1}. Diffusion coefficient from the K_z

model varies three decades between 10^{-4} and 10^{-1} m^2 s^{-1}. On the other hand the K_D model varies 10^{-4} and 10^{-3} m^2 s^{-1}. We think realistic values for the diffusion coefficient may be close to the K_D model.

3 ONE DIMENSIONAL LAGRANGIAN MODEL

3.1 Model

The random walk model is extensively used in simulating particle diffusion and animal aggregation. Skellam (1951) uses the random walk model and the law of diffusion for the study of spatial expansion and distribution of animal population. Our initial step to model the motion of particles follows the conventional random walk. A single particle moves from a position $X(t)$ to an adjacent position $X(t+\Delta t)$ with an instantaneous velocity $V(X,t)$. The cause of movement involves physical, physiological, and social factors. We trace the trajectory of particle every time interval Δt.

$$X(t+\Delta t) = X(t) + \int_{t}^{t+\Delta t} V(X,s)\, ds \tag{15}$$

where t is a continuous time. The discrete form of the above equation may be written as

$$X(n+\Delta n) = X(n) + Z(n) \tag{16}$$

where n is an equally spaced discrete time and $Z(n)$ is an appropriate step size over an fixed time interval Δn. If $Z(n)$ is white noise, the process is the pure random walk. It is convenient to separate $Z(n)$ into biologically induced velocity $Z_B(n)$, e.g. swimming or sinking, and physically induced velocity $Z_P(n)$, e.g. mean current or turbulence, namely

$$Z(n) = Z_B(n) + Z_P(n). \tag{17}$$

We apply a simple random walk diffusion for $Z_P(n)$ if the particle is in the mixed layer, otherwise there is no physical forcing. The step size $Z_P(_n)$ follows a normal distribution with mean zero and standard deviation $(2K_D\Delta n)^{1/2}$. We used $K_D=10^{-4}$ m^2 s^{-1} and $\Delta n=1\ 800$ sec (30 minutes). These diffusion coefficients are approximately for cases $U_{10}=10$ m s^{-1} with $N=0.01$ (see Figure 6) The biological component, $Z_B(n)$, is a constant-speed. The organisms do not interact with each other so that each particle can be traced independently. The depth of mixed layer is set by the Ekman layer model and the turbulent diffusion only happens in the mixed layer with uniform intensity.

3.2 Simulations

At the beginning of the simulation 1 000 particles are located at the surface. Presumably phytoplankton continuously produce new generations. Thus, 1000 particles are added at every 24 hours over 10 day simulation time. At the end of the simulation 11 000 particles were traced. Table 1 summarizes simulation cases.

Figure 7 shows a series of particle distribution profiles at every 12 hours. Particles diffuse like a continuous medium within the mixed layer. No significant change in the density of particle was observed below the mixed layer, 38m, for this case. A slight increase in the descending speed of particle cause drastic difference in the distribution (Figure 8). Because particles sink faster than diffusive effect of turbulence, particles are grouped in a single cluster for each generation. For descending particles under weak wind condition, U_{10}=5 m s^{-1}, a deposit of particles can be found at the base of mixed layer, however, once a particle leaves the turbulent region it never get back to the mixed layer (Figure 9). These results indicate that fast sinking particles distribute rather uniformly inside and below the mixed layer. On the other hand, if the turbulent intensity is not strong enough in the mixed layer for fast sinking particles a non-uniform distribution of particles is created.

Finally, some species of phytoplankton can swim upward and the slight motile may cause a significant difference in the life stage. Due to the active swimming a particle can be entrained back to the mixed layer even if it has been left from the mixed layer. An example of particle trajectory is shown in Figure 10. Although a deposit of particles at the base of mixed layer is growing with time, members of the cluster can be changed over the time. Physiologically this mechanism may act to reduce photo-inhibition. Woods and Onken (1982) showed a particle re-entry mechanism into the mixed layer by introducing diurnal convective mixing. As we have discussed in section 2.2 the diurnal changes in the depth mixed layer is seeming unlikely in the Antarctic ocean.

4. SUMMARY

Our simulation is still in an early stage. No suggestions can be made relating to the distribution of krill. However, we demonstrated the distribution of phytoplankton can be significantly changed depending on the depth mixed layer, the level of turbulence and the sinking/swimming speed of particle. The upper layer in the Antarctic ocean is not as well mixed as we originally thought. Presumably the weak mixing condition allows the phytoplankton to grow sufficiently with almost unlimited nutrition level. Interrelation between physical processes and the primary productivity in the upper ocean must have unique characteristics in the Antarctic ocean.

REFERENCES

BOYD, C.M., M. HEYRAUD and C.N. BOYD. 1984. Feeding of the Antarctic Krill *Euphausia Superba*. Journal of Crustacean Biology 4 (Spec. 1): 123-141.

GARGETT, A.E., T.R. OSBORN and P.W. NASMYTH. 1984. Local isotropy and the decay of turbulence in a stratified fluid. Journal of Fluid Mechanics 144: 231-280.

GORDON, A.L. 1988. Physical oceanographic setting the *Seidlecki* January 1987, South Shetland Island data set, in draft.

GREGG, M.C. 1987. Structures and fluxes in a deep convecting mixed layer. Dynamics of the oceanic surface mixed layer, Proceeding of Hawaiian Winter Workshop, University of Hawaii at Manoa, January 14-16, 1987: 1-24.

HAN, Y.-J., and S.-W. LEE. 1981. A new analysis of monthly mean wind stress over the global ocean, Rep. 26, Climate Research Institute, Oregon State Univ., Corvallis: 148 pp.

LUECK, R.G. 1989. Near surface turbulence during the passage of a storm, in draft.

MORRIS, D.J., I. EVERSON, C. RICKETTS and P. WARD. 1984. Feeding of krill around South Georgia. II. Relations between feeding activity, environment and vertical distribution Marine Ecology -Progress Series 20: 203-206.

MOUM, J.N., D.R. CALDWELL. 1985. Local influences on shear-flow turbulence in the equatorial ocean. Science 230: 315-316.

OSBORN, T.R. 1980. Estimates of the local rate of vertical diffusion from dissipation measurements. Journal of Physical Oceanography 10: 83-89.

ROSS, R.M.. and L.B. QUETIN. 1986. How Productive are Antarctic Krill? BioScinec 36: 264-269.

PLATT, T. and C.L. GALLEGOS. 1980. Modeling primary production. Primary Production in the Sea. FALKOWSKI, P.G. (ed.). Plenum Press, p 339-362.

SKELLAM, J.G. 1951. Random dispersal in theoretical population. Biometrika 38: 196-218.

TENNEKES, H and J.L. LUMLEY. 1972. A First Course in turbulence. MIT press, Cambridge, Massachusetts, 300 pp.

WEBER, L.H. and S.Z. EL-SAYED. 1985. Spatial variability of phytoplankton and the distribution and abundance of krill in the Indian sector of the South Ocean. In SIEGFRIED, W.R., P.R. CONDY, and R.M. LAWS (Eds). Antarctic Nutrient Cycles and Food Webs p 284-293.

WOODS, J.D. and R. ONKEN. 1982. Diurnal variation and primary production in the ocean - preliminary results of a Lagrangian ensemble model. Journal of Plankton Research 4: 735-756.

WROBLEWSKI, J.S. 1982. Interaction of currents and vertical migration in maintaining callanus marshalae in the Oregon upwelling zone - a simulation. Deep-sea Research 29: 665-686.

Table 1: Physical and biological condition for simulations. Swimming (or sinking) speed, W_B, was kept throughout the simulation for each case. The diffusion coefficient K_D was fixed for all simulations. The value is close to a case when wind speed U_{10} is roughly 10 m s^{-1}. Depth of mixing layer was determined from Ekman layer mode.

Case	*A*	*B*	*C*	*D*
W_B (m s^{-1})	10^{-4}	$3.x10^{-4}$	10^{-5}	-10^{-5}
K_D (m^2s^{-1})	10^{-4}	10^{-4}	10^{-4}	10^{-4}
U_{10}(m s^{-1})	10	10	5	5
h_E(m)	38	38	19	19

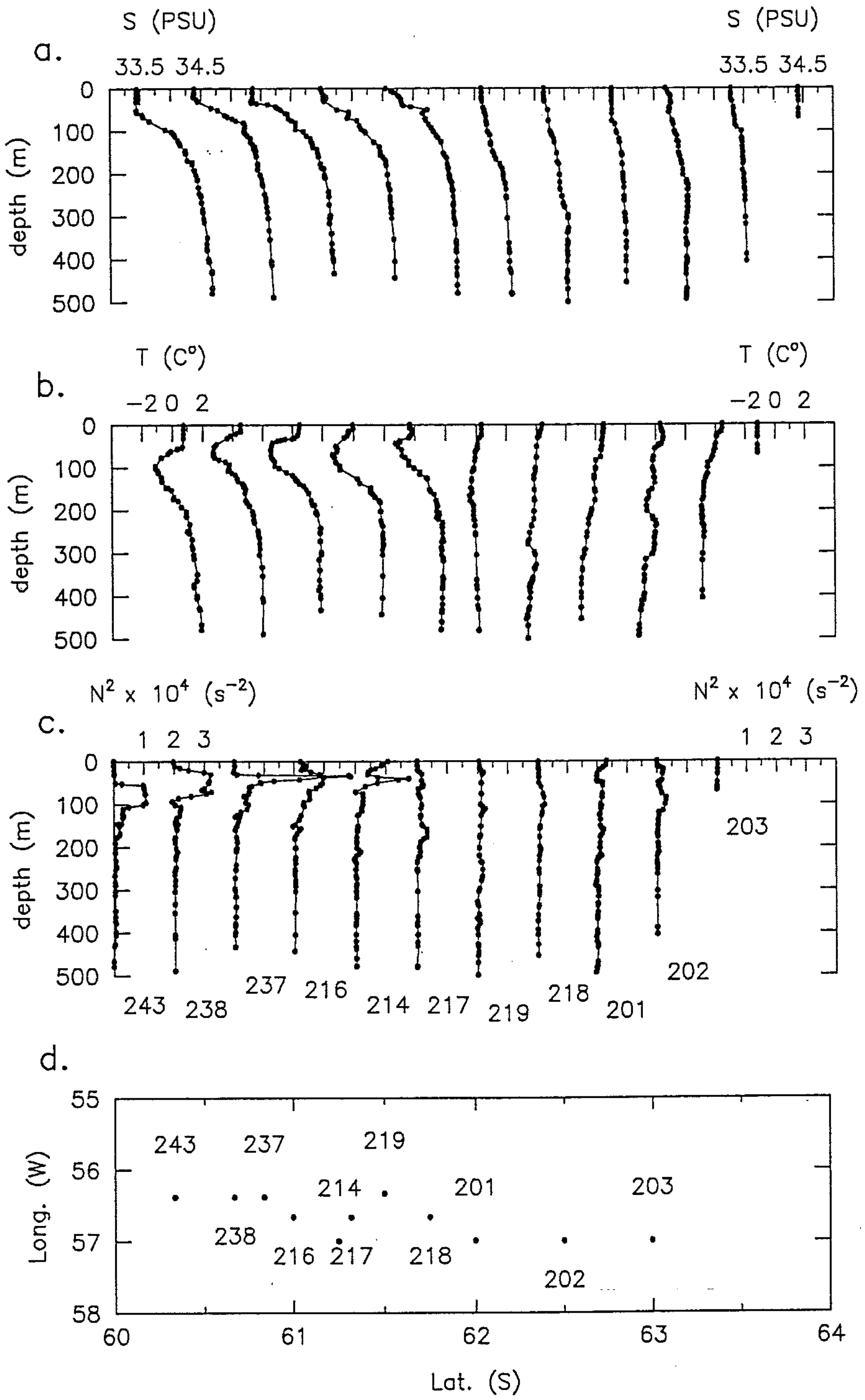

Figure 1: STD profiles along 57°W taken by R/V *Professor Seidlecki* in January 1987. a) Salinity (S) profiles. b) Temperature (T) profiles. c) Buoyancy frequency (N) profiles. d) Location of STD stations. STD station number is shown beneath buoyancy frequency profile.

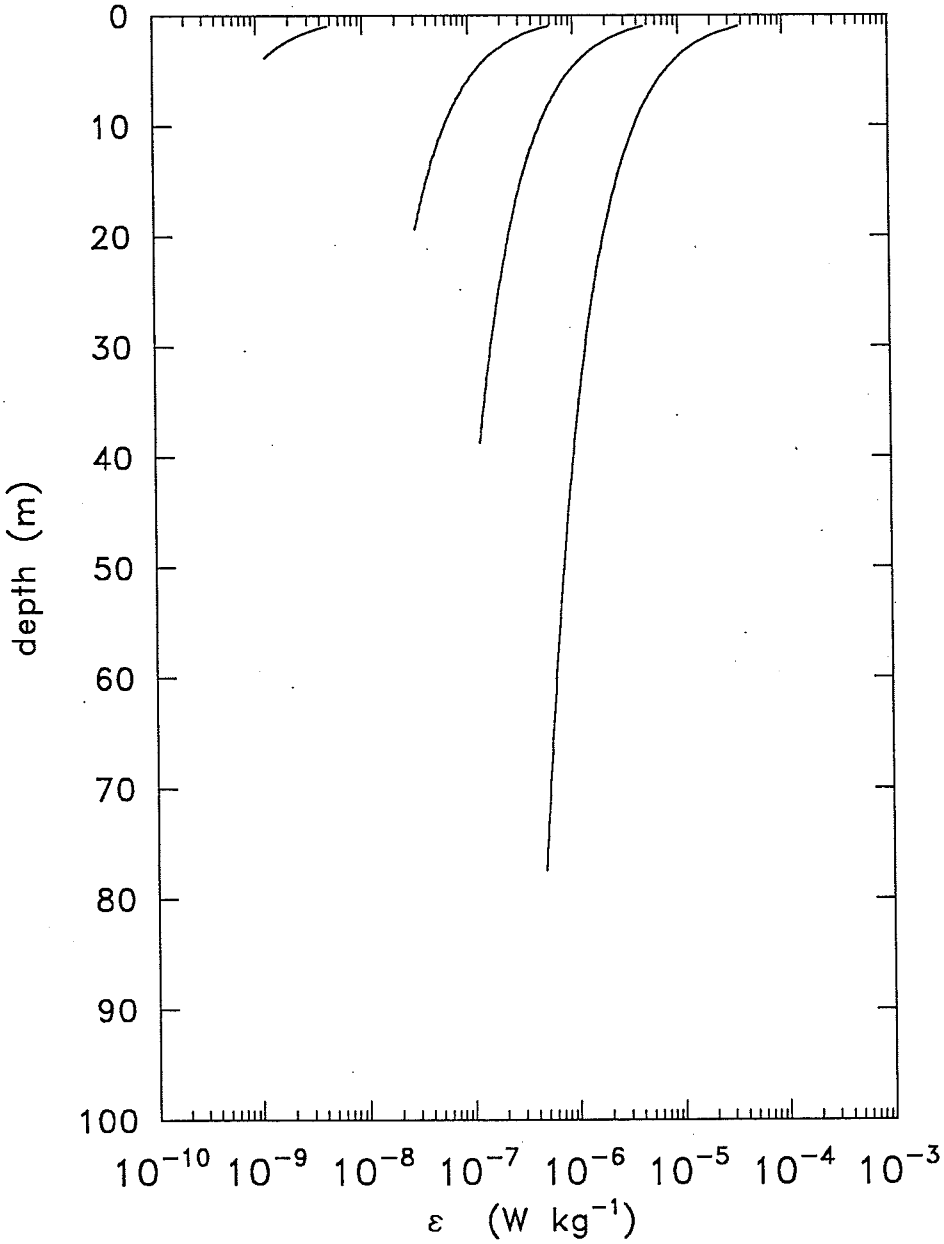

Figure 2: Dissipation profiles between 1 m and the base of the Ekman layer at 61°S. Four wind conditions are used; U_{10} = 1, 5, 10 and 20 m/sec (from the left to the right of profiles).

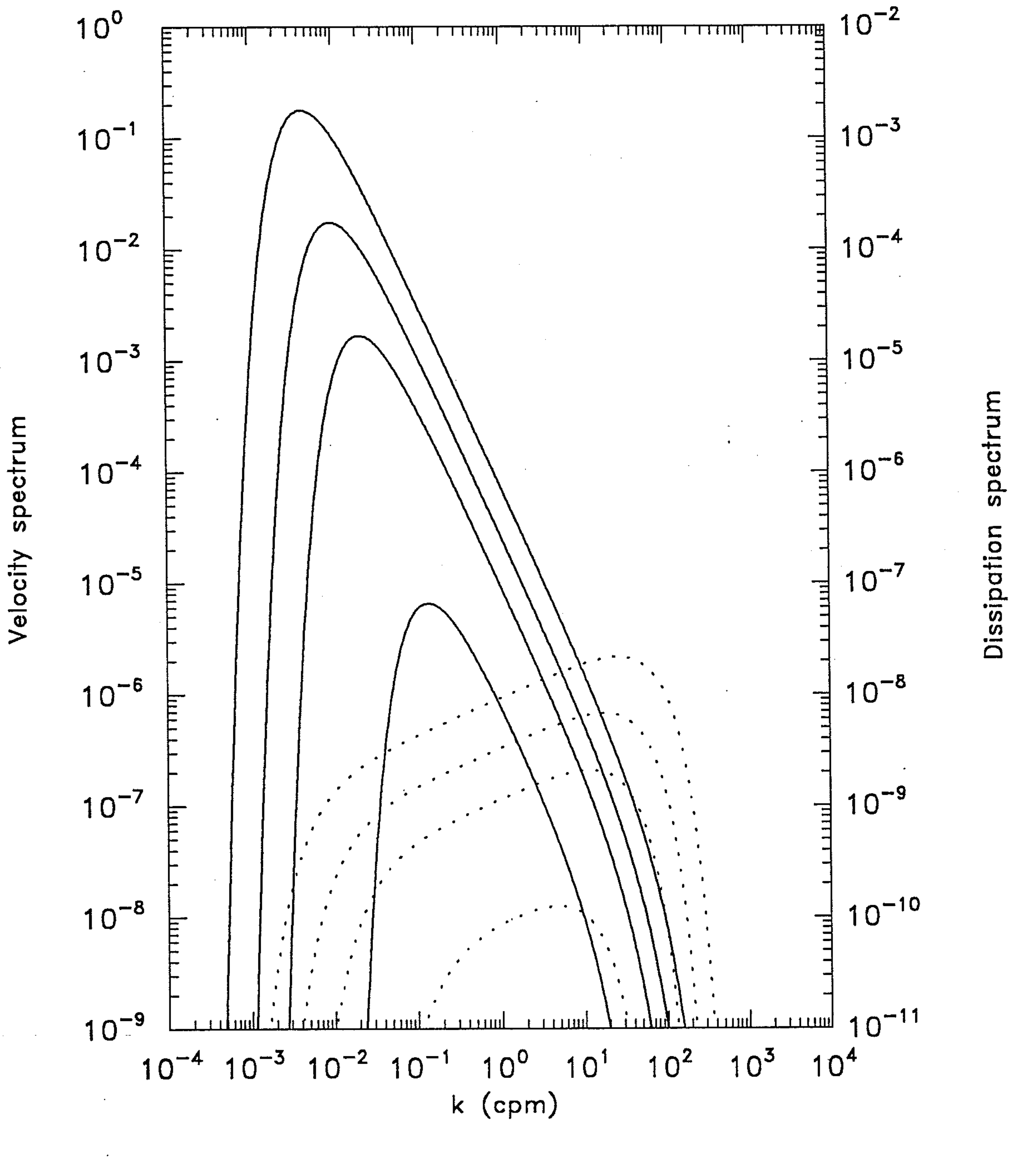

Figure 3: Turbulence velocity spectra (solid lines) and dissipation spectra (dotted lines). The dissipation rates are set by the average dissipation rate from Ekman layer model. Four different wind speeds are used U_{10}=20, 10, 5, and 1 m s^{-1} (from the top to the bottom). The energy contained eddy size is set by the Ozmidov scale $L_o=(\varepsilon N^{-3})^{1/2}$ where N=0.001 rad s^{-1} is used.

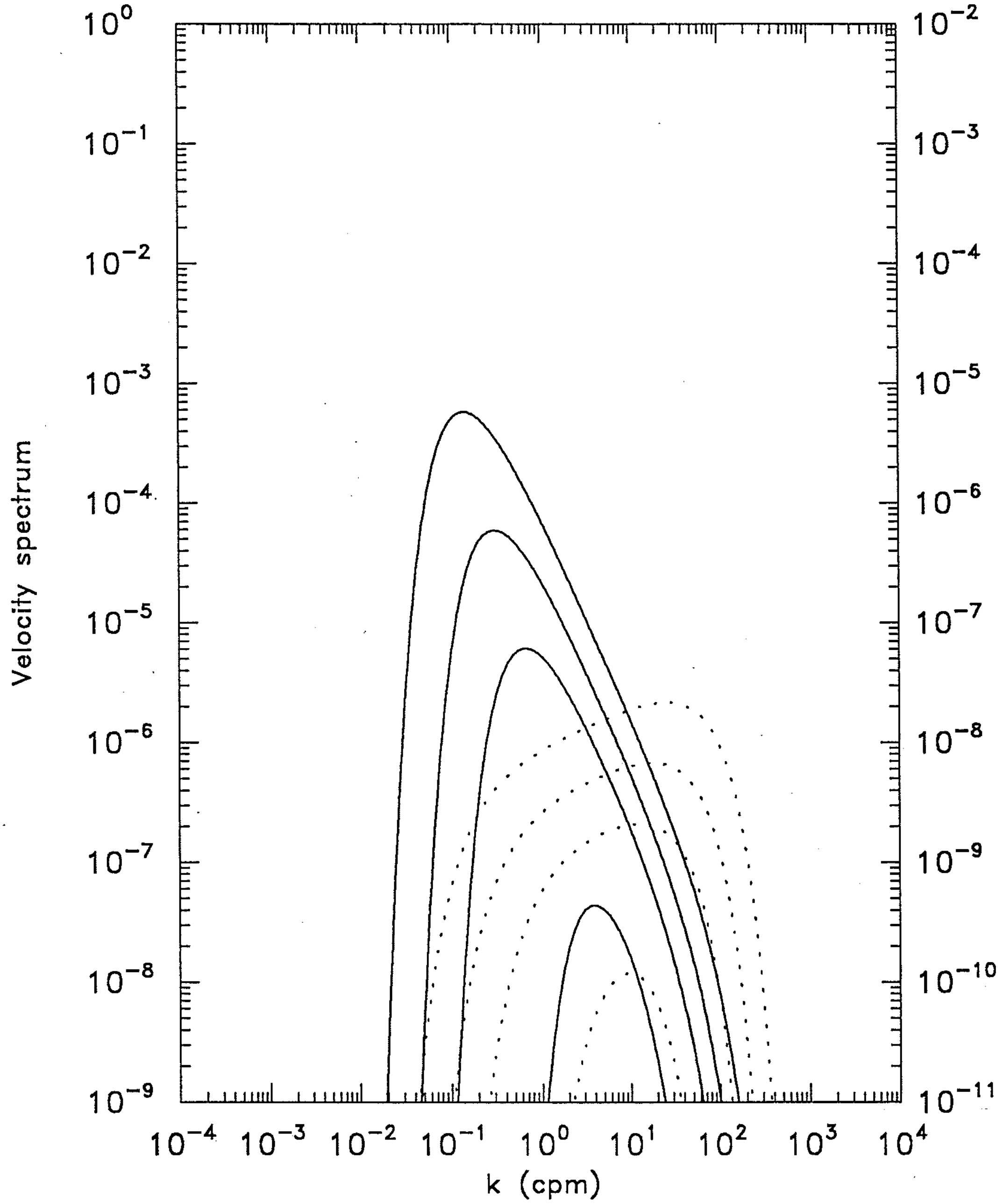

Figure 4: Same as Figure 3 with N=0.01 rad s^{-1}.

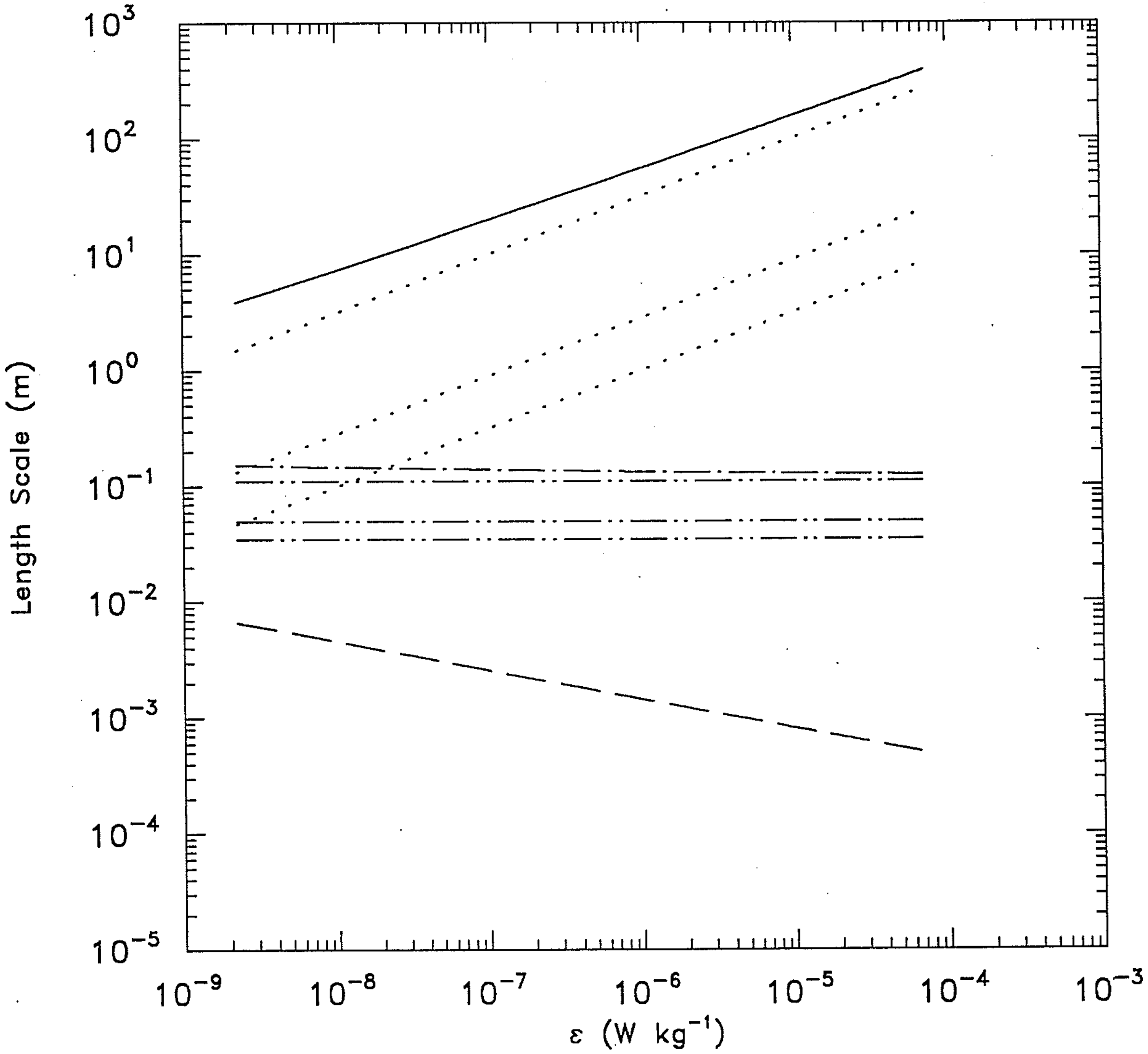

Figure 5: Length scales against dissipation rate. The Ekman layer depth is shown by a solid line and the dissipation rate associated with the length scale is the depth average value. The Ozmidov scale is calculated with three different N=0.001, 0.05 and 0.01 rad s^{-1} and three cases are shown by dotted lines (from the top to the bottom). The Taylor microscale depends on the energy containing eddy size. Two cases are shown the figure. The microscale based on the Ekman depth is shown by single chain dot and the Taylor microscale calculated from the Ozmidov scale appears as three lines of chains with double dots for N=0.001, 0.05 and 0.01 from the top line to the bottom line respectively. The Kolmogorov scale is depicted with a dashed line.

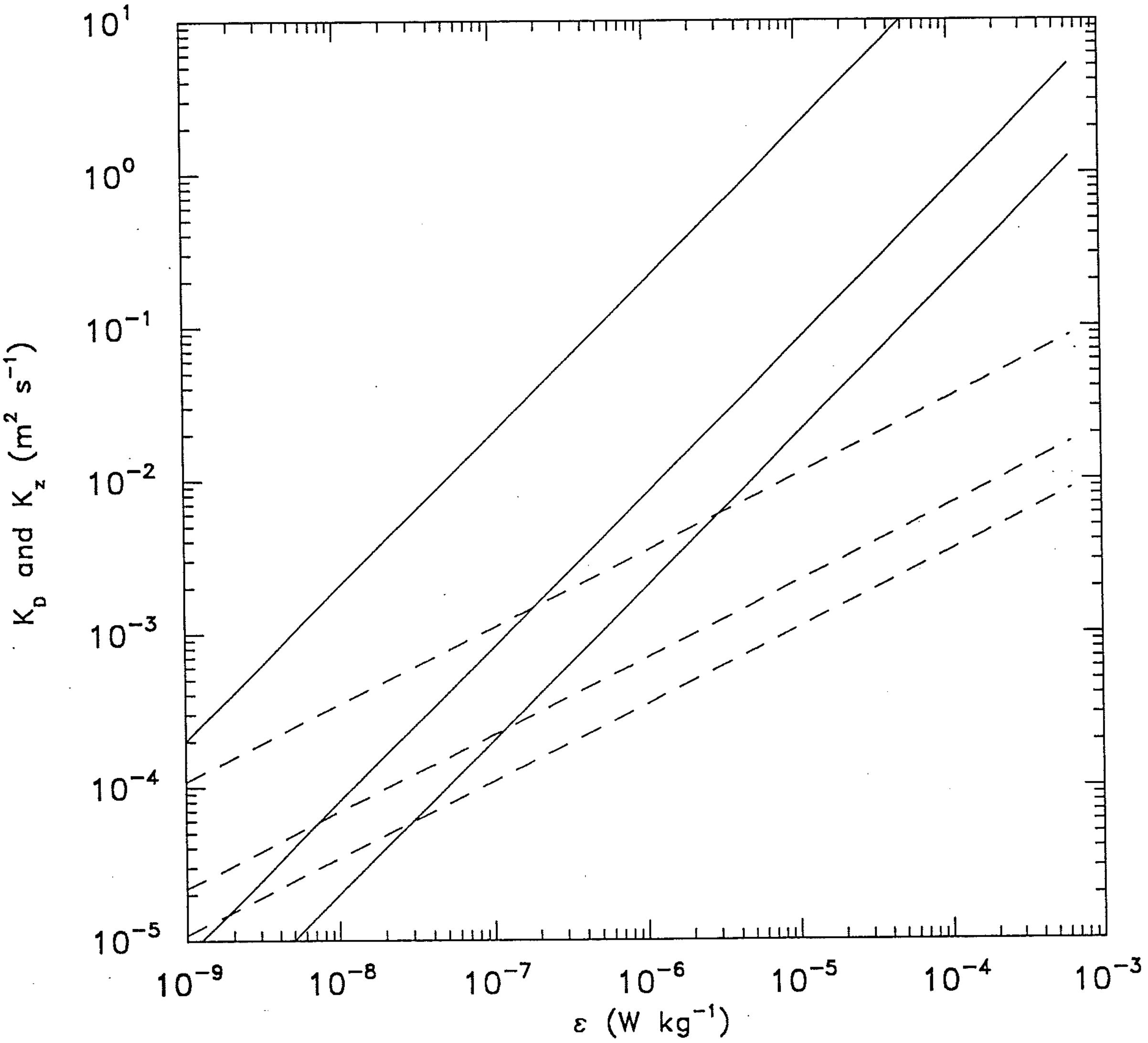

Figure 6: Two diffusion coefficient estimates K_D and K_z against dissipation rates. Solid lines show K_z and dotted lines are K_D. Three different N are used. The top of each line is N=0.001. The middle is N=0.05. The bottom is N=0.01.

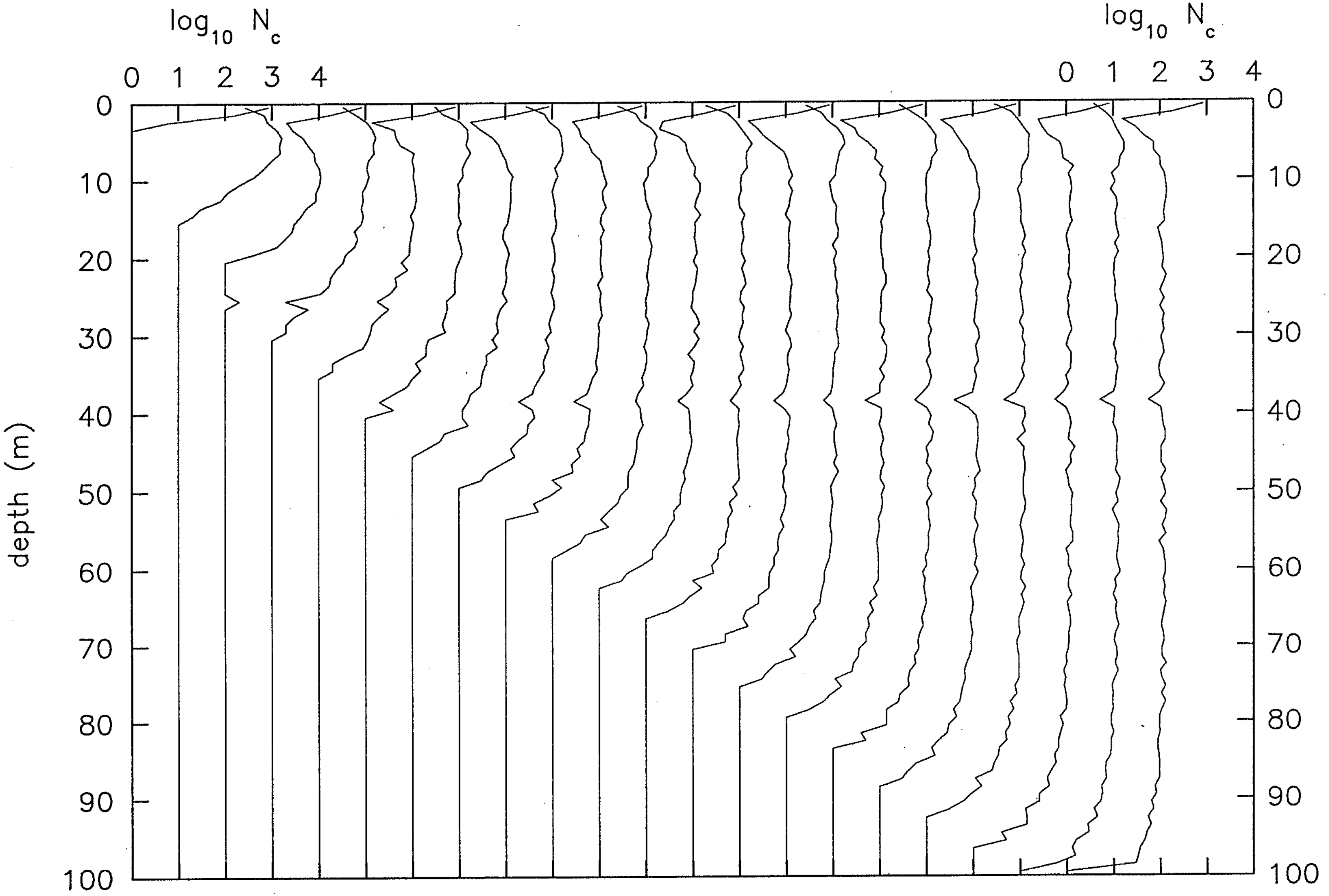

Figure 7: Particle distribution profiles at every 12 hours. Number of particles, N_c, in one-meter bin is shown in logarithmic scale base 10. Each profile offsets by one decade. Simulation Case *A*.

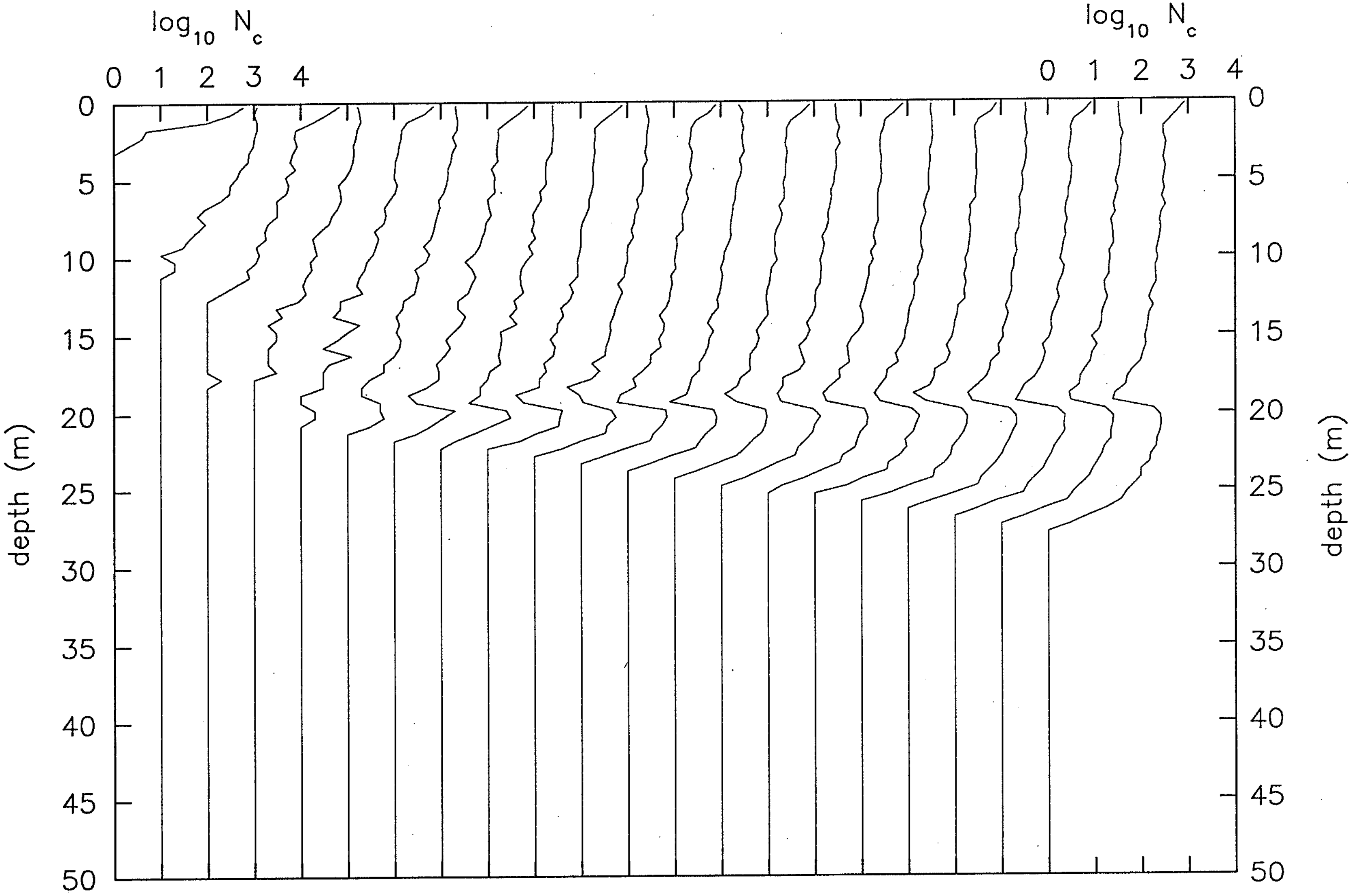

Figure 8: Same as Figure 7 for simulation Case *B*.

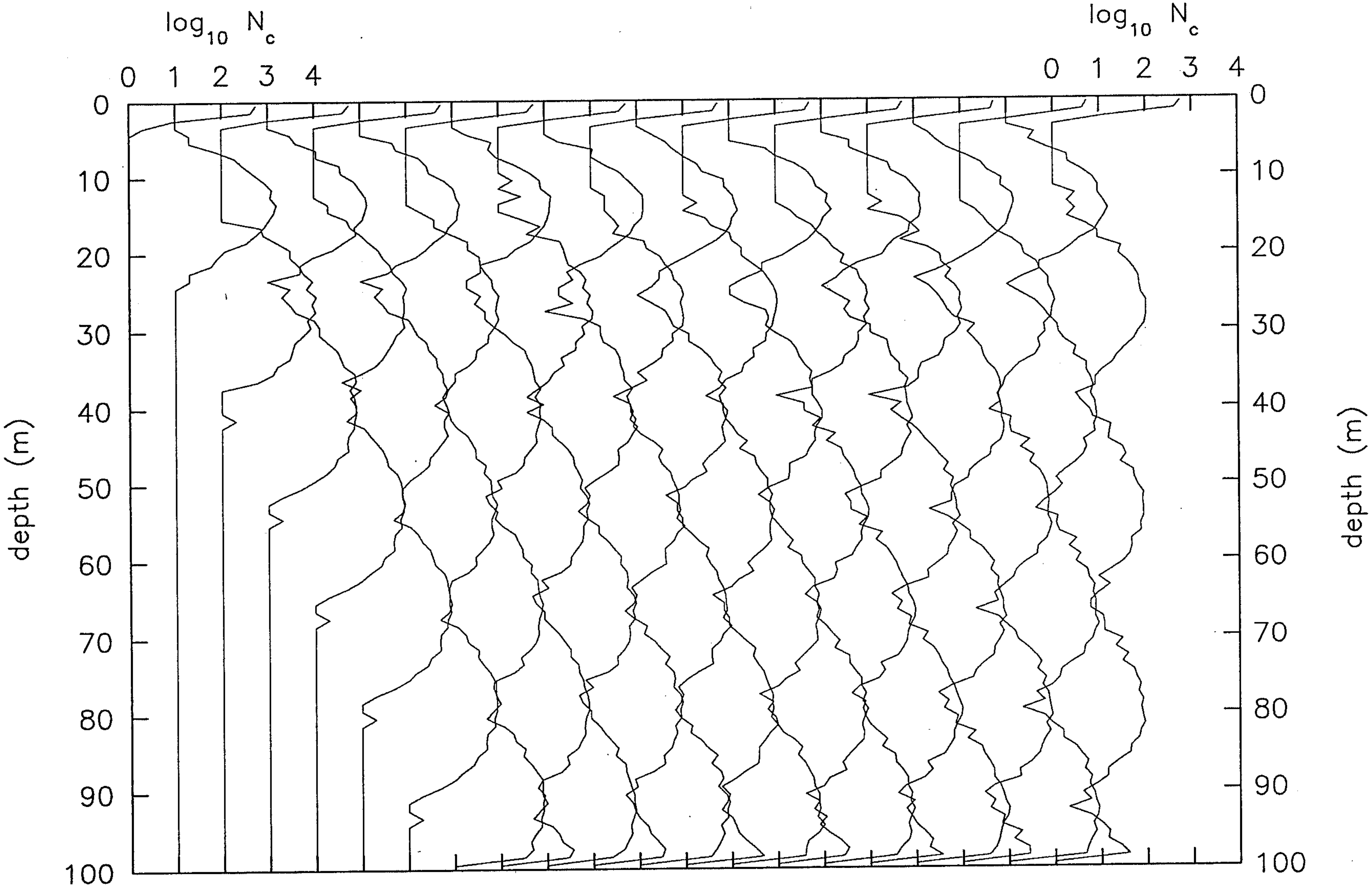

Figure 9: Same as Figure 7 for simulation Case *C*.

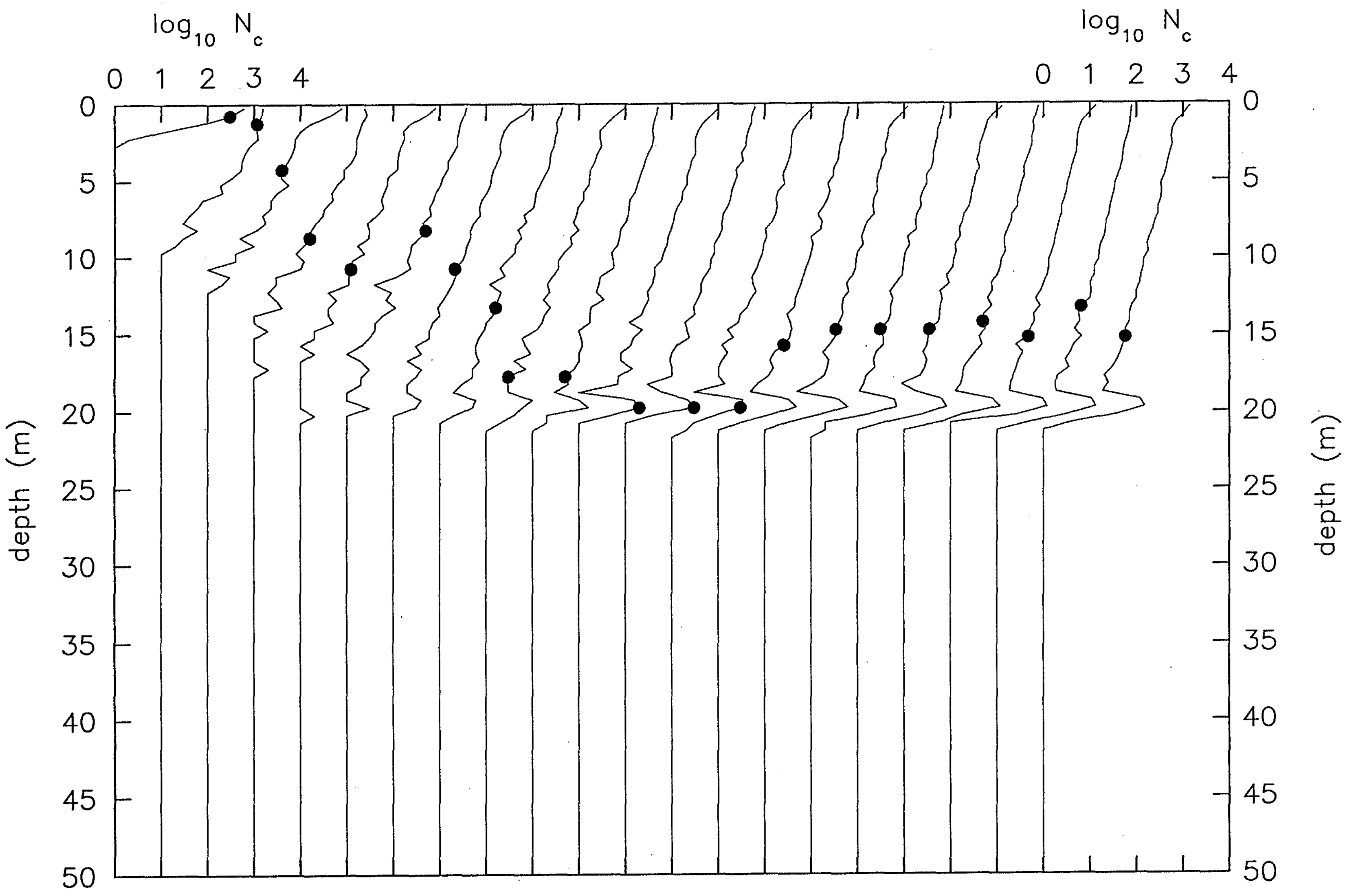

Figure 10: Same as Figure 7 for simulation Case *D*. Solid circles show trajectory of a particle over the whole simulation. The particle leaves the mixed layer roughly after 5 days and is trapped in the base of the mixed layer for a day and half. The particle, then, successfully re-enters in the mixed layer and stays in the mixed layer for the rest of the simulation period.

Légende du tableau

Table 1 Conditions physique et biologique pour les simulations. La vitesse de nage (ou d'enfoncement) W_B, était constante pour toute la simulation dans chaque cas. Le coefficient de diffusion K_D était fixe dans toutes les simulations. La valeur est proche de celle d'un cas où la vitesse du vent U_{10} serait d'environ 10 m/s. La profondeur de la couche de mélange a été déterminée d'après le modèle de couche d'Ekman.

Légendes des figures

Figure 1 Courbes de salinité / température / profondeur le long de 57°O relevées par le navire de recherche *Professor Siedlecki* au mois de janvier 1987. a) Courbes de salinité (S). b) Courbes de température (T). c) Courbes de fréquence de flottabilité (N). d) Emplacement des stations de salinité / température / profondeur Le numéro de la station de salinité / température / profondeur est indiqué sous la courbe de fréquence de flottabilité.

Figure 2. Courbes de dispersion entre 1 m et la base de la couche Ekman à 61°S. Quatre conditions de vents différents ont été utilisées; U_{10} = 1, 5, 10 et 20 m/sec (de la gauche à la droite des courbes).

Figure 3 Spectres de la vitesse de la turbulence (lignes continues) et spectres de dissipation (lignes en pointillé). Les taux de dissipation sont fixés au taux moyen de dissipation du modèle des couches d'Ekman. Quatre vitesses de vent différentes ont été utilisées; U_{10} =1, 5, 10 et 20 m/sec^1. L'énergie a été calculée en tenant compte de la taille du remous, et est fixé par l'échelle Ozmidov $L_o = (eN/^3)^{1/2}$ où N = 0.001 rayon/sec est utilisé.

Figure 4 Identique à la figure 3 avec N = 0.01 rayon sec^{-1}.

Figure 5 Echelles de longueur en fonction du taux de dissipation. La profondeur de la couche Ekman est indiqué par une ligne continue et le taux de dissipation associé avec l'échelle de longueur est la valeur moyenne de profondeur. L'échelle Ozmidov est calculée avec trois différents N = 0.001, 0.05 et 0.01 rayon/sec et trois cas sont indiqués par des lignes pointillées. La micro-échelle Taylor dépend de l'énergie calculée en tenant compte de la taille du remous. Deux cas sont illustrés sur la figure. La base de la micro-échelle sur la profondeur Ekman est indiqué par un pointillé simple et les échelles avec les échelles Ozmidov apparaissent en pointillé double. L'échelle Kolmogorov est representée par une ligne tiretée.

Figure 6 Deux estimations du coefficient de diffusion K_D et K_z en fonction de taux de dissipation. Les lignes continues indiquent K_z et les lignes pointillées, K_D. Trois N différents sont utilisés. Le haut de chaque ligne est N = 0.001. Le centre est N = 0.05. Le bas est N = 0.01.

Figure 7 Courbes de distribution des particules toutes les 12 heures. Le nombre de particules, N_c dans un réceptacle d'un mètre est indiqué sur une échelle logarithmique de base 10. Chaque courbe représente la situation de 10 jours en 10 jours. Cas de simulation *A*.

Figure 8. Identique à la figure 7 pour le cas de simulation *B*.

Figure 9. Identique à la figure 7 pour le cas de simulation *C*.

Figure 10. Identique à la figure 7 pour le cas de simulation *D*. Les cercles pleins montrent la trajectoire d'une particule sur toute la simulation. La particule quitte la couche mixte après environ 5 jours et est bloquée à la base de la couche mixte pour un jour et demi. Ensuite, la particule réussit à rentrer dans la couche mixte et y reste pendant le reste de la période de simulation.

Заголовки к таблицам

Таблица 1 Физические и биологические условия моделирования. Скорость плавания (или погружения), W_B была постоянной для случаев моделирования. Коэффицент рассеивания K_D был постоянным для всех прогонов модели. Его значение близко к случаю, когда скорость ветра U_{10} равнялась приблизительно 10 м/сек. Глубина смешивающего слоя была определена по модели слоя Экмана.

Подписи к рисункам

Рисунок 1 Профили STD вдоль 57°з.д., взятые НИС "Профессор Седлецкий" в январе 1987 г. a) Профили солености (S). b) Профили температуры (T). c) Профили частоты встречаемости слоя с нейтральной плавучестью (N). d) Местонахождение станций STD. Номера станций STD показаны под профилем частоты встречаемости слоя с нейтральной плавучестью.

Рисунок 2 Профили рассеивания между 1 м и основанием слоя Экмана на 61° ю.ш.Используются четыре условия ветра; U_{10} = 1, 5, 10 и 20 м/сек (слева направо по направлению профилей).

Рисунок 3 Спектр скоростей турбулентности (непрерывные линии) и спектры рассеивания (точечные линии).Коэффициенты рассеивания усреднены по модели слоя Экмана. Используется четыре скорости ветра; U_{10} = 1, 5, 10 и 20 м/сек. Отношение между энергией и размером водоворота составлено по шкале Озмидова $L_0 = (\varepsilon/N^3)^{1/2}$, где N=0,001 рад/сек.

Рисунок 4 То же, что изображено на рисунке 3, но в данном случае N=0,01 рад/сек.

Риунок 5 Шкалы длины по отношению к коэффициенту рассеивания. Непрерывная линия указывает глубину слоя Экмана, и коэффициент рассеивания, связанный со шкалой длины, является средним значением глубины. Шкала Озмидова рассчитана по трем разным значениям: N = 0,001, 0,05, и 0,01 рад/сек. Три случая показаны точечными линиями. Микромасштаб Тейлора зависит от размера содержащейся в водовороте энергии. На рисунке представлены два примера. Микромасштаб, основанный на глубине слоя Экмана, отмечен штрих-пунктирной линией и масштабы, основанные на шкале Озмидова, изображаются двойной штрих-пунктирной линией. Шкала Колмогорова изображается пунктирной линией.

Рисунок 6 Две оценки коэффициента распространения K_D и K_Z по отношению к коэффициенту рассеивания. Заштрихованные точки указывают K_Z и точечные линии - K_D Используются три разных N. Верхней точкой каждой линии является N=0,001. Средней точкой - N = 0,05. Нижней точкой - N = 0,01.

Рисунок 7 Профили распределения частиц через каждые 12 часов. Количество частиц N_c в однометровой ячее показано на логарифмической шкале (lg). Расстояние между профилями равно 10 дням. Случай моделирования Фб

Рисунок 8 То же, что на рисунке 7 для случая моделирования *B*.

Рисунок 9 То же, что на рисунке 7 для случая моделирования *C*.

Рисунок 10 То же, что на рисунке 7 для случая моделирования *D*. Заштрихованные точки показывают траекторию частицы в течение всего моделирования Частица покидает смешивающий слой приблизительно через 5 дней и задерживается в основании смешивающего слоя на полтора дня. Затем частица успешно снова входит в смешивающий слой и остается там до окончания периода моделирования.

Encabezamiento de la Tabla

Tabla 1 Condiciones físicas y biológicas para simulaciones. La velocidad de natación (o hundimiento), W_B, se mantuvo durante la simulación de cada caso. Se fijó el coeficiente de difusión K_D para todas las simulaciones. El valor está próximo a un caso cuando la velocidad del viento U_{10} es aproximadamente 10 m s^{-1}. La profundidad de la capa mixta fue determinada a partir de la moda de la capa Ekman.

Leyendas de las Figuras

Figura 1a Perfiles STD (salinidad, temperatura, profundidad) a lo largo de los 57°O tomados por el B/I *Professor Siedlecki* en enero de 1987. a) Salinidad (S) perfiles. b) Temperatura (T) perfiles. c) Frecuencia de flotabilidad (N) perfiles. d) Localización de las estaciones STD. El número de estación STD se muestra debajo del perfil de frecuencia de flotabilidad.

Figura 2 Perfiles de disipación entre 1 m y la base de la capa Ekman a los 61°S. Se usan cuatro condiciones de viento; U_{10} = 1,5,10, y 20 m sec^{-1} (de izquierda a derecha de los perfiles).

Figura 3 Espectro de velocidad de turbulencia (líneas sólidas) y espectro de disipación (líneas de puntos). Los índices de disipación se establecen por el índice de disipación promedio del modelo de la capa Ekman. Se utilizan cuatro velocidades de viento diferentes U_{10} = 1,5,10 y 20 m sec^{-1}. La energía contenida en un remolino de un tamaño dado se establece por la escala Ozmidov $L_o = (N^{-3})^{1/2}$ donde N = 0.001 rad sec^{-1} es utilizado.

Figura 4 Igual que en la Figura 3 con N = 0.01 rad sec^{-1}.

Figura 5	Escala de longitud como función del índice de disipación. La profundidad de la capa Ekman está indicada con una línea sólida y el índice de disipación asociado con la escala de longitud es el valor promedio de profundidad. La escala Ozmidov se calcula con tres N = 0.001, 0.05 y 0.01 rad sec^{-1} diferentes y tres casos están indicados mediante líneas de puntos. La micro escala Taylor depende de la energía que contiene remolinos de un tamaño dado. Se muestran dos casos en la Figura. La base de la micro escala en la profundidad Ekman está indicada por una cadena de puntos sencilla y las escalas Ozmidov aparecen con una cadena de puntos doble. La escala Kolmogorov está representada con una línea quebrada.
Figura 6	Dos estimaciones del coeficiente de difusión K_D y K_Z en relación a los índices de disipación. Las líneas sólidas representan K_Z y las líneas de puntos K_D. Se utilizan tres N diferentes. La parte superior de cada linea es N = 0.001. La parte central es N = 0.05. La parte inferior es N= 0.01.
Figura 7	Perfiles de la distribución de partículars cada 12 horas. Caso de simulación *A*.
Figura 8	Perfiles de la distribución de partículas cada 12 horas. Caso de simulación *B*.
Figura 9	Perfiles de la distribución de partículas cada 12 horas. Caso de simulación *C*.
Figura 10	Perfiles de la distribución de partículas cada 12 horas. Caso de simulación *D*.

JOINT POLISH/AMERICAN HYDROACOUSTIC SURVEY OF ELEPHANT ISLAND AND THE VICINITY OF KING GEORGE ISLAND, 1988

M.C. Macaulay

Abstract

The hydroacoustic survey found a low krill abundance in most areas covered by last years survey. The total biomass in the vicinity of Elephant Island was estimated from 120 kHz data to be 260k tonnes and that in the Bransfield Strait south of King George Island was 39k tonnes for a total of 299k tonnes in the combined areas. The estimated 200 kHz survey data were higher, giving 715k tonnes near Elephant Island and 83k tonnes in the Bransfield Strait. The survey results apply to 7 453 n miles^2 near Elephant Island and 2 894 n miles^2 in the Bransfield Strait. The full survey found (120 kHz data) 385k tonnes (in 7 787 n miles^2) in the Bransfield Strait and the area north of King George Island and 309k tonnes (in 8 836 n m^2) in the expanded area around Elephant Island.

Résumé

Une campagne d'étude hydroacoustique a permis de détecter un niveau d'abondance de krill peu élevé dans la plupart des régions ayant fait l'objet d'une prospection l'année passée. D'après les données établies sur 120 kHz, la biomasse totale aux alentours de l'île de l'Eléphant a été estimée à 260 kilotonnes. Dans le détroit de Bransfield, au sud de l'île du Roi George, elle a été estimée à 39 kilotonnes, soit un total de 299 kilotonnes pour les deux régions. Les données d'étude estimées sur 200 kHz étaient plus élevées, indiquant une biomasse de 715 kilotonnes près de l'île de l'Eléphant et 83 kilotonnes dans le détroit de Bransfield. Les résultats de l'étude s'appliquent à 7453 milles marins carrés près de l'île de l'Eléphant et 2894 mille marins carrés dans le détroit de Bransfield. L'ensemble de l'étude (données obtenues sur 120 kHz) indiquait la présence de 385 kilotonnes (sur 7787 milles marins carrés) dans le détroit de Bransfield et la région au nord de l'île du Roi George, et de 309 kilotonnes (sur 8836 milles marins carrés) dans la région qui s'étend autour de l'île de l'Eléphant.

Резюме

Результаты гидроакустических съемок показали наличие небольшого количества криля в большинстве районов, охваченных съемкой предыдущего года. По данным, полученным при работе на частоте в 120 кГц, общая биомасса в районе острова Элефант была оценена в 260 тысяч тонн, а в проливе Брансфилда, к югу от острова Кинг-Джордж, - в 39 тысяч тонн, что по обоим районам вместе дает 299 тысяч тонн. При работе на частоте 200 кГц оценки были выше: 715 тысяч тонн около острова Элефант и

83 тысячи тонн в проливе Брансфилда. Результаты съемки применимы к акватории в 7453 кв. морских мили у острова Элефант и 2894 кв. морских мили - в проливе Брансфилда. Общие результаты съемок (по данным при работе на частоте в 120 кГц): 385 тысяч тонн (акватория в 7787 кв. морских миль) в проливе Брансфильда и районе к северу от острова Кинг-Джордж и 309 тысяч тонн (акватория в 8836 кв. морских миль) в большем районе вокруг острова Элефант.

Resumen

La prospección hidroacústica encontró una baja abundancia de krill en la mayoría de las áreas cubiertas por la prospección del año pasado. La biomasa total en las proximidades de la isla Elefante estimada a partir de los datos correspondientes a los 120 kHz, resultó ser de 260k toneladas mientras que en el estrecho de Bransfield al sur de la isla Rey Jorge fue de 39k toneladas dando un total de 299k toneladas en las áreas combinadas. Los datos estimados de la prospección en 200 kHz fueron mayores, dando unas 715k toneladas cerca de la isla Elefante y unos 83k toneladas en el estrecho de Bransfield. Los resultados de la prospección corresponden a 7 453 nm^2 cerca de la isla Elefante y a 2 894 nm^2 en el estrecho de Bransfield. La prospección completa (datos correspondientes a 120 kHz) encontró 385k toneladas (en 7 787 nm^2) en el estrecho de Bransfield y en el área al norte de la isla Rey Jorge, y 309k toneladas (en 8 836 nm^2) en el área extendida en los alrededores de la isla Elefante.

1. INTRODUCTION

The joint Polish/American hydroacoustic cruise was conducted as a response to provide input for the CCAMLR Ecosystem Monitoring Program and for providing guidance to the US delegation to the CCAMLR concerning krill and other prey species. This research involves an annual Antarctic field program, analysis and interpretation of data, and preparation of scientific papers. This was the second of a series of similar cruises.

The principal objectives of the cruise focus on priorities identified by the CCAMLR Ecosystem Monitoring Working Group. These include:

(1) Establishment of a standard survey encompassing Elephant Island and King George Island.

(2) Establishment of baseline studies coordinated with predator (e.g. seal and penguin) populations within the survey area.

(3) Establish a longterm monitoring effort for a statistically-based evaluation of net and acoustic sampling gear bias.

The last topic has not been done in a consistent or systematic manner and needs to be addressed to validate the results of any survey effort and to assist with determination of statistical confidence limits about hyrdroacoustic and net estimates of abundance. The survey and baseline studies will permit evaluation of interannual variation in population of krill and other prey as well as monitor distribution. These topics directly respond to identified CCAMLR data needs and will be closely coordinated with us and other nations' research efforts.

2. MATERIALS AND METHODS

The hydroacoustic survey was conducted from 22 January 1988 to 5 February 1988 and covered 1 693 n miles. The area surveyed is shown on the cruise track map (Figure 1). The cruise departed Punta Arenas, Chile on 18 January 1988 and returned to Rio de Janeiro, Brazil on 27 February 1988. The survey of Elephant Island began on 22 January and ended on 31 January. The survey of King George Island and Bransfield Strait began on 31 January and was completed on 5 February. Additional special studies were done north of Elephant Island from 21 January until 22 January and from 5 February until 14 February when the return to Rio was begun. All sampling was done from the R/V *Professor Siedlecki*, a 300 ft stern trawler equipped for fisheries and oceanographic research. The vessel consistently maintained speeds greater than 6 knots (day and night) in all sea states encountered (including force 8 winds and fog).

This joint survey was conducted using simultaneously operated acoustic systems utilizing a towed system (American) and the hull mounted system (Polish) in the R/V *Professor Siedlecki*. There were no indications of interference between systems due to the operating frequencies having no common multiple (50 kHz and 200 kHz, American; 120 kHz Polish). The coverage by frequency/depth/method of integration is as follows: 120 kHz/6-180 m/analog; 50 kHz/6-250 m/digital; 200 kHz/6-250 m/digital. Echo data were processed by analog integrator (120 kHz) or processed using the software and hardware developed at NWAFC (50 kHz and 200 kHz). The methods, constants and target-strengths used for processing the 120 kHz and 200 kHz data presented in this report are included in Appendix.

The areas surveyed were Bransfield Strait in proximity to King George Island (7 787 n miles^2 including 2 894 n miles^2 of areas surveyed in 1987) including the area north of King George Island and the vicinity of Elephant Island (8 836 n miles^2 including 7 453 n miles^2 in areas surveyed in 1987; Figure 1). The survey was conducted 24 hours a day, incorporating minimal interruption of survey mode. These breaks were limited to bongo-net hauls (reduced speed from 6-8 knots to 3 knots for 45 min) spaced approximately every 30 n miles and RMT-8 hauls taken at several locations for length-frequency of ensonified populations. Noon productivity stations incorporating a hydrocast and STD cast were taken daily. The methods used to calculate abundance and biomass are included as an appendix.

3. RESULTS

The results of the analog integration (120 kHz data) gave an estimate of 39k tonnes (in 2 894 n miles^2) in the Bransfield Strait and 260k tonnes (in 7 453 n miles^2) in the Elephant Island area for a total of 299k tonnes in the areas surveyed last year. The full survey found (120 kHz data) 385k tonnes (in 7 787 n miles^2) in the Bransfield Strait and the area north of King George Island and 309k tonnes (in 8 836 n miles^2) in the expanded area around Elephant Island. This is probably a minimum figure because the 120 kHz system had a higher threshold of detection than the 200 kHz system. It is, however, much lower than last year and closer to the estimates observed in 1984 in this area, i.e. a low density. The results from the 50 kHz and 200 kHz systems were stratified to compare with the 120 kHz system and to provide additional independent estimates of abundance and biomass. The areas and statistics for sub-blocks are shown in Table 1 (the geographic boundaries for these areas and sub-blocks are shown in Figure 1). The mean density in each block is shown under the column labelled "Actual Mean, 120 kHz" and is in tonnes per n miles^2. The biomass for each block estimated from 120 kHz data is given under the column labelled "Est. Total, 120 kHz" and is in thousand tonnes. Similar columns are presented for 200 kHz data estimated from the 120 kHz data based on ratios established last year. The 200 kHz data will be presented in the final cruise report as well as the 50 kHz data. Table II presents a complete listing of survey data including the areas not surveyed last year. Table III presents the electrical and acoustic parameters of the systems used.

4. DISCUSSION

The survey in areas covered last year were very comparable (2 894 n miles^2 in 1988 vs 3 000 n miles^2 in 1987 for the Bransfield Strait; 7 453 n miles^2 in 1988 vs 7 346 n miles^2 in 1987 for Elephant Island) (Figure 2). The additional areas covered were to the west of Elephant Island (1 383 n miles^2) and east of Elephant Island (336 n miles^2), and the area north of King George Island (3 239 n miles^2) so that the total survey represents 16 623 n miles^2 in 1988 vs 10 346 n miles^2 in 1987. The mean abundance (tonnes/n miles^2) by block for 120 kHz data and estimated 200 kHz data (Figure 3) is about half that of 1987 as is the total biomass (Figure 4). The distribution of abundance and biomass was much more even between blocks in 1988 instead of highly variable as it was in 1987. The mean abundance and total biomass for 1987 is shown in Figure 5 and the comparison of total biomass in the survey area in 1987 and 1988 (120 kHz data) is shown in Figure 6. A joint scientific paper will report the results of the full comparison of these data.

REFERENCES CITED

JOHANNESSON, K.A. and R.B. MITSON. 1983. Fisheries Acoustics. A practical manual for aquatic biomass estimation. FAO Fisheries Tech. Paper 240. FIRM/t240. 249 PP. FAO Rome.

KRISTENSEN, A. and J. DALEN. 1986. Acoustic estimation of size distribution and abundance of zooplankton. J. Acoust. Soc. Am 80: 601-611.

MACAULAY, M.C., T.S. ENGLISH and O.A. MATHISEN. 1984. Acoustic Characterization of Antarctic krill (*Euphausia superba)* swarms from Elephant Island and Bransfield Strait. J. of Crustacean Biology. Vol 4 (Special No. 1) 16-44 pp.

MACAULAY, M.C., K.L. DALY and O.A. MATHISEN (in prep.) Inter-year variation in the abundance and distribution of Antarctic krill (*Euphausia superba*) near Elephant Island and the South Orkney Islands.

Post-FIBEX Acoustic Workshop. Frankfurt/Mein, FRG 3-14 September 1984. BIOMASS Report Series No. 40: 106 pp.

APPENDIX

CALCULATION OF TARGET STRENGTH AND SYSTEM CONSTANTS

The R/V *Professor Siedlecki* hull mounted system consisted of Simrad[*] EK-120 sounder coupled to a Simrad QM MK II analog echo integrator. A Simrad EK-38 sounder was used for auxiliary observation of targets outside the range of the EK-120 (i.e. below 130 m). Before the cruise, the equipment was calibrated in acoustic and electrical units. These values are presented in Table 2. Echo integration was done for the depths of 6 to 180 m. Because the range of the EK-120 TVG is limited to 110 m, during calculations the results from 110 to 180 m were corrected. The basis for the estimation of krill biomass was the calculation of the mean value of volume back-scattering-strength S_v for each 1 n mile of vessel track following the method described in BIOMASS Report Series No. 40. Mean volume back-scattering is here defined as:

$$\overline{S}_v = -75.81 + 10 \log \overline{I} \qquad 1.0$$

where $\overline{S}_v$ is mean volume back-scattering-strength; $\overline{I}$ is echo integrator deflection for 1 n mile segment (in n miles). The mean abundance of krill per unit of surface area was calculated using:

$$\overline{\sigma} = 10^{0.1(S_v + 10 \log R - TS)} \qquad 1.1$$

where $\overline{\sigma}$ is mean abundance of krill (number/m^2); R is width of integration layer (110 m value was assumed) and TS is mean target strength of ensonified krill. The target strength to length relation used was:

$$\overline{TS} = 19.9 \log \overline{L} - 95.7 \text{ (db)} \qquad 1.2$$

where $\overline{L}$ is the length of krill in mm. Mean surface density or abundance (tonnes/nm^2) was calculated from the following formula:

$$\overline{B} = 3.43 * \overline{\sigma} * \overline{w} \qquad 1.3$$

where $\overline{B}$ is mean surface abundance of biomass; $\overline{w}$ is the mean weight of krill (in g) and is mean density of krill from 1.1 above mean weight of krill was calculated from the relation:

$$\overline{w} = 0.000925 * \overline{L}^{3.55} \qquad 1.4$$

where $\overline{w}$ is weight of krill (mg) and $\overline{L}$ is length of krill (mm).

The towed acoustic systems used from R/V *Professor Siedlecki* consisted of a BIOSONICS Inc. Model 101 sounder operating at 200 kHz and coupled to a Hewlett Packard A900 computer for real-time digital integration of the data. A BIOSONICS Inc. Model 101 sounder operating at 50 kHz was also used. The 50 kHz envelope detected signal was recorded in FM mode on an instrument recorder for post cruise analysis. Before the cruise, the

---

[*] Reference to trade names or commercial firms does not imply endorsement by the National Marine Fisheries Service (NMFS), NOAA.

equipment was calibrated in acoustic and electrical units. These values are presented in Table 2. Analysis of the 200 kHz acoustic data follows the methods of Johanneson and Mitson, 1983 and Macaulay et al, 1984. Measurements of envelope detected voltage for each ping were made every 0.1 m (a digitizing rate of 7.5 kHz), then squared and summed into 1 m depth intervals and averaged for 60 pings (1 min). The estimate of average density in each depth interval and for the total column selected (6-250 m) was then calculated. One-min estimates then were recorded on magnetic disk files for further analyses. Estimates of average density were determined for intervals down to 250 m or bottom whichever occurred first. Provision for elimination of the bottom signal is made in the system by means of a combination software and hardware bottom detection methods. For comparison with 120 kHz data, the data were stratified for the depth bin 6-180 m. The target strength (1.2 above) and length-weight (1.4 above) relations were used for calculations of density and biomass. This was done on the basis of Kristensen and Dalen (1986) which indicates no correction for frequency is necessary between 120 kHz and 200 kHz, unlike that proposed in BIOMASS Report No. 40.

Table 1: Comparative mean abundance and total biomass for blocks also surveyed in 1987.

BLOCK	DIST. n miles	AREA	ACTUAL MEAN 120 kHz	EST. MEAN* 200 kHz	ACTUAL TOTAL 120 kHz tonnes/1000	EST. TOTAL* 200 kHz tonnes/1000
BRANSFIELD STRAIT (BS)						
A5	37.00	567.00	11.02	47.84	6.25	27.13
B5	44.00	811.00	7.06	11.72	5.73	9.50
A6	34.00	826.00	21.27	35.06	17.57	28.96
B6	27.00	690.00	13.12	25.37	9.05	17.51
SUBTOT (BS)	142.00	2894.00	52.47	119.99	38.60	83.10
Avg. (BS)	35.50	723.50	13.12	30.00	9.65	20.77
ELEPHANT ISLAND (EI)						
C1	9.00	223.00	18.70	52.08	4.17	11.61
D1	61.00	446.00	66.98	167.70	29.87	74.79
E1	42.00	446.00	35.89	176.38	16.01	78.67
C2	63.00	734.00	48.64	135.47	35.70	99.43
D2	274.00	881.00	42.25	124.10	37.22	109.33
E2	149.00	882.00	29.50	108.49	26.02	95.69
C3	132.00	1013.00	39.26	89.06	39.77	90.22
D3	109.00	742.00	21.74	34.77	16.13	25.80
E3	99.00	803.00	33.03	83.26	26.52	66.86
C4	62.00	142.00	65.07	80.68	9.24	11.46
D4	25.00	570.00	26.47	66.96	15.09	38.17
E4	56.00	571.00	7.47	22.41	4.27	12.80
SUBTOT (EI)	1081.00	7453.00	435.00	1141.36	260.01	714.82
Avg. (EI)	90.08	621.08	36.25	95.11	21.67	59.57
G. TOTAL	1223.00	10347.00			298.61	797.92

* 200 kHz data estimated from 120 kHz data using 1987 ratios.

Table 2: Mean abundance and total biomass in blocks surveyed in 1988.

BLOCK	DIST. n miles	AREA	ACTUAL MEAN 120 kHz	EST. MEAN* 200 kHz	ACTUAL TOTAL 120 kHz tonnes/1000	EST. TOTAL* 200 kHz tonnes/1000
BRANSFIELD STRAIT (BS)						
AA34	122.00	997.00	86.71	207.75	86.45	207.13
A3	19.00	432.00	91.39	218.96	39.48	94.59
B3	20.00	289.00	57.96	138.85	16.75	40.13
A4	73.00	803.00	139.63	334.53	112.12	268.63
B4	35.00	576.00	38.78	92.90	22.33	53.51
C4	11.00	142.00	65.07	155.88	9.24	22.13
AA5	35.00	579.00	33.05	79.19	19.14	45.85
A5	37.00	567.00	11.02	47.84	6.25	27.13
B5	44.00	811.00	7.06	11.72	5.73	9.50
C5	30.00	420.00	26.13	62.60	10.97	26.29
AA6	18.00	413.00	48.76	116.82	20.14	48.25
A6	34.00	826.00	21.27	35.06	17.57	28.96
B6	27.00	690.00	13.12	25.37	9.05	17.51
C6	20.00	242.00	41.64	99.75	10.08	24.14
SUBTOT (BS)	525.00	7787.00	681.58	1627.22	385.30	913.74
Avg. (BS)	37.50	556.21	48.68	116.23	27.52	65.27
ELEPHANT ISLAND (EI)						
C1	9.00	223.00	18.70	52.08	4.17	11.61
D1	61.00	446.00	66.98	167.70	29.87	74.79
E1	42.00	446.00	35.89	176.38	16.01	78.67
F1	10.00	223.00	46.77	140.32	10.43	31.29
BC2	63.00	734.00	48.64	135.47	35.70	99.43
D2	274.00	881.00	42.25	124.10	37.22	109.33
E2	149.00	882.00	29.50	108.49	26.02	95.69
F2	30.00	441.00	45.77	137.31	20.19	60.55
BC3	132.00	1013.00	39.26	89.06	39.77	90.22
D3	109.00	742.00	21.74	34.77	16.13	25.80
E3	99.00	803.00	33.03	83.26	26.52	66.86
F3	29.00	434.00	27.01	81.04	11.72	35.17
BC4	62.00	142.00	65.07	80.68	9.24	11.46
D4	25.00	570.00	26.47	66.96	15.09	38.17
E4	56.00	571.00	7.47	22.41	4.27	12.80
F4	18.00	285.00	24.58	73.73	7.00	21.01
SUBTOT (EI)	1168.00	8836.00	579.14	1573.76	309.35	862.85
Avg. (EI)	73.00	552.25	36.20	98.36	19.33	63.93
G. TOTAL	1693.00	16623.00			694.65	1776.59

* 200 kHz data estimated from 120 kHz data using 1987 ratios

Table 3: Electro-acoustic characteristics of sounder systems

Manufacturer	BIOSONICS Model 101	BIOSONICS Model 101	SIMRAD EK120
Frequency	50 kHz	200 kHz	120 kHz
Source Level dB//1 uPa ref 1 m	205.4	224.4	219.0
Receiving Sensitivity dB//IV per uPa	-115.7	-132.9	-109.0
Beam pattern (directivity)	12.9	29.5	
Pulse Length (msec)	0.6	0.6	0.6
Time Varied Gain (TVG)	digital	digital	analog

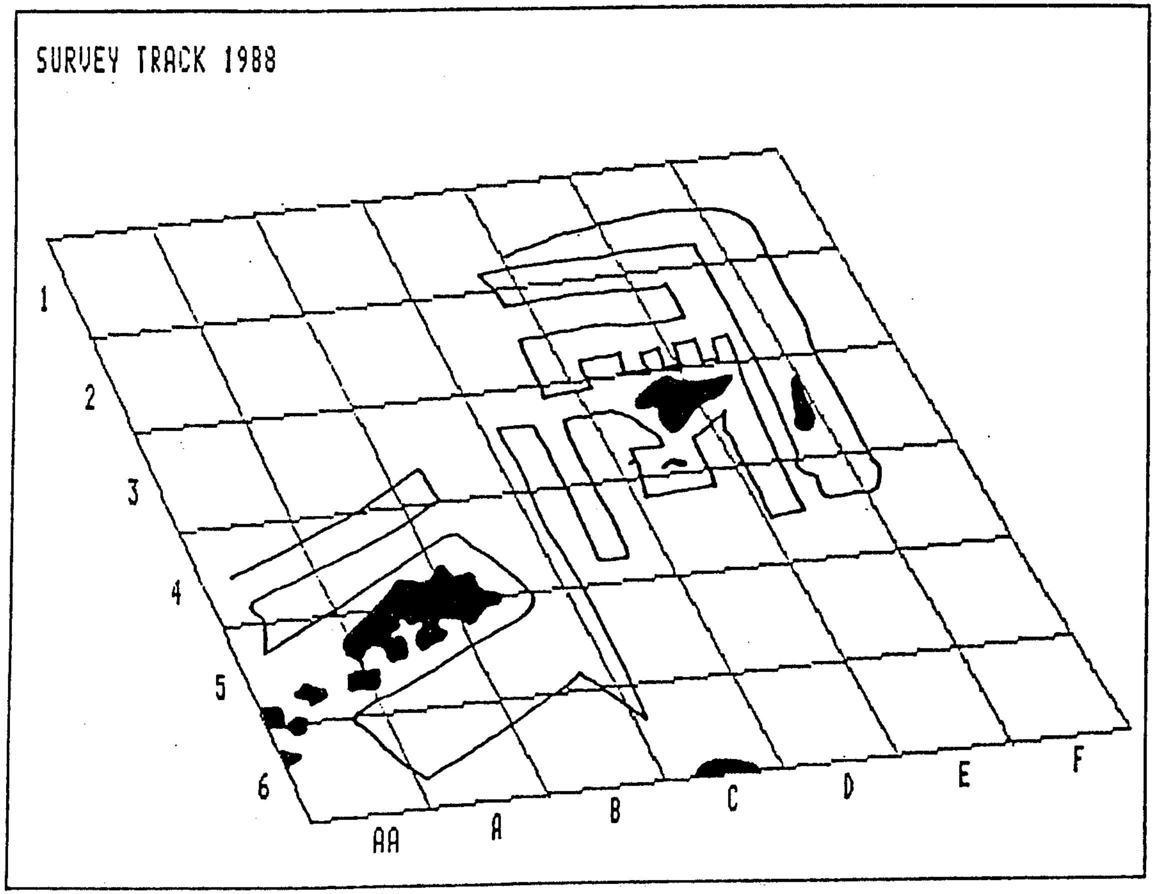

Figure 1: Survey track and block locations in the area of Bransfield Strait and Elephant Island.

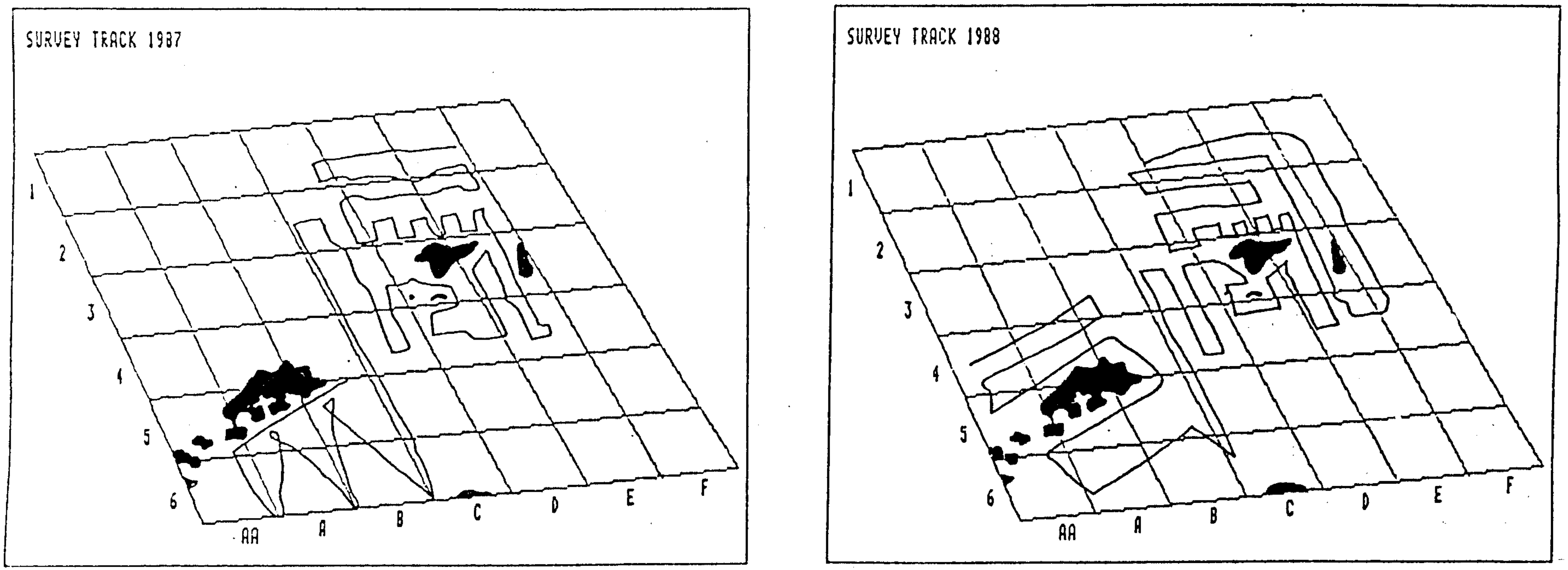

Figure 2: Comparison of cruise tracks in areas surveyed in 1987 and 1988

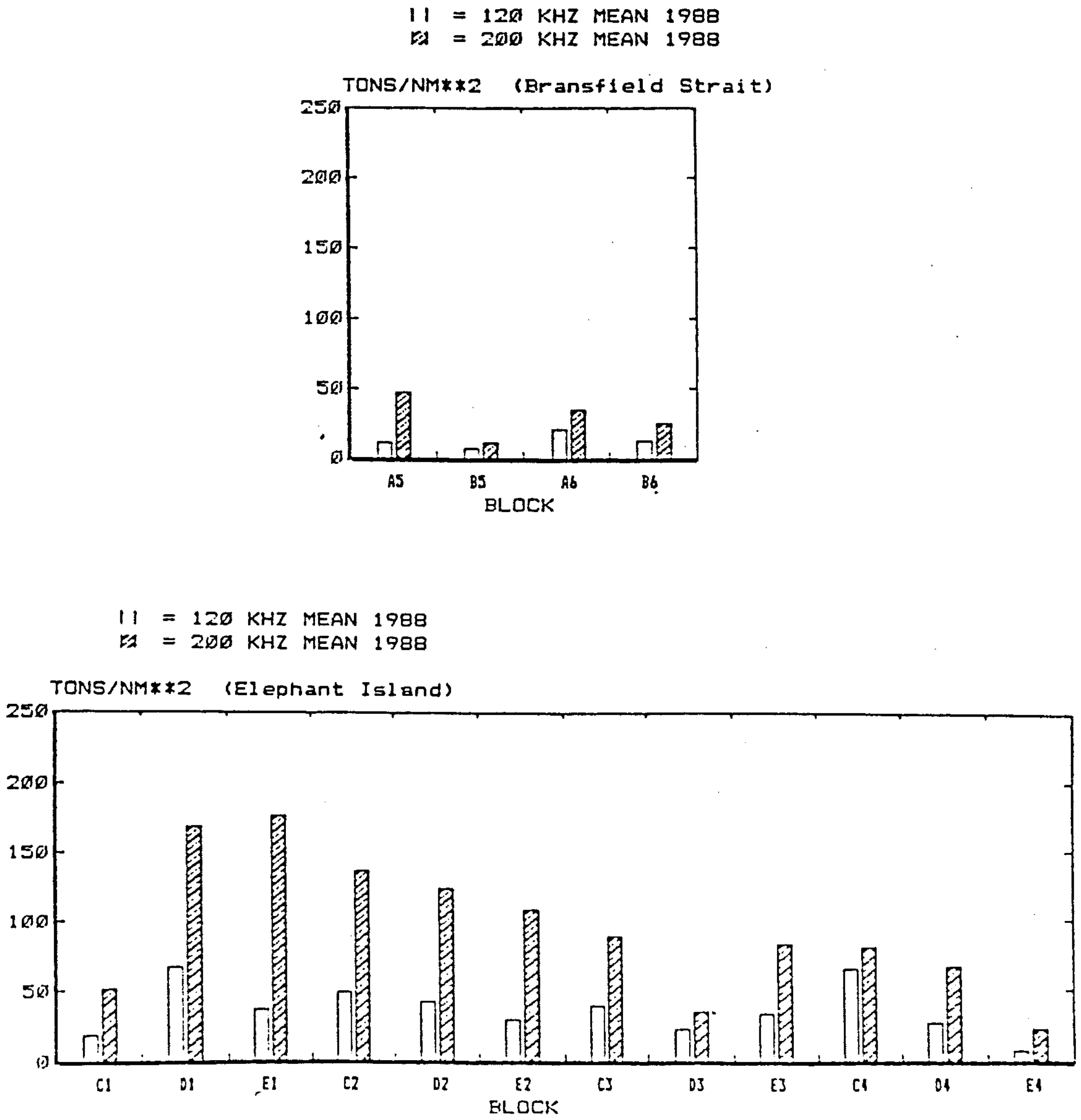

Figure 3: Mean biomass (abundance in tonnes/ n miles^2) for Bransfield Strait and Elephant Island by frequency and block.

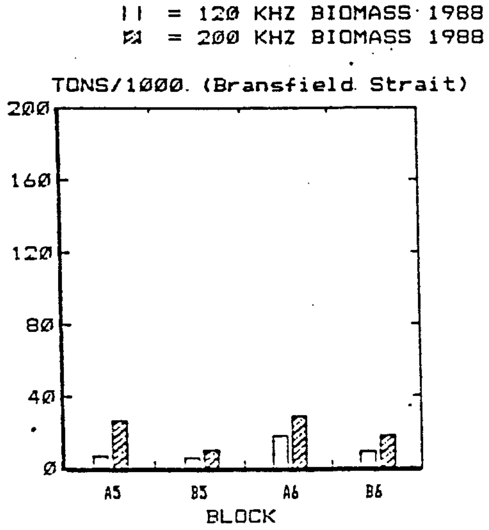

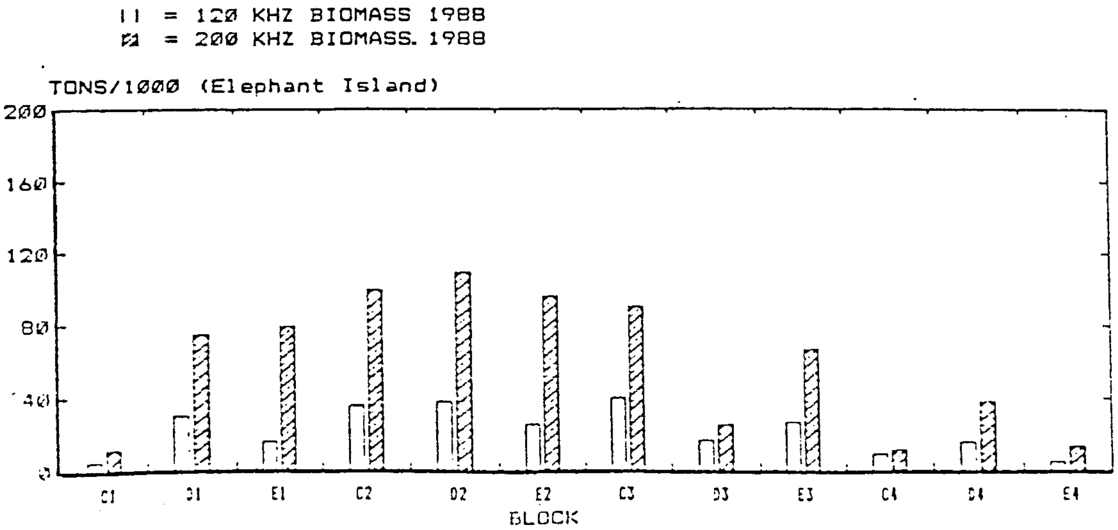

Figure 4: Total biomass (tonnes/1 000) for Bransfield Strait and Elephant Island by frequency and block.

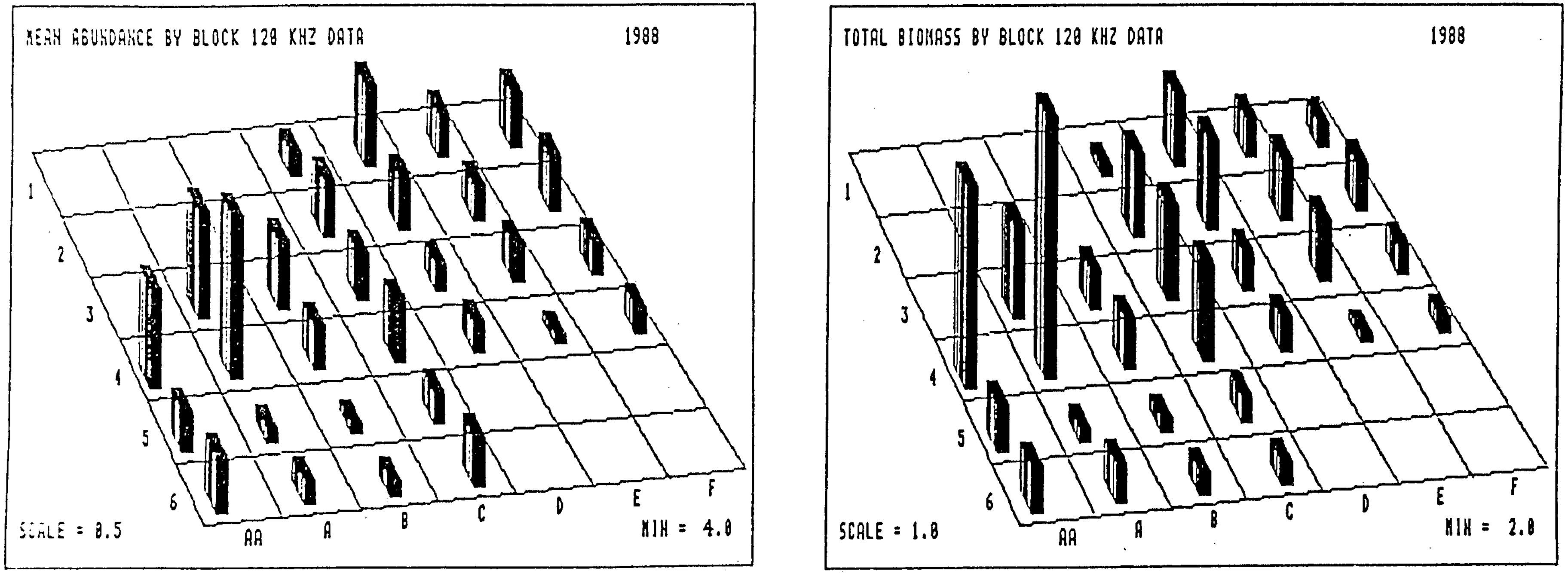

Figure 5: Mean abundance (tonnes/ n miles^2) and total biomass (tonnes/1 000) for 120 kHz data by block.

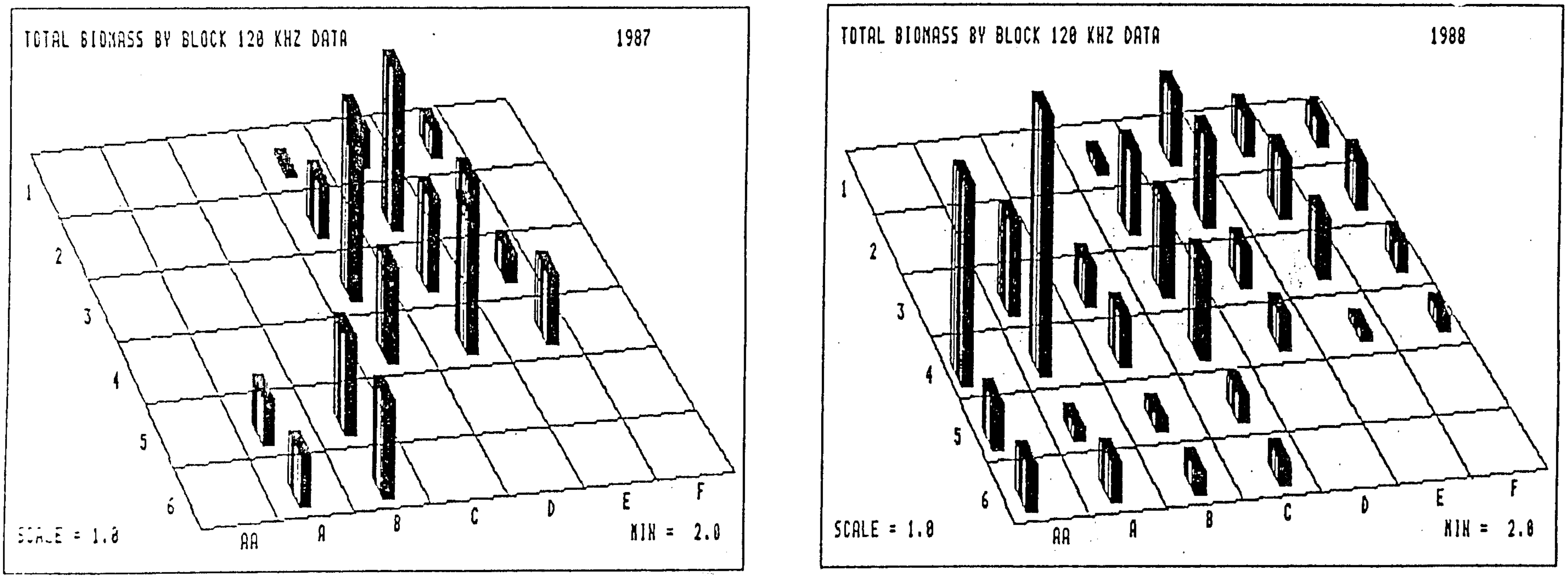

Figure 6: Comparison of total biomass by block for 120 kHz data between 1987 and 1988.

Légendes des tableaux

Tableau 1	Abondance moyenne comparative et biomasse totale pour les aires délimitées étudiées aussi en 1987.
Tableau 2	Abondance moyenne et biomasse totale dans les aires étudiées en 1988.
Tableau 3	Caractéristiques électro-acoustiques des systèmes de sondage.

Légendes des figures

Figure 1	Tracé d'étude et emplacements des aires délimitées dans la zone du détroit de Bransfield et de l'île de l'Eléphant.
Figure 2	Comparaison des trajets de la campagne dans les zone étudiées en 1987 et en 1988.
Figure 3	Biomasse moyenne (tonnes/milles nautiques^2) pour le détroit de Bransfield et l'île de l'Eléphant par fréquence et aire délimitée.
Figure 4	Biomasse totale (tonnes/1 000) pour le détroit de Bransfield et l'île de l'Eléphant par fréquence et aire délimitée.
Figure 5	Abondance moyenne (tonnes/milles nautiques^2) et biomasse totale (1 000 tonnes) pour les données relatives à 120 kHz, par aire délimitée.
Figure 6	Comparaison de la biomasse totale par aire délimitée pour les données à 120 kHz entre 1987 et 1988.

Заголовки к таблицам

Таблица 1	Сравнительная средняя численность и общая биомасса по квадратам, изученным также в 1987 г.
Таблица 2	Средняя численность и общая биомасса по квадратам, изученным также в 1988 г.
Таблица 3	Электроакустические характеристики звуковых систем.

Подписи к рисункам

Рисунок 1	Маршрут съемки и расположения квадратов в районе пролива Брансфилда и острова Элефант.
Рисунок 2	Сравнение маршрутов судов в районах, изученных в 1987 и 1988 гг.
Рисунок 3	Средняя биомасса, измеренная по частоте и квадратам (численность выражена в тоннах/кв.морские мили) для пролива Брансфилда и острова Элефант.
Рисунок 4	Общая биомасса, измеренная по частоте и квадратам (тонны/1000) для пролива Брансфилда и острова Элефант.

Рисунок 5	Средняя численность, (тонны/кв. морские мили) и общая биомасса (1000 тонны), измеренные по квадратам (частота 120кГц).
Рисунок 6	Сравнение общей биомассы, измеренной по квадратам, за 1987 и 1988 гг. (частота 120 кГц).

Encabezamientos de las Tablas

Tabla 1	Abundancia media comparativa y biomasa total para los bloques que fueron también prospeccionados en 1987.
Tabla 2	Abundancia media y biomasa total en los bloques prospeccionados en 1988.
Tabla 3	Características electro-acústicas de los sistemas de sondeo.

Leyendas de las Figuras

Figura 1	Trayectoria de la prospección y localización de los bloques en el área del estrecho de Bransfield y la isla Elefante.
Figura 2	Comparación de las trayectorias del crucero en zonas prospeccionadas en 1987 y 1988.
Figura 3	Biomasa media (abundancia en toneladas/millas náuticas^2) para el estrecho de Bransfield y la isla Elefante por frequencia y bloque.
Figura 4	Biomasa total (toneladas/1 000) para el estrecho de Bransfield y la isla Elefante por frequencia y bloque.
Figura 5	Abundancia media (toneladas/millas náuticas^2) y biomasa total (1 000 toneladas) para los datos de 120 kHz por bloque.
Figura 6	Comparación de la biomasa total por bloque para los datos de 120 kHz entre 1987 y 1988.